

Clinical Gastroenterology
Series Editor: George Y. Wu

Vanessa M. Shami
Michel Kahaleh *Editors*

Endoscopic Ultrasound

 Humana Press

CLINICAL GASTROENTEROLOGY

Series Editor

George Y. Wu

University of Connecticut Health Center, Farmington, CT, USA

For further volumes:

<http://www.springer.com/series/7672>

ENDOSCOPIC ULTRASOUND

Edited by

VANESSA M. SHAMI, MD

*Director of Endoscopic Ultrasound
University of Virginia Health System
Digestive Health Center, USA*

and

MICHEL KAHALEH, MD

*Director of Pancreatico-Biliary Services
University of Virginia Health System
Digestive Health Center, USA*



Humana Press

Editors

Vanessa M. Shami, MD
Associate Professor of Medicine
Director of Endoscopic Ultrasound
Digestive Health Center
University of Virginia Health System
Charlottesville, VA, USA
vms4e@hscmail.mcc.virginia.edu

Michel Kahaleh, MD
Associate Professor of Medicine
Director of Pancreatico-Biliary Services
Digestive Health Center
University of Virginia Health System
Charlottesville, USA
mk5ke@virginia.edu

ISBN 978-1-60327-479-1 e-ISBN 978-1-60327-480-7
DOI 10.1007/978-1-60327-480-7
Springer New York Dordrecht Heidelberg London

Library of Congress Control Number: 2010930043

© Springer Science+Business Media, LLC 2010

All rights reserved. This work may not be translated or copied in whole or in part without the written permission of the publisher (Humana Press, c/o Springer Science+Business Media, LLC, 233 Spring Street, New York, NY 10013, USA), except for brief excerpts in connection with reviews or scholarly analysis. Use in connection with any form of information storage and retrieval, electronic adaptation, computer software, or by similar or dissimilar methodology now known or hereafter developed is forbidden.

The use in this publication of trade names, trademarks, service marks, and similar terms, even if they are not identified as such, is not to be taken as an expression of opinion as to whether or not they are subject to proprietary rights.

Printed on acid-free paper

Humana Press is part of Springer Science+Business Media (www.springer.com)

PREFACE

Endoscopic ultrasound has revolutionized the approach to lesions inside and outside the gastrointestinal tract. It has opened the door for gastroenterologists to explore organs outside of the GI lumen, such as the lymph nodes, lung, pancreas, and liver. Few textbooks provide detailed information on the techniques, indications, and the future of EUS, and the technology is advancing rapidly. The purpose of this text is to provide an updated reference on endoscopic ultrasound, as well as focus on new and expanding technologies related to this field.

The key to understanding endoscopic ultrasound is the instrumentation and technology, which are addressed in the opening chapters. Following chapters describe the utility of EUS in different parts of the body and compartmentalizing it as is done in practice. At the end of the book, the pioneers in the field summarize new studies and the direction of EUS in practice.

By spanning the spectrum of EUS from basics to the new and latest technologies, we believe it will be a valuable resource to physicians and support staff who are beginning EUS, as well as trained ultrasonographers who wish to arm themselves with a comprehensive reference and explore the future of the field.

CONTENTS

Preface	v
Contributors	ix

Part I EUS for Starters

Endosonographic Instrumentation	3
<i>Shawn Mallery</i>	
Probe Ultrasonography	33
<i>Henry C. Ho, Jeffrey L. Tokar, and Irving Waxman</i>	
Radial Endoscopic Ultrasound	63
<i>Scott T. Cooper and Michael K. Sanders</i>	
Linear Endoscopic Ultrasound	91
<i>Jason D. Conway and Girish Mishra</i>	
The Cytopathology of Endoscopic Ultrasound-Guided	
Fine Needle Aspiration	111
<i>Maria Luisa Policarpio-Nicolas, Deborah J. Chute,</i> <i>and Edward B. Stelow</i>	
Pitfalls in Endoscopic Ultrasound	165
<i>Charles E. Dye</i>	

Part II EUS by Location

The Role of EUS in Esophageal Cancer	183
<i>Audrey H. Calderwood and Brain C. Jacobson</i>	
Role of EUS in Mediastinal Nodes, Masses, Cysts, and Lung Cancer	205
<i>David H. Robbins, Babitha Reddy, and Mohamad A. Eloubeidi</i>	
The Role of Endoscopic Ultrasound in Gastric Cancer	227
<i>Sanjay R. Hegde, Oleh Haluszka, and Jeffrey L. Tokar</i>	
The Role of EUS in Subepithelial Lesions	249
<i>Janelle Brown-Chang and Joo Ha Hwang</i>	

<i>Endoscopic Ultrasound of Ampullary and Duodenal Lesions</i>	267
<i>Jessica Trevino and Shyam Varadarajulu</i>	
<i>The Role of EUS in Pancreatic Cancer</i>	283
<i>Vanessa M. Shami, Indu Srinivasan, and Michel Kahaleh</i>	
<i>The Role of EUS in Cystic Lesions of the Pancreas</i>	299
<i>Mohammad Al-Haddad and John DeWitt</i>	
<i>The Role of EUS in the Biliary System</i>	329
<i>Jean-Louis Frossard and Jean-Marc Dumonceau</i>	
<i>The Role of EUS in Rectal Cancer and Fecal Incontinence</i>	371
<i>Uzma D. Siddiqui and Harry R. Aslanian</i>	
<i>Part III Interventional EUS</i>	
<i>Interventional Endoscopic Ultrasound-Guided</i>	
<i>Cholangiopancreatography</i>	
<i>Jennifer L. Maranki, Michel Kahaleh, and Vanessa M. Shami</i>	
<i>Endoscopic Ultrasound-Guided Drainage</i>	
<i>of Pancreatic Fluid Collections</i>	
<i>Jayant P. Talreja and Michel Kahaleh</i>	
<i>Endoscopic Ultrasound-Guided Celiac Plexus Block</i>	
<i>and Celiac Plexus Neurolysis</i>	
<i>Alejandra Castillo-Roth and Frank Gress</i>	
<i>Part IV Innovations in EUS</i>	
<i>Fine Needle Injection Therapy</i>	
<i>Christopher J. DiMaio and William Brugge</i>	
<i>Contrast-Enhanced Endoscopic Ultrasound</i>	
<i>Marc Giovannini</i>	
<i>Endosurgical Applications of EUS</i>	
<i>Annette Fritscher-Ravens and Parupudi V.J. Sriram</i>	
<i>The Future of EUS</i>	
<i>Thomas J. Savides</i>	
<i>Index</i>	527

CONTRIBUTORS

- MOHAMMAD AL-HADDAD, MD • *Assistant Professor of Clinical Medicine
Division of Gastroenterology & Hepatology, Indiana University
School of Medicine, Indianapolis IN, USA*
- HARRY R. ASLANIAN, MD • *Section of Digestive Diseases,
Yale University School of Medicine, New Haven CT, USA*
- JANELLE BROWN-CHANG, MD • *Division of Gastroenterology, Department of
Medicine, University of Washington Medical Center, Seattle, WA, USA*
- WILLIAM BRUGGE, MD • *Professor of Medicine Massachusetts General Hospital,
Boston, MA, USA*
- AUDREY H. CALDERWOOD, MD • *Section of Gastroenterology,
Boston University Medical Center, Boston, MA, USA*
- ALEJANDRA CASTILLO-ROTH, MD • *Clinical Assistant Instructor Division of
Gastroenterology and Hepatology, SUNY Downstate Medical Center,
Brooklyn, NY, USA*
- DEBORAH J. CHUTE, MD • *Assistant Professor Department of Pathology,
Cleveland Clinic, Cleveland, OH, USA*
- JASON D. CONWAY, MD, MPH • *Assistant Professor of Medicine, Section on
Gastroenterology, Wake Forest University Health Sciences, Winston-Salem,
NC, USA*
- SCOTT T. COOPER, MD • *Instructor of Medicine Division of Gastroenterology,
Hepatology and Nutrition, University of Pittsburgh Medical Center,
Pittsburgh, PA, USA*
- JOHN DEWITT, MD, • *Associate Professor of Clinical Medicine
Division of Gastroenterology & Hepatology, Indiana University
School of Medicine, Indianapolis, IN, USA*
- CHRISTOPHER J. DIMAIO, MD • *Massachusetts General Hospital, Boston,
MA, USA*
- JEAN-MARC DUMONCEAU, MD • *Service of Gastroenterology and Hepatology,
Geneva University Hospitals, Micheli-du-Crest street 241205, Geneva,
Switzerland*
- CHARLES E. DYE, MD • *Associate Professor of Medicine Division of
Gastroenterology and Hepatology, MS Hershey Medical Center,
Penn State College of Medicine, Hershey, PA, USA*

- MOHAMAD A. ELOUBEIDI, MD, MHS • *Associate Professor of Medicine and Pathology, Director Endoscopic Ultrasound Program Department of Gastroenterology and Hepatology, The University of Alabama at Birmingham, Birmingham, AL, USA*
- ANNETTE FRITSCHER-RAVENS, MD • *Interdisciplinary Endoscopy Internal Medicine I, University Hospital, Kiel, Germany*
- JEAN-LOUIS FROSSARD, MD • *Service of Gastroenterology and Hepatology, Geneva University Hospitals, Micheli-du-Crest street 241205, Geneva, Switzerland*
- MARC GIOVANNINI, MD • *Head of Endoscopic Unit Paoli-Calmettes Institute, Marseille, France*
- FRANK GRESS, MD • *Professor of Medicine and Chief Division of Gastroenterology and Hepatology, SUNY Downstate Medical Center, Brooklyn, NY, USA*
- OLEH HALUSZKA, MD • *Division of Gastroenterology, Fox Chase Cancer Center, Philadelphia, PA, USA*
- SANJAY R. HEGDE, MD • *Division of Gastroenterology, Fox Chase Cancer Center, Philadelphia, PA, USA*
- HENRY C. HO, MD • *University of Virginia, Charlottesville, VA, USA*
- JOO HA HWANG, MD, PHD • *Assistant Professor Division of Gastroenterology, Department of Medicine, University of Washington Medical Center, Seattle, WA, USA*
- BRIAN C. JACOBSON, MD, MPH • *Section of Gastroenterology, Boston University Medical Center, Boston, MA, USA*
- MICHEL KAHALEH, MD • *Associate Professor of Medicine University of Virginia, Charlottesville, VA, USA*
- SHAWN MALLERY, MD • *Director Division of Gastroenterology, Hennepin County Medical Center, Minneapolis, MN, USA*
- JENNIFER L. MARANKI, MD • *Clinical Fellow University of Virginia, Charlottesville, VA, USA*
- GIRISH MISHRA, MD, MS • *Associate Professor of Medicine Section on Gastroenterology, Wake Forest University Health Sciences, Winston-Salem, NC, USA*
- MARIA LUISA POLICARPIO-NICOLAS, MD • *Department of Pathology, Spectrum Health Hospital, Grand Rapids, MI, USA*
- BABITHA REDDY, DO, MPH • *Division of Gastroenterology, Center for Advanced Therapeutic Endoscopy, Lenox Hill Hospital, New York, NY, USA*
- DAVID H. ROBBINS, MD, MSC • *Division of Gastroenterology, Center for Advanced Therapeutic Endoscopy, Lenox Hill Hospital, New York, NY, USA*
- MICHAEL K. SANDERS, MD • *Assistant Professor of Medicine Division of Gastroenterology, Hepatology and Nutrition, University of Pittsburgh Medical Center, Pittsburgh, PA, USA*
- THOMAS J. SAVIDES, MD • *Professor of Clinical Medicine,*

- University of California, San Diego, CA, USA*
- VANESSA M. SHAMI, MD • *Associate Professor of Medicine, Director of Endoscopic Ultrasound University of Virginia, Charlottesville, VA, USA*
- UZMA D. SIDDIQUI, MD • *Section of Digestive Diseases, Yale University School of Medicine, New Haven, CT, USA*
- INDU SRINIVASAN, MD • *Division of Gastroenterology and Hepatology University of Virginia, Charlottesville, VA, USA*
- PARUPUDI V.J. SRIRAM, MD • *Department of Gastroenterology, Texas Tech University of Health Sciences Center, Lubbock, USA*
- EDWARD B. STELOW, MD • *Professor Department of Pathology, University of Virginia, Charlottesville, VA, USA*
- JAYANT P. TALREJA, MD • *Clinical Fellow University of Virginia, Charlottesville, VA, USA*
- JEFFREY L. TOKAR, MD • *Fox Chase Cancer Center, Philadelphia PA, USA*
- JESSICA TREVINO, MD • *Clinical Fellow Division of Gastroenterology-Hepatology, University of Alabama at Birmingham School of Medicine, Birmingham, AL, USA*
- SHYAM VARADARAJULU, MD • *Associate Professor of Medicine Division of Gastroenterology-Hepatology, University of Alabama at Birmingham School of Medicine, Birmingham, AL, USA*
- IRVING WAXMAN, MD • *Professor of Medicine and Surgery, Center for Advanced Medicine, University of Chicago, Chicago, IL, USA*

Part I
EUS for Starters

Endosonographic Instrumentation

Shawn Mallery, MD

CONTENTS

INTRODUCTION: BASICS OF ULTRASOUND
AND RATIONALE FOR EUS
THE ULTRASOUND TRANSDUCER
RADIAL ARRAY VERSUS LINEAR ARRAY
BASIC ECHOENDOSCOPE DESIGN
LINEAR ARRAY ECHOENDOSCOPES
RADIAL ECHOENDOSCOPES
ENDOBONCHIAL ULTRASOUND DEVICES
OTHER SPECIALIZED DEVICES
EUS MINIPROBES
ULTRASOUND CONSOLES
EUS NEEDLES
CONCLUSION

Abstract

Endoscopic ultrasound is a relatively new technology that has a growing indication which extends beyond the field of gastroenterology. The high degree of resolution and the ability to perform real time imaging during both diagnostic and therapeutic interventions allow ultrasound to remain a highly valuable modality. The first and most important step in performing EUS is to have a thorough understanding on its mechanics as well as the available instrumentation. This chapter sets out to do both.

From: *Clinical Gastroenterology: Endoscopic Ultrasound*,
Edited by: V. M. Shami and M. Kahaleh, DOI 10.1007/978-1-60327-480-7_1,
© Springer Science+Business Media, LLC 2010

Key Words: EUS instrumentation, EUS equipment, Radial EUS, Linear EUS, Fine needle aspiration

INTRODUCTION: BASICS OF ULTRASOUND AND RATIONALE FOR EUS

Diagnostic ultrasonography is a relatively recently developed technology. Initial reports began to appear in the late 1950s and early 1960s (1), and ultrasonography rapidly gained acceptance in the 1970s. As with any technology, diagnostic ultrasound has advantages and disadvantages. When initially introduced, ultrasound provided a relatively unique ability to visualize soft tissue with high degrees of detail. The high degree of resolution and the ability to perform real time imaging during both diagnostic and therapeutic interventions allow ultrasound to remain a highly valuable modality. Advantages include reasonable portability, relatively low cost, and lack of a need for ionizing radiation (as opposed to CT).

Soon after its introduction, several limitations of standard ultrasound became apparent. Ultrasound is unable to image deep to air-filled structures or extremely dense structures such as bone or calculi. As such, ultrasound is of little value in imaging the mediastinum due to the overlying ribs, sternum, and adjacent lungs. Imaging of the pancreas and distal common bile duct is also greatly limited. Another limitation occurs due to a basic principle of sound transmission. Higher resolution imaging requires the use of relatively high frequency sound energy. Unfortunately, higher frequency sound travels poorly through tissue (or other media) – as evidenced by the booming bass sound coming from passing cars with loud stereos without audible treble tones. In order to image structures far from the body surface, standard ultrasound requires the use of relatively low frequency energy (3.5–5 MHz), which as a result produces lower resolution images. In an effort to overcome these limitations, endoscopic ultrasound and transesophageal echocardiography were developed in the early 1980s (2). By placing the ultrasound transducer within the body, it is possible to avoid air-filled or bony structures and reduce the distance between the transducer and the region of interest. As an example, a transducer placed in contact with the duodenal wall will be within 5 mm of the intrapancreatic portion of the distal common bile duct and avoids the interference caused by air in the duodenum, small bowel and colon.

Many issues arose during the initial development of EUS. Should the optical camera view in a forward angle like a standard endoscope or be side-viewing like a duodenoscope? Should the ultrasound transducer

produce images parallel to the long axis of the endoscopy (e.g., a linear or curved linear configuration) or perpendicular to the long-axis (e.g., a radial configuration)? What imaging frequency is ideal? Many of these questions are still debated; however, the currently available echoendoscopes are clearly vastly superior to the initial prototypes. In addition, the development of high-resolution videochip technology has provided higher resolution video imaging (as opposed to older fiberoptic devices) and allows smaller echoendoscopes with larger biopsy channels.

THE ULTRASOUND TRANSDUCER

Although a detailed explanation of the physics of ultrasound is beyond the scope of this article, a basic understanding of ultrasound physics is required. Ultrasound imaging relies upon the use of crystalline material with a unique property called the piezoelectric effect. These crystals vibrate in response to electrical stimulation and, as a result, produce sound. Different crystals produce sound of different frequencies. As important, however, is the reverse phenomenon in which sound energy contacting the crystal will result in the production of electrical current. As a result, the crystals can simultaneously produce a sound beam and “listen” for the portions of this sound energy, which are reflected back to the surface of the crystal. Measurement of the time taken for energy to return, in conjunction with the known speed of sound, allows a calculation of the distance to a given reflecting object. A computer can then display on a map the different locations which produced echoes. Regions which reflect a greater percentage of sound energy is displayed as brighter spots on the map. This is the basis for ultrasound imaging. Imaging with a single piezoelectric crystal will allow probing of a thin line (like a beam from a flashlight) extending from the crystal. By arranging hundreds to thousands of these crystals in an array, a wider region of tissue may be simultaneously imaged.

RADIAL ARRAY VERSUS LINEAR ARRAY

Ultrasound imaging is currently available in two primary imaging planes – radial array and curved linear array (“linear”). These imaging planes are determined by the orientation in which the individual piezoelectric crystals are arrayed on the echoendoscope. Historically, this difference reflected decisions made by separate manufacturers who made different choices with regard to the optimal imaging plane. Early devices produced by Olympus utilized only radial imaging, whereas

early Pentax devices were exclusively linear (although now both companies manufacture both types of devices). Early Olympus mechanical radial-array devices contained a small disc-shaped ultrasound transducer, which was attached to a motor drive and rotated in a plane perpendicular to the long-axis of the endoscope (Fig. 1a, b). This produced a circular image with the endoscope shaft located at the center (Fig. 1c). Pentax linear devices contained a fixed electronic (nonmoving) transducer oriented so as to produce a sector-shaped image parallel to the long-axis of the endoscope (Fig. 2a–c). The majority of early endosonographers learned EUS using the radial devices.

Linear array imaging has one major advantage compared to radial array. This is illustrated in Fig. 2c. A therapeutic device, such as a biopsy needle, which is advanced through the therapeutic channel of the echoendoscope will remain within the imaging beam. As a result, the

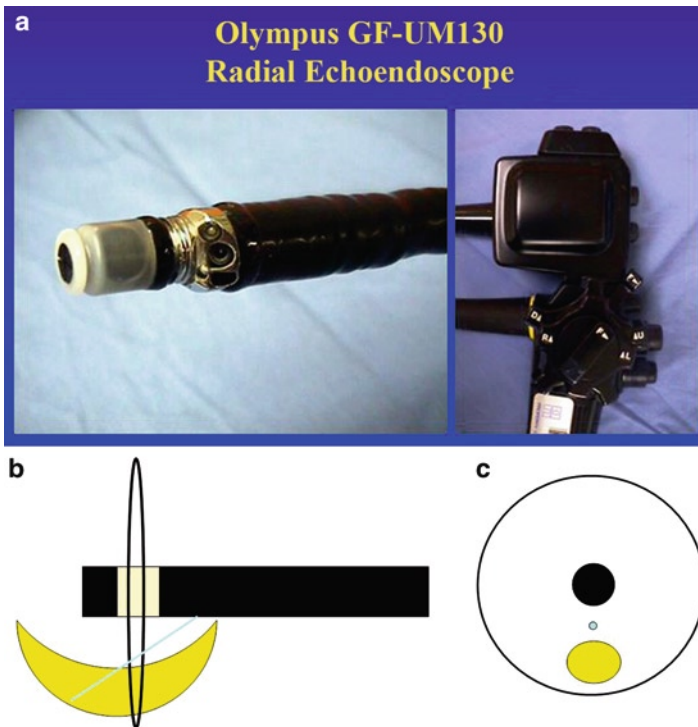


Fig. 1. (a–c) Early Olympus mechanical radial-array devices contain a small disc-shaped ultrasound transducer which is attached to a motor drive and rotated in a plane perpendicular to the long axis of the echoendoscope.

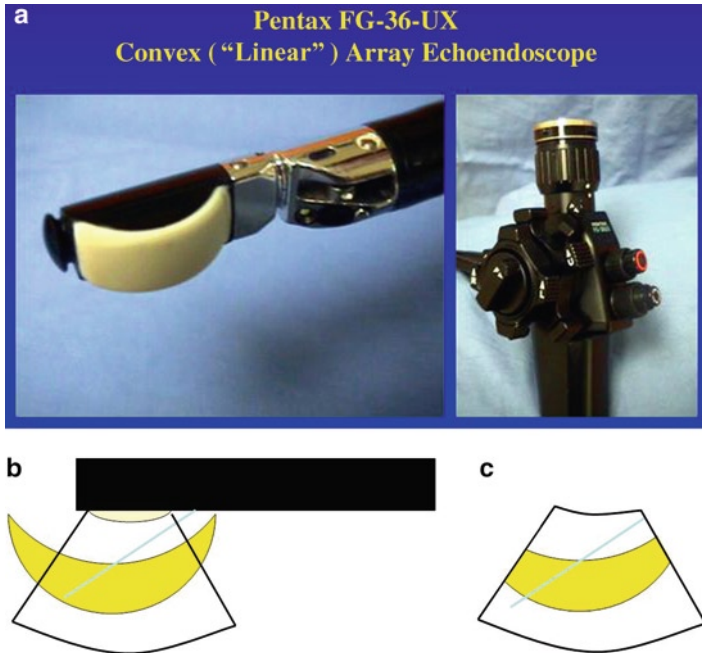


Fig. 2. (a – c) The early Pentax linear devices contain a fixed electronic transducer oriented so as to produce a sector-shaped image parallel to the long-axis of the endoscope. A biopsy needle will remain within the image beam.

entire length of a biopsy needle can be followed continuously as it is advanced through the bowel wall and into adjacent structures of interest. This allows precise placement of a biopsy needle within mass lesions (or other structures, as will be shown in subsequent chapters). This degree of visualization is simply not possible with radial devices. A biopsy needle advanced through a radial device will pass through the imaging beam at roughly a right angle – resulting in a small echogenic spot on the ultrasound image (Fig. 1c). There is no reliable means of determining how far beyond the imaging plane the needle was advanced. Although a few attempts were made to develop techniques for EUS-guided biopsy using radial devices, these approaches were impractical and rapidly abandoned (3).

Because most early endosonographers learned EUS using radial devices, there was significant resistance to adoption of linear EUS. It was often stated that radial EUS was easier to learn than linear, purportedly due to the fact that radial images more closely resembled standard CT imaging planes with which endoscopists were familiar. This is true,

however, only when the echoendoscope is oriented parallel to the spine – an orientation which is often not possible when imaging many abdominal structures such as the pancreas or liver. It was also argued that all EUS cases should be initially performed using a radial echoendoscope, reserving linear devices until a need for biopsy is identified on the radial exam. The argument for this approach was ostensibly due to the superiority of radial imaging, but more likely this indicated greater experience and comfort level with radial devices for the individual endosonographers. In the past 10 years, this practice has changed dramatically at many centers. It is becoming increasingly common to perform a majority of EUS exams entirely with linear devices. This trend likely reflects an increasing familiarity with and availability of linear devices, an increasing acceptance of the clinical utility of EUS-guided tissue sampling (with a concomitant increase in the percentage of cases during which biopsy is performed) and time constraints which discourage the routine use of two separate echoendoscopes for each examination. This discussion is not meant to imply that there is no longer a need for radial EUS. For example, radial array imaging may allow more expeditious screening of large portions of the GI tract wall. Linear imaging does not provide a 360° cross-section of the bowel wall surrounding the endoscope. The resulting blind-spot may be difficult to overcome in some locations without pressing on and distorting the wall – particularly in the antrum and duodenum. The blind spot also makes complete evaluation of the entire surface of circumferential GI tract tumors such as esophageal carcinoma somewhat tedious with a linear device (although in our experience often a critically important feature such as distant metastasis or obvious adventitial invasion can be rapidly identified with a linear device making detailed 360° evaluation unnecessary).

It is prudent to point out that linear and radial imaging are not, by necessity, mutually exclusive. Devices are available for use in transesophageal echocardiography which allows easy, quick rotation between linear and radial imaging. This requires a larger array of crystals, with a resultant larger amount of electrical wiring. At present, the amount of space needed for wiring would preclude the inclusion of other endoscope components which are necessary for EUS, such as biopsy channels and optics. Perhaps someday soon these space limitations will be overcome and a switchable radial/linear EUS scope will become available.

BASIC ECHOENDOSCOPE DESIGN

Although many differences exist between different echoendoscope models, there are many common features. All current echoendoscope models contain a videochip to provide endoscopic imaging, with an

associated light source and water irrigation system for washing the lens. In most instances, the videochip is located proximal to the ultrasound transducer and oriented at an oblique angle to the shaft. The ultrasound transducer is attached to the shaft distal to the optical sensor and oriented in either a linear or radial configuration. It should be noted that older versions of radial devices utilized a rotating disc which spun in a lubricated cap attached to the end of the scope; however, newer devices now use a fixed, annular array of crystals. This eliminates the need for a motor drive, provides clearer images without the potential for motion distortion and allows for color Doppler capability.

As stated earlier, ultrasound imaging is not possible through air. For transcutaneous ultrasound, this air interference is overcome via the application of acoustic coupling gel to the skin surface. It is not feasible, however, to fill the upper GI tract with acoustic coupling gel. Acoustic coupling for EUS is accomplished by either filling the GI tract with water or, alternatively, inflating a water-filled balloon around the transducer which can then be placed in contact with the bowel wall (Fig. 3). These balloons can be inflated using a two-stage water irrigation button – complete depression inflates the balloon while half-depression washes the endoscope lens. Deflation of the balloon involves either a two-stage button (complete depression deflates the balloon) or a switch valve which alternately determines if depression of the suction button empties the bowel lumen or deflates the balloon.



Fig. 3. A water filled balloon around the transducer of an echoendoscope helps to achieve acoustic coupling.

The opposite end of the echoendoscope has two heads. One of these is attached to the light source as with any other endoscope. The other is unique to the echoendoscope and attaches to a separate ultrasound imaging console to transmit the ultrasound data. Each specific manufacturer utilizes a unique ultrasound console; echoendoscopes from one manufacturer are not interchangeable with consoles from a different supplier.

LINEAR ARRAY ECHOENDOSCOPES

A variety of linear devices are now available from multiple manufacturers. These vary in minimal ways, as is detailed in Table 1. The shapes of the transducers vary slightly between suppliers, which influences the shape of the resultant image. The Olympus transducer (Fig. 4) has a more distinct curvature and wider field of view compared to the Pentax device (Fig. 5), providing imaging of more tissue anterior to the echoendoscope. These differences do not necessarily imply a distinct advantage of one type over another. Echoendoscopes are now available in both “diagnostic” and “therapeutic” sizes, determined by the diameter of the device channel. The larger, therapeutic echoendoscopes allow the use of larger therapeutic devices (up to 10 F in diameter) (Fig. 6). This is most relevant with regard to the ability to place large caliber stents directly through the echoendoscope under continuous sonographic guidance (most commonly used for endoscopic drainage of pancreatic pseudocysts). These larger echoendoscopes have, by necessity, a larger overall diameter, and therefore are somewhat more difficult to pass into the esophagus and maneuver through the duodenum.

RADIAL ECHOENDOSCOPES

Several radial array echoendoscopes are currently available, as detailed in Table 2. All except the Olympus GF-UM160 utilize a fixed, nonmoving array of crystals. The GF-UM160 utilizes a rotating disc-shaped transducer (similar to the GF-UM130 shown in Fig. 1a) requiring the use of a motor-drive. Other than this single mechanical-array device the available devices are fairly similar. Pentax radial echoendoscopes place the suction channel and optical sensor at the distal tip of the echoendoscope (Fig. 7) rather than displacing these proximal to the transducer as in the Olympus devices (Fig. 8). This initially led to problems with space limitations in allowing the suction channel and camera wiring to traverse the region of the transducer, requiring a blind spot in the sonographic image (Fig. 9); however, this problem has now been overcome.

Table 1
Linear echoendoscopes

<i>Manufacturer</i>	<i>Model (US processor)</i>	<i>Ultrasound field</i>	<i>Frequency (MHz)</i>	<i>Endoscopic image</i>	<i>Length (mm)</i>	<i>Diameter (maximum) (mm)</i>	<i>Display mode</i>	<i>Channel diameter (mm)</i>
Olympus	GF-UC140P-AL5 (Aloka SSD-Alpha5, Alpha10)	180° Electronic curved linear array	5/6/7.5/10	Video	1,250	14.2	B-mode	2.8
				55° Forward oblique 100° Field of view			M-mode D-mode Flow-mode Powerflow-mode	
Olympus	GF-UCT140-AL5 (Aloka SSD-Alpha5, Alpha10)	180° Electronic curved linear array	5/6/7.5/10	Video	1,250	14.6	B-mode	3.7
				55° Forward oblique 100° Field of view			M-mode D-mode Flow-mode Powerflow-mode	
Olympus	GF-UC160P-OL5 (Olympus EU-C60)	150° Electronic curved linear array	7.5	Video	1,250	14.2	Color power doppler	2.8
				55° Forward oblique 100° Field of view			Color power doppler	
Olympus	GF-UCT160-OL5 (Olympus EU-C60)	150° Electronic curved linear array	7.5	Video	1,250	14.6	Color power doppler	3.7
				55° Forward oblique 100° Field of view			Color power doppler	

(continued)

Table 1
(continued)

<i>Manufacturer</i>	<i>Model (US processor)</i>	<i>Ultrasound field</i>	<i>Frequency (MHz)</i>	<i>Endoscopic image</i>	<i>Length (mm)</i>	<i>Diameter (maximum) (mm)</i>	<i>Display mode</i>	<i>Channel diameter (mm)</i>
Pentax	EG-3630U (Hitachi 5500 or HIVISION 900)	Curved linear array	5/7.5/10	50° Forward	1,250	12.8	B-mode, color doppler	2.4
				oblique 120° Field of view				
Fujinon	EG-3870 UTK (Hitachi 5500 or HIVISION 900)	Curved linear array	5/7.5/10	50° Forward	1,250	12.8	B-mode, color doppler	3.8
				oblique 120° Field of view				
Fujinon	EG-530UT (SU-7000)	110° electronic curved linear array	5/7.5/10/12	40° Forward	1,254	13.9	B-mode, M-mode, Color Doppler, power doppler, PW Doppler, "THI"	3.8
				oblique 140° field of view				



Fig. 4. Olympus linear array echoendoscope.



Fig. 5. Pentax linear array echoendoscope.



Fig. 6. Olympus therapeutic echoendoscope.

Table 2
Radial echoendoscopes

<i>Manufacturer</i>	<i>Model (US processor)</i>	<i>Ultrasound field</i>	<i>Frequency (MHz)</i>	<i>Endoscopic image (all are video)</i>	<i>Length (mm)</i>	<i>Diameter (maximum)</i>	<i>Display mode</i>	<i>Channel diameter (mm)</i>
Olympus	GF-UE160-AL5 (Aloka SSD-Alpha5 or Alpha10)	360° Electronic radial array	5/6/7.5/10	55° Forward oblique 100° Field of view	1,250	13.8	B-mode M-mode D-mode	2.2
	GF-UM160 (Olympus EU ME1 or EU-M60)	360° Mechanical radial	C5/C7.5/ C12/C20 (HyperBand)	50° forward oblique 100° Field of view	1,250	12.7	Flow-mode Powerflow-mode B-mode (no Doppler)	2.2
Pentax	EG-3670URK (Hitachi 5500 or HIVISION 900)	360° electronic radial	5/7.5/10	Forward-viewing 140° Field of View	1,250	12.1	B-mode, Color Doppler, Pulse wave CFA (color flow angio)	2.4
Fujinon	EG-530UR (SU-7000)	360° electronic radial	5/7.5/10/12	Forward-viewing 140° Field of View	1,254	11.5	B-mode M-mode Color Doppler Power Doppler Pulse wave	2.2



Fig. 7. In the Pentax radial echoendoscope, the suction channel and optical sensor is placed at the distal tip of the echoendoscope.



Fig. 8. In the Olympus radial echoendoscope, the suction channel and optical sensor is displaced proximal to the transducer.

ENDOBONCHIAL ULTRASOUND DEVICES

Improvements in technology have recently allowed a significant reduction in the diameter of echoendoscopes. This has allowed a sufficiently small diameter to make insertion into the airway technically feasible (Fig. 10). Ultrasound imaging from within the trachea is clinically relevant because it allows visualization of lymph nodes, which are otherwise unable to be imaged with EUS performed from within the esophagus. Due to the inability to image through air, lymph nodes in the pretracheal region and pulmonary hila cannot be seen via the esophagus. These locations, however, are readily visualized if the transducer is placed in the trachea or main bronchi.



Fig. 9. In the Pentax radial echoendoscope system, placing the suction and optical sensor at the distal end of the echoendoscope led to space limitations in allowing the suction channel and camera wiring to traverse the region of the transducer, requiring a blind spot in the sonographic image.



Fig. 10. Olympus endobronchial ultrasound scope.

There are several relevant differences between endobronchial devices and EUS scopes developed for GI applications. Obviously, endoscopes designed for use in the airway do not need to be as long as devices intended to be inserted into the distal duodenum. The current EBUS scope measures only 600 mm in length compared to 1,250–1,254 mm for currently available EUS devices. Other significant differences include the lack of ability to rinse the endoscope lens and the availability of only up/down deflection without right/left motion capabilities. The water balloon used for acoustic coupling is filled manually via a water-filled syringe attached to the scope, rather than via the use of a two-stage air-water button as with EUS.

Although intended for use in the airway, EBUS devices may have clinical utility in the GI tract as well (4). In particular, the small caliber may allow passage through extremely stenotic esophageal tumors, allowing the evaluation of the distal margin of the mass for complete T-classification. Although the shorter length of the device does not allow passage through the pylorus, the evaluation of the medial portions of the liver and left adrenal is possible to assess for metastatic disease. Assessment of nodal metastasis in the gastrohepatic ligament and celiac region may also be performed. If indicated, the linear orientation of the transducer allows directed needle aspiration for tissue sampling as well. Tissue sampling with this device in the stomach is somewhat challenging due to the extreme flexibility of the shaft, which often results in bowing of the echoendoscope in preference to needle penetration of the gastric wall. In selected cases (such as in patients with prior gastric bypass in whom laparoscopic gastrostomy may be performed to access the gastric remnant), the device may be useful in allowing EUS examination via percutaneous gastrostomies.

OTHER SPECIALIZED DEVICES

Table 3 summarizes the other miscellaneous echoendoscopes. A variety of unique devices have been developed for EUS examination. Not all of these remain clinically available. One of the most useful was the Olympus MH 908 esophagoscope. This ultrathin, short device was designed to allow passage through tightly stenotic esophageal malignancies. The esophagoscope has a much smaller caliber (8.5 mm) than other echoendoscopes. More importantly, the distal tip is tapered and contains a channel which allows the device to be passed over a guidewire through a stricture in a manner similar to a Savary dilator (Fig. 11). The device only allows radial imaging and as such does not allow for EUS-guided tissue sampling. The recent availability of small caliber linear array

Table 3
Miscellaneous echoendoscopes

<i>Manufacturer</i>	<i>Model (US processor)</i>	<i>Ultrasound field</i>	<i>Frequency (MHz)</i>	<i>Endoscopic image</i>	<i>Length (mm)</i>	<i>Diameter (maximum) (mm)</i>	<i>Display mode</i>	<i>Channel diameter (mm)</i>
Olympus	BF-UC160F-OL8 (Olympus EU-C60) for endobronchial US	50°	7.5	Video 35° forward Oblique 80° Field of view	600	6.9	B-mode Color power doppler	2.0
	BF-UC180F (Olympus EU-C60 OR Aloka SSD-Alpha5 or Alpha10) for endo- bronchial US	60° (Alpha5) or 50° (EU-C60)	5/7.5/10/12 MHz (only 7.5 MHz with EU-C60)	Video 35° Forward Oblique 80° Field of view	600	6.9	B-mode Color Power Doppler (with Alpha5: B-mode, M-mode, D-mode, Flow-mode, Powerflow- mode)	2.2

MH-908 Esophagoprobe (Olympus EU ME1 or EU M60)	360° mechanical radial	NA	700	8.5	B-mode	NA
Pentax EB-1970UK Hitachi 5500 or HIVISION 900 for endobronchial US	Curved linear array	Video Forward oblique 100° field of view	600	6.3	B-mode, color Doppler	2.0



Fig. 11. Olympus MH 908 esophagoprobe.



Fig. 12. Olympus end-viewing echoendoscope.

devices (e.g., EBUS scopes) which do allow needle aspiration may well make this device obsolete.

An end-viewing, long, radial-array device has been previously manufactured by Olympus for use in the colon. This has not gained widespread acceptance, probably because there are very few indications for colonic EUS. T-classification of colon cancer does not determine surgical management, and therefore preoperative ultrasound staging of colon cancer is not necessary. T-classification of rectal carcinoma, on the other hand, is critical to management decisions; however, adequate staging of rectal cancer can be performed with currently available echoendoscopes designed for use in the upper GI tract (or dedicated rigid rectal ultrasound probes). The primary indication for ultrasound imaging in the colon proximal to the extent of upper EUS devices is the evaluation of intramural, subepithelial tumors of the colon. These lesions are relatively uncommon, and adequate evaluation

can be performed in most cases using through-the-scope miniprobes (see below) via a two-channel colonoscope. EUS-guided needle aspiration is not possible with this approach (or, for that matter, with the dedicated radial device) but is rarely necessary and thus it is unclear whether the expense of a dedicated EUS colonoscope is warranted. Prototype EUS-duodenoscopes were also developed by Olympus but have never achieved widespread use.

Recently, a prototype end-viewing linear echoendoscope developed by Olympus has received considerable interest. The current prototype device, the Olympus GIF-UCT160J-AL5, measures 14.2 mm in maximal diameter and contains a large-caliber 3.7 mm channel. The combination of a linear imaging plane plus end-viewing optics (Fig. 12) has been touted as providing improved visualization for interventional EUS procedures such as cystgastrostomy. The degree to which the device attains widespread utilization remains to be determined.

EUS MINIPROBES

A variety of small-caliber miniature ultrasound probes are available (Table 4). These miniprobes can be advanced through the channel of a standard diagnostic or therapeutic endoscope or colonoscope. Acoustic coupling may be attained via either instillation of water in the GI tract or the use of specialized balloon sheaths (Fig. 13). Use of a two-channel endoscope is preferred as this allows for simultaneous sonographic imaging with the probe through one channel and water instillation/suctioning through the other. These devices are primarily utilized for the imaging of superficial esophageal, gastric malignancies, or small intramural/subepithelial mass lesions. In this case, the ability to directly place the transducer adjacent to the small structure of interest under endoscopic guidance can be quite useful. These probes cannot be used to perform EUS-guided tissue sampling. A wire-guided version, which can be advanced into the biliary or pancreatic ductal systems at the time of ERCP for intraductal applications, is available.

ULTRASOUND CONSOLES

Each brand of echoendoscope utilizes a specific ultrasound imaging console, and these consoles are not interchangeable. In the past few years, the technical performance and the quality of ultrasound imaging have continued to improve, and endosonographers have demanded imaging quality identical to that available for standard diagnostic ultrasonography.

Table 4
Miniprobos

<i>Probe driver</i>	<i>Model</i>	<i>Frequency (MHz)</i>	<i>Working length (mm)</i>	<i>Outer diameter (mm)</i>
Olympus				
MAJ-935 with EU-M60	UM-2R	12	2,050 (for all)	2.5
or MAJ- 682 with	UM-3R	20		2.5
EU-M30S	UM-G20-29R	20		2.9
or MAJ- 682 with	(wire-guided)	20		2.0
EU-M60	UM-S20-20R	30		2.0
	UM-S30-20R	30		2.4
	UM-S30-25R	20		2.6
	UM-BS20-26R (requires balloon MAJ-643R)			
Fujinon				
SP-702 if Fujinon	P2625	25	2,200 (for all)	2.6
system or	P2620	20		2.6
SP-711	P2615	15		2.6
(interface box	P2612	12		2.6
to Hitachi	P2025	25		2.0
system)	P2020	20		2.0
	P2015	15		2.0
	P2012	12		2.0
	PL2226-7.5	7.5		2.6
	(requires addi- tional adapter)			

The current high-end consoles for Olympus (Aloka Alpha10) (Fig. 14) and Pentax (Hitachi HIVISION 900) (Fig. 15) are exceptional and, in the authors opinion, roughly equivalent. The newest Hitachi console offers a novel diagnostic modality termed “elastography,” which interrogates the relative compressibility of adjacent tissue in response to manual pressure applied with the transducer. Relatively compressible



Fig. 13. With the EUS miniprobe, acoustic coupling may be attained by the use of specialized balloon sheaths.



Fig. 14. Olympus (Aloka Alpha 10) console.



Fig. 15. Pentax (Hitachi HIVISION 900) console.

tissue is displayed as green on the ultrasound image, whereas less compressible (and presumably more likely to be malignant) tissue is displayed as purple (Fig. 16). The clinical applicability of elastography remains to be determined.

A variety of more compact ultrasound consoles are available from Olympus. This includes the Olympus EU-M60 console for use with the mechanical radial array echoendoscope. This console is relatively compact and similar in size to the Olympus light source, but cannot be utilized for the Olympus linear array devices. An even more compact and portable console, the EU-C60, offers an economic alternative to the larger, higher-end Aloka console but with fewer imaging options. For example, this console only allows imaging at 7.5 MHz, and the image resolution is less crisp compared to the higher-end models. Still, the console can be used for both linear and radial echoendoscopes, as well as the EBUS device, and does allow the use of color Doppler imaging. As such, it may provide a reasonable lower cost alternative for lower volume centers or facilities with less available capital.

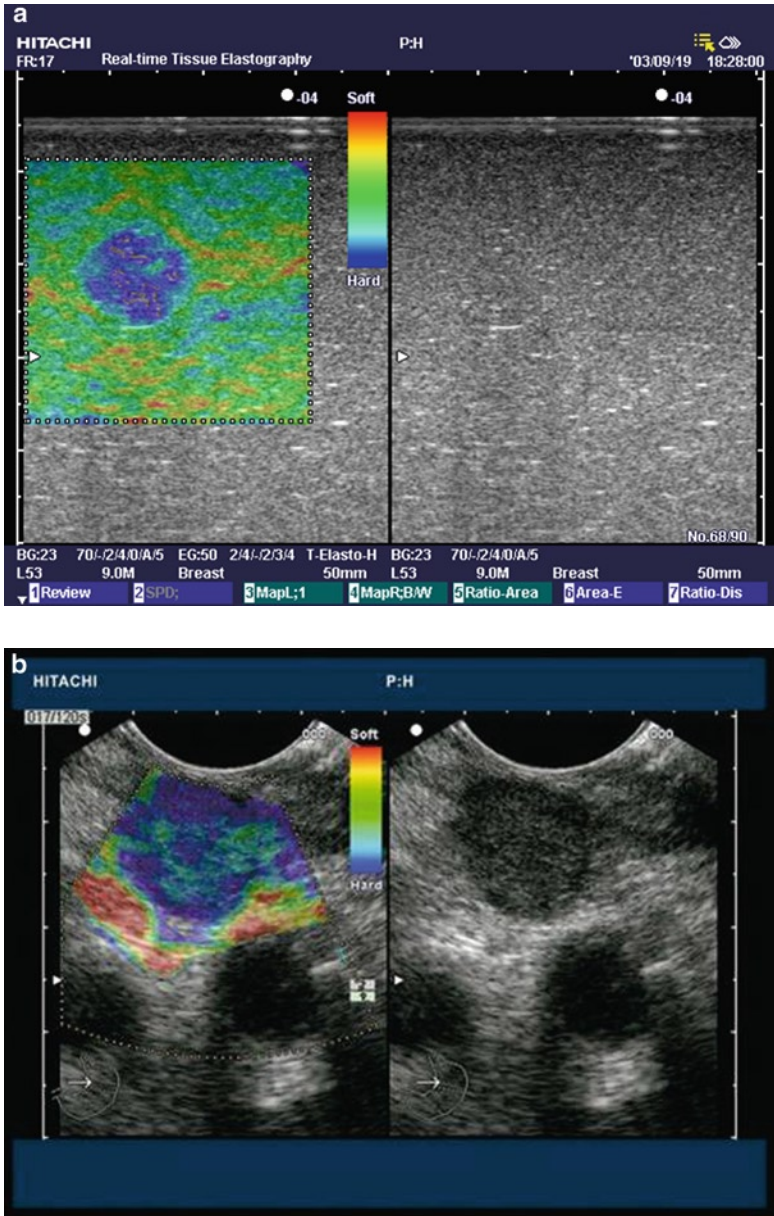


Fig. 16. (a, b) Elastography interrogates the relative compressibility of adjacent tissue in response to manual pressure applied with the transducer. Relatively compressible tissue is displayed as green on the ultrasound image, whereas less compressible (and presumably more likely to be malignant) tissue is displayed as purple.

EUS NEEDLES

EUS-guided intervention requires the use of specialized needles. The needles must be long enough to extend the length of the endoscope channel and must be protected within an outer protective sheath to prevent inadvertent puncture of the endoscope channel (Fig. 17). The needle tip must be long enough to penetrate through the bowel wall and extend into adjacent organs of interest (up to 8 cm to reach hepatic lesions). The needle handle must attach firmly to the echoendoscope handle in order to allow for controlled deployment. Finally, the needle tip is generally roughened or dimpled in order to increase the reflection of the ultrasound beam (Fig. 18).

The first dedicated EUS-FNA needles consisted of a reusable metal sheath and handle assembly into which a single-use needle was loaded (5). In the past few years, entirely disposable models, which have generally supplanted the reusable models, have been released by several vendors.

EUS needles are advanced into the biopsy channel and firmly attached to the echoendoscope via a Luer-lock (Fig. 19). In some models (those made by Cook Medical and Medi-Globe), the extent to which the protective sheath protrudes from the distal end of the echoendoscope may then be adjusted (Fig. 20) to account for subtle differences between echoendoscope manufacturers. It is important that the protective sheath extends beyond the biopsy channel in order to prevent needle damage to the

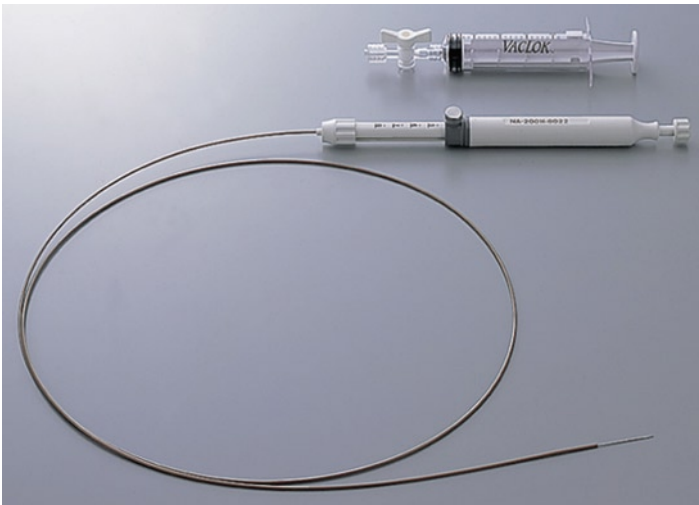


Fig. 17. An EUS needle.



Fig. 18. The needle tip of the EUS needle is often roughened or dimpled to increase reflection of the ultrasound beam.



Fig. 19. EUS needle is attached to the echoendoscope via a Luer-lock.

echoendoscope. The endosonographer should become familiar with the sheath length needed for their echoendoscopes and may initially wish to test this adjustment outside a patient prior to use. It is important to firmly lock the sheath adjustment device prior to needle puncture to prevent inadvertent sheath advancement during the FNA. The needle plunger is

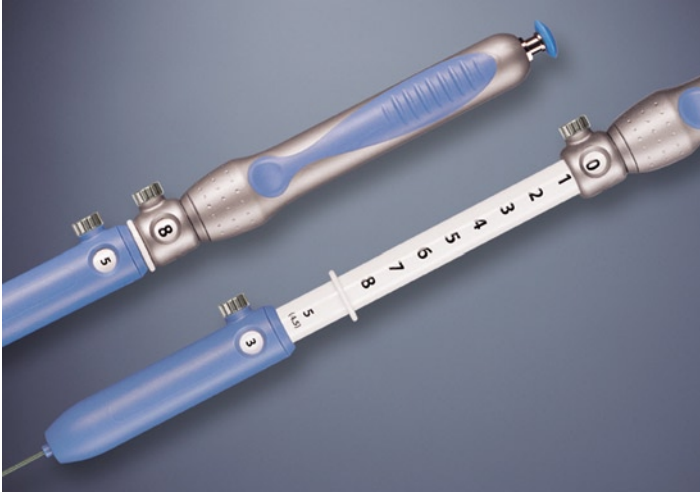


Fig. 20. EUS needle which allows adjustment of the extent to which the protective sheath protrudes from the distal end of the echoendoscope.

then unlocked from the handle assembly, allowing the needle itself to be advanced out of the protective sheath and into the lesion of interest under continuous sonographic guidance. Suction may then be applied either manually or via a preloaded suction syringe.

All currently available needles come packaged with stylets; however, the use of these stylets varies between endosonographers. Some endoscopists choose to keep the stylet in the needle during puncture. In this case, the stylet must be withdrawn a few millimeter into the needle tip so that it no longer protrudes beyond the beveled needle tip prior to puncture. Although some stylets are blunt-tipped and others beveled, it is the authors' experience that the beveled tip of the stylet does not always completely align with the needle bevel and thus needle puncture should not be performed with the stylet fully introduced. Other endoscopists, including the author, do not routinely utilize the stylet. In either case, the stylet should be kept clean as it may be needed later to unclog a needle in case the specimen clots prematurely. Once aspiration is complete, the needle is completely withdrawn into the protective sheath and relocked in place to prevent inadvertent needle advancement and scope trauma as the needle assembly is removed from the echoendoscope.

Several different models of disposable EUS needles are available. Although manufacturers may tout differences in needle visualization, these are minimal in the authors' experience. The needles are available in 25, 22, and 19 ga. Whether these differences in needle gauge result

in difference in cytologic yield is a focus of current study and has not been definitively resolved. In the end, needle choice is based primarily upon experience and endoscopist preference. Needles used for endobronchial ultrasound are, by necessity, shorter in length but of generally similar design.

A 19 gauge core biopsy needle (Quick-Core) has been marketed by Cook Medical (6). This needle is described in detail elsewhere; however, the design includes a permanent stylet with a depressed tissue tray (Fig. 21). The tissue tray/stylet is advanced into the target tissue under continuous sonographic guidance, and then the outer needle is fired forcefully along the outside of the stylet via an automated firing mechanism in order to cut a histologically intact core of tissue into the tray.

Another automated needle, the PowerShot, is manufactured by Olympus (Fig. 22). In this case, the automated, spring-loaded firing mechanism is not intended to obtain a core specimen, but is simply designed to aid in the rapid penetration of target structures with a 22 ga needle for subsequent cytologic aspiration. The needle may be manually advanced for a length up to 6 cm, with the mechanical firing mechanism allowing an additional 3 cm of rapid, automated, forceful penetration. The handle and sheath are reusable. This device may be helpful for the sampling of extremely dense/fibrotic structures or for endoscopists who have difficulty with the manual puncture of routine structures.



Fig. 21. Nineteen gauge core biopsy needle by Cook Medical.

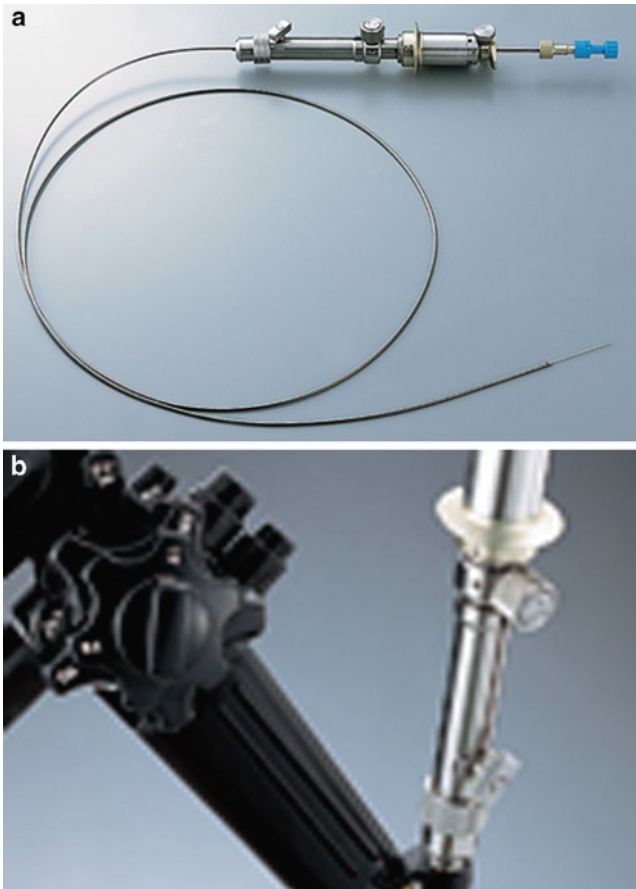


Fig. 22. (a, b) Olympus automated 22 gauge needle.

CONCLUSION

Despite the increasing utilization of endosonography, a relatively limited variety of echoendoscopes and accessories are currently available. As such, the endoscopist should be able to quickly become familiar with the current equipment and rapidly develop a reasonable comfort level with these devices. It is anticipated that an increasing number of specialized echoendoscopes and accessories will become available in the near future, and these developments will be welcomed.

REFERENCES

1. Donald I, MacVicar J, Brown TG. Investigation of abdominal masses by pulsed ultrasound. *Lancet*. 1958;1(7032):1188–95.
2. DiMagno EP, Buxton JL, Regan PT, Hattery RR, Wilson DA, Suarez JR, et al. Ultrasonic endoscope. *Lancet*. 1980;1(8169):629–31.
3. Gress FG, Hawes RH, Savides TJ, Ikenberry SO, Lehman GA. Endoscopic ultrasound-guided fine-needle aspiration biopsy using linear array and radial scanning endosonography. *Gastrointest Endosc*. 1997;45:243–50.
4. Gupta K, Mallery S. Small-caliber endobronchial ultrasonic videoscope: successful transesophageal and transgastric FNA after failed passage of a standard ultrasonic endoscope. *Gastrointest Endosc*. 2007;66:574–7.
5. Vilmann P, Hancke S. A new biopsy handle instrument for endoscopic ultrasound-guided fine-needle aspiration biopsy. *Gastrointest Endosc*. 1996;43:238–42.
6. Levy MJ, Wiersema MJ. EUS-guided trucut biopsy. *Gastrointest Endosc*. 2005;62:417–26.

Probe Ultrasonography

*Henry C. Ho, MD, Jeffrey L. Tokar,
MD,
and Irving Waxman, MD*

CONTENTS

INTRODUCTION
INSTRUMENTS AND EXAMINATION TECHNIQUES
GASTROINTESTINAL WALL ANATOMY
CLINICAL INDICATIONS
INTRADUCTAL ULTRASOUND
TECHNICAL CONSIDERATIONS
BILIARY TRACT ANATOMY
CLINICAL INDICATIONS
PANCREATIC INTRADUCTAL ULTRASOUND
PAPILLA OF VATER INTRADUCTAL ULTRASOUND
FUTURE PROBE TECHNOLOGY
CONCLUSION

Abstract

High frequency ultrasound sonography (HFUS) utilizes probe catheters that operate at a higher frequency than standard endoscopic ultrasonography (EUS). These catheter probes can be passed down the channel of a standard endoscope, or sideview scope during endoscopic retrograde cholangiopancreatography (ERCP), to produce higher resolution ultrasound imaging of the gastrointestinal and pancreaticobiliary tracts. HFUS has an array of clinical applications, like EUS, including the examination of submucosal abnormalities and pancreaticobiliary disease, as well as cancer staging. The improved imaging

From: *Clinical Gastroenterology: Endoscopic Ultrasound*,
Edited by: V. M. Shami and M. Kahaleh, DOI 10.1007/978-1-60327-480-7_2,
© Springer Science+Business Media, LLC 2010

resolution of HFUS, however, results in a loss of imaging depth, thereby limiting its utility in defining deep tissue or distant structures along the GI tract. The extension of HFUS in the pancreaticobiliary tree is intraductal ultrasound (IDUS). IDUS has been shown to have indications in defining choledocholithiasis, evaluating biliary strictures, and local staging of cholangiocarcinoma. IDUS can also be applied as pancreatic IDUS and papilla of Vater IDUS, where it can be useful in the evaluation of pancreatic strictures, pancreatic adenocarcinoma, mucin producing tumors of the pancreas, and papillary tumors.

Key Words: Catheter probe, Probe ultrasonography, High frequency ultrasound sonography (HFUS), Intraductal ultrasound (IDUS), Pancreatic IDUS, Papilla of Vater IDUS

INTRODUCTION

Endoscopic ultrasonography (EUS) incorporates ultrasound technology into the tip of an endoscope to visualize the gastrointestinal wall and surrounding structures. EUS has been used to stage tumors of the gastrointestinal tract, pancreas, and bile ducts (1). Indeed, studies demonstrate that EUS is a highly accurate modality for staging the depth of tumor invasion. Unfortunately, there is difficulty in distinguishing inflammatory versus neoplastic processes via EUS (2). High frequency ultrasound sonography (HFUS) was therefore designed to improve imaging resolution. Typical echo-endoscopes operate from 5 to 20 MHz. HFUS probes, on the other hand, operate with higher frequency (12–30 MHz). HFUS has been demonstrated to produce images with improved resolution in comparison to standard EUS (0.07–0.18 mm) (3–6). One can imagine that more detailed imaging of mucosal and subepithelial lesions of the gastrointestinal tract and pancreaticobiliary tree can be achieved (5). Indeed, the superior definition of HFUS provides images of the wall structure layers resembling those seen on histology (7).

As with all ultrasound technology, the choice of frequency is a trade-off between spatial resolution of the image and imaging depth: higher frequencies produce greater resolution but cannot image deeper into the tissue (8). In fact, the higher frequency image produced using HFUS usually results in a depth of penetration limited to 2–3 cm. Thus, HFUS probes are especially useful in evaluating tumor extension (T stage) of subepithelial lesions (9). The accuracy of staging superficial tumors of the esophagus, stomach, and colon with HFUS probes can be as high as 60–90% (2, 10–14). Moreover, HFUS has been particularly

attractive as the small caliber ultrasound probe (maximum diameter of 2.6 mm) can be passed through the biopsy channel of an endoscope without endoscope exchange (15). In addition, the ability to delineate tumor extension into the muscularis mucosa gives HFUS superior relevance in numerous clinical indications, particularly for tumors that can be cured by endoscopic mucosal resection or photodynamic therapy alone (16, 17).

INSTRUMENTS AND EXAMINATION TECHNIQUES

In general, HFUS probes can be classified by their working mechanism into mechanical or electronic catheters. At the tip of the catheter, mechanical probes have a single ultrasound transducer rotated by a cable, which transmits the signal to an ultrasound processor. When rotating, the ultrasound transducer produces a 360° image, perpendicular to the longitudinal axis of the HFUS catheter. These mechanical HFUS probes are available in various diameters (2–2.9 mm), frequencies (12–30 MHz), and lengths (1,700–2,200 mm) (18, 19). The mean imaging depths based on the 12, 20, and 30 MHz probes have been reported to be 29, 18, and 10 mm, respectively (5, 6, 18–20). These catheters are also capable of linear scanning. Electronic catheters, on the other hand, consist of a probe that contains a number of fixed ultrasound transducers at their tip. These transducers transmit signals via microwires to the image processor. Thus, there is no rotating system; however, these electronic probes can be oriented radially or linearly. Most studies demonstrate experience with these probes in cardiovascular applications. Yet, there appears to be promise in gastrointestinal disease (18, 21, 22).

In order to utilize the HFUS catheter, a standard endoscope is negotiated through the gastrointestinal tract until the area of interest is reached. The HFUS catheter is then advanced through the biopsy channel of the endoscope and placed in contact with the target lesion. A number of techniques have been described to obtain adequate acoustic coupling between the HFUS catheter and the target lesion. The two methods most frequently used are the condom and the balloon techniques. These techniques appear to be especially useful in the esophagus and rectum (23, 24). In the condom technique, a latex condom is attached to the distal end of the endoscope. Unfortunately, the condom prevents visualization and air insufflation. Therefore, endoscopy must be performed prior to employing the condom. Once the condom is applied and the endoscope is advanced to the region of interest, the condom is filled with water through the biopsy channel. The HFUS

probe is then inserted and acoustic coupling is achieved. This technique can suffer from air pockets between the condom and the gut wall causing image degradation (23, 25).

In the balloon technique, a similar concept is used to improve acoustic coupling. In this method, the HFUS catheter is inserted into a latex sheath with a distal balloon that can be instilled with water. Again, air pockets lead to suboptimal image quality (26). If a double channel endoscope is used, however, the endoscopist can suction air pockets and inject water into the gut lumen through the second biopsy channel (27). The suctioning of air in the bowel can lead to collapse of the colon wall and subsequent obscuring of the anatomical relationships of interest. Water immersion over a miniprobe, then, may be the preferable method to decrease image distortion although this technique does not always appear to be necessary (28). There are several other subtleties in examination technique that can improve acoustic coupling. For example, prior to the procedure, the tip of the HFUS probe should be rotated to allow equal distribution of immersion oil that surrounds the transducer cap to maximize image quality. Some endoscopists have used submucosal injections below target lesions, particularly in esophageal and colorectal tumors to improve staging (29). More aggressive manipulation of target lesions such as actual biopsy, however, generally leads to greater artifact imaging. Therefore, the HFUS probe should be used prior to such procedures.

GASTROINTESTINAL WALL ANATOMY

Typical echo-endoscopes operate at frequencies that produce a five layer image of the gastrointestinal wall. The HFUS probe, on the other hand, can identify 9–11 layers in the stomach and five layers in the colon (10, 16, 17, 29, 30). In the stomach, the first (hyperechoic) and second (hypoechoic) layers correspond to the interface with the probe surface and mucosa. The third (hyperechoic) and fourth (hypoechoic) layers are the interface between the mucosa and submucosa. The fifth (hyperechoic) layer is the submucosa. The sixth (hypoechoic) layer represents the inner circular muscle layer. The seventh (hyperechoic) and eighth (hypoechoic) layers are the intramuscular connective tissue interface and outer longitudinal muscle layers, respectively. The ninth (hyperechoic) layer is the subserosa and serosa (Figs. 1 and 2). In the colon, the three layers of the muscularis propria can be visualized. The inner hypoechoic layer is the circular muscle; the middle hyperechoic interface represents the connective tissue; and the outer hypoechoic longitudinal layer is the muscle layer.

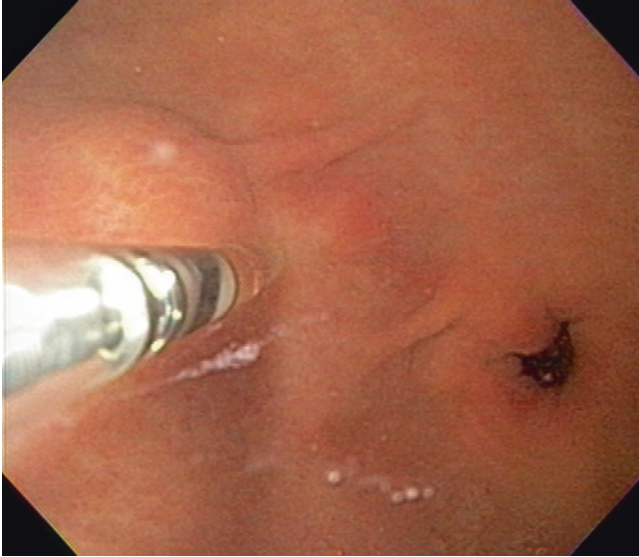


Fig. 1. Endoscopic view of a small, subepithelial mass in the gastric antrum being evaluated with a high-frequency ultrasound miniprobe.

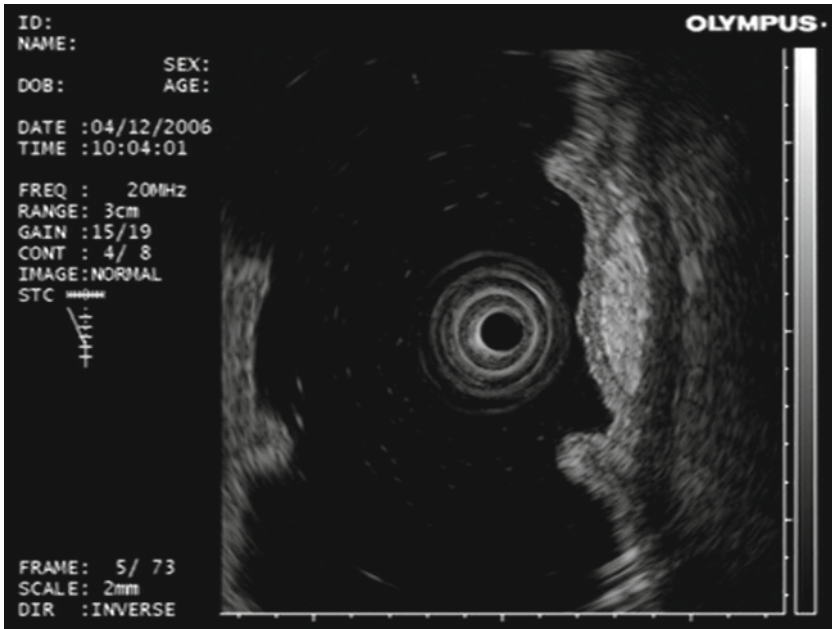


Fig. 2. Endosonographic imaging demonstrates an ovoid, hyperechoic, homogeneous mass in the third echolayer (submucosa) of the gastric antrum. The appearance is typical for a small lipoma.

CLINICAL INDICATIONS

Esophagus

The improved resolution and the ability of HFUS probes to traverse stenotic tumors, which may be inaccessible with dedicated echo-endoscopes, makes HFUS especially attractive in the evaluation of esophageal cancer (20). Indeed, the T staging accuracy of HFUS probes in this setting has been reported up to 85% (10, 17, 31, 32). The accuracy of standard EUS when compared with pathologic staging for superficial (T1) lesions shows a wide range from 50 to 90% (10, 33–35). HFUS probes, on the other hand, have been shown to improve the accuracy of T staging (T1 vs. T2) from 76 to 92% (Figs. 3 and 4) (10). One recent report does suggest, however, that HFUS has limited accuracy in detecting submucosal invasion in early esophageal cancer (36). In addition, the limited depth penetration of HFUS into surrounding tissues (~3 cm) precludes accurate assessment of nodal (N) stage (37). In one study, the accuracy of N staging in patients undergoing preoperative EUS for esophageal cancer was much worse with HFUS than with the standard radial-scanning echo-endoscope (48% vs. 90%) (38). The combined use of a balloon sheathed catheter may improve acoustic coupling and lead to more accurate staging with HFUS in esophageal cancer (23, 26, 27, 37). Unfortunately, HFUS also seems to have limited application in Barrett's esophagus. HFUS has been shown to have diminished accuracy in identifying invasive cancer in patients with high grade dysplasia or intramucosal carcinoma, even with endoscopically visible lesions (30). There are other clinical indications for HFUS in the esophagus including subepithelial lesions (Figs. 5 and 6). HFUS has also been in evaluating esophageal varices, specifically their radius and wall thickness without causing variceal compression (39–41). HFUS has also been useful in evaluation of motility disorders in the esophagus. Under HFUS, hypertrophy or in coordination of the circular and longitudinal muscles can be suggestive of achalasia, diffuse esophageal spasm, or nutcracker esophagus (42–44). Expansion of the esophageal wall and tissue layers (mucosa, submucosa, muscularis propria) has been demonstrated in the early diagnosis of eosinophilic esophagitis (45). In achalasia, the HFUS probe has been used to properly localize the lower esophageal sphincter for botulism toxin injection (46).

Stomach

HFUS has extensive applications beyond the esophagus in the gastrointestinal tract (Figs. 7 and 8). Some reports have indicated that

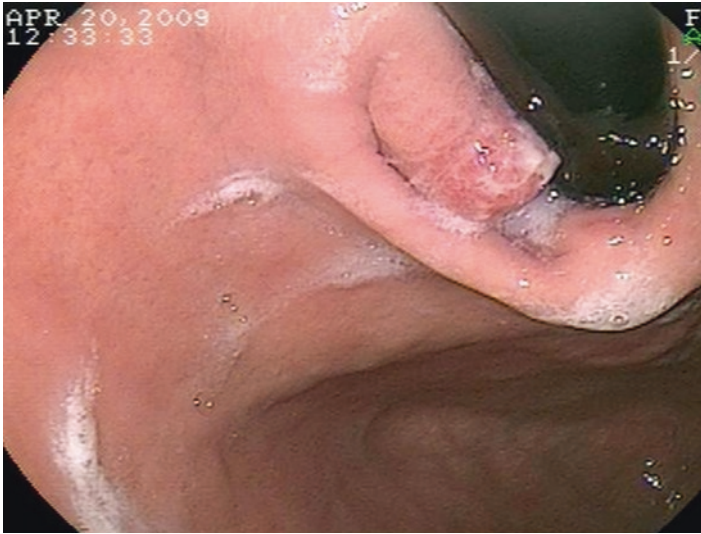


Fig. 3. Retrograde endoscopic view of a nodule involving the gastroesophageal mucosa.

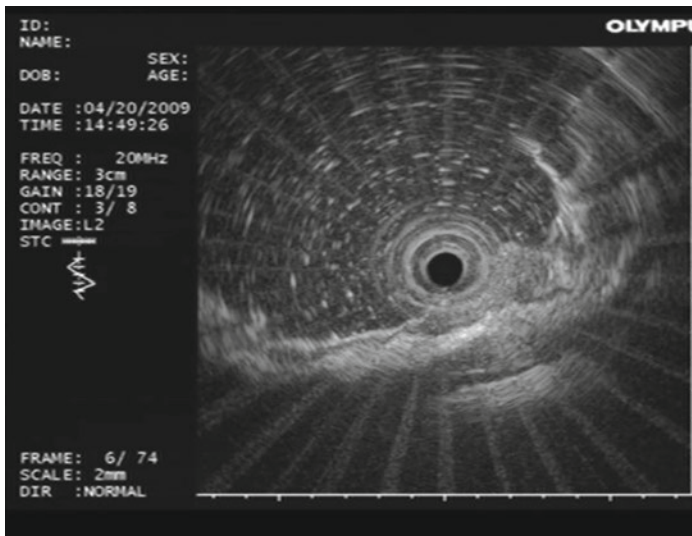


Fig. 4. Evaluation with a high-frequency ultrasound miniprobe demonstrates a hypoechoic mass arising from the second echolayer of the gastric mucosa (deep mucosa). No invasion of the third echolayer (submucosa) is visualized. Endoscopic mucosal resection confirmed a well-differentiated intramucosal adenocarcinoma.



Fig. 5. Endoscopic view of an esophageal granular cell tumor.

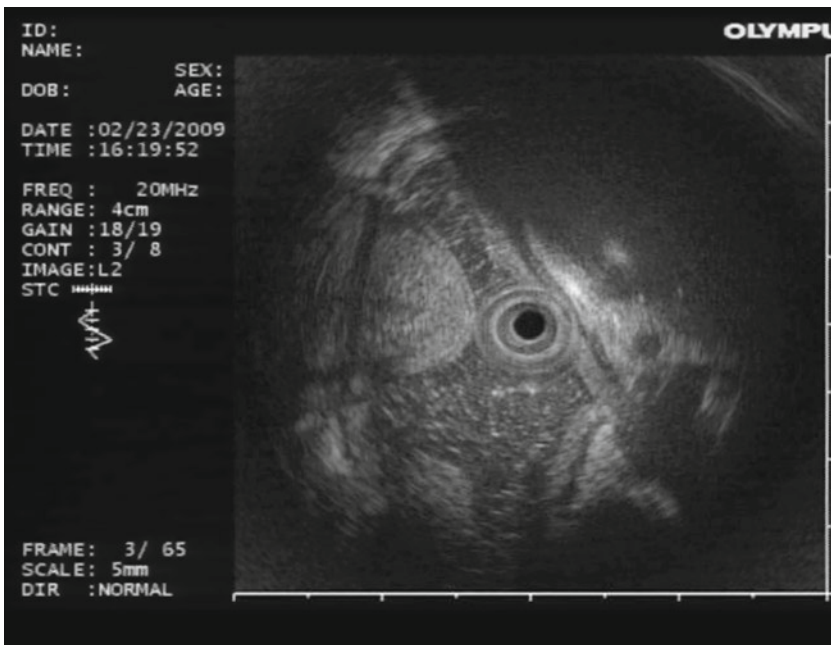


Fig. 6. Hypoechoic, homogenous, subepithelial mass localized to the third echolayer (submucosa) of the esophageal body.

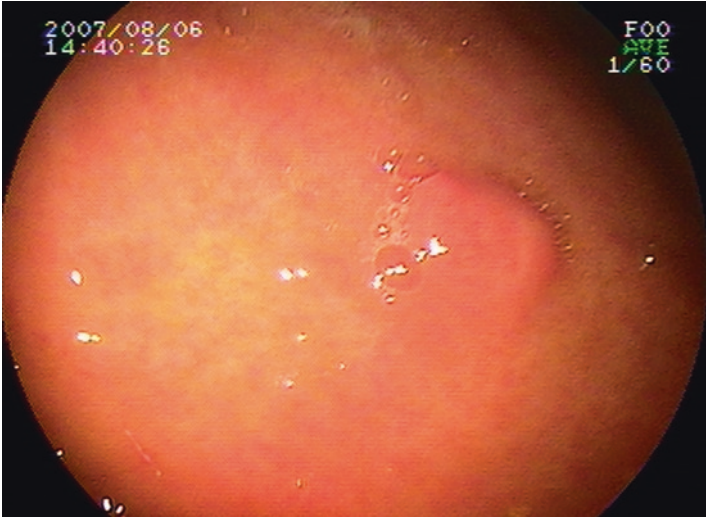


Fig. 7. Endoscopic view of a small subepithelial nodule in the gastric antrum.

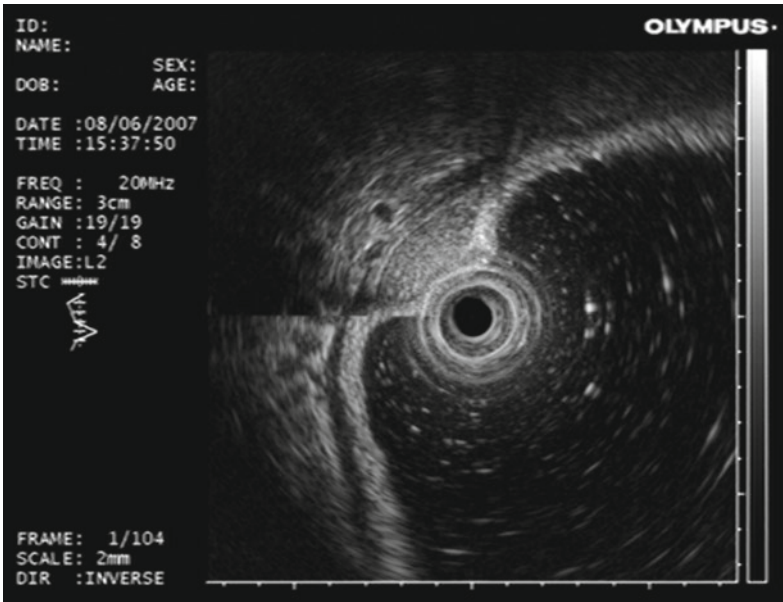


Fig. 8. Endosonographic imaging with a high-frequency ultrasound miniprobe demonstrates an ovoid mass in the third echolayer (submucosa). The submucosal location and shape of the lesion is suggestive of a lipoma, but the echotexture is less hyperechoic. Endoscopic resection demonstrated a submucosal myxoid angioma.

HFUS can aid in the diagnosis of gastric lymphoma, linitis plastica, gastric varices, and Menetrier's gastropathy (47). Under HFUS, lymphoma can be visualized as having thickened mucosa or submucosa with hypertrophic folds. Linitis plastica can appear with marked thickening of the mucosa, submucosa, and muscularis propria while Menetrier's gastropathy can appear sonographically with mucosal thickening and cyst formation (Figs. 9–12). One of the more useful applications of HFUS, though, appears to be T staging of early gastric cancer, particularly those confined to the mucosa or submucosa. The accuracy of T staging using HFUS has been reported as being up to 80% in comparison to 63% accuracy with conventional EUS (47–50). The limitation in depth penetration with HFUS appears to diminish the T staging accuracy in gastric cancer when the lesions invade deeper than 10 mm (51). Thus, subepithelial and well-differentiated lesions are better visualized. Indeed, ulcer scars, dilated glands, local edema, or fibrosis contribute to a large portion of staging errors (50). The HFUS catheters with 3-D imaging capabilities have been reported to have T staging accuracy of almost 90% in superficial gastric cancer (52). The improved accuracy in T staging with HFUS has proven useful in decision-making for endoscopic mucosal resection of early or superficial gastric cancer (53, 54) as early adenocarcinoma confined to the mucosa or submucosa has a 95% 5-year survival rate after resection (55).

Small Bowel and Colon

In the small bowel and colon, HFUS has been shown to be useful in the preoperative diagnosis of pathology such as leiomyoma, leiomyosarcoma, lipoma, lymphoma, and neuroendocrine tumors (56) (Figs. 13 and 14). There has also been evidence that HFUS can be used to assess the severity of active inflammatory bowel disease (57, 58). Some studies suggest that T staging accuracy with HFUS is similar to standard EUS in colorectal cancer (13). One of the largest reports on HFUS in this setting, however, found that tumor staging accuracy was fairly high at 76%. In particular, HFUS probes were more accurate for studying small and flat lesions (<15 mm) (14). In fact, one prospective study found that flat and superficial invasive tumors could be identified with 100% accuracy with HFUS (19). HFUS was even found to be more accurate than high magnification chromoendoscopy for differentiating T1 versus T2 disease (59, 60).

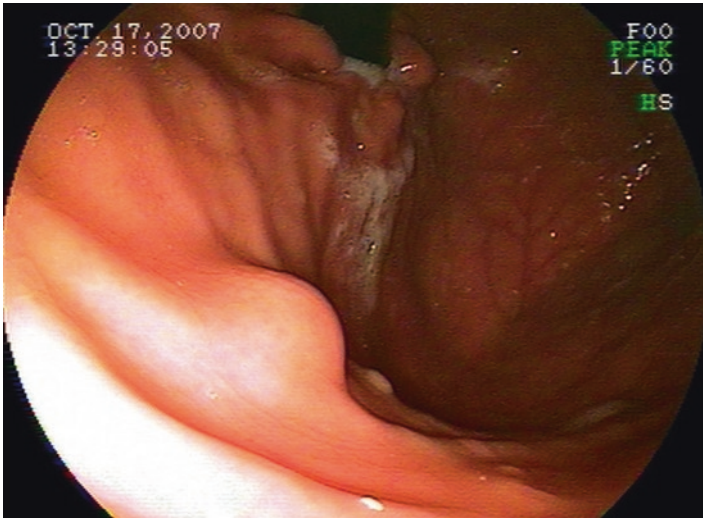


Fig. 9. Retrograde endoscopic view of a small subepithelial mass in the proximal gastric body.

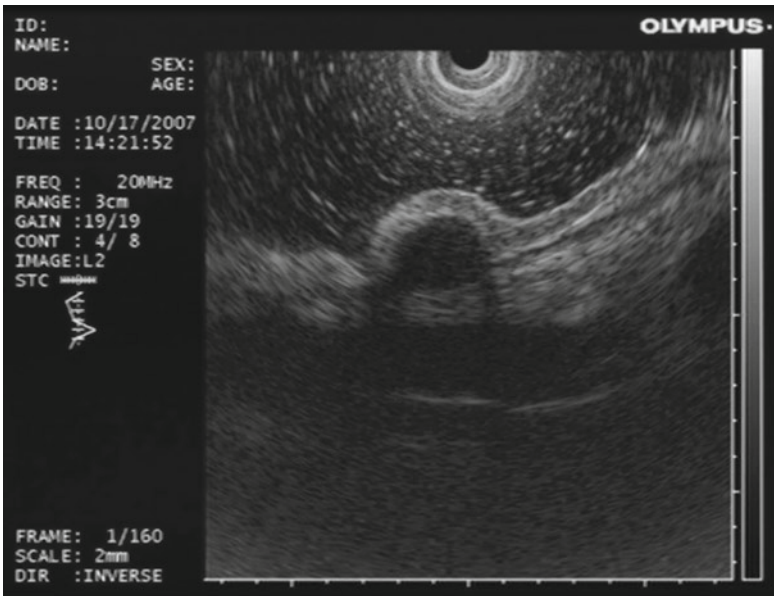


Fig. 10. Endosonographic imaging with a high-frequency miniprobe demonstrates a hypoechoic, homogeneous mass arising from the fourth echolayer (muscularis propria). The differential diagnosis includes a small leiomyoma versus gastrointestinal stromal tumor (GIST).

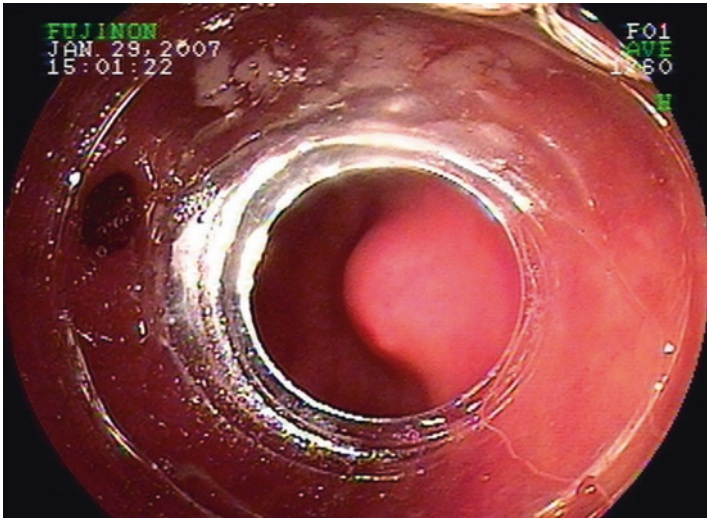


Fig. 11. Endoscopic view of a small, subepithelial mass in the gastric antrum. A clear plastic cap is affixed to the endoscope to facilitate endoscopic resection.



Fig. 12. Endosonographic imaging with a high-frequency miniprobe demonstrates a hypoechoic, mildly heterogeneous mass with indistinct margins in the third echolayer (submucosa). The appearance is consistent with heterotopic pancreatic tissue, “pancreatic rest,” which was confirmed histologically. The punctate an-echoic (black) foci within the mass represent small pancreatic ductal structures.

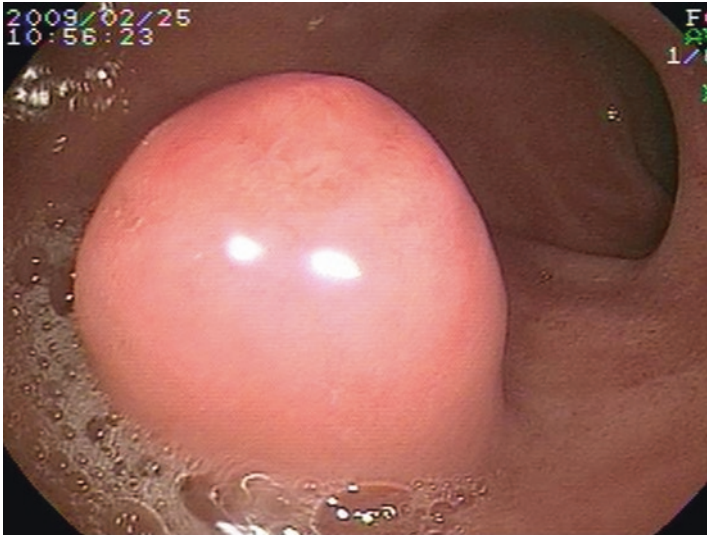


Fig. 13. Endoscopic view of a subepithelial mass in the duodenal bulb. Subepithelial lesions of this nature in the duodenal bulb are frequently found to be carcinoid tumors. However, note the subtle frond-like appearance to the mucosa at the surface of the mass, a feature not typical for carcinoid tumors.

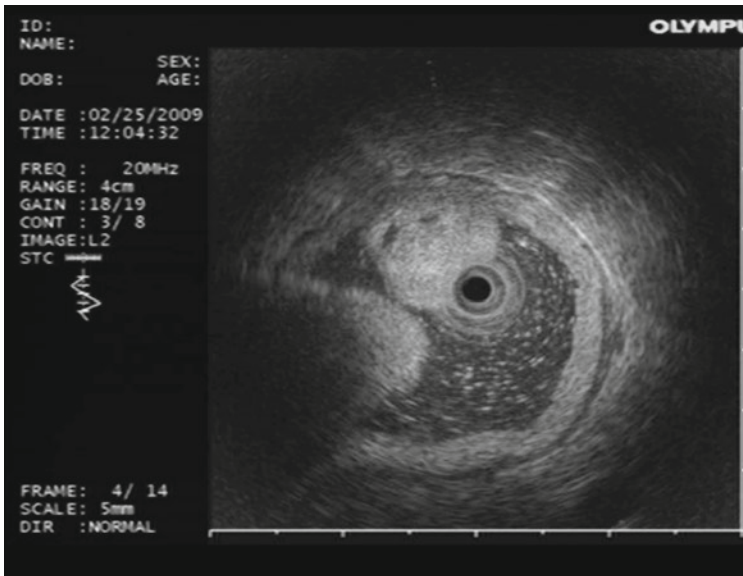


Fig. 14. Endosonographic imaging with a high-frequency miniprobe demonstrates a poorly defined, echogenic mass involving the third echolayer (submucosa). However, the precise echolayer of origin is difficult to determine. Endoscopic resection demonstrated a Brunner's gland adenoma. The small, round anechoic areas within the mass correspond to fluid-filled and dilated glands.

INTRADUCTAL ULTRASOUND

High frequency ultrasound catheters can also be passed over a guide wire into the bile and pancreatic ducts during endoscopic retrograde cholangiopancreatography (ERCP). This is known as intraductal ultrasound (IDUS). This method of ultrasonography utilizes wire-guided miniprobes in 5–10 F diameter with frequencies ranging from 12.5 to 30 MHz. IDUS creates images from within the duct lumen, whose tubular anatomy and surrounding bile and pancreatic fluid facilitates acoustic coupling.

TECHNICAL CONSIDERATIONS

The IDUS probes can be advanced by free cannulation or over a guide-wire; they can be passed through a standard side-viewing endoscope or percutaneously (61–63). Cannulation with the IDUS miniprobe may be difficult without biliary sphincterotomy or use of a guide wire. In some early reports, endoscopic sphincterotomy was required in 10–15% of patients undergoing IDUS (63). New small caliber IDUS catheters, however, seem to permit cannulation without the need for sphincterotomy (62, 64, 65). Still, stenotic strictures may require dilation with a catheter or balloon. It should be noted that, in general, the IDUS procedure time, including catheter insertion and imaging time only adds about 5–10 min to the length of standard ERCP (63, 66). When using IDUS, the usual risks of biliary and pancreatic instrumentation apply, including pancreatitis, reported between 0.4 and 1.5% (63, 67, 68). Complications that are directly attributable to IDUS, however, are rare (62, 63, 66).

BILIARY TRACT ANATOMY

As with HFUS probes, there are different systems available to perform IDUS. Electronic systems use thin, flexible catheters that have no rotating parts. They are 1.1 mm in diameter and 3.5 F. They contain a ring of 64 transducer elements that produce a complete 360° image. The transducer ring detects signal from surrounding tissue and transmits them via microwires to the image processor. In the mechanical system, a single transducer is rotated via a wire producing a 360° image. There are many variations on this basic mechanical system. There are single use probes and multiuse catheters that can vary in design, including the presence of a water-filled protective housing or a water-filled transducer chamber. There are also newer mechanical probes that allow rotating sector and linear scanning.

In IDUS, the normal bile duct appears as either two or three layers, similar to what is visualized under standard EUS (69–72). The sphincter of Oddi appears as a hypoechoic circular thickening within the duodenal wall. When visualized as a two-layer structure, an internal hypoechoic layer represents the mucosa, muscularis propria, and fibrous layer of the subserosa. An outer hyperechoic layer represents the adipose layer of the subserosa, serosa, and interface echo between the serosa and surrounding organs. Unfortunately, it may be difficult to differentiate the fibromuscular layer from the perimuscular connective tissue. This may limit the ability to differentiate between T1 and T2 bile duct cancers although this distinction may not be clinically relevant (73). A third inner hyperechoic layer, representing the interface between the duct mucosa and bile, is occasionally visualized.

CLINICAL INDICATIONS

IDUS is useful in a variety of biliary tract disorders. The most common indications include the evaluation for choledocholithiasis and obstructive jaundice. IDUS is also useful for local tumor staging. In contrast to standard EUS, IDUS is often better in evaluating the proximal biliary system and surrounding structures like the right hepatic artery, portal vein, and hepatoduodenal ligament (69, 74, 75). Like HFUS, more distant structures are difficult to examine secondary to limited depth penetration.

Choledocholithiasis

IDUS has been well described in the evaluation of suspected choledocholithiasis. A number of imaging modalities are available to evaluate these patients, including transabdominal ultrasonography, computed tomography (CT), magnetic resonance (MR), ERCP, and EUS. Initial studies suggested a role for IDUS in patients with suspected choledocholithiasis who have a normal cholangiogram (76, 77). Subsequent studies revealed that the sensitivity of IDUS for suspected choledocholithiasis is superior to ERCP, EUS, or transabdominal ultrasonography (77–79). In some reports, the sensitivity of IDUS was even higher for detecting small stones (<5 mm) (78, 80). Despite the high sensitivity of IDUS for choledocholithiasis, many have questioned the clinical significance of residual sludge and stones observed in several of the aforementioned studies as these may have been small enough to pass spontaneously (81). However, IDUS has been demonstrated to distinguish stones from sludge and air bubbles, altering clinical management in

several studies (79). Unfortunately, the high cost and limited data supporting its utility will likely restrict the use of IDUS in evaluating suspected choledocholithiasis.

Bile Duct Strictures

IDUS has also been shown to distinguish benign from malignant biliary strictures based on bile duct anatomy and unique sonographic imaging characteristics. Features under IDUS that suggest malignancy include a hypoechoic mass (especially if infiltrating surrounding tissue), heterogeneity of the internal echo, notching or irregularity of the outer border, a papillary surface, or disruption of the normal bile duct structure (61, 66, 75, 82–84). There have been several series investigating the utility of IDUS in characterizing bile duct strictures. IDUS has been more accurate than EUS and better able to determine T stage and potential resectability (63). This appears to hold true especially for tumors at the hilum or mid-bile duct (66). IDUS has also been shown to be more accurate, sensitive, and specific when compared to ERCP with tissue sampling in making a final diagnosis (64). Indeed, in a series with patients with suspected malignant strictures but negative tissue sampling by ERCP, the combined use of IDUS resulted in sensitivity and specificity of 90 and 93%, respectively (85). The combination of IDUS and ERCP can improve diagnostic yield, as well. One study found that IDUS in conjunction with ERCP increased the accuracy of characterizing biliary strictures from 58 to 90% (86). A more recent report suggested that IDUS was able to accurately predict malignancy in 86% of patients with negative cytology and histology who were later proven to have malignancy. In fact, IDUS was superior in this setting to digital image analysis (DIA), fluorescence in situ hybridization (FISH), and composite DIA/FISH (87). Even if IDUS fails to provide a final diagnosis, it may be helpful in directing management. For example, some have suggested that identification of disruption of walls by a protruding tumor via IDUS, regardless of tissue sampling results, warrants surgical exploration.

Cholangiocarcinoma

The role of IDUS in primary sclerosing cholangitis is still being determined. IDUS can identify irregular foci within strictures, allowing for focused endoscopic transpapillary biopsy (88). This has not been proven to lead to an earlier diagnosis of cholangiocarcinoma, however

(68). Fortunately, IDUS has been shown to improve the accuracy of local tumor staging of bile duct carcinomas. IDUS is able to detect early lesions, characterize longitudinal tumor extension, and identify tumor spread to adjacent organs and major blood vessels with an accuracy of nearly 100% (69, 72, 75, 89). IDUS has been shown to accurately identify tumor invasion into the pancreatic parenchyma (72, 75, 90), portal vein (69, 72, 90, 91), and right hepatic artery (72, 74, 89, 90). IDUS is superior to standard EUS for T staging (72, 90, 92). In one report, when compared to operative findings, local tumor staging was accurate in 77% of patients with IDUS in comparison to only 54% of patients with EUS (63). The advantages of IDUS over EUS may be even greater for proximal bile duct tumors involving the mid-bile duct to bifurcation as the IDUS miniprobe allows further access (90). Unfortunately, with the limited depth penetration of IDUS, tumor extension outside of the hepatoduodenal ligament is difficult to assess. The use of IDUS in M-staging is therefore limited (69, 93).

Since bile duct carcinomas spread longitudinally, accurate determination of the extent of spread is important for planning operative intervention and margins of resection (94–99). Cholangiography is frequently used; however, this appears to be fairly inaccurate in this setting. In one study, IDUS was significantly more accurate than cholangiography in determining the longitudinal spread of the cancer toward the liver (84% vs. 47%) and toward the duodenum (96% vs. 43%) (62). This was confirmed in another report that cited IDUS as accurately determining the proximal extension of tumor in 92% of patients (61). The superiority of IDUS in comparison to cholangiography in assessing intraductal spread has been shown in other reports as well (75, 90).

It should be mentioned at this point that bile duct wall thickening may result from tumor spread or from peritumoral inflammation (61, 68, 75, 90, 100). This distinction cannot reliably be made with various noninvasive bile duct imaging, including IDUS (75, 89, 90, 101). Some echo-endoscopists have observed that inflammation typically causes symmetrical wall thickening in contrast to malignant infiltration that is typically asymmetric (61, 62). This distinction has not been universally observed, however (68). Another complicating factor in characterizing bile duct wall thickening is the effect of bile duct stents. Biliary stents have been shown to cause reactive changes that can lead to confusion, including overestimation of longitudinal tumor extension (62, 88, 100, 102). Unfortunately, bile duct stents are frequently required to decompress biliary obstruction. Therefore, it is generally recommended to perform IDUS prior to or within a few days of biliary decompression (62).

PANCREATIC INTRADUCTAL ULTRASOUND

Patients who present with signs or symptoms suggestive of a pancreatic neoplasm typically undergo initial transabdominal ultrasound or CT, which can reveal a pancreatic mass or fullness. Additional evaluation using endoscopic procedures such as ERCP and EUS may be required. There is growing evidence that pancreatic IDUS may be helpful for selected patients (67, 83, 103–105). The IDUS probe can usually be placed within the pancreatic duct without prior sphincterotomy (103, 106, 107). It may be difficult, however, to pass the probe into the proximal pancreatic duct since it can be tortuous. On pancreatic IDUS, the main pancreatic duct wall can appear as a single hyperechoic layer or up to three layers. The outer two layers, when visualized, will appear hyperechoic with an intervening hypoechoic layer (71, 103).

Pancreatic Duct Strictures and Pancreatic Adenocarcinoma

IDUS appears useful in characterizing whether pancreatic duct strictures are benign or malignant (83, 108). The accuracy of IDUS in characterizing pancreatic duct strictures has been reported up to 92% (67). In fact, one study demonstrated that IDUS was more sensitive and specific than EUS, CT, or ERCP. IDUS had 100% sensitivity versus 93, 64, and 86% sensitivity, respectively (83). IDUS has also been employed in the detection of pancreatic tumors in early stages. An echo-rich area surrounded by an echo-poor margin is fairly characteristic of pancreatic cancer (109, 110). Chronic pancreatitis, on the other hand, can appear as a ring-like echolucent band surrounded by a fine reticular pattern. The degree of heterogeneity has been described to be in proportion to the degree of fibrosis (83). In one large study, IDUS was found to be more sensitive and specific than EUS, CT, and ERCP in pancreatic imaging (67).

Mucin-Producing and Islet-Cell Tumors

IDUS also appears to have an emerging role in the evaluation of mucin producing tumors of the pancreas. Some of these lesions are premalignant or malignant and may undergo surgical resection. The appropriate diagnosis is crucial as these tumors have a better prognosis than ductal adenocarcinoma. Imaging studies such as transabdominal US, CT, and MR often inadequately differentiate between the cystic neoplasms. Initial experience suggests that EUS can be helpful, though IDUS may be

more accurate (111, 112). Furthermore, IDUS may be helpful in mucin-producing tumors of the ductal branches. For mucinous duct ectasia, IDUS can detect small lesions and determine the extent of intraductal spread and parenchymal invasion. In addition, IDUS can assess the extent of necessary surgery for patients with side-branch disease by identifying papillary tumor projections (67, 107, 113, 114). In one study, comparing IDUS with transabdominal US, CT, EUS, and pancreatoscopy by surgical and pathological confirmation for mucin-producing tumors of different origins, the detection rate of IDUS was superior (106). It should also be briefly mentioned that IDUS has been used with success in localizing pancreatic endocrine tumors (67, 105). These islet-cell tumors typically appear under IDUS as echo-poor, homogenous, well-delineated lesions. In one study, IDUS accurately determined the number of tumors in a patient with multifocal disease that was unrecognized under EUS (67).

PAPILLA OF VATER INTRADUCTAL ULTRASOUND

Lastly, it is worth mentioning the utility of IDUS in characterizing the size and extent of papillary tumors. IDUS has been shown to reliably distinguish the sphincter of Oddi muscle from the remainder of the papilla (115–118). IDUS, then, has great value in clearly visualizing the entire anatomy of the papilla. This was demonstrated in a prospective study of patients with papilla of Vater cancer that underwent surgical resection. IDUS was shown to accurately determine tumor extent at 88% in comparison to transabdominal US and CT, which only detected 9 and 6% of tumors, respectively (117). In another prospective study, IDUS compared favorably to EUS and CT in tumor visualization, diagnosis, and staging (116). Furthermore, in another study in patients with ampullary neoplasms, the accuracy of IDUS in T staging among patients who underwent endoscopic papillectomy was 100%. Overall, IDUS did appear to overestimate tumor staging; however, it appeared useful in therapeutic management (119). These studies indicate that IDUS may be the most accurate modality for diagnosis and local staging of tumors of the papilla of Vater.

FUTURE PROBE TECHNOLOGY

The future of probe ultrasonography may lie in 3-D probes. These instruments are able to obtain up to 120 radial images per minute and produce 3-D figures. Initial reports suggest that 3-D EUS has been

accurate in delineating tumor volume and local invasion, with good explorer agreement and low interobserver variability (120–123). By extension, some reports indicate that 3-D IDUS may better demonstrate biliary tract tumor extension (124–126). In fact, 3-D IDUS may have an added advantage of decreased examination time as less time is spent characterizing relationships between lesions and surrounding structures (127).

CONCLUSION

In summary, continued advancements in ultrasound technology have led to the development of small caliber, catheter probes that can be passed through the accessory channel of a standard endoscope in HFUS or side-view scope in IDUS. These miniprobe operate with a higher frequency than standard EUS creating greater image resolution of mucosal and subepithelial lesions in the gastrointestinal tract and pancreato-biliary tree. Indeed, HFUS appears to offer greater accuracy than standard EUS in T staging of early carcinoma confined to the mucosa or submucosa. As mentioned before, the greater imaging resolution of HFUS results in a loss of imaging depth. This can lead to impaired visualization of distant lymph nodes, and therefore compromised more distal nodal and metastatic staging. Despite these limitations, however, HFUS probes have allowed for more accurate evaluation of superficial tumors and subsequently have influenced therapeutic management such as endoscopic mucosal resection for early stage malignancies.

IDUS, on the other hand, appears to be an effective modality for diagnosing choledocholithiasis, evaluating biliary and pancreatic stenosis, and staging local carcinoma. IDUS can determine the etiology of bile duct strictures with a high sensitivity and specificity and significantly increase the diagnostic accuracy in comparison to other imaging studies or tissue sampling. As a result, IDUS is increasingly becoming an essential tool in the diagnostic work-up of patients with indeterminate biliary duct strictures. For patients with known malignant biliary strictures, IDUS has been shown to be superior to several other modalities in characterizing tumor extension. IDUS shows equal promise in pancreatic diseases, including pancreatic duct stenosis, small pancreatic tumors, intraductal papillary mucinous tumors, and neuroendocrine tumors. Clearly, high frequency ultrasound sonography has been validated in numerous clinical settings and has the potential for growth with further advancements in ultrasound technology.

REFERENCES

1. Gan SI, Rajan E, Adler DG, Baron TH, Anderson MA, Cash BD, Davilla RE, Dominitz JA, Harrison ME 3rd, Ikenberry SO, Lichtenstein D, Qureshi W, Shen B, Zuckerman M, Fanelli RD, Lee KK, Van Guilder T. Role of EUS. *Gastrointest Endosc* 2007;66(3):425–34
2. Yanai H, Yoshida T, Harada T, Matsumoto Y, Nishiaki M, Shigemitsu T, Tada M, Okita K, Kawano T, Nagasaki S. Endoscopic ultrasonography of superficial esophageal cancers using a thin ultrasound probe system equipped with switchable radial and linear scanning modes. *Gastrointest Endosc* 1996;44(5):578–82.
3. Dancygier H, Nattermann C. The role of endoscopic ultrasonography in biliary tract disease: obstructive jaundice. *Endoscopy* 1994;26(9):800–2.
4. Rosch T, Lightdale CJ, Botet JF, Boyce GA, Sivak MV Jr, Yasuda K, Heyder N, Palazzo L, Dancygier H, Schusdziarra V, et al. Localization of pancreatic endocrine tumors by endoscopic ultrasonography. *N Engl J Med* 1992;326(26):1721–6.
5. Kimmey MB, Martin RW, Silverstein FE. Endoscopic ultrasound probes. *Gastrointest Endosc* 1990;36(2 Suppl):S40–6.
6. Schembre D, Ayub K, Jiranek G. High-frequency mini-probe ultrasound: the Rodney Dangerfield of endoscopy? *J Clin Gastroenterol* 2005;39(7):555–6.
7. Odegaard S, Nesje LB, Ohm IM, Kimmey MB. Endosonography in gastrointestinal diseases. *Acta Radiol* 1999;40(2):119–34.
8. Bhutani MS. Interventional endoscopic ultrasonography: state of the art at the new millenium. *Endoscopy* 2000;32(1):62–71.
9. Waxman I, Saitoh Y, Raju GS, Watari J, Yokota K, Reeves AL, Kohgo Y. High-frequency probe EUS-assisted endoscopic mucosal resection: a therapeutic strategy for submucosal tumors of the GI tract. *Gastrointest Endosc* 2002;55(1):44–9.
10. Hasegawa N, Niwa Y, Arisawa T, Hase S, Goto H, Hayakawa T. Preoperative staging of superficial esophageal carcinoma: comparison of an ultrasound probe and standard endoscopic ultrasonography. *Gastrointest Endosc* 1996;44(4):388–93.
11. Takemoto T, Yanai H, Tada M, Aibe T, Fujimura H, Murata N, Karita M, Okita K. Application of ultrasonic probes prior to endoscopic resection of early gastric cancer. *Endoscopy* 1992;24(Suppl 1):329–33.
12. May A, Gunter E, Roth F, Gossner L, Stolte M, Vieth M, Ell C. Accuracy of staging in early oesophageal cancer using high resolution endoscopy and high resolution endosonography: a comparative, prospective, and blinded trial. *Gut* 2004;53(5):634–40.
13. Saitoh Y, Obara T, Einami K, Nomura M, Taruishi M, Ayabe T, Ashida T, Shibata Y, Kohgo Y. Efficacy of high-frequency ultrasound probes for the preoperative staging of invasion depth in flat and depressed colorectal tumors. *Gastrointest Endosc* 1996;44(1):34–9.
14. Yoshida M, Tsukamoto Y, Niwa Y, Goto H, Hase S, Hayakawa T, Okamura S. Endoscopic assessment of invasion of colorectal tumors with a new high-frequency ultrasound probe. *Gastrointest Endosc* 1995;41(6):587–92.
15. Menzel J, Domschke W. Gastrointestinal miniprobe sonography: the current status. *Am J Gastroenterol* 2000;95(3):605–16.

16. Tajima Y, Nakanishi Y, Ochiai A, Tachimori Y, Kato H, Watanabe H, Yamaguchi H, Yoshimura K, Kusano M, Shimoda T. Histopathologic findings predicting lymph node metastasis and prognosis of patients with superficial esophageal carcinoma: analysis of 240 surgically resected tumors. *Cancer* 2000;88(6):1285–93.
17. Murata Y, Suzuki S, Ohta M, Mitsunaga A, Hayashi K, Yoshida K, Ide H. Small ultrasonic probes for determination of the depth of superficial esophageal cancer. *Gastrointest Endosc* 1996;44(1):23–8.
18. Technology Assessment Committee Liu J, Carpenter S, Chuttani R, Croffie J, Disario J, Mergener K, Mishkin DS, Shah R, Somogyi L, Tierney W, Petersen BT. Endoscopic ultrasound probes. *Gastrointest Endosc* 2006;63(6):751–4.
19. Hurlstone DP, Cross SS, Sanders DS. 20-MHz high-frequency endoscopic ultrasound-assisted endoscopic mucosal resection for colorectal submucosal lesions: a prospective analysis. *J Clin Gastroenterol* 2005;39(7):596–9.
20. Chak A, Canto M, Stevens PD, Lightdale CJ, Van de Mierop F, Cooper G, Pollack BJ, Sivak MV Jr. Clinical applications of a new through-the-scope ultrasound probe: prospective comparison with an ultrasound endoscope. *Gastrointest Endosc* 1997;45(3):291–5.
21. Norton ID, Bruce CJ, Seward JB, Vazquez-Sequeiros E, Affi A, Wiersema MJ. Initial experience with a steerable, phased vector array ultrasound catheter in the GI tract. *Gastrointest Endosc* 2001;53(4):496–9.
22. Shamoun DK, Norton ID, Levy MJ, Vazquez-Sequeiros E, Wiersema MJ. Use of a phased vector array US catheter for EUS. *Gastrointest Endosc* 2002;56(3):430–5.
23. Wallace MB, Hoffman BJ, Sahai AS, Inoue H, Van Velse A, Hawes RH. Imaging of esophageal tumors with a water-filled condom and a catheter US probe. *Gastrointest Endosc* 2000;51(5):597–600.
24. Schembre D, Chak A, Stevens P, Isenberg G, Sivak MV Jr, Lightdale CJ. Prospective evaluation of balloon-sheathed catheter US system. *Gastrointest Endosc* 2001;53(7):758–63.
25. Inoue H, Kawano T, Takeshita K, Iwai T. Modified soft-balloon methods during ultrasonic probe examination for superficial esophageal cancer. *Endoscopy* 1998;30(Suppl 1):A41–3.
26. Fockens P, van Dullemen HM, Tytgat GN. Endosonography of stenotic esophageal carcinomas: preliminary experience with an ultra-thin, balloon-fitted ultrasound probe in four patients. *Gastrointest Endosc* 1994;40(2 Pt 1):226–8.
27. Vazquez-Sequeiros E, Wiersema MJ. High-frequency US catheter-based staging of early esophageal tumors. *Gastrointest Endosc* 2002;55(1):95–9.
28. Tseng LJ, Jao YT, Mo LR. Preoperative staging of colorectal cancer with a balloon-sheathed minprobe. *Endoscopy* 2002;34(7):564–8.
29. Watanabe H, Miwa H, Terai T, Imai Y, Ogihara T, Sato N. Endoscopic ultrasonography for colorectal cancer using submucosal saline solution injection. *Gastrointest Endosc* 1997;45(6):508–11.
30. Waxman I, Raju GS, Critchlow J, Antonioli DA, Spechler SJ. High-frequency probe ultrasonography has limited accuracy for detecting invasive adenocarcinoma in patients with Barrett's esophagus and high-grade dysplasia or intramucosal carcinoma: a case series. *Am J Gastroenterol* 2006;101(8):1773–9.

31. Murata Y, Suzuki S, Mitsunaga A, Iizuka Y, Uchiyama M, Uchida K, Nakamura S, Hayashi K, Yoshida K, Toki F, Ide H. Endoscopic ultrasonography in diagnosis and mucosal resection for early esophageal cancer. *Endoscopy* 1998;30 (Suppl 1):A44–6.
32. Hunerbein M, Ulmer C, Handke T, Schlag PM. Endosonography of upper gastrointestinal tract cancer on demand using miniprobe or endoscopic ultrasound. *Surg Endosc* 2003;17(4):615–9.
33. Rosch T. Endosonographic staging of esophageal cancer: a review of literature results. *Gastrointest Endosc Clin N Am* 1995;5(3):537–47.
34. Zuccaro G, Jr Rice TW, Vargo JJ, Goldblum JR, Rybicki LA, Dumot JA, Adelstein DJ, Trolli PA, Blackstone EH. Endoscopic ultrasound errors in esophageal cancer. *Am J Gastroenterol* 2005;100(3):601–6.
35. Rampado S, Bocus P, Battaglia G, Ruol A, Portale G, Ancona E. Endoscopic ultrasound: accuracy in staging superficial carcinomas of the esophagus. *Ann Thorac Surg* 2008;85(1):251–6.
36. Chemaly M, Scalone O, Durivage G, Napoleon B, Pujol B, Lefort C, Hervieux V, Scoazec JY, Souquet JC, Ponchon T. Miniprobe EUS in the pretherapeutic assessment of early esophageal neoplasia. *Endoscopy* 2008;40(1):2–6.
37. Rosch T, Classen M. Pitfalls in endosonographic imaging. In: *Gastrointestinal endosonography*, Van Dam/Sivak, WB Saunders Company; Philadelphia, PA 1999.
38. Nesje LB, Svanes K, Viste A, Laerum OD, Odegaard S. Comparison of a linear miniature ultrasound probe and a radial-scanning echoendoscope in TN staging of esophageal cancer. *Scand J Gastroenterol* 2000;35(9):997–1002.
39. Kane L, Kahaleh M, Shami VM, Caldwell SH, Berg CL, Abdrabbo KM, Yoshida CM, Arseneau KO, Yeaton P. Comparison of the grading of esophageal varices by transnasal endoluminal ultrasound and esophagogastroduodenoscopy. *Clin Gastroenterol Hepatol* 2005;3(8):806–10.
40. Schiano TD, Adrain AL, Cassidy MJ, Mccray W, Liu JB, Baranowski RJ, Bellary S, Black M, Miller LS. Use of high-resolution endoluminal sonography to measure the radius and wall thickness of esophageal varices. *Gastrointest Endosc* 1996;44(4):425–8.
41. Kishimoto H, Sakai M, Kajiyama T, Torii A, Kin G, Tsukada H, Okuma M, Ueda S. Miniature ultrasonic probe evaluation of esophageal varices after endoscopic variceal ligation. *Gastrointest Endosc* 1995;42(3):256–60.
42. Dogan I, Mittal RK. Esophageal motor disorders: recent advances. *Curr Opin Gastroenterol* 2006;22(4):417–22.
43. Mittal RK. Motor and sensory function of the esophagus: revelations through ultrasound imaging. *J Clin Gastroenterol* 2005;39(4 Suppl 2):S42–8.
44. Holloway RH. Esophageal ultrasonography: A new view on esophageal motility. *Am J Gastroenterol* 2007;102(1):146–8.
45. Fox VL, Nurko S, Teitelbaum JE, Badizadegan K, Furuta GT. High-resolution EUS in children with eosinophili “allergic” esophagitis. *Gastrointest Endosc* 2003;57(1):30–6.
46. Hoffman BJ, Knapple WL, Bhutani MS, Verne GN, Hawes RH. Treatment of achalasia by injection of botulinum toxin under endoscopic ultrasound guidance. *Gastrointest Endosc* 1997;45(1):77–9.

47. Akahoshi K, Chijiwa Y, Hamada S, Sasaki I, Nawata H, Kabemura T, Yasuda D, Okabe H. Pretreatment staging of endoscopically early gastric cancer with a 15 MHz ultrasound catheter probe. *Gastrointest Endosc* 1998;48(5):470–6.
48. Yanai H, Noguchi T, Mizumachi S, Tokiyama H, Nakamura H, Tada M, Okita K. A blind comparison of the effectiveness of endoscopic ultrasonography and endoscopy in staging early gastric cancer. *Gut* 1999;44(3):361–5.
49. Hunerbein M, Ghadimi BM, Haensch W, Schlag PM. Transendoscopic ultrasound of exophageal and gastric cancer using miniaturized ultrasound catheter probes. *Gastrointest Endosc* 1998;48(4):371–5.
50. Kida M, Tanabe S, Watanabe M, Kokutou M, Kondou I, Yamada Y, Sakaguchi T, Saigenji K. Staging of gastric cancer with endoscopic ultrasonography and endoscopic mucosal resection. *Endoscopy* 1998;30 Suppl 1:A64–8.
51. Akahoshi K, Chijiwa Y, Tanaka M, Harada N, Nawata H. Endosonography probe-guided endoscopic mucosal resection of gastric neoplasms. *Gastrointest Endosc* 1995;42(3):248–52.
52. Sabet EA, Okai T, Minamoto T, Sawabu N. Endosonographic features of advanced gastric carcinoma invading the colon: is it easy to differentiate from pancreatic invasion? *Endoscopy* 2001;33(2):197.
53. Waxman I, Saitoh Y. Clinical outcome of endoscopic mucosal resection for superficial GI lesions and the role of high-frequency US probe sonography in an American population. *Gastrointest Endosc* 2000;52(3):322–7.
54. Ohashi S, Segawa K, Okamura S, Mitake M, Urano H, Shimodaira M, Takeda T, Kanamori S, Naito T, Takeda K, Itoh B, Goto H, Niwa Y, Hayakawa T. The utility of endoscopic ultrasonography and endoscopy in the endoscopic mucosal resection of early gastric cancer. *Gut* 1999;45(4):599–604.
55. Yasuda K. Endoscopic ultrasonic probes and mucosectomy for early gastric carcinoma. *Gastrointest Endosc* 1996;43(2 Pt 2):S29–31.
56. Watanabe H, Honda S, Kubota H, Higuchi R, Sugimoto K, Iwasaki H, Yoshino G, Kanamaru H, Hanai H, Yoshii S, Kaneko E. Preoperative diagnosis of ileal lipoma by endoscopic ultrasonography probe. *J Clin Gastroenterol* 2000;31(3):245–7.
57. Soweid AM, Chak A, Katz JA, Sivak MV Jr. Catheter probe assisted endoluminal US in inflammatory bowel disease. *Gastrointest Endosc* 1999;50(1):41–6.
58. Hurlstone DP, Sanders DS, Lobo AJ, McAlindon ME, Cross SS. Prospective evaluation of high-frequency mini-probe ultrasound colonoscopic imaging in ulcerative colitis: a valid tool for predicting clinical severity. *Eur J Gastroenterol Hepatol* 2005;17(12):1325–31.
59. Hurlstone DP, Brown S, Cross SS, Shorhouse AJ, Sanders DS. High magnification chromoscopic colonoscopy or high frequency 20 MHz mini probe endoscopic ultrasound staging for early colorectal neoplasia: a comparative prospective analysis. *Gut* 2005;54(11):1585–9.
60. Matsumoto T, Hizawa K, Esaki M, Kurahara K, Mizuno M, Hirakawa K, Yao T, Iida M. Comparison of EUS and magnifying colonoscopy for assessment of small colorectal cancers. *Gastrointest Endosc* 2002;56(3):354–60.
61. Kuroiwa M, Goto H, Hirooka Y, Furukawa T, Hayakawa T, Naitoh Y. Intraductal ultrasonography for the diagnosis of proximal invasion in extrahepatic bile duct cancer. *J Gastroenterol Hepatol* 1998;13(7):715–9.

62. Tamada K, Nagai H, Yasuda Y, Tomiyama T, Ohashi A, Wada S, Kanai N, Satoh Y, Ido K, Sugano K. Transpapillary intraductal US prior to biliary drainage in the assessment of longitudinal spread of extrahepatic bile duct carcinoma. *Gastrointest Endosc* 2001;53(3):300–7.
63. Menzel J, Domschke W. Intraductal ultrasonography (IDUS) of the pancreato-biliary duct system. Personal experience and review of literature. *Eur J Ultrasound* 1999;10(2-3):105–15.
64. Vazquez-Sequeiros E, Baron TH, Clain JE, Gostout CJ, Norton ID, Petersen BT, Levy MJ, Jondal ML, Wiersema MJ. Evaluation of indeterminate bile duct strictures by intraductal US. *Gastrointest Endosc* 2002;56(3):372–9.
65. Ascher SM, Evans SR, Goldberg JA, Garra BS, Benjamin SB, Davros WJ, Zeman RK. Intraoperative bile duct sonography during laparoscopic cholecystectomy: experience with a 12.5-MHz catheter-based US probe. *Radiology* 1992;185(2):493–6.
66. Menzel J, Poremba C, Dietl KH, Domschke W. Preoperative diagnosis of bile duct strictures-comparison of intraductal ultrasonography with conventional endosonography. *Scand J Gastroenterol* 2000;35(1):77–82.
67. Furukawa T, Oohashi K, Yamao K, Naitoh Y, Hirooka Y, Taki T, Itoh A, Hayakawa S, Watanabe Y, Goto H, Hayakawa T. Intraductal ultrasonography of the pancreas: development and clinical potential. *Endoscopy* 1997;29(6):561–9.
68. Gress F, Chen YK, Sherman S, Savides T, Zaidi S, Jaffe P, Lehman G, Wonn MJ, Hawes R. Experience with a catheter-based ultrasound probe in the bile duct and pancreas. *Endoscopy* 1995;27(2):178–84.
69. Tamada K, Ido K, Ueno N, Ichiyama M, Tomiyama T, Nishizono T, Wada S, Noda T, Tano S, Aizawa T, et al. Assessment of portal vein invasion by bile duct cancer using intraductal ultrasonography. *Endoscopy* 1995;27(8):573–8.
70. Fujita N, Noda Y, Kobayashi G, Kimura K, Yago A. Staging of bile duct carcinoma by EUS and IDUS. *Endoscopy* 1998;30(Suppl 1):A132–4.
71. Furukawa T, Naitoh Y, Tsukamoto Y, Mitake M, Yamada M, Ishihara A, Hirooka Y, Satake T, Kanoh J, Tanaka M, et al. New technique using intraductal ultrasonography for the diagnosis of diseases of the pancreatobiliary system. *J Ultrasound Med* 1992;11(11):607–12.
72. Kuroiwa M, Tsukamoto Y, Naitoh Y, Hirooka Y, Furukawa T, Katou T. New technique using intraductal ultrasonography for the diagnosis of bile duct cancer. *J Ultrasound Med* 1994;13(3):189–95.
73. Tamada K, Kanai N, Ueno N, Ichiyama M, Tomiyama T, Wada S, Oohashi A, Nishizono T, Tano S, Aizawa T, Ido K, Kimura K. Limitations of intraductal ultrasonography in differentiating between bile duct cancer in stage T1 and stage T2: in-vitro and in-vivo studies. *Endoscopy* 1997;29(8):721–5.
74. Tamada K, Ido K, Ueno N, Ichiyama M, Tomiyama T, Nishizono T, Wada S, Noda T, Tano S, Aizawa T, et al. Assessment of hepatic artery invasion by bile duct cancer using intraductal ultrasonography. *Endoscopy* 1995;27(8):579–83.
75. Tamada K, Ueno N, Ichiyama M, Tomiyama T, Nishizono T, Wada S, Oohashi A, Tano S, Aizawa T, Ido K, Kimura K. Assessment of pancreatic parenchymal invasion by bile duct cancer using intraductal ultrasonography. *Endoscopy* 1996;28(6):492–6.

76. Das A, Isenberg G, Wong RC, Sivak MV Jr, Chak A. Wire-guided intraductal US: an adjunct to ERCP in the management of bile duct stones. *Gastrointest Endosc* 2001;54(1):31–6.
77. Tseng LJ, Jao YT, Mo LR, Lin RC. Over-the-wire US catheter probe as an adjunct to ERCP in the detection of choledocholithiasis. *Gastrointest Endosc* 2001;54(6):720–3.
78. Ueno N, Nishizono T, Tamada K, Ichiyama M, Wada S, Tomiyama T, Tano S, Aizawa T, Kimura K. Diagnosing extrahepatic bile duct stones using intraductal ultrasonography: a case series. *Endoscopy* 1997;29(5):356–60.
79. Catanzaro A, Pfau P, Isenberg GA, Wong RC, Sivak MV Jr, Chak A. Clinical utility of intraductal US for evaluation of choledocholithiasis. *Gastrointest Endosc* 2003;57(6):648–52.
80. Ohashi S, Ueno N, Tamada K, Tomiyama T, Wada S, Miyata T, Nishizono T, Tano S, Aizawa T, Ido K, Kimura K. Assessment of residual bile duct stones with use of intraductal US during endoscopic balloon sphincteroplasty: comparison with balloon cholangiography. *Gastrointest Endosc* 1999;49(3 Pt 1):328–33.
81. Haber GB. Is seeing believing? *Gastrointest Endosc* 2003;57(6):712–4.
82. Tamada K, Ueno N, Tomiyama T, Ohashi A, Wada S, Nishizono T, Tano S, Aizawa T, Ido K, Kimura K. Characterization of biliary strictures using intraductal ultrasonography: comparison with percutaneous cholangioscopic biopsy. *Gastrointest Endosc* 1998;47(5):341–9.
83. Furukawa T, Tsukamoto Y, Naitoh Y, Mitake M, Hirooka Y, Hayakawa T. Differential diagnosis of pancreatic diseases with an intraductal ultrasound system. *Gastrointest Endosc* 1994;40(2 Pt 1):213–9.
84. Waxman I. Characterization of a malignant bile duct obstruction by intraductal ultrasonography. *Am J Gastroenterol* 1995;90(7):1073–5.
85. Farrell RJ, Agarwal B, Brandwein SL, Underhill J, Chuttani R, Pleskow DK. Intraductal US is a useful adjunct to ERCP for distinguishing malignant from benign biliary strictures. *Gastrointest Endosc* 2002;56(5):681–7.
86. Stavropoulos S, Larghi A, Verna E, Battezzati P, Stevens P. Intraductal ultrasound for the evaluation of patients with biliary strictures and no abdominal mass on computed tomography. *Endoscopy* 2005;37(8):715–21.
87. Levy MJ, Baron TH, Clayton AC, Enders FB, Gostout CJ, Halling KC, Kipp Br, Petersen BT, Roberts LR, Rumalla A, Sebo TJ, Topazian MD, Wiersema MJ, Gores GJ. Prospective evaluation of advanced molecular markers and imaging techniques in patients with indeterminate bile duct strictures. *Am J Gastroenterol* 2008;103(5):1263–73.
88. Brambs HJ. (Intraductal ultrasound of the bile ducts). *Radiologe* 1993;33(7):385–90.
89. Tamada K, Ido K, Ueno N, Ichiyama M, Tomiyama T, Nishizono T, Wada S, Noda T, Tano S, Aizawa T, Kimura K. Assessment of the course and variations of the hepatic artery in bile duct cancer by intraductal ultrasonography. *Gastrointest Endosc* 1996;44(3):249–56.
90. Tamada K, Ido K, Ueno N, Kimura K, Ichiyama M, Tomiyama T. Preoperative staging of extrahepatic bile duct cancer with intraductal ultrasonography. *Am J Gastroenterol* 1995;90(2):239–46.

91. Yasuda K, Mukai H, Nakajima M, Kawai K. Clinical application of ultrasonic probes in the biliary and pancreatic duct. *Endoscopy* 1992;24(Suppl 1):370–5.
92. Menzel J, Domschke W, Brambs HJ, Frank N, Hatfield A, Nattermann C, Odegaard S, Seifert H, Tamada K, Tio TL, Foerster EC. Miniprobe ultrasonography in the upper gastrointestinal tract: state of the art 1995, and prospects. *Endoscopy* 1996;28(6):508–13.
93. Tamada K, Kanai N, Tomiyama T, Ohashi A, Wada S, Satoh Y, Miyata T, Tano S, Ido K, Sugano K. Prediction of the histologic type of bile duct cancer by using intraductal ultrasonography. *Abdom Imaging* 1999;24(5):484–90.
94. Hayashi S, Miyazaki M, Kondo Y, Nakajima N. Invasive growth patterns of hepatic hilar ductal carcinoma. A histologic analysis of 18 surgical cases. *Cancer* 1994;73(12):2992–9.
95. Nimura Y, Kamiya J. Cholangioscopy. *Endoscopy* 1998;30(2):182–8.
96. Sato M, Inoue H, Ogawa S, Ohashi S, Maetani I, Igarashi Y, Sakai Y. Limitations of percutaneous transhepatic cholangioscopy for the diagnosis of the intramural extension of bile duct carcinoma. *Endoscopy* 1998;30(3):281–8.
97. Tamada K, Kurihara K, Tomiyama T, Ohashi A, Wada S, Satoh Y, Miyata T, Ido K, Sugano K. How many biopsies should be performed during percutaneous transhepatic cholangioscopy to diagnose biliary tract cancer? *Gastrointest Endosc* 1999;50(5):653–8.
98. Tamada K, Yasuda Y, Nagai H, Tomiyama T, Tano S, Kanai N, Ohashi A, Aizawa T, Ido K, Kimura K. Limitation of cholangiography in assessing longitudinal spread of extrahepatic bile duct carcinoma to the hepatic side. *J Gastroenterol Hepatol* 1999;14(7):691–8.
99. Yamaguchi K, Chijiwa K, Saiki S, Shimizu S, Takashima M, Tanaka M. Carcinoma of the extrahepatic bile duct: mode of spread and its prognostic implications. *Hepatogastroenterology* 1997;44(17):1256–61.
100. Tamada K, Tomiyama T, Ichiyama M, Oohashi A, Wada S, Nishizono T, Tano S, Aizawa T, Ido K, Kimura K. Influence of biliary drainage catheter on bile duct wall thickness as measured by intraductal ultrasonography. *Gastrointest Endosc* 1998;47(1):28–32.
101. Guibaud L, Bret PM, Reinhold C, Atri M, Barkun AN. Bile duct obstruction and choledocholithiasis: diagnosis with MR cholangiography. *Radiology* 1995;197(1):109–15.
102. Karsten TM, Coene PP, van Gulik TM, Bosma A, van Marle J, James J, Lygidakis NJ, Klopper PJ, van der Heyde MN. Morphologic changes of extrahepatic bile ducts during obstruction and subsequent decompression by endoprosthesis. *Surgery* 1992;111(5):562–8.
103. Furukawa T, Tsukamoto Y, Naitoh Y, Hirooka Y, Katoh T. Evaluation of intraductal ultrasonography in the diagnosis of pancreatic cancer. *Endoscopy* 1993;25(9):577–81.
104. Inui K, Nakazawa S, Yoshino J, Kanemaki N, Okushima K, Nakamura Y, Takashima T. Endoscopy and intraductal ultrasonography. *Semin Surg Oncol* 1998;15(1):33–9.
105. Menzel J, Domschke W. Intraductal ultrasonography may localize islet cell tumours negative on endoscopic ultrasound. *Scand J Gastroenterol* 1998;33(1):109–12.

106. Mukai H, Yasuda K, Nakajima M. Differential diagnosis of mucin-producing tumors of the pancreas by intraductal ultrasonography and peroral pancreatoscopy. *Endoscopy* 1998;30(Suppl 1):A99–102.
107. Taki T, Goto H, Naitoh Y, Hirooka Y, Furukawa T, Hayakawa T. Diagnosis of mucin-producing tumor of the pancreas with an intraductal ultrasonographic system. *J Ultrasound Med* 1997;16(1):1–6.
108. Inui K, Nakazawa S, Yoshino J, Okushima K, Nakamura Y. Endoluminal ultrasonography for pancreatic diseases. *Gastroenterol Clin North Am* 1999;28(3):771–81.
109. Ariyama J, Suyama M, Satoh K, Wakabayashi K. Endoscopic ultrasound and intraductal ultrasound in the diagnosis of small pancreatic tumors. *Abdom Imaging* 1998;23(4):380–6.
110. Itoh A, Goto H, Hirooka Y, Hashimoto S, Hirai T, Niwa K, Takeda K, Hayakawa T. Endoscopic diagnosis of pancreatic cancer using intraductal ultrasonography. *Hepatogastroenterology* 2001;48(40):928–32.
111. Procacci C, Biasiutti C, Carbognin G, Accordini S, Bicego E, Guarise A, Spoto E, Andreis IA, De Marco R, Megibow AJ. Characterization of cystic tumors of the pancreas: CT accuracy. *J Comput Assist Tomogr* 1999;23(6):906–12.
112. Le Borgne J, de Calan L, Partensky C. Cystadenomas and cystadenocarcinomas of the pancreas: a multiinstitutional retrospective study of 398 cases. *French Surgical Association. Ann Surg* 1999;230(2):152–61.
113. Inui K, Nakazawa S, Yoshino J, Yamachika H, Kanemaki N, Wakabayashi T, Okushima K, Taki N, Nakamura Y, Takashima T, Hattori T, Miyoshi H. Mucin-producing tumor of the pancreas-intraluminal ultrasonography. *Hepatogastroenterology* 1998;45(24):1996–2000.
114. Hara T, Yamaguchi T, Ishihara T, Tsuyuguchi T, Kondo F, Kato K, Asano T, Saisho H. Diagnosis and patient management of intraductal papillary-mucinous tumor of the pancreas by using peroral pancreatoscopy and intraductal ultrasonography. *Gastroenterology* 2002;122(1):34–43.
115. Itoh A, Tsukamoto Y, Naitoh Y, Hirooka Y, Furukawa T, Kato T, Kuroiwa M, Hayakawa T. Intraductal ultrasonography for the examination of duodenal papillary region. *J Ultrasound Med* 1994;13(9):679–84.
116. Chak A, Isenberg G, Kobayashi K, Wong RC, Sivak MV Jr. Prospective evaluation of an over-the-wire catheter US probe. *Gastrointest Endosc* 2000;51(2):202–5.
117. Itoh A, Goto H, Naitoh Y, Hirooka Y, Furukawa T, Hayakawa T. Intraductal ultrasonography in diagnosing tumor extension of cancer of the papilla of Vater. *Gastrointest Endosc* 1997;45(3):251–60.
118. Menzel J, Hoepffner N, Sulkowski U, Reimer P, Heinecke A, Poremba C, Domschke W. Polypoid tumors of the major duodenal papilla: preoperative staging with intraductal US, EUS, and CT—a prospective, histopathologically controlled study. *Gastrointest Endosc* 1999;49(3 Pt 1):349–57.
119. Ito K, Fujita N, Noda Y, Kobayashi G, Horaguchi J, Takasawa O, Obana T. Preoperative evaluation of ampullary neoplasm with EUS and transpapillary intraductal US: a prospective and histopathologically controlled study. *Gastrointest Endosc* 2007;66(4):740–7.

120. Vegesna A, Raju R, Asfari W, Korimilli A, Varia A, Orfanidis N, Gaughan J, Ramzan Z, Miller LS. Three-dimensional US volume analysis of gastric pseudo-tumors in a porcine model. *Gastrointest Endosc* 2006;64(4):635–40.
121. Fritscher-Ravens A, Knoefel WT, Krause C, Swain CP, Brandt L, Patel K. Three-dimensional linear endoscopic ultrasound-feasibility of a novel technique applied for the detection of vessel involvement of pancreatic masses. *Am J Gastroenterol* 2005;100(6):1296–302.
122. Kikuchi S, Kida M, Kobayashi K, Yano T, Sakuramoto S, Watanabe M, Kubota K, Isobe Y. New diagnostic imaging of gastrointestinal tumors: a preliminary study of three-dimensional tumor structure and volumetry. *Anticancer Res* 2005;25(4):2935–41.
123. Tsutsui A, Okamura S, Muguruma N, Tsujigami K, Ichikawa S, Ito S, Umino K. Three-dimensional reconstruction of endosonographic images of gastric lesions: preliminary experience. *J Clin Ultrasound* 2005;33(3):112–8.
124. Tamada K, Tomiyama T, Ohashi A, Wada S, Satoh Y, Miyata T, Ido K, Sugano K. Preoperative assessment of extrahepatic bile duct carcinoma using three-dimensional intraductal US. *Gastrointest Endosc* 1999;50(4):548–54.
125. Kanemaki N, Nakazawa S, Inui K, Yoshino J, Yamao J, Okushima K. Three-dimensional intraductal ultrasonography: preliminary results of a new technique for the diagnosis of diseases of the pancreatobiliary system. *Endoscopy* 1997;29(8):726–31.
126. Inui K, Miyoshi H. Cholangiocarcinoma and intraductal sonography. *Gastrointest Endosc Clin N Am* 2005;15(1):143–55.
127. Inui K, Miyoshi H, Yoshino J. Bile duct cancers: what can EUS offer? Intraductal US, 3D-IDUS? FNA-is it possible? *Endoscopy* 2006;38(Suppl 1):S47–9.

Radial Endoscopic Ultrasound

*Scott T. Cooper, MD
and Michael K. Sanders, MD*

CONTENTS

INTRODUCTION
EQUIPMENT
GASTROINTESTINAL TRACT WALL
MEDIASTINUM AND ESOPHAGUS
STOMACH
PANCREAS AND EXTRAHEPATIC BILE DUCT
RECTUM
SUMMARY

Abstract

Over the past decade, radial endoscopic ultrasonography has emerged as a powerful diagnostic tool for evaluating and staging neoplasms of the gastrointestinal tract. Although the initial radial echoendoscopes were heavy, cumbersome instruments, technological advances have resulted in slimmer, lighter scopes with increased agility and a wider range of ultrasound frequencies. Initially, this technology was limited to large, tertiary referral centers due to excessive equipment costs and lack of skilled endosonographers. However, the ever increasing demand for EUS has led to investment in both equipment and experienced endosonographers by some smaller community programs and private practitioners. For the beginner, understanding the basic principles of radial EUS is fundamental for

From: *Clinical Gastroenterology: Endoscopic Ultrasound*,
Edited by: V. M. Shami and M. Kahaleh, DOI 10.1007/978-1-60327-480-7_3,
© Springer Science+Business Media, LLC 2010

establishing the skill set necessary to perform an accurate and efficient exam. A systematic approach to each anatomical station of the digestive tract is critical for assuring a thorough and complete exam. Review of both anatomical and radiologic atlases is helpful for the beginner to understand and accurately interpret ultrasound images. This chapter focuses on the technical details of performing radial EUS on the upper gastrointestinal tract and rectum. Furthermore, attention is directed toward the recognition of common anatomical landmarks in efforts to improve both the efficiency and accuracy of the exam. Although reading a textbook chapter obviously does not substitute for dedicated, supervised hands-on training, a general understanding of the procedure and common anatomical landmarks is crucial to begin EUS training.

Key Words: Endosonography, Radial EUS, EUS stations

INTRODUCTION

Radial endosonography provides a high-resolution, 360° circumferential imaging of the gastrointestinal tract and its surrounding structures. The images created are in a plane perpendicular to the axis of the tip of the endoscope. Therefore, when orienting the echoendoscope along the long axis of the body, images obtained are comparable to those generated with conventional computed tomography (CT) scans. The images produced by the newer radial echoendoscopes rival or surpass other imaging techniques such as magnetic resonance imaging (MRI), CT scans, and transcutaneous ultrasound (1–4). The main disadvantage of radial echoendoscopes, in contrast to linear echoendoscopes, is their inability to allow directed fine needle aspiration or other therapeutic interventions. However, radial endosonography has developed into an invaluable tool for the diagnosis and staging of gastrointestinal neoplasms in the upper gastrointestinal tract and rectum.

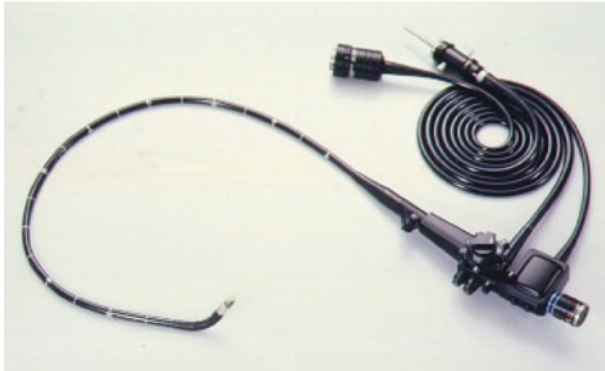
This chapter provides a brief introduction to available radial echoendoscopes as well as some basic principles for radial imaging of the normal upper gastrointestinal tract and rectum. Since the indications for radial EUS are covered in the subsequent chapters, we focus on performing the exam and recognizing common anatomical landmarks. In addition, we have supplied additional references that may provide useful information for the beginner in endosonography (5–7).

EQUIPMENT

Initially, radial echoendoscopes were manufactured with a heavy motor housed in the endoscope handle. The motor drove an ultrasound transducer, which was immersed in an oil bath, located at the tip of the endoscope beyond an oblique-viewing lens. The ultrasound frequencies were limited to 7.5 and 12 MHz. Figure 1 depicts two early fiberoptic echoendoscopes produced by Olympus (Olympus America Inc, Center Valley, PA), which for many years were the standard instruments for endosonography. Later, the motor was incorporated into the umbilical cord connecting the endoscope to the endoscopic processor. In addition, the oil bath was made smaller. These modifications provided the endosonographer with a lighter, slimmer echoendoscope with improved agility and wider range of frequencies (5, 7.5, 12, and 20 MHz) (Fig. 2).



Olympus GF-UM2



Olympus GF-UM20

Fig. 1. GF-UM2 (1984) and GF-UM20 (1991) are two fiberoptic echoendoscopes produced by Olympus (Olympus America Inc, Center Valley, PA). The motor was housed in the handle of the endoscope making these instruments heavier and more cumbersome for the endoscopist. Frequencies were limited to 7.5 and 12 MHz (Photos courtesy of Olympus, Inc.).

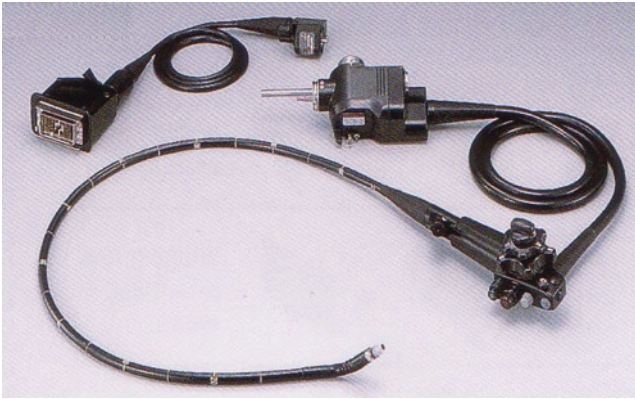


Fig. 2. Olympus GF-UM160 model transferred the motor into the umbilicus providing a light weight instrument with increased agility and wider range of ultrasound frequencies (5, 7.5, 12, and 20 Hz) (Photo courtesy of Olympus, Inc).

More recently, electronic radial echoendoscopes that house an electronic ultrasound transducer immediately beyond an oblique-viewing lens at the tip of the endoscope have been manufactured (Fig. 3). Some feel that electronic radial transducers are less prone to breakage as they lack the mechanical drive shaft and oil bath of mechanical echoendoscopes. Moreover, electronic radial echoendoscopes have the benefit of providing real-time detection of flow (color Doppler), thereby allowing the differentiation between arterial and venous blood flow with pulse Doppler.

For both mechanical and electronic radial echoendoscopes, acoustic coupling between the ultrasound probe and structure of interest is obtained by instilling water into a balloon covering the circumference of the ultrasound probe (Fig. 4). The balloon can be inflated and deflated by valves on the endoscope handle. Once inflated with water, it is extremely important to remove any remaining air bubbles from the balloon to avoid artifact imaging. Acoustic coupling can be further enhanced during the exam by instilling water into the intestinal lumen through the biopsy channel.

For many years, mechanical radial echoendoscopes produced by Olympus were the standard equipment for endosonographers. Pentax (Pentax of America, Montvale, NJ) was the first company to release an electronic radial echoendoscope. Today, there are three leading manufacturers of radial echoendoscopes: Olympus, Pentax, and Fujinon (Fujinon USA Inc, Wayne, NJ). Table 1 lists some of the technical specifications of commonly used radial echoendoscopes (8). For a discussion on ultrasound processors, please refer to the preceding chapter on endosonographic instrumentation.



GF-UE160AL

Fig. 3. Olympus GF-UE160AL has an electronic ultrasound transducer located beyond the oblique-viewing lens. The GF-UE160AL is compatible with the Aloka processor, traditionally used for linear endosonography (Photos courtesy of Olympus, Inc).



Fig. 4. A balloon covers the circumference of the ultrasound probe and can be inflated with water to enhance acoustic coupling.

Table 1
Technical specifications of commonly available radial echoendoscopes

<i>Manufacturer</i>	<i>Pentax</i>	<i>Olympus</i>	<i>Olympus</i>	<i>Olympus</i>	<i>Olympus</i>	<i>Olympus</i>
Model	EG-3630UR	GF UM20	GF UM130	GF UMQ130	GF UM160	GF-UE 160-ALS
Imaging	Video	Fiberoptic	Video	Video	Video	Video
Transducer	Electronic	Mechanical	Mechanical	Mechanical	Mechanical	Electronic
Specifications						
Working length	1,250	1,055	1,250	1,250	1,250	1,250
Insertion tube diameter (mm)	12.1	13.2	12.7	12.7	12.7	11.8
Working channel diameter (mm)	2.4	2	2.2	2.2	2.2	2.2
Tip deflection,	130-60	130	130	130	130	90-130
up-down (degree)						
Tip deflection	60-60	90	90	90	90	90
right-left (degrees)						
Direction of viewing field	Forward	45 forward	50 forward	50 forward	50 forward	55 forward
(degrees)		oblique	oblique	oblique	oblique	oblique
Field of view (degree)	120	80	100	100	100	100
Depth of field (mm)	30-150	3-100	3-100	3-100	3-100	3-100
Acoustic frequency (MHz)	5/7.5/10	7.5/12	7.5/12	7.5/20	5/7.5/12/20	5/6/7.5/10
Scanning angle (degree)	270	360	360	360	360	360

GASTROINTESTINAL TRACT WALL

Unlike other radiographic imaging modalities, endoscopic ultrasound provides superior, detailed imaging of the gastrointestinal wall with five distinct sonographic layers corresponding to their histologic structures (Fig. 5). Previous studies have confirmed the histologic correlates of gastrointestinal ultrasound images (9, 10).

The layer closest to the lumen of the gastrointestinal tract appears as a bright (hyperechoic) structure, which corresponds to the interface between the mucosa and the ultrasound transducer or its surrounding fluid. The second layer of the gastrointestinal tract is a dark (hypoechoic) layer that represents the deep mucosa, or muscularis mucosa. The third sonographic layer corresponds to the submucosa (hyperechoic) and is caused by the acoustic interface between the submucosa

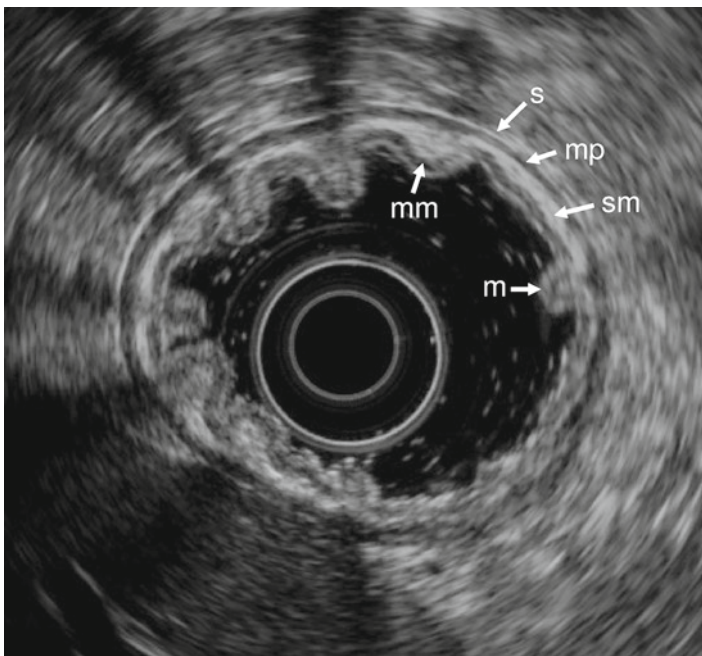


Fig. 5. Ultrasound image of the gastric wall demonstrating five distinct sonographic layers. The superficial mucosa (m) is hyperechoic and represents the first layer. The second layer is the hypoechoic, deep mucosa, or muscularis mucosa (mm). The submucosa (sm) is hyperechoic and corresponds to third layer. The fourth layer, muscularis propria (mp) is hypoechoic. The serosa (s) is the fifth layer and hyperechoic.

and denser muscularis propria. The muscularis propria is hypoechoic and corresponds to the fourth sonographic layer. In some areas of the digestive tract, the fourth layer (muscularis propria) is divided by a thin bright, hyperechoic layer caused by the separation of the inner circular and outer longitudinal muscle layers of the muscularis propria. In these regions, the intestinal wall may demonstrate a seven layer pattern. The last, and deepest, sonographic layer is a bright, hyperechoic structure that corresponds to the serosa in the stomach and small bowel and adventitia in the esophagus. At higher ultrasound frequencies (20–30 MHz), separation of the muscularis mucosa and muscularis propria into the inner circular and outer longitudinal muscle layers may be appreciated, thereby demonstrating a nine layer pattern to the gastrointestinal tract wall (11). Understanding the correlation between the sonographic layers and histologic structures is critical for the diagnosis of subepithelial lesions and staging of gastrointestinal neoplasms.

MEDIASTINUM AND ESOPHAGUS

The previously mentioned five sonographic layers of the gastrointestinal tract wall are easily demonstrated in the esophagus, which is typically about 3 mm thick. Due to its orientation parallel to the long axis of the body, images produced by radial EUS in the esophagus correlate nicely with transverse sections from thoracic CT scans. For the beginner, review of a radiology and/or anatomy atlas can be extremely helpful for interpreting EUS images of the mediastinum.

In order to avoid confusion for the beginner, unless otherwise specified, when describing the anatomical stations for radial EUS, “right” will refer to the patient’s right and “left” will refer to the patient’s left. As with CT imaging, the location of the anatomical structures on the monitor screen is often opposite of the anatomic location.

Distal Esophagus

As with all EUS examinations, a systematic approach should be applied to examine the esophagus and mediastinum, paying close attention to anatomical landmarks for proper orientation. For imaging the upper gastrointestinal tract, generally we begin with a frequency setting between 5 and 7.5 MHz and a range between 6 and 9 cm. These settings provide a general overall view of the anatomy and can be adjusted depending on the lesion of interest. The esophageal exam should begin at the gastroesophageal junction and progress proximally. The balloon

should be inflated to disperse any intraluminal air, and the transducer should be centered in the balloon. One must be careful to avoid overinflation of the balloon as this may compress the esophageal wall and interfere with either detection or staging of neoplasms. The aorta is a constant landmark throughout the exam until withdrawal above the aortic arch. The aorta is seen as a large anechoic structure with hyperechoic walls and measures ~1.5–2 cm in diameter. Maintaining the aorta in the 5–6 o'clock position will simulate anatomical findings observed on transverse CT sections of the mediastinum. As the esophagus is a straight, tubular structure, little manipulation of the ultrasound probe is necessary to maintain proper image orientation.

While maintaining the aorta in the 5 o'clock position, the spine is observed in the 7 o'clock position. Due to its dense nature and poor ultrasound wave penetration, the spine produces an irregular hyperechoic image with significant acoustic artifact. At the 6–12 o'clock position the liver can be seen. In the liver parenchyma, the hepatic veins and intrahepatic bile ducts can be appreciated as completely black (anechoic) structures (Fig. 6). In the distal esophagus, the fundus of the stomach is found in the 1–4 o'clock position (Fig. 7). The stomach can be easily identified by the rugal folds.

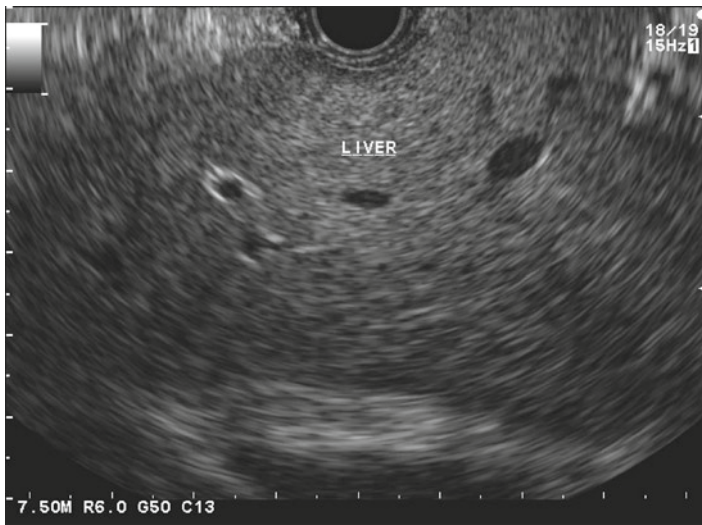


Fig. 6. Left lobe of the liver. The completely black (anechoic) structures within the liver parenchyma represent the hepatic veins and intrahepatic bile ducts.

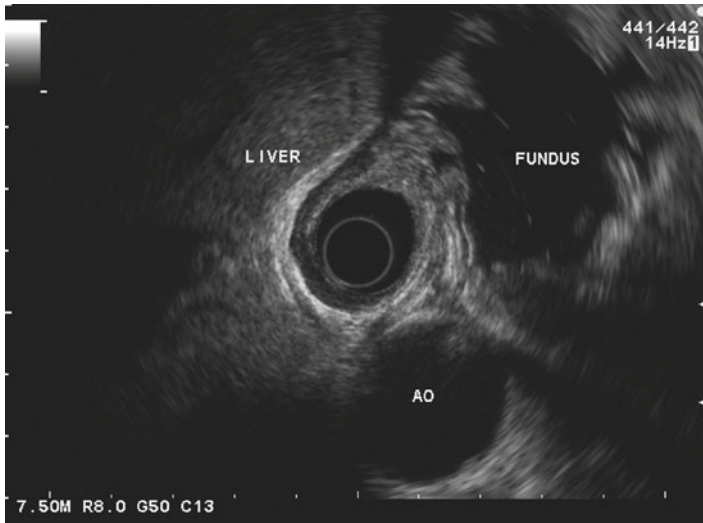


Fig. 7. Imaging of the distal esophagus reveals the fundus, liver, and aorta (AO).

Midesophagus

As the radial echoendoscope is withdrawn to the midesophagus, the left atrium emerges into the 12 o'clock position (Fig. 8). Often, the mitral valve can be visualized as well. The right and left lungs can be seen at the 9 and 2 o'clock positions, respectively, as hyperechoic rings. The azygous vein appears as a hypoechoic structure to the right of the aorta and eventually courses anterior to the spine toward the right lung as the echoendoscope is withdrawn (Fig. 8). The left and right main stem bronchi are seen as hyperechoic rings at the 1 and 11 o'clock positions, respectively, and merge to form the trachea, found in the 12 o'clock position. Significant air artifact is produced by the bronchi and trachea. The inferior tracheobronchial, or carinal lymph nodes are seen at this level, often in the subcarinal space. Normal lymph nodes are seen as hypoechoic, heterogeneous structures with internal hyperechoic foci and poorly defined nodal margins. Benign lymph nodes may also appear to "drape" across the ultrasound transducer in this region. As the echoendoscope is withdrawn further, the arch of the aorta can be seen to the left of the descending aorta (Fig. 9). The aortapulmonary window (APW) can be examined in this region with slight scope tip deflection into the aortic arch and gentle advancement and withdrawal of the echoendoscope (Fig. 10). The APW is an important landmark for nodal staging in upper gastrointestinal malignancies. In the midesophagus, the thoracic duct can also be observed as a small, hypoechoic structure between the aorta and spine (Fig. 11).

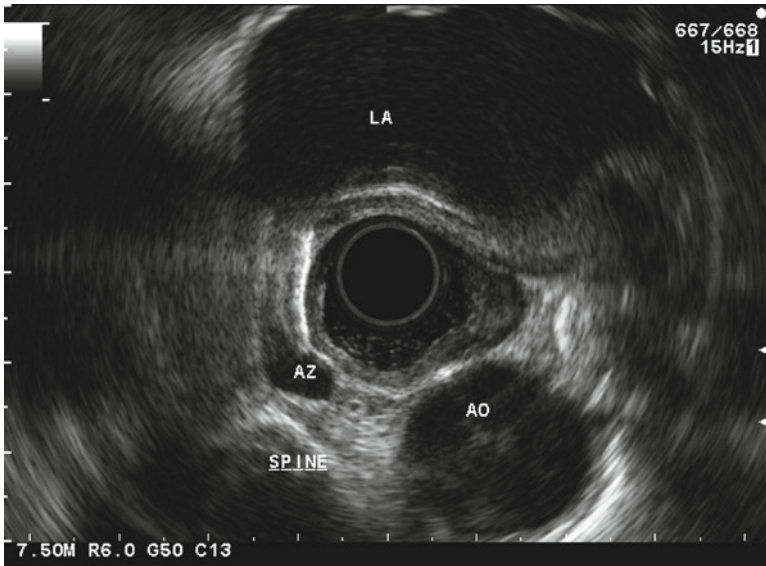


Fig. 8. Views of the midesophagus demonstrating the aorta (AO), left atrium (LA), azygous vein (AZ), and spine.

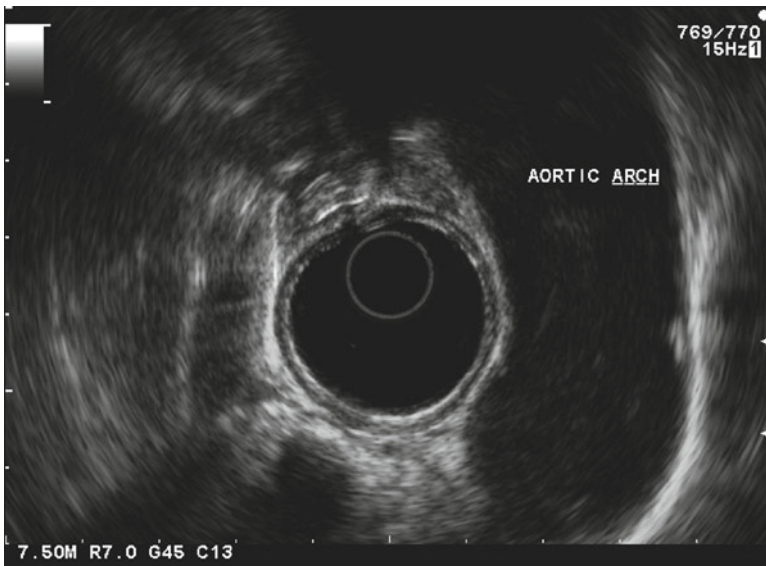


Fig. 9. The aortic arch can be appreciated upon withdrawal from the mid-proximal esophagus.

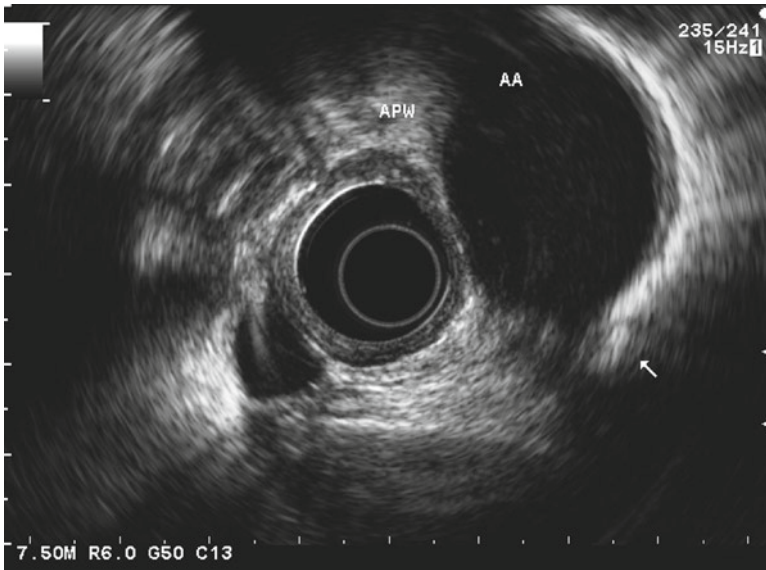


Fig. 10. The aortopulmonary window (APW) is observed at the level of the aortic arch and represents an important landmark for nodal staging.

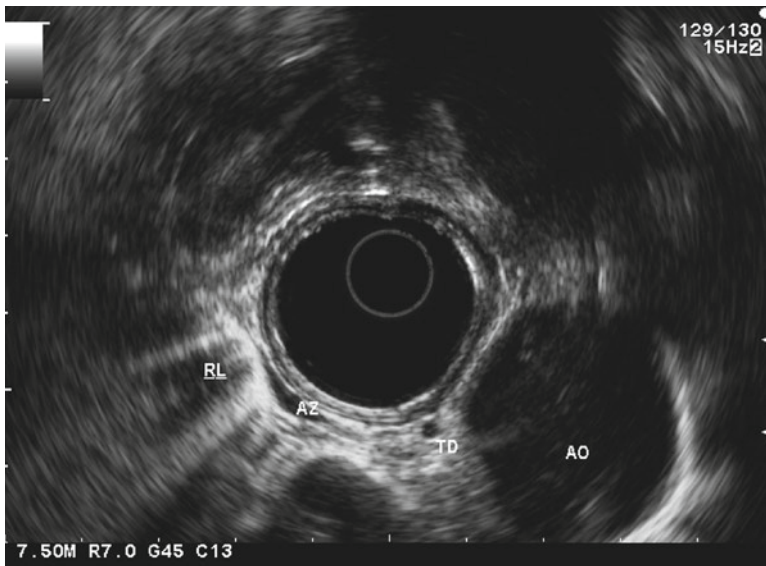


Fig. 11. The thoracic duct (TD) can be observed between the aorta and spine in the midesophagus. The azygous vein (AZ) and right lung (RL) are also demonstrated.

Proximal Esophagus

Just proximal to the aortic arch, one can visualize the left common carotid artery at the 1–2 o'clock position and the left subclavian artery at the 2 o'clock position. As the echoendoscope is withdrawn further, just distal to the upper esophageal sphincter, one can image the thyroid gland, a hyperechoic structure, at the 11 and 1 o'clock position on either side of the trachea, which is seen just to the left of the 12 o'clock position. The thymus can sometimes be visualized just distal to the thyroid.

At this level, one can also image the left and right internal jugular veins located at the 3 and 8 o'clock position, respectively. The left and right carotid arteries are seen just beside and medial to the left and right internal jugular veins. For practical purposes, this region does not contain any significant anatomical landmarks; however, it is extremely important for determining the presence or absence of periesophageal and/or paratracheal lymph nodes when staging upper gastrointestinal malignancies.

STOMACH

Similar to the esophageal exam, examination of the stomach typically begins distally in the prepyloric antrum. The balloon is fully inflated and continuous suction is applied to remove any air from the gastric lumen. Once the gastric wall is collapsed, the echoendoscope is slowly withdrawn to the level of the fundus, paying close attention to both the gastric wall and perigastric structures. Once an abnormality is observed, specific techniques are applied to acquire more detailed imaging.

The five layers of the gastric wall can be easily identified, and typically the wall measures between 3 and 5 mm in diameter. In some regions of the stomach, it may be difficult to achieve perpendicular, high-quality imaging of the gastric wall. This becomes particularly difficult in the antrum, and it may be impossible to adjust either the scope position or tip deflection for adequate imaging. In these circumstances, either a radial miniprobe or instillation of water (100–300 ml) may be necessary to either provide better positioning or enhance acoustic coupling for an adequate exam. When instilling water, the examiner must be aware of the potential aspiration risk and therefore work quickly and efficiently to complete the exam.

When the echoendoscope tip is positioned in the antrum, the anterior wall of the stomach is seen on the left of the ultrasound image and the posterior wall is observed on the right. The gallbladder, which has

three sonographic layers, can be easily imaged from the antrum (Fig. 12). Often times stones, which appear as hyperechoic structures with posterior shadowing (Fig. 13), or sludge, hyperechoic material that lies in the dependent portion of the gallbladder, can be seen. The head and genu of the pancreas along with its surrounding vasculature can also be seen from the antrum.

Withdrawing the echoendoscope into the midbody of the stomach allows visualization of the pancreatic body (Fig. 14). Examination of the pancreas is discussed in further detail in the following section. The splenic hilum, splenic artery and vein, left kidney, portions of the right lobe of the liver, and the entire left lobe of the liver can also be visualized from the stomach. A normal spleen generally has a homogeneous echotexture that is similar to or slightly brighter than the density of the liver. The left kidney contains multiple rings with hyperechoic borders corresponding to the renal calyces (Fig. 15).

When the echoendoscope is positioned immediately below the gastroesophageal junction, the celiac trunk can be seen branching off into the splenic and common hepatic arteries (Fig. 16). Once the celiac axis has been identified, slight withdrawal and clockwise rotation will bring the left adrenal gland into view between the aorta and left kidney

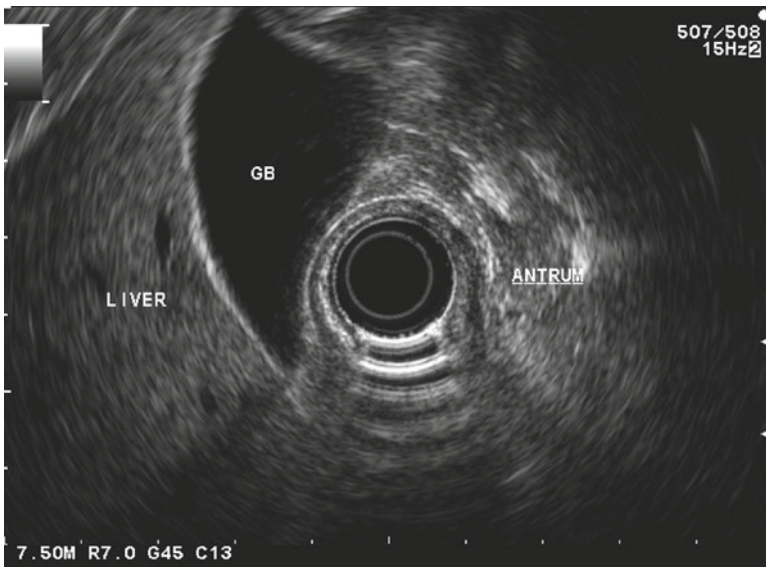


Fig. 12. Ultrasound image from the prepyloric antrum demonstrating the gallbladder (GB) and liver.

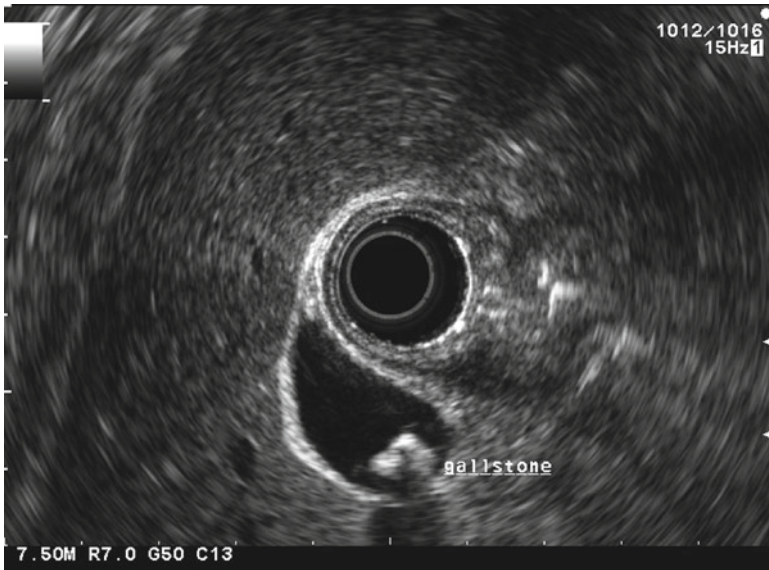


Fig. 13. Gallbladder with hyperechoic gallstones (GS).

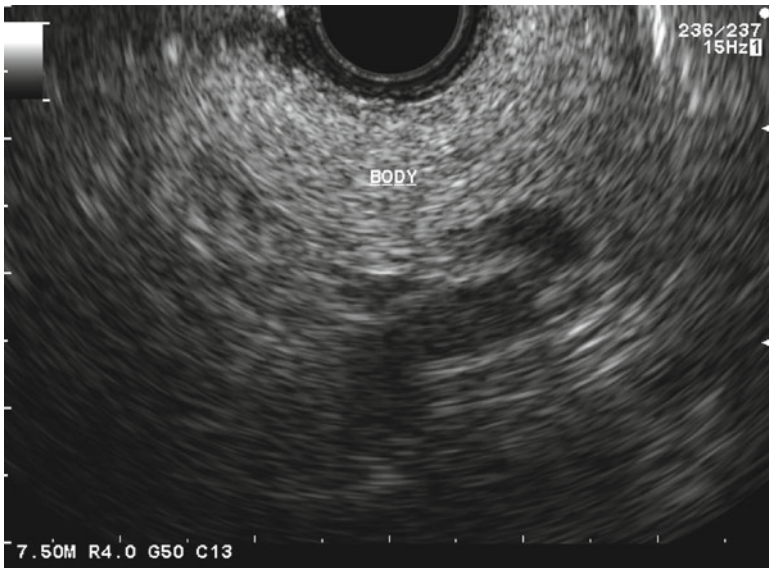


Fig. 14. Body of the pancreas can be seen from the midbody of the stomach. The normal parenchyma displays a fine, speckled pattern often described as having a “salt and pepper” appearance.

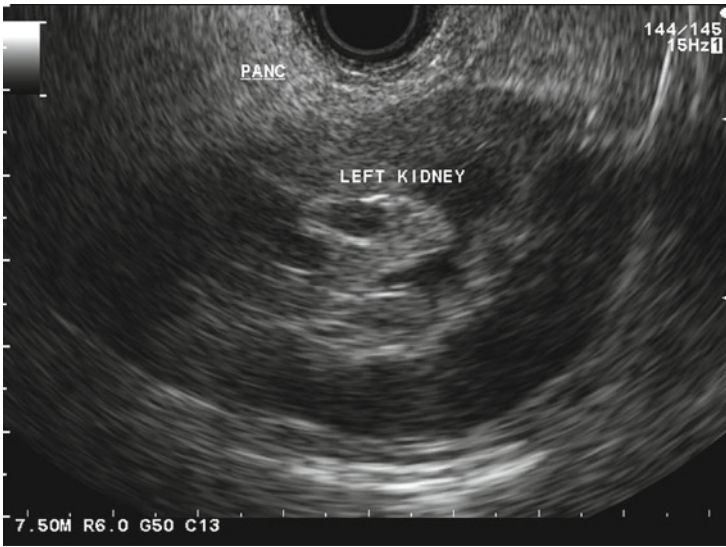


Fig. 15. The left kidney is easily recognizable from the midbody of the stomach. Often times, the pancreatic body (PANC) can be found between the left kidney and ultrasound transducer.

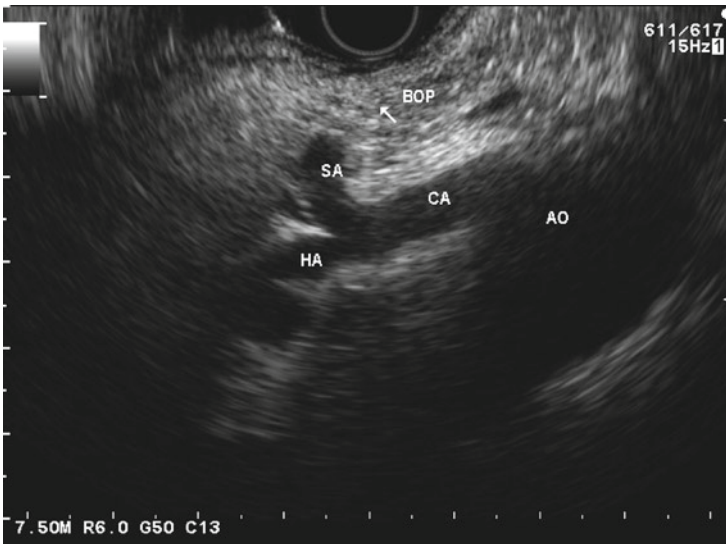


Fig. 16. The celiac artery (CA) arising from the aorta (AO) and bifurcating into the splenic (SA) and common hepatic arteries (HA) observed immediately below the gastroesophageal junction. The splenic artery also serves as a useful landmark for locating the body of the pancreas (BOP).

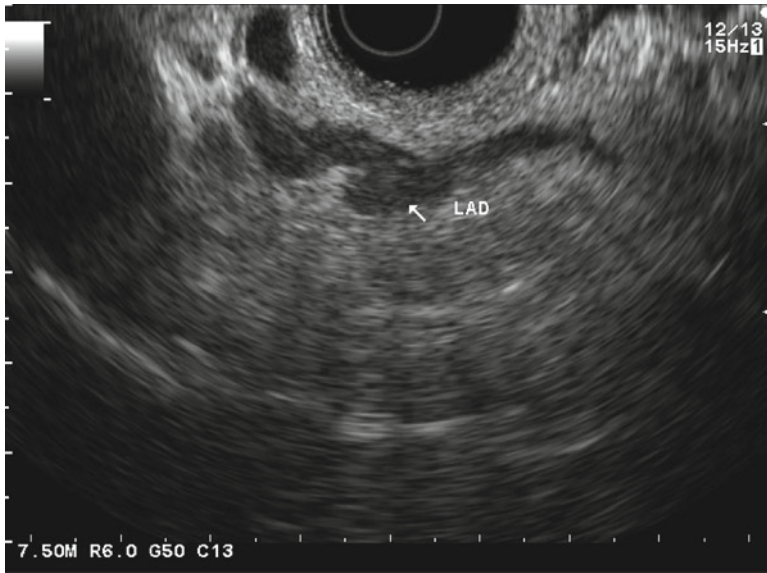


Fig. 17. The left adrenal gland (LAD) is located between the aorta and left kidney. One can appreciate its likening to a “seagull” with outstretched wings.

(Fig. 17). The adrenal gland has been described as a “seagull” with its outstretched wings.

The beginner should quickly become familiar with these important anatomical landmarks as the stomach is large and easily distended, making it simple to become disoriented. Quick recognition of these landmarks will improve both the efficiency and accuracy of your exam.

PANCREAS AND EXTRAHEPATIC BILE DUCT

The pancreas is imaged from both the body of the stomach and duodenum. A normal pancreas has a homogenous, fine speckled pattern that is often described as having a “salt and pepper” appearance (Fig. 14). The border of a normal pancreas is generally smooth. With the echoendoscope, the main pancreatic duct can be traced from the pancreatic head to the tail. As a general rule, the normal pancreatic duct measures between 3 and 4 mm in diameter in the head and tapers to 2 mm in the body and 1 mm in the tail. Usually, the wall of the pancreatic duct is barely perceivable. Side branches may be appreciated

within the pancreatic head. The dorsal pancreas is generally more echogenic than the ventral pancreas. This is thought to be secondary to the higher fat content of the dorsal pancreas. In up to 75% of patients, the ventral anlage which represents the transition zone between the dorsal and ventral pancreas can be seen on EUS (12) (Fig. 18).

Similar to the esophagus and stomach, it is best to begin with a systematic approach when imaging the pancreas. The body and tail can be examined through the posterior wall of the stomach, whereas imaging of the head requires three separate positions within the duodenum: the apex of the duodenal bulb, immediately opposite the papilla, and just distal to the papilla for adequate imaging of the uncinata. Typically, we begin with imaging of the head from the duodenal bulb. Once the echoendoscope is advanced through the pylorus, the balloon is inflated, and the scope tip is deflected slightly downward with advancement of the echoendoscope into the apex. Typically, this maneuver will bring the head of the pancreas into the 6–8 o'clock position. However, if the examiner is having difficulty identifying the pancreatic head, the liver can serve as an excellent landmark from this position and is more easily identifiable. Once the liver is identified, the image should be rotated such that the

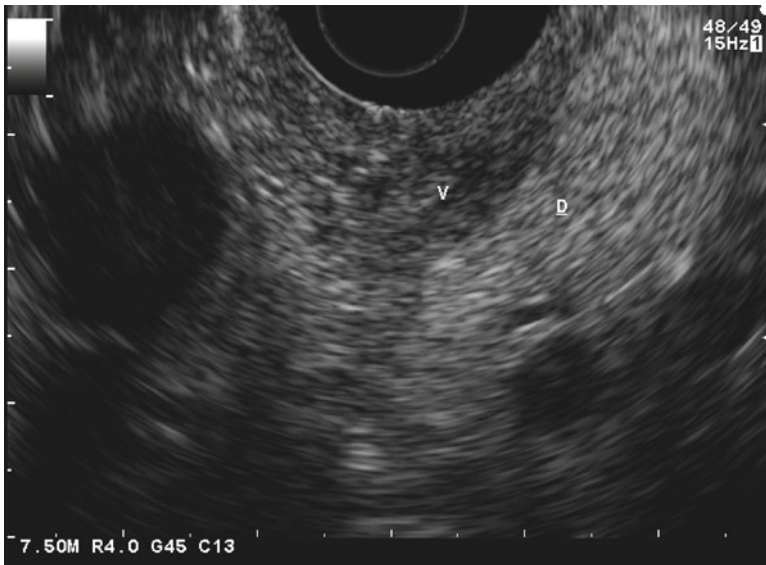


Fig. 18. Ventral anlage represents the transition between the hypoechoic ventral pancreas (V) and the more echogenic dorsal (D) pancreas. This image can be demonstrated best during withdrawal from the second portion of the duodenum.

liver is oriented in the 10 o'clock position. With gentle advancement and withdrawal of the echoendoscope coupled with either upward or downward tip deflection and/or clockwise and counterclockwise torquing, the landmarks in the region should become apparent.

The first landmark should be the common bile duct (CBD) which is a tubular anechoic structure that extends from the duodenal wall upward to the liver. The bile duct travels closest to the transducer and typically measures up to 6 mm in diameter. From this position, withdrawal of the echoendoscope coupled with counterclockwise rotation will allow imaging of the bile duct toward the hilum while gentle advancement and clockwise rotation will trace the bile duct downward to the papilla. The second landmark is the main pancreatic duct, which may be difficult to see in the same plane as the CBD. The pancreatic duct is a smaller tubular structure and may be difficult to visualize, requiring gentle advancement and rotation of the echoendoscope. The portal vein is the largest tubular structure in this region and is positioned furthest from the transducer. The simultaneous view of the bile duct, pancreatic duct and portal vein from the apex of the duodenal bulb has been termed the "stack sign." (13) (Fig. 19). Some authors have reported that the absence of a

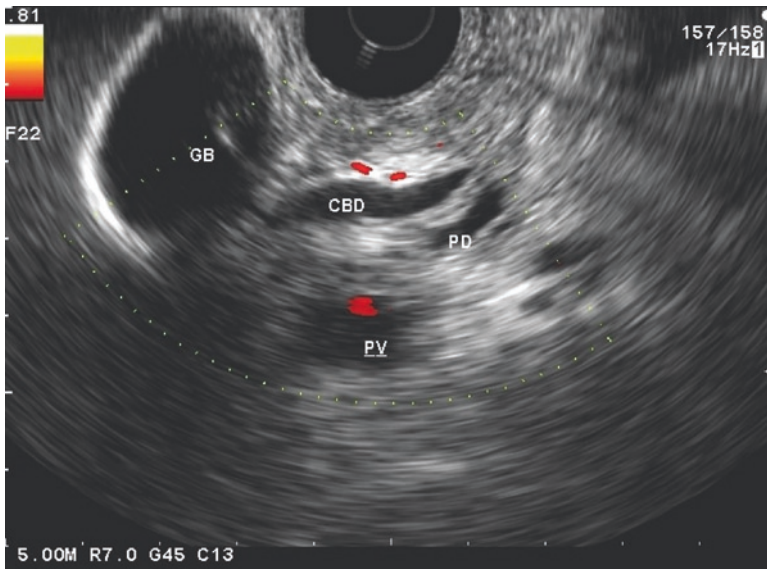


Fig. 19. Simultaneous view of the common bile duct (CBD), main pancreatic duct (PD), and portal vein (PV) from the apex of the duodenal bulb: the so-called stack sign. The gallbladder (GB) is also visualized.

“stack sign” may suggest the presence of pancreas divisum (14). Once the landmarks have been identified from the duodenal bulb, the echoendoscope is carefully advanced into the second portion of the duodenum. Since the radial echoendoscope is an oblique-viewing instrument, the examiner must be careful to avoid injury in this region as endoscopic visualization may be limited.

The second position for imaging the pancreatic head is from the level of the papilla. The papilla is best identified with direct endoscopic visualization followed by the placement of the ultrasound probe on top of the papilla. Balloon inflation followed by gentle advancement and withdrawal of the echoendoscope will allow imaging of the ampulla of Vater and pancreatic head. The bile duct and pancreatic duct can be seen in cross-section from this position with the pancreatic duct deep to the bile duct relative to the ultrasound transducer. This position is critical for accurate staging of ampullary neoplasms. In efforts to improve endosonographic imaging from this position, water may be instilled to enhance acoustic coupling and/or glucagon given to inhibit intestinal motility.

The third position required for a thorough, complete examination of the pancreatic head and uncinate region is located immediately distal to the major papilla. A major anatomical landmark in this region is the abdominal aorta. Once the echoendoscope is positioned beyond the papilla, withdrawal of the scope initially reveals the aorta in its longitudinal axis. Further withdrawal demonstrates the aorta in cross-section with the pancreas seen just to the right of the aorta on the monitor screen. The aorta should be oriented in the 7 o'clock position with the pancreas in the 6 o'clock position. From here, the echoendoscope is slowly withdrawn demonstrating the uncinate, ampulla, CBD, pancreatic duct, and ventral anlage (Fig. 18). As with routine upper endoscopy, a problem that may be encountered upon the withdrawal from the second portion of the duodenum is the tendency to fall back into the antrum. Similar to upper endoscopy, this problem may be avoided with slight withdrawal followed by slight advancement in attempts to maintain a one-to-one reaction with the shaft of the echoendoscope through this region. Despite this maneuver, adequate examination of this region may require several passes with the echoendoscope depending on the patient's anatomy.

After the head has been examined, attention is then focused on the body and tail. Generally, the body and tail are much easier to visualize, and the examination begins immediately below the gastroesophageal junction. The abdominal aorta is identified and oriented into the 6 o'clock position. The echoendoscope is advanced along the wall of the stomach to bring the first branch of the aorta, celiac artery, into view. If resistance is encountered upon advancing the echoendoscope, this

suggests the presence of a hiatal hernia and may require either tip deflection or scope rotation to avoid injury to the gastric wall. Once the bifurcation of the celiac artery is identified, the splenic artery can be traced to the pancreatic body (Fig. 16). Two major anatomical landmarks in this region are the splenoportal confluence and the splenic vein. The splenoportal confluence has been described as having a “club-like” appearance given its unique shape on radial imaging (Fig. 20). Once the splenoportal confluence and pancreatic body have been identified, the gland can be traced toward the genu with counter-clockwise torque and advancement of the scope or toward the tail with gentle withdrawal, clockwise rotation and some upward tip deflection. This produces an elongated view of the pancreas that can be easily traced back and forth with advancement and withdrawal of the echoendoscope. The splenic vein serves as a useful landmark for finding and following the path of the pancreas. In the pancreatic body, the splenic vein courses posterior to the gland, and the parenchyma is visualized between the splenic vein and ultrasound transducer. Toward the tail of the pancreas, as the splenic vein courses to the splenic hilum, the vein crosses the pancreatic tail and courses anteriorly.

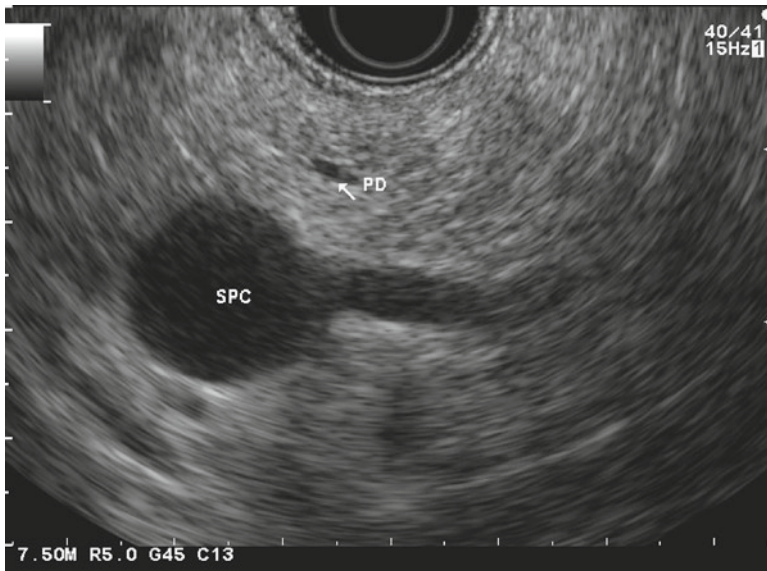


Fig. 20. The splenoportal confluence (SPC) represents a critical landmark for identifying the pancreatic body and genu. The SPC has been described as having a “club-like” appearance.

Obviously, the approach to examining the pancreas may vary among experienced endosonographers; however, the anatomical stations and landmarks remain constant. Quick recognition of these landmarks and understanding their anatomical relation to the pancreas will enable the beginner to regain position quickly if disoriented during the exam.

RECTUM

Rectal endosonography is typically performed to evaluate suspicious polyps, submucosal masses, or stage rectal cancer. Radial EUS can be performed using either a rigid ultrasound probe or standard flexible radial echoendoscope. Rigid probes provide 360° ultrasound imaging similar to standard echoendoscopes. However, rectal probes lack both fiber-optic bundles and charged-couple device (CCD) image sensors, and therefore cannot provide endoscopic images. Due to their rigid nature and lack of endoscopic visualization, rigid probes can only provide sonographic imaging from the rectum and perianal area. Standard, oblique-viewing, flexible radial echoendoscopes can be advanced into the rectum and sigmoid colon under direct endoscopic visualization to provide sonographic imaging from these regions. However, it may be difficult to maneuver the radial echoendoscope beyond the tortuous sigmoid colon due to limited endoscopic visualization and increased risk for perforation.

Patients undergoing EUS of the rectosigmoid colon are typically given an enema or complete bowel preparation to evacuate all stool from the area of interest. The authors prefer a complete bowel preparation as this tends to optimize sonographic imaging and allow endotherapy with electrocautery if necessary. Initially, the patient is placed in the left lateral decubitus position. For the majority of cases, sedation is not necessary but may be preferred depending on the endoscopist and patient preference. Prior to performing the rectal EUS, a flexible sigmoidoscopy is performed to assess the lesion of interest and quality of the bowel preparation. Once the sigmoidoscopy is completed, the radial echoendoscope is gently inserted through the anus and advanced to the sigmoid colon. The balloon is inflated and continuous suction is applied to remove any remaining air within the intestinal lumen. Again, water may be instilled through the biopsy channel to further enhance acoustic coupling. Perpendicular imaging may be difficult in the region of Houston's valves, and therefore, additional water and manipulation of the echoendoscope may be necessary to avoid tangential imaging. From the sigmoid colon, the echoendoscope is slowly withdrawn focusing attention to the intestinal wall and perirectal space.

One of the first landmarks to appear at the level of the distal sigmoid colon is the iliac vessels. The iliac vessels appear as long, tubular, anechoic structures and represent an important landmark for nodal staging in rectal cancer (Fig. 21). Lymph nodes appear as round or oval echogenic structures located in the perirectal space. Usually, lymph nodes can be distinguished from blood vessels by advancing and withdrawing the scope to visualize whether the structure elongates into a long tubular structure suggestive of a vessel or remains fixed like a node. With the development of electronic radial echoendoscopes, the use of Doppler can further aid in discerning nodes from vessels.

When performing rectal endosonography, familiarity with the normal male and female pelvic anatomy is essential. In males, as the echoendoscope is withdrawn from the sigmoid colon into the rectum, the prostate appears as an oval-shaped, hypoechoic, heterogeneous structure located anterior to the rectal wall (Fig. 22). It is not uncommon to observe calcifications within the prostate gland. Once identified, the prostate should be oriented into the 12 o'clock position. With this orientation, the left on the ultrasound image corresponds to the patient's left and right corresponds to the patient's right. Similarly, the top of the image represents the patient's anterior and the bottom represents the patient's posterior. The left and right seminal vesicles are observed just proximal to the prostate and appear as elongated hypoechoic structures located in the 9–12 o'clock and 12 to 3 o'clock positions, respectively. These structures should not be confused with enlarged lymph nodes. In females, the vagina, urethra, uterus, and bladder can also be visualized anterior to the rectum. Similar to the prostate in males, once the uterus is identified, it should be oriented into the 12 o'clock position to obtain proper orientation (Fig. 23).

In the anal canal, the internal and external sphincters are visualized by ultrasound. The internal anal sphincter (IAS) appears as a thin hypoechoic ring surrounding the anal canal. The external anal sphincter (EAS) is seen just lateral to the IAS as a heterogeneous echogenic structure (Fig. 24). In patients with fecal incontinence, trans-anal ultrasound can be useful for evaluating defects in the continuity of the IAS and EAS. Most endosonographers prefer rigid ultrasound probes for optimal evaluation of the anal sphincters.

In addition to suspicious polyps, submucosal masses and rectal cancer, radial EUS can be useful for evaluating perirectal fistulas and abscesses observed in inflammatory conditions such as Crohn's disease (15, 16). Fistulas appear as anechoic or hypoechoic structures within the anorectal region and often demonstrate ultrasound artifact due to air within the fistula. Abscesses may appear as irregularly shaped anechoic or hypoechoic perirectal masses that often have echogenic debris within the

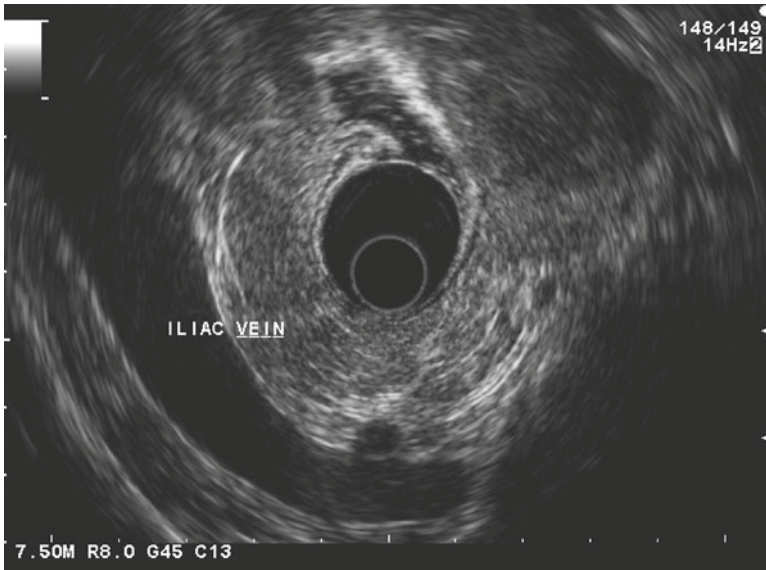


Fig. 21. The iliac vessels appear as long, tubular anechoic structure located in the perirectal space near the rectosigmoid junction. The iliac region is important for nodal staging.

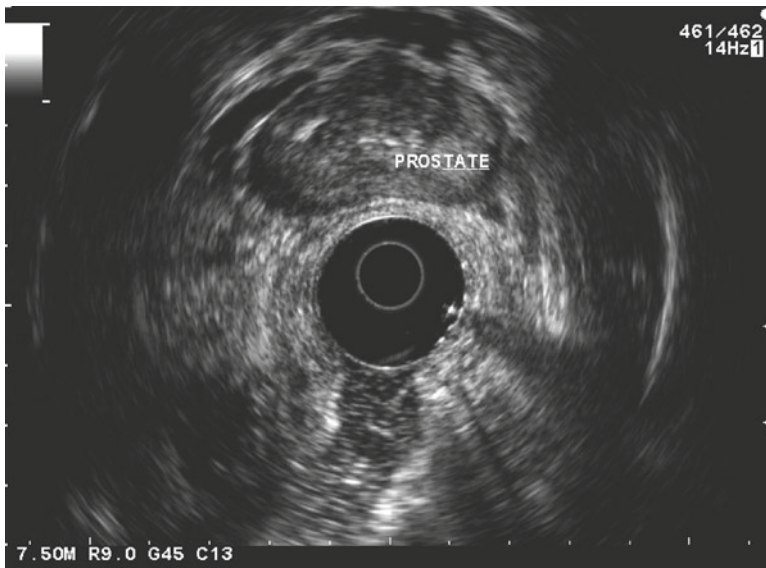


Fig. 22. The oval-shaped prostate is hypoechoic and heterogeneous with well-defined borders. It is not uncommon to see calcifications within the gland.

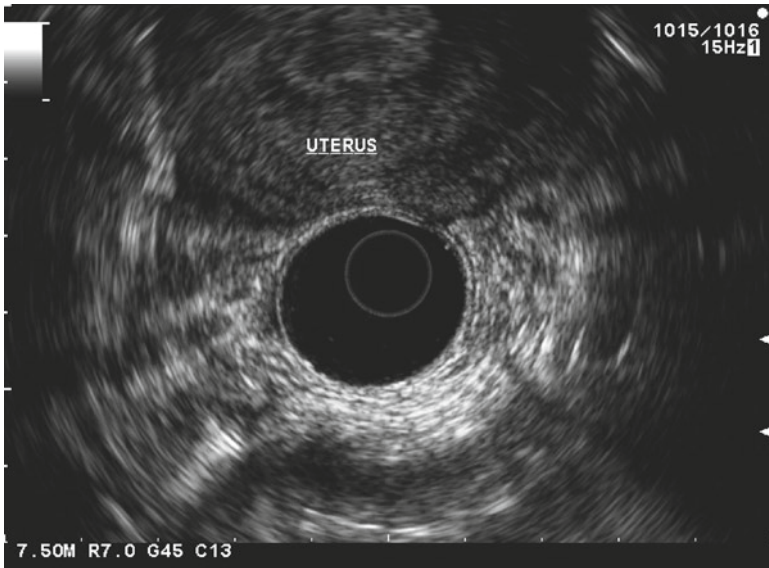


Fig. 23. The uterus is a large hypoechoic structure located anterior to the rectal wall. The vagina may be observed between the uterus and rectal wall upon withdrawal of the scope.

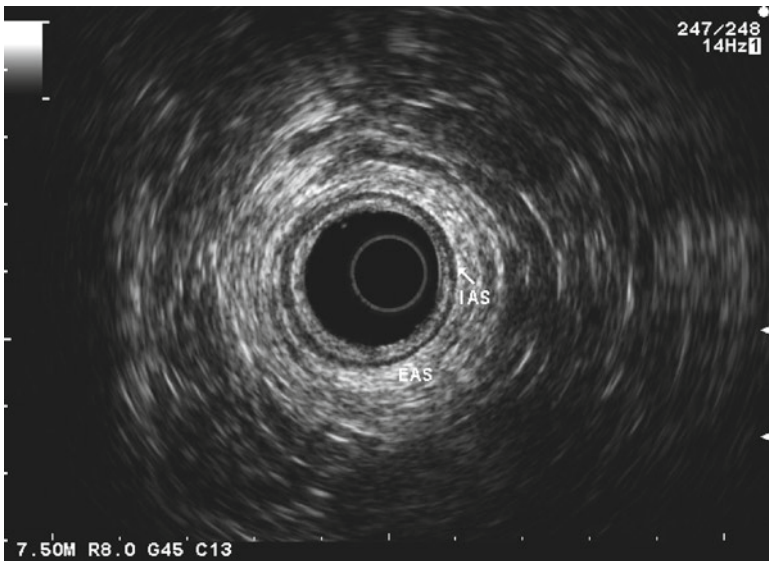


Fig. 24. The internal anal sphincter (IAS) is a thin, hypoechoic ring surrounding the anal canal. The external anal sphincter (EAS) is heterogeneous and echogenic and located just lateral to the IAS.

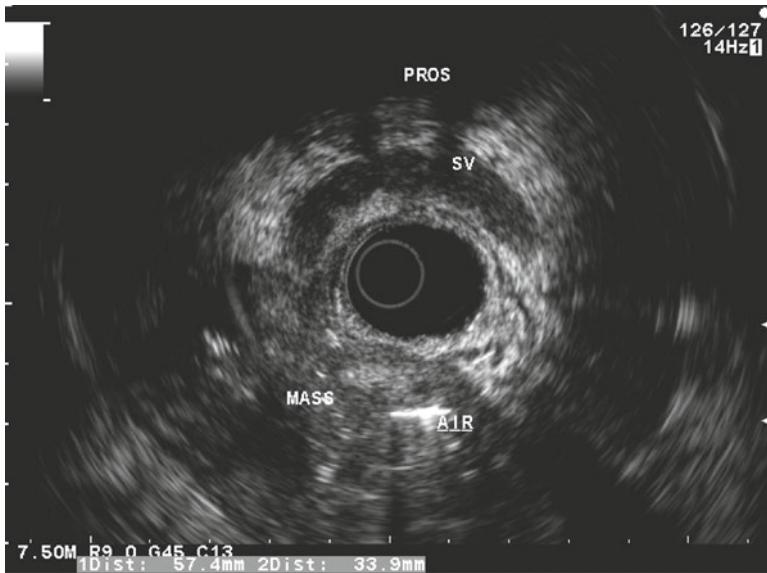


Fig. 25. Large presacral abscess demonstrated as complication from prior colorectal surgery. Note the echogenic debris and air within the abscess. The abscess is located posteriorly as depicted by the anterior position of the prostate (PROS) and seminal vesicles (SV).

abscess cavity (Fig. 25). Abscesses may also be seen as complications from prior colorectal surgery.

SUMMARY

Since its inception over two decades ago, radial EUS has emerged as a powerful diagnostic tool for the evaluation and staging of gastrointestinal neoplasms in both the upper and lower digestive tracts. Although the technology was initially reserved for large, tertiary referral centers, more and more community hospitals are recognizing the increasing demand for EUS, and therefore investing in both equipment and skilled endosonographers. Obviously, reading a textbook chapter or attending a weekend hands-on course is inadequate training for starting an EUS practice. However, textbooks and hands-on courses can serve as excellent adjuncts to dedicated, supervised training. For the beginner, review of an anatomy and radiology atlas is critical for understanding and accurately interpreting the ultrasound images. Acquiring fundamental skills in radial EUS may further assist in learning linear endosonography and

ultimately EUS-guided FNA. Recognizing and remembering the common anatomical landmarks is essential and will ultimately lead to a thorough and efficient exam.

REFERENCES

1. Verma D, Kapadia A, Eisen GM, et al. EUS vs. MRCP for detection of choledocholithiasis. *Gastrointest Endosc.* 2006;64:248–54.
2. McMahon CJ. The relative roles of magnetic resonance cholangiopancreatography (MRCP) and endoscopic ultrasound in the diagnosis of malignant common bile duct strictures: a critically appraised topic. *Abdom Imaging.* 2008;33:10–3.
3. DeWitt J, Devereaux B, Chriswell M, et al. Comparison of endoscopic ultrasonography and multidetector computed tomography for detecting and staging pancreatic cancer. *Ann Intern Med.* 2004;141:753–63.
4. Liu CL, Lo CM, Chan JK, et al. EUS for detection of occult cholelithiasis in patients with idiopathic pancreatitis. *Gastrointest Endosc.* 2000;51:28–32.
5. Gress F, Bhattacharya I, editors. *Endoscopic ultrasonography.* New Jersey: Wiley-Blackwell; 2001.
6. Hawes RH, Fockens P, editors. *Endosonography.* Philadelphia: Saunders Elsevier; 2006.
7. Bhutani MS, Deutsch JC. *Digital human anatomy and endoscopic ultrasonography.* Ashland (OH): People's Medical Publishing House, USA; 2005.
8. Yusuf TE, Tsutaki S, Wagh MS, et al. The EUS hardware store: state of the art technical review of instruments and equipment. *Gastrointest Endosc.* 2007;66:131–43.
9. Kimmey MB, Martin RW, Haggitt RC, et al. Histologic correlates of gastrointestinal ultrasound images. *Gastroenterology.* 1989;96:433–41.
10. Tio TL, Tytgat GN. Endoscopic ultrasonography of normal and pathologic upper gastrointestinal wall structure. Comparison of studies in vivo and in vitro with histology. *Scand J Gastroenterol Suppl.* 1986;123:27–33.
11. Wiersema M, Wiersema L. High-resolution 25 Megahertz ultrasonography of the gastrointestinal wall: histologic correlates. *Gastrointest Endosc.* 1993;39:499–504.
12. Savides TJ, Gress FG, Zaidi AS, et al. Detection of the embryologic ventral pancreatic parenchyma with endoscopic ultrasound. *Gastrointest Endosc.* 1996;43:14–9.
13. Bhutani MS, Hoffman BJ, Van Velse A. Diagnosis of pancreas divisum by endoscopic ultrasound (EUS). In: 10th International Symposium on Endoscopic Ultrasonography. Cleveland, OH, 1995.
14. Bhutani MS, Hoffman BJ, Hawes RH. Diagnosis of pancreas divisum by endoscopic ultrasonography. *Endoscopy.* 1999;31:167–9.
15. Schratte-Sehn AU, Lochs H, Vogelsang H, et al. Endoscopic ultrasonography versus computed tomography in the differential diagnosis of perianorectal complications in Crohn's disease. *Endoscopy.* 1993;25:582–6.
16. Spradlin NM, Wise PE, Herline AJ, et al. A randomized prospective trial of endoscopic ultrasound to guide combination medical and surgical treatment for Crohn's perianal fistulas. *Am J Gastroenterol.* 2008;103:2527–35.

Linear Endoscopic Ultrasound

*Jason D. Conway, MD, MPH
and Girish Mishra, MD, MS*

CONTENTS

INTRODUCTION

TECHNIQUE

ACCESSORIES

ROLE OF LINEAR EUS IN GI DISEASES

SUMMARY

Abstract

The widespread acceptance of endoscopic ultrasound (EUS) has largely been due to the emergence of the linear array echoendoscope. Once endosonographers familiarized themselves with images obtained from the radial echoendoscope with correlative gastrointestinal and extraintestinal anatomy, they reached a certain plateau. Elegant descriptions of lesions and superior staging abilities were soon met by the obvious reality of the need for tissue acquisition. The rapid refinement of the linear array echoendoscope, both in endoscope design and imaging resolution coupled with an improvement in the size of the accessory channels quickly brought this technology to the forefront. This chapter reviews the basic endoscope design of the linear array echoendoscope. The dogma for learning EUS is the need for a systematic approach guided by a “station approach.” We describe the basic techniques used to acquire the necessary images when performing a linear examination. As one masters these maneuvers, performing fine needle aspiration and other therapeutic interventions will seem secondary. The second half of

From: *Clinical Gastroenterology: Endoscopic Ultrasound*,
Edited by: V. M. Shami and M. Kahaleh, DOI 10.1007/978-1-60327-480-7_4,
© Springer Science+Business Media, LLC 2010

this chapter explores the literature, namely asking the question, does the instrument matter and how useful is the linear array endoscope in comparison with the mechanical radial instrument for evaluating esophageal cancer, gastric cancer, pancreatic disorders, suspected common bile duct stones, and lastly rectal cancer. The linear array echoendoscope is an extremely powerful instrument and the benefits derived from using this instrument will be well worth the energy expended in mastering some basic concepts and techniques.

Key Words: Endosonography, Linear EUS, Fine needle aspiration

INTRODUCTION

The linear echoendoscope is an elegant tool designed primarily for fine needle aspiration (FNA) of lesions within the gut wall or adjacent to the lumen of the GI tract. It is also an excellent imaging tool. Continued refinement of the instrument as well as increased experience and establishment of dedicated training programs has led to a dramatic increase in the number of linear EUS procedures being performed over the past 20 years. Not surprisingly, as the number of procedures has increased, so has the number of linear echoendoscope manufacturers. There are currently three manufacturers of linear echoendoscopes: Olympus, Pentax, and Fujinon (1). The recent development of therapeutic roles for EUS relies exclusively on the linear echoendoscope, and these emerging procedures may drive the future evolution of linear endosonography (2). In this chapter, we describe the basic technique for performing linear endosonography to image structures immediately adjacent to the GI tract. We also review the pertinent literature that critically examines the relative merits of the radial echoendoscope over the linear echoendoscope for staging of upper GI malignancies, rectal neoplasms, and benign conditions such as chronic pancreatitis and for evaluating suspected common bile duct (CBD) stones.

TECHNIQUE

Maneuvering the Linear Echoendoscope

Maneuvering a linear echoendoscope through the GI tract is much more challenging than a standard forward viewing endoscope and requires detailed understanding of the construction of the tip of the echoendoscope. The ultrasound transducer is in the shape of a half-circle and placed on the very distal tip of the scope. Just proximal to the transducer and at an oblique angle (between 50 and 60°, based on the

scope model and manufacturer) are the optics, air and water ports, and working channel with elevator¹. The working channel (which varies in diameter from 2 to 3.8 mm) is designed so that, as the FNA needle is advanced, it will be within the plane of scanning and can be visualized as it enters the target tissue. The outer diameters, field of view, scanning frequencies, and degrees of scanning all vary between models and manufacturers (3). Understanding that the transducer is placed distal to the optics and that the optics is oblique is essential to safe insertion and maneuvering of the linear echoendoscope.

Linear EUS examination of the upper GI tract is usually performed with the patient in the left lateral position. Patients should be sedated with conscious sedation or monitored anesthesia care (MAC). The scope should be advanced into the pharynx with all controls unlocked. With the vocal cords in view, the upper esophageal sphincter should be engaged and the scope gently advanced sometimes with a subtle clockwise and counter-clockwise torque of the scope. Flexion of the head and/or anterior thrust of the mandible can also sometimes aid intubation. Excessive pushing force at intubation may lead to pharyngeal perforation (4). If at any time the echoendoscope will not advance, the scope should be removed and the area examined with a standard forward viewing endoscope.

The scope can typically be advanced through the esophagus and into the stomach with gentle pushing and no tip deflection. Angulation of the distal esophagus just proximal to the lower esophageal sphincter and large hiatal hernias can often impede the advancement of the scope into the stomach. Usually, these areas can be traversed with a combination of gentle pressure, subtle tip deflection, and torquing of the scope. It may be helpful to withdraw the scope slightly from these areas of angulation and deflect the tip down with the big wheel in an attempt to visualize the anatomy – though this can be challenging especially in the esophagus.

Advancement through the stomach and into the duodenum is similar to that of a duodenoscope. The pylorus can be traversed by placing it at the very bottom and center of the endoscopic image with tip deflection and gently advancing the scope forward. When the pylorus is engaged, subtle tip down deflection or extension of the tip with the big wheel will aid passage into the duodenal bulb. If the pylorus cannot be engaged, withdrawing the tip of the scope into the antrum and repeat adjustment of the tip to center the pylorus on the bottom of the endoscopic image followed by repeated advancement of the scope may aid passage through the pylorus.

¹All EUS images obtained using the Olympus linear echoendoscope (GF-UC160P, Olympus America, Center Valley, PA) and the Aloka ProSound ALPHA-10 processor scanning at 7.5 MHz (Aloka America, Wallingford, CT).

Advancement through the duodenal sweep is achieved by first advancing the transducer to the apex of the duodenal bulb. The small wheel should then be locked in the right position. With subtle tip up deflection with the big wheel and clockwise torque and slow withdrawal of the scope, the tip will slip around the duodenal sweep and into the second portion of the duodenum. Special care must be taken with this maneuver, as excessive pushing force can lead to perforation of the duodenal bulb (5).

There are other maneuvers unique to linear endosonography used only during the ultrasound examination. Air will interfere with ultrasound imaging and must constantly be suctioned from the lumen of the GI tract. The transducer is pressed against the mucosa by constant tip up deflection with the big wheel. The balloon covering the transducer can be inflated with water to enhance acoustical coupling. Structures are typically examined by a combination of subtle insertion and withdrawal of the scope combined with clockwise and counterclockwise torquing the scope. Unlike standard forward viewing endoscopy, the linear echoendoscope is typically not torqued with the right hand but rather with clockwise and counterclockwise rotation of the endoscopist's torso and/or left hand. These maneuvers can be quite challenging to perform and are best learned from an expert endosonographer (6–10).

Value of a Forward Viewing Endoscopy Prior to EUS

As mentioned above, whenever resistance is encountered with insertion of the linear echoendoscope, the scope should be withdrawn from the patient and the area examined with a standard forward viewing endoscope. If luminal pathology is suspected (e.g., strictures, ulcers, tumors, etc.), forward viewing endoscopy should be performed prior to insertion of the linear echoendoscope. Finally, if the patient has symptoms of obstruction (e.g., dysphagia, nausea and vomiting, etc.), forward viewing endoscopy may rule out luminal pathology prior to passage of the linear echoendoscope.

Mediastinum

The linear echoendoscope is typically used to FNA posterior mediastinal lesions seen on cross-sectional imaging or radial endosonography. Radial EUS survey of the mediastinum just prior to linear EUS and FNA can aid in visualizing the target, determining the depth of scope insertion needed to visualize the target, and identifying adjacent landmarks. Survey of the posterior mediastinum with the linear echoendoscope is very

tedious and requires torquing the scope 180° clockwise followed by 180° counterclockwise at 1–2 cm intervals throughout the entire esophagus. For this reason, survey of the posterior mediastinum is best performed with the radial echoendoscope.

The two most common areas of interest in the posterior mediastinum are the subcarinal space and the aortopulmonary (AP) window. The subcarinal space is located with the scope tip in the distal esophagus at about 35 cm from the incisors and the scope in the neutral position (i.e., with the patient in the left lateral position and no torque or tip deflection applied). The scope is then slowly torqued clockwise and slowly withdrawn. The left atrium will come into view as a large anechoic Doppler positive structure immediately adjacent to the esophagus. The scope should be subtly torqued in either direction and withdrawn, so the largest cross-sectional diameter of the left atrium is centered on the screen. From here, the pulmonary artery is brought into view by slowly withdrawing the scope with subtle tip up deflection to bring a round anechoic Doppler positive structure into the upper right corner of the screen. The subcarinal space is between the left atrium and the pulmonary artery and should be surveyed by clockwise and counterclockwise torque of the scope (see Fig. 1).



Fig. 1. The subcarinal space (SC) with adjacent left atrium (LA) and pulmonary artery (PA).

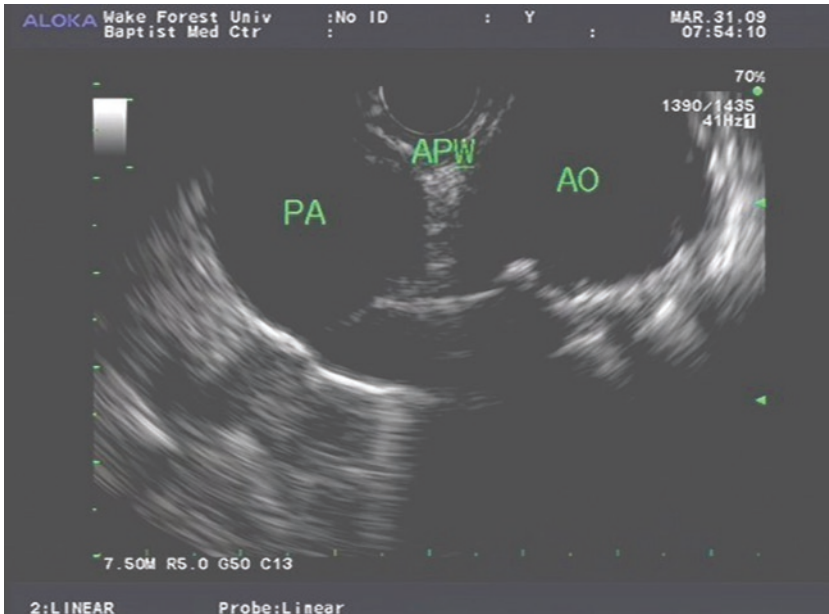


Fig. 2. The aortopulmonary window (APW) with adjacent aorta (AO) and pulmonary artery (PA).

The AP window can be found by inserting the scope to about 30 cm from the incisors in the neutral position. Counterclockwise torque of the scope will find the aorta as a linear Doppler positive anechoic structure immediately adjacent to the esophagus. Staying centered on the aorta, the scope is slowly withdrawn until the aortic arch is immediately below the transducer. The scope is then inserted about 1–2 cm and with slight tip up deflection torqued clockwise. The aorta will go from a linear to a round conformation and the pulmonary artery will be seen just to the left of the aorta on the screen as a round anechoic Doppler positive structure nearly the same diameter as the aorta. The space between the aorta and pulmonary artery is the AP window (see Fig. 2).

Celiac Axis and Adjacent Structures

The celiac axis is found with the tip of the scope in the stomach just below the gastroesophageal junction and in the neutral position. The tip of the scope is deflected slightly up, and the left lobe of the liver is immediately beneath the transducer with the heart seen in the upper

right hand corner of the screen. The scope is torqued clockwise until the aorta will eventually come into view as an anechoic linear Doppler positive structure immediately beneath and nearly parallel to the transducer. The crus of the diaphragm is seen as a thin hypoechoic band parallel to the aorta and lying between the walls of the stomach and aorta. Staying centered on the aorta, the scope is advanced until the celiac axis is seen as the first artery coming off of the aorta. Occasionally, the scope will have to be torqued slightly clockwise and counterclockwise to see if the celiac originates from a more lateral position on the aorta. The superior mesenteric artery can be seen coming off the aorta just to the left of the celiac on the screen (see Fig. 3). The area around the celiac takeoff can be surveyed by clockwise and counterclockwise torque of the scope. Staying centered on the celiac axis, the scope is advanced to reveal the bifurcation of the celiac into the hepatic and splenic arteries.

The left adrenal can be found by first locating the celiac takeoff from the aorta, then withdrawing the scope 1–2 cm and torquing clockwise off the aorta. The left adrenal is a thin “seagull shaped” hypoechoic structure immediately adjacent to the gastric wall.



Fig. 3. The celiac artery (CEL) as it originates from the aorta (AO) with adjacent superior mesenteric artery (SMA).

Liver and Gallbladder

The left lobe of the liver is best seen with the scope along the lesser curvature of the stomach and the tip at the body/antrum junction. The tip is deflected slightly up and the liver will be immediately beneath the transducer. The left lobe is surveyed by slowly withdrawing the scope with clockwise and counterclockwise torque.

The liver hilum is best seen by advancing the scope to the apex of the duodenal bulb and finding the CBD as a circular anechoic Doppler negative structure just below and to the left of the transducer on the screen. Gentle advancement of the scope as well as subtle clockwise and counterclockwise torque may be needed to locate the CBD. When the CBD is located, the scope should be advanced so that the CBD is immediately beneath the transducer. The Doppler positive anechoic structure just to the left of the CBD on the screen is the portal vein (Fig. 4). Keeping the CBD beneath the transducer the scope is torqued counterclockwise. The proximal CBD, confluence of the left and right intrahepatic bile ducts, and liver hilum will then come into view.

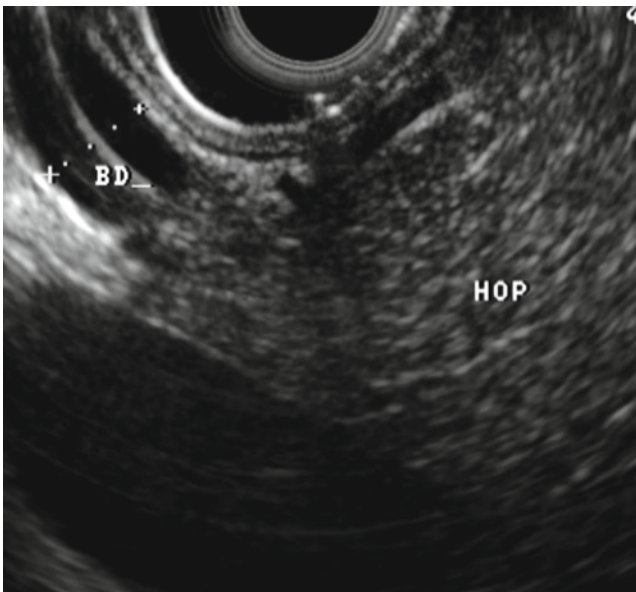


Fig. 4. From the second portion of the duodenum, proximal to the ampulla, the portal vein is seen as the anechoic structure deep to the common bile duct (BD) and running adjacent to the head of the pancreas (HOP).

The right lobe of the liver is more difficult to image. The scope tip should be advanced into the second portion of the duodenum and the aorta found by tip up deflection and subtle clockwise and counterclockwise torque. The aorta will come into view as a linear anechoic Doppler positive structure immediately beneath and in parallel to the transducer. The right lobe of the liver can then be seen by torquing the scope 180° off the aorta and surveyed by clockwise and counterclockwise torque.

The gallbladder is usually best seen by advancing the tip of the scope to the pre-pyloric antrum in the neutral position. The tip is deflected up and the liver is usually seen immediately beneath the transducer. Clockwise and counterclockwise torque and slow withdrawal of the scope will eventually bring the gallbladder into view as a Doppler negative anechoic structure immediately adjacent to the wall of the stomach and surrounded by liver. The gallbladder is surveyed by gentle insertion and withdrawal of the scope and clockwise and counterclockwise torque. In most patients, the gallbladder can also be seen from the duodenal bulb using a similar technique.

Pancreas, Bile Duct, and Ampulla

The body of the pancreas is best seen by finding the celiac axis and following it to the bifurcation as described above. The scope is then advanced a few centimeters and the pancreas body is seen immediately below the transducer. Often the big wheel will need to be released and the tip even deflected downward with the big wheel to advance the scope forward. The pancreas is a homogenous gland with a “salt and pepper” echotexture (see Fig. 5). In some patients, the pancreas can be difficult to discern from the surrounding retroperitoneum. The pancreas duct (PD) is seen as a small (typically 1–3 mm in diameter) round Doppler negative structure in the center of the gland. The pancreas is surveyed by keeping the PD immediately beneath the transducer in the 6 o’clock position by slow advancement and torquing the scope counterclockwise to image the proximal body and genu. The distal body and tail is surveyed by again keeping the PD beneath the transducer and torquing the scope clockwise. The scope will need to be slowly withdrawn to keep the PD immediately beneath the transducer. The left kidney will come into view just below the tail of the pancreas on the screen. By continued withdrawal of the scope and clockwise torque off the tail of the pancreas and following the splenic artery and vein the splenic hilum and spleen can be imaged.



Fig. 5. The normal pancreas body with central pancreas duct (PD) and adjacent splenic artery (SA) and splenic vein (SV).

The pancreas head is best seen from the duodenum. The scope tip is advanced to the apex of the duodenal bulb, and the CBD is found as described above. When the CBD is positioned beneath the transducer in the 6 o'clock position and the scope torqued clockwise, the CBD can be followed to its distal portion and eventually to its intrapancreatic portion which leads to the head of the pancreas. The pancreas head will be directly beneath the transducer and can be surveyed by clockwise and counterclockwise torque of the scope. On the opposite side of the pancreas head from the transducer, the head is bordered by the portal vein, portal confluence, and superior mesenteric vein (see Fig. 6).

The pancreas uncinata is best seen by advancing the scope tip into the second portion of the duodenum and positioning the transducer just distal to the ampulla. The tip of the scope is then deflected up and slowly withdrawn with clockwise and counterclockwise torque until the aorta comes into view, often a round anechoic Doppler positive structure immediately beneath the transducer. Keeping the aorta in view and beneath the transducer, the scope is withdrawn until the aorta changes from a round to a linear conformation immediately beneath

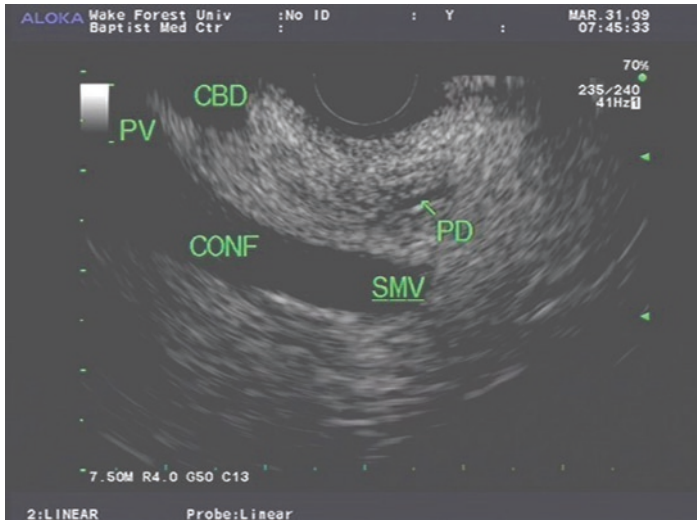


Fig. 6. The head of the pancreas (immediately the transducer) with the pancreas duct (PD) and adjacent common bile duct (CBD). Note how the pancreas head is bordered by the portal vein (PV), confluence (CONF), and superior mesenteric veins (SMV).

and in parallel to the transducer. From here, the scope is torqued just slightly clockwise off the aorta and slowly withdrawn. The pancreas uncinate will come into view directly beneath the transducer. The uncinate can be surveyed by continued slow withdrawal and clockwise and counterclockwise torque of the scope.

The ampulla can be imaged by inserting the scope into the second portion of the duodenum of finding the ampulla endoscopically. The duodenum should be filled with water or saline instilled via a pump or by gravity (e.g., using an IV bag and tubing) through the working channel of the scope. Flushing water into the duodenum with a syringe will cause small air bubbles within the fluid and impede ultrasound imaging. The balloon can also be inflated to displace duodenal air. The tip is kept in the neutral position or deflected slightly down or away from the ampulla, and the scope is slowly withdrawn and simultaneously torqued clockwise and counterclockwise. The ampulla will come into view as a subtle hypoechoic structure in the wall of the duodenum with the CBD and PD arising from it. The ampulla is surveyed by continued slow withdrawal of the scope and clockwise and counterclockwise torque. This position is also the best to see the very distal CBD.

Rectum

As in the mediastinum, linear EUS in the rectum is almost always performed to FNA lesions seen on radial EUS or cross-sectional imaging. Linear EUS is almost always preceded by forward viewing endoscopy to evaluate the rectosigmoid anatomy and luminal pathology. Radial EUS is usually then performed to find the target lesion, determine the depth of scope insertion needed to visualize the target, and to identify adjacent landmarks (e.g., prostate, vagina, seminal vesicals, etc.). Based on this information, the linear echoendoscope is inserted to the appropriate depth; adjacent structures and the target lesion are then found by gentle insertion and withdrawal of the scope and clockwise and counterclockwise torque.

ACCESSORIES

Balloons

Tight fitting latex balloons are often placed over the ultrasound transducer. Depressing the air/water button all the way, instills water into the balloon and can displace air in the lumen and enhance acoustic coupling with the mucosa. After the balloon is placed over the transducer, it should be filled and emptied several times to evacuate all air. Unlike radial endosonography, balloons are not essential to linear endosonography because tip deflection can be used to press the transducer against the mucosa, thereby displacing interfering air. Balloon specifications vary between manufacturers.

Buttons and Caps

The suction and air/water buttons are unique to the echoendoscope and are not interchangeable with standard endoscope buttons. The buttons perform the standard functions of instilling air into the lumen, suction of lumen contents, and washing the lens. Suctioning and washing the lens are performed by partially depressing the appropriate buttons. Additionally, the buttons allow inflation of the balloon with water (air/water button) and suctioning (suction button) of the water from the balloon when completely depressed. The plastic working channel cap for the linear echoendoscope is slightly taller than those used on standard endoscopes. This is due to the metal Luer lock hub on the handle of the echoendoscope being slightly longer than that on a standard endoscope to allow connection of FNA needles.

ROLE OF LINEAR EUS IN GI DISEASES

The widespread use of the linear echoendoscope as the primary and only method for staging as well as performing FNA has been a recent phenomena. In its infancy, the practice of EUS routinely employed a radial exam prior to the intubation of the linear echoendoscope for staging upper GI cancers, submucosal lesions, examination of the pancreas, and for rectal lesions. Although most endosonographers still perform staging exams with the radial echoendoscope, the vast majority of experienced endosonographers rely solely on the linear echoendoscope for interrogating the hepatobiliary and pancreatic regions. Experienced endosonographers would readily admit that it is rarely absolutely necessary to use radial imaging over a linear; a completely obstructing lesion being the exception. In fact, a recent retrospective study specifically compared the use of radial, linear, and miniprobe endosonography equipment during a 10-year prior in a single, large, EUS practice (11). Scope usage was compared between the first 8 years to the last 2 years. These investigators found the radial echoendoscope to be the predominant scope for luminal cancer staging. However, sole use of the linear echoendoscope was increasing, being the preferred scope for pancreaticobiliary and mediastinal indications (33% vs. 76%, $p < 0.001$; 46% vs. 96%, $p < 0.001$). Studies over time have consistently dispelled any claim for superiority of a radial exam over the linear. The ensuing paragraphs review these comparative studies.

Esophageal Cancer

Nearly, all the early seminal studies touting the superior accuracy of EUS for locoregional staging of esophageal cancer were based on radial staging. Arguments against the routine use of the linear echoendoscope for primary staging cite greater difficulty with image interpretation leading to increased procedure time. This premise was challenged by Simsen et al. who conducted a prospective, randomized study to compare the accuracy of curved array and radial EUS for staging of cancers arising in the esophagus and cardia (12). A total of 104 patients underwent EUS; 62 patients had a subsequent surgical exploration. All patients were examined with a radial scanning echoendoscope (UM-3 [first 10 patients], UM-20 [last 94 patients]; Olympus America Corp., Melville, N.Y.) and a curved array scanning echoendoscope (FG32UA; Pentax Precision Instrument Corp., Orangeburg, N.Y.) A single investigator who was blinded to prior imaging results performed every exam. The procedure time was recorded for each exam. If a EUS-FNA was performed, the procedure time for the linear was recorded as the total procedure

time minus the time required for EUS-FNA. The high Kappa coefficient for TNM staging accuracy between these two echoendoscopes is consistent with an overall excellent agreement (T, 0.77; N, 0.75; M, 0.89). When components of the TNM staging were broken down, the staging accuracy for the linear and radial echoendoscopes were, respectively, as follows: T, 72 and 73%, N, 70 and 77%; and M, 61 and 57%. The mean procedure for the curved array was slightly greater (15 min vs. 12; $p < 0.01$)

In another study, Matthes et al. compared the 270° transverse array endosonography (TA-EUS) with linear EUS (L-EUS) for staging of upper GI malignancy in 43 patients (13). There was again, excellent agreement on the T stage between the two modalities in 37 of 42 patients (88%). Linear EUS demonstrated 61 abnormal lymph nodes in 26 patients, with an average of 2.3 nodes per patient, whereas radial EUS demonstrated 85 abnormal lymph nodes with an average of 3.3 nodes per patient ($p = 0.009$). Although statistically significant, the clinical relevance of this difference on patient management has not been thoroughly studied, even though the number of lymph nodes does have prognostic implications (14, 15). Interestingly, there was no difference noted in the ease of esophageal intubation between the two scopes despite a commonly accepted belief that the linear echoendoscope is more challenging to traverse through the upper esophageal sphincter. The choice of endoscope needs, therefore should be individualized to each patient's clinical scenario and presentation (16).

Stomach Cancer

EUS performs well in the staging accuracy for gastric cancers, although its clinical impact continues to be debated. Early gastric cancers are best visualized with high frequency probes. Comparative studies between the radial and linear echoendoscopes in staging gastric cancer are limited and to a great extent focused on the cardia. Given this paucity of data, the relative merits of one approach versus the other are largely based on historical controls. The largest cohort of patients undergoing a linear exam for staging of gastric cancer was reported by Shimoyama et al. (17). These investigators performed a routine endoscopy followed by a forward-viewing echoendoscope with a 7.5 MHz linear probe at the distal end (Machida-Toshiba, Tokyo, Japan). Forty-five patients with gastric cardia cancer who underwent gastrectomy with at least a localized lymphadenectomy were retrospectively analyzed for staging accuracy with nearly half of the patients harboring an early stage malignancy. The overall diagnostic accuracy for the depth

of invasion was 71%. The sensitivity for T1, T2, and T3 lesions was 100, 31, and 75%, respectively. The notoriously poor staging seen in T2 lesions is due to overstaging similar to that encountered in esophageal and rectal cancers. Mucosal (pT1-m) and submucosal (pT1-sm) cancers were correctly identified in 81% of patients. With FNA as an adjunct to linear imaging, the diagnostic accuracy for lymph node involvement was 80%.

Pancreatic Cancer

Perhaps in no other disease state has the widespread use of the linear echoendoscope become more apparent than in pancreatic cancer. In addition to vascular staging, the immediate advantage of tissue confirmation is implicit. The ability to perform primary staging, followed by FNA of either the pancreatic mass itself or of lymph nodes, to the ultimate ability to deem the patient as having distant metastasis to organs such as the liver, makes the linear echoendoscope the preferred instrument. But do we sacrifice staging accuracy without FNA in pancreatic cancers primarily staged by a linear echoendoscope? (Fig. 7).

Several studies that emerged in the late 1990s specifically compared radial scanning with the linear array for primary staging of pancreatic cancer as well as the utility of the linear array scope in both benign and malignant pancreatic lesions. The first study performed by Gress et al. utilized a cohort of 79 patients referred with pancreatic cancer (18). As only 33 patients ultimately had surgical excision, the evaluable groups consisted of 17 patients randomized to linear array and 16 to radial scanning EUS. EUS staging accuracy for linear array was 94% (16 of 17) for T and 71% (12 of 17) for N staging. The staging accuracy for radial scanning was 88% (14 of 16) for T and 75% (12 of 16) for N staging. Surprisingly, radial scanning was more accurate for predicting vascular invasion 100% (16 of 16) than the linear array 94% (16 of 17). These investigators appropriately point out that overall, both EUS designs appear equivalent for staging pancreatic cancer and assessing vascular invasion but with the added power to perform FNA, the linear array would be the preferred instrument for evaluating pancreatic masses. Kochman et al. evaluated the utility of the linear array ultrasound endoscope in the evaluation of suspected pancreatic disease (19). They prospectively compared the linear probe in 26 patients with suspected pancreatic disease with either surgery or long-term clinical follow-up. With the linear probe, the sensitivity and specificity for malignant disease of the pancreas were 80 and 88.9%, respectively.

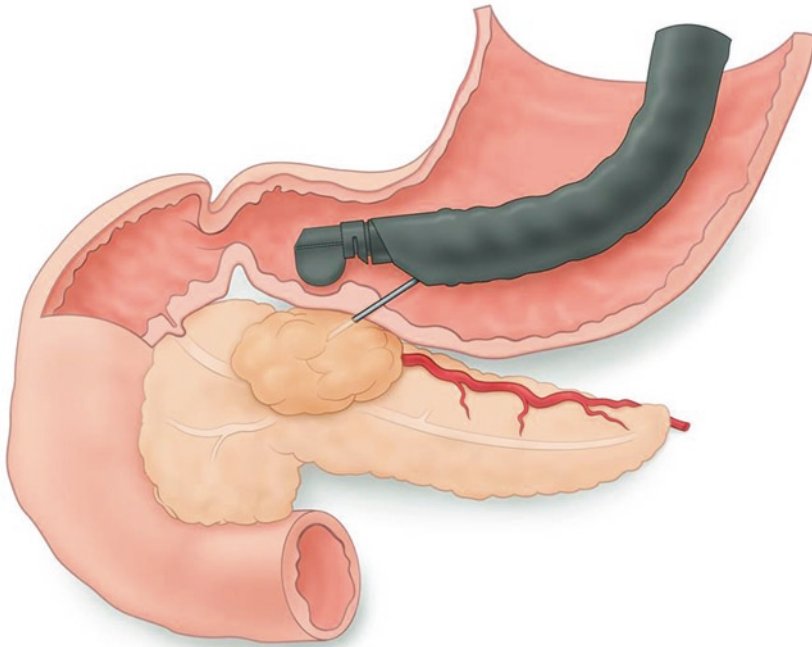


Fig. 7. The scope tip position relative to a pancreas head/genu mass undergoing FNA.

The sensitivity and specificity of linear array for benign disease of the pancreas were 93.8 and 88.2%, respectively. These investigators similarly concluded that the linear array echoendoscope, when employed solely for evaluating pancreatic diseases, is accurate and would have an even greater benefit with its ability to aid in tissue acquisition. Nearly, a decade later, it has become inherently obvious that the linear echoendoscope serves as the default scope for performing pancreatic examinations.

Chronic Pancreatitis and Pancreatic Ductal Anatomy

Standard criteria for diagnosing chronic pancreatitis are based on well-established guidelines using a mechanical radial echoendoscope at 7.5 MHz. Despite standardization, interobserver agreement between 11 experienced endosonographers blinded to the clinical history who were shown videotapes of both patients with chronic pancreatitis and controls, remains moderate, $\kappa=0.45$ (20). Is a linear array exam able to reliably

detect changes of chronic pancreatitis? This question was posed, and unfortunately published only in abstract form (21). This multicenter study, similarly evaluated the interobserver variability between expert endosonographers who were shown (but not informed) videotape examinations of the same patient undergoing both a radial and linear echoendoscope. Lai et al. observed similar interobserver variability with a moderate κ coefficient.

Pancreas divisum remains a challenging diagnosis for endosonographers. An early study suggested the possibility of pancreas divisum in patients undergoing a radial examination in whom a “stack sign” could not be obtained (22). The “stack sign” is an image simultaneously demonstrating the common bile duct, pancreatic duct, and portal vein with the transducer positioned in the duodenal bulb. The overall accuracy for this finding was 80% with a positive predictive value of only 44%. Lai et al. performed a linear-array examination in 162 patients prior to ERCP (23). They were able to adequately visualize the pancreatic duct in 78% of the patients. The overall prevalence of pancreas divisum was 13.6%. The sensitivity, specificity, and positive and negative predictive values for EUS were 95, 97, 86, and 99%, respectively. The EUS examinations were performed at 5MHz (Pentax FG-32UA, FG-36UX, or EG3630U; Pentax Precision Instruments, Orangeburg, N.Y.). A brief mention of the technique is warranted as their technique is elegant but not yet adequately taught or widely known. The scope is advanced into the second portion of the duodenum until the major papilla is identified sonographically. The balloon is then inflated and the scope withdrawn into a short position similar to that in ERCP. The PD is followed continuously from the major papilla to the pancreatic body by gentle withdrawal coupled with clockwise rotation. Pancreas divisum was excluded if the duct was either followed continuously from the major papilla to the body or seen crossing the ventral/dorsal border. We have used this technique with moderate success in determining the presence/absence of pancreas divisum.

Common Bile Duct Stones

EUS has superseded ERCP as the primary endoscopic modality for determining the presence of CBD stones (CBDS); MRCP allows similar accuracy but is limited in stones smaller than 2 mm. Studies in which a radial scanning echoendoscope was used consistently report sensitivities near 90% for the ability of EUS to detect CBDS. Lachter et al. report on 50 patients undergoing a linear array exam (32 FGUA; Pentax, Sci-Lab, Hamburg, Germany) for suspected choledocholithiasis with ERCP serving as the reference (24). EUS had 97% sensitivity,

77% specificity, and 90% accuracy. The authors conclude that “linear array EUS, despite the learning curve, seems to be about equivalent to radial EUS in accuracy.” Another prospective study of 134 patients suspected of CBDS underwent a linear array exam (Pentax FG 32 UA, Tokyo, Japan) followed by ERCP with endoscopic sphincterotomy (127 patients), or choledochoscopy (25). The accuracy for linear array EUS in determining CBDS was 94%; sensitivity, specificity, positive and negative predictive values were 93, 93, 98, and 87%, respectively.

Rectal Cancer

Literature regarding the sole use of the linear array scope for primary staging of rectal cancer is lacking. Certainly, the impact of endorectal ultrasound with FNA (RUS-FNA) is widely documented and accepted. Our experience is probably similar to other centers, namely, the linear echoendoscope can provide acceptable and adequate images for primary staging and is used in cases requiring FNA.

SUMMARY

Performing high quality EUS incorporates both a technical component and an equally important cognitive component. Learning the basics of each component is absolutely vital. This principle is paramount when using the linear array instrument. The basics and “station based” approach will serve as the fundamentals from which one can build the vast library of image recognition with subsequent confidence for performing interventions beyond just FNA. In addition to knowing the images and stations, becoming comfortable with the scope and accessories is crucial. Finally, the technology has to be challenged with science, and the review of the literature strongly supports the equal merits for the linear echoendoscope in staging primary upper GI cancers and for evaluating both benign and malignant pancreatic diseases.

REFERENCES

1. Tierney WM, Adler DG, Chand B, Conway JD, Croffie JM, DiSario JA, et al. Echoendoscopes. *Gastrointest Endosc.* 2007;66(3):435–42.
2. Shami VM, Kahaleh M. Endoscopic ultrasonography (EUS)-guided access and therapy of pancreatico-biliary disorders: EUS-guided cholangio and pancreatic drainage. *Gastrointest Endosc Clin N Am.* 2007;17(3):581–93. vii–viii.

3. Yusuf TE, Tsutaki S, Wagh MS, Waxman I, Brugge WR. The EUS hardware store: state of the art technical review of instruments and equipment (with videos). *Gastrointest Endosc.* 2007;66(1):131–43.
4. Eloubeidi MA, Tamhane A, Lopes TL, Morgan DE, Cerfolio RJ. Cervical esophageal perforations at the time of endoscopic ultrasound: a prospective evaluation of frequency, outcomes, and patient management. *Am J Gastroenterol.* 2009;104(1):53–6.
5. Sanders MK, Malick J, Fasanella KE, Watson AR. Endoscopic closure of iatrogenic duodenal perforation during EUS in a patient with unusual anatomy. *Gastrointest Endosc.* 2008;68(4):802–4.
6. Hawes RH, Fockens P, editors. *Endosonography*. Philadelphia: Saunders Elsevier; 2006. p. 329.
7. Vilmann P. *Endoscopic ultrasonography with curved linear array transducer in diagnosis of cancer in and adjacent to the upper gastrointestinal tract. Scanning and guided fine needle aspiration biopsy*. Copenhagen: Munksgaard; 1998. p. 231.
8. Bhutani MP, Deutsch J, editors. *Human anatomy and endoscopic ultrasonography*. Hamilton, ON: B.C. Decker Inc; 2004. p. 192.
9. Dancygier H, Lightdale CJ, editors. *Endosonography in gastroenterology*. New York: Thieme; 1999. p. 232.
10. Gress FG, Bhattacharya I, editors. *Endoscopic ultrasonography*. Malden, MA: Blackwell Science Inc; 2001. p. 185.
11. Noh KW, Woodward TA, Raimondo M, Savoy AD, Pungpapong S, et al. Changing trends in endosonography: linear imaging and tissue are increasingly the issue. *Dig Dis Sci.* 2007;52:1014–8.
12. Simesen M, Svendsen LB, Knigge U, Vilman P, Jensen F, Rasch L, et al. A prospective randomized comparison of curved array and radial echoendoscopy in patients with esophageal cancer. *Gastrointest Endosc.* 2003;58:671–6.
13. Matthes K, Bounds B, Collier K, Gutierrez A, Brugge WR. EUS staging of upper GI malignancies: results of a prospective randomized trial. *Gastrointest Endosc.* 2006;64:496–502.
14. Eloubeidi MA, Desmond R, Arguedas MR, et al. Prognostic factors for the survival of patients with esophageal carcinoma in the US.: the importance of tumor length and lymph node status. *Cancer.* 2002;95:1434–43.
15. Chen J, Xy R, Hunt GC, Krinsky ML, Savides T. Influence of the number of malignant regional lymph nodes detected by endoscopic ultrasonography on survival stratification in esophageal adenocarcinoma. *Clin Gastroenterol Hepatol.* 2006;5:573–9.
16. Eloubedi MA. Choosing from the expanding EUS armamentarium menu: high-frequency probes, radial, or linear endosonography for staging of upper GI malignancy. *Gastrointest Endosc.* 2006;64:503–4.
17. Shimoyama S, Yasuda H, Hashimoto M, Tatsutomi Y, Aoki F, Mafune K, et al. Accuracy of linear-array EUS for preoperative staging of gastric cardia cancer. *Gastrointest Endosc.* 2004;60:50–5.
18. Gress F, Savides T, Cummings O, Sherman S, Lehman G, Zaidi S, et al. Radial scanning and linear array endosonography for staging pancreatic cancer: a prospective randomized comparison. *Gastrointest Endosc.* 1997;45:138–42.

19. Kochman ML, Elta GH, Bude R, Nostrant TT, Scheiman JM. Utility of a linear array ultrasound endoscope in the evaluation of suspected pancreatic disease. *J Gastrointest Surg.* 1998;2:217–22.
20. Wallace MB, Hawes RH, Durkalski V, Chak A, Mallery S, et al. The reliability of EUS for the diagnosis of chronic pancreatitis: interobserver agreement among experienced endosonographers. *Gastrointest Endosc.* 2001;53:294–9.
21. Lai R, Wiersema MJ, Sahai AV, et al. Blinded comparison of linear and radial endoscopic ultrasound (EUS) for the evaluation of chronic pancreatitis [abstract]. *Gastrointest Endosc.* 2001;53:AB170.
22. Bhutani MS, Hoffman BJ, Hawes RH. Diagnosis of pancreas divisum by endoscopic ultrasonography. *Endoscopy.* 1999;31:167–9.
23. Lai R, Freeman ML, Cass OW, Mallery S. Accurate diagnosis of pancreas divisum by linear-array endoscopic ultrasonography. *Endoscopy.* 2004;36:705–9.
24. Lachter J, Rubin A, Shiller M, Lavy A, et al. Linear EUS for bile duct stones. *Gastrointest Endosc.* 2000;51:51–4.
25. Kohut M, Dulawa EN, Marek T, Kaczor R, Nowak A. Accuracy of endoscopic ultrasonography in the evaluation of patients with suspected common bile duct stones. *Endoscopy.* 2002;34:299–303.

The Cytopathology of Endoscopic Ultrasound-Guided Fine Needle Aspiration

*Maria Luisa Policarpio-Nicolas, MD,
Deborah J. Chute, MD,
and Edward B. Stelow, MD*

CONTENTS

INTRODUCTION
PRINCIPLES OF CYTOLOGY
TERMINOLOGY
BIOPSY OF LUMINAL GUT
BIOPSY OF LYMPH NODES
BIOPSY OF THE LUNG AND MEDIASTINUM
BIOPSY OF THE PANCREAS, EXTRAHEPATIC
BILIARY SYSTEM, AND GALLBLADDER
BIOPSY OF THE LIVER
ADRENAL GLAND
CONCLUSION

Abstract

Cytology plays an integral role with endoscopic ultrasound (EUS) and allows for definitive diagnosis and staging of tumors examined by the technique. This chapter discusses some basic principles of cytology as well as nomenclature. It then discusses, in more depth, the cytologic features of disease processes seen throughout the organs typically sampled by EUS-guided fine needle aspiration.

From: *Clinical Gastroenterology: Endoscopic Ultrasound*,
Edited by: V. M. Shami and M. Kahaleh, DOI 10.1007/978-1-60327-480-7_5,
© Springer Science+Business Media, LLC 2010

Key Words: Adrenal gland, Cytology, Endoscopic ultrasound, Fine needle aspiration, Gut, Liver, Lung, Lymph node, Pancreas, Technique, Terminology

INTRODUCTION

With the naissance of endoscopic ultrasonography, deep-seated masses or lesions have become easily sampled by fine needle aspiration (FNA). Endoscopic ultrasound (EUS) allows for the sonographic imaging of the luminal gut and adjacent structures and coupled with FNA greatly increases the diagnostic yield and even changes therapeutic decisions in approximately 25% of patients with malignancy (1). Overall, the sensitivity of this technique is reported to be between 80 and 90% while the specificity is between 85 and 100% (2).

This chapter discusses EUS-guided FNA (EUS-FNA) from the perspective of the pathologist. It will outline some basic principles of cytology, including terminology and then discuss the cytologic features of the entities encountered with a busy EUS-FNA service. Some organs will be discussed in more detail (e.g., the pancreas) while others will be discussed in a more cursory fashion (e.g., the liver) reflecting the relative frequencies of these organs being sampled.

PRINCIPLES OF CYTOLOGY

Key to the success of EUS-FNA is communication between the gastroenterologists and pathologists. This is particularly facilitated by on-site interpretation which significantly increases the diagnostic yield of EUS-FNA (3). With this interpretation, the diagnostic yield of EUS-FNA increases and sensitivities of greater than 90% can be obtained. This can obviate the need for additional procedures and even result in an overall cost savings (4). Additional material, time, and other resources are available for pathologists at final sign-out that sometimes lead to changes in diagnoses, although this occurs in less than 6% of cases (5, 6). In situations when on-site interpretation is unavailable, the use of such technologies as telepathy may be utilized (7).

Preparations

Optimally prepared slides and cell block are key elements in arriving at the right diagnosis. Prior to the procurement of the sample, proper labeling of slides and specimen containers should be performed.

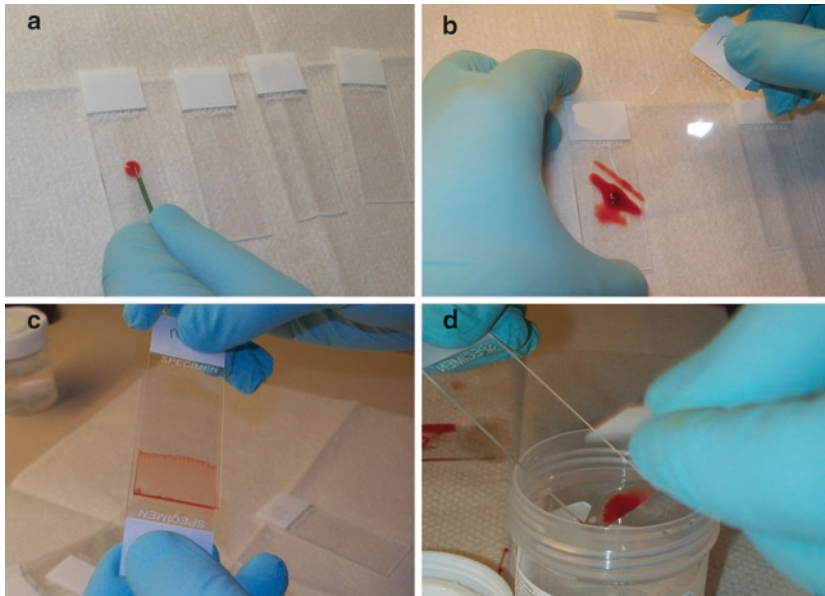


Fig. 1. Smear and cell block preparation during EUS-FNA. (a) Material is placed on a single glass slide from the EUS-FNA needle, (b) a second slide is used to portion out sample and transfer to a third slide for spreading (this can be repeated as needed to create as many slides as needed), (c) the material on the second slide is spread evenly for rapid drying and/or fixation, (d) at the end of the procedure, the clotted material can be scraped into a formalin container for cell block preparation.

In general, it is best if a pathologist or cytotechnologist smears the slides to be used for diagnostic interpretation. The aspirated material should be deposited on the slides by the endosonography team. Depending on the amount of material present, direct smears can then immediately be made or another slide can be used to remove a portion of the deposited material to be smeared onto a separate slide (Fig. 1). This technique allows for additional material to be used for cell block preparation (see below) and usually results in more concentrated material.

Both air-dried smears (stained via a rapid Romanovsky technique) and ethanol-fixed smears (stained via the Papanicolaou method) can be made. Air-dried smears tend to be preferred for on-site interpretation, whereas ethanol-fixed smears, while supplying added cytomorphic detail, tend to be more commonly used at final sign-out.

Uncommonly, pathologists will prefer to use a thin-layer cytologic technique (e.g., ThinPrep) for the interpretation of these specimens. This has the added benefits of obviating the need for immediate smear preparation and creates concentrated preparations (8). Most pathologists, however, prefer not to interpret FNA material prepared as such. The exception is with cyst fluid aspirates, as the specimen can be concentrated and significantly reduces the numbers of slides that must be examined.

As mentioned above, immediate interpretation allows for the proper triaging of aspirated material. Upon review, additional material can be collected for culture (e.g., when necrotizing granulomatous inflammation is seen), for flow cytometry (e.g., when lymphoma is suspected), for cell block (e.g., when histochemical or immunohistochemical stains will be needed), and even for additional unstained smears (when special stains or immunocytochemistry will be attempted). Additionally, material can be gathered for cytogenetic analysis, molecular analysis, and other studies, depending on the clinical situation and on-site interpretation.

TERMINOLOGY

Most FNA cases are signed out with a definitive diagnosis. As such an aspirate may be simply diagnosed as a particular entity (e.g., adenocarcinoma) or it first may be qualified within a tiered system (e.g., positive for malignancy), and then generally followed by a specific diagnosis. Such reports are usually straightforward.

Confusion arises with the use of qualified terminology since it is not always used consistently. Nonetheless, it is convention that the term “atypical” is used when the cytologic features seen in a particular aspirate are qualitatively insufficient for a specific diagnosis (9). The term “suspicious” is then used when the pathologist feels the specimen to be quantitatively insufficient (e.g., there may be only one or two groups of malignant appearing cells seen with an FNA of the pancreas). The terms correlate with calculated diagnostic functions based on pretest probability. For example, an FNA of the pancreas interpreted as “suspicious for adenocarcinoma” in a patient with a mass that is radiographically consistent with malignancy has a positive predictive value of malignancy of nearly 100% (10, 11).

Pathology reports often contain “notes” referred to within the diagnosis. It is important that these “notes” are considered by clinicians when interpreting the pathology report as they are typically used to convey important information regarding the actual diagnosis.

BIOPSY OF LUMINAL GUT

Epithelial Malignancy

Epithelial malignancies of the luminal gut are infrequently sampled by EUS-FNA as they can generally be sampled by forceps biopsy through endoscopy. Occasional epithelial malignancies may have the bulk of the tumor located beneath the mucosa and traditional endoscopic biopsies may fail to yield diagnostic material. This is especially true with diffuse-type gastric adenocarcinomas (i.e., signet ring adenocarcinomas) and carcinoid tumors throughout the GI tract (12, 13).

ADENOCARCINOMA

Adenocarcinomas are epithelial malignancies that form glands. They comprise the majority of distal esophageal, gastric, and small and large intestinal malignancies. Although there are some specific cytologic features that are associated with specific sites, most of the cytologic features are nonspecific. For this reason, when a site of origin is not known, immunohistochemistry can be helpful for localization of the primary malignancy (14). Colorectal adenocarcinomas usually express CK20 and only rarely express CK7 (15). Esophageal, gastric, and small intestinal adenocarcinomas all usually express CK7 and all can express CK20. CDX2 is a homeobox gene that guides intestinal development. While it is most often expressed with colorectal adenocarcinomas, it is also expressed in most esophageal, gastric, and small intestinal adenocarcinomas (16). Furthermore, it is also expressed in a subset of pancreaticobiliary adenocarcinomas.

Cytologic preparations of adenocarcinomas typically show sheets and three-dimensional clusters of cohesive cells (Fig. 2). Architectural regularity is usually lost to some degree. This results in irregular nuclear spacing and overlap, what pathologists sometimes refer to as “loss of honeycomb pattern.” Cells tend to be less mature and thus have higher nuclear to cytoplasmic (N/C) ratios. Evidence of glandular differentiation is typically retained and cytoplasmic vacuolization or lumen formation can usually be identified, at least focally. Nuclei are atypical, enlarged with irregular nuclear contours (membranes). Chromatin pattern can vary, but some coarse granularity is typically seen with prominent nucleoli. Mitotic figures can also be identified. Other less specific features of malignancy include increased overall cellularity, the presence of background necrotic debris, the presence of individual cell necrosis (apoptotic bodies) and the loss of cellular cohesion (i.e., increased numbers of single cells).

Colorectal adenocarcinomas tend to have cells and nuclei which are more elongated and columnar (Fig. 3). These features allow

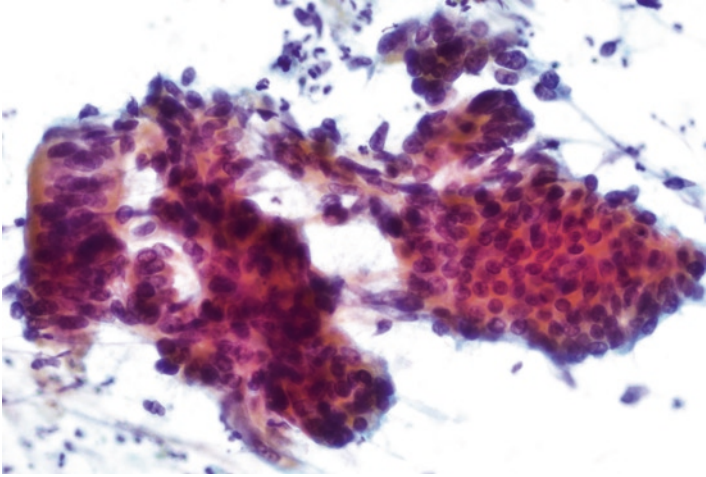


Fig. 2. Aspirates of adenocarcinoma typically have sheets and three-dimensional clusters of epithelial cells which show nuclear enlargement, hyperchromasia, and loss of the normal honeycomb architecture (Pap).

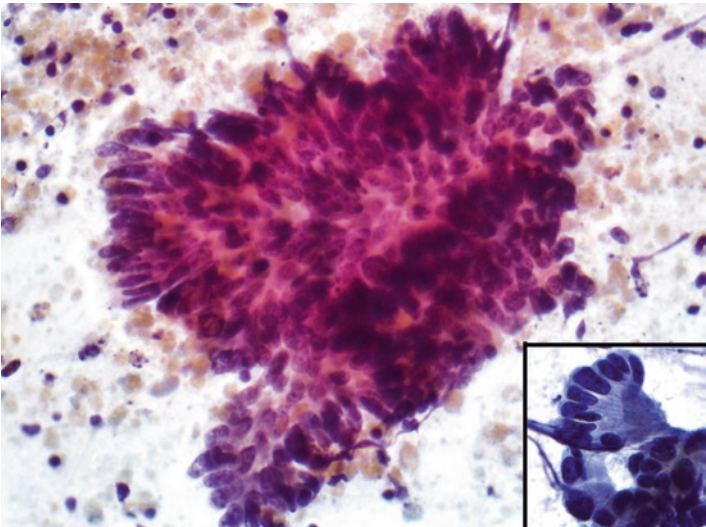


Fig. 3. Aspirates of colonic adenocarcinomas have clusters and strips of columnar cells with hyperchromatic, elongated oval nuclei which are basally located, which impart a "picket-fence" like appearance. The background is notable for "dirty" necrosis. The lower right inset highlights the nuclear atypia frequently seen (Pap).

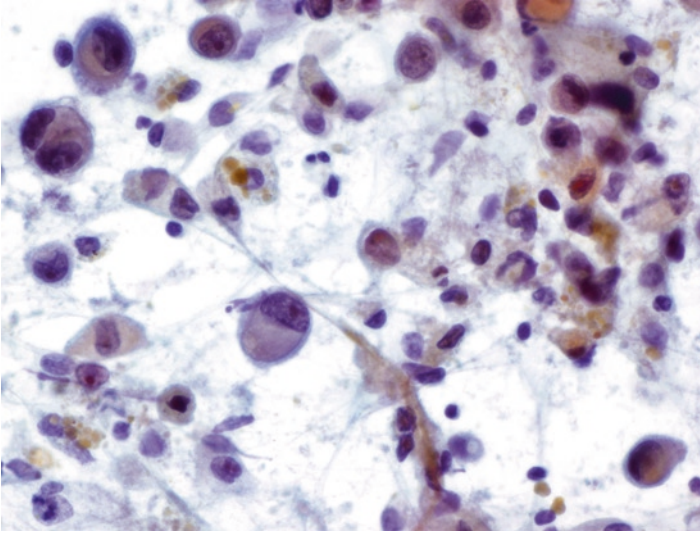


Fig. 4. Aspirates of some poorly differentiated adenocarcinomas can be highly discohesive and have many single cells; when mucin producing, intracytoplasmic mucin droplets can indent the nucleus forming a “signet-ring” appearance (Pap).

pathologists to suggest a primary site for an adenocarcinoma of unknown origin but do not allow for a definitive distinction (17).

Some adenocarcinomas are poorly differentiated or undifferentiated and are composed mostly of single cells (Fig. 4). When the single cells have a large, single intracytoplasmic mucous droplet, a diagnosis of “signet ring carcinoma” can be used. While signet ring carcinomas occur most commonly in the stomach, they can occur anywhere throughout the GI tract, and even outside of the tract. Other cases of adenocarcinoma may appear entirely undifferentiated (e.g., some adenocarcinomas of the stomach driven by Epstein–Barr virus infection) (18). Aspirates will be composed mostly of single cells with the malignant cytologic and nuclear features described above. Immunohistochemistry can be needed with such cases to establish a diagnosis of carcinoma (e.g., immunoreactivity with antibody to keratins) (14).

SQUAMOUS CELL CARCINOMA

The vast majority of squamous cell carcinomas of the luminal gut occur in areas lined by squamous epithelium (i.e., the esophagus and the anus), although they can actually occur anywhere throughout the gut.

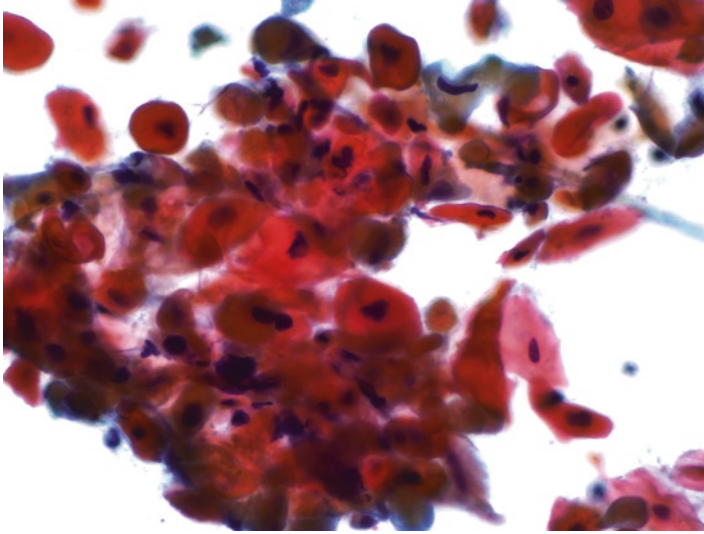


Fig. 5. Aspirates of well-differentiated squamous cell carcinoma have polygonal squamous cells with central enlarged, hyperchromatic nuclei which show irregular nuclear contours. The keratinized cytoplasm will stain distinctively orange on Papanicolaou stain (Pap).

Aspirates of squamous cell carcinomas are similar to those from adenocarcinomas inasmuch as they typically contain sheets of cohesive and atypical cells. The cells usually appear more polygonal in shape, however, and have denser cytoplasm. With the Papanicolaou stain, intracellular and extracellular keratinization is seen with bright orangophilic debris and occasional orangophilic malignant cells (Fig. 5). As with adenocarcinomas, nuclear irregularities, prominent nucleoli, mitotic figures, individual cell necrosis, cellular discohesion, and background necrosis can all be seen. Immunohistochemistry usually cannot be used to determine a tumor's site of origin. It may, however, be helpful for distinguishing poorly differentiated squamous cell carcinomas from other tumors as most squamous cell carcinomas are immunoreactive with antibodies to pankeratin cocktails, CK 5/6, and p63 (14).

SPINDLE CELL (SARCOMATOID) CARCINOMA

Some carcinomas are composed predominately of spindle cells and thus resemble mesenchymal neoplasia. These lesions can occur throughout the GI tract but most commonly involve the esophagus as

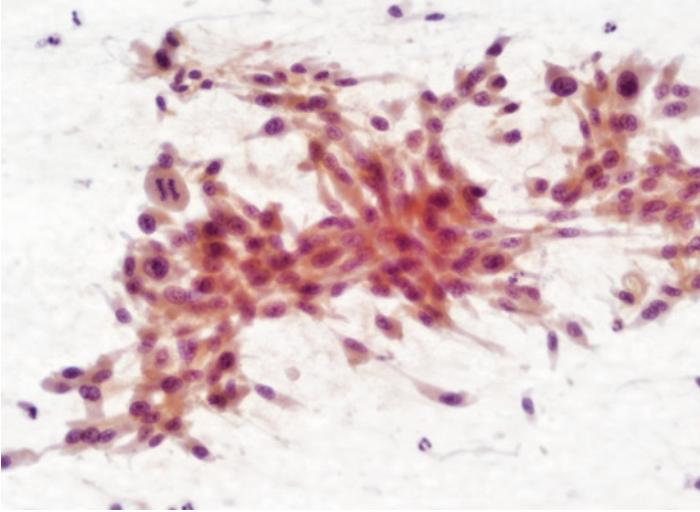


Fig. 6. Aspirates of spindle cell carcinoma show cells with elongated, spindle cytoplasm and oval enlarged hyperchromatic nuclei with variable atypia; in this case, a mitotic figure is apparent in the upper left quadrant (Pap).

polypoid masses (19). Smears are comprised of spindled or stellate cells with a moderate to marked amount of cytologic and nuclear atypia (Fig. 6). That said, spindle cell carcinomas have been noted histologically to show a range in the amount of cytologic atypia present and, furthermore, can be associated with heterologous elements such as cartilage and bone (although this is rare in the esophagus). An epithelial component, usually squamous, may also be seen with the aspirate. Immunohistochemistry can be especially helpful for distinguishing these tumors from true mesenchymal malignancies (i.e., sarcomas) as the spindled cells frequently, but not always, express epithelial antigens, such as cytokeratins (14).

CARCINOID TUMORS AND OTHER WELL-DIFFERENTIATED NEUROENDOCRINE CARCINOMAS

Carcinoid tumors and other specific neuroendocrine tumors (e.g., gastrinomas) are neuroendocrine carcinomas that occur throughout the GI tract (20, 21). Their prognosis is dependent on the site they occur, the specific clinical situation (e.g., a gastric carcinoid tumor arising in a patient with autoimmune gastritis will almost never metastasize), and a number of gross, histological, and immunohistochemical features. In general, tumor size, stage and proliferative activity (mitotic activity or

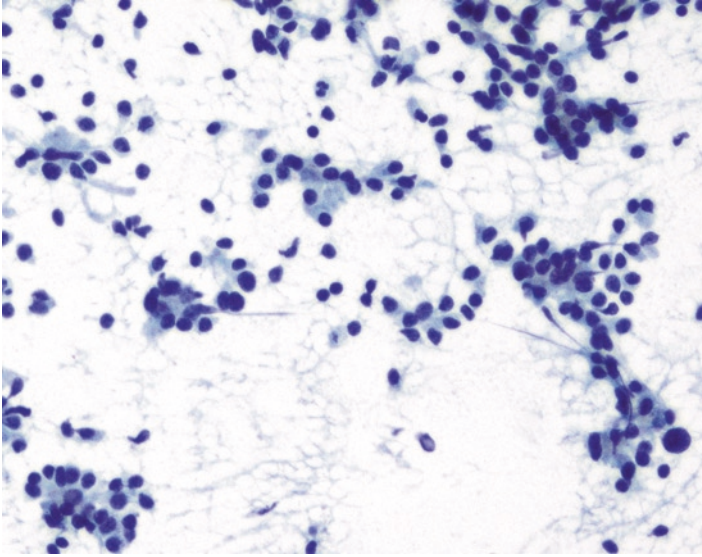


Fig. 7. Aspirates of carcinoid tumors of the GI tract are typically cellular, with discohesive cells forming vague rosettes, and have eccentrically placed nuclei with finely stippled chromatin (Pap).

ki-67 immunolabeling), are the most frequently used pathologic parameters to predict risk.

Aspirates of carcinoid tumors are usually cellular with numerous loose clusters of tumor cells admixed with single cells (Fig. 7) (17). Stripped nuclei are also frequently seen in the background. The tumor cells are usually epithelioid and somewhat monotonous in appearance with a moderate amount of delicate cytoplasm that may have small granules or vacuoles. Nuclei are typically round to oval and eccentrically placed with regular contours and finely stippled chromatin. Necrosis and mitotic figures are uncommonly seen. Although most tumors are composed of epithelioid cells with delicate cytoplasm, some tumors may have spindled, oncocytic, or clear cells.

While smears of carcinoid tumors or other well-differentiated endocrine carcinomas have relatively consistent features, there is frequently some cytologic overlap with other tumors such as well-differentiated adenocarcinomas, epithelioid mesenchymal neoplasms, melanoma, and even some hematolymphoid tumors. Cell block immunohistochemistry can be helpful as carcinoid tumors will be immunoreactive with antibodies to cytokeratins and specific neuroendocrine antigens such as

synaptophysin and chromogranin (20, 21). Specific peptide hormones can also be identified in appropriate cases (e.g., gastrin in gastrinomas). Markers used to predict behavior such as ki-67 should likely be restricted to surgical material.

Mesenchymal Neoplasia

Mesenchymal neoplasms of the luminal gut are uncommon, but are likely the most frequent type of neoplasia sampled of the luminal gut by EUS-FNA. This is because epithelial tumors are so seldom diagnosed by EUS-FNA and because mesenchymal tumors are almost always subepithelial and thus not amenable to sampling by other methods. Although gastrointestinal stromal tumors (GISTs) are the best known of these tumors, other mesenchymal neoplasms have been reported here.

GISTs show a phenotype similar to the interstitial cells of Cajal. The majority are composed of spindle-shaped cells and yield aspirates comprising cellular, small to medium-sized fragments of tumor (Fig. 8) (22–26). The cells have elongated and tapered nuclei. Perinuclear

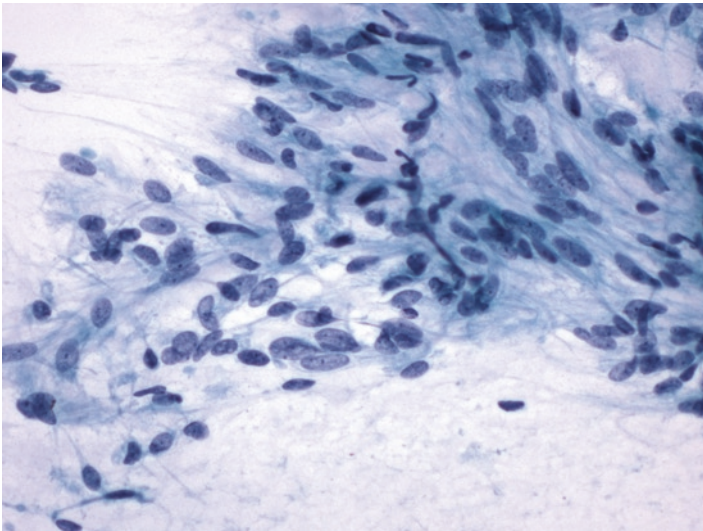


Fig. 8. Gastrointestinal stromal tumors are frequently spindled as seen in this image of an aspirated sample; the cytoplasm is wispy and cell borders are poorly demarcated, and the nuclei are oval with vesicular chromatin (Pap).

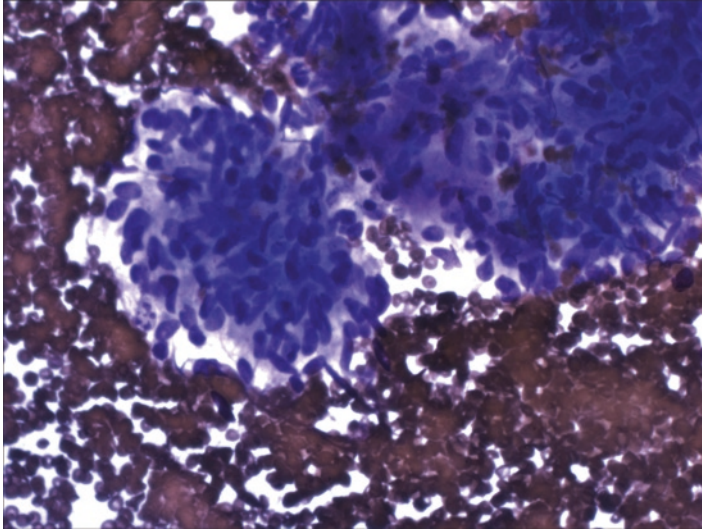


Fig. 9. Aspirates of epithelioid gastrointestinal stromal tumors may contain clusters and large groups of cells that appear akin to an epithelial neoplasm; the cells in this case have plump cytoplasm and round to oval nuclei (DiffQuick (DQ)).

vacuoles can be seen within a delicate cytoplasm. With air-dried, rapid-Romanovsky-stained material, the cytoplasm will sometimes appear metachromatic. Nuclei have delicate chromatin and prominent nucleoli are uncommon. Often, especially adjacent to the tissue fragments, stripped nuclei are present, occasionally with intact single cells. Mitotic figures and necrosis are uncommonly seen and may suggest a more aggressive tumor.

Some GISTs are composed of more round or oval cells and thus have an epithelioid morphology (Fig. 9) (25, 27). The cells have round to oval nuclei with delicate chromatin. As with spindle cell GISTs, necrosis and mitotic figures are uncommon.

A number of articles have been published using conventional cytologic features and/or other ancillary methods to determine the likely behavior of a particular GIST (22, 28, 29). Currently, GIST behavior is predicted with surgical specimens based on the site of the tumor, the size of the tumor, and the tumor's mitotic activity (30). It is thus not surprising that markers of proliferative activity have sometimes been found in some studies to predict behavior.

One reason it is important to distinguish GISTs from other mesenchymal tumors is that they respond to tyrosine kinase inhibition.

There are a number of different mutations that can be found in GISTs and some predict better response (e.g., exon 11 mutations), whereas others predict less response. Material gathered by EUS-FNA can be used for mutational analysis, if desired, to determine if a particular patient should be treated (31).

True smooth muscle tumors (i.e., leiomyomas and leiomyosarcomas) can also be found throughout the GI tract (32, 33). They comprise the majority of mesenchymal tumors of the esophagus. Leiomyomas make up the majority of these tumors. Aspirations of these are similar to those of spindle cell GISTs and are characterized by moderately cellular tissue fragments of spindle cells (Fig. 10) (25). The fragments tend to be a little larger and less cellular than those seen with GISTs and stripped nuclei are less frequently seen. That said, these features cannot be used by themselves to distinguish these tumors and immunohistochemistry is required (see below). Cytologic atypia, necrosis, and mitotic activity are not seen with leiomyomas.

True leiomyosarcomas of the GI tract are very uncommon and the cytologic features have only seldom been reported (33, 34). Aspirates again are composed of cellular fragments of spindled cells; however,

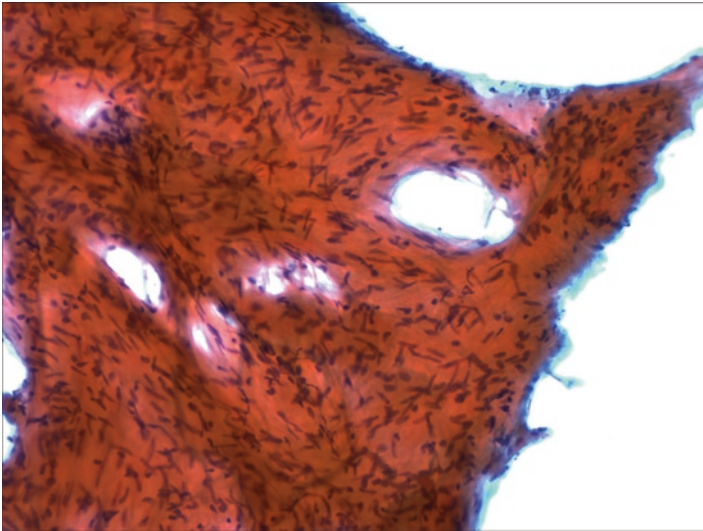


Fig. 10. Leiomyomas tend to smear as cohesive tissue fragments that are less cellular than other spindle cell tumors and contain bland elongated spindle cells (Pap).

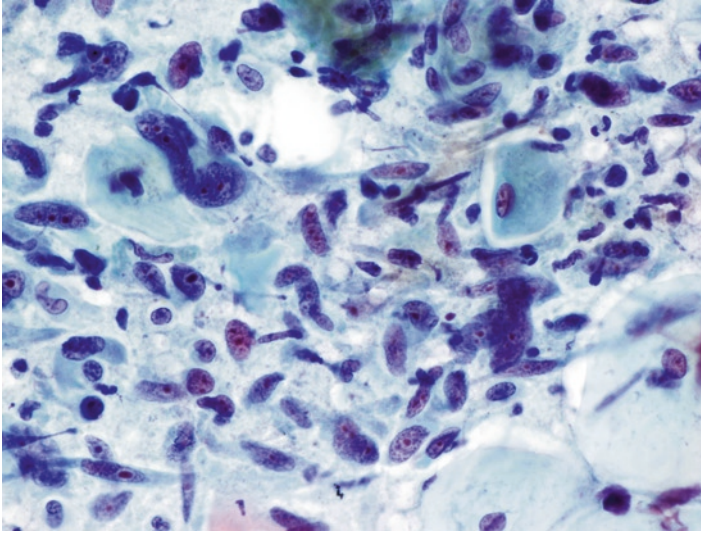


Fig. 11. Aspirates of leiomyosarcomas show cells with frank cytologic malignancy with enlarged, hyperchromatic nuclei with prominent nucleoli, multi-nucleation and bizarre forms (Pap).

obvious cytologic features of malignancy are present (Fig. 11). These include marked cytologic and nuclear atypia, necrosis, cellular discohesion, and numerous mitotic figures.

Peripheral nerve sheath and neural tumors also occur throughout the GI tract and the cytologic features of these tumors have been reported (35, 36). These tumors include schwannomas, mucosal neuromas, malignant peripheral nerve sheath tumors, granular cell tumors, ganglioneuromas, and gangliocytic paragangliomas among other tumors. Aspirates of schwannomas are cytologically indistinguishable from those of GISTs and cells may be either spindled or epithelioid (Fig. 12). Immunohistochemistry is again needed to distinguish these lesions.

A myriad of other mesenchymal tumors can involve the GI tract and could be aspirated by EUS-FNA (2). These include but are not limited to fatty tumors (e.g., lipomas), inflammatory fibroid polyps, inflammatory myofibroblastic tumors, aggressive fibromatoses, solitary fibrous tumors, glomus tumors, synovial sarcomas, clear cell sarcomas, perivascular epithelioid cell tumors (PEComas) and even pediatric small blue cell tumors such as primitive neuroectodermal tumors (PNETs). Immunohistochemistry plays an important role in distinguishing these tumors, as does other ancillary testing, such as FISH, RT-PCR, or

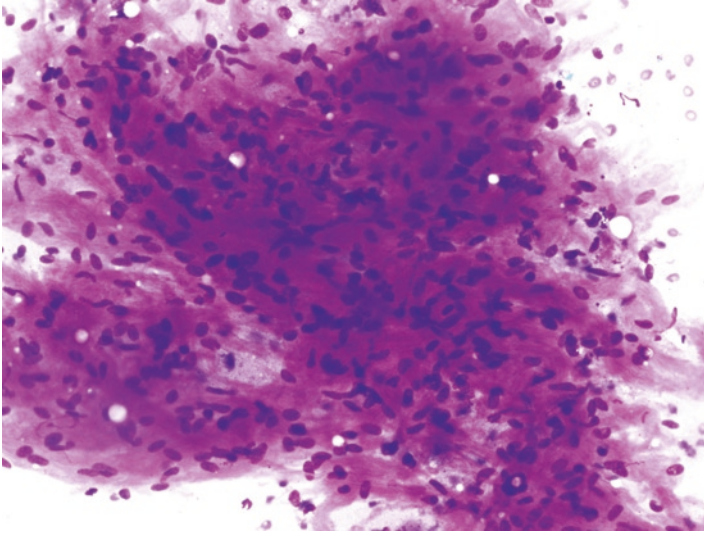


Fig. 12. Aspirates of schwannomas contain clusters of spindle cells with thin, elongated nuclei and indistinct cell borders; a background myxoid matrix (magenta on DiffQuick (DQ) stain) is seen interspersed with the spindle cells.

conventional cytogenetics (e.g., diagnosing clear cell sarcoma, synovial sarcoma or pediatric small blue cell tumors).

As mentioned above, immunohistochemistry is essential for distinguishing the mesenchymal tumors from one another (Table 1) (36). Although results can be somewhat overlapping, given the overall incidence of the various tumors, even a limited panel can have a very high predictive value (Fig. 13).

Lymphoma

Most common types of lymphomas can be adequately classified using cytology and other ancillary techniques, such as flow cytometry and molecular diagnostics or cytogenetics (37, 38). The predictive value of a “negative” result will depend on the overall clinical impression, as it is well known that even with the use of ancillary techniques, some lymphomas, e.g., classical Hodgkin lymphomas, can be difficult to identify.

Most gastric lymphomas are extranodal marginal zone lymphomas (MALT lymphomas) or diffuse large B-cell lymphomas (39). Often these can be diagnosed using forceps biopsy; however, EUS-FNA is

Table 1
Immunohistochemistry of select gastrointestinal/abdominal mesenchymal or pseudomesenchymal lesions

<i>Lesion</i>	<i>CD117</i>	<i>CD34</i>	<i>S100</i>	<i>Actin</i>	<i>Desmin</i>	<i>BCAT^a</i>	<i>HMB45^b</i>	<i>CK^c</i>
Gastrointestinal stromal tumor	+	+	-	-/+	-	-	-	-
Leiomyoma/leiomyosarcoma	-	-	-	+	+	-	-	-
Schwannoma/neural lesion ^d	-	-/+	+	-	-	-	-	-
Glomus tumor	-	-	-	+	-	-	-	-
Inflammatory fibroid polyp	-	+	-	-/+	-	-	-	-
Inflammatory myofibroblastic tumor	-	-	-	+	-	-	-	-
Fibromatosis	+/-	-	-	-/+	-	+	-	-
Melanoma	+/-	-	+	-	-	-	+	-
Sarcomatoid carcinoma ^e	-	-	-	-	-	-	-	+

BCAT beta-catenin, CK (pan) keratin, + positive, +/- often positive, -/+ occasionally positive, - negative

^aNuclear localization

^bOr other more specific melanocytic markers

^cKeratins can occasionally be expressed in diverse mesenchymal lesions. This will depend on a particular laboratory's make-up of their pankeratin (cocktail)

^dGranular cell tumors, neurofibromas, and ganglioneuromas

^eSarcomatoid carcinomas can react with antibodies to a number of mesenchymal antigens depending on their differentiations. This is especially true for actins

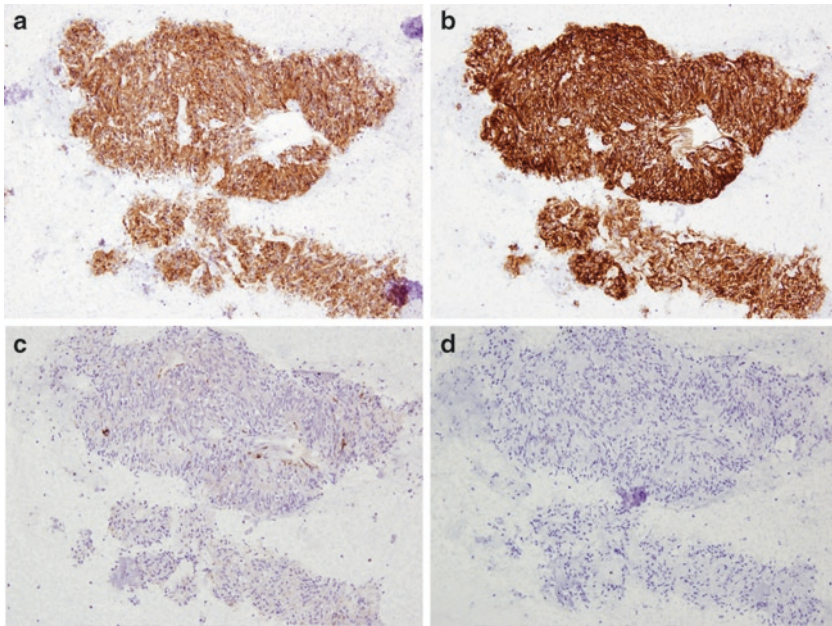


Fig. 13. Immunohistochemistry on cell blocks is helpful in distinguishing spindle cell neoplasms; in this case, the tumor is immunoreactive with antibodies to CD117 (a) and CD34 (b), and not with antibodies to SMA (c) and S100 (d), confirming the diagnosis of gastrointestinal stromal tumor.

sometimes employed when this method fails (2, 40). When EUS-FNA is used, material should be gathered at the time of FNA for flow cytometry (to assess for a monotypic population and for the specific coexpression of diagnostic antigens) and for molecular or cytogenetic analysis (to assess for translocations that are associated with specific types of lymphoma, e.g., the t(11; 14)(q13; q32), seen with mantle cell lymphoma). Additional material for cell block immunohistochemistry can also be helpful.

Aspirates of mature B-cell lymphomas (e.g., extranodal marginal zone lymphoma, follicular lymphoma, and mantle cell lymphoma) tend to have a more monomorphic population of small, mature appearing lymphocytes than reactive, non-neoplastic conditions (Fig. 14) (41, 42); however, admixed non-neoplastic lymphocytes (often T cells) can make this assessment very difficult. Thus, immunophenotyping (generally by flow cytometry) is essential in such cases (43). The identification of a disproportionately overexpressed light chain by flow cytometry usually signifies the diagnosis of a B-cell lymphoma.

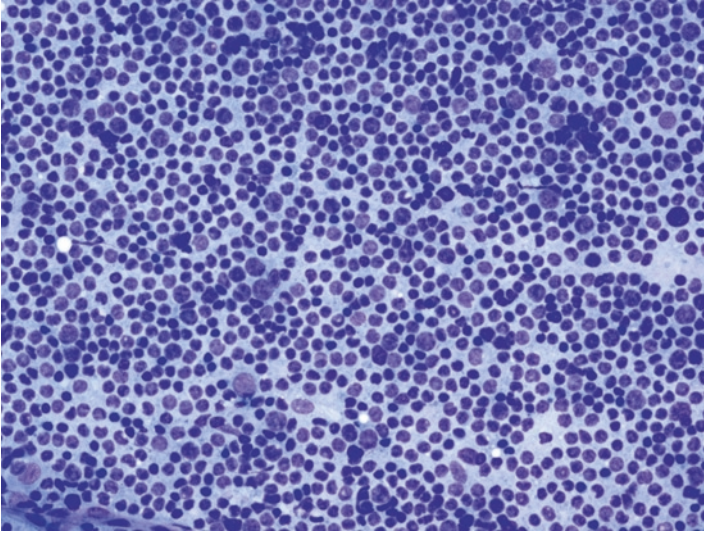


Fig. 14. An aspirate of a follicular lymphoma is characterized by a monotonous population of small to intermediate-sized lymphocytes; note the absence of tangible body macrophages and larger immunoblasts (DiffQuick (DQ)).

Clonality can also be demonstrated using molecular testing, usually through the identification of a single-sized, light chain rearrangement (41). Specific antigen expression can then help subclassify the lymphomas (e.g., mantle cell lymphomas usually express CD5 and do not typically express CD23). An extensive description of this is beyond the scope of this chapter.

Higher grade lymphomas typically yield cells with more cytologic atypia and can usually be recognized as malignant by cytologists (Fig. 15) (41). Mitotic figures, necrosis and apoptotic bodies are usually easy to find. Here, the differential diagnosis usually includes other poorly differentiated malignancies that characteristically have smears composed of malignant single cells (e.g., melanoma). Cell block immunohistochemistry may be all that is needed here as diffuse, large B-cell lymphomas are typically immunoreactive with antibodies to CD45 (leukocyte common antigen) and CD20.

Melanoma

Melanomas of the GI tract are most often found in the anus or rectum; however, they have been reported throughout the tract (44). The tumors

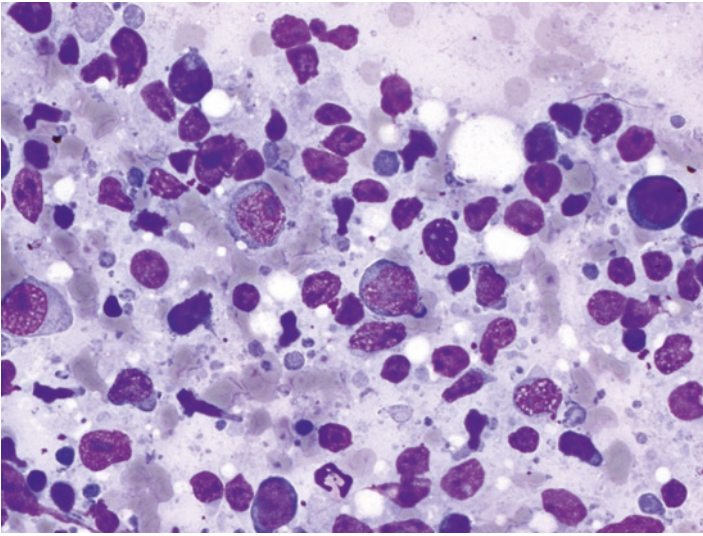


Fig. 15. Aspirates of diffuse large B-cell lymphoma typically have single large atypical cells with scant cytoplasm that have one or more prominent nucleoli and irregular nuclear contours; the discohesive nature of the cells and small fragments of blue cytoplasm in the background (so-called lymphoglandular bodies) help to favor a lymphoproliferative process (DiffQuick (DQ)).

can be composed of epithelioid, spindled and undifferentiated cells (45). Aspirates are typically cellular and composed of numerous single cells, often with some cohesive tissue fragments (Fig. 16), the features recapitulate the histology and malignant cells are typically undifferentiated, epithelioid and/or spindled. The amount of cytoplasm can vary greatly from case to case and many cases, fortunately, will have cytoplasmic pigment, best seen with Papanicolaou-stained material. Nuclei are typically enlarged with irregular contours and prominent nucleoli. Occasional cells will have two nuclei, which, with the prominent nucleoli, render a “bug-eyed” appearance to the cells.

Immunohistochemistry can be used both to diagnose and exclude melanoma. Tumor cells are typically immunoreactive with antibodies to S100 protein and with one or more specific melanoma antigens such as HMB45 or Melan-A (46). Here, a number of caveats should be noted. Melanomas are often immunoreactive with antibody to CD117 and thus a panel of antibodies should be used to exclude GISTs (44). Other tumors, such as clear cell sarcomas, PEComas, and even adrenal cortical

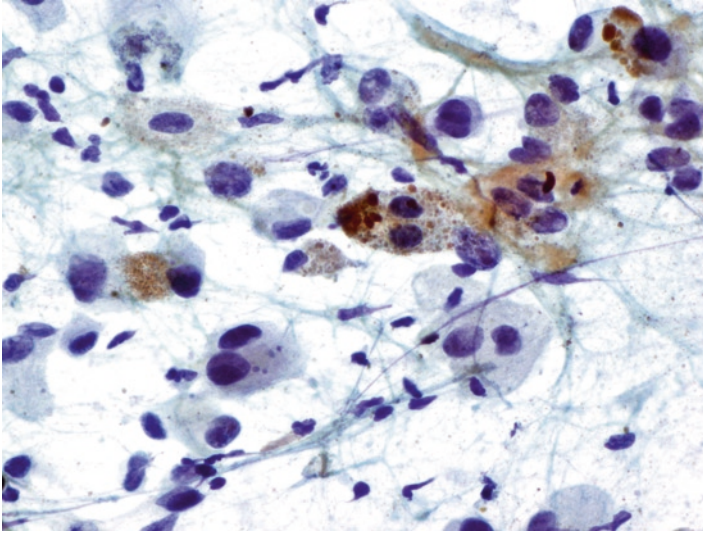


Fig. 16. Malignant melanoma is often called the great mimicker. In this case, cells range from spindled to epithelioid and many cells have binucleation with prominent nucleoli; melanin pigment on Pap stains appears brown, while on DiffQuick (DQ) will appear blue-green (Pap).

neoplasms can express one or more melanocytic markers and need to be excluded with immunohistochemistry or other means.

Other Lesions

Gastrointestinal duplication cysts and bronchogenic cysts are sometimes sampled by EUS-FNA (47). The cytologic features are nonspecific. The background is usually clear or mucoid. Macrophages may be seen, as with any cyst contents. Duplication cysts can be lined by a variety of gastrointestinal epithelia or be lined by ciliated or squamous epithelium, thus the epithelial cells present on aspirate can vary.

Pancreatic heterotopia may present as a mass lesion throughout the upper gastrointestinal tract, most often in the periampullary region but frequently within the stomach (48). These lesions frequently lack acinar tissue, being then composed of only smooth muscle and benign pancreatobiliary-type glands. Aspirates are thus usually nonspecific and a prospective diagnosis based on cytology is usually not possible.

BIOPSY OF LYMPH NODES

The Staging of Malignancy

The biopsy of peri-GI lymph nodes by EUS-FNA is most commonly done to stage known epithelial malignancy (49–53). This includes the staging of esophageal, lung, pancreatic, and rectal malignancies. EUS-FNA can also be used to diagnose adenopathy of unknown origin when the nodes cannot be more easily sampled by other techniques. The specificity of EUS-FNA of lymph nodes for staging is nearly 100% (2, 49–53). Reported sensitivities vary, usually between 80 and 90%, with negative predictive values reported to be usually over 95%.

Metastatic epithelial malignancies have the same cytologic features as their primary tumors, albeit the malignant cells may be few in number and admixed with variable numbers of lymphocytes. One caveat should be noted, however. Treated adenocarcinomas, especially colorectal and esophageal, sometimes leave residual mucous lakes both at the site of the primary tumor and within the lymph nodes (49). Samples from these lakes will show thick mucus sometimes mixed with macrophages. Post-therapeutic specimens are staged based only on the presence of tumor cells and pathologists should note that while the mucus likely signifies past disease, it does not necessarily signify residual tumor.

Adenopathy of Other Etiology

Occasionally lymph nodes are sampled by EUS-FNA for the work-up of adenopathy of unknown cause (49, 52, 54–58). Causes may include metastatic malignancy (of unknown primary at the time of sampling), lymphoma, and reactive/infectious agents. An on-site pathologist is very helpful in these cases as material can be triaged properly based on the cytologic findings. Metastatic carcinoma, melanoma, germ cell malignancy, etc., can all be diagnosed using immunohistochemistry if ample material is present (Fig. 17).

Classification of lymphoproliferative disease is rather complicated and constantly evolving. Currently, there is limited information available regarding the utilization of EUS-FNA in the diagnosis of lymphoproliferative disorders (49, 58, 59). Studies of accuracy are difficult to interpret as pathologists are sometimes able to correctly classify disease as lymphoma, but cannot subclassify the disease. Overall, the sensitivity of EUS-FNA for the diagnosis of lymphoma is probably between 70 and 80%, with a proportion of cases being only partly classifiable (59).

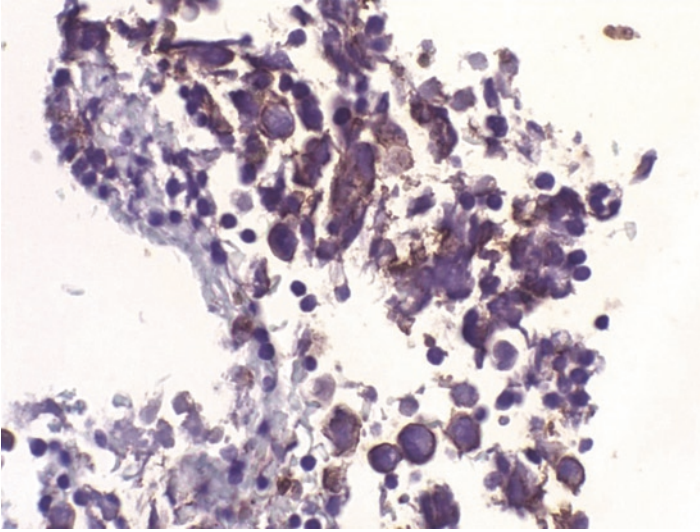


Fig. 17. Cell block preparation of metastatic seminoma to a retroperitoneal lymph node. Neoplastic cells are immunoreactive with antibody to PLAP.

Collecting material for ancillary testing is extremely important for the diagnosis and classification of lymphoma. Indeed, without the use of flow cytometry, the sensitivity of FNA for the diagnosis of lymphoma is much lower than 70–80% (43). A number of studies have shown that sufficient material can be gathered at the time of EUS-FNA to perform flow cytometry in most cases (49, 58, 59).

Both T-cell lymphomas and Hodgkin lymphomas are particularly difficult to diagnose by FNA (41, 42, 60). T-cell lymphomas may be difficult to diagnose by flow cytometry and may not appear cytologically atypical (although most cases do have some atypia). Molecular analysis for a clonal T-cell receptor is helpful in such cases although it will not allow for exact classification of the lymphoma. Hodgkin lymphomas may be difficult to diagnose because of a paucity of the hallmark Reed Sternberg (or Reed Sternberg variant) cells. Indeed, the majority of cells present in aspirates of such cases are usually non-neoplastic leukocytes. Traditional ancillary techniques used for the diagnosis of lymphoma (e.g., flow cytometry, molecular testing and cytogenetics) generally fail to identify the neoplastic cells.

EUS-FNA can also be helpful for diagnosing reactive/infectious causes of adenopathy (49, 52, 54, 55, 57). Causes of infectious lymphadenopathy, most frequently diagnosed by EUS-FNA, are most likely dependent on the patient population seen at a particular hospital. Granulomatous inflammation with clusters of epithelioid macrophages,

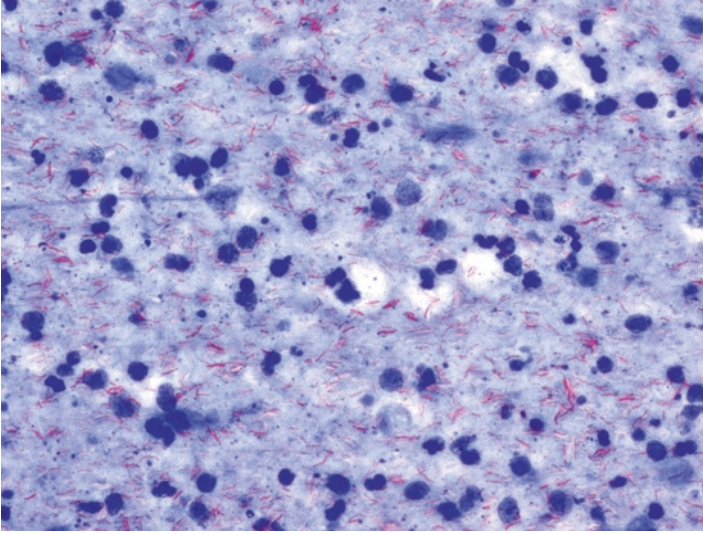


Fig. 18. Aspirate of a lymph node in a patient with atypical mycobacterial infection; A Fite stain highlights beaded rod-like organisms in red, confirming the presence of mycobacteria (Fite stain, alcohol fixed aspirate smear).

lymphocytes, and occasional multinucleated giant cells suggest either Mycobacterial or fungal infection, especially when necrotic debris is also present. Cultures can be obtained at the time of EUS-FNA (again, on-site pathology can be very helpful in determining the need for this). Direct smears can even be made for special histochemical stains that facilitate the identification of specific organisms (e.g., GMS stain to identify fungal elements or a Fite stain to identify mycobacteria) (Fig. 18).

Finally, sarcoidosis is a common cause of adenopathy of unknown cause, especially among African Americans (54). Smears will show tight clusters of epithelioid macrophages (granulomas) admixed with lymphocytes and occasional giant cells (Fig. 19). Necrosis is usually not seen. Sarcoidosis, however, is a diagnosis of exclusion and cytology plays only part of the role of diagnosis. Clinical and laboratory results (such as negative cultures) are also needed to establish a diagnosis.

BIOPSY OF THE LUNG AND MEDIASTINUM

Sampling of the mediastinum, lung and even pleural space is sometimes performed using EUS-FNA. Sampling of the lung is anatomically limited based on proximity to the esophagus (61). It is performed in the vast majority of cases for the diagnosis of epithelial malignancy.

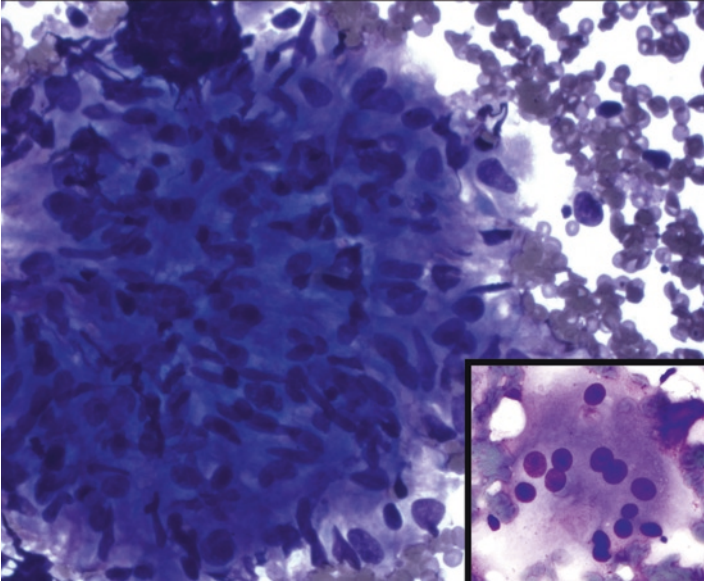


Fig. 19. Aspirates of granulomatous inflammation have aggregates of histiocytes with ill-defined cell borders and bean-shaped nuclei and often contain multinucleated giant cells (lower right insert) (DiffQuick (DQ)).

The term “nonsmall cell carcinoma” encompasses epithelial malignancies other than small cell carcinoma (and carcinoid tumors or other low-grade neuroendocrine carcinomas). It is often used with cytologic samples of the lung, as pathologists struggle to differentiate squamous cell carcinoma, adenocarcinoma, large cell undifferentiated carcinoma, large cell neuroendocrine carcinoma, etc. It usually provides sufficient information to institute proper therapy (surgery, radiation and/or chemotherapy).

The cytologic features of adenocarcinoma and squamous cell carcinoma typically do not differ from those discussed above. Some adenocarcinomas can be very well differentiated and when aspirated will have sheets of epithelial cells that show little cytologic heterogeneity (Fig. 20) (62). Importantly, the cells will not have cilia, like normal bronchial cells. They frequently also have intranuclear cytoplasmic inclusions. Although this is frequently touted as a feature of bronchioloalveolar carcinoma, we believe that specific diagnosis can only be made based on histology (63). Aspirates of large cell undifferentiated carcinomas tend to show more cytologic atypia and cellular discohesion than aspirates of adenocarcinomas or squamous cell carcinomas (64). Prominent nucleoli

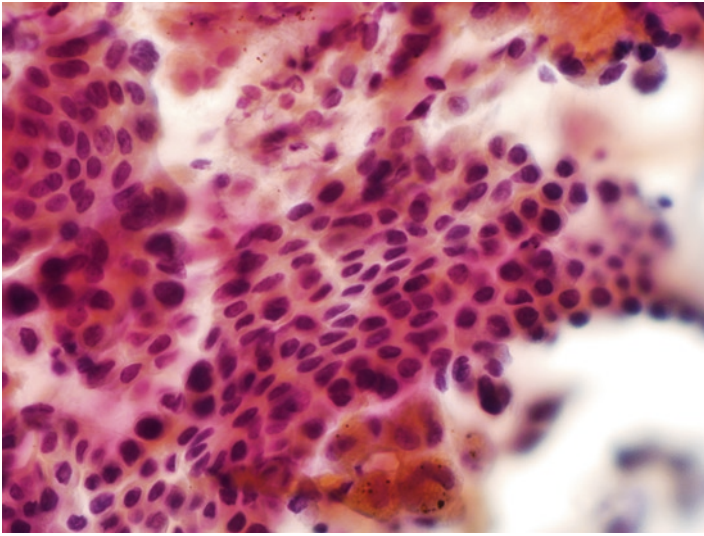


Fig. 20. This aspirate of a well-differentiated adenocarcinomas of the lung has sheets of atypical cells with a disorganized honeycomb appearance, nuclear enlargement and overlap, and nuclear hyperchromasia (Pap). Distinguishing these from normal pneumocytes and bronchial epithelium can be difficult and is helped by the high cellularity and absence of cilia.

are usually present. Multinucleated malignant cells may also be seen and background necrosis is typically present.

Immunohistochemistry can be used to identify the extremely poorly differentiated tumors as most will express keratins and other epithelial antigens. Adenocarcinomas of the lung also frequently express TTF1, a transcription factor important for lung development. This allows many lung adenocarcinomas to be distinguished from metastatic adenocarcinomas (aside from metastatic thyroid carcinomas which also express TTF1) (65).

Large cell neuroendocrine carcinomas should be distinguished from other nonsmall cell carcinomas when possible because of their poor prognosis and possible alternative treatment needs. Aspirates of these tumors typically are cellular with large, fragile mostly discohesive cells (Fig. 21) (66). The cells usually have little cytoplasm. Nuclei have relatively fine chromatin and nucleoli are often inconspicuous. Nuclear molding and crush artifact, as seen with aspirates from small cell carcinomas, usually seen as are mitotic figures and apoptotic bodies. Immunohistochemistry is helpful and neoplastic cells must be reactive with at least one neuroendocrine antigen, such as CD56, synaptophysin or chromogranin.

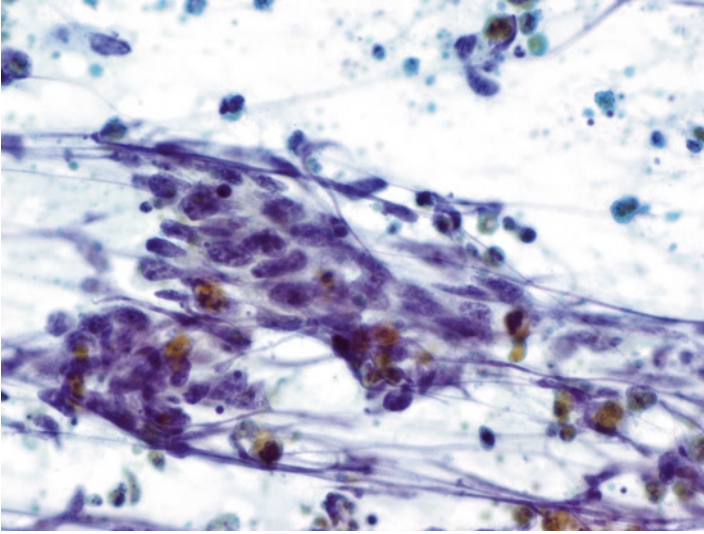


Fig. 21. Large cell neuroendocrine carcinoma of the lung. This aspirate has large cells with fragile cytoplasm that were easily fragmented upon smearing, resulting in nuclear crush artifact and DNA streaking; the large cell size and absence of molding helps to distinguish this from small cell neuroendocrine carcinoma (Pap).

Aspirates of small cell carcinomas have many of the same features as large cell neuroendocrine carcinomas (64). The cells are smaller, however, usually about three to four times the size of a lymphocyte and show less variation in size (Fig. 22). Discohesion, crush artifact, nuclear molding, mitotic figures, and apoptotic bodies are usually seen. Tumor cells often also react with antibodies to neuroendocrine antigens and tend to show prototypical “dot-like” staining with antibodies to cytokeratins. They frequently react with antibodies to TTF-1 and not with antibodies to p63, assisting in their distinction from poorly differentiated or basaloid squamous cell carcinomas (67).

Other primary lung neoplasms may also be sampled by EUS-FNA. Pulmonary carcinoid tumors share cytologic features with carcinoid tumors of the gut.

The mediastinum is primarily sampled to either stage malignancy (usually lung) or to investigate adenopathy of a different etiology (see above) (52). Occasionally, primary mediastinal neoplasia or other pathology is sampled. Here, the pathologist needs to know where in the

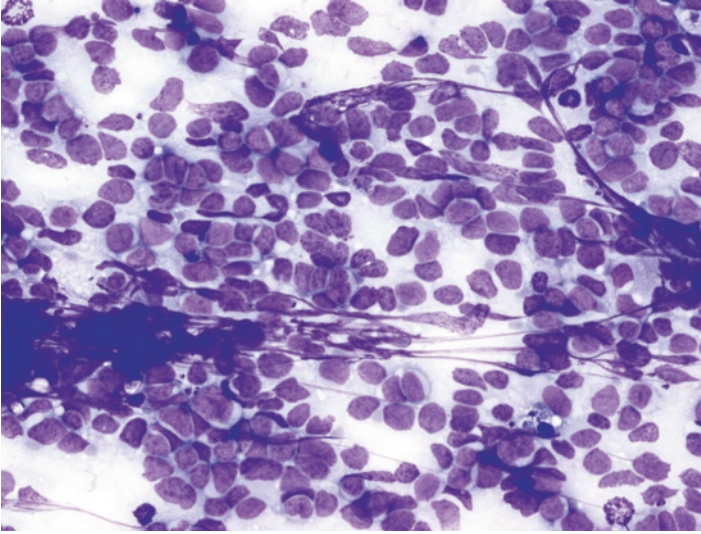


Fig. 22. An aspirate of a small cell neuroendocrine carcinoma, similar to Fig. 21, shows extensive nuclear crush and DNA streaking artifact, increased mitotic activity and fine chromatin; in addition, adjacent cells distort to form flush surfaces rather than overlapping, a process referred to as “molding” (DiffQuick (DQ)).

mediastinum (anterior, middle, or posterior) the lesion is and the radiographic and sonographic characteristics of the lesion.

Rarely, mesenchymal lesions may be sampled, especially of the posterior mediastinum. Schwannomas, ganglioneuromas, paragangliomas, etc., may be sampled (68). Cell block immunohistochemistry is usually needed to make specific diagnoses of these lesions.

BIOPSY OF THE PANCREAS, EXTRAHEPATIC BILIARY SYSTEM, AND GALLBLADDER

Pancreas

The pancreas is one of the most common sites sampled by EUS-FNA. Pathologists need to be well aware of the current WHO classification of tumors of the exocrine and endocrine pancreas and the clinical and radiographic changes associated with different lesions (9). An algorithmic approach to these samples can be helpful with which one begins by knowing whether the lesion is predominately solid or cystic (Fig. 23);

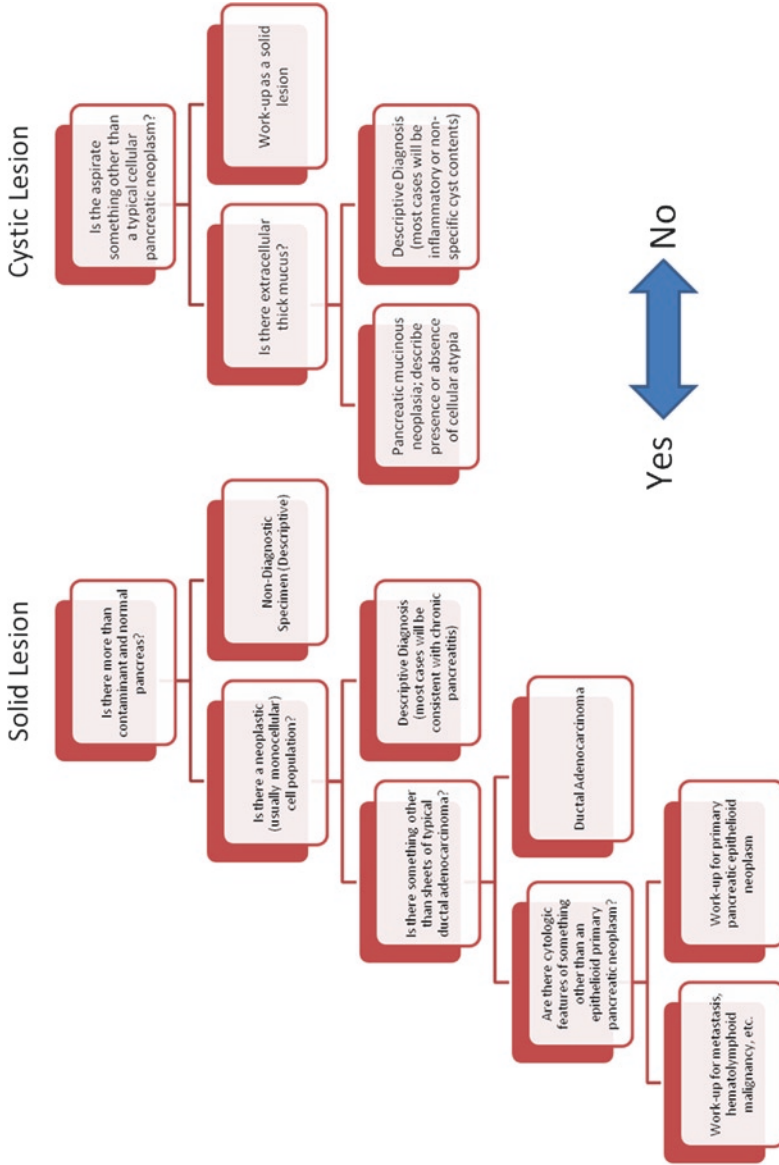


Fig. 23. Simple algorithm for the interpretation of pancreatic cytology specimens.

Table 2
Immunohistochemistry of solid primary pancreatic neoplasms

<i>Neoplasm</i>	<i>CK</i>	<i>CD56</i>	<i>SYN</i>	<i>CG</i>	<i>VIM</i>	<i>TRP</i>	<i>BCAT^a</i>
PEN	+	+	+	+	-/+	-	-
ACC	+	-/+ ^b	-/+ ^b	-/+ ^b	-/+	+	-/+ ^c
SPN	-/+ ^d	+	-/+ ^e	-	+	-/+	+
PB	+	+	-/+	-/+	-	+/-	+/-

PEN pancreatic endocrine neoplasm, ACC acinar cell carcinoma, SPN solid-pseudopapillary neoplasm, PB pancreatoblastoma, CK (pan)cytokeratin, SYN synaptophysin, CG chromogranin, VIM vimentin, TRP trypsin, BCAT beta-catenin, + positive, +/- often positive, -/+ occasionally positive, - negative

^aNuclear immunoreactivity

^bOccasional ACCs demonstrate scattered reactivity with antibodies to neuroendocrine markers

^cRare cases of BCAT nuclear immunoreactivity in ACC have been described

^dSPNs may show weak or focal keratin reactivity

^eSPNs also show occasional, weak reactivity with antibodies to specific neuroendocrine markers

with solid lesions one must first recognize whether lesional tissue is present. The pathologist must then recognize whether the lesional tissue appears neoplastic or not. Pancreatic ductal adenocarcinomas (PDAs), representing by far the most common type of pancreatic neoplasia, need to be recognized (69). Finally, other types of neoplasia need to be sorted out using cytologic and, often, immunohistochemical findings (Table 2).

PANCREATIC DUCTAL ADENOCARCINOMA

The most common pancreatic neoplasm sampled by EUS-guided FNA is the PDA. Unlike non-neoplastic ductal cells, atypical cells seen in PDA show more variability in nuclear size (anisonucleosis) with irregular nuclear membranes, granular chromatin and, often, prominent nucleoli (Fig. 24). As a result of these changes, sheets of cells lose the regular "honeycomb pattern" seen with benign cells and instead nuclei are placed irregularly throughout the sheets, frequently overlapping one another. Necrotic, mucinous and inflammatory debris as well as features of chronic pancreatitis are often seen in the background.

A number of variant patterns can also be present with PDAs that pathologist need to be aware of. Squamous differentiation can be present and even predominate (adenosquamous or squamous cell carcinoma) (70). Abundant mucus can be present such as with an aspirate of a

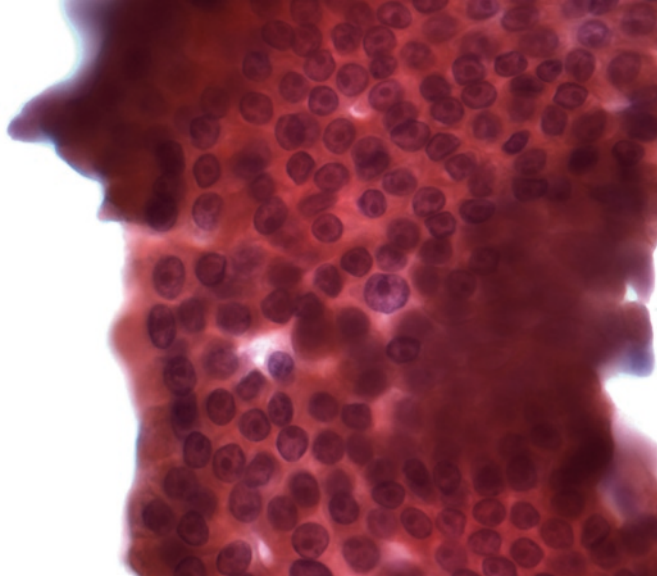


Fig. 24. This aspirate of a well-differentiated pancreatic ductal adenocarcinoma has sheets of cells, but the nuclei show marked variation in size (anisonucleocytosis) and prominent nucleoli (Pap).

colloid carcinoma (71). The cells may be very large with abundant foamy cytoplasm (foamy gland adenocarcinoma) (72). Single cells with large mucin droplets may be seen (signet ring carcinomas). Single markedly atypical cells, sometimes spindled, may predominate such as with anaplastic/undifferentiated carcinomas or undifferentiated carcinomas with osteoclast-like giant cells (Fig. 25) (73–76). Tumors presenting with mostly single cells may require further work-up, often with immunohistochemical staining with antibodies to keratins to prove the epithelial nature of the tumor.

A number of ancillary techniques have been proposed for the diagnosis of PDA in cytologically borderline cases. These include immunohistochemical and molecular testing. A number of proteins are expressed to different degrees in PDA when compared to normal ductal epithelium. These include glycoproteins such as MUC1 and other proteins whose increased expressions were identified through mRNA profiling of tumors, such as mesothelin and prostate stem cell antigen (77–80). Finally, using immunohistochemistry for tumor suppressor proteins known to be lost (or aberrantly expressed when mutated) with high

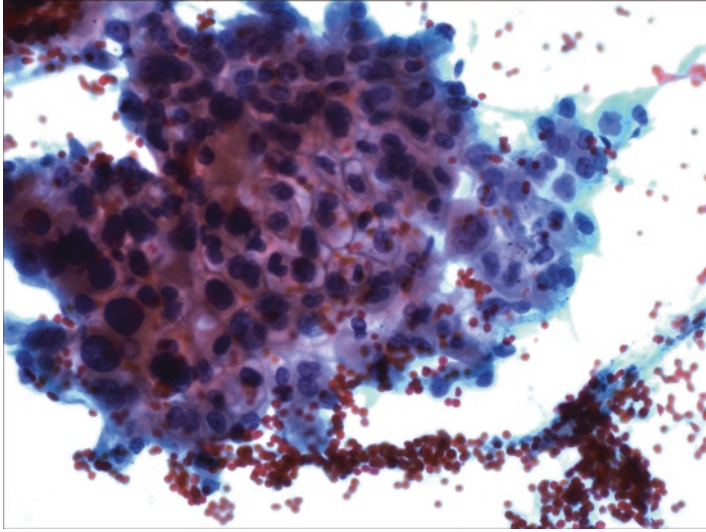


Fig. 25. Aspirates of poorly differentiated pancreatic ductal adenocarcinoma may have both sheets and single cells with marked anisonucleocytopia, hyperchromasia and prominent nucleoli, and loss of the honeycomb architecture (Pap).

frequencies in PDA, such as p16, SMAD4, and p53 has also been shown to be potentially useful (81).

Molecular testing used to assist in the diagnosis of PDA includes KRAS2 sequencing and LOH studies of tumor suppressor gene loci (81, 82). Some have demonstrated that fluorescent in situ hybridization and ploidy analysis with cytologic samples from the pancreas may be helpful for the diagnosis of PDA (83). In spite of the many publications regarding ancillary testing to assist in the diagnosis of PDA with aspirates, it is unclear how the testing is actually used in everyday practice.

OTHER PRIMARY PANCREATIC SOLID NEOPLASMS

Other solid neoplasms of the pancreas are much less common and include acinar cell carcinomas (ACCs), pancreatic endocrine neoplasms (PENs), solid pseudopapillary neoplasms (SPNs), pancreatoblastomas and metastases or lymphomas. While some clinical, radiographic, and cytologic features may suggest a particular diagnosis, cell block immunohistochemistry may be needed to definitively distinguish these lesions (Table 2) (9).

ACCs are very uncommon tumors that occur more often in older men and behave almost as poorly as PDAs (84). Aspirates are frequently very cellular and show a mixture of loosely cohesive cells and single cells (85, 86). Frequently, acinar formation can be seen within the small clusters of cells (Fig. 26). Tumor cells have a moderate amount of granular cytoplasm. Nuclei are enlarged but do not show the degree of atypia typically seen with PDAs. Prominent nucleoli are typically present. The tumors mimic both normal acinar tissue and PENs. Unlike normal acinar tissue, the cells of ACCs tend to be much less cohesive and large groups that resemble normal pancreatic parenchyma should not be present. ACCs usually have more nuclear atypia and prominent nuclei, unlike PENs, although these criteria cannot be entirely relied upon. Indeed, immunohistochemistry is generally recommended for distinguishing these neoplasms (Table 2).

Aspirates of PENs (even when they appear cystic) are typically very cellular with numerous loose clusters of neoplastic cells and single cells (Fig. 27) (85, 87–89). Small rosettes are sometimes seen. Cells typically have a moderate amount of cytoplasm that sometimes has small vacuoles or granules. Nuclei are regular and tend to be eccentrically placed. They

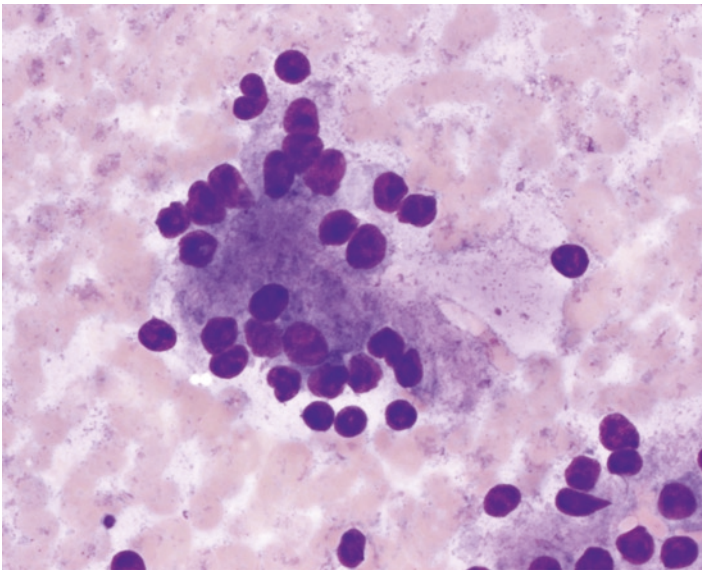


Fig. 26. Aspirates of acinar cell carcinomas are characterized by cells with abundant granular cytoplasm and eccentric round nuclei that form sheets and acinar-like structures; the cells are fragile and frequently disrupt resulting in a granular background (DiffQuick (DQ)).

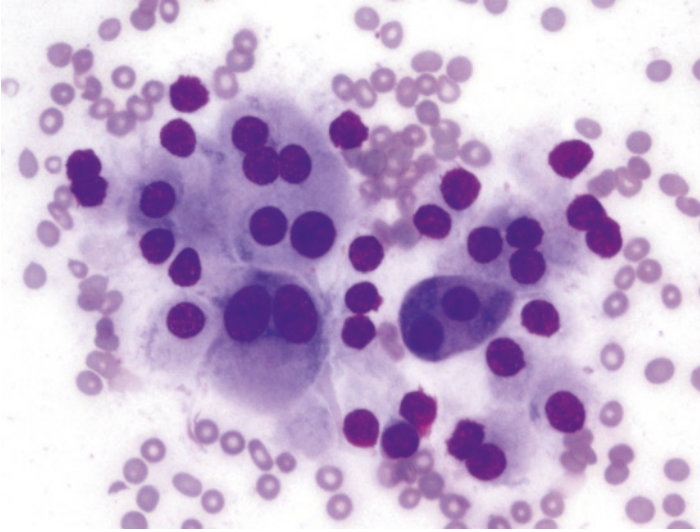


Fig. 27. Pancreatic endocrine tumor aspirates are similar to those of carcinoid tumors of the GI tract (compare to Fig. 8); there are small aggregates and single cells with eccentric round to oval nuclei with minimal pleomorphism is typical (DiffQuick (DQ)).

are round to oval with smooth contours. Occasional cells can have very enlarged and atypical nuclei (endocrine atypia), and some cells may be binucleated. The chromatin can range from fine to more granular. Nucleoli are usually inconspicuous but are sometimes prominent. Mitotic figures are infrequent. Stripped or “naked” nuclei are frequently seen in the background. It is frequently difficult to distinguish PENs from ACCs and SPT and immunohistochemistry may frequently be needed.

Solid pseudopapillary tumors are most frequently found in young to middle-aged women in the tail of the pancreas (90). Aspirates of SPTs are cellular and consist of clusters of cells, single cells, and branching papillary fronds with central capillaries and myxoid stroma lined by uniform cells with round to oval, bland nuclei and rare nuclear grooves (Fig. 28) (91, 92). The cells can also be arranged singly and in groups. Mitotic figures and necrosis are extremely rare. The background can show granular debris, metachromatic globular material, and foam cells. Even though the cytologic features are classic, in most cases, cell block with immunohistochemical studies will be extremely helpful in distinguishing this lesion from PENs and ACCs.

Pancreatoblastomas are almost always found in children and are very rare (93). There are few reports of their cytologic findings (94–96).

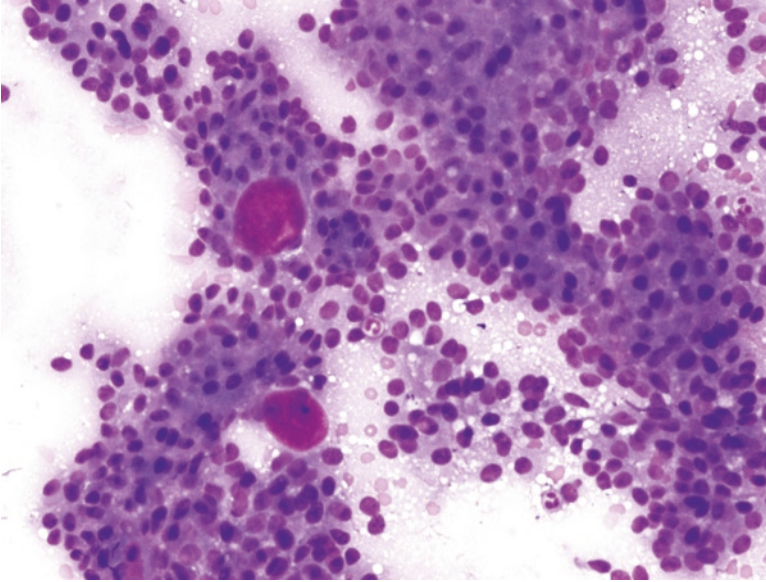


Fig. 28. An aspirate of a solid pseudopapillary neoplasm is characterized by small cells with round to oval, bland nuclei and eccentric cytoplasm that focally form papillary fronds, often associated with metachromatic stroma on DiffQuick (DQ) stains.

Aspirates are cellular and composed of both stromal and epithelial components. Epithelial groups usually form three-dimensional clusters with intermediate to large pleomorphic cells.

Lymphomas can sometimes present as primary pancreatic masses without apparent involvement of other sites (97, 98). Distinguishing these lesions from true primary pancreatic neoplasms is important as lymphomas do not usually require resection. The cytologic features depend on the specific type of lymphoma (see above) that is present but aspirates are generally cellular with mostly discohesive single cells. The most common lymphoma reported to involve the pancreas is the diffuse large B-cell lymphoma and smears usually show numerous large, markedly atypical cells with increased nuclear to cytoplasmic ratios, irregular nuclear contours, and prominent nucleoli with admixed smaller lymphocytes.

Metastatic lesions can present in the pancreas and appear radiographically concerning for primary pancreatic neoplasia (99, 100). Renal cell carcinoma is notorious for presenting late with a metastasis

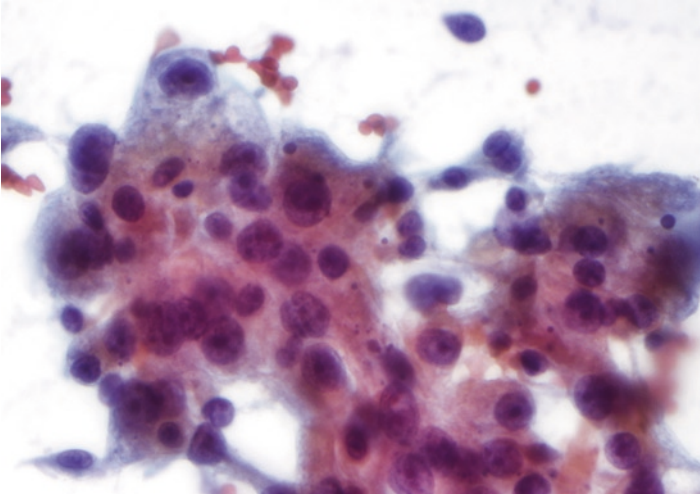


Fig. 29. Aspirates of metastatic renal cell carcinomas typically have cells with abundant cytoplasm and centrally placed large nuclei with prominent nucleoli; the cytoplasm in cases of clear cell RCC is often finely vacuolated as seen in this case (Pap).

to the pancreas (Fig. 29); other tumors include lung, breast, Mullerian, and gastrointestinal carcinomas as well as melanoma and sarcomas. It is imperative for the pathologist to know the patient's history of malignancy if a correct diagnosis is going to be made. Cell block immunohistochemistry can be very helpful for distinguishing these lesions from primary pancreatic malignancies.

SOLID LESIONS MIMICKING SOLID PANCREATIC NEOPLASIA

Acute pancreatitis is diagnosed by clinical, laboratory, and radiological findings. Fine needle aspiration is rarely performed. Occasionally, however, acute pancreatitis can present clinically as ductal obstruction because of an adjacent tumor. The cytologic findings that characterize acute pancreatitis are cellular degeneration, numerous acute inflammatory cells, granular debris, and inflammatory changes of ductal and acinar epithelium (2). Fat necrosis and foam cells may be present. The ductal epithelium may appear markedly atypical; a pathologist should be wary of making a diagnosis of malignancy with a background of obvious acute pancreatitis.

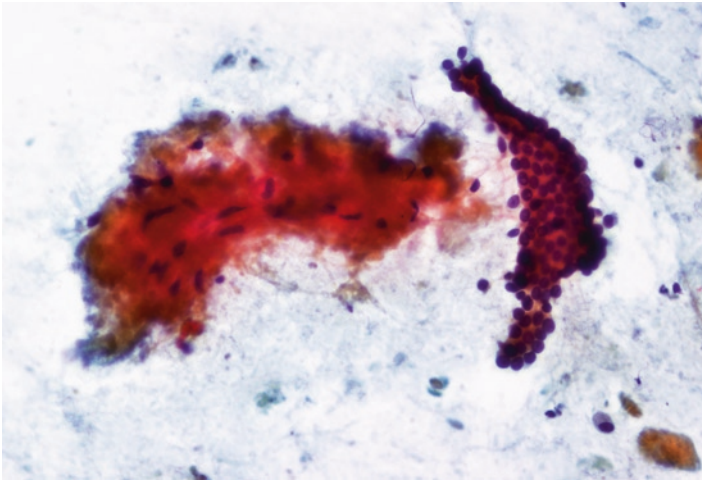


Fig. 30. Aspirates of chronic pancreatitis can be very hypocellular; when present, bland sheets and tubules of normal or slightly reactive ductal cells associated with fibrosis can be seen, often in a background of granular debris due to fat necrosis (Pap).

Chronic pancreatitis is a well-known radiographic and clinical mimicker of pancreatic malignancy (101). Aspirates show fragments of pancreatic parenchyma that contain some degree of fibrosis with acinar tissue splayed apart by spindled cells. In more developed cases, only fragments of fibrotic stroma may be seen (Fig. 30); the background typically shows mixed inflammatory cells, typically with some macrophages, along with calcific debris. Ductal cells may also be present and may show some cytologic atypia that is usually less than that seen with adenocarcinoma.

Autoimmune pancreatitis or lymphoplasmacytic pancreatitis may also present as a mass lesion or bile duct stricture (102). Aspirates have been noted to contain fragments of stromal tissue, often appearing “cellular” due to the increased numbers of lymphocytes and plasma cells. The disease is associated with increased serum levels of IgG4.

Finally, it would be remiss if we did not mention periampullary pancreatitis or “groove pancreatitis” as it may clinically present as a solid and/or cystic mass in the head of the pancreas or periampullary region (103). Reports of cytologic findings are lacking; however, we have seen one case that showed abundant Brunner glands with occasional fragments of mesenchymal tissue (Fig. 31). Rarely, other inflammatory or infectious conditions (e.g., tuberculosis) may present as solid lesions (104).

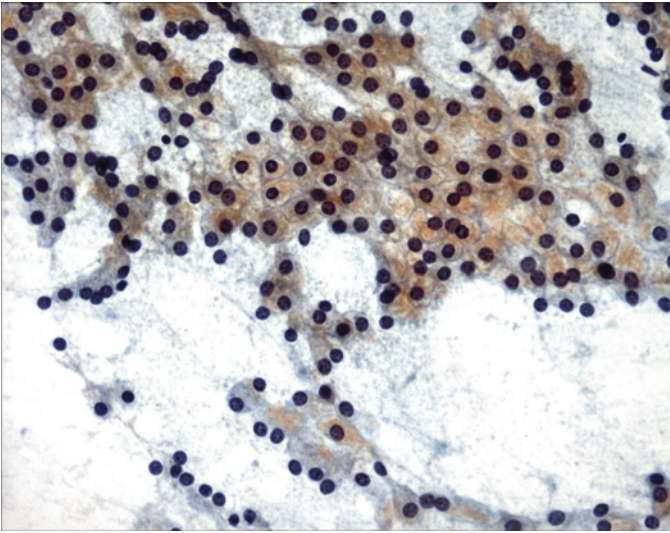


Fig. 31. Groove pancreatitis is associated with hypertrophy of Brunner's glands; these cells can be aspirated and have delicate, cleared cytoplasm with distinct cell membranes and central round nuclei with minimal atypia (Pap).

CYSTIC LESIONS

There is a vast array of cystic lesions in the pancreas (9). The pathologist's role is to generally discriminate neoplastic from non-neoplastic cysts and then to render as specific of a diagnosis as possible. The pathologist should not operate in a vacuum with these lesions and clinical, radiographic, sonographic, and cyst fluid chemistry should be used (Table 3).

The most common cystic-appearing lesion is a pancreatic pseudocyst (2). Aspirates are turbid and brown. Cytologically, they show "dirty" material or granular/calcific debris, proteinaceous material, and variable number of inflammatory cells (usually macrophages and neutrophils). Epithelial cells should be, by definition, absent; however, contamination of gastrointestinal epithelium may be present. Chemical analysis of the cyst fluid is sometimes helpful.

Pathologists should be aware that all typically solid neoplasms, PDAs, PENs, ACCs, SPTs, and metastases may appear predominately cystic (105). Aspirates are typically cellular, or at least more cellular than aspirates of typically cystic neoplasms (2).

The role of cytopathology for the identification of mucinous neoplasia, (intraductal papillary mucinous neoplasms (IPMNs), and mucinous cystic neoplasms (MCNs)) continues to evolve as image techniques

Table 3
Clinical, imaging, and chemical features of selected pancreatic cysts

<i>Lesion</i>	<i>Clinical</i>				<i>Imaging features</i>		<i>Chemistry</i>	
	<i>Symptoms</i>	<i>Age</i>	<i>Sex</i>	<i>Location</i>	<i>Character</i>	<i>CEA</i>	<i>Amylase</i>	
IPMN	Incidental; chronic pancreatitis	>50 years	M>W	Head>tail	Connected to ductal system; main duct may be dilated; usually multiple dilated side branch ducts	High	Variable	
MCN	Incidental; nonspecific symptoms	Adults	W	Body or tail	Multilocular	High	Low	
SC	Incidental; nonspecific symptoms	Adults	W>M	Body or tail	Multilocular, usually with small cysts (microcystic); occasional with larger cysts (macrocytic); central scar; occasional “sunburst” calcification	Low	Low	
Pseudocyst	Pain; chronic pancreatitis	Adults	M>W	Tail>head	Unilocular	Low	Very high	
LEC	Incidental; nonspecific symptoms	Adults	M>W	Throughout	Circumscribed; multilocular or unilocular	Low	Variable; can be very high	
Retention cyst	Chronic pancreatitis; other obstruction	Adults	M=F	Throughout	Unilocular	NA	NA	

IPMN intraductal papillary mucinous neoplasm, MCN mucinous cystic neoplasm, SC serous cystadenoma, LEC lymphoepithelial cyst

advance (106). Cytology is now considered one piece of the puzzle for the identification and management of mucinous neoplasia. Magnetic resonance imaging, ERCP, MRCP, cyst fluid chemical analysis, and even molecular analysis (see below) can be very helpful for identifying these lesions.

Cytologically, aspirates of mucinous neoplasia often show abundant background extracellular mucus that appears more abundant and thicker than typical gastrointestinal contaminant (Fig. 32) (107–110). This is certainly not always the case, however, and with a significant percentage of cases, a definitive atypical extracellular component (mucus) cannot be identified. Aspirates are frequently acellular or paucicellular. Sheets of mucinous epithelium may be present that can range from bland and “normal-appearing” to cytologically malignant (Fig. 33). Bland appearing epithelium is often impossible to distinguish from contaminant GI epithelium (either gastric or duodenal) although some have suggested that immunohistochemistry may be helpful here (111, 112). Such testing may be difficult, however, as the samples are often paucicellular. Cytologic atypia should generally be mentioned and qualified as worsen-

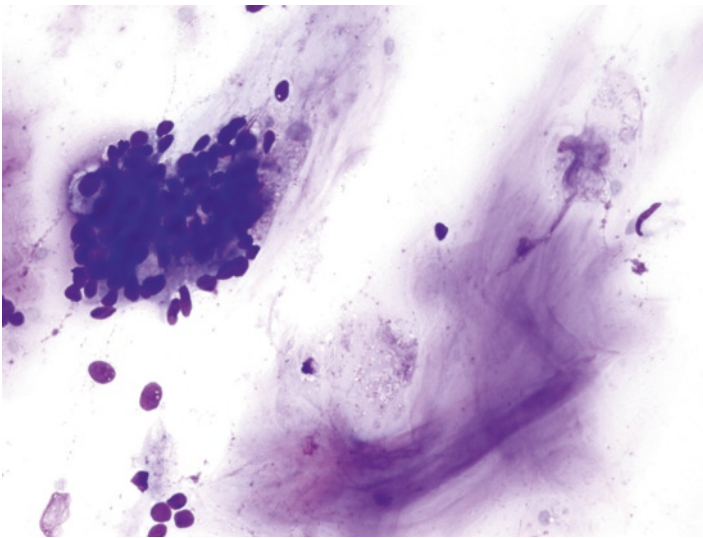


Fig. 32. Aspirates of pancreatic mucinous tumors often contain large quantities of extracellular thick mucin which is best seen on DiffQuick (DQ) stains, and may be very hypocellular; in this case, a few bland columnar epithelial cells are present as well. The tumor was confirmed to be an IPMN on resection.

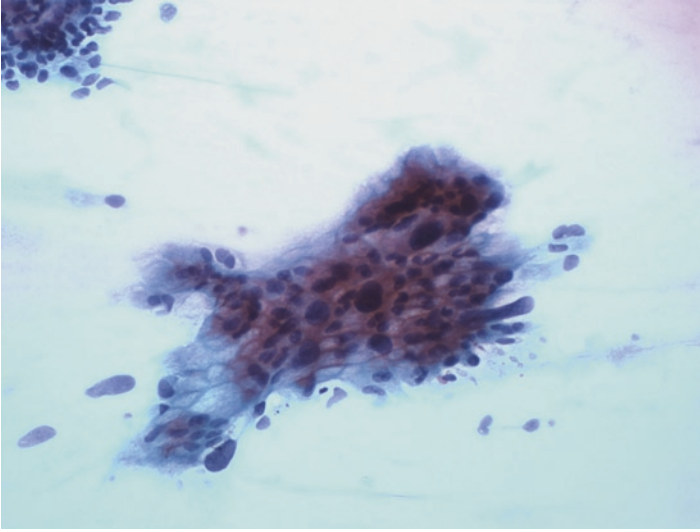


Fig. 33. Aspirates of pancreatic mucinous tumors with epithelial atypia such as seen in this case (enlarged hyperchromatic nuclei with anisonucleocytosis) are more commonly associated with malignancy; on resection this case of IPMN had an area of intraepithelial carcinoma (Pap).

ing atypia has been shown to correlate with malignancy with these lesions (107). It has also been shown that lesions with worsening cytologic atypia tend to yield more cellular samples often with three-dimensional clusters and even papillary fragments. When cytologic features of malignancy are present, it should be mentioned that the presence or absence of invasive disease cannot be assessed. Finally, it should be noted that IPMNs and MCNs cannot be distinguished on FNA as the ovarian-like stroma that defines MCNs histologically is not typically seen on FNA.

Ancillary techniques, including immunohistochemistry, cyst fluid chemical analysis and molecular testing have all been used to aid in the distinction of IPMNs and MCNs from other pancreatic cystic lesions. Cyst fluid chemical analysis is by far the most common ancillary technique used (113). Increased concentrations of CEA have been helpful for both identifying mucinous neoplasia and for predicting malignancy. Increased amylase concentrations are generally associated with pseudocysts but may also be seen with IPMNs. Molecular testing is gaining in popularity. KRAS2 sequencing and LOH studies at multiple tumor suppressor loci have been shown to predict mucinous neoplasia (82, 114).

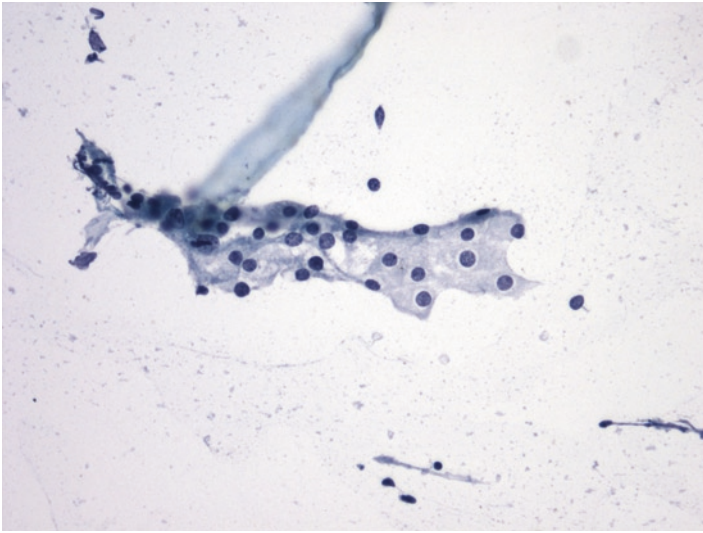


Fig. 34. Rare bland cuboidal cells may be seen with aspirates of serous cystadenomas (DiffQuick (DQ)).

Furthermore, quantitative analysis of mutations has been shown to predict malignancy (115).

Serous neoplasms, either microcystic (more common) or macrocystic (less common) are almost impossible to diagnose based on cytologic features (116, 117). Aspirates have been noted to show clear fluid and be paucicellular with bland sheets of cuboidal to columnar epithelial cells (although some have noted occasional nuclear and cytologic atypia) (Fig. 34). Some have suggested that if abundant cytologic material is present, immunohistochemistry or histochemistry (PAS staining for the identification of cytoplasmic glycogen) may be helpful.

The myriad of other cystic lesions of the pancreas tend to be non-neoplastic and aspirates may show either specific or nonspecific findings. Aspirates of lymphoepithelial cysts typically show keratinous debris, squamous cells, and cholesterol crystals (Fig. 35) (118, 119). Rarely, gastric duplication cysts can involve the pancreas and may show changes similar to those seen with mucinous cysts (120). Retention cysts do not typically show background mucus and may have some bland epithelial sheets. Infectious cysts may simply be abscesses and contain abundant neutrophils and debris or identifiable organisms such as *Giardia* or fluke eggs (121, 122).

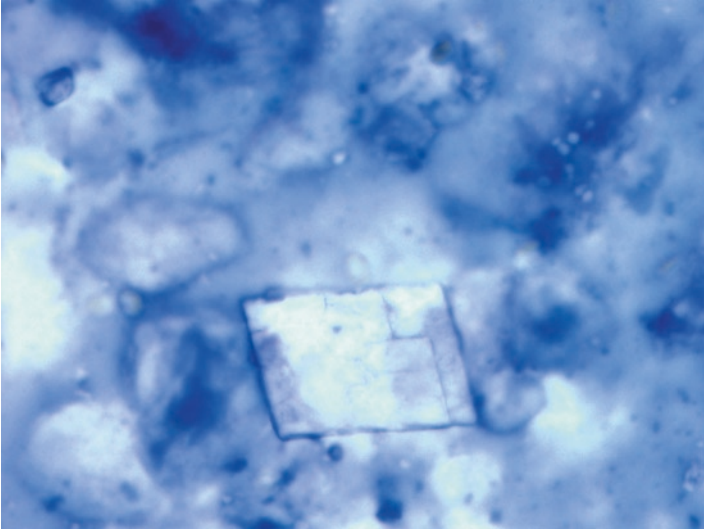


Fig. 35. Aspirates of lymphoepithelial cysts are typically hypocellular and have a background of debris and inflammatory cells; in this case, a large cholesterol crystal is present (DiffQuick (DQ)).

Extrahepatic Biliary System and Gallbladder

EUS-FNA has been shown to be helpful for the diagnosis of extrahepatic cholangiocarcinoma and can be used to diagnose gallbladder carcinoma (123–125). The cytologic features of bile duct and gallbladder adenocarcinomas are similar to PDA and the same variants can be seen (adenosquamous, anaplastic, etc.). There are a few caveats. Both bile duct and gallbladder adenocarcinomas can be exquisitely well differentiated with cytologic atypia that overlaps with reactive epithelium. This is especially concerning for the pathologist, given that abundant non-neoplastic epithelium of the bile duct and gallbladder can be sampled with EUS-FNA, and this epithelium can show significant reactive atypia due to the stent placement and obstruction. These difficulties are akin to those that pathologists face when interpreting bile duct brushing. Rarely, other tumors, such as carcinoid tumors, of the extrahepatic bile duct or gallbladder may be sampled.

BIOPSY OF THE LIVER

The liver is almost always sampled by EUS-FNA for the staging of malignancy, usually epithelial (126). Features of the various malignancies that can metastasize to the liver (e.g., pancreas, luminal gut, and

lung) have already been described. Generally, the cytologic features alone preclude a definitive statement regarding the site of origin, although some malignancies, such as colorectal adenocarcinomas, have cytologic features at least suggestive of the site of origin. If the primary tumor has been previously sampled, either cytologically or histologically, the pathologist can compare the morphologic features of the tumors and note whether they are similar. Cell block immunohistochemistry can also be used to immunophenotype the tumor, and often may suggest a site of origin.

Primary liver malignancies are also sometimes sampled by EUS-FNA, the vast majority of which are hepatocellular carcinomas (HCCs) (126). HCC is the most common primary malignancy of the liver often arising in a background of cirrhosis. It usually presents in older patients as a single mass. Rarely, it can present as multiple masses mimicking metastatic carcinoma. Morphologically, cytologic criteria of malignancy in well-differentiated HCC are the following: numerous stripped atypical nuclei, macronucleoli, increased mitoses, and multinucleation (127, 128). Architectural criteria in smears include widened trabeculae, well-defined capillaries traversing tissue fragments, and solid islands of hepatocytes rimmed by endothelial cells (Fig. 36).

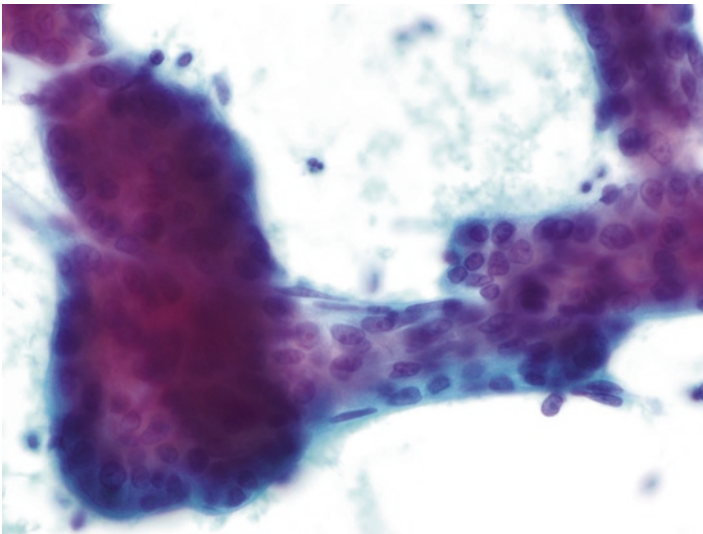


Fig. 36. This aspirate of a well-differentiated hepatocellular carcinomas has thickened hepatic plates (>3 cells thick); the cords of hepatocytes are lined by endothelial cells which give the appearance of a sharp cellular border (Pap).

Intrahepatic cholangiocarcinomas share cytologic features with extrahepatic cholangiocarcinomas and thus pancreatobiliary carcinomas in general (129). Aspirates show sheets of glandular cells with a loss of architectural regularity (loss of honeycomb pattern) and varying degrees of nuclear abnormalities. Cytologically, they are impossible to distinguish from metastases, especially from the pancreatobiliary system. Their immunophenotype is also nonspecific and a definitive diagnosis usually rests on a combination of cytologic and clinical findings.

ADRENAL GLAND

The left adrenal gland can be easily imaged and sampled by EUS-FNA. Sampling is most often performed for the diagnosis of metastatic malignancy, most often lung (130–133). Often the difficulty for the pathologist will be to determine the site of origin of the tumor or distinguish the lesion from a primary adrenal tumor.

The cytologic features of the various epithelial malignancies that may metastasize to the adrenal gland have already been discussed. As with the diagnosis of both primary and metastatic lesions at other sites, comparison to other available histologic materials can be helpful as can be the construction of a cell block for immunohistochemical staining. Occasionally, lymphoma or infectious disease (e.g., histoplasmosis) will be present in the adrenal gland. Diagnosis of these lesions is as discussed above.

Pheochromocytoma is an uncommon neoplasm and when it presents, it may either be sporadic or familial (134). Smears show loose aggregates of polymorphic cells (cuboidal, elongated, or multinucleated) with eosinophilic granular cytoplasm and anisonucleosis. Some cells have coarse chromatin with prominent nucleoli and others have bland nuclear features. Immunohistochemical studies performed on cell block show the neoplastic cells to be immunoreactive with antibodies to chromogranin and synaptophysin, often with tell-tale sustentacular cells exhibiting immunoreactivity with antibodies to S100 protein. The neoplastic cells are not reactive with antibodies to cytokeratins.

Other uncommon adrenal neoplasms, such as myelolipomas, vascular tumors, ganglioneuromas, and neuroblastomas, could also be sampled by EUS-FNA. The discussion of their cytologic features is beyond the scope of this chapter.

CONCLUSION

This chapter discussed the most common sites and entities sampled by EUS-FNA. It was the aim of this chapter to discuss the more common difficulties faced by pathologists as they interpret EUS-FNA specimens.

Indeed the cytopathologist is integral for a well-functioning EUS-FNA service. Communication between the gastroenterologist and pathologist is paramount for the correct classification of disease and thus, the appropriate management of patients. How well a EUS-FNA service functions at a particular institution will depend greatly on the skills of the gastroenterologist and pathologist and their ability to work together.

REFERENCES

1. Chang KJ, Katz KD, Durbin TE, Erickson RA, Butler JA, Lin F, et al. Endoscopic ultrasound-guided fine-needle aspiration. *Gastrointest Endosc.* 1994;40(6):694–9.
2. Bardales RH, Stelow EB, Mallery S, Lai R, Stanley MW. Review of endoscopic ultrasound-guided fine-needle aspiration cytology. *Diagn Cytopathol.* 2006;34(2):140–75.
3. Klapman JB, Logrono R, Dye CE, Waxman I. Clinical impact of on-site cytopathology interpretation on endoscopic ultrasound-guided fine needle aspiration. *Am J Gastroenterol.* 2003;98(6):1289–94.
4. Nasuti JF, Gupta PK, Baloch ZW. Diagnostic value and cost-effectiveness of on-site evaluation of fine-needle aspiration specimens: review of 5, 688 cases. *Diagn Cytopathol.* 2002;27(1):1–4.
5. Woon C, Bardales RH, Stanley MW, Stelow EB. Rapid assessment of fine needle aspiration and the final diagnosis – how often and why the diagnoses are changed. *Cytojournal.* 2006;3:25.
6. Eloubeidi MA, Tamhane A, Jhala N, Chhieng D, Jhala D, Crowe DR, et al. Agreement between rapid onsite and final cytologic interpretations of EUS-guided FNA specimens: implications for the endosonographer and patient management. *Am J Gastroenterol.* 2006;101(12):2841–7.
7. Kerr SE, Bellizzi AM, Stelow EB, Frierson Jr HF, Policarpio-Nicolas ML. Initial assessment of fine-needle aspiration specimens by telepathology: validation for use in pathology resident-faculty consultations. *Am J Clin Pathol.* 2008;130(3):409–13.
8. de Luna R, Eloubeidi MA, Sheffield MV, Eltoum I, Jhala N, Jhala D, et al. Comparison of ThinPrep and conventional preparations in pancreatic fine-needle aspiration biopsy. *Diagn Cytopathol.* 2004;30(2):71–6.
9. Bellizzi AM, Stelow EB. Pancreatic cytopathology: a practical approach and review. *Arch Pathol Lab Med.* 2009;133:388–404.
10. Enayati PG, Traverso LW, Galagan K, Thirlby RC, Larson J, Hauptman EM, et al. The meaning of equivocal pancreatic cytology in patients thought to have pancreatic cancer. *Am J Surg.* 1996;171(5):525–8.

11. Shin HJ, Lahoti S, Sneige N. Endoscopic ultrasound-guided fine-needle aspiration in 179 cases: the M.D. Anderson Cancer Center experience. *Cancer*. 2002;96(3):174–80.
12. Tio TL. Large gastric folds evaluated by endoscopic ultrasonography. *Gastrointest Endosc Clin N Am*. 1995;5(3):683–91.
13. Lucido M, Lai R, Mallery S. Endoscopic ultrasound-guided fine needle aspiration in the diagnosis of linitis plastica. *Dig Endosc*. 2004;16:A66.
14. Dabbs DJ. Immunohistology of metastatic carcinoma of unknown primary. In: Dabbs DJ, editor. *Diagnostic Immunohistochemistry*. 2nd ed. Philadelphia: Churchill Livingstone; 2006. p. 180–226.
15. Chu P, Wu E, Weiss LM. Cytokeratin 7 and cytokeratin 20 expression in epithelial neoplasms: a survey of 435 cases. *Mod Pathol*. 2000;13(9):962–72.
16. Werling RW, Yaziji H, Bacchi CE, Gown AM. CDX2, a highly sensitive and specific marker of adenocarcinomas of intestinal origin: an immunohistochemical survey of 476 primary and metastatic carcinomas. *Am J Surg Pathol*. 2003;27(3):303–10.
17. Wang HH. Gastrointestinal tract. In: Cibas ES, Ducatman BS, editors. *Cytology: diagnostic principles and clinical correlates*. 2nd ed. Edinburgh: Saunders; 2003. p. 189–214.
18. Herath CH, Chetty R. Epstein–Barr virus-associated lymphoepithelioma-like gastric carcinoma. *Arch Pathol Lab Med*. 2008;132(4):706–9.
19. Gabbert HE, Shimoda T, Hainaut P, Nakamura Y, Field JK, Inoue H. Squamous cell carcinoma of the oesophagus. In: Hamilton SR, Aaltonen LA, editors. *Pathology and genetics of tumours of the digestive system*. Lyon: IARC Press; 2000. p. 11–9.
20. Capella C, Solcia E, Sobin LH, Arnold R. Endocrine tumours of the stomach. In: Hamilton SR, Aaltonen LA, editors. *Pathology and genetics of tumours of the digestive system*. Lyon: IARC Press; 2000. p. 53–7.
21. Capella C, Solcia E, Sobin LH, Arnold R. Endocrine tumours of the small intestine. In: Hamilton SR, Aaltonen LA, editors. *Pathology and genetics of tumours of the digestive system*. Lyon: IARC Press; 2000. p. 77–82.
22. Ando N, Goto H, Niwa Y, Hirooka Y, Ohmiya N, Nagasaka T, et al. The diagnosis of GI stromal tumors with EUS-guided fine needle aspiration with immunohistochemical analysis. *Gastrointest Endosc*. 2002;55(1):37–43.
23. Boggino HE, Fernandez MP, Logrono R. Cytomorphology of gastrointestinal stromal tumor: diagnostic role of aspiration cytology, core biopsy, and immunohistochemistry. *Diagn Cytopathol*. 2000;23(3):156–60.
24. Gu M, Ghafari S, Nguyen PT, Lin F. Cytologic diagnosis of gastrointestinal stromal tumors of the stomach by endoscopic ultrasound-guided fine-needle aspiration biopsy: cytomorphologic and immunohistochemical study of 12 cases. *Diagn Cytopathol*. 2001;25(6):343–50.
25. Stelow EB, Stanley MW, Mallery S, Lai R, Linzie BM, Bardales RH. Endoscopic ultrasound-guided fine-needle aspiration findings of gastrointestinal leiomyomas and gastrointestinal stromal tumors. *Am J Clin Pathol*. 2003;119(5):703–8.
26. Wieczorek TJ, Faquin WC, Rubin BP, Cibas ES. Cytologic diagnosis of gastrointestinal stromal tumor with emphasis on the differential diagnosis with leiomyosarcoma. *Cancer*. 2001;93(4):276–87.

27. Dong Q, McKee G, Pitman M, Geisinger K, Tambouret R. Epithelioid variant of gastrointestinal stromal tumor: diagnosis by fine-needle aspiration. *Diagn Cytopathol.* 2003;29(2):55–60.
28. Debol SM, Stanley MW, Mallery JS. Can fine needle aspiration cytology adequately diagnose and predict the behavior of gastrointestinal stromal tumors? *Adv Anat Pathol.* 2001;8(2):93–7.
29. Meara RS, Cangiarella J, Simsir A, Horton D, Eltoum I, Chhieng DC. Prediction of aggressiveness of gastrointestinal stromal tumours based on immunostaining with bcl-2, Ki-67 and p53. *Cytopathology.* 2007;18(5):283–9.
30. Fletcher CD, Berman JJ, Corless C, Gorstein F, Lasota J, Longley BJ, et al. Diagnosis of gastrointestinal stromal tumors: a consensus approach. *Hum Pathol.* 2002;33(5):459–65.
31. Gomes AL, Bardales RH, Milanezi F, Reis RM, Schmitt F. Molecular analysis of c-Kit and PDGFRA in GISTs diagnosed by EUS. *Am J Clin Pathol.* 2007;127(1):89–96.
32. Miettinen M, Kopczynski J, Makhlof HR, Sarlomo-Rikala M, Gyorffy H, Burke A, et al. Gastrointestinal stromal tumors, intramural leiomyomas, and leiomyosarcomas in the duodenum: a clinicopathologic, immunohistochemical, and molecular genetic study of 167 cases. *Am J Surg Pathol.* 2003;27(5):625–41.
33. Miettinen M, Sarlomo-Rikala M, Sobin LH, Lasota J. Esophageal stromal tumors: a clinicopathologic, immunohistochemical, and molecular genetic study of 17 cases and comparison with esophageal leiomyomas and leiomyosarcomas. *Am J Surg Pathol.* 2000;24(2):211–22.
34. Stelow EB, Jones DR, Shami VM. Esophageal leiomyosarcoma diagnosed by endoscopic ultrasound-guided fine-needle aspiration. *Diagn Cytopathol.* 2007;35(3):167–70.
35. Stelow EB, Lai R, Bardales RH, Linzie BM, Mallery S, Stanley MW. Endoscopic ultrasound-guided fine-needle aspiration cytology of peripheral nerve-sheath tumors. *Diagn Cytopathol.* 2004;30(3):172–7.
36. Stelow EB, Murad FM, Debol SM, Stanley MW, Bardales RH, Lai R, et al. A limited immunocytochemical panel for the distinction of subepithelial gastrointestinal mesenchymal neoplasms sampled by endoscopic ultrasound-guided fine-needle aspiration. *Am J Clin Pathol.* 2008;129(2):219–25.
37. Hehn ST, Grogan TM, Miller TP. Utility of fine-needle aspiration as a diagnostic technique in lymphoma. *J Clin Oncol.* 2004;22(15):3046–52.
38. Austin RM, Birdsong GG, Sidawy MK, Kaminsky DB. Fine needle aspiration is a feasible and accurate technique in the diagnosis of lymphoma. *J Clin Oncol.* 2005;23(35):9029–30. author reply 9030–1.
39. Wotherspoon A, Chott A, Gascoyne RD, Muller-Hermelink HK. Lymphoma of the stomach. In: Hamilton SR, Aaltonen LA, editors. *Pathology and genetics of the digestive system.* Lyon: IARC Press; 2000. p. 57–61.
40. III Vander Noot MR, Eloubeidi MA, Chen VK, Eltoum I, Jhala D, Jhala N, et al. Diagnosis of gastrointestinal tract lesions by endoscopic ultrasound-guided fine-needle aspiration biopsy. *Cancer.* 2004;102(3):157–63.
41. Young NA, Al-Saleem T. Diagnosis of lymphoma by fine-needle aspiration cytology using the revised European-American classification of lymphoid neoplasms. *Cancer.* 1999;87(6):325–45.

42. Young NA, Al-Saleem TI, Ehya H, Smith MR. Utilization of fine-needle aspiration cytology and flow cytometry in the diagnosis and subclassification of primary and recurrent lymphoma. *Cancer*. 1998;84(4):252–61.
43. Nicol TL, Silberman M, Rosenthal DL, Borowitz MJ. The accuracy of combined cytopathologic and flow cytometric analysis of fine-needle aspirates of lymph nodes. *Am J Clin Pathol*. 2000;114(1):18–28.
44. Chute DJ, Cousar JB, Mills SE. Anorectal malignant melanoma: morphologic and immunohistochemical features. *Am J Clin Pathol*. 2006;126(1):93–100.
45. Morrison C, Young DC, Wakely Jr PE. Cytopathology of malignant melanoma in conventional and liquid-based smears. *Am J Clin Pathol*. 2002;118(3):435–41.
46. Wick MR. Immunohistology of melanocytic neoplasms. In: Dabbs DJ, editor. *Diagnostic immunohistochemistry*. 2nd ed. Philadelphia: Churchill Livingstone; 2006. p. 162–79.
47. Eloubeidi MA, Cohn M, Cerfolio RJ, Chhieng DC, Jhala N, Jhala D, et al. Endoscopic ultrasound-guided fine-needle aspiration in the diagnosis of foregut duplication cysts: the value of demonstrating detached ciliary tufts in cyst fluid. *Cancer*. 2004;102(4):253–8.
48. Rodriguez FJ, Abraham SC, Allen MS, Sebo TJ. Fine-needle aspiration cytology findings from a case of pancreatic heterotopia at the gastroesophageal junction. *Diagn Cytopathol*. 2004;31(3):175–9.
49. Stelow EB, Lai R, Bardales RH, Mallery S, Linzie BM, Crary G, et al. Endoscopic ultrasound-guided fine-needle aspiration of lymph nodes: the Hennepin County Medical Center experience. *Diagn Cytopathol*. 2004;30(5):301–6.
50. Eloubeidi MA, Wallace MB, Reed CE, Hadzijahic N, Lewin DN, Van Velse A, et al. The utility of EUS and EUS-guided fine needle aspiration in detecting celiac lymph node metastasis in patients with esophageal cancer: a single-center experience. *Gastrointest Endosc*. 2001;54(6):714–9.
51. Shami VM, Parmar KS, Waxman I. Clinical impact of endoscopic ultrasound and endoscopic ultrasound-guided fine-needle aspiration in the management of rectal carcinoma. *Dis Colon Rectum*. 2004;47(1):59–65.
52. Fritscher-Ravens A, Sriram PV, Bobrowski C, Pforte A, Topalidis T, Krause C, et al. Mediastinal lymphadenopathy in patients with or without previous malignancy: EUS-FNA-based differential cytodiagnosis in 153 patients. *Am J Gastroenterol*. 2000;95(9):2278–84.
53. Cahn M, Chang K, Nguyen P, Butler J. Impact of endoscopic ultrasound with fine-needle aspiration on the surgical management of pancreatic cancer. *Am J Surg*. 1996;172(5):470–2.
54. Fritscher-Ravens A, Sriram PV, Topalidis T, Hauber HP, Meyer A, Soehendra N, et al. Diagnosing sarcoidosis using endosonography-guided fine-needle aspiration. *Chest*. 2000;118(4):928–35.
55. Itaba S, Yoshinaga S, Nakamura K, Mizutani T, Honda K, Takayanagi R, et al. Endoscopic ultrasound-guided fine-needle aspiration for the diagnosis of peripancreatic tuberculous lymphadenitis. *J Gastroenterol*. 2007;42(1):83–6.
56. Williams DB, Sahai AV, Aabakken L, Penman ID, van Velse A, Webb J, et al. Endoscopic ultrasound guided fine needle aspiration biopsy: a large single centre experience. *Gut*. 1999;44(5):720–6.

57. Yasuda I, Tsurumi H, Omar S, Iwashita T, Kojima Y, Yamada T, et al. Endoscopic ultrasound-guided fine-needle aspiration biopsy for lymphadenopathy of unknown origin. *Endoscopy*. 2006;38(9):919–24.
58. Pugh JL, Jhala NC, Eloubeidi MA, Chhieng DC, Eltoun IA, Crowe DR, et al. Diagnosis of deep-seated lymphoma and leukemia by endoscopic ultrasound-guided fine-needle aspiration biopsy. *Am J Clin Pathol*. 2006;125(5):703–9.
59. Ribeiro A, Vazquez-Sequeiros E, Wiersema LM, Wang KK, Clain JE, Wiersema MJ. EUS-guided fine-needle aspiration combined with flow cytometry and immunocytochemistry in the diagnosis of lymphoma. *Gastrointest Endosc*. 2001;53(4):485–91.
60. Chhieng DC, Cangiarella JF, Symmans WF, Cohen JM. Fine-needle aspiration cytology of Hodgkin disease: a study of 89 cases with emphasis on false-negative cases. *Cancer*. 2001;93(1):52–9.
61. Hernandez A, Kahaleh M, Olazagasti J, Jones DR, Daniel T, Stelow E, et al. EUS-FNA as the initial diagnostic modality in centrally located primary lung cancers. *J Clin Gastroenterol*. 2007;41(7):657–60.
62. Otori NP, Santa Maria EL. Cytopathologic diagnosis of bronchioloalveolar carcinoma: does it correlate with the 1999 World Health Organization definition? *Am J Clin Pathol*. 2004;122(1):44–50.
63. Atkins KA. The diagnosis of bronchioloalveolar carcinoma by cytologic means. *Am J Clin Pathol*. 2004;122(1):14–6.
64. French CA. Respiratory tract. In: Cibas ES, Ducatman BS, editors. *Cytology: diagnostic principles and clinical correlates*. 2nd ed. Edinburgh: Saunders; 2003. p. 61–96.
65. Roh MS, Hong SH. Utility of thyroid transcription factor-1 and cytokeratin 20 in identifying the origin of metastatic carcinomas of cervical lymph nodes. *J Korean Med Sci*. 2002;17(4):512–7.
66. Jimenez-Heffernan JA, Lopez-Ferrer P, Vicandi B, Marino A, Tejerina E, Nistal M, et al. Fine-needle aspiration cytology of large cell neuroendocrine carcinoma of the lung: a cytohistologic correlation study of 11 cases. *Cancer*. 2008;114(3):180–6.
67. Wu M, Szporn AH, Zhang D, Wasserman P, Gan L, Miller L, et al. Cytology applications of p63 and TTF-1 immunostaining in differential diagnosis of lung cancers. *Diagn Cytopathol*. 2005;33(4):223–7.
68. Wakely Jr PE. Cytopathology-histopathology of the mediastinum II. Mesenchymal, neural, and neuroendocrine neoplasms. *Ann Diagn Pathol*. 2005;9(1):24–32.
69. Kloppel G, Hruban RH, Longnecker DS, Adler G, Kern SE, Partanen TJ. Ductal adenocarcinoma of the pancreas. In: Hamilton SR, Aaltonen LA, editors. *World Health Organization classification of tumours. Pathology and genetics of tumours of the digestive system*. Lyon: IARC Press; 2000. p. 221–30.
70. Rahemtullah A, Misdraji J, Pitman MB. Adenosquamous carcinoma of the pancreas: cytologic features in 14 cases. *Cancer*. 2003;99(6):372–8.
71. Adsay NV, Pierson C, Sarkar F, Abrams J, Weaver D, Conlon KC, et al. Colloid (mucinous noncystic) carcinoma of the pancreas. *Am J Surg Pathol*. 2001;25(1):26–42.
72. Stelow EB, Pambuccian SE, Bardales RH, Debol SM, Mallery S, Lai R, et al. The cytology of pancreatic foamy gland adenocarcinoma. *Am J Clin Pathol*. 2004;121(6):893–7.

73. Gupta RK, Wakefield SJ. Needle aspiration cytology, immunocytochemistry, and electron microscopic study of unusual pancreatic carcinoma with pleomorphic giant cells. *Diagn Cytopathol.* 1992;8(5):522–7.
74. Mullick SS, Mody DR. “Osteoclastic” giant cell carcinoma of the pancreas. Report of a case with aspiration cytology. *Acta Cytol.* 1996;40(5):975–9.
75. Silverman JF, Dabbs DJ, Finley JL, Geisinger KR. Fine-needle aspiration biopsy of pleomorphic (giant cell) carcinoma of the pancreas. Cytologic, immunocytochemical, and ultrastructural findings. *Am J Clin Pathol.* 1988;89(6):714–20.
76. Silverman JF, Finley JL, MacDonald Jr KG. Fine-needle aspiration cytology of osteoclastic giant-cell tumor of the pancreas. *Diagn Cytopathol.* 1990;6(5):336–40.
77. Chhieng DC, Benson E, Eltoum I, Eloubeidi MA, Jhala N, Jhala D, et al. MUC1 and MUC2 expression in pancreatic ductal carcinoma obtained by fine-needle aspiration. *Cancer.* 2003;99(6):365–71.
78. Giorgadze TA, Peterman H, Baloch ZW, Furth EE, Pasha T, Shiina N, et al. Diagnostic utility of mucin profile in fine-needle aspiration specimens of the pancreas: an immunohistochemical study with surgical pathology correlation. *Cancer.* 2006;108(3):186–97.
79. Jhala N, Jhala D, Vickers SM, Eltoum I, Batra SK, Manne U, et al. Biomarkers in diagnosis of pancreatic carcinoma in fine-needle aspirates. *Am J Clin Pathol.* 2006;126(4): 572–9.
80. McCarthy DM, Maitra A, Argani P, Rader AE, Faigel DO, Van Heek NT, et al. Novel markers of pancreatic adenocarcinoma in fine-needle aspiration: mesothelin and prostate stem cell antigen labeling increases accuracy in cytologically borderline cases. *Appl Immunohistochem Mol Morphol.* 2003;11(3):238–43.
81. van Heek T, Rader AE, Offerhaus GJ, McCarthy DM, Goggins M, Hruban RH, et al. K-ras, p53, and DPC4 (MAD4) alterations in fine-needle aspirates of the pancreas: a molecular panel correlates with and supplements cytologic diagnosis. *Am J Clin Pathol.* 2002;117(5):755–65.
82. Khalid A, Finkelstein S, McGrath K. Molecular diagnosis of solid and cystic lesions of the pancreas. *Clin Lab Med.* 2005;25(1):101–16.
83. Levy MJ, Clain JE, Clayton A, Halling KC, Kipp BR, Rajan E, et al. Preliminary experience comparing routine cytology results with the composite results of digital image analysis and fluorescence in situ hybridization in patients undergoing EUS-guided FNA. *Gastrointest Endosc.* 2007;66(3):483–90.
84. Klimstra DS, Longnecker D. Acinar cell carcinoma. In: Hamilton SR, Aaltonen LA, editors. *World Health Organization classification of tumours. Pathology and genetics of tumours of the digestive system.* Lyon: IARC Press; 2000. p. 241–3.
85. Labate AM, Klimstra DL, Zakowski MF. Comparative cytologic features of pancreatic acinar cell carcinoma and islet cell tumor. *Diagn Cytopathol.* 1997;16(2):112–6.
86. Stelow EB, Bardales RH, Shami VM, Woon C, Presley A, Mallery S, et al. Cytology of pancreatic acinar cell carcinoma. *Diagn Cytopathol.* 2006;34(5):367–72.
87. al-Kaisi N, Weaver MG, Abdul-Karim FW, Siegler E. Fine needle aspiration cytology of neuroendocrine tumors of the pancreas. A cytologic, immunocytochemical and electron microscopic study. *Acta Cytol.* 1992;36(5):655–60.

88. Collins BT, Cramer HM. Fine-needle aspiration cytology of islet cell tumors. *Diagn Cytopathol.* 1996;15(1):37–45.
89. Gu M, Ghafari S, Lin F, Ramzy I. Cytological diagnosis of endocrine tumors of the pancreas by endoscopic ultrasound-guided fine-needle aspiration biopsy. *Diagn Cytopathol.* 2005;32(4):204–10.
90. Kloppel G, Luttges J, Klimstra D, Hruban R, Kern S, Adler G. Solid-pseudopapillary neoplasm. In: Hamilton SR, Aaltonen LA, editors. World Health Organization Classification of Tumours. Pathology and Genetics of Tumours of the Digestive System. Lyon: IARC Press; 2000. p. 246–8.
91. Bardales RH, Centeno B, Mallery JS, Lai R, Pochapin M, Guiter G, et al. Endoscopic ultrasound-guided fine-needle aspiration cytology diagnosis of solid-pseudopapillary tumor of the pancreas: a rare neoplasm of elusive origin but characteristic cytomorphologic features. *Am J Clin Pathol.* 2004;121(5):654–62.
92. Pettinato G, Di Vizio D, Manivel JC, Pambuccian SE, Somma P, Insubato L. Solid-pseudopapillary tumor of the pancreas: a neoplasm with distinct and highly characteristic cytological features. *Diagn Cytopathol.* 2002;27(6):325–34.
93. Klimstra DS, Longnecker D. Pancreatoblastoma. In: Hamilton SR, Aaltonen LA, editors. World Health Organization classification of tumours. Pathology and genetics of tumours of the digestive system. Lyon: IARC Press; 2000. p. 244–5.
94. Henke AC, Kelley CM, Jensen CS, Timmerman TG. Fine-needle aspiration cytology of pancreatoblastoma. *Diagn Cytopathol.* 2001;25(2):118–21.
95. Pitman MB, Faquin WC. The fine-needle aspiration biopsy cytology of pancreatoblastoma. *Diagn Cytopathol.* 2004;31(6):402–6.
96. Zhu LC, Sidhu GS, Cassai ND, Yang GC. Fine-needle aspiration cytology of pancreatoblastoma in a young woman: report of a case and review of the literature. *Diagn Cytopathol.* 2005;33(4):258–62.
97. Nayer H, Weir EG, Sheth S, Ali SZ. Primary pancreatic lymphomas: a cytopathologic analysis of a rare malignancy. *Cancer.* 2004;102(5):315–21.
98. Volmar KE, Routbort MJ, Jones CK, Xie HB. Primary pancreatic lymphoma evaluated by fine-needle aspiration: findings in 14 cases. *Am J Clin Pathol.* 2004;121(6):898–903.
99. Mesa H, Stelow EB, Stanley MW, Mallery S, Lai R, Bardales RH. Diagnosis of nonprimary pancreatic neoplasms by endoscopic ultrasound-guided fine-needle aspiration. *Diagn Cytopathol.* 2004;31(5):313–8.
100. Volmar KE, Jones CK, Xie HB. Metastases in the pancreas from nonhematologic neoplasms: report of 20 cases evaluated by fine-needle aspiration. *Diagn Cytopathol.* 2004;31(4):216–20.
101. Stelow EB, Bardales RH, Lai R, Mallery S, Linzie BM, Crary GS, et al. The cytological spectrum of chronic pancreatitis. *Diagn Cytopathol.* 2005;32(2):65–9.
102. Deshpande V, Mino-Kenudson M, Brugge WR, Pitman MB, Fernandez-del Castillo C, Warshaw AL, et al. Endoscopic ultrasound guided fine needle aspiration biopsy of autoimmune pancreatitis: diagnostic criteria and pitfalls. *Am J Surg Pathol.* 2005;29(11):1464–71.
103. Adsay NV, Zamboni G. Paraduodenal pancreatitis: a clinico-pathologically distinct entity unifying “cystic dystrophy of heterotopic pancreas”, “para-duodenal wall cyst”, and “groove pancreatitis”. *Semin Diagn Pathol.* 2004;21(4): 247–54.

104. Ahlawat SK. EUS-guided FNA diagnosis of pancreatic tuberculosis. *Gastrointest Endosc.* 2007;65(3):557–8.
105. Adsay NV, Klimstra DS. Cystic forms of typically solid pancreatic tumors. *Semin Diagn Pathol.* 2000;17(1):81–8.
106. Tanaka M, Chari S, Adsay V, Fernandez-del Castillo C, Falconi M, Shimizu M, et al. International consensus guidelines for management of intraductal papillary mucinous neoplasms and mucinous cystic neoplasms of the pancreas. *Pancreatology.* 2006;6(1–2):17–32.
107. Michaels PJ, Brachtel EF, Bounds BC, Brugge WR, Pitman MB. Intraductal papillary mucinous neoplasm of the pancreas: cytologic features predict histologic grade. *Cancer.* 2006;108(3):163–73.
108. Stelow EB, Stanley MW, Bardales RH, Mallery S, Lai R, Linzie BM, et al. Intraductal papillary-mucinous neoplasm of the pancreas. The findings and limitations of cytologic samples obtained by endoscopic ultrasound-guided fine-needle aspiration. *Am J Clin Pathol.* 2003;120(3):398–404.
109. Recine M, Kaw M, Evans DB, Krishnamurthy S. Fine-needle aspiration cytology of mucinous tumors of the pancreas. *Cancer.* 2004;102(2):92–9.
110. Layfield LJ, Cramer H. Fine-needle aspiration cytology of intraductal papillary-mucinous tumors: a retrospective analysis. *Diagn Cytopathol.* 2005;32(1):16–20.
111. Nagle JA, Wilbur DC, Pitman MB. Cytomorphology of gastric and duodenal epithelium and reactivity to B72.3: a baseline for comparison to pancreatic lesions aspirated by EUS-FNAB. *Diagn Cytopathol.* 2005;33(6):381–6.
112. Nawgiri RS, Nagle JA, Wilbur DC, Pitman MB. Cytomorphology and B72.3 labeling of benign and malignant ductal epithelium in pancreatic lesions compared to gastrointestinal epithelium. *Diagn Cytopathol.* 2007;35(5):300–5.
113. van der Waaij LA, van Dullemlen HM, Porte RJ. Cyst fluid analysis in the differential diagnosis of pancreatic cystic lesions: a pooled analysis. *Gastrointest Endosc.* 2005;62(3):383–9.
114. Khalid A, McGrath KM, Zahid M, Wilson M, Brody D, Swalsky P, et al. The role of pancreatic cyst fluid molecular analysis in predicting cyst pathology. *Clin Gastroenterol Hepatol.* 2005;3(10):967–73.
115. Khalid A, Zahid M, Finkelstein SD, Leblanc JK, Kaushik N, Ahmad N, et al. Pancreatic cyst fluid DNA analysis in evaluating pancreatic cysts: a report of the PANDA study. *Gastrointest Endosc.* 2009;69(6):1095–102.
116. Belsley NA, Pitman MB, Lauwers GY, Brugge WR, Deshpande V. Serous cystadenoma of the pancreas: limitations and pitfalls of endoscopic ultrasound-guided fine-needle aspiration biopsy. *Cancer.* 2008;114(2):102–10.
117. Huang P, Staerckel G, Sneige N, Gong Y. Fine-needle aspiration of pancreatic serous cystadenoma: cytologic features and diagnostic pitfalls. *Cancer.* 2006;108(4):239–49.
118. Centeno BA, Stockwell JW, Lewandrowski KB. Cyst fluid cytology and chemical features in a case of lymphoepithelial cyst of the pancreas: a rare and difficult preoperative diagnosis. *Diagn Cytopathol.* 1999;21(5):328–30.
119. Policarpio-Nicolas ML, Shami VM, Kahaleh M, Adams RB, Mallery S, Stanley MW, et al. Fine-needle aspiration cytology of pancreatic lymphoepithelial cysts. *Cancer.* 2006;108(6):501–6.

120. Woon CS, Pambuccian SE, Lai R, Jessurun J, Gulbahce HE. Ciliated foregut cyst of pancreas: cytologic findings on endoscopic ultrasound-guided fine-needle aspiration. *Diagn Cytopathol.* 2007;35(7):433–8.
121. Lai R, Linzie B, Mallery S. Pancreatic clonorchiasis diagnosed by EUS-guided pancreatic duct aspiration. *Gastrointest Endosc.* 2001;54(2):241–4.
122. Carter JE, Nelson JJ, Eves M, Boudreaux C. *Giardia lamblia* infection diagnosed by endoscopic ultrasound-guided fine-needle aspiration. *Diagn Cytopathol.* 2007;35(6):363–5.
123. Jacobson BC, Pitman MB, Brugge WR. EUS-guided FNA for the diagnosis of gallbladder masses. *Gastrointest Endosc.* 2003;57(2):251–4.
124. Eloubeidi MA, Chen VK, Jhala NC, Eltoun IE, Jhala D, Chhieng DC, et al. Endoscopic ultrasound-guided fine needle aspiration biopsy of suspected cholangiocarcinoma. *Clin Gastroenterol Hepatol.* 2004;2(3):209–13.
125. Meara RS, Jhala D, Eloubeidi MA, Eltoun I, Chhieng DC, Crowe DR, et al. Endoscopic ultrasound-guided FNA biopsy of bile duct and gallbladder: analysis of 53 cases. *Cytopathology.* 2006;17(1):42–9.
126. Cameron SEH, Evans RA, Debol SM, Mallery S, Stelow EB. Endoscopic ultrasound-guided fine needle aspiration of the liver. *Mod Pathol.* 2007;20:220A.
127. Das DK. Cytodiagnosis of hepatocellular carcinoma in fine-needle aspirates of the liver: its differentiation from reactive hepatocytes and metastatic adenocarcinoma. *Diagn Cytopathol.* 1999;21(6):370–7.
128. de Boer WB, Segal A, Frost FA, Sterrett GF. Cytodiagnosis of well differentiated hepatocellular carcinoma: can indeterminate diagnoses be reduced? *Cancer.* 1999;87(5): 270–7.
129. Chaudhary HB, Bhanot P, Logrono R. Phenotypic diversity of intrahepatic and extrahepatic cholangiocarcinoma on aspiration cytology and core needle biopsy: case series and review of the literature. *Cancer.* 2005;105(4):220–8.
130. DeWitt J, Alsatie M, LeBlanc J, McHenry L, Sherman S. Endoscopic ultrasound-guided fine-needle aspiration of left adrenal gland masses. *Endoscopy.* 2007;39(1): 65–71.
131. Jhala NC, Jhala D, Eloubeidi MA, Chhieng DC, Crowe DR, Roberson J, et al. Endoscopic ultrasound-guided fine-needle aspiration biopsy of the adrenal glands: analysis of 24 patients. *Cancer.* 2004;102(5):308–14.
132. Kramer H, Groen HJ. Diagnosis of mediastinal and left adrenal abnormalities with endoscopic ultrasonography. *Respir Med.* 2005;99(7):926–8.
133. Stelow EB, Debol SM, Stanley MW, Mallery S, Lai R, Bardales RH. Sampling of the adrenal glands by endoscopic ultrasound-guided fine-needle aspiration. *Diagn Cytopathol.* 2005;33(1):26–30.
134. Stelow EB, Stanley MW, Mallery S. Synchronous primary pancreatic endocrine neoplasm and adrenal pheochromocytoma diagnosed by EUS-guided FNA. *Gastrointest Endosc.* 2004;59(1):136–9.

Pitfalls in Endoscopic Ultrasound

Charles E. Dye, MD

CONTENTS

SEDATION
ENDOSCOPE INTUBATION AND PASSAGE
ORIENTATION
TECHNICAL ISSUES
EUS INDICATIONS
EQUIPMENT SELECTION
FNA CONSIDERATIONS
CONCLUSION

Abstract

Endoscopic ultrasound (EUS) has a prolonged learning curve. Essential components include mastery of new endoscopic and radiographic skills as well as becoming familiar with anatomic relationships and variables. Additionally, providers must help train technicians and nurses, refine sedation strategies, and create productive relationships with cytopathologists. Aims of this chapter are to provide practical advice, hopefully to speed progression through the learning curve and to help improve safety and exam quality. Common EUS pitfalls and simple solutions are organized and presented in the following categories: sedation, endoscopic intubation and passage, orientation, technical issues, potential problem indications, choosing the right equipment for each case, and fine needle aspiration. Pitfalls are particularly salient for beginners, but many have pertinence for advanced endosonographers, including those moving to a new practice site. Selected take home points are highlighted with case examples and figures.

From: *Clinical Gastroenterology: Endoscopic Ultrasound*,
Edited by: V. M. Shami and M. Kahaleh, DOI 10.1007/978-1-60327-480-7_6,
© Springer Science+Business Media, LLC 2010

Key Words: Pitfalls, Endoscopic orientation, Sedation, Intubation, Scope passage, Indications, Equipment, Ultrasound settings, Image quality, Fine needle aspiration, Coagulopathy, Endoscopy unit staff

SEDATION

Endoscopic ultrasound (EUS) examinations take longer and entail more noxious stimuli than standard upper endoscopy, especially when performed by beginners. Risk factors for sedation-limited exams should prompt precautions to minimize patient discomfort and obtain good outcomes. Heightened patient anxiety, alcohol or controlled substance use, and failure to tolerate prior endoscopy should be among a series of screening questions prior to exams. Additionally, severe cardiopulmonary disease warrants special consideration, such as seeking the assistance of an anesthesiologist.

Anesthesiology assistance and propofol are perhaps ideal solutions. When such luxuries are not available, more aggressive sedation initially with careful planning of exams to limit time and noxious stimuli may provide an adequate outcome. As an example, for a patient with a pancreatic head mass requiring tissue sampling, one strategy would be to apply a topical anesthesia block, achieve moderate sedation incorporating meperidine as a narcotic agent whenever possible, then pass the linear scope with fine needle aspiration (FNA) capability and proceed immediately to the appropriate EUS windows to begin tissue sampling. For such an exam, it would not be unusual to exceed 100 mg of meperidine and 8 mg of midazolam during 20–30 min of procedure time. Premedication, the addition of diazepam during exams, and adjunctive medication such as diphenhydramine are sedation strategies used by some providers. Adding inapsine (droperidol®) has fallen out of favor due to heightened concerns for QT prolongation and sudden death.

ENDOSCOPE INTUBATION AND PASSAGE

A major pitfall of EUS may be encountered when attempting to pass the echoendoscope. Several characteristics, including rigid and less rounded tips, oblique viewing optics, and larger diameters, can make this difficult. Intubation difficulties are less commonly encountered with newer generation scopes, featuring smaller diameters and more favorable tip configurations. Standard EGD neck positioning maneuvers are often helpful. A jaw thrust may allow easier esophageal intubation, particularly in patients where cervical spine disease precludes other positioning maneuvers. Unique solutions include partially inflating the

balloon on the echoendoscope and then applying a gentle torquing pressure (1). Another is to pass a standard forward viewing endoscope, then insert a guide wire and remove the scope. After the transfer of the wire through a catheter protecting the echoendoscope accessory channel, gentle traction can be applied on the wire during echoendoscope passage to achieve safe intubation (2).

Histories warranting special attention include prior difficulty passing endoscopes, dysphagia, and potential gastric outlet obstruction. Consider evaluating the anatomy and luminal integrity with a quick standard endoscopy exam. When necessary, dilation to at least 15 mm can be performed. For staging esophageal malignancy, a common indication requiring dilation, using hydrostatic balloons appears to be a safe option allowing complete EUS evaluations, including celiac lymph node sampling (3, 4). Maneuvers with a partially inflated EUS balloon or a guide wire, as mentioned previously, can also facilitate safe passage in some cases of luminal stenosis (1, 5). Use of a thinner caliber endobronchial ultrasound scope has been recently described to allow staging of celiac nodes in stenotic esophageal tumors (6). Some authors advocate high frequency probe use for stenotic esophageal tumors, avoiding the potential risks of dilation. Arguments against probe use include difficulties visualizing deeper tissue structures and the inability to perform FNA for confirmation of node status (7).

ORIENTATION

Probably, the most frustrating pitfall of EUS is becoming disoriented when learning to examine extraluminal structures, particularly when performing examinations in the duodenum. A good knowledge of cross-sectional anatomy with emphasis on vascular relationships is a prerequisite. An endosonographer can then follow the “roadmap” conferred by central arterial and mesenteric venous anatomy, serving as the frame of reference for many standard EUS views of surrounding structures. By convention, the aorta is positioned near 6 o’clock on the monitor, creating a situation where structures at 12 o’clock are anterior. From certain standard positions corresponding to anatomic landmarks, the examiner can coordinate exams and clarify pathology. Useful standard positions include:

- (1) Esophagus at ~26 cm from the gums - aortic arch and aortopulmonary window slightly proximal to the carina;
- (2) Proximal stomach ~40–45 cm from the gums - aorta giving off the celiac axis (Fig. 1);
- (3) Duodenum distal to the major papilla - aorta closely associated with the uncinate process of the pancreas (Fig. 2);



Fig. 1. Proximal stomach: aorta and celiac axis (cel axis) situated posteriorly. From this position, pushing slightly and angling the scope tip along the posterior wall of the stomach will bring the splenic vessels and body of the pancreas into view. The splenic vein is oriented along the inferior margin of the pancreatic body and tail.

- (4) Rectum at ~7–9 cm insertion revealing the prostate in men and at ~9–11 cm insertion revealing the uterus in women (Fig. 3).

Of course, when anatomy has been surgically altered, visualizing structures may be difficult or impossible. An example is attempting to visualize the pancreatic head and common bile duct in a patient who has undergone distal gastrectomy and gastrojejunostomy.

Also remember that reproducing standard views of the gut wall and extraluminal structures involve more than putting the scope tip at the corresponding level of the gastrointestinal tract. With both radial and linear echoendoscopes, the ultrasound probe has to be positioned along a specific axis to convey a desired view. The axis necessary to generate standard views often changes little when imaging within linear organs such as the esophagus. In contrast, major scope tip adjustments may be necessary when imaging in the stomach and duodenum. Increasing numbers of examinations and familiarity with the anatomy will eventually relegate this concept to second nature. When learning, however, concentrating on standard positions to orient surrounding anatomy and pathology will help diminish uncertainty and frustration. For example,

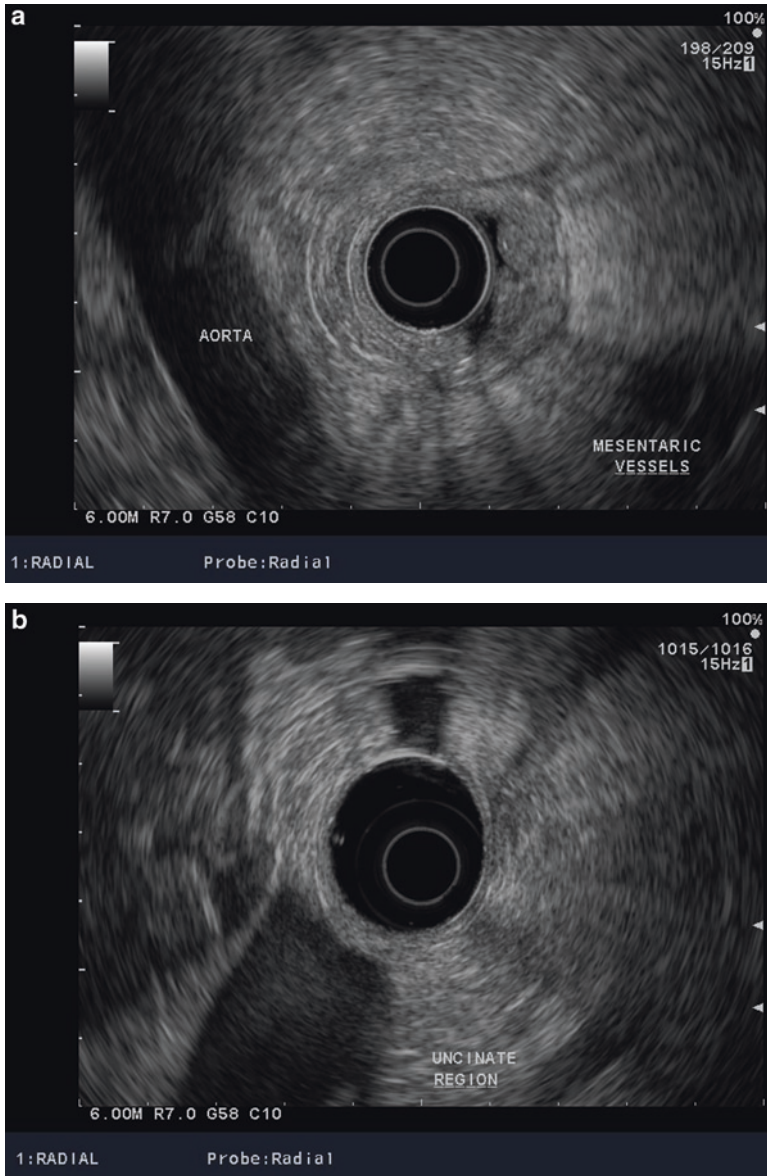


Fig. 2. (a) Deep duodenum: aorta with longitudinal view on the left side of the screen. The superior mesenteric vein and artery are often visible on the bottom right side of the screen. (b) Deep Duodenum: Aorta with cross-sectional view on the left side of the screen. The mesenteric vein may be seen deep to a portion of the uncinate process and pancreatic head on the bottom right side of the screen. (c) Mid Duodenum: Aorta with cross-sectional view highlighted by color doppler on the left side of the screen. The closely related common bile duct (CBD) and pancreatic duct (PD) may be visible on the bottom of the screen before they join at the major papilla.

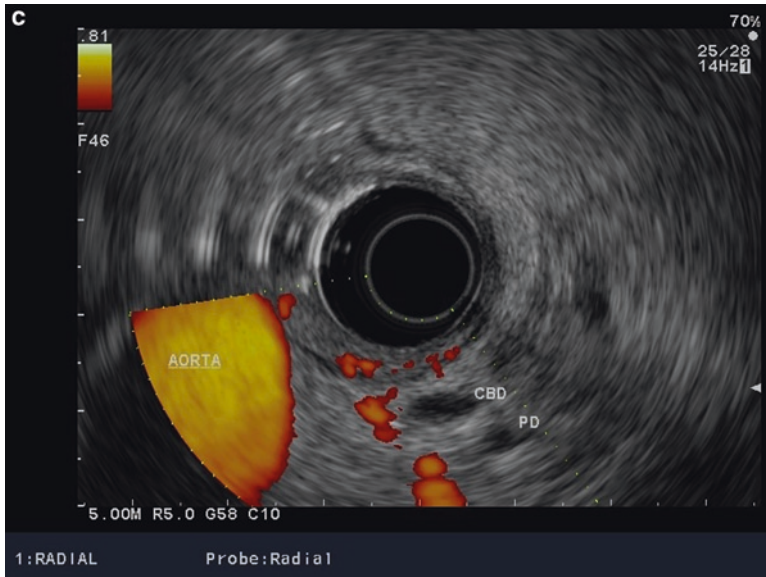


Fig. 2. (continued)

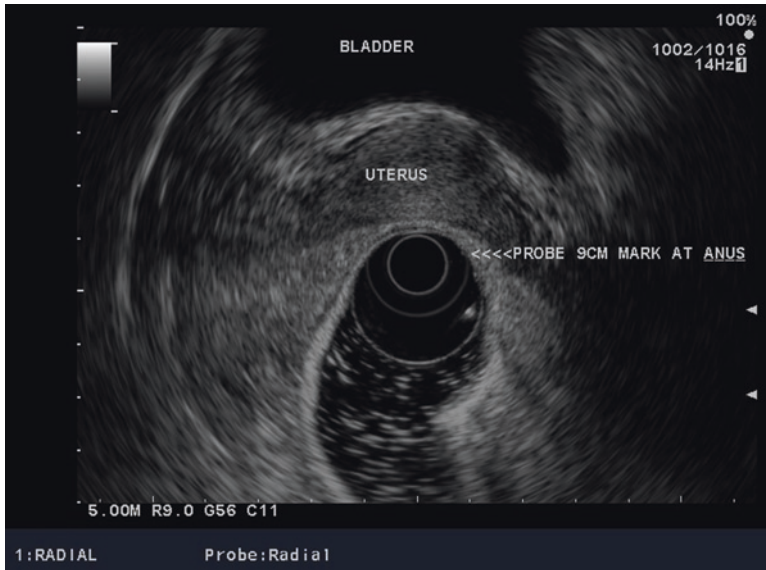


Fig. 3. Female rectum: 9 cm proximal to the anus with the uterus immediately anterior and the bladder deeper to the rectal wall. These structures can be oriented along the top of the screen to establish the anterior reference for the remainder of the exam.

the aorta and celiac axis are good starting points when attempting to evaluate the body of the pancreas. From the celiac axis, pushing distally should bring the body of the pancreas into view, with the splenic vessels and splenoportal confluence framing the gland along its inferior margin. Pitfalls associated with this particular maneuver include: the deeper celiac axis precluding adequate visualization, and a proximal gastric configuration where the scope lodges at the fundus-body junction instead of sliding along the greater curve. Solutions include using appropriate tip deflection and torque: downward deflection while attempting to visualize the deep celiac axis and upward deflection with rightward torque to follow the greater curve distally.

TECHNICAL ISSUES

There are a few technical solutions to improve image quality. Acoustic coupling is an important ultrasound concept particularly relevant to EUS, as the transducer is often in an air-filled lumen. Because ultrasound waves do not penetrate air, eliminating air from the equation is imperative. Air elimination begins before the scope is passed, while testing the balloon covering the ultrasound transducer. The water bottle attached to the scope should be full. Ensure the balloon is completely filled with water and aspirated several times while manipulating air bubbles toward the suction port in order to expel them. In the patient, the balloon should be filled with water to varying degrees at nearly all stages of the EUS exam. Care should also be taken to minimize insufflation of air through the scope and to suction air from the lumen of the GI tract whenever possible. Even after appropriate precautions, air bubbles within the scope balloon may be an issue limiting exams. Options include withdrawal of the scope to attempt to clear the bubble(s) followed by repeat passage, or proceeding with the image field defect and compensating by scope tip manipulations precluding interference with the anatomic view of interest.

In patients with a history of significant latex allergy, it is not recommended to use standard endoscope balloons for acoustic coupling. In such cases, water instillation into the lumen may be used to “submerge” the ultrasound transducer and replace air in the lumen. Water instillation is also useful when attempting to generate detailed views of the gut wall layers, such as clarifying small subepithelial lesions and staging ampullary neoplasms. Remember that water instillation into the upper GI tract is an aspiration risk. Position the patient appropriately and use oral suction diligently. On this note, be cognizant of the aspiration pitfall during any upper EUS exam, particularly in patients with potential gastric outlet obstruction or after induction of deeper sedation.

EUS systems have variable control settings to obtain better quality images. Until providers gain the depth of knowledge created by supplemental reading and experience, complex manipulations of the system settings should be avoided while in search of the perfect image. Routinely performing complex manipulations potentially wastes time and may force a trip by a company ultrasound technician to reset the system. There are a few controls that are standard with all systems and easy to manipulate. Among these are the frequency settings. Low frequencies increase the ability to resolve structures at greater distances from the transducer (such as a lesion deep in the liver), while high frequencies increase the ability to resolve structures close to the transducer (such as gut wall layers). Magnification is another control, and conveys maximal image detail of a point of interest at a given distance from the transducer. Finally, gain and contrast settings allow focusing and the ability to adjust brightness. Keep in mind that even when settings are properly utilized, some structures are harder or impossible to clearly image in certain patients. An example is the pancreas that cannot be differentiated from surrounding tissues because it is infiltrated by fat, appearing brighter than usual and amorphous. In this instance, anatomic landmarks such as vasculature are helpful.

EUS INDICATIONS

Failure to understand diagnostic limitations of EUS can result in pitfalls. Most of these pitfalls are avoidable if limitations are understood and discussed with patients and referring physicians prior to examinations. Although EUS may heighten diagnostic accuracy, it is important to note that EUS providers should not overlook the clinical history and standard radiographic data. Even more critical, EUS is not a substitute for histology. For example, when attempting to identify the etiology of nonhealing gastric ulceration or thickened folds of the stomach, the absence of muscularis propria expansion and perigastric lymphadenopathy may reassure against malignancy, but standard endoscopic biopsy information and surveillance may still be indicated. It is perilous to perceive EUS as able to “rule out” cancer in this situation. Another example is a patient with abdominal pain, weight loss, and a limited quality computerized tomography (CT) scan revealing fullness of the pancreatic head. In this scenario, a hypodense expansion of the pancreatic head on EUS could be secondary to malignancy or pancreatitis. Even if fine needle aspiration (FNA) is performed, there may be false negative sampling errors or nondiagnostic samples (8, 9). Furthermore, sampling acute pancreatitis with or without fluid collections may confer additional risks, including

infectious complications (10, 11). The full history with supporting lab data and perhaps a better quality pancreatic protocol CT scan as a surveillance measure may be indicated. In some cases, surgical exploration should be considered if the history and CT findings are consistent with a malignant process, even if the FNA results are reassuring.

In summary, a thorough clinical history and good quality radiographic data are essential for proper case selection and to help formulate more accurate EUS impressions and recommendations. Sometimes, proper evaluation of data obtained noninvasively will prevent unnecessary EUS exams, or allow EUS to be delayed in order to maximize the clinical utility and safety of the exam.

For tumor staging, several pitfalls are important to keep in mind, as data may be paramount to oncology team members' treatment decisions regarding resectability and neoadjuvant therapy. One important pitfall is overstaging due to tumor inflammatory changes, particularly when attempting to differentiate between T1/T2 and T2/T3 lesions. Understaging lesions is also a potential problem, often when dealing with early node metastasis where the nodes are subcentimeter and less abnormal appearing (12, 13). Difficulty predicting vascular involvement of the mesenteric vessels in pancreatic cancer staging is another pitfall (14, 15). Staging after chemotherapy and radiation therapy is inaccurate because EUS cannot distinguish tumor from scarring (16). A repeat exam after neoadjuvant therapy, however, can sometimes be helpful to reassure against persistence of widespread nodal disease and new metastatic disease (17). An example would be an older patient, with locally advanced esophageal cancer and marginal performance status, who has completed neoadjuvant therapy and apparently has stable disease by repeat CT and positron emission tomography (PET). CT scans and PET scans may have difficulty characterizing lesions less than one centimeter, particularly metastatic lymph nodes in this size range, although this is an evolving topic (18–20). If a repeat EUS exam with FNA proves that multiple locoregional nodes remain diseased, this poor prognostic information may affect the decision to proceed with surgery. Even more importantly, if metastatic disease were proven by FNA in the celiac or cervical regions after neoadjuvant therapy, most centers would not proceed with surgery.

EQUIPMENT SELECTION

Choosing the appropriate equipment for the particular indication can avoid pitfalls. Probes are often useful for intramural lesions and superficial cancers to provide T-staging information while radial exams have been

advocated to help detect locoregional lymphadenopathy, particularly for esophageal and rectal cancer (21, 22). Linear scopes have advantages resolving extra luminal structures such as liver lesions and in visualizing vascular involvement by tumors. Furthermore, linear scopes are necessary for tissue sampling to heighten metastatic disease staging accuracy or provide definitive diagnosis of deep wall lesions such as gastrointestinal stromal tumors (23, 24).

In general, linear scopes should be used when the etiology is strongly suspected by cross sectional imaging and tissue sampling is the indication for the exam. A clear example is a patient with back pain and weight loss, positive serum tumor markers, and a pancreatic body mass encasing the celiac axis and SMA. A less clear example arises in esophageal cancer staging, particularly when confronted with a moderate stenosis and the need to clarify upper abdominal node status. Initial use of the linear EUS scope will expedite definitive tissue sampling and may be safer if the compromised esophageal lumen is crossed only once with an EUS scope and sedation is limited. However, omitting the radial exam may compromise staging accuracy, and it is possible that FNA will not be indicated during the exam.

Some complicated disease processes may benefit from radial exams, particularly when cross-sectional imaging suggests the normal anatomy may be obscured and/or there has been a significant time interval since the most recent cross sectional imaging. In such cases, radial exams confer the benefit of a 360° view, which may facilitate EUS interpretation, particularly for radiologists and surgeons using EUS data to facilitate clinical decision-making. Examples include pancreatic and gallbladder mass lesions in patients with recent clinical histories consistent with inflammatory etiologies.

Endoscopy unit efficiency is also a consideration when choosing equipment. An example is thickened gastric folds or small superficial appearing gastric wall lesions. If an EUS probe is applied, it can clarify a need for deeper wall sampling attempts or mucosectomy. The endoscope necessary to perform these maneuvers is already in position. Savings may include exam and equipment reprocessing time.

FNA CONSIDERATIONS

Bleeding risks and management of anticoagulants are often debated in the periprocedure period. Data suggest that bleeding complications are rare, but appear to have a higher incidence when sampling cystic lesions and pancreatitis (25). More recent publications and societal guidelines emphasize that antiplatelet agents may be safely continued

for many therapeutic endoscopy procedures, including polypectomy and dilation (26, 27). Providers should attempt to make evidence-based decisions as data evolve. At present, it appears that a strict policy of several days off antiplatelet and anticoagulant medications before or after FNA procedures should be reconsidered in patients at high risk for cardiovascular events. Often, continuing monotherapy with either aspirin or another platelet inhibitor may be an option. Heparin and/or coumadin may be safely restarted immediately after the procedure if there are no signs of postprocedure complications. Prudent endosonographers should involve cardiologists and primary physicians in patients at higher risk for periprocedure cardiovascular events. Avoid the pitfall of standardized written or verbal instructions to stop platelet inhibiting medications and coumadin five days prior to procedures or delay the use of these agents after procedures.

Passage of the FNA sheath through the scope once in position can be compromised by angulation of the scope tip. Few things are more frustrating than spending 10 min locating a pancreatic head lesion, only to be stymied by the inability to advance and lock the FNA sheath in place. Corrective measures include losing position by straightening the scope tip to pass the device, or using a more flexible FNA sheath and needle. Penetration of the GI wall while maintaining visualization of the target may also be difficult. Corrective actions include opposing the scope tip more completely against the wall with an upward control deflection after suctioning all air from the lumen followed by a quick forceful thrust with the needle as opposed to a slow and controlled push. If these measures fail, the stylet may be pulled back, so only the sharp bevel of the needle is presented against the wall. Removal of the stylet during needle passage increases the probability that lesion samples will be contaminated by gut epithelium. Finally, a 25-gauge needle may allow easier puncture of the wall layers and access to a lesion, while maintaining EUS visualization.

Poor visualization of the needle may also result if aiming adjustments are made by turning the tip of the scope right or left to bring a target into view. Avoid this pitfall by using torque on the scope, instead of the right and left turn dial, as the linear EUS array will provide a better view of the needle path to the target. A bent FNA needle may be very hard to visualize en route to the target, and the easiest adjustment is to replace it with a new apparatus. Although more flexible sheaths and needles, as previously mentioned, are tremendous assets to ease passage through scopes, they are more easily bent. Adjusting the scope tip position so less elevator lift is required to hit the target will help prevent “crooked arrow” mishaps, and is also likely to decrease costs (Fig. 4).

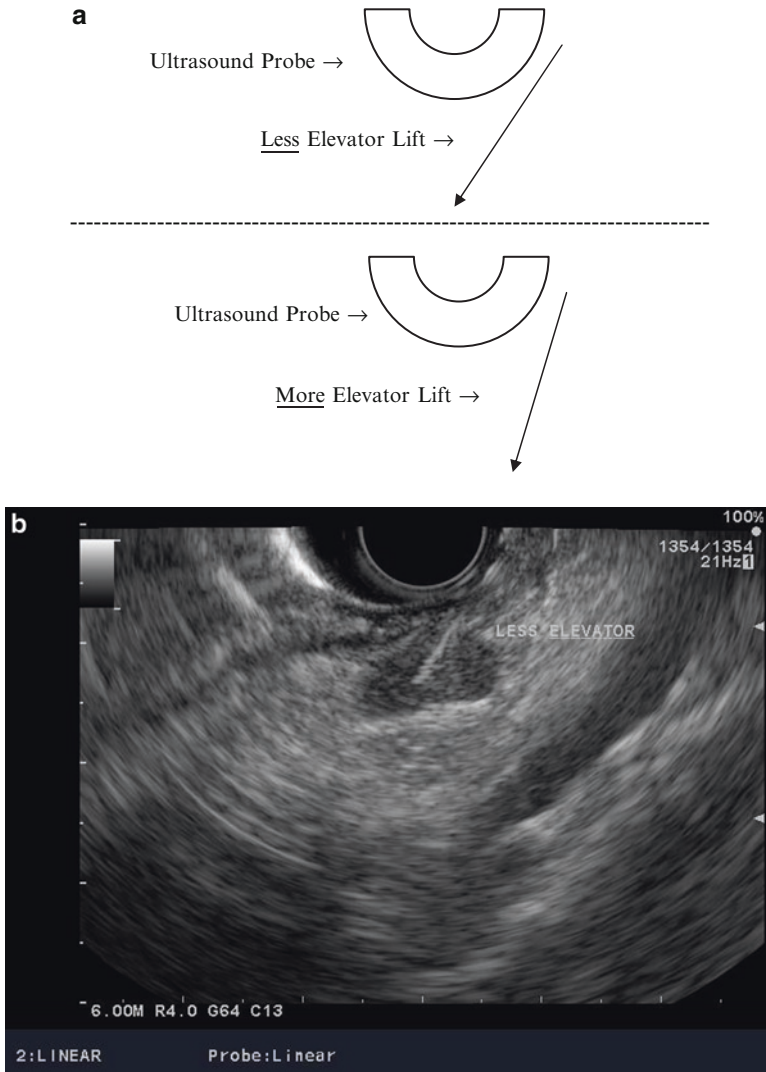


Fig. 4. (a) Targeting lesions: Note the angle between the center of the EUS probe and the needle. This angle is influenced by variables, including the depth of scope insertion, degree of tip deflection toward the target, and the amount of elevator deflection on the needle sheath. (b) Mediastinal node sampling with less tip deflection toward the target and less elevator pressure on the needle sheath. (c) Same mediastinal node but sampled with more tip deflection toward the target and more elevator pressure on the needle sheath. (d) Bent FNA needle sheath resulting from more elevator pressure in targeting a lesion.

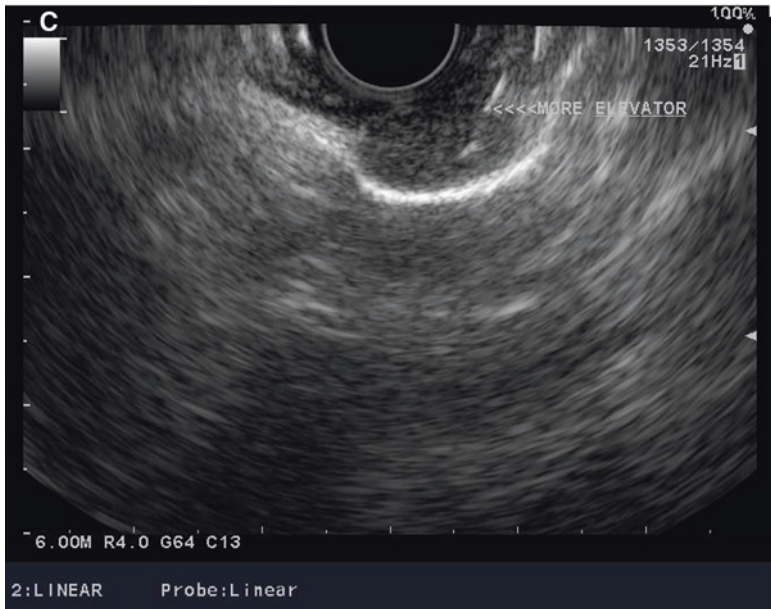


Fig. 4. (continued)

In order to mitigate the nondiagnostic pitfalls of FNA, form a good working relationship with cytology staff. It has been clearly shown that the presence of cytopathology staff on-site to assist in preparation and interpretation of specimens will increase diagnostic FNA accuracy

(28–31). The minimum possible number of FNA passes can be obtained in this fashion, which may decrease procedure time and complications. Additionally, there will be less need for repeat sampling procedures. Because physical presence is less cost-effective for billing by cytology staff, it has been debated whether having on-site cytopathology interpretation is more cost-effective in general (32, 33). For endosonographers, patients, and third party payers, it appears clear that on-site cytopathology preparation and interpretation is optimal practice (34).

Endoscopy unit staff requirements may also depend upon the relationship that is established with cytopathology. Equipment setup and processing combined with patient care typically require both an endoscopy technician and endoscopy nurse for EUS FNA procedures, even if an anesthesiologist or CRNA is involved. If a cytopathologist and/or cytopathology technician is actively involved with slide preparation, endoscopy unit staffing requirements may be less rigorous.

CONCLUSION

In summary, pitfalls of EUS are many and varied. Concentrating on patient specific and equipment-related issues will be particularly beneficial to those learning EUS. Providers concerned with endoscopy unit management should thoroughly consider select topics, including sedation, equipment choice, and FNA. Hopefully, most pitfalls in practice will not feel as deep after reviewing this chapter, promoting less frustration and greater satisfaction for practitioners employing this exciting technology.

REFERENCES

1. Sahai AV. Balloon-assisted esophageal intubation to prevent cervical perforation during EUS. *Gastrointest Endosc.* 2002;55:140–1.
2. Dabezies MA. Esophageal intubation over a guide wire. *Gastrointest Endosc.* 1993;39(4):597.
3. Parmar KS, Zwischenberger TB, Reeves AL, Waxman I. Clinical impact of endoscopic ultrasound-guided fine needle aspiration of celiac axis lymph nodes (M1a disease) in esophageal cancer. *Ann Thorac Surg.* 2002;73(3):916–20.
4. Jacobson BC, Shami VM, Faigel KO, Larghi A, Kahaleh M, Dye C, et al. Through-the-scope balloon dilation for endoscopic ultrasound staging of stenosing esophageal cancer. *Dig Dis Sci.* 2007;52(3):817–22.
5. Huck H, Goldberg M, Ruchim M. The “Hansel and Gretel” technique for access problems during ERCP. *Gastrointest Endosc.* 1994;40(3):387–8.
6. Gupta K, Mallery S. Small caliber endobronchial ultrasonic videoscope: successful transesophageal and transgastric FNA after failed passage of a standard ultrasound endoscope. *Gastrointest Endosc.* 2007;66(3):574–7.

7. Menniger R, Tuebergen D, Kochler G, Sauerland C, Senninger N, Bruewer M. Endoscopic ultrasound with conventional probe and miniprobe in pre-operative staging of esophageal cancer. *J Gastrointest Surg.* 2008;12(2):256–62.
8. Fritscher-Ravens A, Brand L, Knofel WT, Bobrowski C, Topalidis T, Thonke F, et al. Comparison of EUS-guided FNA for focal pancreatic lesions in patients with normal parenchyma and chronic pancreatitis. *Am J Gastroenterol.* 2002;97(11):2768–75.
9. Eloubeidi MA, Varadarajulu S, Desai S, Shirley R, Heslin MJ, Mehra M, et al. A prospective evaluation of an algorithm incorporating routine pre-operative EUS-FNA in suspected pancreatic cancer. *J Gastrointest Surg.* 2007;11(7):813–9.
10. Gress F, Michael H, Gelrud D, Patel P, Gottlieb K, Singh F, et al. EUS-guided fine-needle aspiration of the pancreas: evaluation of pancreatitis as a complication. *Gastrointest Endosc.* 2002;56:864–7.
11. Wiersema MJ, Vilmann P, Giovannini M, Chang KJ, Wiersema LM. Endosonography-guided fine-needle aspiration biopsy: diagnostic accuracy and complication assessment. *Gastroenterology.* 1997;112:1087–95.
12. Shami VM, Waxman I. Endoscopic ultrasound-guided fine needle aspiration in esophageal cancer. *Minerva Chir.* 2002;57(6):811–8.
13. Rosenberg J, White GE, Shami V, Villaflor V, Ferguson M, Dye C. Accuracy and utility of Endoscopic Ultrasound (EUS) in clinical stage T2N0 Esophageal Cancer. *Am J Gastroenterol.* 2008;103(S1):A74. S31.j.
14. Wiersema MJ. Identifying contraindications to resection in patients with pancreatic carcinoma: the role of endoscopic ultrasound. *Can J Gastroenterol.* 2002;16(2):109–14.
15. Bao PQ, Johnson JC, Lindsey EH, Schuartz DA, Arildsen RC, Grzeszcz K, et al. EUS and CT predictors of pancreatic cancer resectability. *J Gastrointest Surg.* 2008;12(1):10–6.
16. Vanagunas A, Lin DE, Stryker SJ. Accuracy of endoscopic ultrasound for restaging rectal cancer following neoadjuvant chemoradiation therapy. *Am J Gastroenterol.* 2004;99(1):109–12.
17. Zuccaro Jr G. Endoscopic ultrasound classification of esophageal cancer after chemotherapy or chemoradiotherapy. *Am J Gastroenterol.* 2006;101(6):1222–33.
18. Sandha GS, Severin D, Postema E, McEwan A, Stewart K. Is positron emission tomography useful in locoregional staging of esophageal cancer? Results of a multidisciplinary initiative comparing CT, positron emission tomography, and EUS. *Gastrointest Endosc.* 2008;67(3):402–9.
19. Facey K, Bradbury I, Laking G, Payne E. Overview of the clinical effectiveness of positron emission tomography imaging in selected cancers. *Health Technol Assess.* 2007;11(44):iii–iv. xi–267.
20. Jamil LH, Gill KRS, Wallace MB. Staging and restaging of advanced esophageal cancer. *Curr Opin Gastroenterol.* 2008;24(4):530–4.
21. Rampado S, Bocus P, Battaglia G, Ruol A, Portale G, Ancona E. Endoscopic ultrasound: accuracy in staging superficial carcinomas of the esophagus. *Ann Thorac Surg.* 2008;85(1):251–6.
22. Hünerbein M, Totkas S, Ghadimi BM, Schlag PM. Preoperative evaluation of colorectal neoplasms by colonoscopic miniprobe ultrasonography. *Ann Surg.* 2000;232(1):46–50.

23. Shami VM, Parmer KS, Waxman I. Clinical impact of endoscopic ultrasound and endoscopic ultrasound-guided fine-needle aspiration in the management of rectal carcinoma. *Dis Colon Rectum*. 2004;7(1):59–65.
24. Vilmann P, Khattar S, Hancke S. EUS examination of the upper GI tract using a curved array transducer: a preliminary report. *Surg Endosc*. 1991;5(2):79–82.
25. Shah JN, Muthusamy R. Minimizing complications of endoscopic ultrasound and EUS-guided fine needle aspiration. *Gastrointest Endosc Clin N Am*. 2007;17:129–43.
26. American Society for gastrointestinal endoscopy guideline. Guideline on the management of anticoagulation and antiplatelet therapy for endoscopic procedures. *Gastrointest Endosc*. 2002;55(7):775–9.
27. American Society for gastrointestinal endoscopy guideline. The management of low-molecular-weight heparin and nonaspirin antiplatelet agents for endoscopic procedures. *Gastrointest Endosc*. 2005;61(2):189–94.
28. Jhala NC, Eltoun IA, Eloubeidi MA, Meara R, Chhieng DC, Crowe DR, et al. Providing on-site diagnosis of malignancy in endoscopic-ultrasound-guided fine-needle aspirates: should it be done? *Ann Diagn Pathol*. 2007;11(3):176–81.
29. Klapman JB, Logrono R, Dye CE, Waxman I. Clinical impact of on-site cytopathology interpretation on endoscopic ultrasound-guided fine needle aspiration. *Am J Gastroenterol*. 2003;98:1289–94.
30. Layfield LJ, Bentz JS, Gopez EV. Immediate on-site interpretation of fine needle aspiration smears. *Cancer Cytopathol*. 2001;93:319–22.
31. Logrono R, Waxman I. Interactive role of the cytopathologist in EUS-guided fine needle aspiration: an efficient approach. *Gastrointest Endosc*. 2001;54:485–90.
32. Nasuti JF, Gupta PK, Baloch ZW. Diagnostic value and cost-effectiveness of on-site evaluation of fine needle aspiration specimens. *Diagn Cytopathol*. 2002;27:1–4.
33. Stelow EB, Bardales RH, Stanley MW. Pitfalls in endoscopic ultrasound-guided fine-needle aspiration and how to avoid them. *Adv Anat Pathol*. 2005;12(2):62–73.
34. Jhala NC, Jhala DN, Chieng DC, Eloubeidi MA, Eltoun IA. Endoscopic ultrasound-guided fine-needle aspiration. A cytopathologist's perspective. *Anat Pathol*. 2003;120:351–67.

Part II

EUS by Location

The Role of EUS in Esophageal Cancer

*Audrey H. Calderwood, MD
and Brian C. Jacobson, MD, MPH*

CONTENTS

INTRODUCTION
DIAGNOSIS
STAGING ESOPHAGEAL CANCER
T STAGING
N STAGING
M STAGING
RETAGING
DETECTING TUMOR RECURRENCE
BARRETT'S ESOPHAGUS
QUALITY INDICATORS
CONCLUSION

Abstract

Esophageal cancer is the fifth most common gastrointestinal cancer and the ninth leading cause of cancer death in the United States. The incidence of esophageal adenocarcinoma is on the rise. Accurate staging of esophageal cancer is critical for the selection of appropriate treatment. Endoscopic ultrasound (EUS) plays an important role in the staging of esophageal cancer. EUS provides a detailed view of the esophageal wall, helps determine tumor depth of infiltration, and can

From: *Clinical Gastroenterology: Endoscopic Ultrasound*,
Edited by: V. M. Shami and M. Kahaleh, DOI 10.1007/978-1-60327-480-7_7,
© Springer Science+Business Media, LLC 2010

characterize lymph nodes as malignant or benign. As such, EUS is the most accurate modality for regional staging of esophageal cancer and is more accurate than computed tomography and positron emission tomography scan for the characterization of nodal status. EUS plays a limited role in the detection of metastatic disease and restaging after neoadjuvant therapy. This chapter elaborates on the role of EUS in the care of patients with esophageal cancer.

Key Words: EUS, Esophageal cancer, Staging, Barrett's esophagus

INTRODUCTION

Esophageal cancer is the fifth most common gastrointestinal cancer and the ninth leading cause of cancer death in the United States. Every year, there are ~14,000 new cases of esophageal cancer diagnosed, of which ~8,000 are adenocarcinoma and 6,000 are squamous cell cancers. Adenocarcinoma of the esophagus has one of the fastest rising incidence rates of any malignancy in the United States (1). The outcome of esophageal cancer is strongly linked to its stage at diagnosis and the overall 5-year survival rate remains less than 20% (2). Accurate staging of esophageal cancer is critical for the selection of appropriate treatment. Endoscopic ultrasound (EUS) plays a central role in the staging of esophageal cancer and may also be important in detecting disease recurrence.

DIAGNOSIS

The role of EUS in the initial diagnosis of esophageal cancer is limited to cases in which routine endoscopy has failed to make a diagnosis (3). Specifically, if biopsies or brush cytology during endoscopy are nondiagnostic and the clinical suspicion remains high for malignancy, then EUS can be performed with or without fine needle aspiration (FNA) for a definitive diagnosis (4).

STAGING ESOPHAGEAL CANCER

Esophageal cancer is staged according to the TNM system established by the American Joint Committee on Cancer (AJCC) and the International Union Against Cancer (UICC) (Tables 1–3) (5, 6). This system incorporates the depth of invasion of the primary tumor (T classification), the status of regional lymph nodes (N classification) and the presence or absence of distant metastases (M classification). The TNM classifications are then grouped into stages according to prognosis (Tables 2 and 3). The 5-year survival rate is more than 95%

Table 1
TNM classification of esophageal cancer

T	Primary tumor
Tx	Tumor cannot be assessed
T0	No evidence of primary tumor
Tis	High-grade dysplasia
T1	Tumor invades the lamina propria, muscularis mucosae (T1a) or submucosa (T1b), but does not breach the submucosa
T2	Tumor invades the muscularis propria, but does not breach the muscularis propria
T3	Tumor invades the adventitia
T4	Tumor invades adjacent structures; T4a: resectable tumor invading the pleura, pericardium, or diaphragm, T4b: unresectable tumor invading other adjacent structures, such as aorta, vertebral body, trachea, etc.
N	Regional lymph nodes
NX	Regional lymph nodes cannot be assessed
N0	No regional lymph node metastases
N1	Metastasis in 1–2 regional lymph nodes
N2	Metastasis in 3–6 regional lymph nodes
N3	Metastasis in seven or more regional lymph nodes
M	Distant metastasis
M0	No distant metastasis
M1	Distant metastasis

Used with the permission of the American Joint Committee on Cancer (AJCC), Chicago, Illinois. The original source for this material is the AJCC Cancer Staging Manual, Seventh Edition (2010) published by Springer Science and Business Media LLC, <http://www.springerlink.com> (5)

Table 2
Anatomic stage/prognostic groups squamous cell carcinoma^a

<i>Stage</i>	<i>T</i>	<i>N</i>	<i>M</i>	<i>Grade</i>	<i>Tumor location</i>
0	Tis (HGD)	N0	M0	1, X	Any
IA	T1	N0	M0	1, X	Any
IB	T1	N0	M0	2–3	Any
	T2-3	N0	M0	1, X	Lower, X

^aOr mixed histology including a squamous component or NOS

(continued)

Table 2
(continued)

<i>Stage</i>	<i>T</i>	<i>N</i>	<i>M</i>	<i>Grade</i>	<i>Tumor location</i>
IIA	T2-3	N0	M0	1,X	Upper, middle
	T2-3	N0	M0	2-3	Lower, X
IIB	T2-3	N0	M0	2-3	Upper, middle
	T1-2	N1	M0	Any	Any
IIIA	T1-2	N2	M0	Any	Any
	T3	N1	M0	Any	Any
	T4a	N0	M0	Any	Any
IIIB	T3	N2	M0	Any	Any
IIIC	T4a	N1-2	M0	Any	Any
	T4b	Any	M0	Any	Any
	Any	N3	M0	Any	Any
IV	Any	Any	M1	Any	Any

^bLocation of the primary cancer site is defined by the position of the upper (proximal) edge of the tumor in the esophagus

Table 3
Anatomic stage/prognostic groups adenocarcinoma

<i>Stage</i>	<i>T</i>	<i>N</i>	<i>M</i>	<i>Grade</i>
0	Tis (HGD)	N0	M0	1,X
1A	T1	N0	M0	1-2, X
1B	T1	N0	M0	3
	T2	N0	M0	1-2, X
IIA	T2	N0	M0	3
IIB	T3	N0	M0	Any
	T1-2	N1	M0	Any
IIIA	T1-2	N2	M0	Any
	T3	N1	M0	Any
	T4a	N0	M0	Any
IIIB	T3	N2	M0	Any
IIIC	T4a	N1-2	M0	Any
	T4b	Any	M0	Any
	Any	N3	M0	Any
IV	Any	Any	M1	Any

for stage 0 disease, 50–80% for stage I disease, 30–40% for stage IIA disease, 10–30% for stage IIB disease and 10–15% for Stage III disease (7). The median survival for patients with metastatic disease treated with palliative chemotherapy is less than 1 year (8).

Accurate staging is therefore important for determining prognosis, guiding appropriate therapy, and allowing the evaluation of treatment protocols. Increasing T classification itself corresponds to worsening 5-year survival rates. The 5 year-survival rate is 46, 30, 22, and 7% for T1, T2, T3, and T4 tumors, respectively (9). By guiding appropriate therapy and avoiding unnecessary treatment, accurate staging may also reduce the costs of care of esophageal cancer. A retrospective review of cases of esophageal cancer referred for preoperative staging identified 26% of patients with stage I and stage IV tumors that could be spared neoadjuvant chemoradiotherapy and surgery, respectively for an average cost savings of \$3443 per patient (10).

T STAGING

EUS is the most accurate modality for regional staging of esophageal cancer. It provides a detailed view of the esophageal wall and helps determine tumor depth of infiltration.

Standard endoscopes operating at frequencies of 7.5 and 12 MHz are able to visualize the esophageal wall as a five-layered structure. Understanding the ultrasound appearance of the five layers of the normal esophagus allows us to recognize the degree of tumor infiltration into the wall layers and thus stage the primary lesion. The first hyperechoic layer of the esophagus seen on EUS corresponds to the superficial mucosa, the second hypoechoic layer corresponds to the deep mucosa, the third hyperechoic layer corresponds to the submucosa, the fourth hypoechoic layer to the muscularis propria, and the fifth hyperechoic layer corresponds to the adventitia (11). T1a lesions invade the lamina propria or muscularis mucosae, while T1b lesions invade the submucosa. By EUS, this appears as a hypodense lesion that extends into the second or third layer, but not through the third layer (Fig. 1). T2 lesions invade but do not breach the muscularis propria, which corresponds to the invasion of the fourth ultrasound layer (Fig. 2). T3 lesions invade the periesophageal tissue, but do not invade adjacent structures. By EUS, this corresponds to invasion beyond the fourth echolayer (Fig. 3). Lastly, T4a lesions are generally considered resectable and invade the pleura, pericardium, or diaphragm while T4b lesions are considered unresectable lesions that invade other adjacent structures such as the aorta, vertebral body, trachea, etc. (Fig. 4).

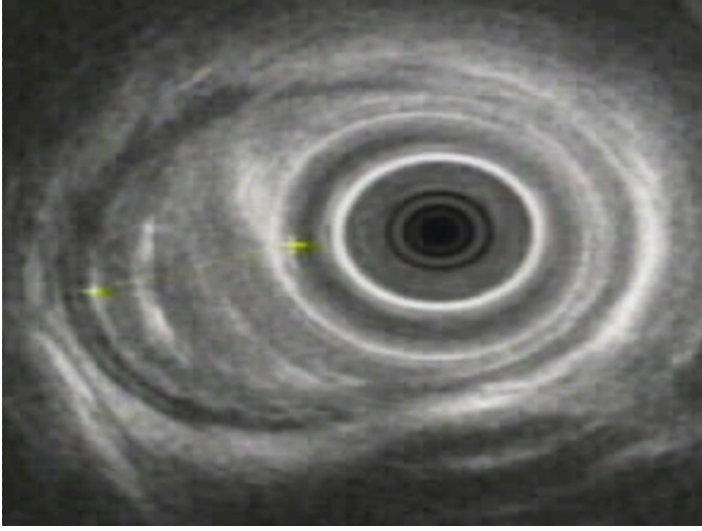


Fig. 1. T1b mass invading the submucosa but sparing the hypoechoic muscularis propria.

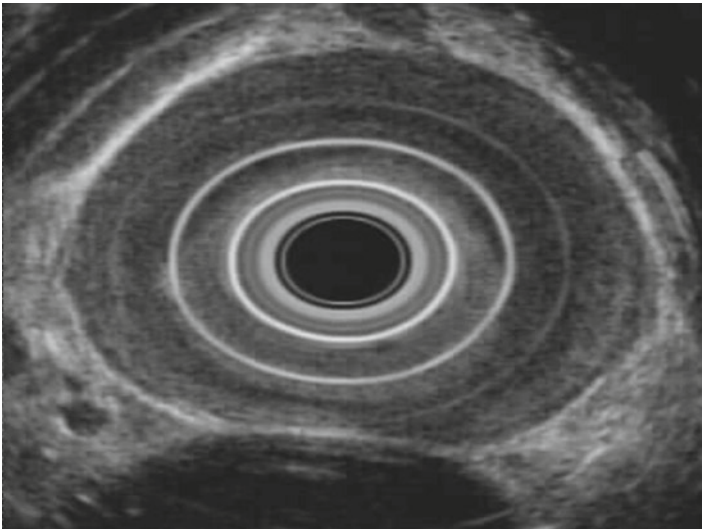


Fig. 2. A T2 cancer. The muscularis propria is involved, but the surrounding adventitia is not invaded.

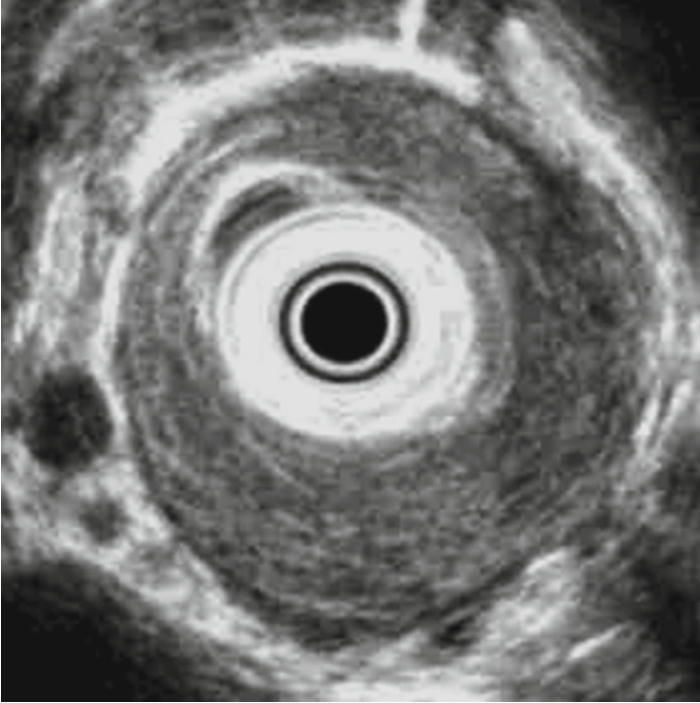


Fig. 3. A T3 tumor. The outer border of the tumor is irregular with pseudopod-like extension of tumor noted at the 6 o'clock position.

The choice of using either a transverse- or linear-array echoendoscope for esophageal cancer staging is likely influenced more by operator experience than superiority of one instrument over the other. One prospective study with 43 patients compared staging of esophageal and gastric cancers using transverse-array and linear-array echoendoscopes (12). Both instrument types provided similar T classifications; however, transverse-array instruments yielded better detection of lymph nodes. Another prospective study with 104 patients found excellent agreement in TNM staging between linear and radial endoscopes with similar accuracy stage for stage (13). Overall, the choice of echoendoscope should be tailored to each patient's clinical scenario and ideally, one should maintain efficiency while maximizing the quality of the exam (14). For example, a T3 tumor with suspected celiac nodes based on computed tomography (CT) may be best staged with only a linear-array echoendoscope to permit both T staging and FNA of the celiac nodes. A suspected T1 lesion without nodes on CT may be better staged with a transverse-array or radial echoendoscope.

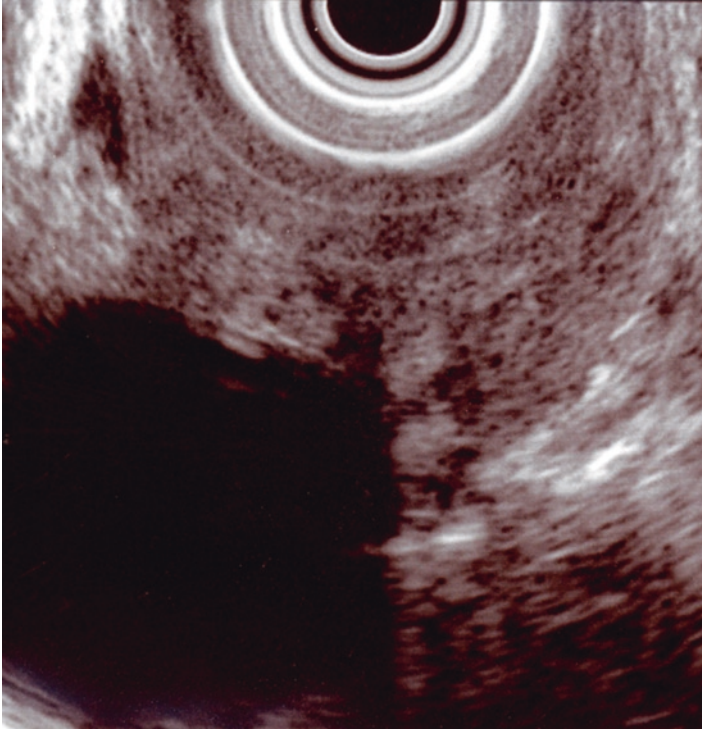


Fig. 4. A T4b tumor with invasion into the aorta noted by the loss of interface between the tumor and the great vessel.

A large body of literature supports EUS as the most accurate modality for local staging of esophageal cancer when compared to direct visualization endoscopy, CT, and positron emission tomography (PET) scanning. A review of 21 series found that EUS was 84% accurate for the prediction of T class (15). Other studies have found that the accuracy of EUS for T staging with most radial scanning 7.5–12 MHz transducers is between 75 and 92% compared to CT which has an accuracy of 42–60% (16–20).

However, the accuracy of EUS for staging of esophageal cancer varies by T classification (21). EUS is more reliable for staging T3 and T4 tumors, with accuracies of 89–94% and 88–100%, respectively, than it is for T1 and T2 tumors, with accuracies of 75–84% and 64–85%, respectively (16, 22). In particular, T2 lesions appear to be the most challenging because they are subject to overstaging (22, 23). EUS can differentiate T1 and T2 lesions from T3 or T4 lesions with 87% accuracy, 82% sensitivity, and 91% specificity (24).

High frequency miniprobe catheters (15–30 MHz) provide a more detailed visualization of the mucosa and submucosa, and their use therefore increases the accuracy of staging T1 and T2 tumors to 83–94% (25). One study of 22 patients compared preoperative staging by miniprobe with EUS, using surgical pathology as the gold standard. The accuracy of T staging was 86% for mucosal carcinoma and 94% for submucosal carcinoma using the miniprobe compared to 71% for mucosal carcinoma and 78% for submucosal carcinoma using standard frequency echoendoscopes (26). Therefore, miniprobes play an important role in the evaluation of superficial lesions being considered for nonsurgical treatment, including endoscopic mucosal resection (EMR) or photodynamic therapy (PDT). If disease is limited to the mucosa by EUS, EMR may be undertaken to provide pathologic staging useful in the management of early cancer or high grade dysplasia (27).

N STAGING

The TNM system for nodal staging of esophageal cancer has recently changed with an emphasis on both the location of lymph nodes as well as the number of lymph nodes since the data demonstrate that the number of regional lymph nodes containing metastases is the most important prognostic factor (Fig. 5). Regional lymph nodes extend from



Fig. 5. FNA of a subcarinal lymph node. The needle is the white line entering the hypoechoic node at the 1 o'clock position lymph node.

periesophageal cervical nodes to celiac nodes. A major difference between the old and new (as of 2010) staging system is that the involvement of a celiac lymph node is considered regional (N) and no longer metastatic disease (M1a).

An increasing number of malignant regional lymph nodes detected by EUS are associated with poorer survival in patients with esophageal cancer. In a retrospective case series of 85 patients with esophageal adenocarcinoma, those with 0, 1–2, and >2 malignant-appearing lymph nodes had median survivals of 66, 14.5, and 6.5 months, respectively (28).

EUS is one of the most accurate modalities available for the staging of regional lymph nodes. When examining lymph nodes by EUS, there are several features that can help predict malignancy. Size greater than 1 cm, round shape, sharply demarcated borders, and hypoechoic echotexture are all suggestive of malignancy. When all four features are present, the accuracy of these predictors is 80%; however, only a minority of lymph nodes will have all four features present at once (29, 30). The overall accuracy of EUS for N staging is 75–80% compared to CT scan, which has an overall accuracy of 51–74% (15, 17–19, 22). EUS is also superior to PET scan, which has an accuracy of 37–90% (31–34). In a prospective study of 75 patients with newly diagnosed esophageal cancer, the sensitivity and specificity for nodal involvement by modality were 86 and 67% for EUS, 84 and 67% for CT, and 82 and 60% for PET (20).

There are subtle differences in the ability of EUS to differentiate benign from malignant lymph nodes based on location. For example, EUS is more accurate when staging celiac lymph nodes than mediastinal lymph nodes. EUS has a sensitivity of 83%, specificity of 98%, and an accuracy of 95% for celiac lymph nodes compared to mediastinal lymph nodes, for which EUS has a sensitivity of 79%, specificity of 63% and an accuracy of 73% (35). The accuracy of N1 classification is higher than for N0 (89% vs. 69%) (15).

The use of FNA improves the ability of EUS to confirm malignant adenopathy. In a large multicenter trial of 171 patients with upper GI lesions, EUS with FNA for N classification was found to have a sensitivity of 92%, specificity of 92%, positive predictive value of 100%, and a negative predictive value of 86% with an overall accuracy of 92% (36). EUS with FNA has a superior accuracy to EUS alone with a rate of 87% compared to 74%, respectively in one series (37). In patients who have already undergone CT scan for staging of their esophageal cancer, EUS with FNA may change the tumor stage in a significant number of cases (38% in one series) (37). When performing FNA, at least three passes should be made to maximize sensitivity (38).

One limitation of FNA is the inability to aspirate lymph nodes that are located behind the primary tumor. Passage of a needle through the tumor to access the lymph node for aspiration can lead to contamination of the specimen with malignant cells from the primary tumor itself. Complications from FNA for staging of esophageal cancer are rare (39).

A selective approach to EUS-FNA for preoperative nodal staging of esophageal cancer has been evaluated in an attempt to minimize cost and address situations in which EUS-FNA is not technically feasible. Vazquez-Sequeiros et al. performed a prospective study of 144 patients with esophageal cancer who were evaluated with EUS. They found that a modified set of criteria, including the four standard criteria for malignant adenopathy (size, shape, borders, echotexture) helped predict malignancy (20, 40). The additional features included in their prediction model were the presence or absence of celiac lymph nodes, the number of lymph nodes (>5 vs. ≤ 5) and EUS T stage (T3/T4 vs. T1/T2). When the presence of at least one criterion was used as indicating N1 stage, sensitivity approached 100%, and when the presence of ≥ 6 criteria was used to indicate N1 stage, specificity approached 100%. In this study, the investigators found that a selective use of FNA might have avoided performing FNA in 42% of patients. These modified criteria may help the endosonographer better select which lymph nodes to target in order to enhance the diagnostic yield of EUS-FNA. The current standard of care is to perform EUS-FNA whenever feasible to maximize staging accuracy (41, 42).

In addition to FNA, elastography is emerging as another technique with the potential to improve staging. Elastography uses concepts similar to ultrasonography to convey information about the firmness of a tissue in response to compression (43). The clinical utility of elastography is based on the fact that malignant tissues are typically harder than benign tissues. Elastography software can be incorporated into EUS processors, making it an adjunctive technique during EUS, just as Doppler has become integrated into endosonography. Elastography may help distinguish benign from malignant lymph nodes, thereby allowing the endoscopist to select which nodes should be preferentially aspirated. It may also prove useful when staging nodes deemed inaccessible due to intervening vessels or adjacent tumor (44).

One study using EUS-elastography to distinguish benign from malignant nodes found a sensitivity and specificity of 100 and 50%, respectively (45). In another study with 78 lymph nodes (cervical, mediastinal, and abdominal), investigators found a sensitivity of 85%, specificity of 92%, and an accuracy of 88.5% (46). Before elastography becomes universally accepted, technical improvements must be made and reliable diagnostic algorithms will need to be established.

Staging in the Setting of Malignant Strictures

Complete assessment by EUS may be limited in the setting of esophageal obstruction. The incidence of malignant strictures that restrict the passage of an echoendoscope is ~30% (47). Studies suggest that failure to traverse such a stricture results in significantly decreased accuracy for both T and N staging (48, 49). Similarly, failure to pass an echoendoscope beyond a malignant stricture is an accurate predictor of advanced T classification and poorer survival. More than 90% of patients with a nontraversable stricture have stage III or IV disease (49). Median survival in patients with a nontraversable stricture is ~10 months compared to those without a stenosis, who have a median survival of ~20 months (50).

When faced with an obstructing malignant stricture, the endosonographer can choose to limit the EUS exam to the proximal tumor margin, perform esophageal dilation to permit passage of the echoendoscope, or attempt staging with a miniprobe (under direct visualization if a standard endoscope can traverse the stricture or blindly through the stricture). Stricture dilation may permit complete cancer staging, including the evaluation of the celiac axis, but it carries a risk of perforation estimated to range from 0 to 24% (48, 49, 51–53). Esophageal dilation may be performed using Savary-type wire-guided dilators or through-the-scope (TTS) balloon dilators.

In one study of 267 EUS examinations, 81 patients (30%) required dilation. Dilation was performed using Savary-Guillard wire-guided dilators in a gradual, step-wise fashion to a diameter of 9–18 mm. Successful dilation allowing the passage of the echoendoscope was accomplished in 85% of all patients and 94% of cases where the stricture was dilated to ≥ 14 mm (52). There were no complications. The accuracy of T staging after dilation, however, was only 61% which may indicate that trauma from the procedure disrupted normal tissue planes. In another study with 42 cases, Savary wire-guided dilations were carried out without fluoroscopy to a maximum diameter of 16 mm and no complications occurred (53). Dilation provided critical staging information in 19% of cases, including the detection of metastases (seven cases) and upstaging of a T3 tumor to T4 (one case). In 45% of these cases, celiac or retroperitoneal lymph nodes were found. Dilation to at least 14 mm diameter provided complete staging in 87% of patients. Dilation to 12.8 mm was insufficient to complete EUS with a 74% failure rate.

TTS balloon dilators may help complete staging in up to 95% of patients. In a multicenter retrospective study with 272 cases, 28% of cases required dilation (54). EUS was performed with a radial echoendoscope and FNA was then performed with a curved linear echoendoscope where

appropriate. Dilation was performed through at least two balloon sizes, but usually through three sizes of a single balloon without fluoroscopy. In this series, there were two perforations, one during EUS with dilation, and one during EUS without dilation. The perforation associated with dilation occurred when a TTS balloon was inflated directly to 16.5 mm. Nineteen percent of patients who required dilation had celiac adenopathy (previously considered M1a disease), and the authors concluded these nodes would have been missed had dilation not been undertaken. TTS balloon dilators may have advantages over bougienage because it does not require repeated esophageal intubations or fluoroscopy.

An alternative to dilation is to use either catheter miniprbes or, when available, a 7.5 MHz nonoptical, wire-guided esophagoprobe made by Olympus (MH908; Olympus America, Melville, NY). Mallery and Van Dam compared EUS outcomes at one institution before and after the introduction of the wire-guided MH908 esophagoprobe (47). They found the rate of complete staging increased from 60 up to 90% with an increased detection rate for metastatic disease (34% vs. 11%). One drawback of the use of such radial-array EUS probes in this setting is the inability to perform FNA of any visualized lymph nodes.

M STAGING

Patients with distant metastasis are not amenable to surgical resection and are candidates for palliative treatment only. Distant metastases from esophageal cancer occur in nonregional lymph nodes, the liver (35%), the lungs (20%), bone (9%), adrenal glands (2%), the brain (2%), and the spleen, pancreas, stomach, and pericardium (1%) (55).

The AJCC TNM M classification is characterized by the presence (M1) or absence (M0) of metastases. With the new classification, M1 is no longer further subdivided into distant lymph node metastases (M1a) and other metastases (M1b) as this was not found to be useful (Table 1). In the past, this distinction between M1a and M1b was felt to be clinically relevant as the treatment may differ between the two. In many tertiary care centers, M1a disease is treated with induction chemoradiotherapy followed by surgery with the goal of cure, whereas M1b stage is treated with palliative measures only. M1a tumors have a better 5-year survival than M1b disease (6 vs. 2%) (56). In the new classification system, celiac lymph node involvement is considered regional nodal disease (N), while all distant disease is considered metastatic (M1).

Radiological imaging, with PET or CT scanning, is superior to EUS when screening for M1 disease. PET scan may be the most accurate tool

in this setting. In one study of 100 patients with esophageal cancer, PET scanning had a sensitivity of 69%, and an accuracy of 84% compared with CT scanning which had a sensitivity of 45% and an accuracy of 63% (57). A recent prospective study of 75 patients with newly diagnosed esophageal cancer evaluated by PET, CT, and EUS found similar performance for the detection of metastatic disease with PET and CT scan, which were both superior to EUS (20). PET scanning and CT scanning had sensitivity of 81% and specificity of 91 and 82%, respectively, for the detection of metastatic disease compared to sensitivity of 73% and specificity of 86% with EUS.

Some data suggests that EUS may be useful in screening for occult liver metastasis, which when small (<1 cm), can be missed by CT and even PET. Detection of occult liver metastases may help avoid unnecessary surgery. EUS, however, can only adequately assess the left hepatic lobe.

In a retrospective study of 98 patients with cancer of the esophagus or cardia, EUS found lesions suspicious for metastases in 7% of cases (58). FNA confirmed metastatic disease in four patients, while the fifth patient had a liver metastasis missed because of a falsely negative fine needle aspirate. The median size of the metastatic liver lesions was 5 mm, and they were all missed by CT or PET. Another study found that EUS detected metastatic liver lesions overlooked by conventional, cross-sectional CT imaging in 2% of cases (59).

RESTAGING

Tumor restaging by EUS after neoadjuvant chemoradiotherapy may help identify patients whose tumors have progressed in stage to T4 or M1, and who are thus no longer surgical candidates. However, PET scan is emerging as the most accurate modality for predicting pathologic tumor response and serves as an independent predictor of survival. The accuracy of PET and integrated PET/CT in this setting ranges from 76 to 89% (60, 61).

EUS is inaccurate for restaging after neoadjuvant therapy as chemotherapy and radiation result in significant inflammation and fibrosis that can have the same sonographic appearance as tumor. The inflammatory response and necrosis within the esophageal wall may be most pronounced within 2 weeks of completing neoadjuvant therapy, making this a particularly inaccurate period for EUS. In one retrospective study of 97 patients treated with neoadjuvant chemoradiotherapy, posttreatment EUS was only 27% accurate in predicting stage (62). Downstaging by EUS did not predict the absence of residual tumor at surgery. In another

retrospective study of 49 patients with stage II or III esophageal cancer, EUS was able to distinguish T1/T2 tumors from T3 tumors in only 26% of cases (63). The authors found that using the criterion of a greater than 50% reduction in tumor thickness by EUS was only 44% sensitive and 75% specific to predict down staging (63). A second limitation of EUS after neoadjuvant therapy is that lymph nodes may shrink in size but still contain micrometastases that will be missed by endosonography. In one study, the accuracy of EUS without FNA for detecting malignant adenopathy after chemotherapy was only 64% (62).

Some have hoped that EUS after neoadjuvant treatment might at least help predict survival. For example, Chak et al. evaluated the change in maximal cross-sectional area of a tumor as measured by EUS before and after chemoradiotherapy in 59 patients (64). They considered a 50% reduction in area as a response. They then followed patients for a median of 19 months and found a significant difference in survival between responders, whose median survival was 17.6 months, and nonresponders, whose median survival was 14.5 months. In another prospective study of 41 patients, a 50% reduction in maximal tumor cross-sectional area correlated with pathologic tumor regression (65). EUS correctly predicted a positive response in 87% of patients and correctly predicted failure to respond in 77% of patients. However, the clinical utility of this information may be limited, and the routine measuring of tumor cross-sectional area has not become a widespread practice.

DETECTING TUMOR RECURRENCE

Tumor recurrence is the most common cause of mortality in patients who have undergone resection. Approximately 50% of patients develop recurrent disease within 2 years of surgery. Postsurgery surveillance with EUS, or even standard endoscopy, is not part of routine follow-up care. However, studies have shown that EUS can detect cancer recurrence with a positive predictive value of 75–100% (66, 67). EUS is more sensitive than endoscopy in detecting locoregional recurrence, as recurrent disease is often extramucosal. In addition, fibrosis may be misinterpreted as recurrent cancer on CT, leading to misdiagnosis. In a study of 40 patients who underwent surgical resection of esophageal cancer, 10% had an unsuspected anastomotic recurrence diagnosed by EUS despite a negative CT (66). Similarly, in a study of 43 patients undergoing routine surveillance EUS every 6 months for at least 2 years after surgery, two-thirds did not have symptoms when recurrent disease was found (67). Whether or not the early detection of cancer recurrence after surgery impacts survival remains unknown.

BARRETT'S ESOPHAGUS

Barrett's esophagus is the most important risk factor for the development of adenocarcinoma of the esophagus. Patients with high-grade dysplasia or early adenocarcinoma are candidates for local endoscopic therapy with EMR or PDT. The role of EUS in Barrett's esophagus is to accurately diagnose superficial lesions in order to guide local, organ-sparing therapy and to exclude those with lymph node involvement that warrant surgical treatment.

Buskens et al. retrospectively examined preoperative EUS results from 77 patients who underwent subtotal esophagectomy for high-grade dysplasia or T1 adenocarcinoma (68). The authors found that EUS correctly predicted the absence of lymph node metastases in 93% of patients. Tumors that did not penetrate beyond the first third of the submucosal layer (m1, m2, m3, or sm1) did not have lymph node metastases. The negative predictive value of EUS for submucosal invasion and lymph node metastases was 95 and 93%, respectively. Infiltration of the tumor beyond the first third of the submucosal layer on EUS was a significant predictor of the presence of lymph node metastases. A study of 22 patients with Barrett's esophagus complicated by high-grade dysplasia or intramucosal carcinoma compared preoperative EUS findings to surgical pathologic evaluation (69). The authors found that preoperative EUS had 100% sensitivity, 94% specificity, and 100% negative predictive value for submucosal invasion and 100% sensitivity, 81% specificity, and 100% negative predictive value for lymph node involvement. EUS has also been shown to be superior to CT scan for T and N staging in early Barrett's cancers (70). EUS has not been shown to be effective for surveillance in Barrett's esophagus with high grade dysplasia or early carcinoma after the treatment with PDT (71).

QUALITY INDICATORS

The combined American Society of Gastrointestinal Endoscopy/American College of Gastroenterology Taskforce on Quality in Endoscopy developed several quality indicators specifically related to EUS in the setting of esophageal cancer staging (42). These include (1) using the AJCC/UICC TNM staging system when describing tumor and node findings, (2) documentation of celiac axis visualization in cases without obstruction, and (3) performing EUS-guided FNA of suspicious celiac lymph nodes when staging an intrathoracic tumor.

CONCLUSION

EUS plays an important role in the care of patients with esophageal cancer. In particular, EUS is essential in staging of the primary esophageal tumor and its nodal status. Although there is no consensus on an optimal staging strategy, EUS, CT scan, and PET scan should be considered complimentary modalities in the accurate staging of esophageal cancer. EUS in this setting is safe, with risks similar to standard upper endoscopy. Advancements in technology, such as elastography, may help further enhance the accuracy and efficiency of EUS. Future studies should address the impact of EUS on patient outcomes.

REFERENCES

1. Pera M, Cameron A, Tratek V, et al. Increasing incidence of adenocarcinoma of the esophagus and esophago-gastric junction. *Gastroenterology*. 1993;104:510–3.
2. Vollweiler J, Zuccaro G. Staging of Esophageal Cancer. In: Faigel DO, Kochman ML, editors. *Endoscopic Oncology*. Totowa, NJ: Humana; 2006.
3. Jacobson BJ, Hirota W, Baron TH, et al. The role of endoscopy in the assessment and treatment for esophageal cancer. *Gastrointest Endosc*. 2003;57:817–22.
4. Faigel DO, Deveney C, Phillips D, et al. Biopsy-negative malignant esophageal stricture: diagnosis by endoscopic ultrasound. *Am J Gastroenterol*. 1998;93:2257–60.
5. Edge SB, Byrd DR, Compton CC, et al. *AJCC Cancer Staging Manual*. 7th ed. New York: Springer; 2010.
6. Sobin L, Wittekind C. *TNM Classification of malignant tumours*. 6th ed. New York: Wiley; 2002.
7. Reed CE. Surgical management of esophageal carcinoma. *Oncologist*. 1999;4:95–105.
8. Enzinger PC, Ilson DH, Kelsen DP. Chemotherapy in esophageal cancer. *Semin Oncol*. 1999;26:12–20.
9. American Joint Committee on Cancer. Esophagus. In: Beahrs OH, Hansen DE, Hutter RVP, et al., editors. *Manual for staging of cancer*. 4th ed. Philadelphia: Lippincott Williams and Wilkins; 1992.
10. Shumaker DA, de Garmo P, Faigel DO. Potential impact of preoperative EUS on esophageal cancer management and cost. *Gastrointest Endosc*. 2002;56:391–6.
11. Kimmey MB, Martin RW, Haggitt RC, et al. Histologic correlates of gastrointestinal ultrasound images. *Gastroenterologica*. 1989;96:433–41.
12. Matthes K, Bounds BC, Collier K, et al. EUS staging of upper GI malignancies: results of a prospective randomized trial. *Gastrointest Endosc*. 2006;64:496–502.
13. Siemsen M, Svendsen LB, Knigge U, et al. A prospective randomized comparison of curved array and radial echoendoscopy in patients with esophageal cancer. *Gastrointest Endosc*. 2003;58:671–6.
14. Eloubeidi MA. Choosing from the expanding EUS armamentarium menu: high-frequency probes, radial or linear endosonography for staging of upper GI malignancy? *Gastrointest Endosc*. 2006;64:503–4.

15. Rosch T. Endosonographic staging of esophageal cancer: a review of the literature results. *Gastrointest Endosc Clin N Am.* 1995;5(3):537–47.
16. Rosch T. Esophageal cancer: the munich experience. In: Van Dam J, Sivak M, editors. *Gastrointestinal endosonography.* Philadelphia: WB Saunders; 1999.
17. Botet JF, Lightdale CJ, Zauber AG, et al. Preoperative staging of esophageal cancer: comparison of endoscopic US and dynamic CT. *Radiology.* 1991;181:419–25.
18. Kienle P, Buhl K, Kuntz C, et al. Prospective comparison of endoscopy, endosonography and computed tomography for staging of tumours of the oesophagus and gastric cardia. *Digestion.* 2002;66:230–6.
19. Tio TL, Cohen P, Coene PP, et al. Endosonography and computed tomography of esophageal carcinoma. Preoperative classification compared to the new (1987) TNM system. *Gastroenterology.* 1989;96:1478–86.
20. Lowe VJ, Booya F, Fletcher JG, et al. Comparison of positron emission tomography, computed tomography, and endoscopic ultrasound in the initial staging of patients with esophageal cancer. *Mol Imaging Biol.* 2005;7:422–30.
21. Saunders HS, Wolfman NT, Ott DJ. Esophageal cancer. Radiologic staging. *Radiol Clin North Am.* 1997;35:281–94.
22. Heidemann J, Schilling MK, Schmassmann A, et al. Accuracy of endoscopic ultrasonography in preoperative staging of esophageal carcinoma. *Dig Surg.* 2000;17:219–24.
23. Vollweiler J, Zuccaro G. Staging of esophageal cancer. In: Faigel DO, Kochman ML, editors. *Endoscopic oncology: gastrointestinal endoscopy and cancer management.* Totowa, NJ: Humana; 2006. p. 31–42.
24. Rice TW, Blackstone EH, Adelstein DJ, et al. Role of clinically determined depth of tumor invasion in the treatment of esophageal carcinoma. *J Thorac Cardiovasc Surg.* 2003;125:1091–102.
25. Murata Y, Suzuki S, Ohta M, et al. Small ultrasonic probes for determination of the depth of superficial esophageal cancer. *Gastrointest Endosc.* 1996;44:23–8.
26. Hasegawa N, Niwa Y, Arisawa T, et al. Preoperative staging of superficial esophageal carcinoma: comparison of an ultrasound probe and standard endoscopic ultrasonography. *Gastrointest Endosc.* 1996;44:388–93.
27. Larghi A, Lightdale CJ, Memeo L, et al. EUS followed by EMR for staging of high-grade dysplasia and early cancer in Barrett's esophagus. *Gastrointest Endosc.* 2005;62:16–23.
28. Chen J, Xu R, Hunt GC, et al. Influence of the number of malignant regional lymph nodes detected by endoscopic ultrasonography on survival stratification in esophageal adenocarcinoma. *Clin Gastroenterol Hepatol.* 2006;4:573–9.
29. Catalano MF, Sivak Jr MV, Rice T, et al. Endosonographic features predictive of lymph node metastasis. *Gastrointest Endosc.* 1994;40:442–6.
30. Bhutani MS, Hawes RH, Hoffman BJ. A comparison of the accuracy of echo features during endoscopic ultrasound (EUS) and EUS-guided fine-needle aspiration for diagnosis of malignant lymph node invasion. *Gastrointest Endosc.* 1997;45:474–9.
31. Block MI, Patterson GA, Sundaresan RS, et al. Improvement in staging of esophageal cancer with the addition of positron emission tomography. *Ann Thorac Surg.* 1997;64:770–6. discussion 776–7.

32. Kole AC, Plukker JT, Nieweg OE, et al. Positron emission tomography for staging of oesophageal and gastroesophageal malignancy. *Br J Cancer*. 1998;78:521–7.
33. Luketich JD, Schauer PR, Meltzer CC, et al. Role of positron emission tomography in staging esophageal cancer. *Ann Thorac Surg*. 1997;64:765–9.
34. Rankin SC, Taylor H, Cook GJ, et al. Computed tomography and positron emission tomography in the pre-operative staging of oesophageal carcinoma. *Clin Radiol*. 1998;53:659–65.
35. Catalano MF, Alcocer E, Chak A, et al. Evaluation of metastatic celiac axis lymph nodes in patients with esophageal carcinoma: accuracy of EUS. *Gastrointest Endosc*. 1999;50:352–6.
36. Wiersema MJ, Vilmann P, Giovannini M, et al. Endosonography-guided fine-needle aspiration biopsy: diagnostic accuracy and complication assessment. *Gastroenterology*. 1997;112:1087–95.
37. Vazquez-Sequeiros E, Wiersema MJ, Clain JE, et al. Impact of lymph node staging on therapy of esophageal carcinoma. *Gastroenterology*. 2003;125:1626–35.
38. Wallace MB, Kennedy T, Durkalski V, et al. Randomized controlled trial of EUS-guided fine needle aspiration techniques for the detection of malignant lymphadenopathy. *Gastrointest Endosc*. 2001;54:441–7.
39. Adler DG, Jacobson BC, Davila RE, et al. ASGE guideline: complications of EUS. *Gastrointest Endosc*. 2005;61:8–12.
40. Vazquez-Sequeiros E, Levy MJ, Clain JE, et al. Routine vs. selective EUS-guided FNA approach for preoperative nodal staging of esophageal carcinoma. *Gastrointest Endosc*. 2006;63:204–11.
41. Eloubeidi MA. Routine EUS-guided FNA for preoperative nodal staging in patients with esophageal carcinoma: is the juice worth the squeeze? *Gastrointest Endosc*. 2006;63:212–4.
42. Jacobson BC, Chak A, Hoffman B, et al. Quality indicators for endoscopic ultrasonography. *Am J Gastroenterol*. 2006;101:898–901.
43. Taylor LS, Porter BC, Rubens DJ, et al. Three-dimensional sonoelastography: principles and practices. *Phys Med Biol*. 2000;45:1477–94.
44. Jacobson BC. Pressed for an answer: has elastography finally come to EUS? *Gastrointest Endosc*. 2007;66:301–3.
45. Giovannini M, Hookey LC, Bories E, et al. Endoscopic ultrasound elastography: the first step towards virtual biopsy? Preliminary results in 49 patients. *Endoscopy*. 2006;38:344–8.
46. Saftoiu A, Vilmann P, Ciurea T, et al. Dynamic analysis of EUS used for the differentiation of benign and malignant lymph nodes. *Gastrointest Endosc*. 2007;66:291–300.
47. Mallery S, Van Dam J. Increased rate of complete EUS staging of patients with esophageal cancer using the nonoptical, wire-guided echoendoscope. *Gastrointest Endosc*. 1999;50:53–7.
48. Catalano MF, Van Dam J, Sivak Jr MV. Malignant esophageal strictures: staging accuracy of endoscopic ultrasonography. *Gastrointest Endosc*. 1995;41:535–9.
49. Van Dam J, Rice TW, Catalano MF, et al. High-grade malignant stricture is predictive of esophageal tumor stage. Risks of endosonographic evaluation. *Cancer*. 1993;71:2910–7.

50. Hiele M, De Leyn P, Schurmans P, et al. Relation between endoscopic ultrasound findings and outcome of patients with tumors of the esophagus or esophagogastric junction. *Gastrointest Endosc.* 1997;45:381–6.
51. Kallimanis GE, Gupta PK, al-Kawas FH, et al. Endoscopic ultrasound for staging esophageal cancer, with or without dilation, is clinically important and safe. *Gastrointest Endosc.* 1995;41:540–6.
52. Pfau PR, Ginsberg GG, Lew RJ, et al. Esophageal dilation for endosonographic evaluation of malignant esophageal strictures is safe and effective. *Am J Gastroenterol.* 2000;95:2813–5.
53. Wallace MB, Hawes RH, Sahai AV, et al. Dilation of malignant esophageal stenosis to allow EUS guided fine-needle aspiration: safety and effect on patient management. *Gastrointest Endosc.* 2000;51:309–13.
54. Jacobson BC, Shami VM, Faigel DO, et al. Through-the-scope balloon dilation for endoscopic ultrasound staging of stenosing esophageal cancer. *Dig Dis Sci.* 2007;52:817–22.
55. Quint LE, Hepburn LM, Francis IR, et al. Incidence and distribution of distant metastases from newly diagnosed esophageal carcinoma. *Cancer.* 1995;76:1120–5.
56. Christie NA, Rice TW, DeCamp MM, et al. M1a/M1b esophageal carcinoma: clinical relevance. *J Thorac Cardiovasc Surg.* 1999;118:900–7.
57. Luketich JD, Friedman DM, Weigel TL, et al. Evaluation of distant metastases in esophageal cancer: 100 consecutive positron emission tomography scans. *Ann Thorac Surg.* 1999;68:1133–6. discussion 1136–7.
58. McGrath K, Brody D, Luketich J, et al. Detection of unsuspected left hepatic lobe metastases during EUS staging of cancer of the esophagus and cardia. *Am J Gastroenterol.* 2006;101:1742–6.
59. Prasad P, Schmulewitz N, Patel A, et al. Detection of occult liver metastases during EUS for staging of malignancies. *Gastrointest Endosc.* 2004;59:49–53.
60. Swisher SG, Maish M, Erasmus JJ, et al. Utility of PET, CT, and EUS to identify pathologic responders in esophageal cancer. *Ann Thorac Surg.* 2004;78:1152–60. discussion 1152–60.
61. Cerfolio RJ, Bryant AS, Ohja B, et al. The accuracy of endoscopic ultrasonography with fine-needle aspiration, integrated positron emission tomography with computed tomography, and computed tomography in restaging patients with esophageal cancer after neoadjuvant chemoradiotherapy. *J Thorac Cardiovasc Surg.* 2005;129:1232–41.
62. Agarwal B, Swisher S, Ajani J, et al. Endoscopic ultrasound after preoperative chemoradiation can help identify patients who benefit maximally after surgical esophageal resection. *Am J Gastroenterol.* 2004;99:1258–66.
63. Ribeiro A, Franceschi D, Parra J, et al. Endoscopic ultrasound restaging after neoadjuvant chemotherapy in esophageal cancer. *Am J Gastroenterol.* 2006;101:1216–21.
64. Chak A, Canto MI, Cooper GS, et al. Endosonographic assessment of multimodality therapy predicts survival of esophageal carcinoma patients. *Cancer.* 2000;88:1788–95.
65. Willis J, Cooper GS, Isenberg G, et al. Correlation of EUS measurement with pathologic assessment of neoadjuvant therapy response in esophageal carcinoma. *Gastrointest Endosc.* 2002;55:655–61.

66. Catalano MF, Sivak Jr MV, Rice TW, et al. Postoperative screening for anastomotic recurrence of esophageal carcinoma by endoscopic ultrasonography. *Gastrointest Endosc.* 1995;42:540–4.
67. Fockens P, Manshanden CG, van Lanschot JJ, et al. Prospective study on the value of endosonographic follow-up after surgery for esophageal carcinoma. *Gastrointest Endosc.* 1997;46:487–91.
68. Buskens CJ, Westerterp M, Lagarde SM, et al. Prediction of appropriateness of local endoscopic treatment for high-grade dysplasia and early adenocarcinoma by EUS and histopathologic features. *Gastrointest Endosc.* 2004;60:703–10.
69. Scotinotis IA, Kochman ML, Lewis JD, et al. Accuracy of EUS in the evaluation of Barrett's esophagus and high-grade dysplasia or intramucosal carcinoma. *Gastrointest Endosc.* 2001;54:689–96.
70. Pech O, May A, Gunter E, et al. The impact of endoscopic ultrasound and computed tomography on the TNM staging of early cancer in Barrett's esophagus. *Am J Gastroenterol.* 2006;101:2223–9.
71. Savoy AD, Wolfsen HC, Raimondo M, et al. The role of surveillance endoscopy and endosonography after endoscopic ablation of high-grade dysplasia and carcinoma of the esophagus. *Dis Esophagus.* 2008;21:108–13.

Role of EUS in Mediastinal Nodes, Masses, Cysts, and Lung Cancer

*David H. Robbins, MD, MSc,
Babitha Reddy, DO, MPH, and
Mohamad A. Eloubeidi, MD, MHS*

CONTENTS

INTRODUCTION
ROLE OF FNA
THE LUNG MASS
LUNG CANCER
RATIONALE FOR EUS
BEFORE YOU START
WHICH TEST IS BEST?
CROSS-SECTIONAL IMAGING
FUNCTIONAL IMAGING
FAILED BRONCHOSCOPY AND EUS RESCUE
EUS AND MEDIASTINOSCOPY
MEDICAL MEDIASTINOSCOPY
ENDOBONCHIAL ULTRASOUND
SHOULD EUS BE EMPLOYED IN SUSPECTED
EARLY LUNG CANCER?
THE LINEAR EXAM
THE FNA TECHNIQUE
SELECTIVE NODAL TARGETING
DOES EUS PREDICT T4 DISEASE?
EUS AFTER INDUCTION THERAPY

From: *Clinical Gastroenterology: Endoscopic Ultrasound*,
Edited by: V. M. Shami and M. Kahaleh, DOI 10.1007/978-1-60327-480-7_8,
© Springer Science+Business Media, LLC 2010

NEW APPLICATIONS
COST EFFECTIVENESS OF EUS IN LUNG CANCER
TRAINING
CONCLUSION

Abstract

Full minimally invasive evaluation of all lymph node stations (with the exception of station 6) is now possible with the advent of endobronchial and trans-esophageal endoscopic ultrasound. Endoscopic ultrasound fine-needle aspiration (EUS-FNA) allows sampling of mediastinal lymph nodes relevant to lung cancer staging, particularly in the subcarinal area (station 7), lower para-esophageal lymph nodes (station 8), inferior pulmonary ligament lymph nodes (station 9), and celiac lymph nodes. EUS-FNA is an extremely powerful nonsurgical option for sampling metastatic nodes, sarcoidosis, and lymphoma. Both adrenal glands can be sampled by EUS-FNA through the trans-gastric approach or the trans-duodenal approach. EUS-FNA is also able to sample central primary lung masses abutting the esophagus, particularly when other techniques fail. EBUS-FNA has the distinct advantage to reach areas that have proven inaccessible to EUS. These stations include the right and left upper and lower para-tracheal areas (4R and 4L; 2R and 2L), right and left hilar areas (station 10) and the right and left interlobar stations (station 11). It is best to work in a multidisciplinary fashion with colleagues in thoracic surgery, pulmonary, radiology, and oncology to individualize the best staging approach for the patient.

Key Words: Lung cancer, Lung cancer staging, Mediastinal lymph node, Endoscopic ultrasound, Endobronchial ultrasound, Fine needle aspiration, Adrenal gland, Lymphoma, Sarcoidosis, Mediastinal cyst, Duplication cyst

INTRODUCTION

Trans-esophageal endoscopic ultrasound (EUS) is the most accurate, efficient, and safe tool for evaluating the posterior mediastinum. The surging interest in mediastinal EUS is fueled by the rising demand for precise staging of nonsmall cell lung carcinoma (NSCLC), as well as uninvestigated mediastinal adenopathy and centrally located chest masses.

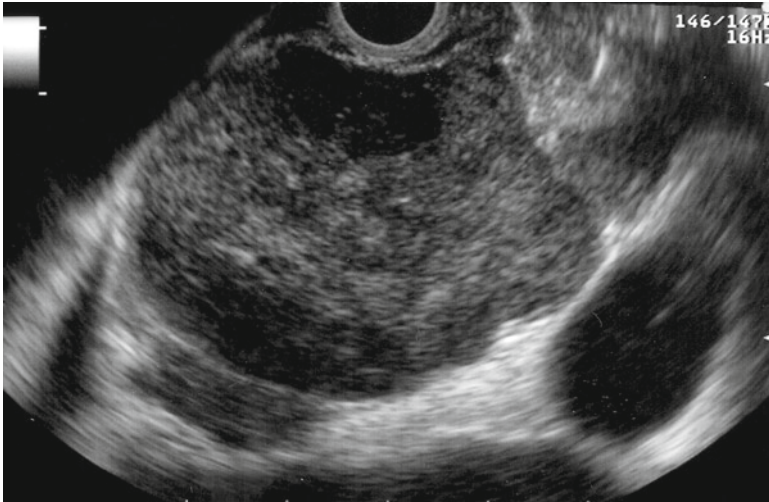


Fig. 1. Melanoma. EUS-FNA along with immunostains confirmed recurrent metastatic melanoma to the mediastinum.

Since the differential diagnosis of posterior mediastinal abnormalities includes benign and malignant etiologies, tissue acquisition by fine-needle aspiration (EUS-FNA) is essential. Benign entities include tuberculosis, granulomatous disease, sarcoidosis, histoplasmosis, and lymphoma (1). Metastases include primary carcinoma of the lung and esophagus, as well as extrathoracic sites such as the head and neck, breast, melanoma (Fig. 1) and subdiaphragmatic sites such as renal (Fig. 2) (2), gastric and pancreatic cancer (3). This chapter reviews the role of EUS in the mediastinum and in evaluating patients with known or suspected lung cancer.

Mediastinal Cysts

EUS can distinguish cystic lesions (bronchogenic or duplication cysts) from solid mediastinal masses seen on cross-sectional imaging. Foregut duplication cysts account for up to 15% of primary mediastinal masses. Bronchogenic cysts usually reveal one of two echogenic patterns: anechoic and simple (the majority are filled with a clear liquid) or anechoic pattern admixed with solid debris (4).

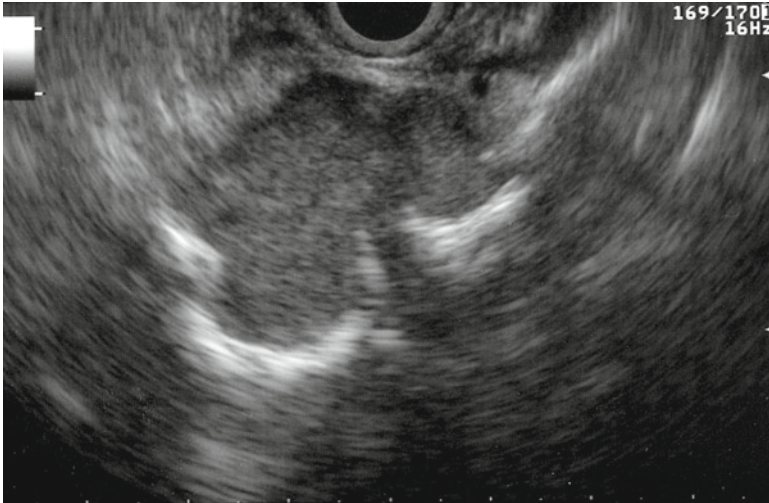


Fig. 2. RCC metastasis. EUS-FNA (with immunostains) diagnosed renal cell carcinoma metastatic to the spine.

ROLE OF FNA

We do not advocate aspirating simple cysts since they have a classic appearance by EUS and can be accurately identified by CT (4). Unlike trans-gastric aspiration, the relatively higher pH in the esophagus and the high oral bacterial load may promote infection of the mediastinal cyst. The approach to heterogeneous cysts is not, however, as straightforward since these cysts are often incorrectly interpreted as solid masses by cross-sectional imaging (CT or MRI). Such cysts are usually filled with thick echogenic and tenacious debris seen as hyperechoic reflectors. Aspiration usually results in a frothy, brownish fluid. The high viscosity can limit the yield to just a few drops for interpretation. The rationale to aspirate such lesions is to rule out a cystic metastasis. Prophylactic antibiotics should be given (5–7) as there have been case reports of infection without antibiotic coverage.

THE LUNG MASS

Another important indication for EUS is sampling primary lung masses, particularly when the lesion is close to the esophagus or for those not otherwise amenable to percutaneous or surgical approaches (8). This approach has been shown to provide tissue diagnosis of primary lung masses when other modalities have failed and when neoadjuvant therapy

is planned for borderline or unresectable masses. It can be especially helpful in obviating surgery in small cell lung carcinoma (Figs. 3 and 4). Surprisingly, we have not encountered complications of pneumothorax in sampling primary lung masses (9).

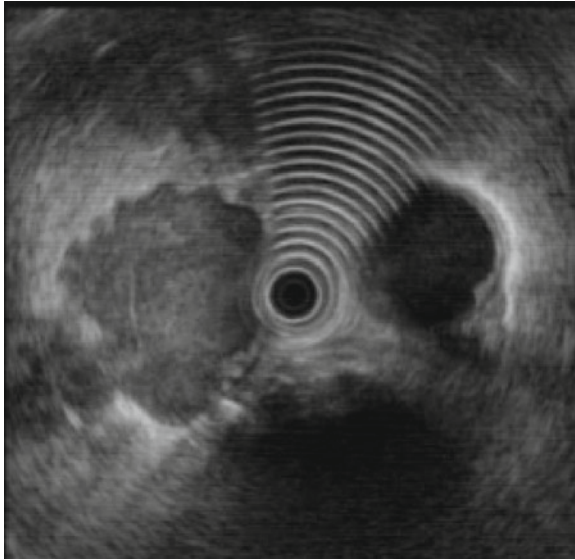


Fig. 3. Subcarinal mass invading the mediastinum.

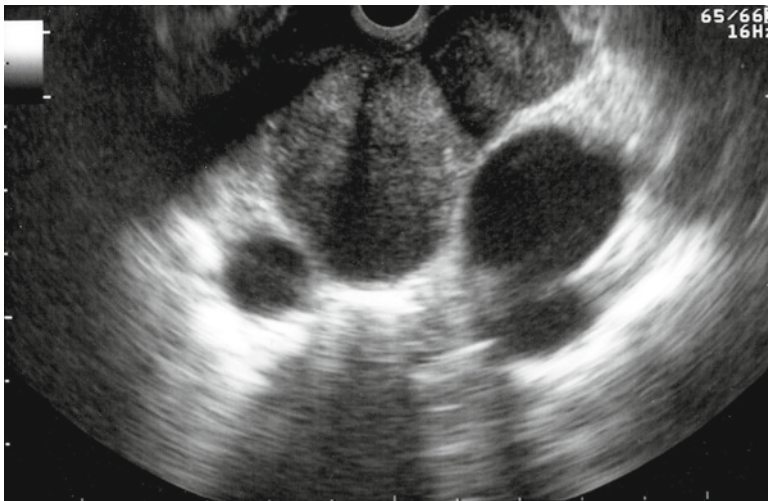


Fig. 4. Bulky N2 disease. EUS-FNA confirmed N2 disease in a patient with NSCLC.

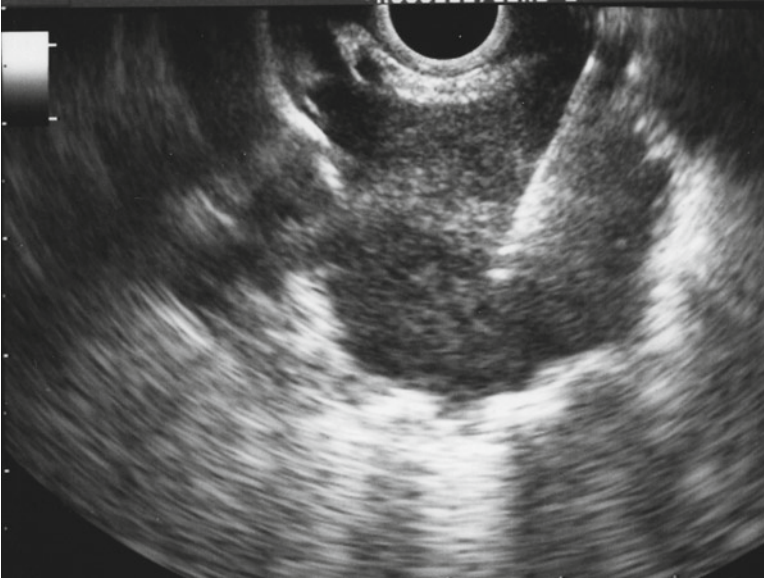


Fig. 5. Primary lung mass: EUS-FNA of a centrally located mass confirmed primary NSCLC.

LUNG CANCER

NSCLC (Fig. 5) is the number one cause of cancer death worldwide. Despite improvements in cross-sectional and functional imaging and attempts to screen those at high risk, the incidence and mortality rate of NSLC are unchanged. For the vast majority of patients, surgery with or without neoadjuvant therapy is the only hope for cure. For most, with the exception of the earliest stage tumors, the likelihood of cure after surgery remains poor (10).

The frequently inexorable progression of disease across all stages is driven by unrecognized metastases. Node positive NSCLC confirmed by EUS-FNA is more likely to receive neoadjuvant chemotherapy versus surgery compared to node negative lung cancer. Early, routine EUS-FNA provides important prognostic information and determines the most effective management (11).

RATIONALE FOR EUS

Mediastinal lymph node metastases are common (up to one third of patients) and generally indicate unresectable disease. Ipsilateral or subcarinal mediastinal nodal metastases (N2) or contralateral mediastinal

lymph node involvement (N3, stage IIIB) generally obviates surgical resection (12). Primary surgery is reserved for the minority of patients without nodal and/or distant metastases (stage I–II) (10).

Accurate staging minimizes unnecessary surgery, provides prognosis, and determines eligibility for clinical trials. Despite the increasing variety of competitive and complementary staging techniques, there is no broadly accepted consensus on how best to stage patients with the greatest accuracy and least morbidity. Reliance on chest computed tomography (CT) and integrated positron emission tomography (PET) scanning alone to stage and evaluate surgical candidacy is plagued by false positive results and potentially over-treatment or delayed surgery. Pathologic confirmation of enlarged or PET positive lymph node findings should be systematically pursued prior to surgical resection.

BEFORE YOU START

EUS for lung cancer staging requires a thorough understanding of the tumor, node, and metastasis (TNM) classification which has been revised in 2010 (Table 1) (13). Endosonographers should be especially familiar with the nodal staging. Additionally, familiarity with the Mountain–Dressler regional lymph node classification system (Fig. 6) (14, 15) as well as a new international lymph node map defining the anatomical boundaries for lymph node stations is necessary (13). Whenever possible, radiographs must be reviewed prior to embarking upon EUS and target “the worst first” – those metastases which impart the most advanced stage.

In general, the lower posterior mediastinum is ideally suited to EUS. EUS can access the lower para-tracheal space (station 4R and L), the subcarina (station 7), distal para-esophageal nodes (station 8), the pulmonary ligament (station 9), and varying the AP window (station 5). An “unsung” advantage of EUS is its ability to detect and sample celiac, left and right adrenal glands, hepatic, and ascitic or pleural fluid metastases otherwise (16) missed by cross-sectional imaging (17). These areas are uniquely in the domain of EUS and have significant impact in the treatment decision and prognosis in patients with NSCLC.

Evaluation of the anterior and right-sided mediastinum is limited by intervening tracheal and proximal bronchial air (stations 2 and 4R). These locations should be considered for bronchoscopic sampling, particularly with endobronchial ultrasound (EBUS) as discussed below. A recent summary of 13 prospective studies underscores the high accuracy of EUS (18).

Table 1
TNM classification of lung cancer

Regional lymph nodes (N)

NX	Regional lymph nodes cannot be assessed
N0	No regional lymph node metastases
N1	Metastatic in ipsilateral peribronchial and/or ipsilateral hilar lymph nodes and intrapulmonary nodes, including involvement by direct extension
N2	Metastasis in ipsilateral mediastinal and/or subcarinal lymph node(s)
N3	Metastasis in contralateral mediastinal, contralateral hilar, ipsilateral or contralateral scalene, or supraclavicular lymph node(s)

Anatomic stage/prognostic groups

Occult carcinoma	TX	N0	M0
Stage 0	Tis	N0	M0
Stage IA	T1a	N0	M0
	T1b	N0	M0
Stage IB	T2a	N0	M0
Stage IIA	T2b	N0	M0
	T1a	N1	M0
	T1b	N1	M0
Stage IIIA	T2a	N1	M0
	T1a	N2	M0
	T1b	N2	M0
	T2a	N2	M0
	T2b	N2	M0
	T3	N1	M0
	T3	N2	M0
Stage IIIb	T4	N0	M0
	T4	N1	M0
	T1a	N3	M0
	T1b	N3	M0
	T2a	N3	M0
	T2b	N3	M0
	T3	N3	M0
Stage IV	Any T	Any N	M1a
	Any T	Any N	M1b

Used with the permission of the American Joint Committee on Cancer (AJCC), Chicago, Illinois. The original source for this material is the AJCC Cancer Staging Manual, Seventh Edition (2010) published by Springer Science and Business Media LLC, <http://www.springerlink.com>

A recent case series suggested a single trans-aortic EUS-FNA for intrapulmonary tumors, and enlarged lymph nodes lateral to the aorta (station 6) was feasible. Malignancy was confirmed in 64% of patients, who otherwise would have undergone mediastinotomy or an open procedure (19).

WHICH TEST IS BEST?

Patients with newly diagnosed NSCLC face a dizzying array of invasive staging options and no modality is perfect or universally available. Mediastinoscopy (MS) and trans-bronchial fine-needle aspiration (TBNA) are widely established but are primarily limited respectively by increased invasiveness and a modest negative predictive value (NPV). EUS-FNA has emerged as a diagnostic and staging tool because

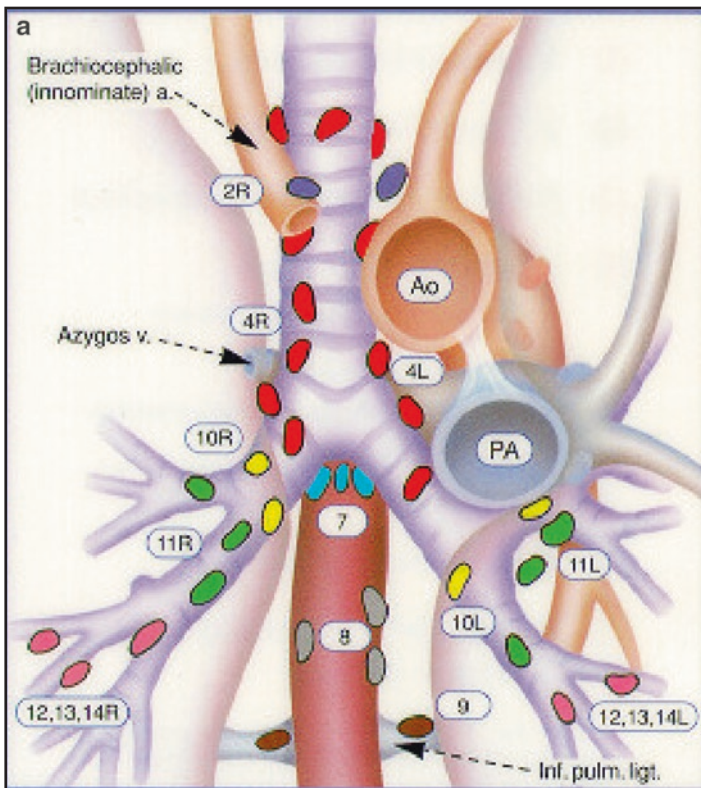


Fig. 6. The Mountain and Dressler regional lymph node classification (a) anterior view, (b) posterior view.

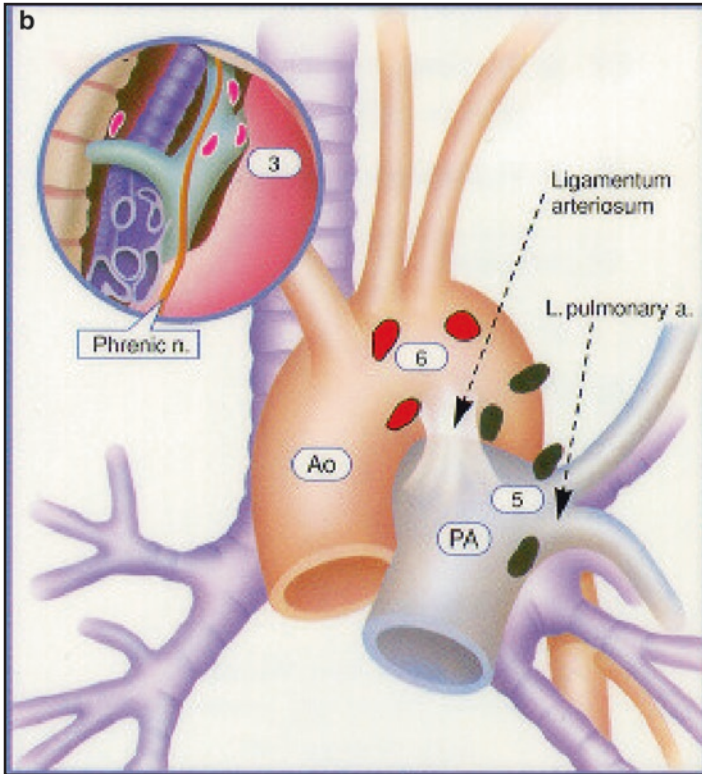


Fig. 6. (continued)

of its safety, accuracy, and patient convenience. For those endosonographers embarking a new programmatic application, integration of EUS into institutional clinical pathways is best achieved by participation in a multidisciplinary thoracic tumor board.

CROSS-SECTIONAL IMAGING

CT is the most common initial staging modality due to its widespread availability and ease of interpretation. While excellent for distant metastatic staging, the performance of CT in evaluating the mediastinum is not optimal (20). A meta-analysis, including 3,829 patients across 20 studies, revealed a NPV of 82% (18% were found to have advanced disease at surgical staging) (21). The sensitivity and specificity of CT for mediastinal nodes ranges from 57 to 82% (22).

CT and EUS should be considered complementary approaches. CT is most useful for primary tumor imaging and for a “lay of the land” while EUS provides a focused exam of select metastatic sites. Direct comparisons between EUS and CT in detecting mediastinal adenopathy have been performed (23–25) and the sensitivity of EUS for mediastinal lymph node detection was consistently above 90%. It is crucial to note that in patients with an unremarkable chest CT, EUS-FNA detected advanced disease and obviated the need for more invasive staging in a significant portion of patients (17, 26). In the absence of extrathoracic metastases, EUS-FNA is useful regardless of CT findings.

FUNCTIONAL IMAGING

CT with integrated 18F-fluorodeoxyglucose positron emission tomography (PET–CT) has become the noninvasive gold standard. Despite initial enthusiasm that functional imaging might obviate the need for tissue sampling or FNA, PET–CT findings are not recognized as definitive proof of N2-N3 disease (27). PET is widely thought to be more accurate than CT, but false positives are common (up to 39%) (28).

Despite these shortcomings, PET–CT remains an excellent and irreplaceable part of the metastatic evaluation. A meta-analysis of 18 studies with 1,045 patients reported a pooled sensitivity, specificity, positive predictive value (PPV), and NPV of PET for staging mediastinal lymph nodes in NSCLC patients of 84, 89, 79, and 93%, respectively (29).

EUS-FNA can be used to document suspicious findings on PET–CT with great accuracy (97% accuracy (28), 93% sensitivity, and 100% specificity) (14). In that study, EUS confirmed N2/N3 disease in 69% of patients who were PET avid in the mediastinum. Importantly, one third of these lesions were outside the reach of surgical MS. More than a quarter of PET avid patients were found to have no nodal metastases after EUS-FNA, and 70% of “PET suspicious” patients had no mediastinal spread at surgery. These results underscore the point that functional imaging cannot replace tissue confirmation.

Furthermore, in unexplained mediastinal lymphadenopathy, EUS-FNA complemented PET findings by improving specificity and thus accuracy of diagnosis. The PPV approached 100% with overall accuracy 97% in lymph node pathology. Equivocal PET findings are particularly suited for minimally invasive EUS-FNA in which tissue diagnosis is invaluable (30).

FAILED BRONCHOSCOPY AND EUS RESCUE

TBNA is a widely employed blind technique with a poorly defined diagnostic yield (31, 32). It is associated with complications such as bleeding and pneumothorax (31). EUS-FNA “rescue” can be done immediately after an unrevealing TBNA if on-site cytology demonstrates a nondiagnostic specimen.

EUS AND MEDIASTINOSCOPY

Mediastinoscopy long considered the gold standard, is the most invasive staging technique. It is relatively costly, requires general anesthesia, and may require hospital admission. While safe, it carries the greatest procedural risk (33, 34). In a sense, EUS-FNA and MS are both competing and complementary techniques, although the future of lung cancer staging is likely to exclude surgical staging altogether. Two prospective studies directly compared EUS-FNA to MS (22, 25) in one the combination of EUS-FNA and MS increased the sensitivity to 86% compared to EUS-FNA alone (61%) or MS alone (53%) (25). Compared to MS, EUS-FNA offers wider access to the posterior mediastinum, including the subcarina, the inferior mediastinum, and the aortopulmonary window (APW).

MEDICAL MEDIASTINOSCOPY

Combined with EBUS (Fig. 7) for interrogation of the anterior mediastinum, the concept of complete “medical mediastinoscopy” is likely to largely replace surgical staging (35). Up to 10% of thoracotomies with intent to resect result in “open and shut” without resection; an additional 25–35% are ultimately futile on the basis of postoperative recurrence. In a recent study, the sensitivity and specificity approached 100% when EUS-FNA was combined with EBUS-TBNA (Table 2) (17, 36).

ENDOBONCHIAL ULTRASOUND

EBUS is a novel diagnostic tool for mediastinal staging. Two prospective studies combined EUS-FNA with endobronchial ultrasound guided trans-bronchial needle biopsy (EBUS-TBNA) (37). The difference in sensitivity between the two procedures was not statistically

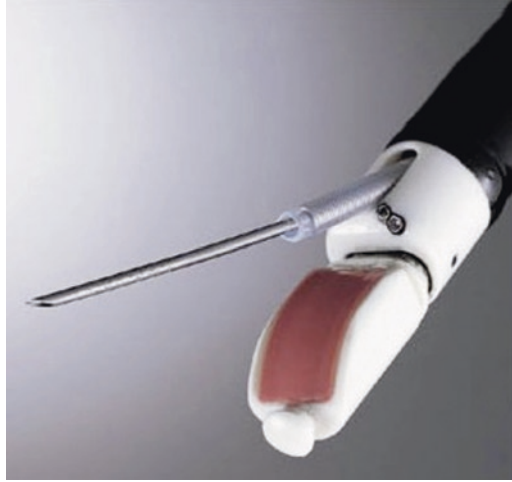


Fig. 7. Tip of endobronchial echoendoscope (EBUS) with FNA needle.

Table 2
Comparison of EUS-FNA, EBUS-FNA and combined approaches (medical mediastinoscopy) in the evaluation of mediastinal lesions

	<i>Sensitivity</i> (%)	<i>Specificity</i> (%)	<i>PPV</i> (%)	<i>NPV</i> (%)	<i>Accuracy</i> (%)
EUS-FNA	80	100	100	66	86
EBUS-TBNA	85	100	100	72	89
Combined	100	100	100	100	100

significant and the combined approach had higher sensitivity and accuracy than either modality alone.

Additional larger trials are necessary to evaluate the utility of combined approach in unselected populations. We suspect combined EUS-FNA and EBUS-TBNA will be shown to provide total “medical mediastinoscopy” and in most cases obviate the need for surgical exploration.

Addition of EUS to a routine work-up in a small study which included chest CT, TBNA and, in some circumstances PET, reduced the need for surgical staging by an estimated 78% in patients with enlarged posterior mediastinal nodes (35).

SHOULD EUS BE EMPLOYED IN SUSPECTED EARLY LUNG CANCER?

The role of EUS-FNA after a high quality, negative PET-CT remains controversial in the patient with a small peripheral carcinoma. EUS-FNA has been reported to upstage an otherwise resectable patient (29). Such cases suggest the utility of EUS-FNA even in patients with no significant mediastinal lymph node metastases on PET. However, the yield of EUS-FNA and MS in a negative integrated PET-CT may be low (37).

EUS can be used, however, in a subgroup of patients that might harbor undetected N2 disease such as those whose tumor have high SUV >10 and those with poorly differentiated tumors (37).

THE LINEAR EXAM

A linear mediastinal exam typically begins 30 cm from the incisors. At this level, one should appreciate the cardiac motion from the left atrium and ventricle. Pulling back slightly will bring in to view the subcarinal space where the left atrium drains into the pulmonary artery. Remember that clockwise rotation of the scope along its axis brings left-sided structures into view. Gentle pullback will then reveal the APW, the space defined by its two named great vessels. The aorta can be seen to round off into its oblong appearing arch by turning clockwise about 90° and pulling back about 2 cm from the APW.

The descending aorta is identified with the CLA echoendoscope at about 35 cm from the incisor. A continuous and steady push of the CLA endoscope to about 45 cm – while the aorta is maintained in view – leads to the identification of the celiac axis bifurcation. A gentle clockwise maneuver will lead to the “seagull” shaped organ, the left adrenal gland. In patients with metastasis to the adrenal, the gland loses its normal shape and takes the form of a mass (Figs. 8 and 9). Occasionally, one limb of the adrenal is slightly enlarged; commonly this is a benign adenoma.

Recent reports suggest that those nodes lacking a central Doppler signal (intranodal blood vessel) are much more likely to be malignant (38, 39).

THE FNA TECHNIQUE

The sensitivity and specificity of EUS without FNA for diagnosing mediastinal lymph node metastases ranges between 54–75% and 71–98%, respectively (6, 7). The introduction of FNA for tissue confirmation

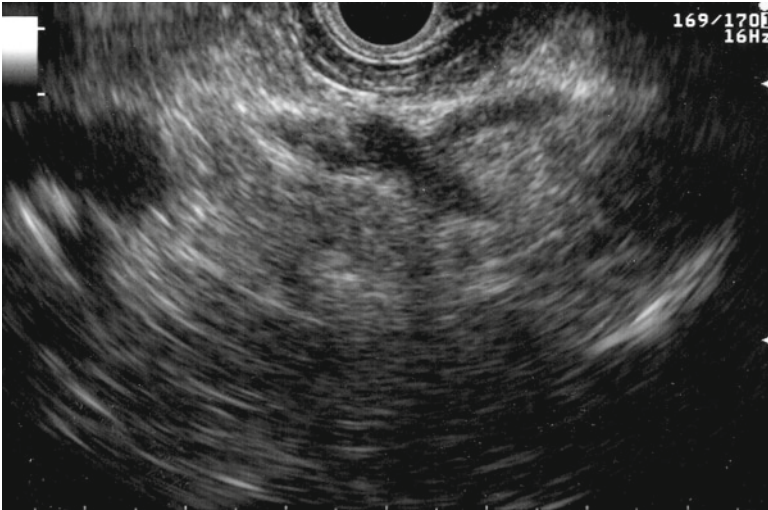


Fig. 8. Normal appearing “seagull” adrenal gland (curvilinear echoendoscope).



Fig. 9. Adrenal metastasis. An 11 mm nodule in the left wing of the left adrenal gland.

markedly improved the accuracy to 94–95% (Fig. 10) (9, 10, 12). Typically, 3–4 passes is sufficient for lymph nodes, a primary mass may require additional sampling. We use the smallest gauge needle possible (25-ga)

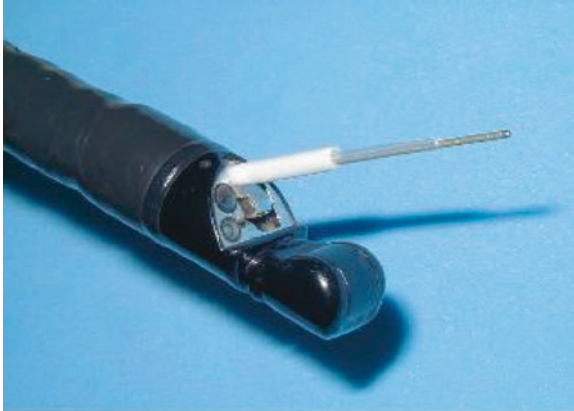


Fig. 10. Tip of linear echoendoscope with FNA needle.

to minimize hemorrhagic contamination yet still provide sufficient material. Adjunctive use of negative suction through the supplied syringe can increase overall cytologic yield but may also draw in more contaminating blood. In cases when EUS-FNA is nondiagnostic, a 19-gauge Trucut biopsy needle designed for use in conjunction with an echo endoscope may be useful to procure larger specimens for histopathological analysis. This approach is particularly useful in evaluating patients with Hodgkin's lymphoma (40).

SELECTIVE NODAL TARGETING

There has been a great deal of interest in defining nodal echo qualities that best predict the likelihood of harboring metastatic disease. In general, suspicious features include sharp borders, a uniformly hypoechoic appearance, rounded shape, and a short axis diameter of >1 cm (Fig. 11). EUS-FNA sampling of smaller suspicious lymph nodes undetected by CT imaging offers equivalent diagnostic sensitivity to larger malignant lymph nodes. This has great impact, particularly in unexpected locally advanced disease (41). The PPV for lymph nodes that meet all criteria is quite good (80%), but sensitivity is imperfect. Only about 25% of lymph nodes in one study exhibited all of these features (40). It is important to remember small triangular lymph nodes in the subaortic space (station 5) are relatively common and usually benign, especially in smokers, urban dwellers, and those with chronic lung disease.

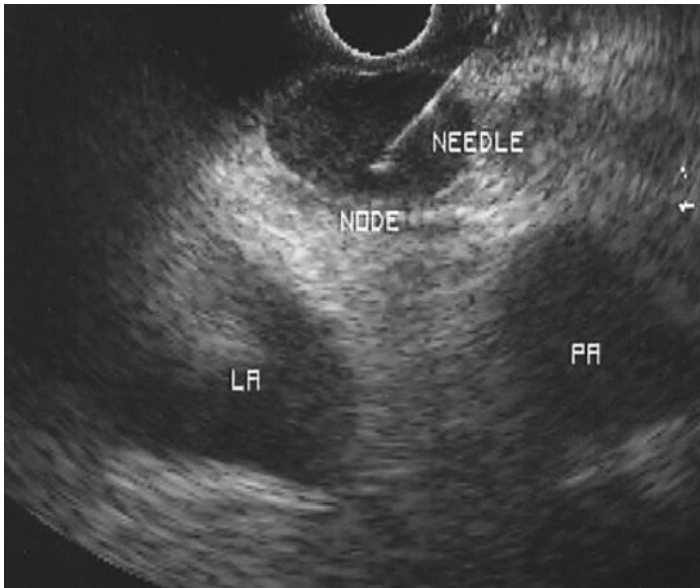


Fig. 11. EUS-FNA of lymph node.

DOES EUS PREDICT T4 DISEASE?

Studies have also demonstrated high sensitivity and specificity of EUS-FNA for advanced tumors (T4 by direct invasion of the mediastinum, heart, great vessels, trachea, esophagus, vertebral body, or carina) or malignant pleural effusion retrospectively (42) and prospectively (25). Surgery is generally contraindicated in T4 disease. The role of EUS in defining T4 disease, however, remains unclear. One retrospective study assessed the accuracy of EUS in discriminating T4 disease. Among 175 patients, 8 were diagnosed at surgery as T4, including 2 with malignant pleural effusions by EUS-FNA. The sensitivity, specificity, PPV, and NPV of EUS for T4 extent were 87.5, 98, 70, and 99%, respectively. Three of five patients, thought to have mediastinal invasion at EUS, were surgically staged as T2, highlighting the risk of over-staging. Caution should be exercised when staging primary lung or mediastinal masses by EUS since over-staging may occur particularly for mediastinal invasion.

EUS AFTER INDUCTION THERAPY

Patients who have completed induction therapy, in anticipation of surgery with intent to cure, present a unique challenge. The problem of “restaging” after therapy relates to scarring and inflammatory change.

CT is particularly inaccurate (58%). Such scarring limits subsequent surgical staging such as MS with an incompleteness rate as high as 40% (17, 43). A few studies have examined the role of EUS-FNA to evaluate the mediastinal response to neoadjuvant chemotherapy (17, 36). A recent study of 28 patients demonstrated that postinduction EUS-FNA had a high NPV with 93% accuracy. Although concordant with PET-CT restaging findings, invaluable pathological confirmation with this minimally invasive procedure (avoiding MS) establishes its superiority and confidence in selecting the most appropriate preoperative “intent to cure” surgical candidates (33).

NEW APPLICATIONS

EUS-guided fiducial placement of CyberKnife radiotherapy of mediastinal and abdominal malignancies is a newer application which further expands the role of EUS. Eleven of thirteen patients underwent successful placement of three to six fiducials through a 19-gauge fine needle for directed radiation therapy. One infectious complication was reported (34). Further studies are forthcoming in defining this EUS application.

COST EFFECTIVENESS OF EUS IN LUNG CANCER

Cost-efficacy has been evaluated prospectively (17) and in decision analysis modeling (31). The studies demonstrated a cost benefit with EUS-FNA compared to MS and concluded EUS-FNA could reduce the cost of staging by 16–40%. The cost of MS in these studies was, however, quite conservative, as calculations were based on the assumption that patients would stay in a hospital for a total of 3 days (15, 17).

TRAINING

Performing EUS at a high level requires the completion of a dedicated fourth year fellowship. Among the various indications for EUS, mediastinal exams are among the most readily learned. In one study, the learning curve of EUS-FNA was assessed using two residents (17). Two residents each performed 29 and 25 procedures and, not surprisingly, failed to reach the ability of experienced operators. The American Society for Gastrointestinal Endoscopy (ASGE) recommends a minimum of 150 cases of supervised EUS, 50 of which should include FNA (32). Equally controversial is defining who should be performing

trans-esophageal lung cancer staging. Since lung cancer is not in the clinical domain of most gastroenterologists, other specialists are pursuing training in trans-esophageal EUS. Short courses in mediastinal EUS are increasingly available to both pulmonologists and thoracic surgeons.

CONCLUSION

EUS has redefined the way we evaluate patients with posterior mediastinal lesions and especially those with NSCLC. Despite the broad evidence base supporting its utility, the integration of routine EUS in patients with NSCLC outside of tertiary care centers has not been rapidly adopted. In time more data will better define the role of EUS in the diagnosis of mediastinal masses as well as the diagnosis and staging of lung cancer.

REFERENCES

1. Annema JT, Veselic M, Rabe KF. Endoscopic ultrasound-guided fine-needle aspiration for the diagnosis of sarcoidosis. *Eur Respir J*. 2005 Mar;25(3):405–9.
2. Kramer H. Screening for kidney disease in adults with diabetes mellitus: don't forget serum creatinine. *Am J Kidney Dis*. 2004 Nov;44(5):921–3.
3. Pungpapong S, Noh KW, Wallace MB. Endoscopic ultrasonography in the diagnosis and management of cancer. *Expert Rev Mol Diagn*. 2005 Jul;5(4):585–97.
4. Eloubeidi MA, Cohn M, Cerfolio RJ, Chhieng DC, Jhala N, Jhala D, et al. Endoscopic ultrasound-guided fine-needle aspiration in the diagnosis of foregut duplication cysts: the value of demonstrating detached ciliary tufts in cyst fluid. *Cancer*. 2004 Aug 25;102(4):253–8.
5. Fazel A, Moezardalan K, Varadarajulu S, Draganov P, Eloubeidi MA. The utility and the safety of EUS-guided FNA in the evaluation of duplication cysts. *Gastrointest Endosc*. 2005 Oct;62(4):575–80.
6. Annema JT, Veselic M, Versteegh MI, Rabe KF. Mediastinitis caused by EUS-FNA of a bronchogenic cyst. *Endoscopy*. 2003 Sep;35(9):791–3.
7. Wildi SM, Hoda RS, Fickling W, Schmulewitz N, Varadarajulu S, Roberts SS, et al. Diagnosis of benign cysts of the mediastinum: the role and risks of EUS and FNA. *Gastrointest Endosc*. 2003 Sep;58(3):362–8.
8. Hernandez A, Kahaleh M, Olazagasti J, Jones DR, Daniel T, Stelow E, et al. EUS-FNA as the initial diagnostic modality in centrally located primary lung cancers. *J Clin Gastroenterol*. 2007 Aug;41(7):657–60.
9. Varadarajulu S, Hoffman BJ, Hawes RH, Eloubeidi MA. EUS-guided FNA of lung masses adjacent to or abutting the esophagus after unrevealing CT-guided biopsy or bronchoscopy. *Gastrointest Endosc*. 2004 Aug;60(2):293–7.
10. Spira A, Ettinger DS. Multidisciplinary management of lung cancer. *N Engl J Med*. 2004 Jan 22;350(4):379–92.

11. Eloubeidi MA, Desmond R, Desai S, Mehra M, Bryant A, Cerfolio RJ. Impact of staging transesophageal EUS on treatment and survival in patients with non-small-cell lung cancer. *Gastrointest Endosc*. 2008 Feb;67(2):193–8.
12. Jett JR, Scott WJ, Rivera MP, Sause WT. Guidelines on treatment of stage IIIB non-small cell lung cancer. *Chest*. 2003 Jan;123(1 Suppl):221S–5S.
13. Edge SB, Byrd DR, Compton CC, Fritz AG, Greene FL, Trotti A, et al. *AJCC cancer staging manual*. 7th ed. New York: Springer; 2010.
14. Mountain CF. Revisions in the International System for Staging Lung Cancer. *Chest*. 1997 Jun;111(6):1710–7.
15. Mountain CF, Dresler CM. Regional lymph node classification for lung cancer staging. *Chest*. 1997 Jun;111(6):1718–23.
16. Eloubeidi MA, Morgan DE, Cerfolio RJ, Eltoum IA. Transduodenal EUS-guided FNA of the right adrenal gland. *Gastrointest Endosc*. 2008 Mar;67(3):522–7.
17. Wallace MB, Ravenel J, Block MI, Fraig M, Silvestri G, Wildi S, et al. Endoscopic ultrasound in lung cancer patients with a normal mediastinum on computed tomography. *Ann Thorac Surg*. 2004 May;77(5):1763–8.
18. Ogita S. Endoscopic ultrasound fine-needle aspiration in the staging of non-small-cell lung cancer: Williston Park; 2006.
19. von Bartheld MB, Rabe KF, Annema JT. Transaortic EUS-guided FNA in the diagnosis of lung tumors and lymph nodes. *Gastrointest Endosc*. 2009 Feb;69(2):345–9.
20. Spiro SG, Porter JC. Lung cancer—where are we today? Current advances in staging and nonsurgical treatment. *Am J Respir Crit Care Med*. 2002 Nov 1;166(9):1166–96.
21. Micames CG, McCrory DC, Pavey DA, Jowell PS, Gress FG. Endoscopic ultrasound-guided fine-needle aspiration for non-small cell lung cancer staging: A systematic review and metaanalysis. *Chest*. 2007 Feb;131(2):539–48.
22. Toloza EM, Harpole L, McCrory DC. Noninvasive staging of non-small cell lung cancer: a review of the current evidence. *Chest*. 2003 Jan;123(1 Suppl):137S–46S.
23. Annema JT, Versteegh MI, Veselic M, Voigt P, Rabe KF. Endoscopic ultrasound-guided fine-needle aspiration in the diagnosis and staging of lung cancer and its impact on surgical staging. *J Clin Oncol*. 2005 Nov 20;23(33):8357–61.
24. Rosenberg JM, Perricone A, Savides TJ. Endoscopic ultrasound/fine-needle aspiration diagnosis of a malignant subcarinal lymph node in a patient with lung cancer and a negative positron emission tomography scan. *Chest*. 2002 Sep;122(3):1091–3.
25. Savides TJ, Perricone A. Impact of EUS-guided FNA of enlarged mediastinal lymph nodes on subsequent thoracic surgery rates. *Gastrointest Endosc*. 2004 Sep;60(3):340–6.
26. LeBlanc JK, Devereaux BM, Imperiale TF, Kesler K, DeWitt JM, Cummings O, et al. Endoscopic ultrasound in non-small cell lung cancer and negative mediastinum on computed tomography. *Am J Respir Crit Care Med*. 2005 Jan 15;171(2):177–82.
27. Silvestri GA, Tanoue LT, Margolis ML, Barker J, Detterbeck F. The noninvasive staging of non-small cell lung cancer: the guidelines. *Chest*. 2003 Jan;123(1 Suppl):147S–56S.

28. Toloza EM, Harpole L, Detterbeck F, McCrory DC. Invasive staging of non-small cell lung cancer: a review of the current evidence. *Chest*. 2003 Jan;123(1 Suppl): 157S–66S.
29. Graeter TP, Hellwig D, Hoffmann K, Ukena D, Kirsch CM, Schafers HJ. Mediastinal lymph node staging in suspected lung cancer: comparison of positron emission tomography with F-18-fluorodeoxyglucose and mediastinoscopy. *Ann Thorac Surg*. 2003 Jan;75(1):231-5; discussion 5–6.
30. Kalade AV, Eddie Lau WF, Conron M, Wright GM, Desmond PV, Hicks RJ, et al. Endoscopic ultrasound-guided fine-needle aspiration when combined with positron emission tomography improves specificity and overall diagnostic accuracy in unexplained mediastinal lymphadenopathy and staging of non-small-cell lung cancer. *Intern Med J*. 2008 Nov;38(11):837–44.
31. Schenk DA, Bower JH, Bryan CL, Currie RB, Spence TH, Duncan CA, et al. Transbronchial needle aspiration staging of bronchogenic carcinoma. *Am Rev Respir Dis*. 1986 Jul;134(1):146–8.
32. Shure D, Fedullo PF. The role of transcarinal needle aspiration in the staging of bronchogenic carcinoma. *Chest*. 1984 Nov;86(5):693–6.
33. Stigt JA, Oostdijk AH, Timmer PR, Shahin GM, Boers JE, Groen HJ. Comparison of EUS-guided fine needle aspiration and integrated PET-CT in restaging after treatment for locally advanced non-small cell lung cancer. *Lung Cancer*. 2009 Nov;66(2):198–204.
34. Pishvaian AC, Collins B, Gagnon G, Ahlawat S, Haddad NG. EUS-guided fiducial placement for CyberKnife radiotherapy of mediastinal and abdominal malignancies. *Gastrointest Endosc*. 2006 Sep;64(3):412–7.
35. Larsen SS, Vilmann P, Krasnik M, Dirksen A, Clementsen P, Maltbaek N, et al. Endoscopic ultrasound guided biopsy performed routinely in lung cancer staging spares futile thoracotomies: preliminary results from a randomised clinical trial. *Lung Cancer*. 2005 Sep;49(3):377–85.
36. Vilmann P, Puri R. The complete “medical” mediastinoscopy (EUS-FNA + EBUS-TBNA). *Minerva Med*. 2007 Aug;98(4):331–8.
37. Cerfolio RJ, Bryant AS, Eloubeidi MA. Routine mediastinoscopy and esophageal ultrasound fine-needle aspiration in patients with non-small cell lung cancer who are clinically N2 negative: a prospective study. *Chest*. 2006 Dec;130(6):1791–5.
38. Sawhney MS, Debold SM, Kratzke RA, Lederle FA, Nelson DB, Kelly RF. Central intranodal blood vessel: a new EUS sign described in mediastinal lymph nodes. *Gastrointest Endosc*. 2007 Apr;65(4):602–8.
39. Hall JD, Kahaleh M, White GE, Talreja J, Northup PG, Shami VM. Presence of lymph node vasculature: a new EUS criterion for benign nodes? *Dig Dis Sci*. 2009 Jan;54(1):118–21.
40. Bhutani MS, Hawes RH, Hoffman BJ. A comparison of the accuracy of echo features during endoscopic ultrasound (EUS) and EUS-guided fine-needle aspiration for diagnosis of malignant lymph node invasion. *Gastrointest Endosc*. 1997 Jun;45(6):474–9.
41. Tournoy KG, Ryck FD, Vanwalleghem L, Praet M, Vermassen F, Maele GV, et al. The yield of endoscopic ultrasound in lung cancer staging: does lymph node size matter? *J Thorac Oncol*. 2008 Mar;3(3):245–9.

42. Eloubeidi MA, Cerfolio RJ, Chen VK, Desmond R, Syed S, Ojha B. Endoscopic ultrasound-guided fine needle aspiration of mediastinal lymph node in patients with suspected lung cancer after positron emission tomography and computed tomography scans. *Ann Thorac Surg.* 2005 Jan;79(1):263–8.
43. Mateu-Navarro M, Rami-Porta R, Bastus-Piulats R, Cirera-Nogueras L, Gonzalez-Pont G. Remediastinoscopy after induction chemotherapy in non-small cell lung cancer. *Ann Thorac Surg.* 2000 Aug;70(2):391–5.

The Role of Endoscopic Ultrasound in Gastric Cancer

*Sanjay R. Hegde, MD,
Oleh Haluszka, MD,
and Jeffrey L. Tokar, MD*

CONTENTS

INTRODUCTION
GASTRIC CANCER STAGING SYSTEMS
DIAGNOSIS AND STAGING OF GASTRIC CANCER
EUS TECHNIQUE
PRIMARY TUMOR ASSESSMENT (T-STAGE)
OF GASTRIC CANCER BY EUS
LYMPH NODE ASSESSMENT (N-STAGING)
OF GASTRIC CANCER BY EUS
ASSESSMENT OF DISTANT METASTASES
(M-STAGING) OF GASTRIC CANCER BY EUS
TECHNICAL LIMITATIONS OF EUS
FOR TNM STAGING OF GASTRIC CANCER
COMPARISON OF EUS TO OTHER IMAGING
MODALITIES FOR STAGING OF GASTRIC
CANCER
EUS IN THE EVALUATION OF EARLY GASTRIC
CANCER
EUS IN THE EVALUATION OF LOCALLY
ADVANCED GASTRIC CANCER
CONCLUSION

From: *Clinical Gastroenterology: Endoscopic Ultrasound*,
Edited by: V. M. Shami and M. Kahaleh, DOI 10.1007/978-1-60327-480-7_9,
© Springer Science+Business Media, LLC 2010

Abstract

Accurate staging of gastric cancer is vital in guiding treatment decisions. Endoscopic ultrasound (EUS) has emerged as the most accurate means of locally staging gastric cancer. In this review, we discuss the role of EUS in the management of gastric cancer, focusing on EUS technique for Tumor Node Metastasis (TNM) staging, comparison of EUS to other imaging modalities used for staging, and specific clinical scenarios (early and advanced gastric cancer) in which EUS is performed.

Key Words: Endoscopic ultrasound, EUS, Gastric cancer, TNM staging

INTRODUCTION

Gastric adenocarcinoma remains an important cause of cancer-related death despite falling incidence and mortality rates over the past 70 years. It is the fourth most common cancer and the second most common cause of cancer-related death worldwide (1). Incidence and mortality rates are higher in developing countries and are particularly high in Asia. In Japan, gastric cancer is still the most common cause of cancer related death (2).

Adenocarcinoma accounts for greater than 90% of all gastric cancers. These can be further classified histologically as (1) intestinal-type, well-differentiated and (2) diffuse, poorly-differentiated cancers, the latter carrying a worse prognosis (3). In the United States, there has been an increase in the incidence of proximal gastric cancers, whereas distal tumors predominate in Japan (1, 4). Previously described risk factors include *Helicobacter pylori* infection, atrophic gastritis, pernicious anemia, subtotal gastrectomy, gastric polyps, blood type A, male gender, older age, increased dietary intake of nitrate rich food, family history, and several hereditary syndromes (Diffuse Hereditary Gastric Cancer, HNPCC, FAP, and Peutz-Jeghers syndrome) (1).

Prognosis correlates with stage of disease and is best with early lesions (5). In the United States, patients tend to present with more advanced disease than those in Japan where there are well-established screening programs for gastric cancer (6). Five-year survival rates are 61% for localized disease and 3% with advanced disease in the United States (5). Accurate staging is important in planning appropriate treatment. Endoscopic ultrasound (EUS) has emerged as the most accurate means of staging localized gastric cancer and is useful in determining which lesions may be amenable to endoscopic resection.

GASTRIC CANCER STAGING SYSTEMS

The two most commonly used staging systems for gastric cancer are the American Joint Committee on Cancer (AJCC)/International Union Against Cancer (IAUC) system (7) and the Japanese Gastric Cancer Association System (8). The AJCC system is the most commonly used system in the United States, and the new staging system for 2010 is shown in Table 1. It utilizes a Tumor Node Metastasis (TNM)

Table 1
TNM classification of gastric cancer

<i>T-stage</i>	<i>Description</i>
TX	Primary tumor cannot be assessed
Tis	Carcinoma in situ: intraepithelial tumor without invasion of the lamina propria
T1	Tumor invades lamina propria, muscularis mucosae, or submucosa
T1a	Tumor invades lamina propria or muscularis mucosae
T1b	Tumor invades submucosa
T2	Tumor invades muscularis propria
T3	Tumor penetrates subserosal connective tissue without invasion of visceral peritoneum or adjacent structures
T4	Tumor invades serosa (visceral peritoneum) or adjacent structures
T4a	Tumor invades serosa (visceral peritoneum)
T4b	Tumor invades adjacent structures
N-stage	
NX	Regional lymph node (s) cannot be assessed
N0	No regional lymph node metastasis
N1	Metastasis in 1–2 regional lymph nodes
N2	Metastasis in 3–6 regional lymph nodes
N3	Metastasis in seven or more regional lymph nodes
N3a	Metastasis in 7–15 regional lymph nodes
N3b	Metastasis in 16 or more regional lymph nodes
M stage	
M0	No distant metastasis
M1	Distant metastasis

(continued)

Table 1
(continued)

<i>T-stage</i>	<i>Description</i>
AJCC stage groupings	
Group stage	TNM stage
0	Tis, N0, M0
IA	T1, N0, M0
IB	T2, N0, M0
	T1, N1, M0
IIA	T3, N0, M0
	T2, N1, M0
	T1, N2, M0
IIB	T4a, N0, M0
	T3, N1, M0
	T2, N2, M0
	T1, N3, M0
IIIA	T4a, N1, M0
	T3, N2, M0
	T2, N3, M0
IIIB	T4b, N0, M0
	T4b, N1, M0
	T4a, N2, M0
	T3, N3, M0
IIIC	T4b, N2, M0
	T4b, N3, M0
	T4a, N3, M0
IV	Any T, Any N, M1

Used with the permission of the American Joint Committee on Cancer (AJCC), Chicago, Illinois. The original source for this material is the AJCC Cancer Staging Manual, Seventh Edition (2010) published by Springer Science and Business Media LLC, <http://www.springerlink.com>

classification scheme, and the most recent revision designates four categories of nodal involvement (N0–N3) based on the absolute number of involved regional lymph nodes (7). The Japanese Staging System incorporates the number and location of the primary gastric tumor(s), a macroscopic description of tumor morphology, a depth of tumor invasion

(T-stage) system similar to AJCC/IUAC, and a detailed classification schema for nodal (N) and metastatic (M) extension. The macroscopic description of tumor morphology is useful in determining whether or not a particular lesion may be amenable to endoscopic therapy (9). Studies comparing these two systems suggest that the AJCC/IUAC system is better at predicting patient prognosis (8, 10–12).

DIAGNOSIS AND STAGING OF GASTRIC CANCER

Standard upper endoscopy with biopsies remains the gold standard for diagnosing gastric cancer (13). Unless EUS is available and can be performed at the time of the initial endoscopy, the staging workup for a newly diagnosed cancer should begin with non-invasive radiologic imaging (e.g., computerized tomography (CT), magnetic resonance imaging (MRI), combined positron emission tomography with CT (PET-CT)). These tests should be performed prior to EUS, since detection of unresectable disease (e.g., metastases) eliminates the need for endosonographic evaluation.

EUS TECHNIQUE

Endosonographic evaluation of gastric cancers requires the establishment of a good acoustic interface between the echoendoscope and the area of interest. This can be achieved by insufflation of the water-filled balloon on the echoendoscope and instillation of 200–500 mL of deaerated water into the gastric lumen (while elevating the patient's head to decrease the risk of aspiration). Optimal imaging is achieved by orienting the ultrasound transducer perpendicular to the target lesion since tangential imaging may cause the normal gastric wall layers to appear pathologically thickened. This perpendicular orientation can be difficult to achieve for lesions located in certain portions of the stomach (e.g., antrum and fundus).

Higher ultrasound frequencies provide greater near-field resolution but sacrifice the depth of penetration, while the converse is true for lower frequencies. Thus, high frequency transducers can provide greater resolution of the gastrointestinal wall layers, but provide limited information about regional lymph nodes and adjacent organs. Lower frequency transducers (e.g., 5–7.5 MHz) should be positioned roughly 2–3 cm from the target lesion, while high-frequency transducers (e.g., 20 MHz) provide the best images when positioned 1–2 cm from the structure being evaluated.

Most studies evaluating EUS for staging of gastric cancer have employed radial echoendoscopes with frequencies of 7.5–12 MHz. These frequencies generate a five-layer image of the gastric wall, composed of alternating bright (hyperechoic) and dark (hypoechoic) layers, including a mucosal interface layer (layer 1, bright), a deeper mucosal layer which contains the muscularis mucosa (layer 2, dark), the submucosa (layer 3, bright), muscularis propria (layer 4, dark), and serosa (layer 5, bright). The five-layer wall pattern of the normal gastric wall is shown in Fig. 1.

Reusable high frequency miniprobcs (20–30 MHz) are small diameter catheter-based ultrasound devices that can be advanced through the working channel of a conventional forward-viewing optical endoscope. Under optimal circumstances, these high-frequency miniprobcs produce a nine-layered resolution of the GI tract wall, and they can be ideal for imaging small gastric lesions, but their limited depth of pen-



Fig. 1. Normal five-layer wall pattern from gastric antrum. Layer 1: Interface layer, superficial mucosa (hyperechoic/bright). Layer 2: Deep mucosa (hypoechoic/dark). Layer 3: Submucosa (hyperechoic/bright). Layer 4: Muscularis propria (hypoechoic/dark). Layer 5: Serosa (hyperechoic/bright).

etration can be disadvantageous in the evaluation of larger lesions (>2 cm) (14, 15). Unlike radial echoendoscopes, curvilinear (aka, linear) echoendoscopes allow fine needle aspiration (FNA) for diagnostic tissue sampling of lymph nodes and other extra-gastric pathology. FNA can provide information that is crucial to accurate gastric cancer staging. FNA of the gastric wall itself can be useful in patients with suspected scirrhous gastric cancers, since conventional forceps biopsies of these tumors are frequently nondiagnostic (16).

PRIMARY TUMOR ASSESSMENT (T-STAGE) OF GASTRIC CANCER BY EUS

Staging of gastric cancer via EUS begins with the evaluation of the primary tumor with particular attention to the depth of invasion (T-staging) (17–19). The typical endosonographic appearance of T1–T4 tumors is as follows (18):

- T1: Thickening of the mucosal layers (layers 1 and 2) (T1a) or invasion into the submucosa (layer 3) (T1b). The muscularis propria (layer 4) is not involved by tumor; hence the thickness of layer 4 is normal. Depressed or flat lesions can be seen as an irregularity of the first layer and slightly thickened second layer. High-frequency transducers may help characterize the degree of mucosal and submucosal involvement. Figure 2 shows the endoscopic, endosonographic, and histologic features of a lesion with submucosal involvement (T1b).
- T2: Tumor infiltrates into the muscularis propria (layer 4) is associated with the loss of hyperechoic submucosal interface between the tumor and the muscularis propria. The muscularis propria is typically abnormally thickened, but the hyperechoic serosal layer (layer 5) is preserved.
- T3: Tumor penetrates through the serosa, which is manifested as disruption of the hyperechoic fifth layer.
- T4: Tumor invades the serosa (visceral peritoneum) (layer 5) (T4a) or directly into structures adjacent to the stomach (T4b), such as the pancreas, transverse colon, liver, spleen, left kidney, aorta, and upper abdominal vasculature. Endosonographic findings that raise concern for T4 disease include abutment of and loss of the plane of interface between the tumor and adjacent structures, or discernible tumor invasion into the adjacent structure.

Table 2 shows the results of studies from 1989 to 2006 describing the diagnostic accuracy for EUS for T-staging of gastric cancer. During this time period, the reported accuracy of EUS for T-staging ranged from 68 to 92%, with a mean accuracy of 80% (20–43). A recent meta-analysis

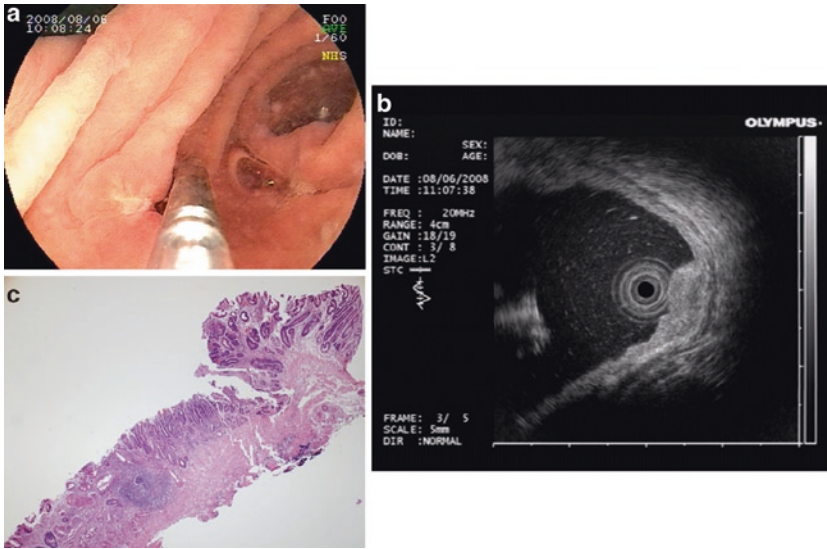


Fig. 2. Gastric cancer with submucosal involvement (T1). (a) Endoscopic appearance of ulcerated lesion in gastric antrum during evaluation with ultra-sound mini-probe. (b) EUS appearance demonstrates central ulceration, irregular contour, and involvement of the submucosa (layer 3) with an intact muscularis propria (layer 4). (c) Histologic appearance of lesion demonstrates invasion the submucosa.

of 22 studies from 1986 to 2006 evaluated pooled sensitivities and specificities of EUS for T-staging of gastric cancer, and also evaluated the effect of changes in EUS technology and EUS criteria for tumor staging over this time period. The pooled sensitivities and specificities for each T-stage were as follows: T1 (88.1% sensitivity, 100% specificity), T2 (82.3% sensitivity, 95.6% specificity), T3 (89.7% sensitivity, 94.7% specificity), and T4 (99.2% sensitivity, 96.7% specificity). In assessing the effects of technology advancements on the diagnostic accuracy of EUS for T-staging, studies were grouped between 1986 and 1994, 1995 and 1999, and 2000 and 2006. Pooled sensitivities and specificities for all T-stages were noted to increase from 1986 to 2006, highlighting the importance of improvements in technology and increased experience with EUS on its diagnostic accuracy for staging gastric cancers (44).

One criticism of these studies is that the endoscopists performing the EUS examinations have not routinely been blinded to the results of other imaging modalities performed prior to the EUS (i.e., the macroscopic

Table 2
Diagnostic accuracy of EUS for tumor (T) and nodal (N) staging
of gastric cancer. Adapted with permission from M. Kida (18)

<i>Reference</i>	<i>Year</i>	<i>N</i>	<i>T-staging (%)</i>	<i>N-staging (%)</i>
Aibe et al. (20)	1989	67	73	69
Tio et al. (21)	1989	72	84	68
Heintz et al. (22)	1991	19	79	72
Botet et al. (23)	1991	50	92	78
Akahoshi et al. (24)	1991	74	81	50
Cerizzi et al. (25)	1992	29	90	57
Rosch et al. (26)	1992	41	71	75
Caletti et al. (27)	1993	42	91	69
Nattermann et al. (28)	1993	50	82	78
Ziegler et al. (29)	1993	108	86	74
Grimm et al. (30)	1993	147	78	87
Dittler et al. (31)	1993	254	83	66
De Angelis et al. (32)	1994	86	80	75
Massari et al. (33)	1996	65	89	68
Wang et al. (34)	1998	119	70	65
Mancino et al. (35)	2000	79	76	67
Willis et al. (36)	2000	116	78	77
Xi et al. (37)	2003	32	80	69
Shinoyama et al. (38)	2004	45	71	80
Javaid et al. (39)	2004	112	83	64
Bhandari et al. (40)	2004	63	88	79
Ganapathi et al. (41)	2006	109	80	77
Tsenduren et al. (42)	2006	41	68	100
Potrc et al. (43)	2006	82	68	57
Total patients	–	1,820	–	–
Mean accuracy	–	–	80	72

tumor appearance on white-light endoscopy, CT scan findings). The information obtained by these other modalities can potentially introduce a source of bias by influencing the endosonographer's decision-making and their ultimate tumor staging classification. This potential bias was evaluated in a retrospective study of 33 patients who underwent videotaped EUS examinations for the evaluation of gastric cancer.

All of the patients in this study, with the exception of one, had surgically resected specimens for correlation with histopathologic T-stage. These videotaped examinations were subsequently blindly reviewed by endosonographers (without review of CT and endoscopy images) and their interpretations were compared with those of a nonblinded endosonographer that had performed the initial EUS assessment. For nonblinded EUS evaluation, the overall T-staging accuracy (compared to histopathology) was 66.7%, but this fell to 45.5% under blinded evaluation (45). The same authors performed a follow-up study of 55 videotaped EUS examinations of gastric cancer patients with five examiners, blinded as described above, and described significant inter-observer variability among endosonographers within each T-stage designation; with kappa values of 0.47, 0.38, 0.39, and 0.34 for T1, T2, T3, and T4 lesions, respectively (46). In clinical practice, it is impractical to perform EUS in the absence of endoscopic and cross-sectional imaging data. These studies highlight the subjective component of EUS and the potential impact that knowledge of other test results can have on the diagnostic accuracy of EUS (20–43). Despite these limitations, EUS remains the most studied and consistently accurate method for local T-staging for gastric cancer.

LYMPH NODE ASSESSMENT (N-STAGING) OF GASTRIC CANCER BY EUS

Endosonographic N-staging of gastric cancer requires careful inspection of several peri-gastric regions, including those adjacent to the greater and lesser curvatures (including the suprapyloric and infrapyloric areas), the celiac axis (including the left gastric and the common hepatic arteries), the gastrohepatic ligament, and the splenic hilum (being cautious not to confuse benign splenules with pathologic lymph nodes). Several endosonographic features have been described as being predictive of malignant lymph nodes, as listed in Table 3. If all four of these features are present, they have an accuracy of diagnosing a malignant lymph node of 80%. However, only 25% of malignant lymph nodes have all four features, and the presence of any one of these features can help independently predict malignant involvement (47). It has recently been suggested that the presence of intact intranodal vasculature correlates with benign lymph node status, and may be a fifth distinguishing EUS criteria (48). EUS-guided FNA of abnormal appearing regional lymph nodes is an additional important adjunct in determining malignant involvement (47, 49). FNA is a safe and effective method of tissue

acquisition, and should be considered if any suspicious lymph nodes are identified, but care should be taken to avoid traversing the primary gastric tumor to prevent inadvertent tumor seeding along the needle tract and contamination of the cytology sample by malignant cells.

EUS appears to be less accurate for N-staging than T-staging (Table 4). Table 5 shows reported EUS accuracy rates of N-staging for gastric cancer, with an average accuracy of 72% (20–43).

Many of these studies used the older 1987 TNM classification in which the N-stage was determined by the distance of the involved nodes in relation to the primary tumor, rather than the absolute number of malignant regional nodes as advocated in the 2010 guidelines (7, 50).

Table 3
Comparison of EUS features of malignant vs. benign lymph nodes

<i>Malignant</i>	<i>Benign</i>
Round or oval	Flat, triangular, “draping”
Homogeneous, hypoechoic	Heterogeneous, centrally hyperechoic
Sharp borders	Poorly defined borders
Size >10 mm	Size <10 mm
	Intact intranodal vasculature

Table 4
Comparison of EUS vs. CT/MRI for gastric cancer tumor staging (T-staging) accuracy. Adapted with permission from M. Kida (18)

<i>Reference</i>	<i>Year</i>	<i>N</i>	<i>EUS (%)</i>	<i>CT (%)</i>	<i>MRI (%)</i>
Botet et al. (23)	1991	50	92	42	
Grimm et al. (30)	1991	118	82	11	
Ziegler et al. (29)	1993	108	86	43	
Kuntz et al. (59)	1999	82	73	51	48
Kang et al. (60)	2000	46			83
Sohn et al. (61)	2000	30		67	73
Polkowski et al. (62)	2004	88	63	44	
Bhandari et al. (40)	2004	63	88	83	
Zhong et al. (63)	2005	15			71
Total/mean		509	81	49	69

Table 5
Comparison of EUS vs. CT/MRI for gastric cancer nodal staging
(N-staging) accuracy. Adapted with permission from M. Kida (18)

<i>Reference</i>	<i>Year</i>	<i>N</i>	<i>EUS (%)</i>	<i>CT (%)</i>	<i>MRI (%)</i>
Botet et al. (23)	1991	50	78	48	
Grimm et al. (30)	1991	118	88	21	
Ziegler et al. (29)	1993	108	74	51	
Kuntz et al. (59)	1999	82	87	65	69
Kang et al. (60)	2000				
Sohn et al. (61)	2000			55	59
Polkowski et al. (62)	2004	88	30	47	
Bhandari et al. (40)	2004	63	79	75	
Zhong et al. (63)	2005	15			57
Total/mean		509	72	52	62

ASSESSMENT OF DISTANT METASTASES (M-STAGING) OF GASTRIC CANCER BY EUS

Cross-sectional imaging studies such as CT and MRI are the preferred modalities in the initial evaluation for metastatic disease in gastric cancer patients. The addition of PET scanning to measure 18-Fluorodeoxyglucose (FDG) uptake to conventional CT scanning has improved the detection rates of metastatic disease (51–53). EUS has a relatively limited role in this setting. The application of EUS for the evaluation of liver metastases has been described, but data is limited (54). Since the liver is the most frequently involved metastatic site that can be visualized during EUS, it should be inspected carefully. Less common sites for distant metastatic disease that also can be evaluated using EUS and FNA include the posterior mediastinum, left adrenal gland, pancreas, and upper abdominal ascites (55, 56).

TECHNICAL LIMITATIONS OF EUS FOR TNM STAGING OF GASTRIC CANCER

While EUS can be an accurate means of determining T- and N-stage for gastric cancer, several factors have been associated with over- or understaging, including the presence of ulceration, inflammation, peri-tumoral

fibrosis, and tumor localization along the lesser curvature and posterior gastric wall (34, 57). The absence of a serosal layer along the lesser curvature and posterior wall may lead to erroneous overstaging of tumors in these locations (i.e., characterizing a T2 lesion as a T3 lesion). T2 lesions near the gastrocolic or gastrohepatic ligaments can be similarly overstaged (19). Other factors associated with inaccurate staging include large tumor size (>3 cm), which is more commonly associated with overstaging, and poorly differentiated tumor histology, which is most often associated with under-staging (58).

COMPARISON OF EUS TO OTHER IMAGING MODALITIES FOR STAGING OF GASTRIC CANCER

Studies evaluating EUS, CT, and MRI for staging of gastric cancer have generally shown that EUS is more accurate for both T- and N-staging (23, 29, 30, 40, 59–64). These data are listed in Tables 4 and 5. In one study evaluating T-staging accuracy of all three modalities, EUS had the highest overall accuracy for T-staging (73%) and N-staging (87%), MRI had the lowest accuracy (48%) for T-staging, N-staging accuracies for MRI and CT scan were comparable (69 and 65%, respectively) (59). More recent studies using multidetector CT and MRI have shown improved accuracy for T-staging, however, until more data becomes available, EUS remains the most accurate imaging modality for this purpose (64). Nonetheless, CT and/or MRI are the best initial studies for the evaluation of metastases, thus the complementary role of cross-sectional imaging and EUS in staging of gastric cancers must be underscored.

EUS IN THE EVALUATION OF EARLY GASTRIC CANCER

Early gastric cancer is defined as gastric adenocarcinoma limited to the gastric mucosa or submucosa (8). In Japan, early gastric cancer represents nearly 50% of diagnosed cases, whereas most cases in the US represent advanced disease (1, 5, 6). The potential macroscopic appearances of such lesions based on the Japanese classification system are depicted in Fig. 3. Patients with early gastric cancer have a favorable prognosis and survival has been reported as high as 90% with curative surgical resection (65). EUS is helpful in determining which tumors may be amenable to curative endoscopic resection. Recently, higher frequency miniproboscopes (30 MHz) have been shown to accurately

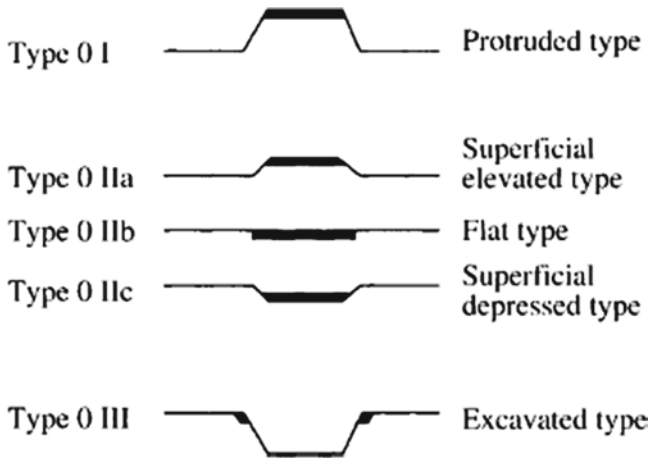


Fig. 3. Japanese classification of gastric cancer based on endoscopic appearance. Type 0: Superficial, flat tumors with or without minimal elevation or depression. Type 0 I: Protruded type (lesion thickness $>2\times$ normal mucosal thickness). Type 0 IIa: Superficial elevated type (lesion thickness $\leq 2\times$ normal mucosal thickness). Type 0 IIb: Flat type. Type 0 IIc: Superficial depressed type. Type III: Excavated type.

diagnose lesions with minute submucosal invasion with an accuracy as high as 92%, an improvement over 12 MHz (81%) and 20 MHz probes (86%) (66).

In recent years, endoscopic resection (ER) techniques have become a part of the management of early gastric cancers. ER can be considered in patients with any of the following (8, 9, 67):

1. Well-differentiated intramucosal adenocarcinoma without ulceration or ulcer scar (no size limitation)
2. Well-differentiated intramucosal carcinoma with ulceration or ulcer scar <3 cm
3. Tumor diameter <2 cm in type IIa lesions and <1 cm in type IIb and IIc lesions
4. Patients with sm1 lesions (minute submucosal invasion <500 μm) with well-differentiated carcinoma <3 cm
5. Patients with no evidence of lymphatic or venous involvement

Conventional cap-based ER of larger lesions (>1.5 cm) may involve piecemeal resection, which can make it impossible to determine histologically whether a complete resection (R0) was achieved (68). In addition, the healing process following cap-based ER can result in submucosal

fibrosis, which can impede subsequent endoscopic efforts to resect the residual neoplasm. Endoscopic submucosal dissection (ESD) is a newer technique performed with insulated-tip needle knives (IT knives), enabling en bloc resection of these larger diameter early-stage cancers (9, 67). ESD has enjoyed widespread acceptance and application in Japan, but IT knives are not yet widely available for use in the United States. However, since the risk of concomitant lymph node with tumor invasion into the submucosa is ~20%, surgical resection should strongly be considered for patients who are medically fit to undergo surgery (69).

EUS IN THE EVALUATION OF LOCALLY ADVANCED GASTRIC CANCER

The Borrmann classification is a commonly utilized system for the macroscopic classification of locally advanced gastric cancers, subdividing them into four subtypes (70):

- Type I: Polypoid
- Type II: Fungating
- Type III: Ulcerated
- Type IV: Diffusely infiltrative

Tumors classified as Type IV based on their macroscopic appearance are histologically characterized as poorly differentiated, scirrhous adenocarcinomas. When the entire stomach is involved with Type IV disease the term “linitis plastica” is used and refers to the “leather bottle” appearance of the stomach on barium radiography (71). Much of the data regarding EUS in the evaluation of infiltrative or scirrhous gastric cancer comes from the studies of EUS in the evaluation of thickened gastric folds (72, 73). The gastric wall is considered thickened when total wall thickness exceeds 3.6 mm (Fig. 4) (73). Diffuse thickening that is limited to the first two layers (i.e., mucosa and deep mucosa), is most frequently attributable to a benign process (72, 73). In one study that compared patients with scirrhous type gastric cancer to patients with hypertrophic gastritis, those with scirrhous gastric cancer had overall preservation of the five-layer gastric wall pattern with irregular hypoechoic thickening of the third and fourth layers (i.e., submucosa and muscularis propria). Patients with hypertrophic gastritis, on the other hand, demonstrate wall thickening confined to the mucosa (74). Unexplained thickening of the muscularis propria (layer 4) is often a pathologic finding on EUS, and can be seen in both infiltrating gastric carcinoma and gastric lymphoma (72, 73, 75, 76). Contrary to linitis

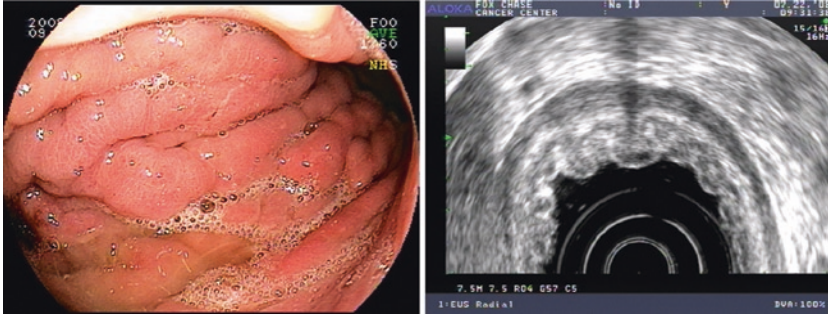


Fig. 4. Infiltrative scirrhus gastric cancer (linitis plastica). (a) Endoscopic appearance demonstrates thickened gastric folds. (b) EUS appearance demonstrates pathologic thickening of muscularis propria (layer 4) with relative preservation of five-layer gastric wall pattern.

plastica, wherein the five-layer structure can often still be discerned on EUS, infiltrating gastric lymphomas often disrupt or obliterate the five-layer pattern. Infiltrative carcinomas may also show a more vertical growth pattern into the gastric wall, while lymphomas may demonstrate a more horizontal pattern (16). Tissue acquisition using EUS-guided FNA of the gastric wall is another means by which EUS can help delineate benign from malignant causes of thickened gastric folds, since endoscopic forceps biopsies can be nondiagnostic even when infiltrating malignancy is present (16, 73).

Finally, with regard to T-staging of scirrhus gastric cancers, designation of T-stage on the basis of the deepest wall layer showing thickening or irregularity has been reported to have an overall accuracy of 88% (77). Endosonography also plays a role in the staging of noncarcinomatous neoplasms of the stomach, such as lymphomas that involve the mucosa-associated lymphoid tissue (i.e., MALT lymphomas), but further description of the role of EUS in these settings is beyond the scope of this review.

CONCLUSION

The diagnosis of gastric cancer should be established endoscopically and confirmed histologically. Once distant metastatic disease has been ruled out using non-invasive cross-sectional imaging, loco-regional staging with EUS should be considered. Endosonography, particularly using higher-frequency ultrasound miniprobosc (e.g., 30 MHz), plays a role in the assessment of early gastric cancers confined to the mucosa

and submucosa and can help select patients for endoscopic resection. EUS is also useful in the evaluation of patients with suspected infiltrative scirrhous gastric cancer or linitis plastica and helps differentiate it from other conditions that cause “thickened gastric folds.” While the accuracy of EUS can be influenced by the presence of ulcer, fibrosis, peritumoral inflammation, and a variety of technical factors, EUS is still the most well-studied and consistently accurate imaging modality for the local staging of gastric cancer and remains the first-choice test for this purpose in the absence of metastatic disease.

REFERENCES

1. Crew KD, Neugut AI. Epidemiology of gastric cancer. *World J Gastroenterol*. 2006;12(3):354–62.
2. Parkin DM. International variation. *Oncogene*. 2004;23(38):6329–40.
3. Lauren P. The two histological main types of gastric carcinoma: diffuse and so-called intestinal-type carcinoma. An attempt at a histo-clinical classification. *Acta Pathol Microbiol Scand*. 1965;64:31–49.
4. Wilkinson N, Howe J, Gay G, Patel-Parekh L, Scott-Conner C, Donohue J. Differences in the pattern of presentation and treatment of proximal and distal gastric cancer: results of the 2001 gastric patient care evaluation. *Ann Surg Oncol*. 2008;15(6):1644–50.
5. Jemal A, Siegel R, Ward E, et al. Cancer statistics, 2008. *CA Cancer J Clin*. 2008; 58(2):71–96.
6. Kawai K, Watanabe Y. The impact of mass screening on gastric cancer mortality in Japan. *Gastrointest Endosc*. 1998;47(3):320–3.
7. Edge SB, Byrd DR, Compton CC, et al. *AJCC cancer staging manual*. 7th ed. New York: Springer; 2010.
8. JGCA. Japanese classification of gastric carcinoma – 2nd English edition. *Gastric Cancer*. 1998;1(1):10–24.
9. Nakajima T. Gastric cancer treatment guidelines in Japan. *Gastric Cancer*. 2002;5:1–5.
10. Katai H, Yoshimura K, Maruyama K, Sasako M, Sano T. Evaluation of the new international union against cancer TNM staging for gastric carcinoma. *Cancer*. 2000;88(8):1796–800.
11. Hayashi H, Ochiai T, Suzuki T, et al. Superiority of a new UICC-TNM staging system for gastric carcinoma. *Surgery*. 2000;127(2):129–35.
12. Ichikura T, Tomimatsu S, Uefuji K, Kimura M, Uchida T, Morita D, et al. Evaluation of the new American joint committee on cancer/International union against cancer classification of lymph node metastasis from gastric carcinoma in comparison with the Japanese classification. *Cancer*. 1999;86(4):553–8.
13. Kurtz R, Sherlock P. The diagnosis of gastric cancer. *Semin Oncol*. 1985;12(1): 11–8.
14. Yanai H, Tada M, Karita M, Okita K. Diagnostic utility of 20-megahertz linear endoscopic ultrasonography in early gastric cancer. *Gastrointest Endosc*. 1996;44(1): 29–33.

15. Okamura S, Tsutsui A, Muguruma N, Ichikawa S, Sogabe M, Okita Y, et al. The utility and limitations of an ultrasonic miniprobe in the staging of gastric cancer. *J Med Invest.* 1999;46:49–53.
16. Caletti G, Fusaroli P, Togliani T, Bocus P, Roda E. Endosonography in gastric lymphoma and large gastric folds. *Eur J Ultrasound.* 2000;11(1):31–40.
17. Hawes R, Fockens P. How to perform EUS in the stomach. In: Hawes RH, Fockens PJ, editors. *Endosonography.* Philadelphia, PA: Saunders; 2006.
18. Kida M. EUS in gastric cancer. In: Hawes RH, Fockens P, editors. *Endosonography.* Philadelphia, PA: Saunders; 2006.
19. Olds G, Chak AC. Endoscopic ultrasound for staging gastric cancer. In: Faigel DO, Kochman ML, editors. *Endoscopic oncology.* Totowa, NJ: Humana; 2006.
20. Aibe T, Fujimura H, Noguchi T, et al. Endosonographic detection and staging of early gastric cancer. In: Dancygier H, Classen M, editors. *Fifth International Symposium on EUS.* Munich, Germany; 1989. p. 71–8.
21. Tio TL, Schouwink MH, Cikot RJ, Tytgat GN. Preoperative TNM classification of gastric carcinoma by endosonography in comparison with the pathological TNM system: a prospective study of 72 cases. *Hepatogastroenterology.* 1989;36:51–6.
22. Heintz A, Junginger T. Endosonographic staging of cancers of the esophagus and stomach. Comparison with surgical and histopathologic staging. *Bildgebung.* 1991;58:4–8.
23. Botet JF, Lightdale CJ, Zauber AG, et al. Preoperative staging of gastric cancer: comparison of endoscopic US and dynamic CT. *Radiology.* 1991;181(2):426–32.
24. Akahoshi K, Misawa T, Fujishima H, et al. Preoperative evaluation of gastric cancer by endoscopic ultrasound. *Gut.* 1991;32(5):479–82.
25. Cerizzi A, Crosta C, Botti F, Carrara A, Alloni R, Taschieri AM. Preoperative staging of gastric carcinoma using endosonography (EUS). *Ann Ital Chir.* 1992;63(4):465–9.
26. Rösch T, Lorenz R, Zenker K, von Wichert A, Dancygier H, Höfler H, et al. Local staging and assessment of resectability in carcinoma of the esophagus, stomach, and duodenum by endoscopic ultrasonography. *Gastrointest Endosc.* 1992;38(4):460–7.
27. Caletti G, Ferrari A, Brocchi E, Barbara L. Accuracy of endoscopic ultrasonography in the diagnosis and staging of gastric cancer and lymphoma. *Surgery.* 1993;113(1):14–27.
28. Nattermann C, Galbenu-Grunwald R, Nier H, Dancygier H. Endoscopic ultrasound in TN staging of stomach cancer. A comparison with computerized tomography and conventional ultrasound. *Z Gesamte Inn Med.* 1993;48(2):60–4.
29. Ziegler K, Sanft C, Zimmer T, et al. Comparison of computed tomography, endosonography, and intraoperative assessment in TN staging of gastric carcinoma. *Gut.* 1993;34(5):604–10.
30. Grimm H, Binmoeller KF, Hamper K, Koch J, Henne-Bruns D, Soehendra N. Endosonography for preoperative locoregional staging of esophageal and gastric cancer. *Endoscopy.* 1993;25(3):224–30.
31. Dittler HJ, Siewert JR. Role of endoscopic ultrasonography in gastric carcinoma. *Endoscopy.* 1993;25(2):162–6.
32. De Angelis C, Gindro T, Recchia S, et al. Value and limitations of preoperative endoscopic ultrasonography in predicting stage and resectability of gastric cancer. *Gastroenterology.* 1994;106:380 (abstract).

33. Massari M, Cioffi U, De Simone M, Bonavina L, D'elia A, Rosso L, et al. Endoscopic ultrasonography for preoperative staging of gastric carcinoma. *Hepatogastroenterology*. 1996;43(9):542–6.
34. Wang J-Y, Hsieh J-S, Huang Y-S, Huang C-J, Hou M-F, Huang T-J. Endoscopic ultrasonography for preoperative locoregional staging and assessment of resectability in gastric cancer. *Clin Imaging*. 1998;22(5):355–9.
35. Mancino G, Bozzetti F, Schicci A, et al. Preoperative endoscopic ultrasonography in patients with gastric cancer. *Tumori*. 2000;86(2):139–41.
36. Willis S, Truong S, Gribnitz S, Fass J, Schumpelick V. Endoscopic ultrasonography in the preoperative staging of gastric cancer. *Surg Endosc*. 2000;14(10):951–4.
37. Xi WD, Zhao C, Ren GS. Endoscopic ultrasonography in preoperative staging of gastric cancer: determination of tumor invasion depth, nodal involvement and surgical resectability. *World J Gastroenterol*. 2003;9(2):254–7.
38. Shimoyama S, Yasuda H, Hashimoto M, et al. Accuracy of linear-array EUS for preoperative staging of gastric cardia cancer. *Gastrointest Endosc*. 2004;60(1):50–5.
39. Javaid G, Shah OJ, Dar MA, Shah P, Wani NA, Zargar SA. Role of endoscopic ultrasonography in preoperative staging of gastric carcinoma. *ANZ J Surg*. 2004;74(3):108–11.
40. Bhandari S, Sup Shim CH, Hoon Kim J, et al. Usefulness of three-dimensional, multidetector row CT (virtual gastroscopy and multiplanar reconstruction) in the evaluation of gastric cancer: a comparison with conventional endoscopy, EUS, and histopathology. *Gastrointest Endosc*. 2004;59(6):619–26.
41. Ganpathi I, So J, Ho KY. Endoscopic ultrasonography for gastric cancer. *Surg Endosc*. 2006;20(4):559–62.
42. Tsendsuren T, Jun SM, Mian XH. Usefulness of endoscopic ultrasonography in preoperative TNM staging of gastric cancer. *World J Gastroenterol*. 2006;12(1):43–7.
43. Potrč S, Skalicky M, Ivanecz A. Does endoscopic ultrasound staging already allow individual treatment regimens in gastric cancer. *Wien Klin Wochenschr*. 2006;118:48–51.
44. Puli S, Batapati JKR, Bechtold ML, Antillon MR, Ibdah JA. How good is endoscopic ultrasound for TNM staging of gastric cancers? A meta-analysis and systematic review. *World J Gastroenterol*. 2008;14(25):4011–9.
45. Meining A, Dittler HJ, Wolf A, et al. You get what you expect? A critical appraisal of imaging methodology in endosonographic cancer staging. *Gut*. 2002;50(5):599–603.
46. Meining A, Rösch T, Wolf A, et al. High interobserver variability in endosonographic staging of upper gastrointestinal cancers. *Z Gastroenterol*. 2003;41:391–4.
47. Bhutani MS, Hawes RH, Hoffman BJ. A comparison of the accuracy of echo features during endoscopic ultrasound (EUS) and EUS-guided fine-needle aspiration for diagnosis of malignant lymph node invasion. *Gastrointest Endosc*. 1997;45(6):474–9.
48. Hall JD, Kahaleh M, White GE, Talreja J, Northup PG, Shami VM. Presence of lymph node vasculature: a new EUS criterion for benign nodes? *Dig Dis Sci*. 2009;54(1):118–21.

49. ten Berge J, Hoffman BJ, Hawes RH, et al. EUS-guided fine needle aspiration of the liver: indications, yield, and safety based on an international survey of 167 cases. *Gastrointest Endosc.* 2002;55(7):859–62.
50. Hermanek P, Sobin LH. UICC TNM classification of malignant tumors. 4th ed. Berlin: Springer; 1987.
51. Kinkel K, Lu Y, Both M, Warren RS, Thoeni RF. Detection of hepatic metastases from cancers of the gastrointestinal tract by using noninvasive imaging methods (US, CT, MR imaging, PET): a meta-analysis. *Radiology.* 2002;224(3):748–56.
52. Yeung HW, Macapinlac H, Karpeh M, Finn RD, Larson SM. Accuracy of FDG-PET in gastric cancer. Preliminary experience. *Clin Positron Imaging.* 1998;1(4):213–22.
53. Chen J, Cheong JH, Yun MJ, Kim J, Lim JS, Hyung WJ, et al. Improvement in preoperative staging of gastric adenocarcinoma with positron emission tomography. *Cancer.* 2005;103(11):2383–890.
54. Prasad P, Schmulewitz N, Patel A, et al. Detection of occult liver metastases during EUS for staging of malignancies. *Gastrointest Endosc.* 2004;59(1):49–53.
55. Chen CH, Yang CC, Yeh YH. Preoperative staging of gastric cancer by endoscopic ultrasound: the prognostic usefulness of ascites detected by endoscopic ultrasound. *J Clin Gastroenterol.* 2002;35(4):321–7.
56. Chu K-M, Kwok K-F, Law S, Wong K-H. A prospective evaluation of catheter probe EUS for the detection of ascites in patients with gastric carcinoma. *Gastrointest Endosc.* 2004;59(4):471–4.
57. Yanai H, Matsumoto Y, Harada T, et al. Endoscopic ultrasonography and endoscopy for staging depth of invasion in early gastric cancer: a pilot study. *Gastrointest Endosc.* 1997;46(3):212–6.
58. Kim J-H, Song KS, Youn YH, et al. Clinicopathologic factors influence accurate endosonographic assessment for early gastric cancer. *Gastrointest Endosc.* 2007;66(5):901–8.
59. Kuntz C, Herfarth C. Imaging diagnosis for staging of gastric cancer. *Semin Surg Oncol.* 1999;17(2):96–102.
60. Kang B, Kim JH, Kim KW, Lee DY, Baek SY, Lee SW, et al. Value of the dynamic and delayed MR sequence with Gd-DTPA in the T-staging of stomach cancer: correlation with the histopathology. *Abdom Imaging.* 2000;25(1):14–24.
61. Sohn K-M, Lee JM, Lee S-Y, Ahn B-Y, Park S-M, Kim K-M. Comparing MR Imaging and CT in the staging of gastric carcinoma. *Am J Roentgenol.* 2000;174(6):1551–7.
62. Polkowski M, Palucki J, Wronska E, Szawlowski A, Nasierowska-Guttmejer A, Butruk E. Endosonography versus helical computed tomography for locoregional staging of gastric cancer. *Endoscopy.* 2004;36(7):617–23.
63. Zhong L, Lei LI, Jian Hua SUN, Jian Rong XU. Preoperative diagnosis of gastric cancer using 2-D magnetic resonance imaging with 3-D reconstruction techniques. *Chin J Dig Dis.* 2005;6(4):159–64.
64. Kwee RM, Kwee TC. Imaging in local staging of gastric cancer: a systematic review. *J Clin Oncol.* 2007;25(15):2107–16.
65. Fujiwara M, Kodera Y, Misawa K, Kinoshita M, Kinoshita T, Miura S, et al. Longterm outcomes of early-stage gastric carcinoma patients treated with laparoscopy-assisted surgery. *J Am Coll Surg.* 2008;206(1):138–43.

66. Ichikawa T, Kudo M, Matsui S, Okada M, Kitano M. Endoscopic ultrasonography with three miniature probes of different frequency is an accurate diagnostic tool for endoscopic submucosal dissection. *Hepatogastroenterology*. 2007;54(73):325–8.
67. Soetikno RM, Gotoda T, Nakanishi Y, Soehendra N. Endoscopic mucosal resection. *Gastrointest Endosc*. 2003;57(4):567–79.
68. Yokoi C, Gotoda T, Hamanaka H, Oda I. Endoscopic submucosal dissection allows curative resection of locally recurrent early gastric cancer after prior endoscopic mucosal resection. *Gastrointest Endosc*. 2006;64(2):212–8.
69. Ichikura T, Uefuji K, Tomimatsu S, Okusa Y, Yahara T, Tamakuma S. Surgical strategy for patients with gastric carcinoma with submucosal invasion. A multivariate analysis. *Cancer*. 1995;76(6):935–40.
70. Borrmann R. Geshwulste des magens und duodenums. In: Henke F, Lubarsch O, editors. *Handbuch der speziellen pathologischen Anatomie und Histologie*, vol. 4. Berlin: Springer; 1926.
71. Levine M, Kong V, Rubesin SE, Laufer I, Herlinger H. Scirrhous carcinoma of the stomach: radiologic and endoscopic diagnosis. *Radiology*. 1990;175:151–4.
72. Mendis R, Gerdes H, Lightdale CJ, Botet JF. Large gastric folds: a diagnostic approach using endoscopic ultrasonography. *Gastrointest Endosc*. 1994;40(4):437–41.
73. Caletti G, Fusaroli P, Bocus P. Endoscopic ultrasonography in large gastric folds. *Endoscopy*. 1998;30 Suppl 1:A72–5.
74. Fujishima H, Misawa T, Chijiwa Y, Maruoka A, Akahoshi K, Nawata H. Scirrhous carcinoma of the stomach versus hypertrophic gastritis: findings at endoscopic US. *Radiology*. 1991;181(1):197–200.
75. Chen T, Wu CH, Lee CL, Lai YC, Yang SS. Endoscopic ultrasonography in the differential diagnosis of giant gastric folds. *J Formos Med Assoc*. 1999;98(4):261–4.
76. Songür Y, Okai T, Watanabe H, Motoo Y, Sawabu N. Endosonographic evaluation of giant gastric folds. *Gastrointest Endosc*. 1995;41(5):468–74.
77. Saito N, Takeshita K, Habu H, Endo M. The use of endoscopic ultrasound in determining the depth of cancer invasion in patients with gastric cancer. *Surg Endosc*. 1991;5(1):14–9.

The Role of EUS in Subepithelial Lesions

*Janelle Brown-Chang, MD
and Joo Ha Hwang, MD, PhD*

CONTENTS

INTRODUCTION
EXTRAMURAL LESIONS
INTRAMURAL LESIONS
CONCLUSIONS

Abstract

Subepithelial masses are often encountered when performing endoscopy. The differential diagnosis for subepithelial masses includes lesions that are benign, premalignant, or malignant. Evaluation of subepithelial lesion with EUS allows further characterization of the lesion by ultrasound imaging, providing valuable information to help guide further management.

Key Words: Endoscopy, Endoscopic ultrasound, Subepithelial masses

INTRODUCTION

The term subepithelial lesion refers to any mass, bulge, or impression visible within the lumen of the gastrointestinal tract that is covered by normal appearing mucosa (Fig. 1). While the term “submucosal” rather than subepithelial is occasionally used, this is less accurate as the lesion may arise from any of the layers of the gastrointestinal wall or even from extrinsic

From: *Clinical Gastroenterology: Endoscopic Ultrasound*,
Edited by: V. M. Shami and M. Kahaleh, DOI 10.1007/978-1-60327-480-7_10,
© Springer Science+Business Media, LLC 2010

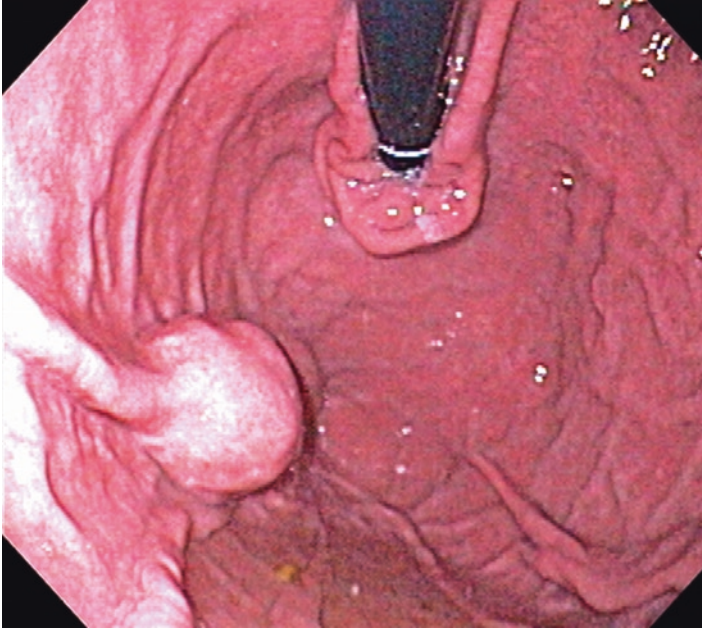


Fig. 1. Endoscopic image of a gastric subepithelial mass.

compression, not just the submucosa. The prevalence of subepithelial lesions detected on routine endoscopy is unknown; however, one retrospective study reported that subepithelial gastric lesions were found in 0.36% of esophagogastroduodenoscopies performed between 1976 and 1984 (1). The differential diagnosis for a gastrointestinal subepithelial lesion is broad and includes malignant tumors, premalignant lesions, benign masses, and normal structures – which are potentially indistinguishable from one another by simple endoscopic evaluation. Experienced gastroenterologists can make educated guesses as to the cause of a subepithelial bulge; using tricks such as probing with forceps to elicit a “pillow sign” (suggestive of lipoma) or evaluating for smooth tapered edges versus sharper cut-offs at the borders of the mass are of only limited effectiveness. In fact, two prospective studies have shown a sensitivity of 89–98% and specificity of 29–64% in the ability of endoscopists to determine intramural causes of subepithelial masses (2, 3). While the final diagnosis of many of these lesions is made on biopsy or resection, EUS alone can often yield a specific diagnosis, especially in the case of extrinsic compression. EUS imaging of the gastrointestinal tract typically identifies five distinct layers – though up to seven to nine can be seen

Table 1
The histologic structures associated with the five layers appreciated on EUS evaluation of the gastrointestinal wall

<i>EUS layer</i>	<i>Histologic structure</i>
1	Superficial mucosa
2	Deep mucosa
3	Submucosa plus acoustic interface between submucosa and muscularis propria
4	Muscularis propria minus acoustic interface between submucosa and muscularis propria
5	Serosa and subserosal fat

depending on the region of the GI tract being evaluated and the frequency of the ultrasound transducer. These layers have a histological correlation as described in Table 1 (4). Size, layer of origin, and echotexture (Table 2) can all be used to help identify intramural lesions or direct further management (surgical resection, endoscopic submucosal resection/dissection) or studies (special stains and immunohistochemical evaluation of tissue samples) to aid in their accurate identification. Extension between layers, irregular margins, or invasion into adjacent structures have all been used to suggest malignant lesions further expanding the information available to guide treatment (5, 6). The goal of this chapter is to discuss the various causes of subepithelial lesions and the role of EUS in identifying and directing management for these lesions.

EXTRAMURAL LESIONS

Extraluminal compression by the spleen or splenic vessels is the most common etiology for a subepithelial lesion found to be of extramural origin (Fig. 2 a,b) (2, 3, 7). Other normal anatomic variants such as left lobe of the liver, gallbladder, pancreas or loops of bowel are also potential causes for extraluminal compression. Occasionally, enlarged uterine fibroids, pancreatic pseudocysts, aneurysms, and enlarged lymph nodes can also sometimes be interpreted as subepithelial lesions. Identification of these extramural lesions is straightforward with the use of EUS.

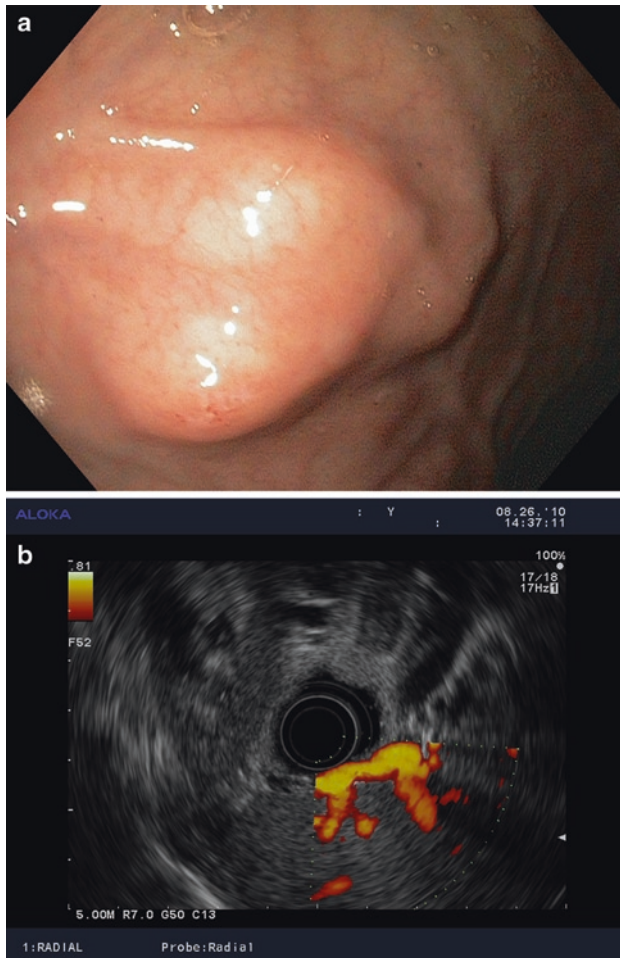


Fig. 2. (a) Endoscopic view of extrinsic compression of the stomach. (b) Radial EUS image of prominent splenic vessels causing extrinsic compression. The use of color doppler confirms vessel flow.

INTRAMURAL LESIONS

Benign

LIPOMA

Lipomas are common, benign, slow growing fatty tumors most commonly found in the right side of the colon, but can be seen anywhere in the GI tract (8, 9). They are often seen to have a

Table 2
Intramural subepithelial masses and their EUS characteristics

<i>Subepithelial lesion</i>	<i>EUS layer^a</i>	<i>Echogenicity</i>
Malignant or potentially malignant lesions		
GIST	4 (rarely 2)	Hypoechoic
Lymphoma	2, 3 or 4	Hypoechoic
Glomus tumor	3 or 4	Hypoechoic
Metastatic carcinoma	Any	Hypoechoic
Granular cell tumor	2 or 3	Hypoechoic
Carcinoid	2 or 3	Hypoechoic
Benign lesions		
Leiomyoma	2 or 4	Hypoechoic
Fibroma	3	Hyperechoic
Neurofibroma	3 or 4	Hyperechoic
Osteochondroma	3	Hyperechoic
Lipoma	3	Intensely hyperechoic
Lymphangioma	3 or 4	Hypoechoic
Fibrovascular polyp	3 or 4	Hyperechoic
Pancreatic rest	2 or 3	Hypoechoic
Duplication cyst	Any or extramural	Anechoic
Varices	2 or 3	Anechoic

^aRefer to Table 1 for histological structure corresponding to EUS layer. (Adapted from Hwang and Kimmey (71))

yellowish hue on endoscopy and can exhibit the so-called pillow sign when probed with a closed forcep. One study has suggested that there is a high specificity of 98% but a relatively low sensitivity of 40% for a positive pillow sign (2). While a classic appearing solitary, yellowish lesion that exhibits a pillow sign may require no confirmation with EUS, it can be more confusing in reality. There are reports of lipomas which become ulcerated and large enough to obstruct or even cause intussusception (8–12). On EUS, lipomas are found to be intensely hyperechoic and well circumscribed (Fig. 3). They arise from the submucosal layer – typically the third layer on EUS imaging. The characteristic appearance on EUS is diagnostic and no further evaluation, including biopsy is indicated.

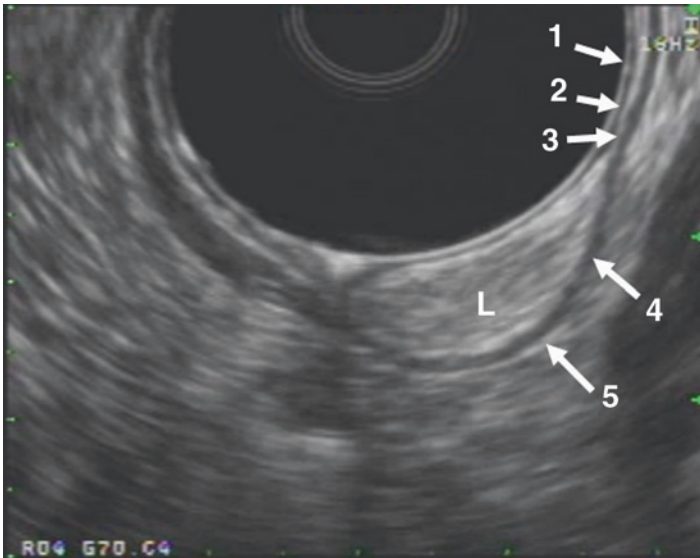


Fig. 3. Radial scanning EUS image of a lipoma. The mass (L) is hyperechoic and continuous with the third US layer (submucosa). Also identified by numbered arrows are the superficial mucosa (1), deep mucosa (2), submucosa (3), muscularis propria (4), and serosa (5).

LEIOMYOMA

Benign tumors composed of well-differentiated smooth muscle cells, true leiomyomas are more commonly found in the esophagus and small intestine but have been found throughout the GI tract, including the appendix (13, 14). A single center case series reported “polypoid” leiomyomas, arising from the muscularis mucosae, were more common in the rectosigmoid, whereas “submucosal” leiomyomas were more common in the distal esophagus and proximal stomach (15). Older literature often over estimated the presence of leiomyomas, especially in the stomach, as Gastrointestinal intestinal stromal tumors (GISTs) were often misclassified as their benign cousins (16). With immunohistochemical staining it is now possible to confirm these diagnoses. True leiomyomas stain positively for α -smooth muscle actin (SMA) and desmin and negatively for CD117, CD34, and S100 (Table 3). They appear as hypoechoic well-circumscribed masses in the muscularis propria or the muscularis mucosae (the fourth and second EUS layers, respectively, Fig. 4). Leiomyomas require tissue sampling with both histologic and immunohistochemical analysis for diagnosis since they

Table 3
Immunohistochemical (IHC) staining for markers
of gastrointestinal mesenchymal tumors

<i>Tumor</i>	<i>Positive IHC markers</i>
GIST	CD-117 (C-KIT), CD-34
Smooth muscle tumor	Smooth muscle actin, desmin
Schwannoma (Granular cell tumor)	S-100
Glomus tumor	Smooth muscle actin, vimentin

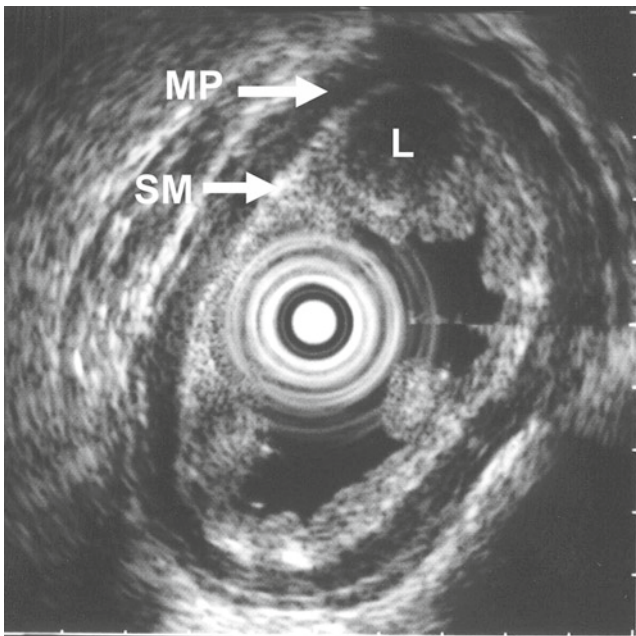


Fig. 4. Small esophageal subepithelial mass identified using a 20 MHz catheter probe. The lesion (L) is homogeneous, hypoechoic, and confined to the second and third EUS layer [deep mucosa and submucosa (SM)]. The lesion was removed by endoscopic submucosal resection and identified as an esophageal leiomyoma by histology and immunohistochemistry. [Reproduced from (71), with permission from Elsevier.]

appear similar to GIST lesions on EUS imaging. While they are benign, leiomyomas can grow to be large enough to cause intestinal obstruction and can require surgical resection depending on the size and location of the mass.

VARICES

While esophageal varices are characteristic enough in appearance to avoid requiring EUS evaluation, varices of other areas of the bowel can be less obvious. Gastric varices can masquerade as a subepithelial mass or large gastric fold on endoscopy (17). Varicose vessels can also be found in less common locations such as the duodenum, surgical anastomotic sites, rectum, and sigmoid colon. Clues such as thorough patient history and portal hypertensive gastropathy can lead to an accurate diagnosis of ectopic varices. Other endoscopic clues include a blue tint to the subepithelial mass, and soft consistency when probed with a closed forceps. EUS examination with Doppler flow can confirm or make the diagnosis when there is doubt. EUS will reveal a round or tubular hypoechoic or anechoic structure in the submucosa (the third EUS layer) that demonstrates venous flow when evaluated with Doppler. EUS is also being explored as a guide in the treatment of bleeding varices. There are small case series by using EUS to guide cyanoacrylate injection and case reports of EUS-guided coiling of refractory bleeding varices (18, 19).

PANCREATIC REST

Ectopic pancreatic tissue within the gastric wall is known as a pancreatic rest. Endoscopically, a subepithelial nodule with a central umbilication is the classic finding (Fig. 5a), though the sensitivity and specificity of this finding is unclear. Pancreatic rests are typically found in the gastric antrum and on EUS evaluation will have a heterogeneous echotexture that is hypoechoic in relation to the surrounding tissue. They are usually located within the submucosal layer – the third EUS layer (Fig. 5b) (20). While pancreatic rests are most often asymptomatic incidental findings on endoscopy, they have been reported to present with nausea, epigastric pain, weight loss, hematemesis, and gastric outlet obstruction (20, 21). Although pancreatic rests are benign lesions, there are rare case reports of adenocarcinoma arising in one of these heterotopic areas of pancreatic tissue (22–26). While the endoscopic appearance and EUS findings may be suggestive of a diagnosis, as the list of hypoechoic lesions in the third layer includes several malignant entities, a firm cytologic or pathologic proven diagnosis is important. Cap-assisted endoscopic mucosal

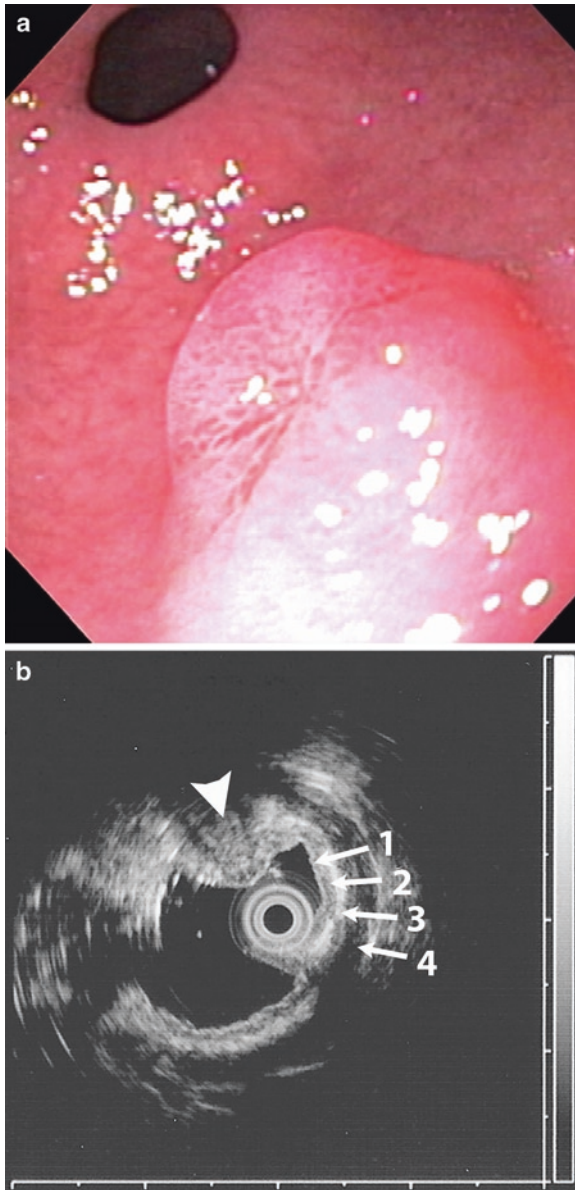


Fig. 5. Pancreatic rest. **(a)** Endoscopic image of an umbilicated subepithelial mass in the gastric antrum. **(b)** EUS image of a hypoechoic heterogeneous mass in the second and third EUS layers (white arrow head) as imaged using a 20 MHz catheter probe. Also identified by numbered arrows are the superficial mucosa (1), deep mucosa (2), submucosa (3), and muscularis propria (4).

resection is an effective manner of obtaining adequate tissue for histologic diagnosis (27).

DUPLICATION CYST

While found most commonly in children, gastrointestinal duplication cysts are also identified throughout adulthood (28, 29). The cysts are benign lesions resulting from an error in the embryonic development of the foregut and can be found either within or adjacent to the wall of the gastrointestinal tract. As the name implies, duplication cysts are lined with intact gastrointestinal epithelium (30). As the cyst lumen is not in continuity with the intestinal lumen, the cysts can enlarge with time secondary to secretions resulting in mass effect, rupture, or bleeding (28, 31, 32). A duplication cyst is often anechoic, smooth, spherical, or tubular structure with a well-defined wall by EUS (33, 34) (Fig. 6).

INFLAMMATORY FIBROID POLYP

Inflammatory fibroid polyps (IFP) are rare nonneoplastic localized lesions that originate in the submucosa. The lesion is composed of multiple small blood vessels and diffuse inflammatory cells, often eosinophils, loosely arranged in edematous stroma without a capsule (35, 36). IFPs are most

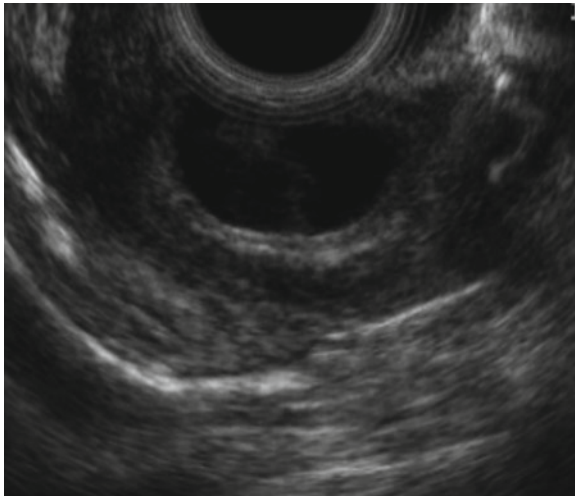


Fig. 6. Linear EUS image of an anechoic, smooth, and spherical structure arising from the gastric wall consistent with a duplication cyst.

commonly found in the stomach but are also seen in the large and small intestines and rarely in the esophagus (37). The polyps are located in the deep mucosal or submucosal layers (second and third EUS layers) with no involvement of the muscularis propria (35). They are usually hypoechoic with a homogenous echotexture with indistinct borders on EUS – however, they will occasionally appear slightly hyperechoic secondary to the multiple penetrating blood vessels throughout the polyp.

Malignant or Premalignant

GASTROINTESTINAL STROMAL TUMOR

Approximately 5,000–6,000 new cases of gastrointestinal stromal tumor (GIST) are diagnosed each year with 10–30% being malignant at the time of diagnosis (38). This makes GISTs among the most frequently identified intramural subepithelial masses. While all GISTs are felt to carry malignant potential, their natural history is not fully understood and many GISTs will never metastasize. This leads to some controversy over management. Initially, GISTs were thought to be smooth muscle cell tumors; however, they are now felt to arise from the interstitial cells of Cajal. Immunohistochemical staining for CD117, also known as C-KIT, can be used to identify GISTs. Given these new tools in diagnosis, a study of archived histologic slides of gastric tumors previously diagnosed as smooth muscle tumors revealed that most were actually GISTs (16).

Most commonly found in the stomach, GISTs usually develop in the muscularis propria but can also rarely be seen arising from the muscularis mucosa (38, 39). On EUS imaging, GISTs are seen as a hypoechoic mass with a homogenous echotexture that is continuous with the muscularis propria (EUS layer 4, Fig. 7). While certain characteristics such as size greater than 3 cm, irregular extraluminal border, cystic changes, heterogeneous echotexture and enlarged neighboring lymph nodes can suggest malignancy, even small GISTs have the potential to be malignant and metastasize (5, 6, 40–42). Only histologic examination is able to provide the definitive malignant potential of a GIST. When such a subepithelial lesion is being evaluated, EUS-FNA or core needle biopsy is indicated (43, 44). If the lesion is diagnosed as a GIST then the patient should be evaluated for possible surgical resection.(45).

CARCINOID TUMOR

Carcinoid tumors are neuroendocrine tumors arising from the enterochromaffin-like (ECL) cells and can be found anywhere in the GI tract. Endoscopically, carcinoids will appear as polypoid subepithelial lesions

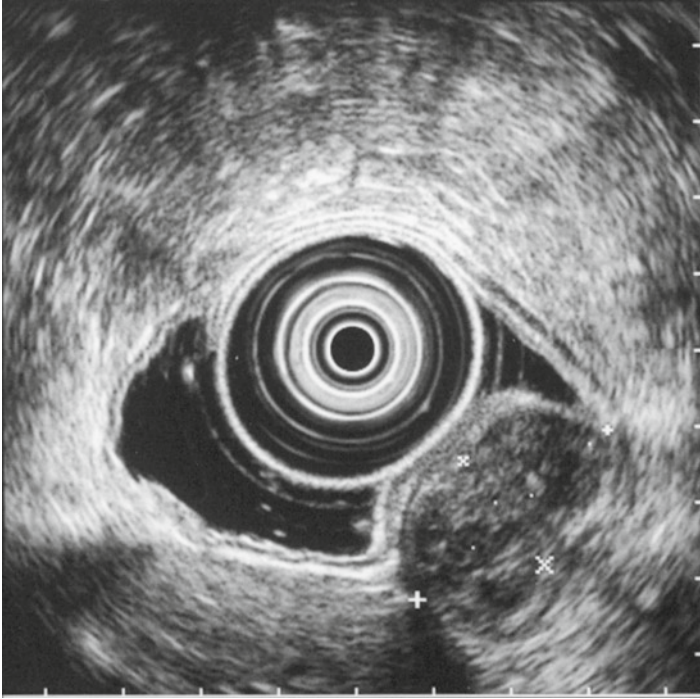


Fig. 7. Radial scanning EUS image of a GIST located in the fourth US layer corresponding to the muscularis propria. Marks on image represent size measurements of the tumor (17×33 mm). [Reproduced from (71), with permission from Elsevier].

(46). On EUS, carcinoid tumors are hypoechoic lesions originating in the deep mucosa or submucosa (second or third EUS layer). They may have the classic “salt and pepper” pattern. EUS evaluation can help determine the presence and depth of invasion and the presence of nodal metastasis (47, 48). Carcinoid tumors from different areas of the GI tract will have potentially varying presentation and symptoms. Rectal carcinoids are often incidental findings on colonoscopy and size of the lesion is a key factor in risk for metastasis. Lesions less than 1 cm have rarely metastasized, and endoscopic resection is potentially curative (48, 49). Gastric carcinoids are often seen in the setting of hypergastrinemia due to gastrinoma or autoimmune atrophic gastritis. In this setting, there are often multiple carcinoids but the overall potential for malignancy and metastasis is significantly lower than in the case of a solitary, even small, gastric carcinoid tumor (50–52).

LYMPHOMA

Primary lymphomas of the GI tract are usually of B-cell varieties, including diffuse large B-cell, mantle cell, Burkitt's, and mucosa associated lymphoid tissue (MALT) type lymphoma (53, 54). While MALT type lymphomas most frequently occur in the stomach, mantle cell lymphomas more commonly involves the colon. Presentation of GI tract lymphoma can vary from ulcerated masses to thickened folds, fleshy polyps, and subepithelial masses, thus EUS is often crucial in diagnosis as standard biopsies are often not enough to obtain sufficient tissue. EUS with FNA can also be used to collect samples for flow cytometry to further aid in diagnosis (55). On EUS, gastrointestinal lymphoma usually appears as a hypoechoic lesion in the deep mucosa or submucosa (second or third EUS layer) (56).

GLOMUS TUMORS

Originating from modified vascular smooth muscle cells, glomus tumors are usually found in peripheral soft tissue but can also be found in the gastrointestinal tract (57, 58). While usually benign, these lesions do have malignant potential and can also present with ulceration and bleeding like many subepithelial lesions. Case series and case reports have described glomus tumors causing extensive bleeding and death secondary to liver metastasis (57, 59). On evaluation by EUS, glomus tumors are located in the submucosa and muscularis propria – also rarely in the serosa (third, fourth, and fifth EUS layers, respectively). The tumors appear well circumscribed and are typically hypoechoic though sometimes heterogeneous with prominent internal Doppler signals suggesting the hypervascularity of these lesions (59, 60). As these findings are insufficient to obtain a firm diagnosis and cannot be used to predict malignant potential, fine-needle aspiration with cytologic and immunohistochemical staining positive for smooth muscle actin and vimentin and negative for CD117 helps differentiate this lesion (57, 61).

GRANULAR CELL TUMORS

Granular cell tumors are rare lesions thought to arise from Schwann cells and are most often seen in the skin or soft tissues but occasionally found in the GI tract. Usually benign, there are reports of malignant transformation (62). Endoscopically, they appear as firm subepithelial lesions. On EUS imaging, they are described as hypoechoic lesions within the deep mucosa or submucosa (second and third EUS layers). Some case series also describe a marginal halo surrounding the hypoechoic center (63). As the marginal halo is not always detected, these

lesions are similar in appearance to other intramural masses and tissue diagnosis should be obtained. In addition to cytologic or histopathologic evaluation, staining for S-100 can be helpful in differentiating this tumor (64).

METASTASIS

Overall, the incidence of metastatic spread of malignancies to the gastrointestinal tract is rare. However, localized spread, invasion, and metastasis of gynecologic cancers to the stomach and rectosigmoid are more common (65–68). Malignant melanoma and carcinomas of the breast, lung, and kidneys have been documented to metastasize to the GI tract (69, 70). The main role of EUS in this setting is to aid in obtaining tissue to either confirm spread of a known tumor or to help guide further studies to determine the primary cancer.

CONCLUSIONS

There are many entities that give rise to subepithelial lesions – the most common of which have been discussed above and are summarized in Table 2. Table 3 reviews some of the immunohistochemical markers used to help in their identification. While the specificity of the appearance of subepithelial lesions on EUS is low, it is currently the best test to help direct further diagnostics and management when a subepithelial mass is encountered on routine endoscopy.

REFERENCES

1. Hedenbro JL, Ekelund M, Wetterberg P. Endoscopic diagnosis of submucosal gastric lesions. The results after routine endoscopy. *Surg Endosc.* 1991;5:20–3.
2. Hwang JH, Saunders MD, Rulyak SJ, et al. A prospective study comparing endoscopy and EUS in the evaluation of GI subepithelial masses. *Gastrointest Endosc.* 2005;62:202–8.
3. Rösch T, Kapfer B, Will U, Buomus W, Strobel M, Lorenz R, et al. Accuracy of endoscopic ultrasonography in upper gastrointestinal submucosal lesions: a prospective multicenter study. *Scan J Gastroenterol.* 2002;37:856–62.
4. Kimmey MB, Martin RW, Haggitt RC, et al. Histologic correlates of gastrointestinal ultrasound images. *Gastroenterology.* 1989;96:433–41.
5. Chak A, Canto MI, Rösch T, Dittler HJ, Hawes RH, Tio TL, et al. Endosonographic differentiation of benign and malignant stromal cell tumors. *Gastrointest Endosc.* 1997;45:468–72.
6. Palazzo L, Landi B, Cellier C, Cuillerier E, Roseuu G, Barbier JP. Endosonographic features predictive of benign and malignant gastrointestinal stromal cell tumours. *Gut.* 2000;46:88–92.

7. Motoo Y, Okai T, Ohta H, et al. Endoscopic ultrasonography in the diagnosis of extraluminal compressions mimicking gastric submucosal tumors. *Endoscopy*. 1994;26:239–42.
8. Fernandez MJ, Davis RP, Nora PF. Gastrointestinal lipoma. *Arch Surg*. 1983;118:1081–3.
9. Hancock BJ, Vajcner A. Lipomas of the colon: a clinicopathologic review. *Can J Surg*. 1988;31:178–81.
10. Thompson WM, Kende AI, Levy AD. Imaging characteristics of gastric lipomas in 16 adult and pediatric patients. *AJR Am J Roentgenol*. 2003;181:981–5.
11. Maderal F, Hunter F, Fuselier G, et al. Gastric lipomas – an update of clinical presentation, diagnosis and treatment. *Am J Gastroenterol*. 1984;79:964–7.
12. Deeth TM, Madden PN, Dodds WJ. Multiple lipomas of the stomach and duodenum. *Am J Dig Dis*. 1975;20:771–4.
13. Valls C, Sancho C, Bechini J, Dominguez J, Montana X. Intestinal leiomyomas: angiographic imaging. *Gastrointest Radiol*. 1992;17:220–2.
14. Gill SS, Heuman DM, Mihas AA. Small intestinal leiomyomas. *J Clin Gastroenterol*. 2001;33:267–82.
15. Agaimy A, Wunsch PH. True smooth muscle neoplasms of the gastrointestinal tract: morphological spectrum and classification in a series of 85 cases from a single institute. *Langenbecks Arch Surg*. 2007;392:75–81.
16. Miettinen M, Sobin LH, Sarlomo-Rikala M. Immunohistochemical spectrum of GISTs at different sites and their differential diagnosis with a reference to CD117 (KIT). *Mod Pathol*. 2000;13:1134–42.
17. Mendis RE, Gerdes H, Lightdale CJ, Botet JF. Large gastric folds: a diagnostic approach using endoscopic ultrasonography. *Gastrointest Endosc*. 1994;40:437–41.
18. Romero-Castro R, Pellicer-Bautista FJ, Jimenez-Saenz M, Marcos-Sanchez F, Caunedo-Alvarez A, Ortiz-Moyano C, et al. EUS-guided injection of cyanoacrylate in perforating feeding veins in gastric varices: results in 5 cases. *Gastrointest Endosc*. 2007;66:402–7.
19. Levy MJ, Wong Kee Song LM, Kendrink ML, Misra S, Gostout CJ. EUS-guided coil embolization for refractory ectopic variceal bleeding (with videos). *Gastrointest Endosc*. 2008;67:572–4.
20. Thoeni RF, Gedgaudas RK. Ectopic pancreas: usual and unusual features. *Gastrointest Radiol*. 1980;5:37–42.
21. Lai EC, Tompkins RK. Heterotopic pancreas. Review of a 26 year experience. *Am J Surg*. 1986;151:697–700.
22. Goldfarb WB, Bennett D, Monafu W. Carcinoma in a heterotopic gastric pancreas. *Ann Surg*. 1963;158:56–9.
23. Tanumura A, Yamamoto H, Shibata H, Sano E. Carcinoma in heterotopic gastric pancreas. *Acta Path Jpn*. 1979;29:251–7.
24. Hickman DM, Frey CF, Carson HW. Adenocarcinoma arising in gastric heterotopic pancreas. *West J Med*. 1981;135:57–61.
25. Jeng KS, Yang KC, Kuo SH. Malignant degeneration of heterotopic pancreas. *Gastrointest Endosc*. 1991;37:196–8.
26. Ura H, Denno R, Hirata K, et al. Carcinoma arising from ectopic pancreas in the stomach: endosonographic detection of malignant change. *J Clin Ultrasound*. 1998;26:265–8.

27. Faigel DO, Gopal D, Weeks DA, Corless C. Cap-assisted endoscopic submucosal resection of a pancreatic rest. *Gastrointest Endosc.* 2001;54:782-4.
28. Lamont AC, Starinsky RM, Cremin BJ. Ultrasonic diagnosis of duplication cysts in children. *Br J Radiol.* 1984;57:463-7.
29. Hulnick DH, Balthazar EJ. Gastric duplication cyst: GI series and CT correlation. *Gastrointest Radiol.* 1987;12:106-8.
30. Mathur M, Gupta SD, Bajpai M, Rohatagi M. Histochemical pattern in alimentary tract duplications of children. *Am J Gastroenterol.* 1991;86:1419-23.
31. Ott DJ, Wolfman NT, Wu WC, Chen MY, White WL. Endoscopic ultrasonography of benign esophageal cyst simulating leiomyoma. *J Clin Gastroenterol.* 1992;15:85-7.
32. Stringer MD, Dinwiddie R, Hall CM, Spitz L. Foregut duplication cysts: a diagnostic challenge. *J R Soc Med.* 1993;86:174-5.
33. Geller A, Wan KK, DiMagna EP. Diagnosis of foregut duplication cysts by endoscopic ultrasonography. *Gastroenterology.* 1995;109:838-42.
34. Faigel DO, Burke A, Ginsberg GG, et al. The role of endoscopic ultrasound in the evaluation and management of foregut duplications. *Gastrointest Endosc.* 1997;45:99-103.
35. Kim YI, Kim WH. Inflammatory fibroid polyps of gastrointestinal tract. Evolution of histologic patterns. *Am J Clin Pathol.* 1988;89:721-7.
36. Matsushita M, Hajiro K, Okazaki K, Takakuwa H. Gastric inflammatory fibroid polyps: endoscopic ultrasonographic analysis in comparison with the histology. *Gastrointest Endosc.* 1997;46:53-7.
37. Ozolek JA, Sasatomi E, Swalsky PA, Rao U, Kraskinskas A, Finkelstein SD. Inflammatory fibroid polyps of the gastrointestinal tract: clinical, pathologic and molecular characteristic. *Appl Immunohistochem Mol Morphol.* 2004;12:59-66.
38. Miettinen M, Sarlomo-Rikala M, Lasota J. Gastrointestinal stromal tumors: recent advances in understanding of their biology. *Hum Pathol.* 1999;30:1213-20.
39. Fletcher CD, Berman JJ, Corless C, Gorstein F, Lasota J, Longley BJ. Diagnosis of gastrointestinal stromal tumors: a consensus approach. *Hum Pathol.* 2002;33:459-65.
40. Meesters B, Pauwels PA, Pijnenburg AM, Vlasveld LT, Repelaer van Driolog. Metastasis in a 'benign' duodenal stromal tumour. *Eur J Surg Oncol.* 1998;24:334-5.
41. Trupiano JK, Stewart RE, Misick C, Appelman HD, Goldblum JR. Gastric stromal tumors: a clinicopathologic study of 77 cases with correlation of features with nonaggressive and aggressive clinical behaviors. *Am J Surg Pathol.* 2002;26:705-514.
42. Evans HL. Smooth muscle tumors of the gastrointestinal tract. A study of 56 cases followed for a minimum of 10 years. *Cancer.* 1985;56:2242-50.
43. Levy AD, Remotti HE, Thompson WM, Sobin LH, Miettinen M. Gastrointestinal stromal tumors: radiologic features with pathologic correlation. *Radiographics.* 2003;23:283-304.
44. Ando N, Goto H, Niwa Y, Hirooka Y, Ohmiya N, Nagasaka T, et al. The diagnosis of GI stromal tumors with EUS-guided fine needle aspiration with immunohistochemical analysis. *Gastrointest Endosc.* 2002;55:37-43.
45. Hwang JH, Rulyak SJ, Kimmey MB. AGA technical review: management of gastric subepithelial masses. *Gastroenterology.* 2006;130:2217-28.

46. Nakamura S, Lida M, Yao T, Fujishima M. Endoscopic features of gastric carcinoids. *Gastrointest Endosc.* 1991;37:535–8.
47. Matsumoto T, Iida M, Suekane H, Tominaga M, Yao T, Fujishima M. Endoscopic ultrasonography in rectal carcinoid tumors: contribution to selection of therapy. *Gastrointest Endosc.* 1991; 37:539–42.
48. Soga J. Early-stage carcinoids of the gastrointestinal tract: an analysis of 1914 reported cases. *Cancer.* 2005;103:1587–95.
49. Kwaan MR, Goldberg JE, Bleday R. Rectal carcinoid tumors: review of results after endoscopic and surgical treatment. *Arch Surg.* 2008;143:471–5.
50. Rindi G, Azzoni C, La Rosa S, Klersy C, Paolotti D, Rappel S, et al. ECL cell tumor and poorly differentiated endocrine carcinoma of the stomach: prognostic evaluation by pathological analysis. *Gastroenterology.* 1999;116:532–42.
51. Rindi G, Luinetti O, Cornaggia M, Capella C, Solcia E. Three subtypes of gastric argyrophil carcinoid and the gastric neuroendocrine carcinoma: a clinicopathologic study. *Gastroenterology.* 1993;104:994–1006.
52. Soga J. Gastric carcinoids: a statistical evaluation of 1094 cases collected from the literature. *Surg Today.* 1997;27:892–901.
53. Brooks JJ, Enterline HT. Primary gastric lymphomas. A clinicopathologic study of 58 cases with long-term follow-up and literature review. *Cancer.* 1983;51:701–11.
54. Lewin KJ, Ranchod M, Dorfman RF. Lymphomas of the gastrointestinal tract: a study of 117 cases presenting with gastrointestinal disease. *Cancer.* 1978;42: 693–707.
55. Vander Noot III MR, Eloubeidi MA, Chen VK, Eltoun I, Jhala D, Syed S, et al. Diagnosis of gastrointestinal lesions by endoscopic ultrasound-guided fine-needle aspiration biopsy. *Cancer.* 2004;102:157–63.
56. Bolondi L, Casanova P, Caletti GC, et al. Primary gastric lymphoma versus gastric carcinoma: endoscopic US evaluation. *Radiology.* 1987;165:821–6.
57. Miettinen M, Paal E, Lasota J, Sobin LH. Gastrointestinal glomus tumors: a clinicopathologic, immunohistochemical, and molecular genetic study of 32 cases. *Am J Surg Pathol.* 2002;26:301–11.
58. Tsuneyoshi M, Enjoji M. Glomus tumor: a clinicopathologic and electron microscopic study. *Cancer.* 1982;50:1601–7.
59. Yan SL, Yen YR, Chen CH, Yank CC, Kuo CL, Wu HS. Gastric glomus tumor: a hypervascular submucosal tumor on power Doppler endosonography. *J Clin Ultrasound.* 2007;35:164–8.
60. Imamura A, Tochiwara M, Natsui K, Murashima Y, Suga T, Yaoaka T, et al. Glomus tumor of the stomach: endoscopic ultrasonographic findings. *Am J Gastroenterol.* 1994;89:272.
61. Debol SM, Stanley MW, Mallery S, Sawinski E, Bardales RH. Glomus tumor of the stomach: cytologic diagnosis by endoscopic ultrasound-guided fine-needle aspiration. *Diagn Cytopathol.* 2003;28:316–21.
62. Yoshizawa A, Ota H, Sakaguchi N, Kanai S, Nakayama J, Matsuzawa K, et al. Malignant granular cell tumor of the esophagus. *Virchows Arch.* 2004;444:304–6.
63. Jung MK, Jeon SW, Cho CM, et al. Gastric schwannomas: endosonographic characteristics. *Abdom Imaging.* 2008;33:388–90.
64. Prematilke IV, Piris J, Shah KA. Fine needle aspiration cytology of a granular cell tumour of the oesophagus. *Cytopathology.* 2004;15:120–1.

65. Kadakia SC, Parker A, Canales L. Metastatic tumors to the upper gastrointestinal tract: endoscopic experience. *Am J Gastroenterol.* 1992;87:1418–23.
66. Saunders NJ. Haematemesis due to gastric involvement by metastatic ovarian carcinoma 30 years after removal of the primary tumour. *Br J Clin Pract.* 1986;40:298–9.
67. Taylor RR, Phillips WS, O'Connor DM, Harrison CR. Unusual intramural gastric metastasis of recurrent epithelial ovarian carcinoma. *Gynecol Oncol.* 1994;55:152–5.
68. Sangha S, Georgeos F, Freter R, Paiva LL, Jacobson BC. Diagnosis of ovarian cancer metastatic to the stomach by EUS-guided FNA. *Gastrointest Endosc.* 2003;58:933–5.
69. Taal BG, Peterse H, Boot H. Clinical presentation, endoscopic features, and treatment of gastric metastases from breast carcinoma. *Cancer.* 2000;89:2214–21.
70. Panagiotou I, Brountzos END, Bafaloukos D, et al. Malignant melanoma metastatic to the gastrointestinal tract. *Melanoma Res.* 2002;12:169–73.
71. Hwang JH, Kimmey MB. The incidental upper gastrointestinal subepithelial mass. *Gastroenterology.* 2004;126:301–7.

Endoscopic Ultrasound of Ampullary and Duodenal Lesions

*Jessica Trevino, MD
and Shyam Varadarajulu, MD*

CONTENTS

INTRODUCTION
AMPULLA OF VATER
TECHNIQUE OF EUS EXAMINATION
STAGING ACCURACY OF EUS
TREATMENT
DUODENAL LESIONS
CONCLUSIONS

Abstract

Neoplastic transformation of the intestinal mucosa occurs more commonly in the ampulla of Vater than any other area in the small intestines. Given its proximity to vital structures of the pancreaticobiliary system, management of pathology involving the ampulla of Vater is a clinical challenge. This chapter reviews the role of EUS in the evaluation of different pathology involving the ampullary and duodenal segments of the gastrointestinal (GI) tract.

Key Words: Major duodenal papilla, Endoscopic ultrasound, Duodenal pathology

From: *Clinical Gastroenterology: Endoscopic Ultrasound*,
Edited by: V. M. Shami and M. Kahaleh, DOI 10.1007/978-1-60327-480-7_11,
© Springer Science+Business Media, LLC 2010

INTRODUCTION

Endoscopic Ultrasonography (EUS) is a useful tool for the evaluation of ampullary lesions. The anatomy of the ampulla of Vater is complex, as it consists of three epithelia that encompass the bile duct, the pancreatic duct and the duodenal mucosa (1). In comparison with more traditional modalities, such as Computed Tomography (CT) and Ultrasonography (US), the diagnostic accuracy of EUS has consistently been shown to be superior. When considering treatment options, it is imperative to be precise, specifically when deciding on surgical resectability versus palliation. Additionally, the option of endoscopic papillectomy can be addressed and performed if deemed feasible by EUS. This chapter reviews the role of EUS in the evaluation of different pathology involving the ampullary and duodenal segments of the gastrointestinal (GI) tract.

AMPULLA OF VATER

Benign Lesions of the Ampulla of Vater

Despite the ampulla's small size, it harbors the highest incidence for neoplastic transformation in the small bowel. Autopsy studies have revealed that benign neoplasms of the ampulla of Vater occur in 0.04–0.21% of patients, usually in the age range of the mid 50s (1–3). A majority of the benign lesions are adenomatous in nature. These are premalignant lesions that follow the adenoma-carcinoma sequence. It has been reported that malignancy within an adenoma of the papilla frequents close to 26% (1). Additionally, in patients with familial adenomatous polyposis (FAP), there is a high prevalence of duodenal lesions, predominantly found in the periampullary region. These periampullary adenomas will occur invariably in patients with FAP and this location is second only to the colorectum for malignancy, occurring in 4.5–8.5% of patients (4). Due to this increased risk, screening duodenoscopy is recommended for patients with polyposis syndromes with both a forward and side-viewing endoscope (5). Other rare benign diseases involving the major papilla include lipomas, fibromas, leiomyomas, lymphangiomas, hamartomas, and hemangiomas (1, 4) (Table 1). Several studies have shown that biopsy alone is insufficient for the identification of ampullary lesions, with the percentage of false-negative biopsies ranging from 17 to 40% (6). The reasons for this are threefold: one, the tumor may be endoampullary in location, thereby requiring a biliary sphincterotomy to expose the tumor for performing biopsies; two, it may be difficult to reliably differentiate a benign stricture from dysplasia in the setting

Table 1
Lesions involving the major duodenal ampulla

<i>Benign</i>	<i>Malignant</i>
Adenoma	Adenocarcinoma
Lipoma	Neuroendocrine carcinoma
Carcinoid	Acinar cell carcinoma
GIST	Signet ring cell
Fibroma	Lymphoma
Lymphangioma	Metastatic lesions:
Leiomyoma/leiomyofibromas	Melanoma
Hamartoma	Hypernephroma
Hemangiomas	Bladder cell carcinoma

of inflammation; and three, benign adenomas may harbor a foci of adenocarcinoma that may be difficult to diagnose by standard biopsies.

Malignant Lesions of the Ampulla of Vater

Ampullary carcinoma accounts for 7–10% of all peripancreatic lesions, occurring in approximately six million persons per year (3, 7–9). Overall, adenocarcinoma of the ampulla of Vater represents 5% of all gastrointestinal carcinomas (10). It has been estimated that 35–90% of ampullary adenocarcinomas develop from preexisting ampullary adenomas (10). Treatment and prognosis can vary, so it is imperative to differentiate an ampullary malignancy from carcinoma of the head of the pancreas or bile duct. Patients typically present with pain, weight loss and/or early jaundice. Five year survival rates vary widely in the literature, from 30 to 70% (8, 9). Poor prognostic factors are patient age greater than 70 years, larger tumor size, vascular invasion, lymph node metastasis, and perineural microscopic invasion (7). Unfortunately, recurrence of carcinoma of the ampulla of Vater, despite pancreatoduodenectomy, is as high as 50% (7, 11, 12). It has been linked to T and N stages as well as tumor characteristics and has been shown to metastasize to the liver, peritoneum, and the tumor bed (7, 11). Other malignant lesions involving the ampulla of Vater (Table 1) range from lymphoma to rarely described signet-ring cell carcinoma (4, 13–15). It is important to note that hyperplasia of Brunner's glands or adenofibromatosis can clinically, endoscopically, and radiologically mimic a malignancy of the ampulla of Vater

(4, 16, 17). Surgical resection is necessary for definitive diagnosis of these pseudotumors and tends to provide treatment for clinical symptoms of obstruction (4). One large study evaluated 3,292 ampullary cancer presentations (8). Of these patients, 40% underwent surgical resection with a 5 year survival rate of 36.8%. This is in comparison with a 16% survival rate in patients undergoing resection of pancreatic head cancers (18). Using EUS not only to diagnose, but also to stage and distinguish ampullary from pancreatic cancers is an important component of appropriate management. However, the diagnosis of an ampullary cancer by endoscopy or EUS is not always straightforward. In the setting of acute duodenal inflammation in pancreatitis or after passage of common bile stones or in the presence of an endobiliary stent, it may be difficult to reliably identify an ampullary growth at endoscopy. Likewise, studies have shown that very few criteria can reliably diagnose ampullary cancer at EUS. The presence of tumor infiltration of the duodenal muscularis propria and intraductal involvement of the bile or pancreatic ducts at EUS is criteria specific for an invasive ampullary tumor (19).

Lesions Involving the Minor Duodenal Ampulla

Minor papilla pathology is rarely described in the literature. However, there have been some case reports of minor papilla adenomas as well as additional lesions, including carcinoid and paragangliomas (17, 20–26). The largest series included three patients with minor papilla adenomas where EUS was utilized prior to attempting endoscopic removal of lesions limited to the papilla (17). EUS was performed primarily to exclude ductal involvement and to identify pancreas divisum. This study concluded that minor papilla lesions could be removed safely when the pathology is confined to the mucosal layers and in the absence of ductal involvement.

TECHNIQUE OF EUS EXAMINATION

The ampulla is best evaluated using the radial echoendoscope. Shortening the echoendoscope after advancing it to the second portion of the duodenum usually brings the ampulla in line with the EUS transducer. After suctioning air from the lumen of the small bowel, the balloon is inflated and the transducer is tipped up to investigate the ampulla which is seen as a “mound”. It is oftentimes necessary to inject water via the biopsy channel to obtain better acoustic coupling. It is important not to compress the ampulla with the balloon as it may create tangential imaging. Once the ampullary mound is identified, it is

essential to investigate the individual ampullary wall layers thoroughly. In general, lesions invading the muscularis layer are better managed surgically. Also, the pancreatic and bile duct termination within the ampulla requires close inspection. The presence of ductal dilation is suggestive of an occlusive duct. In these patients, it is important to rule out ductal involvement by the tumor mass (Fig. 1a, b). Patients with intraductal tumor involvement more often require a Whipple's procedure and are not candidates for any endoscopic intervention. While performing EUS, it is also important to evaluate for regional lymphadenopathy, vascular invasion, and ascites. The presence of any of the three features excludes the possibility of performing an endoscopic ampullectomy. While the superior mesenteric vein can be identified easily while performing the uncinate pull through maneuver, it can sometimes be difficult to identify the invasion of the superior mesenteric artery. The presence of ascites in the setting of malignancy raises the possibility of peritoneal carcinomatosis, and the fluid should be aspirated for cytopathological analysis.

EUS-Guided FNA

Although EUS-guided FNA is now a standard practice for the diagnosis of pancreatic, gastrointestinal, and mediastinal malignancies, its role in the evaluation of ampullary neoplasms is unclear (27). Most experts believe that ampullary neoplasms are better diagnosed by histology, as these lesions are readily accessible for endoscopic biopsy. In the experience of these authors, an EUS-guided FNA is useful only for the evaluation of intraductal or deep seated tumors when repeated biopsies do not yield a diagnosis. One retrospective study concluded that FNA of ampullary lesions establishes a definitive diagnosis, and thereby alters clinical management in one-third of patients undergoing EUS examinations (28). Another retrospective review of using EUS for the diagnosis of ampullary lesions documented that the average number of passes for diagnosis was 2.4, with no false positive results (10). While performing EUS-guided FNA (Fig. 2a, b), the ampullary mound should be targeted and the sample procured if possible without applying suction. As the tumor is predominantly superficial in nature, applying aggressive suction makes the specimen bloody and of poor diagnostic quality.

Intraductal Ultrasound

Intraductal ultrasound (IDUS) has a role in cases where local resection may be reasonable when EUS indicates the lesion to spare the muscularis layer.

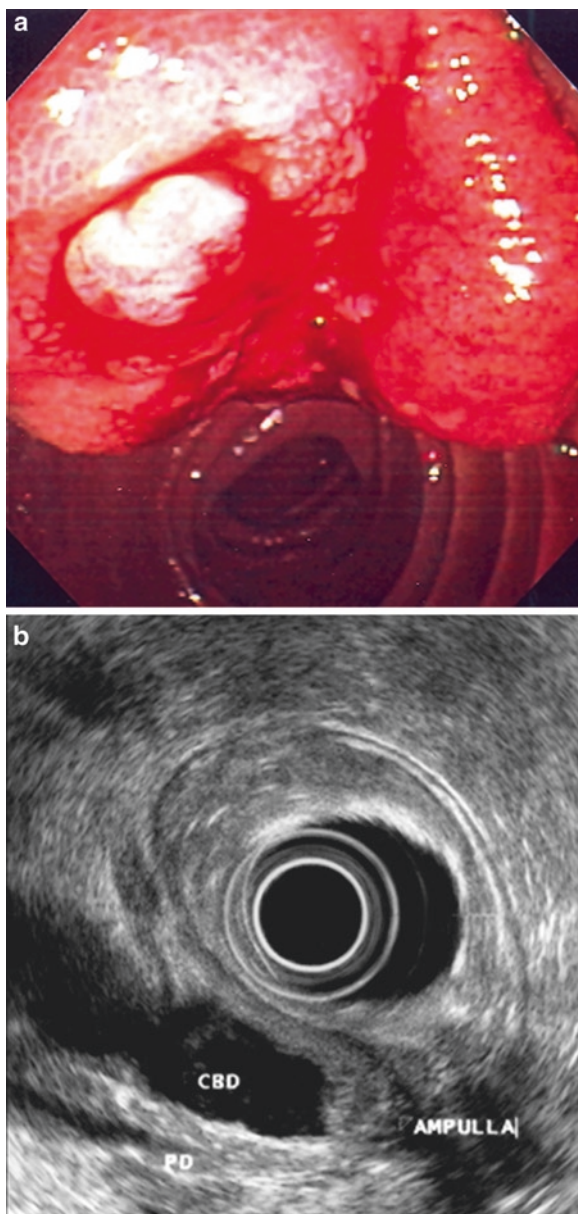


Fig. 1. (a) Endoscopic view of cancer of the major duodenal papilla. (b) On EUS, the tumor is seen to invade the distal CBD.

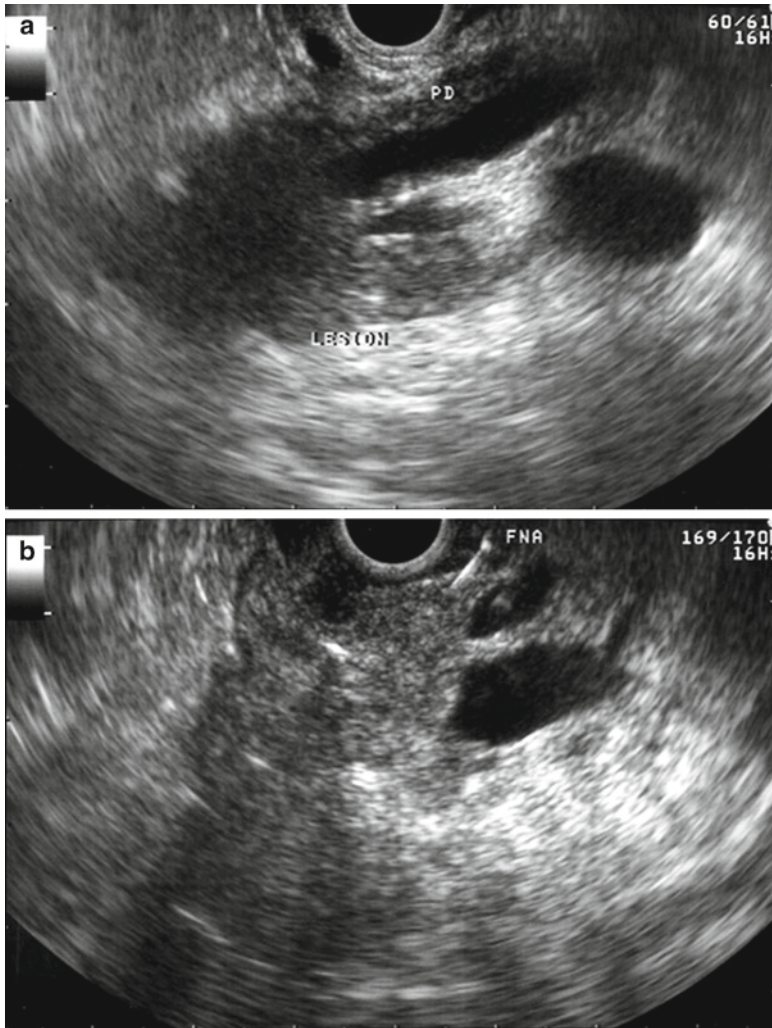


Fig. 2. (a) Ampullary mass as seen using a linear echoendoscope. The common bile duct appears dilated. (b) EUS-guided FNA of the ampullary mass. Both the bile and pancreatic ducts are dilated due to tumor invasion.

IDUS enables more accurate assessment of bile or pancreatic duct involvement by the tumor and aids in evaluating the extent of the disease. Select studies have looked at using IDUS as an adjuvant to EUS when evaluating these tumors (29–31). Two studies looked at diagnostic accuracy of IDUS with surgical resection and found IDUS staging accu-

racy at 88 and 93% (30, 31). Also, in patients with endoampullary growth, IDUS may be the only reliable technique to identify the lesion as it enables visualization of the muscle layer of the sphincter of Oddi in a distinct plane (30). The probe images at a frequency of 20 MHz. The procedure is performed at endoscopic retrograde cholangiopancreatography (ERCP) by passing the IDUS probe over a 0.035 inch guidewire into the biliary or pancreatic ductal systems. The probe is then gradually withdrawn and the ductal wall layers and disease extent are studied (Fig. 3a–c). In patients who have undergone a sphincterotomy, the presence of air bubbles may cause imaging artifacts. In such cases, water can be instilled using an ERCP cannula and imaging undertaken so as to obtain better acoustic coupling (32). The procedure is technically easy and safe to perform. A major limitation of the technology is that the life expectancy of the IDUS probe is only up to 50 examinations. Also, it is important to make sure that the elevator of the duodenoscope is kept lowered so as to prevent accidental damage of the probe.

STAGING ACCURACY OF EUS

According to the TNM classification that is used to stage ampullary cancers, T1 corresponds to tumors localized to the sphincter of Oddi, T2 tumors are those invading the muscularis propria, T3 includes those invading the pancreas by less than 2 cm and T4 includes those invading the pancreas more deeply or involving adjacent vessels and organs (Table 2) (33). Multiple studies have confirmed the superior role of EUS in the evaluation of ampullary lesions (18, 29, 34–42). When comparing CT and US with EUS for adequate recognition of ampullary masses, EUS has the highest accuracy (29). One study revealed a detection rate of only 7% using US as compared to 29% and 93% with CT and EUS, respectively (29). Another study of 50 patients with ampullary neoplasms compared the staging accuracy of EUS with CT and MRI/angiography. Using surgical histopathology as the gold standard, EUS was more accurate (78%) in T staging than both CT and MRI (24% and 46%, respectively) (34). Under staging of T3 lesions or over staging of T2 carcinomas accounted for most of the inaccuracies in T staging and may be related to the presence of an endobiliary stent which causes shadowing artifacts or desmoplastic peritumoral pancreatitis that cannot be differentiated from cancer by EUS imaging alone (38). This differentiation between T2 and T3 may not be very important as clinical management does not change. From a practical standpoint, it is more important to know if a lesion can be resected by

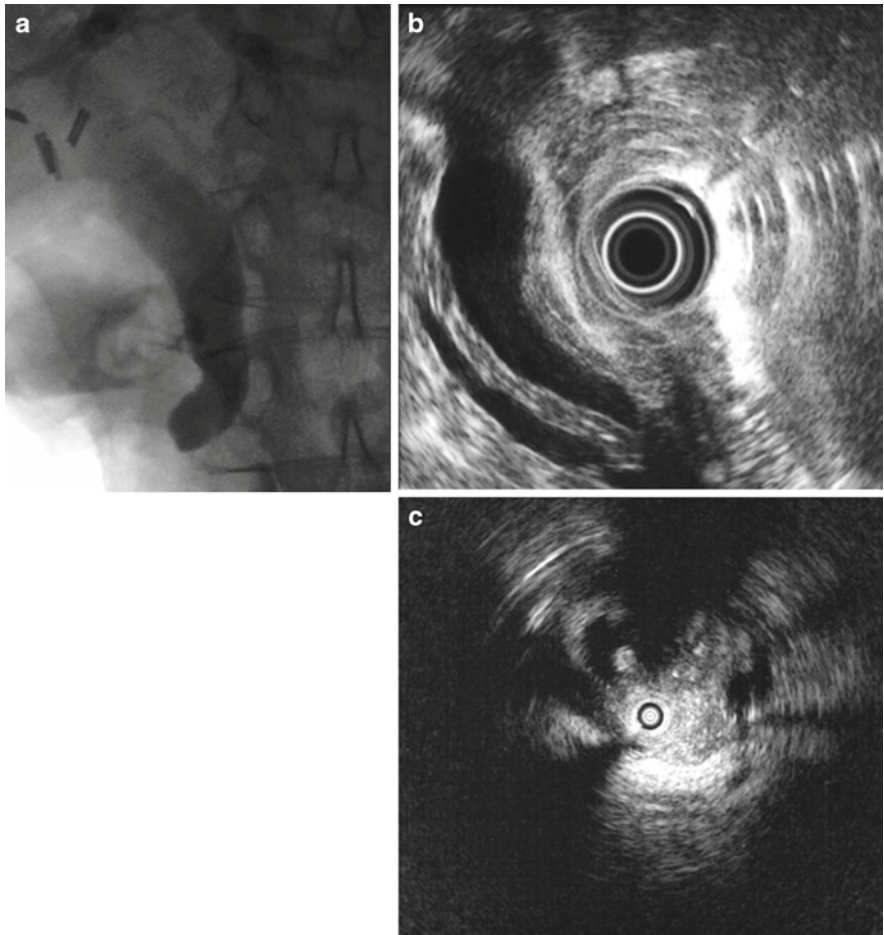


Fig. 3. (a) Cholangiogram reveals abrupt termination of the bile duct with poor drainage of contrast. (b) At EUS, borderline dilation of the bile and pancreatic ducts are noted without the obvious presence of a tumor mass. (c) On intraductal ultrasound, a 1 cm endoampullary mass is noted as a papillary projection. At surgery, this patient was found to have a 1 cm ampullary cancer invading the distal CBD.

endoscopy or not, as any lesion beyond T1 will require surgery. The accuracy of EUS in differentiating T1 tumors from more advanced disease ranges between 87 and 94%. There are no significant differences in the accuracy of N staging between EUS and CT scan (34–37). A major limitation of EUS is its inability to evaluate tumor involvement

Table 2
The TNM classification for ampullary cancer

T	(Primary tumor)
Tx	Primary tumor cannot be assessed
T0	No evidence of primary tumor
Tis	Carcinoma in situ
T1	Tumor limited to ampulla of Vater or sphincter of Oddi
T2	Tumor invades duodenal wall
T3	Tumor invades pancreas
T4	Tumor invades peripancreatic soft tissues or other adjacent organs or structures other than pancreas
N	(Regional lymph nodes)
Nx	Regional lymph nodes cannot be assessed
N0	No regional lymph node metastasis
N1	Regional lymph node metastasis
M	(Distant metastasis)
M0	No distant metastasis
M1	Distant metastasis

Adapted from Ref. 33.

in the sphincter of Oddi. IDUS is a complimentary technique that provides an accurate assessment of the sphincter site. Select studies have looked at using intraductal ultrasound (IDUS) as an adjuvant to EUS when evaluating ampullary tumors (29–31). In a study of 32 patients, IDUS had a diagnostic accuracy of 87.5% and its sensitivity and specificity for assessing nodal involvement were 66.7% and 91.3%, respectively (30). The T staging accuracy rates were 100% for tumors confined to the sphincter, 92.3% for those involving the duodenal submucosa, 100% for those involving the duodenal muscle layer and 75% for those involving the pancreas. Intraductal ultrasound was 100% accurate in identifying ductal involvement. A subsequent study confirmed similar findings, with overall tumor accuracy at 88.9% (31). More recently, a prospective study of 40 patients comparing EUS and IDUS, revealed an overall T stage accuracy at only 78% for IDUS, as compared with EUS at 63%. Identification of ductal involvement using IDUS and EUS for biliary and pancreatic ducts was 90% and 88–90%, respectively (29).

TREATMENT

When considering the treatment of ampullary lesions, historically, patients have required surgical intervention. A Whipple or pylorus-preserving pancreaticoduodenectomy have been the standard treatment options (29). Recently, localized ampullary masses which are discovered early may have the option of endoscopic resection. If the histology reveals adenoma, it is fairly well accepted to attempt endoscopic resection of the lesion. However, when dealing with high grade intraepithelial neoplasia or carcinoma in situ, there is still some variability on the decision tree (43). One study evaluated the question of applying endoscopic resection in early ampullary cancer (44). Of 106 patients with ampullary neoplasia (109 lesions: adenoma n=92, carcinoma n=4, hyperplastic n=12, lymphangioma n=1) that included those with and without intraductal growth, endoscopic resection was curative at a mean follow up of 43 months in 83% of patients. In patients with intraductal growth, the authors had a 46% cure rate and suggested this could be accomplished if the intraductal growth is less than 1 cm (44). In general, the success rate for endoscopic ampullectomy with a curative intent is between 70 and 80% (45–48). The procedure is associated with a morbidity rate between 6 and 36% and almost no mortality. The recipe for endoscopic success is appropriate selection of patients. One study did investigate whether there were predictable factors for endoscopic resection of ampullary lesions (49). A total of 56 patients undergoing interventional endoscopy for an ampullary neoplasia were evaluated, including 29 adenomas, 20 adenocarcinomas, 4 adenomyomas, 2 paragangliomas, and 1 neuroendocrine tumor. While the authors did discover that EUS T stage and the inability to obtain a cleavage plane were predictive of malignancy, there were no factors which were predictive of successful endoscopic excision for benign lesions (49).

We recommend performing an EUS first to assess the T and N stage, rule out vascular or nodal involvement, and exclude the possibility of ductal invasion. If the patient is deemed a candidate suitable for endoscopic resection, an IDUS may then be performed during ERCP to confirm the absence of ductal involvement or duodenal submucosal infiltration by the tumor.

DUODENAL LESIONS

A majority of lesions involving the duodenum are submucosal and benign in nature. These include lipomas, polyps, carcinoid tumors, Brunner's gland hyperplasia, heterotopic pancreas, and stromal cell tumors (50).

Malignant lesions include primary adenocarcinoma and metastasis from melanoma, renal cell cancer, and breast cancer (50). Most malignant lesions involving the proximal duodenum cause gastric outlet obstruction and are managed by a Whipple's procedure, localized resection or palliative gastric bypass procedure. Since endoscopic biopsy is sufficient to provide a tissue diagnosis in most patients, the role of EUS is confined mainly to the evaluation of benign lesions.

Benign Lesions of the Duodenum

In general, lesions larger than 2 cm in size are evaluated using a radial echoendoscope and those smaller than 2 cm using an ultrasound probe (7.5–12 MHz) that is passed via the biopsy channel of a therapeutic endoscope. While EUS enables accurate assessment of tumor characteristics such as size and depth of wall layer involvement, it can sometimes be difficult to reliably differentiate the various lesions based on morphology alone. An exception to this rule may be the diagnosis of duodenal varices, lipomas, stromal cell tumors, and extrinsic organs causing luminal compression that can be easily differentiated by EUS. A resection specimen is oftentimes required in others to establish a definitive diagnosis. As performing FNAs on small lesions can be technically challenging, the role of EUS is mainly to assess the tumor depth so as to facilitate safe endoscopic removal (Fig. 4a–c). The most common indication for EUS-guided FNA of a duodenal mass is the procurement of tissue for c-kit staining in patients with stromal cell tumors. Carcinoid tumors that measure more than 2 cm in size are generally removed surgically, whereas endoscopic resection can be attempted in those smaller than 2 cm or not invading the muscularis layer. In the largest series that evaluated the utility of EUS in 169 patients with protruding duodenal lesions, the diagnostic accuracy of EUS was 93.3% (50).

CONCLUSIONS

Overall, EUS has definitively established its role in investigating ampullary and duodenal lesions. The staging accuracy of EUS has been shown to be superior to CT and US for the evaluation of ampullary lesions. EUS and IDUS enables more accurate assessment of ductal involvement, thereby facilitating endoscopic resection of ampullary masses that otherwise would require an extended surgical resection.

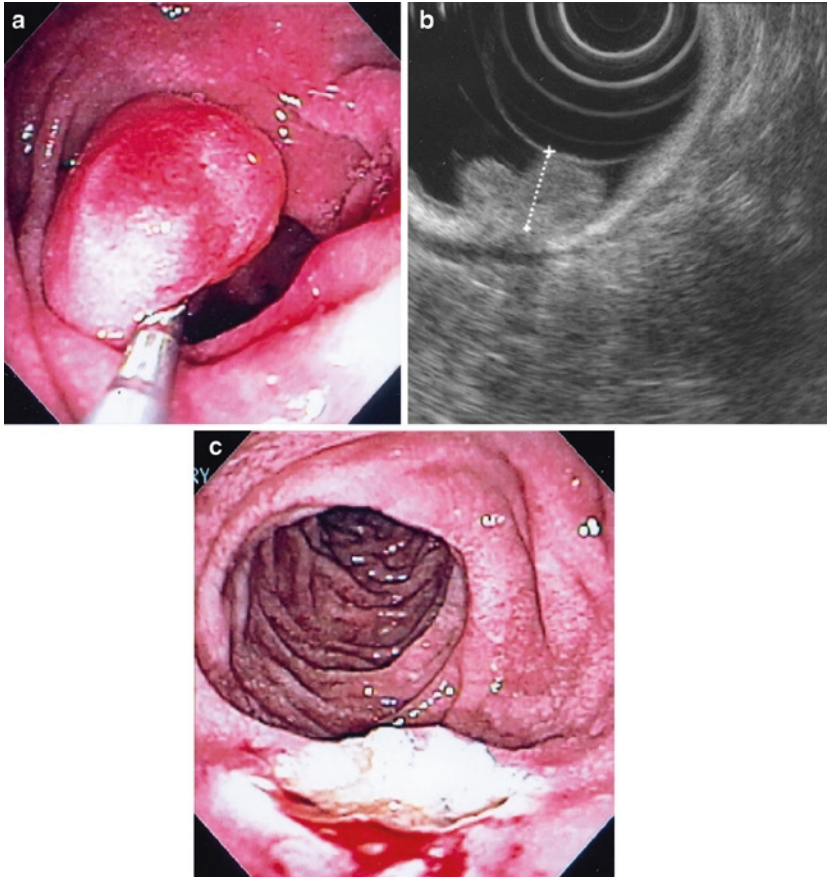


Fig. 4. (a) Small polypoid lesion in the duodenal bulb on endoscopic view. (b) At EUS, the lesion appears hypoechoic and is confined to the mucosal layer. (c) Successful removal of the lesion by injection-assisted polypectomy. Pathology revealed adenomatous polyp with low grade dysplasia.

REFERENCES

1. Treitschke F, Beger H. Local resection of benign periampullary tumors. *Ann Onc.* 1999;10(S4):S212–4.
2. Feldman M, Friedman L, Bradnt L. *Sleisenger and Fordtran's gastrointestinal and liver disease: pathophysiology, diagnosis, management.* Elsevier Health Sciences 2006; 8.
3. Grobmyer S, Stasik C, Draganov P, et al. Contemporary results with ampullectomy for 29 “benign” neoplasms of the ampulla. *J Am Coll Surg.* 2008;206(3):466–71.

4. Kim M, Lee S, Seo D, et al. Tumors of the major duodenal papilla. *Gastrointest Endosc.* 2001;54(5):609–19.
5. ASGE guideline. The role of endoscopy in the surveillance of premalignant conditions of the upper GI tract. *Gastrointest Endosc.* 2006;63(4):570–80.
6. Heidecke C, Rosenberg R, Bauer M, et al. Impact of grade dysplasia in villous adenomas of Vater's papilla. *World J Surg.* 2002;26:709–14.
7. Chiche L, Alkofer B, Parienti J, et al. Usefulness of follow-up after pancreatoduodenectomy for carcinoma of the ampulla of Vater. *HPB.* 2007;9:140–5.
8. O'Connell JB, Maggard M, Manunga J, et al. Survival after resection of ampullary carcinoma: a national population-based study. *Ann Surg Oncol.* 2008;15(7):1820–7.
9. Howe J, Klimstra D, Moccia R, Conlon KC, Brennan MF. Factors predictive of survival in ampullary carcinoma. *Ann Surg.* 1998;228(1):87–94.
10. Defrain C, Chang C, Srikureja W, Nguyen PT, Gu M. Cytologic features and diagnostic pitfalls of primary ampullary tumors by endoscopic ultrasound-guided fine needle aspiration. *Cancer.* 2005;105(5):289–97.
11. Tanaka S, Hirohashi K, Tanaka H, et al. Prognostic factors in patients with carcinoma of the papilla of Vater. *Hepatogastroenterology.* 2002;49(46):1116–9.
12. de Castro S, Kuhlmann K, van Heek T, et al. Recurrent disease after microscopically radical (r0) resection of periampullary adenocarcinoma in patients without adjuvant therapy. *J Gastrointest Surg.* 2004;8(7):775–84.
13. Akatsu T, Aiura K, Takahashi S, et al. Signet-ring cell carcinoma of the ampulla of Vater: report of a case. *Surg Today.* 2007;37:1110–4.
14. Kawakami H, Kuwatani M, Onodera M, et al. Primary acinar cell carcinoma of the ampulla of Vater. *J Gastroenterol.* 2007;42:694–7.
15. Green D, Roswell C, Cohen L. Metastatic bladder carcinoma to ampulla of Vater. *Gastrointest Endosc.* 2008;68(1):199–200.
16. Kim MH, Lee SK, Lee SY, Min YI. A case of adenofibromatous hyperplasia of the major duodenal papilla hardly differentiated from carcinoma [in Korean with English abstract]. *Korean J Gastroenterol.* 1993;25:1333–6.
17. Mayoral W, Salcedo JA, Montgomery B, Al-Kawas FH. Biliary obstruction and arid pancreatitis caused by Brunner's gland hyperplasia of the major duodenal papilla: a case report and review of the literature. *Endoscopy.* 2000;32:998–1001.
18. Yusef T, Bhutani M. Role of endoscopic ultrasonography in diseases of the extrahepatic biliary system. *J Gastroenterol Hepatol.* 2004;19:243–50.
19. Keriven O, Napoleon B, Souquet JC, Pujol B, Fouque P, Ponchon T. Patterns of the ampulla of Vater at endoscopic ultrasonography (abstract). *Gastrointest Endosc.* 1993;39:290.
20. Trevino J, Wilcox CM, Varadarajulu S. Endoscopic resection of minor papilla adenomas (with video). *Gastrointest Endosc.* 2008;68(2):383–6.
21. Loew BJ, Lukens FJ, Navarro F, et al. Successful endoscopic resection of gangliocytic paraganglioma of the minor papilla in a patient with pancreas divisum and pancreatitis (video). *Gastrointest Endosc.* 2007;65:547–50.
22. House MG, Yeo CJ, Schulick RD. Periampullary pancreatic somatostatinoma. *Ann Surg Oncol.* 2002;9:869–74.
23. Cheng CL, Sherman S, Fogel EL, et al. Endoscopic snare papillectomy for tumors of the duodenal papillae. *Gastrointest Endosc.* 2004;60:757–64.

24. Nakamura T, Ozawa T, Kitagawa M, et al. Endoscopic resection of gangliocytic paraganglioma of the minor duodenal papilla: case report and review. *Gastrointest Endosc.* 2002;55:270–3.
25. Sugiyama M, Kimura W, Muto T, Yahagi N, Ichinose M, Miki K. Endoscopic resection of adenoma of the minor papilla. *Hepatogastroenterology.* 1999; 46:189–92.
26. Lucena JF, Alvarez OA, Gross GW. Endoscopic resection of heterotrophic pancreas of the minor duodenal papilla: case report and review of the literature. *Gastrointest Endosc.* 1997;46:69–72.
27. Anand D, Barroeta J, Gupta P, Kochman M, Baloch ZW. Endoscopic ultrasound guided fine needle aspiration of non-pancreatic lesions: an institutional experience. *J Clin Pathol.* 2007;60:1254–62.
28. Muthusamy R, Jafri S, Cristian N. Endoscopic ultrasound guided fine-needle aspiration in the diagnosis and staging of ampullary neoplasms. *Gastrointest Endosc.* 2001;53(5):AB176.
29. Ito K, Fujita N, Noda Y, et al. Preoperative evaluation of ampullary neoplasm with EUS and transpapillary intraductal US: a prospective and histopathologically controlled study. *Gastrointest Endosc.* 2007;66(4):740–7.
30. Itoh A, Goto H, Naitoh Y, Hirooka Y, Furukawa T, Hayakawa T. Intraductal ultrasonography in diagnosing tumor extension of cancer of the papilla of Vater. *Gastrointest Endosc.* 1997;45(3): 251–9.
31. Menzel J, Hoepffner N, Sulkowski U, et al. Polypoid tumors of the major duodenal papilla: preoperative staging with intraductal US, EUS and CT – a prospective, histopathologically controlled study. *Gastrointest Endosc.* 1999;49(3):349–57.
32. Varadarajulu S. A modified technique to overcome the limitations of intraductal ultrasound for diagnosis of common bile duct stones. *Endoscopy.* 2008;40(2):E152.
33. Edge SB, Byrd DR, Compton CC, et al. *AJCC cancer staging manual.* 7th ed. New York: Springer; 2010.
34. Cannon M, Carpenter S, Elta G, et al. EUS compared with CT, magnetic resonance imaging, and angiography and the influence of biliary stenting on staging accuracy of ampullary neoplasms. *Gastrointest Endosc.* 1999;50(1):27–33.
35. Skordilis P, Mouzas I, Dimoulios P, Alexandrakis G, Moschandrea J, Kouroumalis E. Is endosonography an effective method for detection and local staging of the ampullary carcinoma? A prospective study. *BMC Surg.* 2002;2:1–8.
36. Midwinter MJ, Beveridge CJ, Wilsdon JB, Bennett MK, Baudouin CJ, Charnley RM. Correlation between spiral computed tomography, endoscopic ultrasonography and findings at operation in pancreatic and ampullary tumours. *Br J Surg.* 1999;86:189–93.
37. Rosch T, Braig C, Gain T, Feuerbach S, Siewert J, Schusdziarra V. Staging of pancreatic and ampullary carcinoma by endoscopic ultrasonography. *Gastroenterology.* 1992;102:188–99.
38. Tio TL, Sie LH, Kallimanis G, et al. Staging of ampullary and pancreatic carcinoma: comparison between endosonography and surgery. *Gastrointest Endosc.* 1996;44:706–13.
39. Chen CH, Yang CC, Yeh YH, Chou DA, Nien CK. Reappraisal of endosonography of ampullary tumors: correlation with transabdominal sonography, CT and MRI. *J Clin Ultrasound.* 2009;37(1):18–25.

40. Mukai H, Nakajima M, Yasuda K, Mizuno S, Kawai K. Evaluation of endosonographic ultrasonography in the pre-operative staging of carcinoma of the ampulla of Vater and common bile duct. *Gastrointest Endosc.* 1992;38(6):676–83.
41. Chen CH, Tseng LJ, Yang CC, Yeh YH, Mo LR. The accuracy of endoscopic ultrasound, endoscopic retrograde cholangiopancreatography, computed tomography and transabdominal ultrasound in the detection and staging of primary ampullary tumors. *Hepatogastroenterology.* 2001;48(42):1750–3.
42. Chen CH, Tseng LJ, Yang CC, Yeh YH, Mo LR. Preoperative evaluation of peri-ampullary tumors by endoscopic sonography, transabdominal sonography and computed tomography. *J Clin Ultrasound.* 2001;29(6):313–231.
43. Seewald S, Omar S, Soehendra N. Endoscopic resection of tumors of the ampulla of Vater: how far and how deep down can we go? *Gastrointest Endosc.* 2006;63(6):789–91.
44. Bohnacker S, Seitz U, Nguyen D, et al. Endoscopic resection of benign tumors of the duodenal papilla without and with intraductal growth. *Gastrointest Endosc.* 2005;62(4):551–60.
45. Saurin JC, Chavaillon A, Napoleon B, et al. Long-term follow-up of patients with endoscopic treatment of sporadic adenomas of the papilla of Vater. *Endoscopy.* 2003;35:402–6.
46. Binmoeller K, Boaventura S, Ramsperger K, Soehendra N. Endoscopic snare excision of the benign adenomas of the papilla of Vater. *Gastrointest Endosc.* 1993;39:127–31.
47. Zadorova Z, Dvofak M, Hajer J. Endoscopic therapy of benign tumors of the papilla of Vater. *Endoscopy.* 2001;33:345–47.
48. Norton I, Gostout C, Baron T, Geller A, Petersen BT, Wiersema MJ. Safety and outcome of endoscopic excision of the major duodenal papilla. *Gastrointest Endosc.* 2002;56:239–43.
49. Kahaleh M, Shami VM, Brock A, et al. Factors predictive of malignancy and endoscopic resectability in ampullary neoplasia. *Am J Gastroenterol.* 2004;99:2335–9.
50. Xu GQ, Wu YQ, Wang LJ, Chen HT. Values of endoscopic ultrasonography for diagnosis and treatment of duodenal protruding lesions. *J Zhejiang Univ Sci B.* 2008;9:329–34.

The Role of EUS in Pancreatic Cancer

*Vanessa M. Shami, MD,
Indu Srinivasan, MD,
and Michel Kahaleh, MD*

CONTENTS

INTRODUCTION
PRESENTATION AND INITIAL EVALUATION
RADIOGRAPHIC IMAGING STUDIES
ENDOSCOPIC ULTRASOUND (EUS)

Abstract

Several advances in diagnosis, treatment and palliation of pancreatic cancer have occurred in the last decade. A multidisciplinary approach of the management of pancreatic cancer is required. Cross sectional imaging is usually the first imaging modality for diagnosis and staging. Endoscopic ultrasonography (EUS) with its superiority in detecting smaller lesions, lymph node metastasis, and vascular infiltration has become the next imaging modality. The adjunction of fine needle aspiration to EUS, with its relatively low risk profile, has increased the accuracy of this technique and helped differentiate pancreatic adenocarcinoma from other pancreatic neoplasms which may influence treatment as well as prognosis. Finally, EUS-FNA allows the performance of celiac plexus neurolysis for unremitting pain in these patients.

Key Words: Pancreatic cancer, Pancreatic mass, Obstructive jaundice, Pancreatic cancer staging

From: *Clinical Gastroenterology: Endoscopic Ultrasound*,
Edited by: V. M. Shami and M. Kahaleh, DOI 10.1007/978-1-60327-480-7_12,
© Springer Science+Business Media, LLC 2010

INTRODUCTION

Pancreatic cancer is the fourth most common cause of cancer death in the United States and second leading cause of death among all of the gastrointestinal malignancies (1). It has been estimated that about 38,000 Americans were diagnosed with pancreatic cancer in 2008 (1). According to the latest data from the American Cancer Society, 1 and 5 year survival rates at all stages of diagnosis were 24% and 5%, respectively. In view of the dismal survival statistics, early diagnosis and proper assessment of tumor resectability hold the key to increased survival. Unfortunately, even with surgical resection, the prognosis does not increase dramatically. Furthermore, the high cost of pancreatic surgery and its potential morbidity emphasize the need to identify tumors amenable to resection while avoiding surgical procedures on inoperable tumors (2, 3). The aim of this chapter is to review the role of EUS in the current day evaluation and management of patients with suspected pancreatic cancer.

PRESENTATION AND INITIAL EVALUATION

Pancreatic ductal adenocarcinoma accounts for over 90% of pancreatic tumors (4). The peak incidence is between the ages of 60 and 80 years. More than 80% of patients present with pain which is predominantly felt in the upper abdomen commonly radiating to the back (5, 6). Significant and rapid loss of weight is a characteristic feature of pancreatic cancer (5, 6). Symptoms from pancreatic cancer depend upon the location of the tumor. Tumors arising from the head of the pancreas present with symptoms of biliary obstruction such as cholestasis, pruritus, and jaundice (4), while tumors arising from the body, tail, or the uncinate process present with nonspecific symptoms such as early satiety, anorexia, and asthenia (5, 6). In the presence of these nonspecific symptoms, attempts must be made to rule out various conditions presenting similarly, i.e., other primary tumors (ampullary, gallbladder, biliary, etc.), metastatic cancers to either the pancreas (melanoma, breast and lung cancer), or the portahepatis (i.e., colon cancer) and finally, benign lesions such as chronic pancreatitis or peptic ulcer disease. Additionally, new onset diabetes mellitus in a patient with no apparent predisposing factors such as family history and obesity might be an indication of underlying malignancy (7). While examining these patients, emphasis should be on the detection of a palpable gallbladder in the presence of jaundice (Courvoisier sign), metastatic lymph nodes such as Virchow's node (left supraclavicular node) or periumbilical nodes, ascites, or rarely the presence of unexplained thrombophlebitis.

Less than 5% of pancreatic tumors are neuroendocrine tumors, (8) which are part of the APUD (amine precursor uptake and decarboxylation) group. These tumors are divided into two types: hormonally hyperfunctioning and nonhyperfunctioning, depending on whether they produce a clinical and biochemical picture related to excessive hormone production. The symptoms for hyperfunctioning endocrine tumors depend on the hormones that are elevated such as insulin, glucagon, vasoactive intestinal peptides, and somatostatins. (9). Insulinomas present with fasting hypoglycemia and neuropsychiatric symptoms while gastrinomas present with peptic ulcer, diarrhea, and steatorrhea. The nonhyperfunctioning endocrine tumors are more common than hyperfunctioning endocrine tumors and typically present late with abdominal pain, jaundice, or GI obstruction (10, 11). It is important to diagnose these patients as treatment and prognosis is different than with patients who have pancreatic adenocarcinoma. Pancreatic neuroendocrine tumors appear as a homogeneous mass with distinct margins and hypoechoic to the normal pancreatic parenchyma (12) (Fig. 1a, b). However, sometimes they may appear as an isoechoic or hyperechoic mass (13) making the diagnosis solely on the basis of EUS very challenging. Often times FNA is needed as these tumors appear essentially identical to adenocarcinoma.

The current 2010 AJCC TNM Staging of pancreatic neuroendocrine tumors, carcinoid tumors, and exocrine tumors are summarized in Table 1 (14). This is the first time that endocrine and exocrine tumors of the pancreas have been grouped under the same staging system.

Primary pancreatic lymphoma comprises less than 0.5% of pancreatic cancers (15). However, its diagnosis is extremely important as the primary treatment is systemic versus surgical therapy. Pancreatic lymphoma usually presents as a mass occupying the pancreas and often involves the peripancreatic lymph nodes (Fig. 2). The absence of palpable superficial and mediastinal lymphadenopathy as well as the absence of hepatic or splenic involvement in conjunction with a normal white cell count may differentiate it from nonhodgkin's lymphoma invading the pancreas (16). The challenging thing is that pancreatic lymphoma also typically presents with nonspecific symptoms such as weight loss, abdominal pain, nausea, and vomiting (16). Rarely, jaundice, acute pancreatitis, and small bowel obstruction are manifestations of pancreatic lymphoma (17). The nonspecific symptoms make it difficult to be differentiated from pancreatic adenocarcinoma (17). This differentiation is crucial since the treatment of pancreatic lymphoma is chemotherapy. Some authors have also suggested the use of adjuvant surgery (16, 18) and radiotherapy. Pancreatic lymphoma has a better prognosis than pancreatic adenocarcinoma and the use of multimodality treatments has increased the cure rate to as high as 30% (18).

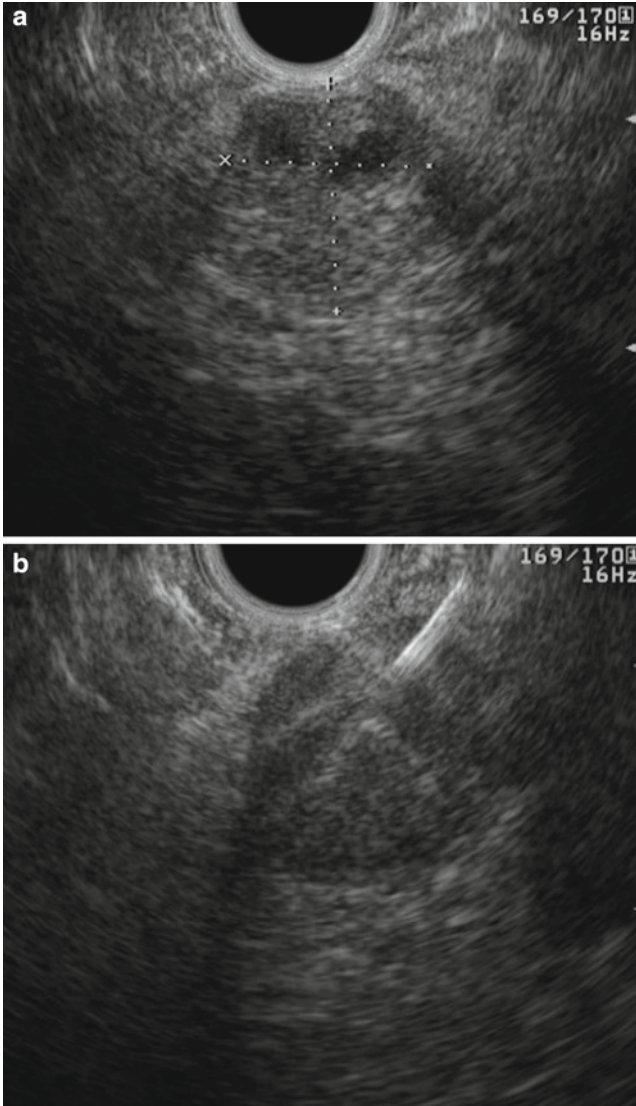


Fig. 1. (a) A hypoechoic mass representing a neuroendocrine tumor can be seen in the body of the pancreas. (b) FNA is being performed of the hypoechoic neuroendocrine tumor.

Rarely, pancreatic masses may represent metastasis from other sites. The most common cancers are renal cell carcinoma (Fig. 3), lung cancer, and breast cancer. Sometimes, melanoma can metastasize to the pancreas as well (Fig. 4). Since these masses are indistinguishable from pancreatic adenocarcinoma, FNA for cytology is mandatory.

Table 1

T	(Primary tumor)
Tx	Primary tumor cannot be assessed
T0	No evidence of primary tumor
Tis	Carcinoma in situ
T1	Tumor limited to the pancreas, 2 cm or less in greatest dimension
T2	Tumor limited to the pancreas, more than 2 cm in greatest dimension
T3	Tumor extends beyond the pancreas but without involvement of the celiac axis or the superior mesenteric artery
T4	Tumor involves the celiac axis or the superior mesenteric artery (unresectable primary tumor)
N	(Regional lymph nodes)
Nx	No regional lymph node metastasis
N1	Regional lymph node metastasis
M	(Distant Metastasis)
M0	No distant metastasis
M1	Distant metastasis

Adapted from Ref. 14.

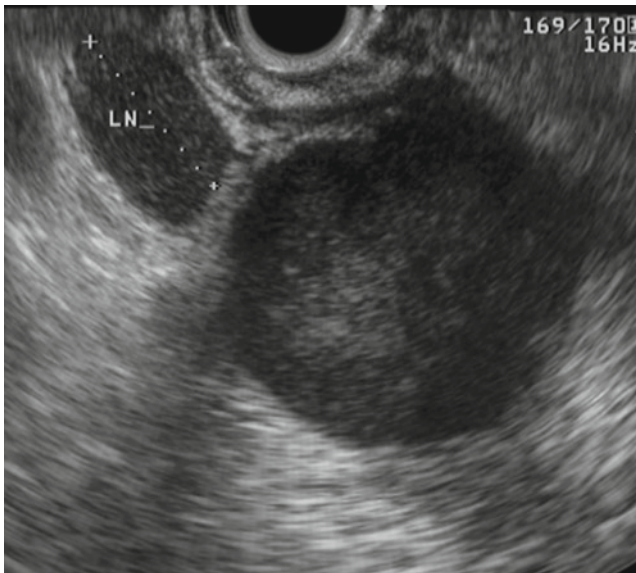


Fig. 2. A hypoechoic mass which represents a B-cell lymphoma with an adjacent peritumoral lymph node is noted.

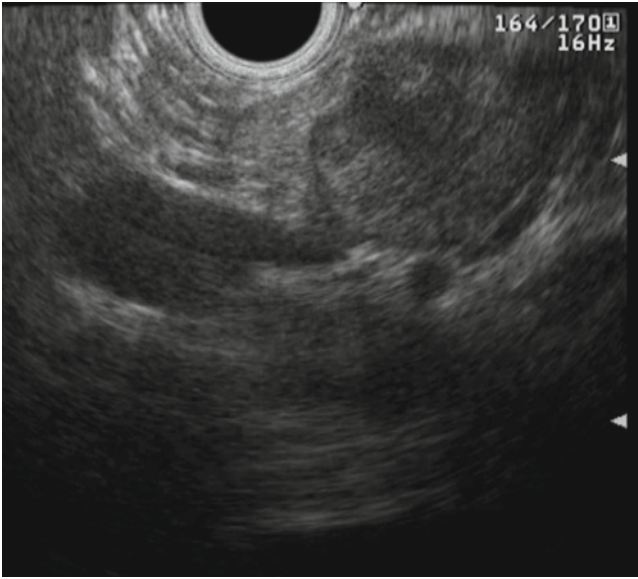


Fig. 3. A hypoechoic pancreatic mass can be visualized and represents metastatic renal cell carcinoma.

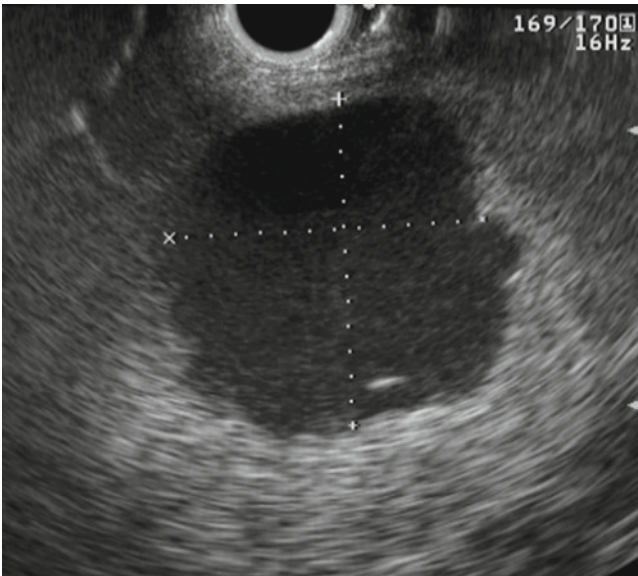


Fig. 4. An EUS image revealing metastatic melanoma to the pancreas.

RADIOGRAPHIC IMAGING STUDIES

Often when a patient presents with abdominal pain or jaundice, transabdominal US (TUS) is the initial investigation of choice. It is a noninvasive and a cost-effective method, which provides excellent imaging of the porta hepatis, gallbladder, liver, pancreatic head and proximal extrahepatic bile ducts as well as allows the assessment of the relationship of the tumor to the pancreatic duct, bile duct, and regional vessels. However, suboptimal visualization of distal bile duct, body and tail of pancreas due to overlying bowel gas and variable skill of the operator limit its use. For instance, TUS has a sensitivity of only 76% for the detection of pancreatic tumors (19, 20). Therefore, TUS needs to be supplemented with better imaging tools. CT is the most commonly used imaging modality for the detection and staging of pancreatic cancer. Though CT depicts the local extension of cancer along with the involvement of regional vasculature, its main limitation is its inability to reveal liver and lymph node metastasis (21–23). Recent usage of multidetector CT scans allows the use of extremely thin collimation to procure high resolution scans during multiple phases of contrast enhancement (24–26). Multiplanar reconstruction of these images helps in the optimal staging of the pancreatic cancer as well as to rule out metastatic disease. Despite the technological advances, the ability to detect pancreatic lesions smaller than 2.5 cm remains suboptimal (27, 28). Gadolinium and mangafodipir sodium-enhanced 3.0 Tesla MRI, may be used as an adjunct to helical CT for detecting smaller lesions (29, 30). A meta-analysis conducted in 2005 showed that the sensitivity of MRI and helical CT for the diagnosis of adenocarcinoma was 84% and 91% respectively, while their respective sensitivity for the resectability of the tumor is 82% and 81% (31). Thus, the inability to offer dramatic improvement in diagnosis combined with the increased cost and lack of availability, restricted the use of MRI to patients with equivocal CT findings or those with suspected pancreatic cystic neoplasms or in whom knowledge of pancreaticobiliary ductal anatomy was desired. Of late, certain authors have advocated the combining of 18F-fluorodeoxyglucose-positron emission tomography with CT scan for increased sensitivity (32). The cost and lack of availability of PET-CT, however, limits its usage.

ENDOSCOPIC ULTRASOUND (EUS)

EUS has been one of the most dynamic innovations of gastrointestinal endoscopy during the last 25 years, providing the endoscopist with the unique opportunity to visualize the gastrointestinal wall layers and surrounding organs.

There are three basic echoendoscope designs utilized – the radial array system, a curvilinear array system, and high frequency catheter-based miniprobes. Miniprobes have no setting in the diagnosis of pancreatic cancer unless performed in an intraductal fashion (Refer to Chap. 2). Although very few studies have been conducted comparing the efficacy of the radial versus the curvilinear array systems (33), their ability to detect and stage cancer has been similar (34). The radial array system provides a 360° circumferential image of the gastrointestinal system which aids in obtaining complete images that are easy to interpret. It also aids in better visualization of the papilla, longitudinal view of the common bile duct, and submucosal lesions. The curvilinear array, on the other hand, provides a 180° view parallel to the shaft. Though the images are sectoral and more difficult to orient, it is highly beneficial for tracing the path of the needle when inserted out of the working channel of the echoendoscope. Thus, while radial arrays are used for the initial evaluation and staging of the cancer, the linear array, with its ability to perform EUS-FNA, EUS-guided injection therapies, and EUS-guided drainage procedures, has become the preferred choice of echoendoscopy (33). Recently, a new generation of radial scan electronic device and lower frequency mechanical devices with Doppler application have been introduced. Their efficacy, however, still needs to be evaluated prospectively.

For the appropriate use of the echoendoscope, it is pertinent to know both the normal anatomy of the pancreatobiliary system as well as the standard imaging techniques. After crossing the EG junction, the echoendoscope should be rotated clockwise to visualize the body of the pancreas in between the celiac and superior mesenteric arteries. Here, the pancreas can be traced to the splenic hilum using the splenic vein as a landmark where the pancreatic tail is revealed. On counterclockwise rotation the pancreatic neck, body, and tail appear between the splenic vein and posterior gastric wall. The scope is then advanced toward the angle of the stomach following the portal vein and the bile duct, and on crossing the duodenal bulb, the head of pancreas can be visualized (35) (Refer to Chaps. 3 and 4). Typically, pancreatic adenocarcinoma appears as an inhomogeneous hypoechoic mass with irregular borders in the pancreatic parenchyma (Fig. 5). If the mass is located in the head of the pancreas, it often obstructs the pancreatic and common bile duct with resultant proximal dilation (Fig. 6). Additionally, EUS is very useful in detecting vessel involvement, including SMV, PV (Fig. 7), and SMA involvement. Inspection of the celiac axis, as well as both liver lobes (Fig. 8), and the detection of ascites (Fig. 9) are crucial. If any of these regions are aspirated and cytology positive, it portends more advanced disease.

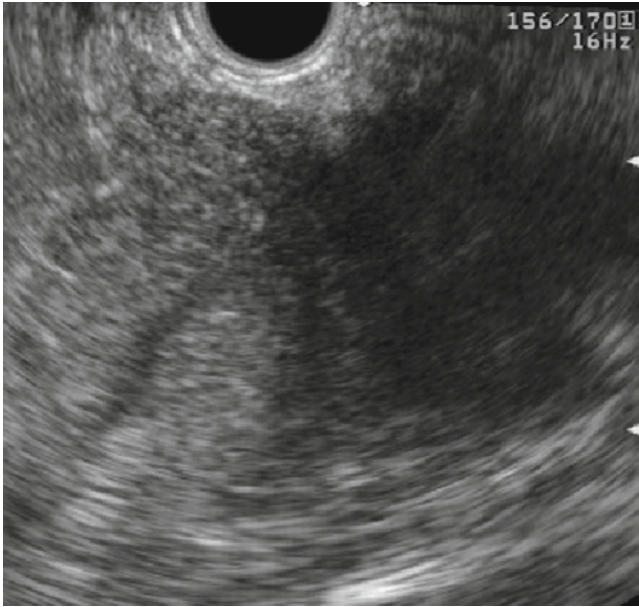


Fig. 5. An irregular hypoechoic mass is visualized in the head of the pancreas representing adenocarcinoma.

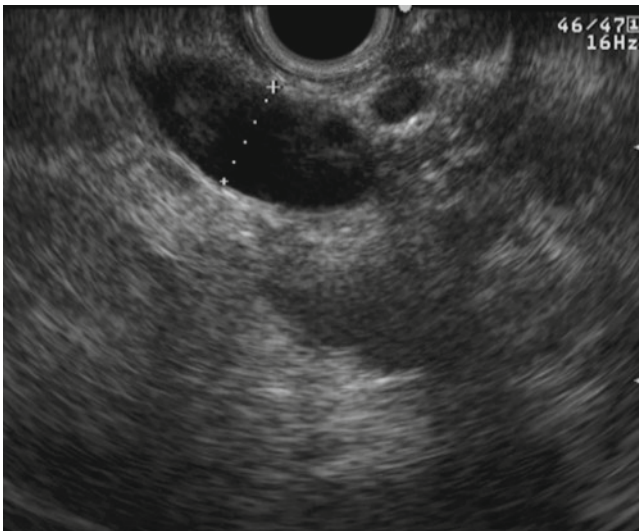


Fig. 6. Marked biliary duct dilation secondary to downstream obstruction by the pancreatic mass.

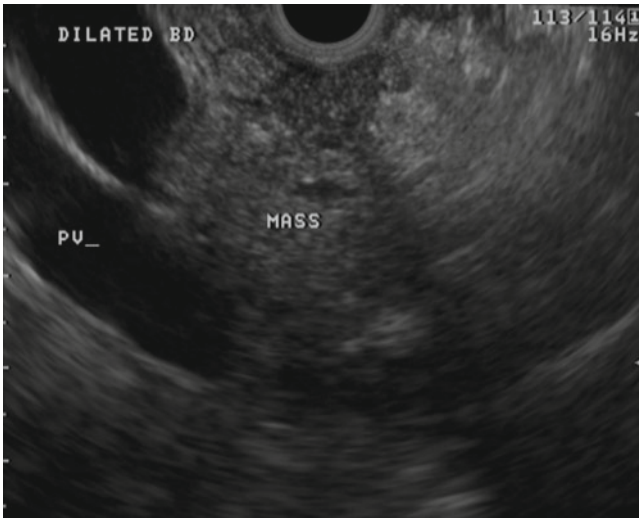


Fig. 7. A hypoechoic pancreatic mass invading the portal confluence.

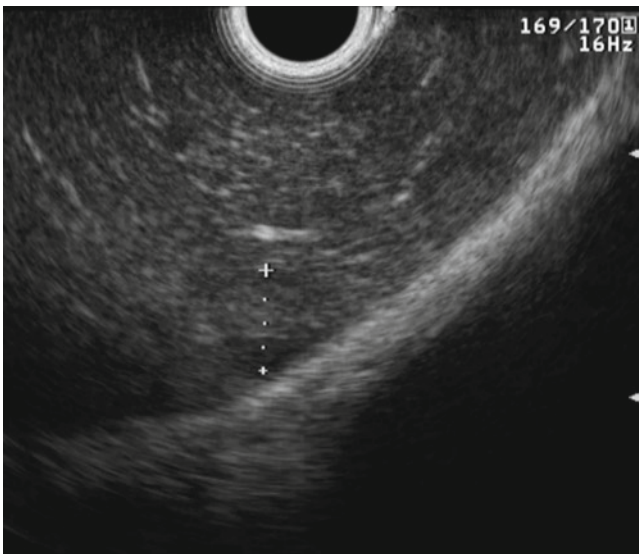


Fig. 8. A round, isoechoic lesion can be seen in the left lobe of the liver which represents metastasis.

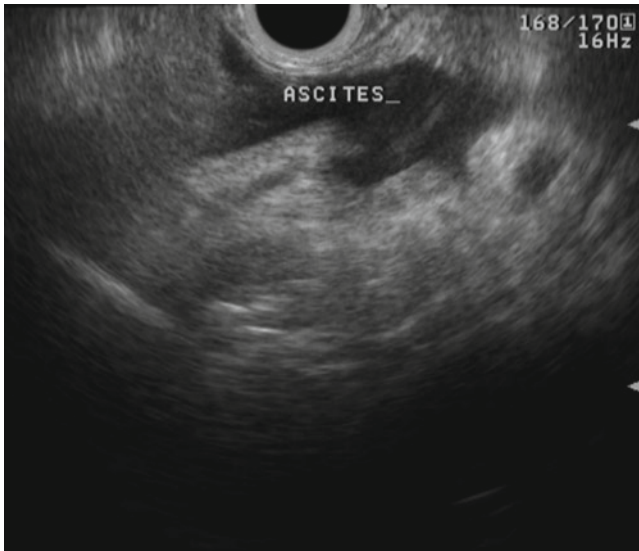


Fig. 9. A small pocket of ascites is detected, and cytology reveals adenocarcinoma.

EUS is superior to CT in the detection of pancreatic tumors especially with a diameter of less than 25 mm (20, 36–41). Recently, however, with the advent of MDCT, this difference has reduced (24, 42). EUS can also locate lymph node metastasis and vascular infiltration with a higher sensitivity than CT (43). The potential major drawbacks of EUS include – operator dependence, limited visualization of the right hepatic lobe and peritoneal metastasis. Additionally, it may be difficult to detect tumor in patients with concomitant chronic pancreatitis, or when the cancer is diffusely infiltrating the whole gland (40, 44). Despite these limitations, some authors have documented that the negative predictive value of EUS for tumor detection is as high as 100% (45). EUS is particularly helpful in demonstrating the presence of neuroendocrine tumors with a sensitivity of more than 80% (46, 47). It not only localizes the tumor, but also differentiates it from adenocarcinoma (48) which has a worse prognosis. EUS has a higher sensitivity for diagnosing the tumors located in the head of the pancreas than the tumors located at body or tail of the pancreas (49, 50).

A recent review by DeWitt et al., comparing the role of EUS and CT in staging of the pancreatic cancer depicted EUS as superior to CT for T(tumor) staging (20, 27) and for detecting the invasion of the portal

vein while the invasion of celiac and superior mesenteric arteries were better detected by CT scan (13). However, the study demonstrated equal efficacy of both EUS and CT scan in N (nodal) staging (21) and determining the tumor resectability (13).

Studies have shown that the sensitivity of cytology obtained during ERCP to be less than 70%. Therefore, ERCP should be performed only for biliary decompression (51, 52). EUS-guided FNA is the preferred procedure due to its ability to detect and stage the lesion, assess resectability, obtain FNA for cytologic confirmation, and finally to carry out EUS-guided celiac neurolysis in the presence of unresectable tumor with unremitting pain (53, 54).

EUS-FNA of pancreatic masses is low risk with a reported complication rate of 1–2%. Most complications are minor and include self-limited bleeding, abdominal pain, and acute pancreatitis.

Although a relatively safe procedure, routine preoperative tissue sampling is not always required in surgically fit patients. For example, EUS-FNA of resectable pancreatic body and tail tumors has been associated with possible tumor seeding in the gastric wall.

When performing FNA of pancreatic masses, it is important to keep in mind that making simple hematoxylin–eosin stains of the specimen may not be sufficient for diagnosis in all cases. For example, in cases where lymphoma is suspected, it is important to perform extra FNA passes, so the cytologists have enough cells for flow cytometry (17, 55). Rarely, endoscopic ultrasound-guided trucut biopsy should be considered in cases where the diagnosis is equivocal (56).

The sensitivity and specificity of EUS-FNA for the diagnosis of pancreatic cancer is 85% and 98%, respectively (20) and remains extremely accurate even after previously negative tissue sampling from ERCP and percutaneous biopsies (57). Despite its excellent sensitivity, the negative predictive value of EUS-FNA does not completely exclude the possibility of malignancy; this is particularly true in conditions when pancreatitis accompanies pancreatic cancer.

In summary, EUS is very useful in the diagnosis and locoregional staging of nonmetastatic pancreatic masses. It is especially superior over cross-sectional imaging for tumors less than 2.5 cm. Fine needle aspiration of pancreatic masses should be performed in instances where the diagnosis is equivocal, or when the tumor is suspected to represent a malignant process other than adenocarcinoma such as lymphoma, a neuroendocrine tumor, or metastasis.

REFERENCES

1. Jemal A, Siegel R, Ward E, Hao Y, Xu J, Murray T, et al. Cancer statistics, 2008. *CA Cancer J Clin.* 2008;58:71–96.
2. Pedrazzoli S, DiCarlo V, Dionigi R, Mosca F, Pederzoli P, Pasquali C, et al. Standard versus extended lymphadenectomy associated with pancreatoduodenectomy in the surgical treatment of adenocarcinoma of the head of the pancreas: a multicenter, prospective, randomized study. Lymphadenectomy Study Group. *Ann Surg.* 1998;228:508–17.
3. Yeo CJ, Cameron JL, Lillemoe KD, Sohn TA, Campbell KA, Sauter PK, et al. Pancreaticoduodenectomy with or without distal gastrectomy and extended retroperitoneal lymphadenectomy for periampullary adenocarcinoma, part 2: randomized controlled trial evaluating survival, morbidity, and mortality. *Ann Surg.* 2002;236:355–66. discussion 366–8.
4. Kloppel G, Solicic E, Longnecker DS, Capella C, Sobin LH. Histological typing of tumors of the exocrine pancreas. Berlin: Springer; 1996.
5. Kalser MH, Barkin J, MacIntyre JM. Pancreatic cancer. Assessment of prognosis by clinical presentation. *Cancer.* 1985;56:397–402.
6. Bakkevold KE, Arnesjo B, Kambestad B. Carcinoma of the pancreas and papilla of Vater: presenting symptoms, signs, and diagnosis related to stage and tumour site. A prospective multicentre trial in 472 patients. Norwegian Pancreatic Cancer Trial. *Scand J Gastroenterol.* 1992;27:317–25.
7. Chari ST, Leibson CL, Rabe KG, Ransom J, de Andrade M, Petersen GM. Probability of pancreatic cancer following diabetes: a population-based study. *Gastroenterology.* 2005;129:504–11.
8. Fesinmeyer MD, Austin MA, Li CI, De Roos AJ, Bowen DJ. Differences in survival by histologic type of pancreatic cancer. *Cancer Epidemiol Biomarkers Prev.* 2005;14:1766–73.
9. Goldin SB, Aston J, Wahi MM. Sporadically occurring functional pancreatic endocrine tumors: review of recent literature. *Curr Opin Oncol.* 2008;20:25–33.
10. Dralle H, Krohn SL, Karges W, Boehm BO, Brauckhoff M, Gimm O. Surgery of resectable nonfunctioning neuroendocrine pancreatic tumors. *World J Surg.* 2004;28:1248–60.
11. Hochwald SN, Zee S, Conlon KC, Colleoni R, Louie O, Brennan MF, et al. Prognostic factors in pancreatic endocrine neoplasms: an analysis of 136 cases with a proposal for low-grade and intermediate-grade groups. *J Clin Oncol.* 2002;20:2633–42.
12. Gorman B, Charboneau JW, James EM, Reading CC, Galiber AK, Grant CS, et al. Benign pancreatic insulinoma: preoperative and intraoperative sonographic localization. *AJR Am J Roentgenol.* 1986;147:929–34.
13. Bottger TC, Junginger T. Is preoperative radiographic localization of islet cell tumors in patients with insulinoma necessary? *World J Surg.* 1993;17:427–32.
14. Edge SB, Byrd DR, Compton CC, et al. *AJCC Cancer Staging manual.* 7th ed. New York: Springer; 2010.

15. Baylor SM, Berg JW. Cross-classification and survival characteristics of 5,000 cases of cancer of the pancreas. *J Surg Oncol.* 1973;5:335–58.
16. Behrns KE, Sarr MG, Strickler JG. Pancreatic lymphoma: is it a surgical disease? *Pancreas.* 1994;9:662–7.
17. Nayer H, Weir EG, Sheth S, Ali SZ. Primary pancreatic lymphomas: a cytopathologic analysis of a rare malignancy. *Cancer.* 2004;102:315–21.
18. Brown PC, Hart MJ, White TT. Pancreatic lymphoma, diagnosis and management. *Int J Pancreatol.* 1987;2:93–9.
19. Rickes S, Unkrodt K, Neye H, Ocran KW, Wermke W. Differentiation of pancreatic tumours by conventional ultrasound, unenhanced and echo-enhanced power Doppler sonography. *Scand J Gastroenterol.* 2002;37:1313–20.
20. DeWitt J. EUS and pancreatic tumors. In: Hawes R, Fockens P, editors. *Endosonography.* London: Elsevier Press; 2006.
21. Valls C, Andia E, Sanchez A, Fabregat J, Pozuelo O, Quintero JC, et al. Dual-phase helical CT of pancreatic adenocarcinoma: assessment of resectability before surgery. *AJR Am J Roentgenol.* 2002;178:821–6.
22. Roche CJ, Hughes ML, Garvey CJ, Campbell F, White DA, Jones L, et al. CT and pathologic assessment of prospective nodal staging in patients with ductal adenocarcinoma of the head of the pancreas. *AJR Am J Roentgenol.* 2003;180:475–80.
23. Andersson R, Vagianos C, Williamson R. Preoperative staging and evaluation of resectability in pancreatic ductal adenocarcinoma. *HPB (Oxford).* 2004;6:5–12.
24. Catalano C, Laghi A, Fraioli F, Pediconi F, Napoli A, Danti M, et al. Pancreatic carcinoma: the role of high-resolution multislice spiral CT in the diagnosis and assessment of resectability. *Eur Radiol.* 2003;13:149–56.
25. Prokesch RW, Chow LC, Beaulieu CF, Nino-Murcia M, Mindelzun RE, Bammer R, et al. Local staging of pancreatic carcinoma with multi-detector row CT: use of curved planar reformations initial experience. *Radiology.* 2002;225:759–65.
26. Vargas R, Nino-Murcia M, Trueblood W, Jeffrey Jr RB. MDCT in pancreatic adenocarcinoma: prediction of vascular invasion and resectability using a multiphase technique with curved planar reformations. *AJR Am J Roentgenol.* 2004;182:419–25.
27. DeWitt J, Devereaux BM, Lehman GA, Sherman S, Imperiale TF. Comparison of endoscopic ultrasound and computed tomography for the preoperative evaluation of pancreatic cancer: a systematic review. *Clin Gastroenterol Hepatol.* 2006;4:717–25. quiz 664.
28. DeWitt J, Devereaux B, Chriswell M, McGreevy K, Howard T, Imperiale TF, et al. Comparison of endoscopic ultrasonography and multidetector computed tomography for detecting and staging pancreatic cancer. *Ann Intern Med.* 2004;141:753–63.
29. Schima W. MRI of the pancreas: tumours and tumour-simulating processes. *Cancer Imaging.* 2006;6:199–203.
30. Schima W, Ba-Ssalamah A, Goetzinger P, Scharitzer M, Koelblinger C. State-of-the-art magnetic resonance imaging of pancreatic cancer. *Top Magn Reson Imaging.* 2007;18:421–9.
31. Bipat S, Phoa SS, van Delden OM, Bossuyt PM, Gouma DJ, Lameris JS, et al. Ultrasonography, computed tomography and magnetic resonance imaging for

- diagnosis and determining resectability of pancreatic adenocarcinoma: a meta-analysis. *J Comput Assist Tomogr.* 2005;29:438–45.
32. Casneuf V, Delrue L, Kelles A, Van Damme N, Van Huisse J, Berrevoet F, et al. Is combined 18F-fluorodeoxyglucose-positron emission tomography/computed tomography superior to positron emission tomography or computed tomography alone for diagnosis, staging and restaging of pancreatic lesions? *Acta Gastroenterol Belg.* 2007;70:331–8.
 33. Gress F, Savides T, Cummings O, Sherman S, Lehman G, Zaidi S, et al. Radial scanning and linear array endosonography for staging pancreatic cancer: a prospective randomized comparison. *Gastrointest Endosc.* 1997;45:138–42.
 34. Kochman ML, Elta GH, Bude R, Nostrant TT, Scheiman JM. Utility of a linear array ultrasound endoscope in the evaluation of suspected pancreatic disease. *J Gastrointest Surg.* 1998;2:217–22.
 35. Vilmann P, Hancke S. Endoscopic ultrasound scanning of the upper gastrointestinal tract using a curved linear array transducer: “the linear anatomy”. *Gastrointest Endosc Clin N Am.* 1995;5:507–21.
 36. Rosch T, Lorenz R, Braig C, Feuerbach S, Siewert JR, Schusdziarra V, et al. Endoscopic ultrasound in pancreatic tumor diagnosis. *Gastrointest Endosc.* 1991;37:347–52.
 37. Palazzo L, Roseau G, Gayet B, Vilgrain V, Belghiti J, Fekete F, et al. Endoscopic ultrasonography in the diagnosis and staging of pancreatic adenocarcinoma. Results of a prospective study with comparison to ultrasonography and CT scan. *Endoscopy.* 1993;25:143–50.
 38. Yasuda K, Mukai H, Nakajima M. Endoscopic ultrasonography diagnosis of pancreatic cancer. *Gastrointest Endosc Clin N Am.* 1995;5:699–712.
 39. Hunt GC, Faigel DO. Assessment of EUS for diagnosing, staging, and determining resectability of pancreatic cancer: a review. *Gastrointest Endosc.* 2002;55:232–7.
 40. Muller MF, Meyenberger C, Bertschinger P, Schaer R, Marincek B. Pancreatic tumors: evaluation with endoscopic US, CT, and MR imaging. *Radiology.* 1994;190:745–51.
 41. Legmann P, Vignaux O, Dousset B, Baraza AJ, Palazzo L, Dumontier I, et al. Pancreatic tumors: comparison of dual-phase helical CT and endoscopic sonography. *AJR Am J Roentgenol.* 1998;170:1315–22.
 42. Del Frate C, Zanardi R, Morteale K, Ros PR. Advances in imaging for pancreatic disease. *Curr Gastroenterol Rep.* 2002;4:140–8.
 43. Rosewicz S, Wiedenmann B. Pancreatic carcinoma. *Lancet.* 1997;349:485–9.
 44. Bhutani MS, Gress FG, Giovannini M, Erickson RA, Catalano MF, Chak A, et al. The No Endosonographic Detection of Tumor (NEST) Study: a case series of pancreatic cancers missed on endoscopic ultrasonography. *Endoscopy.* 2004;36:385–9.
 45. Klapman JB, Chang KJ, Lee JG, Nguyen P. Negative predictive value of endoscopic ultrasound in a large series of patients with a clinical suspicion of pancreatic cancer. *Am J Gastroenterol.* 2005;100:2658–61.
 46. Chatzipantelis P, Salla C, Konstantinou P, Karoumpalis I, Sakellariou S, Doumani I. Endoscopic ultrasound-guided fine-needle aspiration cytology of pancreatic neuroendocrine tumors: a study of 48 cases. *Cancer.* 2008;114:255–62.

47. Ardengh JC, de Paulo GA, Ferrari AP. EUS-guided FNA in the diagnosis of pancreatic neuroendocrine tumors before surgery. *Gastrointest Endosc.* 2004;60:378–84.
48. McLean AM, Fairclough PD. Endoscopic ultrasound in the localisation of pancreatic islet cell tumours. *Best Pract Res Clin Endocrinol Metab.* 2005;19:177–93.
49. Rosch T, Lightdale CJ, Botet JF, Boyce GA, Sivak Jr MV, Yasuda K, et al. Localization of pancreatic endocrine tumors by endoscopic ultrasonography. *N Engl J Med.* 1992;326:1721–6.
50. Soria MT, Gines A, Belda J, Sole M, Pellise M, Bordas JM. Usefulness of endoscopic ultrasound-guided fine needle aspiration (EUS-G FNA) in diagnosing the extension of non-small cell lung cancer. *Arch Bronconeumol.* 2002;38:536–41.
51. Ponchon T, Gagnon P, Berger F, Labadie M, Liaras A, Chavaillon A, et al. Value of endobiliary brush cytology and biopsies for the diagnosis of malignant bile duct stenosis: results of a prospective study. *Gastrointest Endosc.* 1995;42:565–72.
52. Pugliese V, Conio M, Nicolo G, Saccomanno S, Gatteschi B. Endoscopic retrograde forceps biopsy and brush cytology of biliary strictures: a prospective study. *Gastrointest Endosc.* 1995;42:520–6.
53. Santo E. Pancreatic cancer imaging: which method? *JOP.* 2004;5:253–7.
54. Horwhat JD, Paulson EK, McGrath K, Branch MS, Baillie J, Tyler D, et al. A randomized comparison of EUS-guided FNA versus CT or US-guided FNA for the evaluation of pancreatic mass lesions. *Gastrointest Endosc.* 2006;63:966–75.
55. Saif MW. Primary pancreatic lymphomas. *JOP.* 2006;7:262–73.
56. Gines A, Wiersema MJ, Clain JE, Pochron NL, Rajan E, Levy MJ. Prospective study of a Trucut needle for performing EUS-guided biopsy with EUS-guided FNA rescue. *Gastrointest Endosc.* 2005;62:597–601.
57. Gress F, Gottlieb K, Sherman S, Lehman G. Endoscopic ultrasonography-guided fine-needle aspiration biopsy of suspected pancreatic cancer. *Ann Intern Med.* 2001;134:459–64.

The Role of EUS in Cystic Lesions of the Pancreas

Mohammad Al-Haddad, MD and John DeWitt, MD

CONTENTS

INTRODUCTION
EUS VERSUS OTHER IMAGING MODALITIES IN
THE DIAGNOSIS OF CPLS
EUS-FNA OF CPLS: TECHNIQUE
EUS-GUIDED TRUCUT BIOPSIES
CYST FLUID EVALUATION
SEROUS CYSTIC NEOPLASMS
MUCINOUS CYSTIC NEOPLASMS
INTRADUCTAL PAPILLARY MUCINOUS
NEOPLASMS
OTHER RARE TYPES OF CPLS
TREATMENT OF CPLS
CONCLUSION

Abstract

Cystic pancreatic lesions (CPLs) are increasingly recognized in clinical practice. Although inflammatory cysts are most commonly encountered, mucinous CPLs are important to identify and follow due to the risk of progression to malignancy. Endoscopic ultrasound (EUS) is widely accepted as the test of choice for the diagnosis and follow-up of CPLs. Not only does EUS permit close high quality images of the cyst, but also allows for fine needle aspiration (FNA) of cyst fluid,

From: *Clinical Gastroenterology: Endoscopic Ultrasound*,
Edited by: V. M. Shami and M. Kahaleh, DOI 10.1007/978-1-60327-480-7_13,
© Springer Science+Business Media, LLC 2010

where cytological exam is performed to determine malignancy. More recently, certain tumor markers and DNA analysis of genetic markers of cyst fluid became available and could help differentiate mucinous from nonmucinous lesions. Management of CPLs takes into account the risk of malignancy and the benefit of pancreatic resection. This decision usually depends on multiple factors, including the type of cyst, presence of clinical symptoms, suspected underlying malignancy, and patient's overall health status. Recent development of minimally invasive treatment alternatives like cyst epithelium ablation with alcohol, appear safe and effective in high risk lesions although larger long-term studies are needed to demonstrate clinical utility.

Key Words: Pancreatic cysts, Mucinous cystic neoplasms of the pancreas, IPMN, Serous cystadenomas

INTRODUCTION

Cystic pancreatic lesions (CPLs) are increasingly detected due to the widespread use of cross-sectional imaging modalities like computed tomography (CT) and magnetic resonance imaging (MRI). It is estimated that up to 1.2% of the general population have pancreatic cysts based on large scale imaging observational studies (1) and up to 24% based on autopsy studies (2). While the majority of these lesions are benign, about 10–15% can be classified as cystic neoplasms and may require further evaluation, management, and follow-up (3, 4). The differential diagnosis of cystic lesions of the pancreas remains wide. Based on surgical pathology, CPLs can be classified by the type of epithelium lining the cyst. Pseudocysts are not classified as a CPL since these are nonepithelial inflammatory fluid collections that are associated with acute or chronic pancreatitis (3). Pseudocysts constitute more than 75% of pancreatic cysts that are diagnosed and are discussed in depth in another chapter of this book. The rest of CPLs are mainly cystic neoplasms that include intraductal papillary mucinous neoplasms (IPMN), serous cystadenomas (SCA), mucinous cystadenomas (MCN), mucinous cystadenocarcinomas (MCAC), solid pseudopapillary tumors (SPT), and few other rare types (5). The ability of the different cross-sectional imaging modalities to characterize these lesions is variable but remains limited. Endoscopic ultrasound (EUS) has emerged as a real-time imaging technique that provides high resolution images and morphologic details of CPLs. The combination of fine-needle aspiration cytology with other recently available diagnostic markers has further increased its diagnostic accuracy. In this chapter, we describe the role

of EUS in the diagnosis and management of CPLs and provide an overview and management alternatives of commonly encountered CPLs in clinical practice.

EUS VERSUS OTHER IMAGING MODALITIES IN THE DIAGNOSIS OF CPLS

The large number of incidental and asymptomatic CPLs noted on routine cross-sectional imaging studies challenge clinicians to identify the type of cyst, stratify the risk of malignancy and the need for surgery. Studies describing the role of noninvasive imaging like CT and MRI in the diagnosis of CPLs have been mostly small and retrospective in design. Relying on radiologic imaging characteristics alone in CPLs has been shown to be misleading, with up to 40% of serous and mucinous lesions being misdiagnosed as pseudocysts (3, 6) (Table 1). Reported overall diagnostic accuracy for these lesions has been highly variable ranging between 20 and 83% (7–9). In one study of 50 patients, three radiologists independently and prospectively interpreted CT scans in patients with a variety of CPLs with subsequent surgical pathology confirmation (10). These authors found that only 27% of SCA were correctly diagnosed when a consensus of two out of three radiologists was used for the diagnosis. In other small, retrospective studies evaluating a mixed type of CPLs, higher diagnostic accuracy was described using CT scan, and reached 82% in one study of 18 patients (11). In the same study, endoscopic retrograde pancreatography was diagnostic in only 53%. In a large multicenter French study of 398 patients with a variety of CPLs who underwent surgical resection, preoperative radiological exams were diagnostic in only 20% of SCA, 30% of MCN, and 29% of MCAC (7). The majority of misclassified CPLs were mistaken for pseudocysts (9% of MCAs and 15% of MCACs). There are few studies using head-to-head comparison of imaging modalities, such as CT and MRI, for the diagnosis of CPLs. In one small study of patients with both serous and mucinous cystadenomas (12), MRI was found to be slightly superior to CT in diagnosing cystic neoplasms, but CT scan was superior to MRI in detecting calcification within the wall and septa seen in mucinous lesions. For IPMN, MRCP has been reportedly found to be superior to ERCP for the evaluation of the morphology of side branches and associated cysts, including communication with the main pancreatic duct, but the two modalities were similar in assessing for cyst septations or nodules (13). These results were reproduced in a recent study of 18 patients with IPMN, where MRCP was found to be superior to CT in delineating pancreatic ductal anatomy and associated changes (14).

Table 1
Characteristics of cyst fluid in the main types of CPLs

<i>Lesion</i>	<i>Location</i>	<i>Fluid color</i>	<i>Viscosity</i>	<i>Cytology</i>	<i>CEA</i>	<i>CA 19-9</i>	<i>Amylase</i>
Pseudocyst	Anywhere	Dark yellow to Brown	Thin	Inflammatory cells with debris, macrophages but typically no mucin	Low to minimally increased	Variable	High
Serous cystadenoma	Body/tail > head	Colorless with blood contaminant	Thin	Usually acellular. Small glycogen staining cuboidal cells may be seen in the background	Undetectable to low	Low	Low
Mucinous cystadenoma	Body/tail > head	Colorless	Thick	May be acellular with background mucin. Mucinous epithelia cells may be seen	Moderate increase	Variable	Variable
Mucinous cystadenocarcinoma	Body/tail > head	Colorless	Thick	Malignant mucinous epithelia cells	Marked increase	High	Variable
Intraductal papillary mucinous neoplasm	Main duct or side branch, head > body and tail	Colorless	Thick	Acellular with background of mucin. Occasionally mucinous epithelial cells with papillary projections and variable atypia may be seen	Moderate increase	Variable	High

EUS permits close, high resolution imaging of CPLs morphology that may not be readily visualized by CT or MRI. Diagnostic accuracy of EUS imaging alone for detecting malignant or premalignant lesions is reportedly 82–96% (15–20). Earlier literature described several EUS features of pancreatic cysts associated with increased malignancy risk, including thick wall, protruding tumor, presence of nodule or mass and thick septations (15, 16). Subsequent studies, however, uncovered the shortcomings of relying on EUS alone in differentiating benign from malignant CPLs. For example, in one study, blinded expert endosonographers reviewed EUS videotapes of pathologically confirmed pancreatic cystic neoplasms and noted cyst features, type, and malignancy potential (18). The interobserver agreement was moderately good in detecting solid lesions but only fair for detecting pancreatic duct abnormalities, septations, and the diagnosis of neoplastic versus nonneoplastic lesions. Expert agreement on the diagnosis of SCAs was moderately good ($\kappa=0.46$) but only fair for the remainder of the lesions. The agreement on the presence or absence of solid component was moderately good ($\kappa=0.43$), and the overall accuracy rates for the diagnosis of neoplastic versus nonneoplastic lesions ranged from 40 to 93%. A large prospective multicenter US study found that the accuracy of EUS imaging features alone for the diagnosis of mucinous lesions was only 51% (20). Given the above limitations, EUS morphology alone is generally considered inadequate for further characterization of CPLs or predicting their malignancy potential.

EUS-FNA OF CPLS: TECHNIQUE

EUS-guided fine needle aspiration (EUS-FNA) has been shown to be an effective and safe sampling method of CPLs. Its safety has been confirmed by multiple studies and complication rates in recent literature were found to be around 1% or less (21–24).

EUS-FNA for CPLs is performed using the linear array echoendoscope under conscious sedation and appropriate cardiorespiratory monitoring (25). The ultrasound transducer on the distal tip of the echoendoscope permits needle advancement into the lesion under real-time guidance. A variety of commercially available FNA needles is available and range in size between 19 and 25 gauge. It is recommended that Doppler is used to examine the projected path of the needle to avoid puncturing intervening blood vessels, while trying to minimize the amount of normal pancreatic tissue that has to be traversed. Once the gastric or duodenal wall is punctured and the needle enters the cyst, the stylet is withdrawn and suction is applied. If possible, complete cyst aspiration

using only one biopsy is recommended. The needle is then withdrawn back into the sheath and assembly is removed. The material retrieved from the aspiration is then expressed on two glass slides: one slide is air-dried for immediate staining and on-site review while the other slide is alcohol-fixed for later pathologic exam. The presence of on-site cytopathology for rapid interpretation is recommended and has been shown to improve the diagnostic yield (26). The risk of infection from EUS-FNA of pancreatic cysts was initially reported to be as high as 14% in early studies (27). Therefore, it has become routine practice to administer IV antibiotics (such as a fluoroquinolone) prior to or immediately after EUS-FNA followed by oral antibiotics for 3–5 days to limit this risk. Recent studies have shown that this practice may limit this complication to less than 3% (24).

A recently developed cytobrush device (Echobrush®, Cook Medical Inc., Winston-Salem, NC) has been approved for use with a 19-gauge EUS-FNA needle. Suitable CPLs for cytobrush use include those that are at least 2 cm in diameter and located in the neck, body, or tail of the pancreas. These limitations mainly reflect the difficulty of using the relatively stiff 19-gauge needle to aspirate head and uncinata lesions. Once the needle is in the cyst, the stylet is withdrawn and the brush is advanced through the sheath under ultrasound guidance. The brush is moved back and forth several times to ensure adequate tangential contact with the cyst wall or any mural nodules. Patients on anticoagulation are usually excluded due to higher risk of bleeding shown in the pilot study (28). Prophylactic antibiotics are administered as described above.

EUS-GUIDED TRUCUT BIOPSIES

EUS-guided Trucut biopsy (EUS-TCB) permits the acquisition of a tissue fragment with preserved histologic architecture and has been shown to be safe for tissue sampling from a variety of solid organs (29, 30). The Quick-Core® (Cook Medical Inc., Winston-Salem, NC) is a commercially available TCB device that is a 19-gauge needle equipped with a spring-loaded cutting sheath and a tissue tray (29, 30). Initial human experience showed that EUS-TCB provides superior diagnostic accuracy for submucosal lesions, lymphoma, and autoimmune pancreatitis compared to standard EUS-FNA (31). The same studies suggested that the use of TCB in solid lesions of the pancreas may provide a diagnosis in fewer passes.

In CPLs, the TCB may offer a histological specimen from the wall cyst, supporting stroma, or any other solid components of the cyst. The use of EUS-TCB for CPLs was initially described by Levy et al. (32)

in ten patients and was found to be diagnostic in six patients, partially diagnostic in one and nondiagnostic in the remaining three. No complications were reported in this small study. The authors recommend its use only when the histologic findings are likely to change patient management. Until further randomized prospective trials become available, EUS-FNA remains the mainstay of sampling CPLs for cytology and obtaining tumor markers.

CYST FLUID EVALUATION

Cytology

Due to the inherent limitations of EUS morphology alone in accurately diagnosing CPLs, the use of FNA for cytology and fluid analysis of these lesions has been extensively evaluated. The specificity of EUS-FNA cytology for the diagnosis of CPLs is excellent and exceeds 90% in most published studies (19, 20, 33). On the other hand, the sensitivity of EUS-FNA remains widely variable with most studies reporting a sensitivity of <50% (19, 20, 33, 34). Brandein et al. reported EUS-FNA sensitivity, specificity, and an accuracy of 50%, 100%, and 89%, respectively, for the diagnosis of malignancy in 26 patients with different types of CPLs (33). In another report of 18 patients with surgical pathology correlation, Sedlack et al. (34) reported sensitivity, specificity, and an accuracy of 27%, 100%, and 55%, respectively; however, in this study FNA was only performed when there was diagnostic uncertainty. Frossard et al. (19) reported that EUS-FNA correctly identified 65 of 67 (97%) CPLs when a dedicated on-site pathologist reviewed all cytologic preparations. In a study of 48 patients from our institution, the sensitivity, specificity, and frequency of cases correctly identified by EUS-FNA cytology for the diagnosis of mucinous cystic neoplasms were 12.5%, 90.6%, and 64.6%, respectively (35). Finally, in a prospective, multicenter study, Brugge et al. (20) reported the results of EUS-FNA cytology and tumor markers in 112 patients who underwent surgery. This study reported a sensitivity and specificity of cytology of 35% and 83%, respectively. The sensitivity of EUS-FNA for the diagnosis of malignancy in mucinous lesions was only 22%. Possible reasons for this wide variation in the reported sensitivity of EUS-FNA cytology for the diagnosis of CPLs may include the variable use of on-site cytology interpretation and cytopathologist expertise, lesion sampling error, sporadic distribution of malignant epithelium in the cyst, presence of gastrointestinal contaminant, and variability of endosonographers' experience. In a recent pilot study,

CPLs cytobrushings were shown to be superior to standard cytology specimens obtained via FNA in seven out of ten patients (28). Recently updated data from a prospective blinded study comparing FNA to cytobrushings showed mucinous epithelium in 16 out of 22 patients compared to six out of 22 using FNA alone, including two cases of high grade dysplasia seen exclusively on cytobrushings (36).

Tumor Markers

Tumor markers in pancreatic cysts that have been evaluated in various studies include: carcinoembryonic antigen (CEA), CA19-9, CA 72-4, and CA 125. The most commonly evaluated marker is CEA, and this is generally found in high levels in mucinous lesions, but is lower in pseudocysts and nonmucinous tumors. An early study found that a CEA level less than 5 ng/mL provided 100% sensitivity and 86% specificity for distinguishing mucinous neoplasms from other cystic lesions (37). The same study demonstrated that a CA 19-9 level >50,000 U/mL had 75% sensitivity and 90% specificity for distinguishing mucinous from nonmucinous tumors. The same authors later reported that a cyst fluid CA 72-4 >40 U/mL had a 63% sensitivity and 98% specificity for distinguishing SCA from mucinous cystadenomas and cystadenocarcinoma (38). Frossard et al. reported that a CA19-9 level exceeding 50,000 U/mL had 15% sensitivity and 81% specificity in differentiating mucinous from other cystic lesions (19). The same study demonstrated a CEA level >400 ng/mL to offer sensitivity and specificity levels of 13% and 75%, respectively, to distinguish mucinous from nonmucinous cystic lesions. Sperti et al. (39) reported multiple tumor marker levels in both serum and cyst fluid in 48 patients with pancreatic cysts. Cyst fluid CA 72-4 levels were significantly higher in mucinous cystic tumors, with 95% specificity and 80% sensitivity in detecting mucinous or malignant cysts. The results of cyst fluid CEA were less accurate than CA 72-4, with a sensitivity of 38% and a specificity of 100% in detecting benign and malignant mucinous lesions. The largest prospective study to date (20) determined that a cut-off of cyst fluid CEA of 192 ng/mL provided a sensitivity of 73% and specificity of 84% for differentiating mucinous from nonmucinous CPLs in 112 patients who underwent surgery. Cyst fluid CA 19-9 level of 2,900 offered a sensitivity of 68% and specificity of 62% for differentiating mucinous from nonmucinous tumors. No other combination of factors, including cytology, morphology, and CEA levels was found to be more accurate than CEA levels alone.

Biochemical markers such as amylase and lipase may be evaluated in these patients. Amylase is usually elevated in inflammatory cysts like

pseudocysts and IPMN due to the communication with the pancreatic duct. In a pooled analysis from 12 studies, an amylase concentration <250 U/L supported a diagnosis of SCA, MCA, or MCAC (sensitivity 44%, specificity 98%) and thus virtually excluded pseudocysts (40). In the same analysis, a CEA level <5 ng/mL suggested a SCA or pseudocyst (sensitivity 50%, specificity 95%) and a CEA >800 ng/mL strongly suggested MCN (sensitivity 48%, specificity 98%). A CA 19-9 <37 U/mL strongly suggested pseudocyst or SCA (sensitivity 19%, specificity 98%).

From the above studies, we recommend the evaluation of cyst fluid from EUS-FNA for CEA, cytology, and amylase tests whenever sufficient fluid (about 1–1.5 mL) is obtained. If less fluid is obtained, cytology should always be obtained and then CEA if enough fluid remains. Other cyst fluid tumor markers such as CA 19-9 appear to offer inferior diagnostic results compared to CEA alone and their use is not currently recommended.

Genetic Markers

In recent years, there has been increased interest in identifying specific genetic markers that are associated with higher risk of malignancy in CPLs. Modeled after the adenoma-carcinoma sequence in colon cancer, IPMNs are believed to follow a similar transformation from hyperplasia to dysplasia and carcinoma (41). K-ras gene mutation has been well studied and appears to occur early in the transformation sequence (41). As with other cancers, more than one “hit” is believed to be required for the progression of precancerous cystic tumors to malignancy. In IPMN, this is reported to be a result of tumor suppressor gene inactivation, which is represented by the loss of heterozygosity at 9p12 (p16) and 17 p13 (p53) (42). Other studies have investigated the specific genetic markers of SCA and MCN. Moore et al. (43) described allelic losses on chromosome 10q in 50% of cases and on chromosome 3p in 40% of cases. No K-ras or p53 mutations were noted in any of the 21 SCA studied. Kim et al. (44) found that one-third of MCN were associated with K-ras mutations and further variable changes in tumor suppressor genes like p16 and p53, but were not observed in any SCA.

The use of the above markers has been evaluated in clinical applications. It was found that pancreatic juice contains K-ras mutations in high frequency (60%) in patients with IPMN (45, 46). Similar to pancreatic juice, PCL fluid contains DNA shed from the epithelial lining (47). Khalid et al. (48) initially reported data from 36 PCLs with confirmed

histology showing that cyst fluid examination for K-ras mutations and microsatellite allelic loss was feasible and predictive of malignancy. In a multicenter, prospective study (49), the same author evaluated the role of DNA analysis in 124 patients undergoing EUS-FNA with malignant cytology or later confirmed surgical pathology. This study found that an elevated quantity of good quality DNA and high amplitude mutations were associated with malignant cystic neoplasms. Very high amounts of mutated DNA and mutational sequence of K-ras followed by allelic loss was very specific for malignant cysts. High amplitude and K-ras mutations were very specific for mucinous cysts. Recent data in abstract form compared the accuracy of CEA to DNA analysis in 100 patients with CPLs and found only fair agreement between those two methods. CEA alone had the highest sensitivity (82%) compared to 11% for K-ras mutation and 70% for allelic imbalance (50). The CEA and DNA analyses in this study were complementary and together identified all mucinous cysts included. A commercially available genetic test (RedPath® IP, Pittsburgh, PA) is available to identify the above genetic markers in free floating DNA which may help to provide additional information of CPLs and stratify their risk of malignancy. The role of cyst fluid DNA analysis in clinical practice, however, remains to be determined.

In the next part of the chapter, we will be discussing the common types of CPLs individually while focusing on the EUS features, cytology, and tumor markers' characteristics.

SEROUS CYSTIC NEOPLASMS

SCAs are most commonly seen in females in the seventh decade of life and are typically asymptomatic. They may be found incidentally on imaging studies performed for other reasons or may become manifested if the lesion compresses adjacent structures such as the gastrointestinal tract. Although most reports indicate a preponderance to occur in the body and tail (51), some authors report a higher incidence in the head and neck (52). The conventional endosonographic appearance of a microcystic SCA is a well-delineated lesion with multiple, small fluid filled cavities (typically less than 5 mm in size) with thin septa (Fig. 1). A central scar (usually referred to as sunburst calcification but could be only fibrosis) may be present in up to one quarter of the cases (Fig. 2) (53). The presence of any intramural nodules, cyst wall thickening, floating debris or mucin or associated pancreatic ductal dilation is unusual and could indicate an underlying mucinous lesion (16, 54).

The diagnostic yield of EUS-FNA for SCA is usually poor due to the small size of the cystic compartments and the relatively vascular intercystic

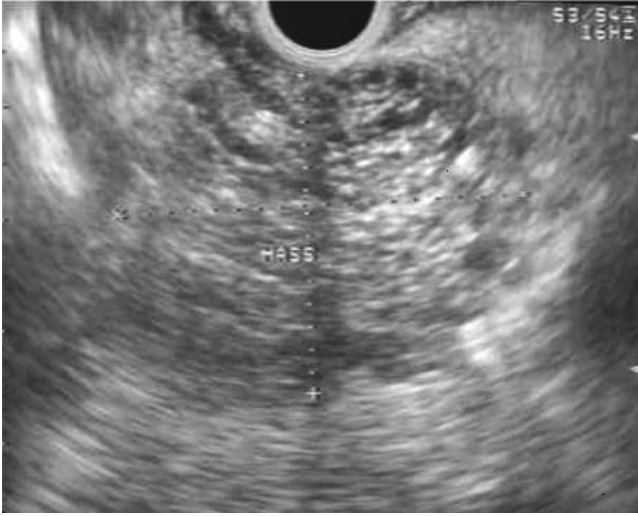


Fig. 1. Characteristic endoscopic ultrasound appearance of a microcystic serous cystadenoma in the head of the pancreas in an asymptomatic 65-year-old female patient. The lesion contains multiple small cysts separated by thin septa.

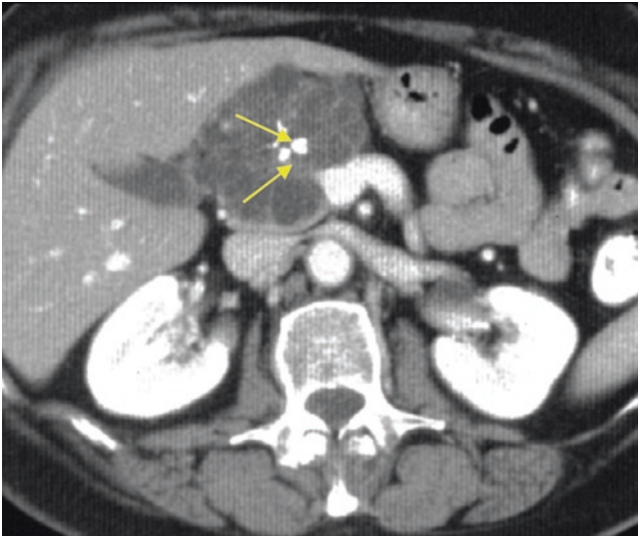


Fig. 2. CT scan of the abdomen of an incidentally detected serous cystadenoma. Central calcifications (arrows) and lobulated multicystic appearance are typical CT findings.

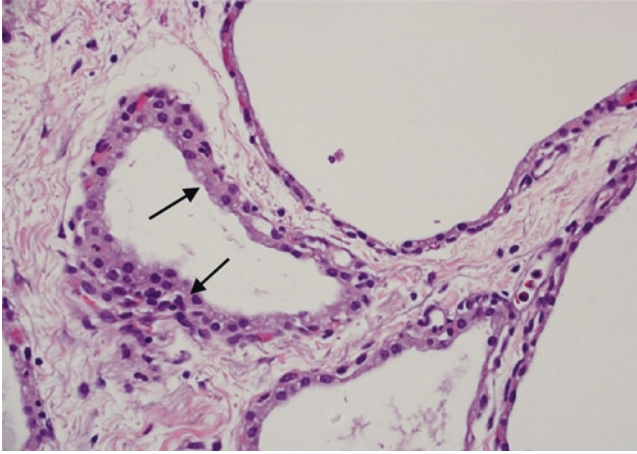


Fig. 3. Histopathology of serous cystadenoma. Cuboidal epithelial cells (arrows) are seen to line small cystic spaces. (H&E, $\times 400$).

septa. Due to the distinctive endosonographic appearance of microcystic SCA, cyst sampling is generally not needed. If necessary, EUS-FNA of SCA should target the larger cystic compartments for fluid analysis. Fluid obtained is often thin, nonviscous and is colorless. Cellularity is usually very low, and if any, cuboidal epithelial cells have been described on aspirate that stain positive for glycogen but not mucin (Fig. 3) (55). CEA levels are usually low (less than 20 ng/mL) (56). The macrocystic variant of SCA cannot be distinguished morphologically from mucinous cystic lesions, and therefore FNA of these lesions is recommended. Generally, clinical observation alone is sufficient for SCA as these cystic lesions seldom undergo malignant transformation (57). Surgery is recommended for larger symptomatic cysts or when there is uncertainty about the diagnosis.

MUCINOUS CYSTIC NEOPLASMS

MCNs include mucinous cystadenomas and carcinomas. These tumors are usually associated with extracellular mucin production with variable degrees of atypia. Females are often more affected than males, particularly in their fifth and sixth decade (58, 59), and the lesions most commonly occur in the pancreatic body and tail. The specific histopathology hallmark of these tumors is the presence of ovarian stroma and is required to differentiate this from IPMN (60). MCNs are premalignant lesions but the risk of malignant degeneration is likely less than that

of IPMN (60). MCNs can be completely asymptomatic when incidentally noted on imaging studies, but can also be present with obstructive symptoms due to large size, or weight loss and jaundice. When jaundice is present, the suspicion of malignant transformation is raised. Main pancreatic duct communication is rarely present with MCN.

The morphology of MCN on EUS can be variable but are commonly associated with a visible wall and septations of variable thickness (Fig. 4). Peripheral calcifications can be seen in up to 15% of cases (Figs. 5 and 6) (58). The presence of thick or irregular cyst wall, intramural nodules or solid components and larger size have been associated with malignancy (16). EUS-FNA is advised for confirmation of all suspected MCN. Cytology may reveal columnar epithelial cells in up to half of the patients associated with mucin (Fig. 7) (40, 61). Mucin identified cytologically by EUS-FNA can be difficult to differentiate from gastric contaminant mucinous epithelium, therefore we recommend cyst aspiration from the duodenum whenever feasible. Cyst fluid from MCNs is typically clear but is often viscous with relatively elevated CEA levels and low amylase. The risk of malignancy in these tumors described in a recent series of 163 patients was found to be 17.5% (5.5% with carcinoma in situ and 12% with invasive cancer) (62).

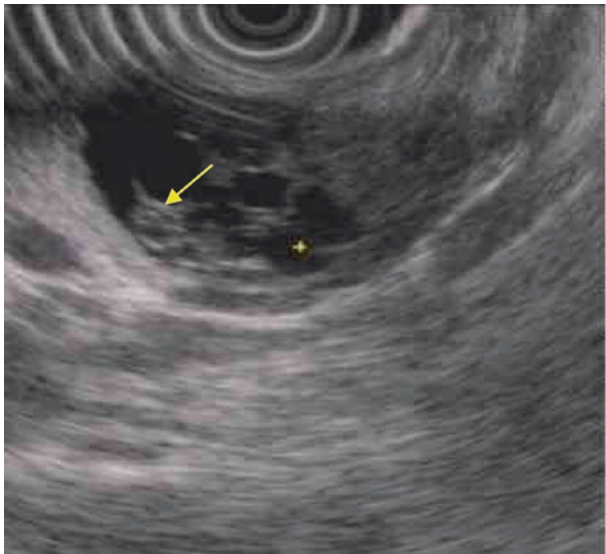


Fig. 4. EUS findings in a middle age female patient with a mucinous cystic neoplasm in the body of the pancreas. A cyst wall is present and few intracystic nodules arising from the wall (arrow) could represent a solid lesion or mucous.

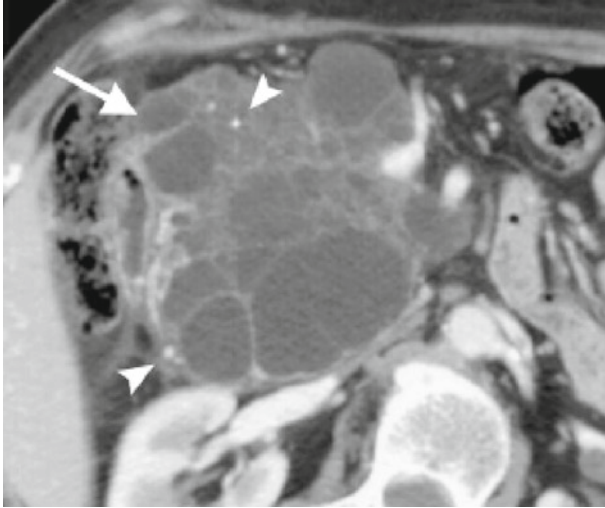


Fig. 5. CT scan findings of a patient with mucinous cystic neoplasm. Multiple cystic spaces with variable thickness septations are apparent (arrow) and generally considered a risk of malignancy. Peripheral calcifications (arrowheads) within the septa are noted in up to 15% of patients.

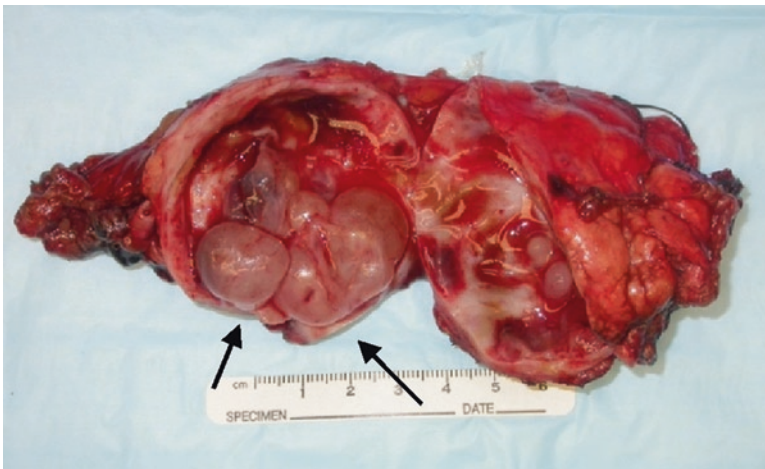


Fig. 6. Gross surgical specimen in a patient with mucinous cystic neoplasm. Multiple cystic compartments filled with mucin (arrows) are noted. No malignancy was detected in this specimen.

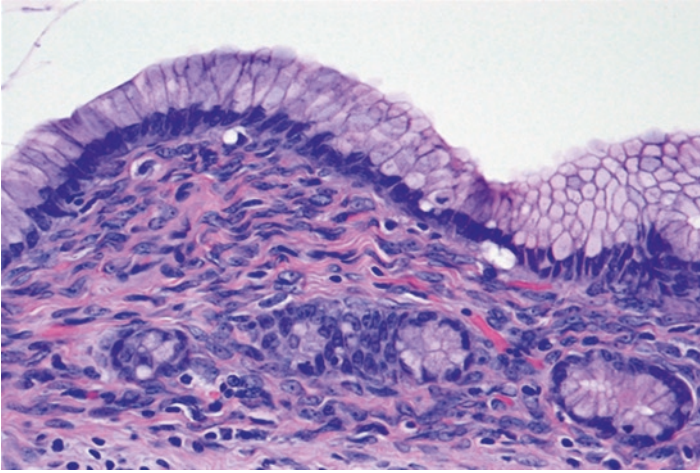


Fig. 7. Photomicrograph of a mucinous cystadenoma (H&E, $\times 400$). Columnar mucinous epithelial cells are seen overly ovarian stroma. Ovarian stroma is the pathological hallmark of these tumors.

Therefore, surgical resection is recommended whenever feasible. The prognosis after surgery for MCN that have not undergone malignant transformation is excellent and the 5 year survival for mucinous cystadenocarcinomas postresection exceeds 60% (7, 53).

INTRADUCTAL PAPILLARY MUCINOUS NEOPLASMS

IPMN are premalignant mucinous cystic lesions that arise from the main pancreatic duct, side branch or both and are associated with ductal ectasia, intraductal papillary growth, and mucin production (63). IPMN is most prevalent in the sixth to seventh decade of life and affects males and females equally (64).

The main duct IPMN is typically easy to differentiate in EUS (Fig. 8) and ERCP (Fig. 9) due to the diffuse dilation of the pancreatic duct (Fig. 10), mural tumor growth and occasionally intraductal filling defects due to mucin production. EUS imaging of branched duct IPMN usually demonstrates visible communication of the cyst with the main pancreatic duct. However, in the absence of duct communication, branched duct IPMN may be morphologically indistinguishable from MCNs. Any visible mucin extruding from a patulous papilla supports the diagnosis and the classic “fish mouth deformity” is considered diagnostic. During EUS, any intraductal mass, mural nodule or projections

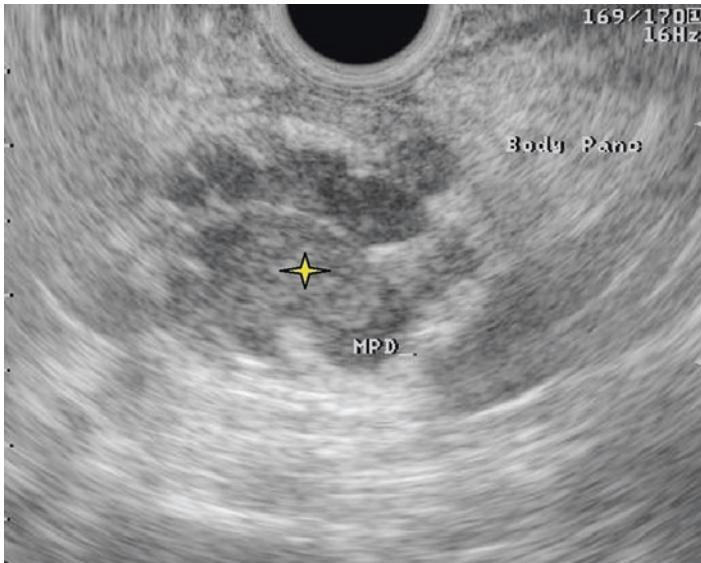


Fig. 8. Intraductal papillary mucinous neoplasm affecting the main pancreatic duct and side branches in a male patient with acute recurrent pancreatitis. EUS showed a dilated pancreatic duct within the body of the pancreas (star) with intraductal tumor growth. (MPD main pancreatic duct).

noted within the main duct or off a cyst wall should be the target of FNA. If no visible lesions are noted, the main duct or branch can be punctured for cytology and tumor markers. Cytology usually reveals thick mucin but may be thin and completely acellular (65). Occasionally, fragments of papillary mucinous epithelium can be seen on FNA (Fig. 11) or cytobrushings. Cyst fluid resembles that obtained from MCN with a relatively elevated CEA; however, amylase tends to be higher due to the ductal communication.

The risk of malignancy within IPMN is well described in the literature, although most of the earlier studies included mixed populations with both side branch and main duct IPMN. The risk of malignancy in the main duct type has been reported to range from 57% to 92% (66–70), and therefore surgery is recommended for these patients. The natural history of the side branch type remains less established. An adenoma to carcinoma sequence is believed to account for the slow growth of these tumors and the lag time observed between the detection of these lesions and the development of invasive cancer (64). Risk factors associated with invasive cancer have been described and include older age, presence of symptoms such as jaundice and weight loss, intramural nodules, and



Fig. 9. ERCP appearance of a dilated main pancreatic duct in a patient with main duct IPMN. Filling defects are seen consistent with mucin.

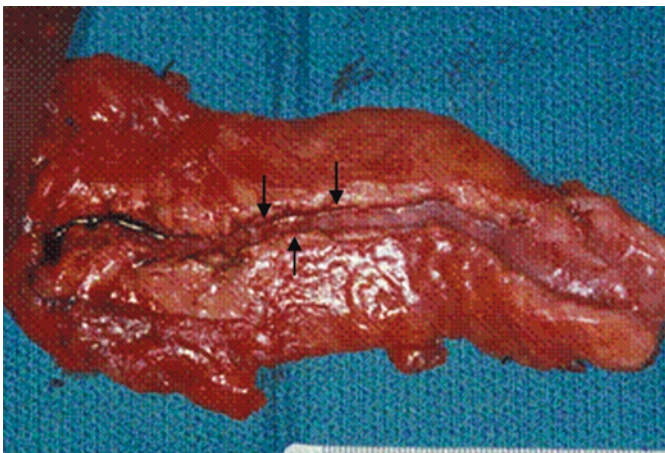


Fig. 10. Longitudinal section of a pancreas resection specimen demonstrating the diffuse dilation of the main pancreatic duct (arrows) in a patient with intraductal papillary mucinous neoplasm.

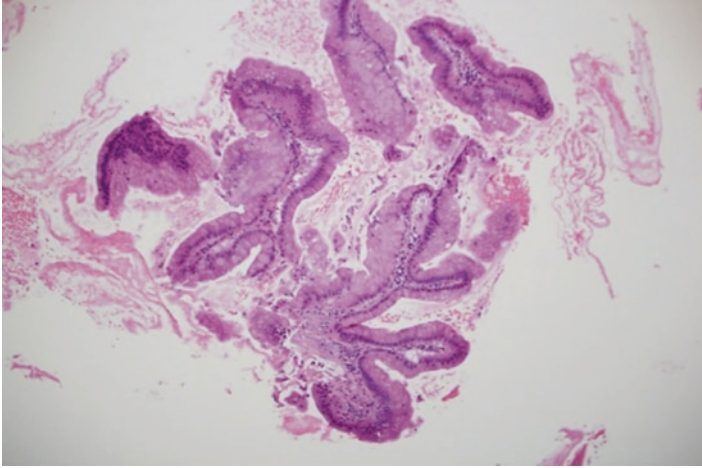


Fig. 11. Fine needle aspiration cytology smear (H&E, $\times 4$) in a patient with a side branch intraductal papillary mucinous neoplasm. A small fragment of papillary mucinous epithelium is occasionally noted and was diagnostic in this case.

progressive dilation of the main duct. Unfortunately, a major limitation of EUS-FNA in detecting invasive malignancy preoperatively is its low sensitivity, which has been reported to be as low as 44% in two studies (40, 71). In one study by our group, Pais et al. (72) reported an EUS sensitivity as high as 75% in detecting malignancy within IPMN; however, three quarters of the patients with malignancy had an associated solid mass. This same study reported that CEA levels from IPMN could not reliably distinguish benign from invasive IPMN. Another study (73) showed that the combination of EUS and ERCP cytology samples had a 91% sensitivity for invasive IPMN carcinoma but only 40% for minimally invasive disease like carcinoma in situ/high grade dysplasia. Recently, few studies have described the role of intraductal ultrasonography (IDUS) in the diagnosis of IPMN. Hara et al. (74) reported IDUS sensitivity, specificity, and an accuracy of 68%, 89%, and 78%, respectively, for lesions protruding 4 mm or more within the duct. However, there was no statistically significant difference between carcinoma in situ and invasive carcinoma, and a differential diagnosis was not possible based on IDUS findings alone.

This inability to reliably diagnose IPMN with variable degrees of dysplasia preoperatively appears to have a higher significance in small lesions (<3 cm in size) where the general recommendations have been

to observe. In a recent study of 147 patients with only branched IPMN, the malignancy rate was 12% in patients who underwent surgical resection (75). In this same study, cyst size (>3 cm) and the presence of pancreas-related symptoms had no effect on the risk of malignancy. Two other studies have shown that the risk of malignancy in side branch lesions is 6% and 46%, respectively (67, 68) and that invasive cancer can be detected in lesions <3 cm in size (76–78).

OTHER RARE TYPES OF CPLS

Solid pseudopapillary tumors (PST) are rare neoplasms of the pancreas that affect mainly young females. Small lesions may be diagnosed incidentally while asymptomatic (Fig. 12) but could enlarge and present with symptoms due to mass effect (79–83). EUS may show a purely solid (Fig. 13) or a mixed solid and cystic mass. FNA usually shows branching papillae with myxoid stroma which is best seen on cell block slides (Fig. 14). A recent multicenter study reported that EUS-FNA with or without immunochemistry preoperatively diagnosed 75% of 28 patients (83). On immunohistochemistry, the tumor cells typically react to Vimentin and cellblock preparation is recommended when the diagnosis

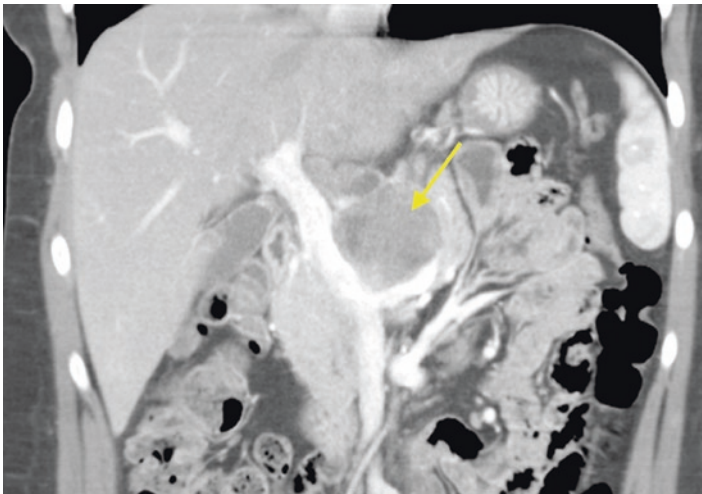


Fig. 12. CT scan of the abdomen demonstrating a solid pseudopapillary tumor in a young female patient slightly compressing the portal venous confluence under the neck and body of the pancreas.

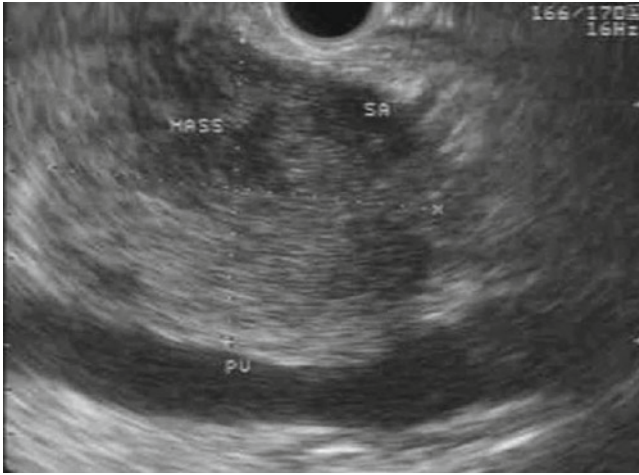


Fig. 13. EUS appearance of the solid pseudopapillary tumor in the same patient. The tumor is seen to abut the portal vein (PV) and encase the splenic artery (SA).

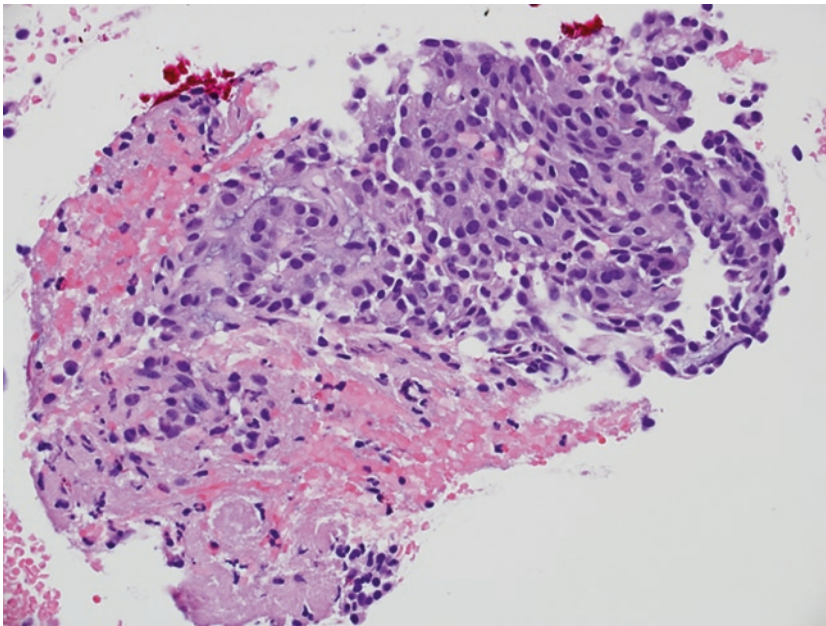


Fig. 14. Core biopsy histology of a pseudopapillary tumor. Myxoid stroma and branching papillae are seen. (H&E, $\times 400$).

is considered. The overall prognosis after surgical resection is excellent and is generally recommended due to the risk of malignant transformation (up to 15%) and the relatively young age of the patients. Metastatic disease is rarely seen and prognosis remains good after surgical resection of metastatic lesions (84).

Approximately 10% of all pancreatic neuroendocrine tumors of the pancreas have a cystic component (85). Lesions vary in size and morphology, and therefore FNA is recommended. Cytology shows a small homogenous small cell population with round nuclei that should stain positive for chromogranin and synaptophysin. Routine cell block preparation is therefore recommended in these patients. Other rare CPLs include metastatic lesions (from renal cell carcinoma or melanoma), (86) teratomas, choriocarcinomas, teratomas, lymphoepithelial cysts (87), and lymphoceles (88).

TREATMENT OF CPLS

Expectant Management

Recent literature supports expectant observation in low risk PCLs with benign EUS features, negative FNA and, low tumor markers. In a study of 539 patients with various CPLs, the risk of progression to malignancy among those lesions <3 cm in size without a solid component was found to be 3% (89), which is similar to the mortality associated with surgical resection of the pancreas. Recently, published practice guidelines (90) take into consideration this balance between the risk of malignancy and the benefit of pancreatic resection. The proposed approach incorporates the information obtained from cross-sectional imaging, EUS, and cyst fluid analysis to differentiate mucinous (pre-malignant) and nonmucinous cystic lesions.

Practically, the decision to follow rather than resect a PCL is a clinical judgment and is based on consideration of the patient age, comorbidities, and an estimation of the cancer risk in the lesion. CT scan, MRI and MRCP are generally considered safe and reliable in providing follow-up data on cyst and pancreatic duct size, but are less sensitive in detecting intramural nodules, which are better evaluated by the use of EUS-FNA (89, 91). Therefore, an EUS-based algorithm is recommended for the initial evaluation and follow-up of PCLs of indeterminate behavior (92). However, in studies evaluating the outcome of conservatively managed IPMNs, for example, lack of long-term follow-up remains a major limitation, with median follow-up of 10–45 months reported (68, 75).

Surgical Management

The mainstay of treatment of malignant and premalignant PCLs remains surgical resection. Recently, reported surgical mortality rates associated with pancreatic surgery have decreased compared to earlier studies, and currently is under 3% at referral centers (93, 94). Morbidity from surgical resection, however, remains over 20% in most series. In one high-volume surgical center, the rate of complications following pancreatic cyst surgery in a group of 170 patients was 22% with a mortality rate of 0.6% (89). In the recent years, enucleation has emerged as a less invasive alternative, with reduced operative times and blood loss without increasing postoperative morbidity (95, 96). However, this approach remains limited to certain tertiary care centers and to a selective population of patients.

Alternate Nonsurgical Management and Future Developments

Alternative nonoperative therapies for CPLs have been described in the recent years. In a pilot study of 25 patients, Gan et al. (97) reported their experience using incrementally increasing concentrations of ethanol injection into CPLs. No complications were reported with this technique. Twenty three patients underwent follow-up with either surgical resection (five patients) or repeat imaging. Eight out of 23 patients had complete resolution of the cysts on radiology studies. Variable degrees of cyst epithelial ablation were reported in the five surgical cases. Subsequently, a multicenter randomized double-blinded study of 39 patients (98) with suspected mucinous or nonmucinous CPLs and pseudocysts were randomized to lavage with ethanol (23 patients) or saline (16 patients). This study found that ethanol lavage led to a statistically significant decrease in cyst surface area compared to saline lavage. Surgical pathology in three patients who underwent surgical resection following ethanol lavage demonstrated 50–100% ablation of the cyst lining. Overall 33% of patients in this series had complete cyst resolution by follow-up imaging. Two patients developed acute pancreatitis (overall 4% incidence) following ethanol lavage. The authors concluded that ethanol lavage could be a safe and effective method to ablate CPLs. Other lavage agents have been reported in renal and thyroid cystic lesions like acetic acid (99) and polydocanol (100), but no trials have been reported to date on use in CPLs.

Oh and his coworkers described the use of paclitaxel after ethanol for injecting ten patients presumed CPLs that do not communicate with the pancreatic duct (101). After a median follow-up of 6 months,

imaging showed complete resolution of cysts in six patients, partial resolution in three and no change in one. However, none of the patients underwent surgical resection to confirm the ablation. One patient was hospitalized with focal pancreatitis, and one had vague but transient abdominal pain.

CONCLUSION

CPLs are being increasingly recognized in symptomatic and asymptomatic patient populations. Diagnosis and management of such lesions should involve a multidisciplinary approach with gastroenterologists, radiologists, and surgeons. Utilization of cyst morphology by cross-sectional imaging studies or EUS alone cannot reliably differentiate benign from malignant cysts. Therefore, we recommend the routine use of EUS-FNA in the management of CPLs. Cytology, tumor markers, including CEA and DNA analysis can further characterize these lesions and increase the diagnostic accuracy of mucinous and malignant cysts. Recent advances in EUS for cyst epithelium ablation are a promising minimally invasive alternative treatment of high risk lesions.

REFERENCES

1. Spinelli KS, Fromwiller TE, Daniel RA, Kiely JM, Nakeeb A, Komorowski RA, et al. Cystic pancreatic neoplasms: observe or operate. *Ann Surg.* 2004;239:651–7. discussion 657–9.
2. Kimura W, Nagai H, Kuroda A, Muto T, Esaki Y. Analysis of small cystic lesions of the pancreas. *Int J Pancreatol.* 1995;18:197–206.
3. Warshaw AL, Rutledge PL. Cystic tumors mistaken for pancreatic pseudocysts. *Ann Surg.* 1987;205:393–8.
4. Brugge WR, Lauwers GY, Sahani D, Fernandez-del Castillo C, Warshaw AL. Cystic neoplasms of the pancreas. *N Engl J Med.* 2004;351:1218–26.
5. Kloppel G, Luttges J. WHO-classification 2000: exocrine pancreatic tumors. *Verh Dtsch Ges Pathol.* 2001;85:219–28.
6. Mathieu D, Guigui B, Valette PJ, Dao TH, Bruneton JN, Bruel JM, et al. Pancreatic cystic neoplasms. *Radiol Clin North Am.* 1989;27:163–76.
7. Le Borgne J, de Calan L, Partensky C. Cystadenomas and cystadenocarcinomas of the pancreas: a multiinstitutional retrospective study of 398 cases. French Surgical Association. *Ann Surg.* 1999;230:152–61.
8. Procacci C, Biasutti C, Carbognin G, Accordini S, Bicego E, Guarise A, et al. Characterization of cystic tumors of the pancreas: CT accuracy. *J Comput Assist Tomogr.* 1999;23:906–12.
9. Bassi C, Salvia R, Molinari E, Biasutti C, Falconi M, Pederzoli P. Management of 100 consecutive cases of pancreatic serous cystadenoma: wait for symptoms and see at imaging or vice versa? *World J Surg.* 2003;27:319–23.

10. Curry CA, Eng J, Horton KM, Urban B, Siegelman S, Kuszyk BS, et al. CT of primary cystic pancreatic neoplasms: can CT be used for patient triage and treatment? *AJR Am J Roentgenol.* 2000;175:99–103.
11. Kehagias D, Smyrniotis V, Kalovidouris A, Gouliamos A, Kostopanagiotou E, Vassiliou J, et al. Cystic tumors of the pancreas: preoperative imaging, diagnosis, and treatment. *Int Surg.* 2002;87:171–4.
12. Minami M, Itai Y, Ohtomo K, Yoshida H, Yoshikawa K, Iio M. Cystic neoplasms of the pancreas: comparison of MR imaging with CT. *Radiology.* 1989;171:53–6.
13. Koito K, Namieno T, Ichimura T, Yama N, Hareyama M, Morita K, et al. Mucin-producing pancreatic tumors: comparison of MR cholangiopancreatography with endoscopic retrograde cholangiopancreatography. *Radiology.* 1998;208:231–7.
14. Waters JA, Schmidt CM, Pinchot JW, White PB, Cummings OW, Pitt HA, et al. CT vs MRCP: optimal classification of IPMN type and extent. *J Gastrointest Surg.* 2008;12:101–9.
15. Koito K, Namieno T, Nagakawa T, Shyonai T, Hirokawa N, Morita K. Solitary cystic tumor of the pancreas: EUS-pathologic correlation. *Gastrointest Endosc.* 1997;45:268–76.
16. Gress F, Gottlieb K, Cummings O, Sherman S, Lehman G. Endoscopic ultrasound characteristics of mucinous cystic neoplasms of the pancreas. *Am J Gastroenterol.* 2000;95:961–5.
17. Ahmad NA, Kochman ML, Lewis JD, Ginsberg GG. Can EUS alone differentiate between malignant and benign cystic lesions of the pancreas? *Am J Gastroenterol.* 2001;96:3295–300.
18. Ahmad NA, Kochman ML, Brensinger C, Brugge WR, Faigel DO, Gress FG, et al. Interobserver agreement among endosonographers for the diagnosis of neoplastic versus non-neoplastic pancreatic cystic lesions. *Gastrointest Endosc.* 2003;58:59–64.
19. Frossard JL, Amouyal P, Amouyal G, Palazzo L, Amaris J, Soldan M, et al. Performance of endosonography-guided fine needle aspiration and biopsy in the diagnosis of pancreatic cystic lesions. *Am J Gastroenterol.* 2003;98:1516–24.
20. Brugge WR, Lewandrowski K, Lee-Lewandrowski E, Centeno BA, Szydlowski T, Regan S, et al. Diagnosis of pancreatic cystic neoplasms: a report of the cooperative pancreatic cyst study. *Gastroenterology.* 2004;126:1330–6.
21. Al-Haddad M, Wallace MB, Woodward TA, Gross SA, Hodgins CM, Toton RD, et al. The safety of fine-needle aspiration guided by endoscopic ultrasound: a prospective study. *Endoscopy.* 2008;40:204–8.
22. Giovannini M, Seitz JF, Monges G, Perrier H, Rabbia I. Fine-needle aspiration cytology guided by endoscopic ultrasonography: results in 141 patients. *Endoscopy.* 1995;27:171–7.
23. Wiersema MJ, Kochman ML, Cramer HM, Tao LC, Wiersema LM. Endosonography-guided real-time fine-needle aspiration biopsy. *Gastrointest Endosc.* 1994;40:700–7.
24. Lee LS, Saltzman JR, Bounds BC, Poneris JM, Brugge WR, Thompson CC. EUS-guided fine needle aspiration of pancreatic cysts: a retrospective analysis of complications and their predictors. *Clin Gastroenterol Hepatol.* 2005;3:231–6.
25. DeWitt J. EUS-FNA of cystic pancreatic tumors. *Tech Gastrointest Endosc.* 2005;7:181–7.

26. Klapman JB, Logrono R, Dye CE, Waxman I. Clinical impact of on-site cytopathology interpretation on endoscopic ultrasound-guided fine needle aspiration. *Am J Gastroenterol.* 2003;98:1289–94.
27. Wiersema MJ, Vilmann P, Giovannini M, Chang KJ, Wiersema LM. Endosonography-guided fine-needle aspiration biopsy: diagnostic accuracy and complication assessment. *Gastroenterology.* 1997;112:1087–95.
28. Al-Haddad M, Raimondo M, Woodward T, Krishna M, Pungpapong S, Noh K, et al. Safety and efficacy of cytology brushings versus standard FNA in evaluating cystic lesions of the pancreas: a pilot study. *Gastrointest Endosc.* 2007; 65:894–8.
29. Levy MJ, Jondal ML, Clain J, Wiersema MJ. Preliminary experience with an EUS-guided trucut biopsy needle compared with EUS-guided FNA. *Gastrointest Endosc.* 2003;57:101–6.
30. Wiersema MJ, Levy MJ, Harewood GC, Vazquez-Sequeiros E, Jondal ML, Wiersema LM. Initial experience with EUS-guided trucut needle biopsies of perigastric organs. *Gastrointest Endosc.* 2002;56:275–8.
31. Levy MJ, Reddy RP, Wiersema MJ, Smyrk TC, Clain JE, Harewood GC, et al. EUS-guided trucut biopsy in establishing autoimmune pancreatitis as the cause of obstructive jaundice. *Gastrointest Endosc.* 2005;61:467–72.
32. Levy MJ, Smyrk TC, Reddy RP, Clain JE, Harewood GC, Kendrick ML, et al. Endoscopic ultrasound-guided trucut biopsy of the cyst wall for diagnosing cystic pancreatic tumors. *Clin Gastroenterol Hepatol.* 2005;3:974–9.
33. Brandwein SL, Farrell JJ, Centeno BA, Brugge WR. Detection and tumor staging of malignancy in cystic, intraductal, and solid tumors of the pancreas by EUS. *Gastrointest Endosc.* 2001;53:722–7.
34. Sedlack R, Affi A, Vazquez-Sequeiros E, Norton ID, Clain JE, Wiersema MJ. Utility of EUS in the evaluation of cystic pancreatic lesions. *Gastrointest Endosc.* 2002;56:543–7.
35. Attasaranya S, Pais S, LeBlanc J, McHenry L, Sherman S, DeWitt JM. Endoscopic ultrasound-guided fine needle aspiration and cyst fluid analysis for pancreatic cysts. *JOP.* 2007;8:553–63.
36. Gill KR, Al-Haddad M, Krishna M, Gross SA, Jamil LH, Woodward TA, et al. Cytologic evaluation of cystic pancreatic lesions (CPL): comparison of echobrush vs. standard EUS-FNA techniques in a blinded prospective study. *Gastrointest Endosc.* 2008;67:AB97.
37. Hammel P, Levy P, Voitot H, Levy M, Vilgrain V, Zins M, et al. Preoperative cyst fluid analysis is useful for the differential diagnosis of cystic lesions of the pancreas. *Gastroenterology.* 1995;108:1230–5.
38. Hammel P, Voitot H, Vilgrain V, Levy P, Ruzsniwski P, Bernades P. Diagnostic value of CA 72-4 and carcinoembryonic antigen determination in the fluid of pancreatic cystic lesions. *Eur J Gastroenterol Hepatol.* 1998;10:345–8.
39. Sperti C, Pasquali C, Guolo P, Polverosi R, Liessi G, Pedrazzoli S. Serum tumor markers and cyst fluid analysis are useful for the diagnosis of pancreatic cystic tumors. *Cancer.* 1996;78:237–43.
40. van der Waaij LA, van Dullemen HM, Porte RJ. Cyst fluid analysis in the differential diagnosis of pancreatic cystic lesions: a pooled analysis. *Gastrointest Endosc.* 2005;62:383–9.

41. Gerdes B, Wild A, Wittenberg J, Barth P, Ramaswamy A, Kersting M, et al. Tumor-suppressing pathways in cystic pancreatic tumors. *Pancreas*. 2003; 26:42–8.
42. Wada K, Takada T, Yasuda H, Amano H, Yoshida M, Sugimoto M, et al. Does “clonal progression” relate to the development of intraductal papillary mucinous tumors of the pancreas? *J Gastrointest Surg*. 2004;8:289–96.
43. Moore PS, Zamboni G, Brighenti A, Lissandrini D, Antonello D, Capelli P, et al. Molecular characterization of pancreatic serous microcystic adenomas: evidence for a tumor suppressor gene on chromosome 10q. *Am J Pathol*. 2001; 158:317–21.
44. Kim SG, Wu TT, Lee JH, Yun YK, Issa JP, Hamilton SR, et al. Comparison of epigenetic and genetic alterations in mucinous cystic neoplasm and serous microcystic adenoma of pancreas. *Mod Pathol*. 2003;16:1086–94.
45. Berthelemy P, Bouisson M, Escourrou J, Vaysse N, Rumeau JL, Pradayrol L. Identification of K-ras mutations in pancreatic juice in the early diagnosis of pancreatic cancer. *Ann Intern Med*. 1995;123:188–91.
46. Tada M, Teratani T, Komatsu Y, Kawabe T, Shiratori Y, Omata M. Quantitative analysis of ras gene mutation in pancreatic juice for diagnosis of pancreatic adenocarcinoma. *Dig Dis Sci*. 1998;43:15–20.
47. Tateishi K, Tada M, Yamagata M, Isayama H, Komatsu Y, Kawabe T, et al. High proportion of mutant K-ras gene in pancreatic juice of patients with pancreatic cystic lesions. *Gut*. 1999;45:737–40.
48. Khalid A, McGrath KM, Zahid M, Wilson M, Brody D, Swalsky P, et al. The role of pancreatic cyst fluid molecular analysis in predicting cyst pathology. *Clin Gastroenterol Hepatol*. 2005;3:967–73.
49. Khalid A, Finkelstein S, McGrath K. Molecular diagnosis of solid and cystic lesions of the pancreas. *Clin Lab Med*. 2005;25:101–16.
50. Sawhney M, Devarajan S, O’Farrell R, Cury M, Rabi Kundu R, Girish Anand G, et al. Comparison of CEA and DNA analysis in 100 consecutive patients with pancreatic cysts. *Gastrointest Endosc*. 2008;67:AB209.
51. Pyke CM, van Heerden JA, Colby TV, Sarr MG, Weaver AL. The spectrum of serous cystadenoma of the pancreas. Clinical, pathologic, and surgical aspects. *Ann Surg*. 1992;215:132–9.
52. Sarr MG, Kendrick ML, Nagorney DM, Thompson GB, Farley DR, Farnell MB. Cystic neoplasms of the pancreas: benign to malignant epithelial neoplasms. *Surg Clin North Am*. 2001;81:497–509.
53. Warshaw AL, Compton CC, Lewandrowski K, Cardenosa G, Mueller PR. Cystic tumors of the pancreas. New clinical, radiologic, and pathologic observations in 67 patients. *Ann Surg*. 1990;212:432–43. discussion 444–5.
54. Song MH, Lee SK, Kim MH, Lee HJ, Kim KP, Kim HJ, et al. EUS in the evaluation of pancreatic cystic lesions. *Gastrointest Endosc*. 2003;57:891–6.
55. Carlson SK, Johnson CD, Brandt KR, Batts KP, Salomao DR. Pancreatic cystic neoplasms: the role and sensitivity of needle aspiration and biopsy. *Abdom Imaging*. 1998;23:387–93.
56. Centeno BA, Lewandrowski KB, Warshaw AL, Compton CC, Southern JF. Cyst fluid cytologic analysis in the differential diagnosis of pancreatic cystic lesions. *Am J Clin Pathol*. 1994;101:483–7.

57. Matsumoto T, Hirano S, Yada K, Shibata K, Sasaki A, Kamimura T, et al. Malignant serous cystic neoplasm of the pancreas: report of a case and review of the literature. *J Clin Gastroenterol.* 2005;39:253–6.
58. Sarr MG, Carpenter HA, Prabhakar LP, Orchard TF, Hughes S, van Heerden JA, et al. Clinical and pathologic correlation of 84 mucinous cystic neoplasms of the pancreas: can one reliably differentiate benign from malignant (or premalignant) neoplasms? *Ann Surg.* 2000;231:205–12.
59. Zamboni G, Scarpa A, Bogina G, Iacono C, Bassi C, Talamini G, et al. Mucinous cystic tumors of the pancreas: clinicopathological features, prognosis, and relationship to other mucinous cystic tumors. *Am J Surg Pathol.* 1999; 23:410–22.
60. Reddy RP, Smyrk TC, Zapiach M, Levy MJ, Pearson RK, Clain JE, et al. Pancreatic mucinous cystic neoplasm defined by ovarian stroma: demographics, clinical features, and prevalence of cancer. *Clin Gastroenterol Hepatol.* 2004;2:1026–31.
61. Sperti C, Pasquali C, Pedrazzoli S, Guolo P, Liessi G. Expression of mucin-like carcinoma-associated antigen in the cyst fluid differentiates mucinous from nonmucinous pancreatic cysts. *Am J Gastroenterol.* 1997;92:672–5.
62. Crippa S, Salvia R, Warshaw AL, Dominguez I, Bassi C, Falconi M, et al. Mucinous cystic neoplasm of the pancreas is not an aggressive entity: lessons from 163 resected patients. *Ann Surg.* 2008;247:571–9.
63. D'Angelica M, Brennan MF, Suriawinata AA, Klimstra D, Conlon KC. Intraductal papillary mucinous neoplasms of the pancreas: an analysis of clinicopathologic features and outcome. *Ann Surg.* 2004;239:400–8.
64. Sohn TA, Yeo CJ, Cameron JL, Hruban RH, Fukushima N, Campbell KA, et al. Intraductal papillary mucinous neoplasms of the pancreas: an updated experience. *Ann Surg.* 2004;239:788–97. discussion 797–9.
65. Stelow EB, Stanley MW, Bardales RH, Mallery S, Lai R, Linzie BM, et al. Intraductal papillary-mucinous neoplasm of the pancreas. The findings and limitations of cytologic samples obtained by endoscopic ultrasound-guided fine-needle aspiration. *Am J Clin Pathol.* 2003;120:398–404.
66. Kobari M, Egawa S, Shibuya K, Shimamura H, Sunamura M, Takeda K, et al. Intraductal papillary mucinous tumors of the pancreas comprise 2 clinical subtypes: differences in clinical characteristics and surgical management. *Arch Surg.* 1999;134:1131–6.
67. Doi R, Fujimoto K, Wada M, Imamura M. Surgical management of intraductal papillary mucinous tumor of the pancreas. *Surgery.* 2002;132:80–5.
68. Matsumoto T, Aramaki M, Yada K, Hirano S, Himeno Y, Shibata K, et al. Optimal management of the branch duct type intraductal papillary mucinous neoplasms of the pancreas. *J Clin Gastroenterol.* 2003;36:261–5.
69. Sugiyama M, Izumisato Y, Abe N, Masaki T, Mori T, Atomi Y. Predictive factors for malignancy in intraductal papillary-mucinous tumours of the pancreas. *Br J Surg.* 2003;90:1244–9.
70. Salvia R, Fernandez-del Castillo C, Bassi C, Thayer SP, Falconi M, Mantovani W, et al. Main-duct intraductal papillary mucinous neoplasms of the pancreas: clinical predictors of malignancy and long-term survival following resection. *Ann Surg.* 2004;239:678–85. discussion 685–7.

71. Maire F, Couvelard A, Hammel P, Ponsot P, Palazzo L, Aubert A, et al. Intraductal papillary mucinous tumors of the pancreas: the preoperative value of cytologic and histopathologic diagnosis. *Gastrointest Endosc.* 2003;58:701–6.
72. Pais SA, Attasaranya S, Leblanc JK, Sherman S, Schmidt CM, DeWitt J. Role of endoscopic ultrasound in the diagnosis of intraductal papillary mucinous neoplasms: correlation with surgical histopathology. *Clin Gastroenterol Hepatol.* 2007;5:489–95.
73. Wiesenauer CA, Schmidt CM, Cummings OW, Yiannoutsos CT, Howard TJ, Wiebke EA, et al. Preoperative predictors of malignancy in pancreatic intraductal papillary mucinous neoplasms. *Arch Surg.* 2003;138:610–7. discussion 617–8.
74. Hara T, Yamaguchi T, Ishihara T, Tsuyuguchi T, Kondo F, Kato K, et al. Diagnosis and patient management of intraductal papillary-mucinous tumor of the pancreas by using peroral pancreatoscopy and intraductal ultrasonography. *Gastroenterology.* 2002;122:34–43.
75. Pelaez-Luna M, Chari ST, Smyrk TC, Takahashi N, Clain JE, Levy MJ, et al. Do consensus indications for resection in branch duct intraductal papillary mucinous neoplasm predict malignancy? A study of 147 patients. *Am J Gastroenterol.* 2007;102:1759–64.
76. Kubo H, Chijiwa Y, Akahoshi K, Hamada S, Harada N, Sumii T, et al. Intraductal papillary-mucinous tumors of the pancreas: differential diagnosis between benign and malignant tumors by endoscopic ultrasonography. *Am J Gastroenterol.* 2001;96:1429–34.
77. Serikawa M, Sasaki T, Fujimoto Y, Kuwahara K, Chayama K. Management of intraductal papillary-mucinous neoplasm of the pancreas: treatment strategy based on morphologic classification. *J Clin Gastroenterol.* 2006;40:856–62.
78. Kawamoto S, Lawler LP, Horton KM, Eng J, Hruban RH, Fishman EK. MDCT of intraductal papillary mucinous neoplasm of the pancreas: evaluation of features predictive of invasive carcinoma. *AJR Am J Roentgenol.* 2006;186:687–95.
79. Chen X, Zhou GW, Zhou HJ, Peng CH, Li HW. Diagnosis and treatment of solid-pseudopapillary tumors of the pancreas. *Hepatobiliary Pancreat Dis Int.* 2005;4:456–9.
80. Cheng DF, Peng CH, Zhou GW, Tao ZY, Chen X, Lei RQ, et al. Clinical misdiagnosis of solid pseudopapillary tumour of pancreas. *Chin Med J (Engl).* 2005;118:922–6.
81. Peng CH, Chen DF, Zhou GW, Yang WP, Tao ZY, Lei RQ, et al. The solid-pseudopapillary tumor of pancreas: the clinical characteristics and surgical treatment. *J Surg Res.* 2006;131:276–82.
82. Peng CH, Cheng DF, Zhou GW, Yang WP, Lei RQ, Jin XL, et al. The surgical treatment of the solid-pseudopapillary tumor of pancreas: report of 21 cases. *Zhonghua Wai Ke Za Zhi.* 2005;43:145–8.
83. Jani N, Dewitt J, Eloubeidi M, Varadarajulu S, Appalaneni V, Hoffman B, et al. Endoscopic ultrasound-guided fine-needle aspiration for diagnosis of solid pseudopapillary tumors of the pancreas: a multicenter experience. *Endoscopy.* 2008;40:200–3.
84. Alexandrescu DT, O’Boyle K, Feliz A, Fueg A, Wiernik PH. Metastatic solid-pseudopapillary tumour of the pancreas: clinico-biological correlates and management. *Clin Oncol (R Coll Radiol).* 2005;17:358–63.

85. Kongkam P, Al-Haddad M, Attasaranya S, O'Neil J, Pais S, Sherman S, et al. EUS and clinical characteristics of cystic pancreatic neuroendocrine tumors. *Endoscopy*. 2008;40:602–5.
86. DeWitt J, Jowell P, Leblanc J, McHenry L, McGreevy K, Cramer H, et al. EUS-guided FNA of pancreatic metastases: a multicenter experience. *Gastrointest Endosc*. 2005;61:689–96.
87. Capitanich P, Iovaldi ML, Medrano M, Malizia P, Herrera J, Celeste F, et al. Lymphoepithelial cysts of the pancreas: case report and review of the literature. *J Gastrointest Surg*. 2004;8:342–5.
88. Lim WC, Leblanc JK, Dewitt J. EUS-guided FNA of a peripancreatic lymphocele. *Gastrointest Endosc*. 2005;62:459–62.
89. Allen PJ, D'Angelica M, Gonen M, Jaques DP, Coit DG, Jarnagin WR, et al. A selective approach to the resection of cystic lesions of the pancreas: results from 539 consecutive patients. *Ann Surg*. 2006;244:572–82.
90. Khalid A, Brugge W. ACG practice guidelines for the diagnosis and management of neoplastic pancreatic cysts. *Am J Gastroenterol*. 2007;102:2339–49.
91. Rodriguez JR, Salvia R, Crippa S, Warshaw AL, Bassi C, Falconi M, et al. Branch-duct intraductal papillary mucinous neoplasms: observations in 145 patients who underwent resection. *Gastroenterology*. 2007;133:72–9. quiz 309–10.
92. Oh HC, Kim MH, Hwang CY, Lee TY, Lee SS, Seo DW, et al. Cystic lesions of the pancreas: challenging issues in clinical practice. *Am J Gastroenterol*. 2008;103:229–39. quiz 228, 240.
93. Lillemoe KD, Kaushal S, Cameron JL, Sohn TA, Pitt HA, Yeo CJ. Distal pancreatectomy: indications and outcomes in 235 patients. *Ann Surg*. 1999;229:693–8. discussion 698–700.
94. Yeo CJ, Cameron JL. Improving results of pancreaticoduodenectomy for pancreatic cancer. *World J Surg*. 1999;23:907–12.
95. Madura JA, Yum MN, Lehman GA, Sherman S, Schmidt CM. Mucin secreting cystic lesions of the pancreas: treatment by enucleation. *Am Surg*. 2004;70:106–12. discussion 113.
96. Kiely JM, Nakeeb A, Komorowski RA, Wilson SD, Pitt HA. Cystic pancreatic neoplasms: enucleate or resect? *J Gastrointest Surg*. 2003;7:890–7.
97. Gan SI, Thompson CC, Lauwers GY, Bounds BC, Brugge WR. Ethanol lavage of pancreatic cystic lesions: initial pilot study. *Gastrointest Endosc*. 2005;61:746–52.
98. DeWitt J, McGreevy K, Schmidt CM, Collier K, Brugge W. Ethanol pancreatic injection of cysts (EPIC): preliminary results of a prospective multicenter, randomized, double blinded study. *Gastrointest Endosc*. 2007;65:106.
99. Seo TS, Oh JH, Yoon Y, Lim JW, Park SJ, Chang SG, et al. Acetic acid as a sclerosing agent for renal cysts: comparison with ethanol in follow-up results. *Cardiovasc Intervent Radiol*. 2000;23:177–81.
100. Brunken C, Pfeiffer D, Tauber R. Long term outcome after percutaneous sclerotherapy of renal cysts with polidocanol. *Urologe A*. 2002;41:263–6.
101. Oh HC, Seo DW, Lee TY, Kim JY, Lee SS, Lee SK, et al. New treatment for cystic tumors of the pancreas: EUS-guided ethanol lavage with paclitaxel injection. *Gastrointest Endosc*. 2008;67:636–42.

The Role of EUS in the Biliary System

Jean-Louis Frossard, MD
and Jean-Marc Dumonceau, MD

CONTENTS

TECHNIQUE OF BILIARY IMAGING
GALLSTONE DISEASE
BILIARY STRICTURES
GALLBLADDER

Abstract

Standard endoscopic ultrasound (EUS) and intraductal ultrasonography (IDUS) are, with magnetic resonance, the best techniques currently available to image the extrahepatic bile ducts and the gallbladder. In this chapter, we review current knowledge about gallstone disease, bile duct strictures, and gallbladder lesions.

In patients at high risk of having bile duct stones, endoscopic retrograde cholangio-pancreatography (ERCP) is the most cost-effective procedure, whereas EUS is indicated when the clinical index of suspicion for stones is low or intermediate (to spare costs and morbidity associated with ERCP). Sensitivity and specificity of EUS for the diagnosis of choledocholithiasis are close to 95%. In cases of unexplained acute pancreatitis, EUS provides a diagnosis in a majority of patients; in particular by detecting gallstone disease that had not been suspected at percutaneous ultrasonography.

From: *Clinical Gastroenterology: Endoscopic Ultrasound*,
Edited by: V. M. Shami and M. Kahaleh, DOI 10.1007/978-1-60327-480-7_14,
© Springer Science+Business Media, LLC 2010

For the diagnosis of malignant vs. benign biliary strictures, the accuracy of EUS without fine needle aspiration (FNA) is not as high (80%), but EUS-FNA (in particular of lymph nodes) alters patient management in a significant proportion of cases. IDUS is the best technique for assessing the longitudinal tumor extent as well as T (but not N) categories. IDUS may also assist in diagnosing malignant transformation in primary sclerosing cholangitis.

Gallbladder polypoid lesions are frequent and can better be assessed by EUS than by percutaneous ultrasonography. EUS may be useful to examine lesions measuring 5–10 mm in diameter.

Finally, the accuracy of EUS for staging gallbladder cancer is in the range of 80–90%; it is particularly useful to distinguish between T1 and T2 tumors because the therapeutic planning is markedly different between these two categories.

Key Words: Endoscopic ultrasonography, Endoscopic ultrasonography-guided fine needle aspiration, Gallstone disease, Cholangiocarcinoma, Gallbladder cancer, Primary sclerosing cholangitis

TECHNIQUE OF BILIARY IMAGING

Standard Endoscopic Ultrasonography

Endoscopic ultrasonography (EUS) is performed after an overnight fast, usually with the patient in left lateral decubitus position and under intravenous sedation. If a biliary stricture is suspected, it is useful to have previous cross-sectional imaging studies (in particular magnetic resonance cholangiopancreatography [MRCP] if available) to assess the level of biliary obstruction and the presence of a mass or lymph nodes. Whether a radial or a linear scanning echoendoscope is used, the extrahepatic bile ducts can be visualized completely in the majority of the patients by inserting the echoendoscope in two positions, namely the “apical” position and the “kissing the papilla” position. During the introduction of the instrument, little air inflation is required and many echoendoscopists mainly look at the EUS view even at this stage (the endoscopic view may be placed as a “picture in picture” on the main screen if a radial instrument is used). Once a position is achieved, suctioning air and inflating the balloon at the tip of the instrument enhance acoustic coupling. Using high frequencies (7.5, 12, or even 20 MHz), a spasmolytic drug (N-butyl hyoscine or glucagon) and color Doppler are useful to obtain better imaging and to avoid confusion between a nondilated bile duct and adjacent vessels.

The “apical” position is obtained by inserting the transducer into the apex of the duodenal bulb; the balloon is then inflated until it occludes the duodenal lumen and the instrument is maneuvered to visualize five landmarks: (1) the “duodenal fall-off,” which corresponds to the duodenal wall; (2) the bile duct, adjacent to the transducer; (3) the Wirsung’s duct (deeper); (4) the superior mesenteric/portal veins; and (5) the gallbladder.

The “kissing the papilla” position is obtained by entering the second portion of the duodenum, distal to the papilla, and then pulling back the instrument in the “short-route” position to place the transducer close to the papilla (as is done for endoscopic retrograde cholangio-pancreatography [ERCP]). At this time, it is useful to have a rapid look at the endoscopic view of the papilla. If the papilla is located in a paradiverticular position, abundant water instillation may be useful to avoid artifacts. This position is ideal to detect a stone impacted into the distal portion of the bile duct or into the papilla.

Particularities relative to the radial- and linear-scanning echoendoscope are as follows: with a radial echoendoscope, EUS is always begun in the “apical” position because the bile duct is readily recognized (usually within 30 s) by delicately pressing the instrument, balloon inflated, against the apex of the duodenal bulb and slightly moving the up/down and right/left knobs. The bile duct courses immediately adjacent to the transducer, presents as a three-layer wall (not always detectable), and may be tracked up to the hilum by slightly withdrawing the instrument while applying counterclockwise torque (inverse movements to track the bile duct down to the papilla) (Fig. 1). If the bile duct is thin, it may be difficult to visualize its full course in a single view; in this case, partly deflating the balloon may be useful to avoid compressing the bile duct. The gallbladder appears as an anechoic crescent when pulling the instrument from the apical position to the pylorus. In the “kissing the papilla” position, the instrument is slightly withdrawn while moving the up/down and right/left knobs to follow the convergence of the biliary and pancreatic ducts into the papilla (Fig. 2).

With a linear echoendoscope, in the “apical” position, the main maneuver performed to track the bile duct consists in torquing the instrument (advancing/withdrawing the instrument is less useful). Some echoendoscopists directly start the examination in the “kissing the papilla” position, and track the bile duct proximally up to the liver hilum by withdrawing the instrument into the duodenal bulb/pyloric region while simultaneously applying counterclockwise torquing (balloon inflation and a relatively long endoscope position may help to prevent it from slipping into the stomach). As complete imaging of the bile duct with a linear instrument requires more experience than with a radial instrument, it may be



Fig. 1. Radial EUS image (5 MHz) showing the normal anatomy of the common hepatic duct (arrows) emerging from the convergence.

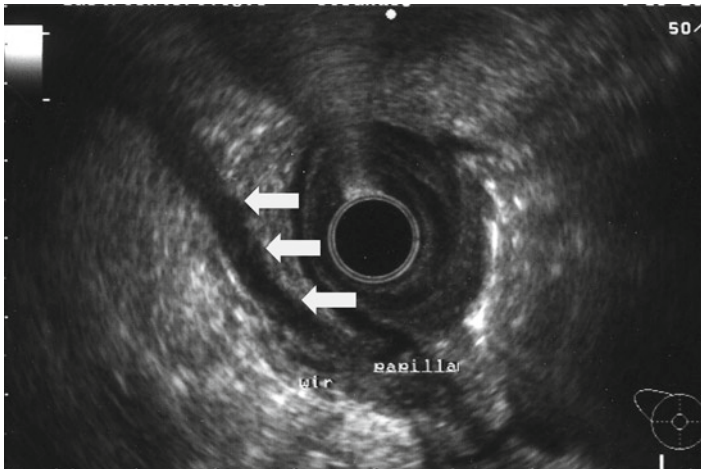


Fig. 2. Radial EUS image (7.5 MHz) showing the normal anatomy of the common bile duct (arrows) and Wirsung's duct down to the ampulla of Vater.

useful to perform the first examinations in patients who have a biliary stent in place. The liver hilum is usually imaged at the lowest frequency available (5 MHz) because it is located at 4–5 cm from the transducer. As in other gastrointestinal locations, EUS-guided fine needle aspiration (EUS-FNA) is performed after color Doppler examination of the anticipated needle tract. EUS-FNA in the region of the liver hilum is more demanding than in other segments of the bile duct; it is usually performed from the post pyloric (or, infrequently, the prepyloric) region while advancing the instrument to lean against the greater curvature of the stomach.

The principal limitations of biliary EUS include (1) difficulties in performing a biliary examination after Billroth II gastrectomy; (2) poor visualization of the right hepatic duct (plus the hilum in some cases, as well as the distal portion of the bile duct in case of chronic calcified pancreatitis); (3) limited accuracy in case of pneumobilia (e.g., previous biliary sphincterotomy); and (4) operator-dependency.

Intraductal Ultrasonography

Intraductal ultrasonography (IDUS) provides high-resolution images of the biliary tree because high-frequency (20–30 MHz) probes are generally used. These probes may be inserted into the bile ducts during endoscopic or percutaneous cholangiography. Wire-guided IDUS probes are strongly advised because they can be inserted without biliary sphincterotomy in virtually all cases (and without dilation in many cases of biliary stricture [stricture dilation or sampling is preferably performed after IDUS]) (1). In practice, for two-dimensional IDUS, a high-frequency, 20-MHz, wire guided, probe (e.g., UM-G20-29R, Olympus, Tokyo, Japan) is inserted “over-the-wire” with the minimal use of the elevator to avoid damaging this fragile and costly probe (Fig. 3). Continuous imaging is obtained during slow withdrawal of the probe, with the elevator in low position to minimize friction (fluoroscopy may be used to locate the radiopaque tip of the probe). IDUS adds a mean of 5 min to ERCP (2).

Three-dimensional IDUS (3D-IDUS) has emerged as an interesting alternative to two-dimensional IDUS. Probes that allow 3D-IDUS present an outer, immobile, sheath and an inner, mobile, radial transducer; they must be connected to a specific driving unit. The most recent models of 3D-IDUS probes (e.g., UM-DG20-31R, Olympus) are wire guided. After inserting the probe up to the hilum, the driving unit is activated and the ultrasonic transducer is progressively withdrawn inside the immobile outer sheath at a constant speed (generally, over a 40-mm length). Two or



Fig. 3. Endoscopic view of the insertion into the bile duct of a three-dimensional IDUS probe (outer diameter, 2.9 mm). Probe insertion is performed over-the-wire and without previous biliary sphincterotomy (papilla below two diverticulae).

three passes are generally required to image the whole bile duct. Various types of 3D reconstructions, including dual plane, oblique, and surface rendering reconstructions may be performed in real-time. Electronic storage of data acquired during all passes allows, together with the standardization of the procedure, to interpret 3D-IDUS after completing ERCP. Data acquisition is thus quicker than with conventional IDUS and images may be interpreted with an experienced echoendoscopist even if he/she has not attended the procedure.

Complications specifically attributable to IDUS are exceptional, likely because no fluid irrigation is required owing to the presence of bile (in contrast, cholangioscopy requires fluid irrigation and has been associated with increased complication rates) (3). However, IDUS requires ERCP with its associated morbidity (plus biliary stenting to relieve obstruction after biliary contamination if a stricture is present).

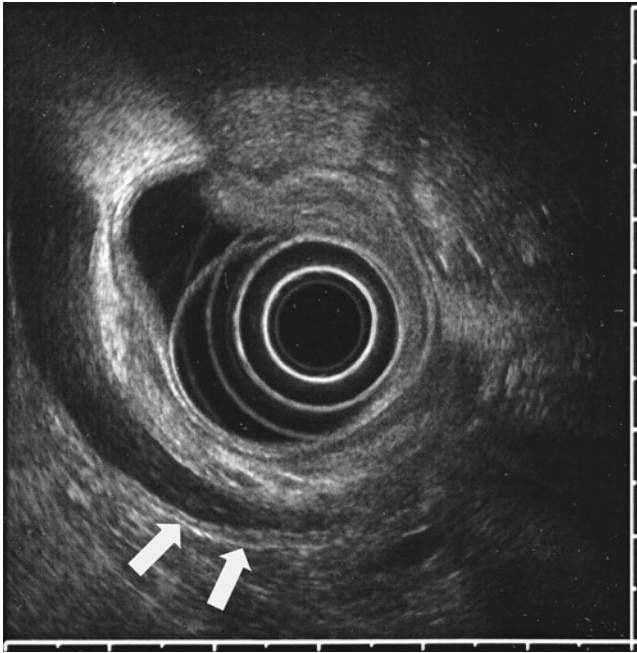


Fig. 4. Radial EUS image (12 MHz) showing the three endosonographic layers of the common bile duct, best identified at high frequencies (arrows).

Normal Findings

Two or three endosonographic layers are identified in the normal bile duct wall (Fig. 4) (4–7). The inner hyperechoic layer corresponds to biliary mucosa and the interface between the bile duct wall and bile (this layer may not be visible); the middle hypoechoic layer corresponds to the fibromuscular layer, and the outer hyperechoic layer corresponds to the adipose layer of the subserosa, the serosa, and the interface echo between the serosa and surrounding organs (thus, it is not part of the bile duct itself). In some patients, the fibromuscular layer cannot be distinguished from the perimuscular connective tissue, particularly in the intrapancreatic portion of the bile duct, and these appear as a single hypoechoic layer (6). The bile duct wall thickness is measured at the level of the middle hypoechoic layer; it is 0.6 mm in normal subjects, and the upper limit of normal is 1.8 mm (7, 8). The thickness of the normal bile duct wall is not significantly different when measured upstream from an obstruction or in case of choledocholithiasis, but it is

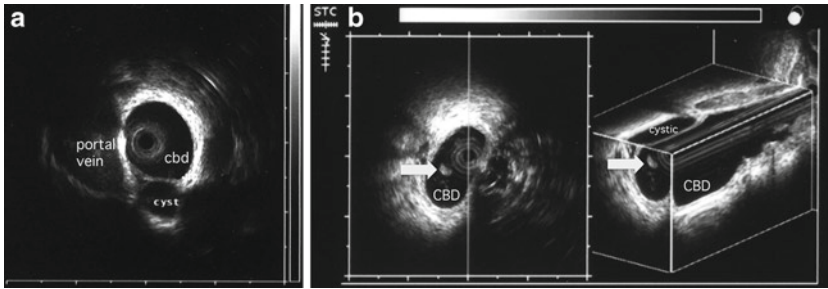


Fig. 5. Normal anatomy of the common bile duct (CBD) as shown by a two-dimensional or a three-dimensional 20 MHz IDUS probe. **(a)** Two-dimensional IDUS probe; the cystic duct (Cyst) and the portal vein are seen in cross-section; **(b)** three-dimensional IDUS probe (composite image, as rendered in real-time); the cystic duct runs parallel to the CBD (note the presence in the CBD of a hyperechoic spot without postacoustic shadow (arrow) that corresponds to a microlithiasis).

increased when a biliary drain is left in place for >2 weeks or in case of primary sclerosing cholangitis (PSC) (mean thickness, 2.0 and 2.5 mm, respectively) (8, 9).

Imaging of the right hepatic artery, portal vein, and hepatoduodenal ligament are easier to obtain with IDUS compared to EUS. During probe withdrawal, the following peribiliary structures can be identified: right hepatic artery (longitudinal, vascular structure crossing behind the common hepatic duct), portal vein (longitudinal vascular structure behind the right hepatic artery that is larger and presents a thinner wall), the cystic duct (in continuity with the CBD) (Fig. 5), the main pancreatic duct and surrounding pancreatic parenchyma, the inferior vena cava (posterior to the pancreatic parenchyma), and the sphincter of Oddi (circular, hypoechoic thickening within the duodenal wall). Demonstration of the common and left hepatic arteries is most often not possible because probes commonly used for biliary imaging work at high frequencies and have a limited penetration depth.

GALLSTONE DISEASE

Introduction

Symptomatic gallstone disease may be related to sludge, microlithiasis and calculi. Biliary sludge is considered to be a suspension of various items, including crystals, mucin, and cellular debris within bile while

Table 1
Risk factors for common bile duct (CBD) stones in patients awaiting cholecystectomy

<i>Low risk (0–5%)</i>	<i>Intermediate risk (5–50%)</i>	<i>High risk (>50%)</i>
Normal ultrasonography	Hyperbilirubinemia (>30 $\mu\text{mol/L}$)	Cholangitis
Normal liver tests	Increased alkaline phosphatase	Jaundice
	Increased ALAT	Dilated CBD
	Pancreatitis	
	Cholecystitis	
	Age >55 years	

microlithiasis is defined as stones <3 mm in diameter (10, 11). Many authors use the term microlithiasis or sludge interchangeably, likely because sludge is considered to be a precursor to microlithiasis and both have the same clinical significance.

Gallstone disease is one of the most prevalent digestive diseases in Western countries, but only 2–4% of patients become symptomatic each year (12, 13). CBD lithiasis is found in 10–15% of patients undergoing cholecystectomy (14), and is associated with potentially severe complications, including pancreatitis and cholangitis. ERCP is the preferred procedure to treat CBD stones, but it is being abandoned as a diagnostic test due to its attendant morbidity (5–10%) and imperfect sensitivity (85–90%) (15, 16). In a prospective cost-minimization study that enrolled 485 patients with suspected CBD stones investigated by EUS, EUS followed by ERCP in case of positive finding was the least costly strategy (ERCP was avoided in about half patients) (17). However, “ERCP first” became the least costly strategy if the risk of CBD stones were >60% (e.g., cholangitis). However, this requires the ability to accurately assess the risk of CBD stone based on non-invasive tests (Table 1), and may vary according to local costs.

Technique

Biliary sludge produce low-amplitude echoes without a postacoustic shadow that layer in the dependent portion of the gallbladder or CBD and shift with positional changes (Fig. 6); microlithiasis is observed as tiny hyperechoic materials (0.5–3 mm) without a postacoustic shadow, and stones produce echoes of high amplitude ≥ 3 mm with a postacoustic

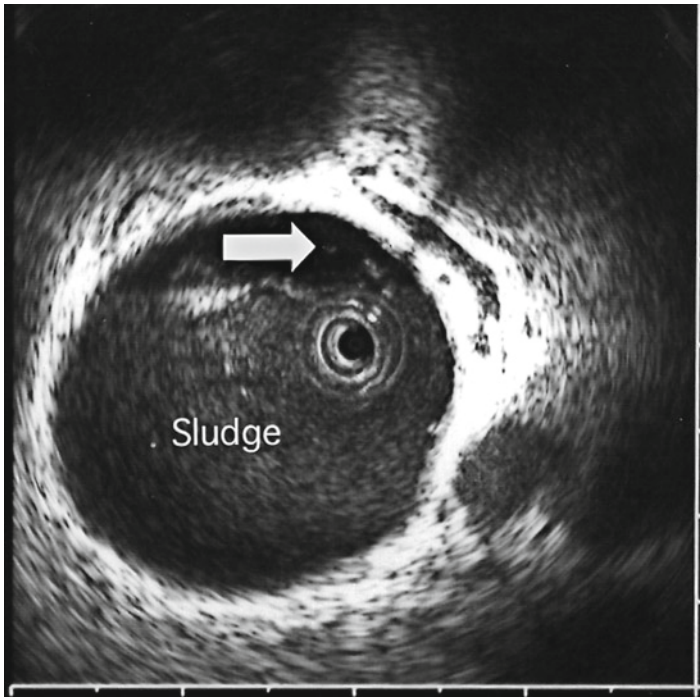


Fig. 6. Two-dimensional IDUS image (20 MHz) showing abundant sludge (low-amplitude echoes without a postacoustic shadow), plus microlithiasis that floats above the bile-sludge level in the common bile duct (tiny hyperechoic materials without a postacoustic shadow, arrow).

shadow and may move within the gallbladder or the CBD (Fig. 7). Mirizzi's syndrome is a condition that should be diagnosed preoperatively because it is associated with an increased risk of bile duct injury at laparoscopic cholecystectomy (18). It is identified as a compression of the CBD by a cystic stone or a large gallbladder stone responsible for upstream dilation of the common hepatic duct (Fig. 8).

Results

A meta-analysis assessed the results of EUS specifically for the diagnosis of CBD stones (19). Twenty-seven prospective cohort studies were included, totaling 2,673 patients with suspected choledocholithiasis (mean prevalence, 36% [15–86%]). Pooled sensitivity and specificity for the diagnosis of choledocholithiasis by EUS were 94% (95%

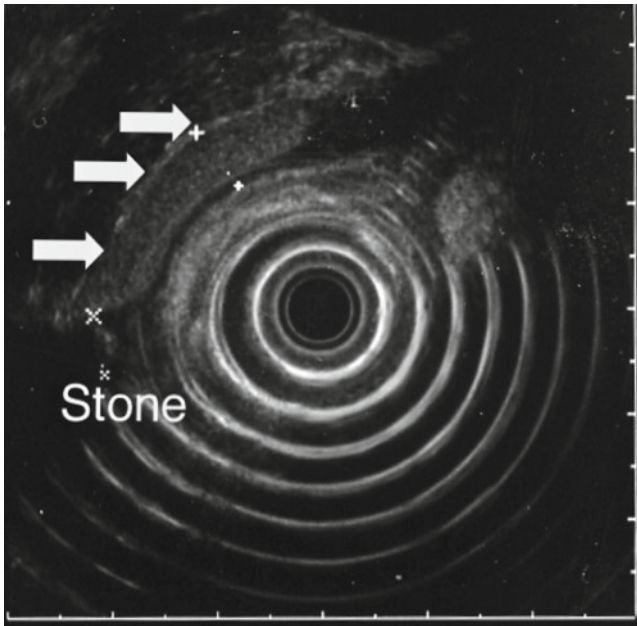


Fig. 7. Radial EUS image (12 MHz) showing an obstructing stone in the common bile duct (high amplitude echo with a postacoustic shadow), associated with an upstream accumulation of dense, sedimented, sludge (arrows).

confidence interval, 93–96%) and 95% (95% confidence interval, 94–96%), respectively. These results concur with those of a previous meta-analysis that showed that EUS had higher sensitivity (89%) and specificity (94%) for the diagnosis of choledocholithiasis compared to malignancy (sensitivity, 78%; specificity, 84%) (20). In the most recent meta-analysis (19), the quality of the 27 studies that qualified for inclusion was generally judged as low because only 33% of studies satisfied all of three predefined criteria to qualify as a high-quality study. In that meta-analysis, three variables were associated with a better accuracy of EUS. These included a clinical context of suspected biliary pancreatitis (as compared to contexts of suspected biliary obstruction or of suspected CBD stones), a time interval between EUS and gold-standard that was <72 h (stones spontaneously pass into the duodenum as time elapses) (21), and the presence of a verification bias (i.e., if patients with stones detected at EUS only were verified by the gold-standard, other patients being verified by clinical follow-up). A limitation of this meta-analysis is that all studies that were included had been performed in tertiary care

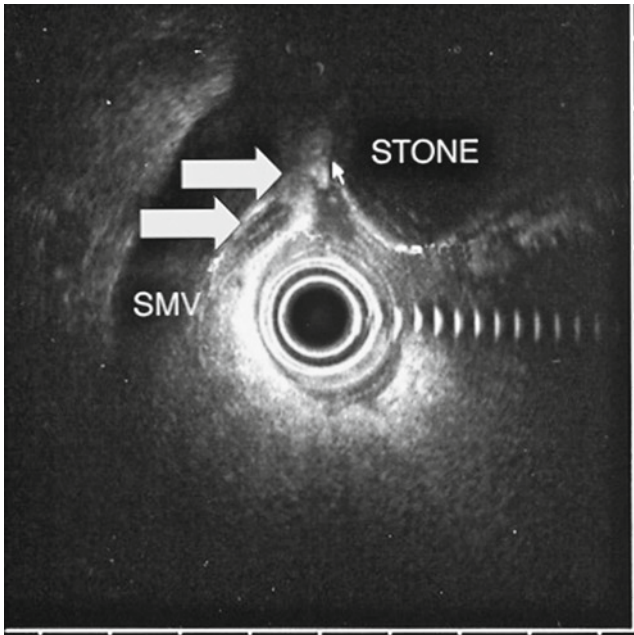


Fig. 8. Radial EUS image (12 MHz) showing a Mirizzi's syndrome. Note the presence of a high amplitude echo with a postacoustic shadow in the gallbladder, corresponding to a large stone that compresses the common bile duct (arrows). SMV superior mesenteric vein.

settings so that it is unknown if these results can be transferred to the community.

Contrary to EUS, MRCP is completely noninvasive, and it also presents an excellent accuracy for the detection of CBD stones (Table 2) (22–29). A systematic review of five prospective randomized blinded trials that compared EUS with MRCP for the detection of CBD stones found no significant differences between both tests (30). The authors concluded that clinicians should choose between tests based on local resource availability (that is much larger for MRCP compared to EUS), experience and costs. An advantage specific to EUS is that, in properly organized endoscopy units, therapeutic ERCP may immediately follow diagnostic EUS. This approach allows saving costs as compared to the “MRCP followed by ERCP” approach in low-to-moderate risk patients (31). EUS is also recommended for the detection of small stones or stones impacted into the papilla in case of negative

Table 2
Comparison of EUS vs. magnetic resonance cholangiopancreatography for the detection of common bile duct stones

<i>First author</i>	<i>No patients</i>	<i>EUS</i>			<i>Magnetic resonance cholangiopancreatography</i>		
		<i>Sensitivity</i>	<i>Specificity</i>	<i>Accuracy</i>	<i>Sensitivity</i>	<i>Specificity</i>	<i>Accuracy</i>
Ainsworth (22)	163	0.89	0.98	0.93	0.90	0.92	0.91
Aubé (23)	47	0.94	0.97	0.94	0.88	0.97	–
De Lédinghen (24)	32	1	0.95	0.91	1	0.73	0.82
Fernández-Esparrach (29)	72	0.93	0.81	0.86	0.87	0.95	0.92
Kondo (25)	28	1	0.50	0.93	0.88	0.75	0.86
Materne (26)	50	0.97	0.88	0.94	0.91	0.94	0.92
Scheiman (27)	30	0.80	0.95	–	0.40	0.96	–
Schmidt (28)	57	0.97	0.94	0.97	0.95	0.95	0.95

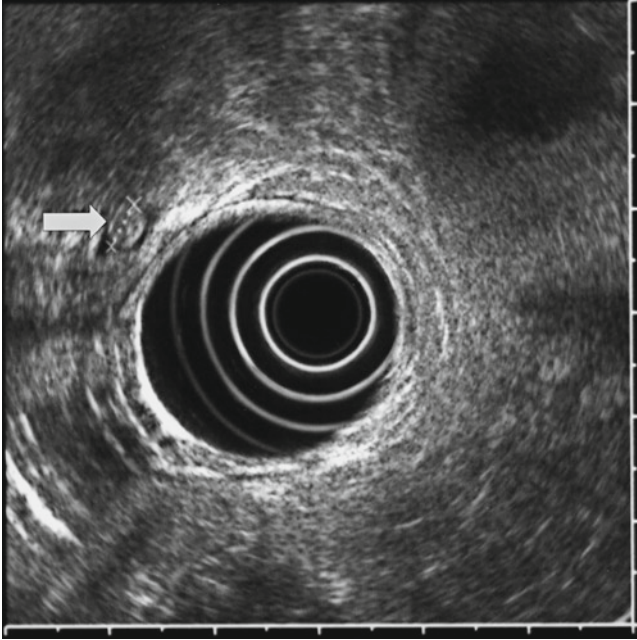


Fig. 9. Radial EUS image (12 MHz) showing a 4-mm in diameter stone impacted into the ampulla (arrow). Note the absence of postacoustic shadow.

MRCP because the spatial resolution of MRCP is lower than that of EUS (1.5 mm vs. 0.1 mm), and the ampullary region is more difficult to examine at MRCP (Figs. 9 and 10) (32).

Finally, (1) the accuracy of MRCP is dependent on experience in image interpretation and on magnetic resonance imaging techniques (similar to EUS), and (2) MRCP is contraindicated in patients with incompatible material such as pacemakers (and it is very difficult to perform in case of claustrophobia) (27, 32).

Particular Case: “Idiopathic” Acute Pancreatitis

EUS is particularly useful to investigate “idiopathic” acute pancreatitis. Standard investigation of acute pancreatitis, including percutaneous ultrasonography (US) and CT scan, does not find the cause of acute pancreatitis in 10–20% of cases (33). A significant proportion of these cases are unrecognized biliary pancreatitis. This is supported, among other factors (33), by the identification, at microscopic examination, of

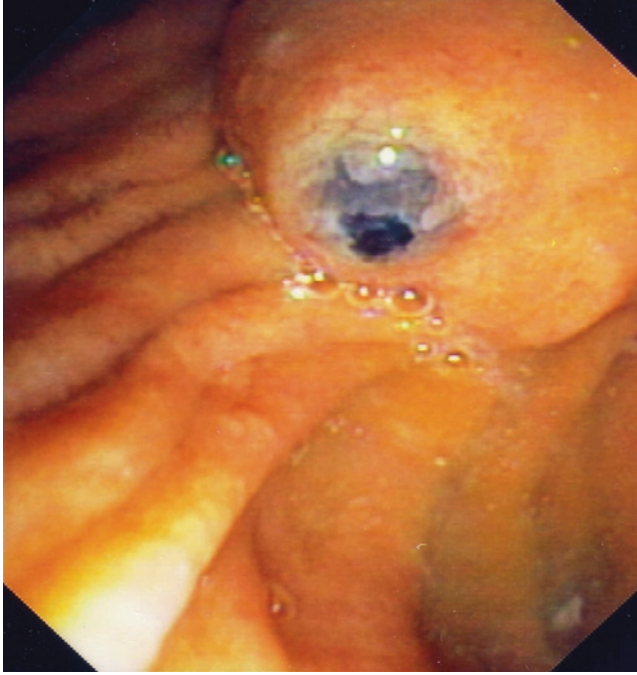


Fig. 10. Endoscopic view of a stone impacted into the papilla, as seen when entering the second portion of the duodenum (black pigment stone related to hemolytic disease in a patient with sickle cell anemia).

crystals in bile sampled from the bile duct or gallbladder in up to 80% of cases (34).

In five studies that have analyzed the results of EUS for acute pancreatitis diagnosed as “idiopathic” after a standard work-up, gallstones were found in 170 (27%) of 631 patients (Fig. 11) (35–39). In addition to this, other lesions were detected in another 220 patients, for an overall yield of EUS of 62%. The likelihood of finding gallstone disease at EUS in idiopathic pancreatitis is similar for a first attack or in case of relapsing disease, but it is low in case of previous cholecystectomy (39).

Recognizing the biliary origin of acute pancreatitis is critical as recurrences develop in 33–61% of cases in the absence of treatment (40, 41). To this end, Wilcox et al. recently concluded that EUS should be considered to evaluate patients with a first attack of “idiopathic” acute pancreatitis (33).

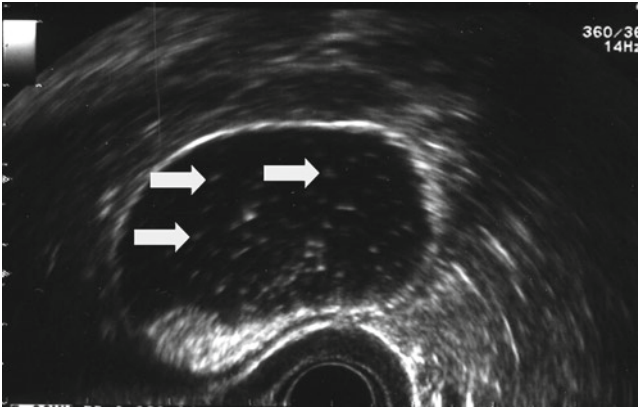


Fig. 11. Linear EUS image (7.5 MHz) showing a microlithiasis of the gallbladder (hyperechoic spots without postacoustic shadow, arrows). Note that hyperechoic spots accumulate in the lower part of the gallbladder and form a hyperechoic pseudopolyp (left hand side). Percutaneous ultrasonography had revealed no abnormality in this obese patient after a first attack of acute pancreatitis, and this had been diagnosed as “idiopathic” acute pancreatitis.

BILIARY STRICTURES

Standard Endoscopic Ultrasonography

DETECTION AND CHARACTERIZATION OF BILIARY STRICTURES AND LYMPH NODES

In the absence of a pancreatic mass, two characteristics of the bile duct wall are used to discriminate malignant from benign biliary strictures at EUS (42). These are (1) a maximal thickness ≥ 3 mm and (2) the presence of irregular outer margins. In a prospective study of 40 patients with a bile duct stricture of unknown origin, Lee et al. found that a bile duct wall thickness ≥ 3 mm had sensitivity and specificity for diagnosing malignancy of 79% each (Fig. 12) (42). An irregular outer edge of the bile duct wall is also indicative of malignancy but, in contrast, echo features are similar for both benign and malignant strictures (most lesions are hypoechoic compared to the liver) (43).

In a recent meta-analysis (20), Garrow et al. reviewed 36 studies that analyzed the ability of EUS (without FNA) to detect the presence and etiology of a biliary obstruction in 3,532 patients. Accuracy of EUS was high for the detection of a biliary obstruction (sensitivity, 88%; specificity, 90%), but lower for differentiating benign from malignant causes (sensitivity, 78%; specificity, 84%). Linear and radial EUS were

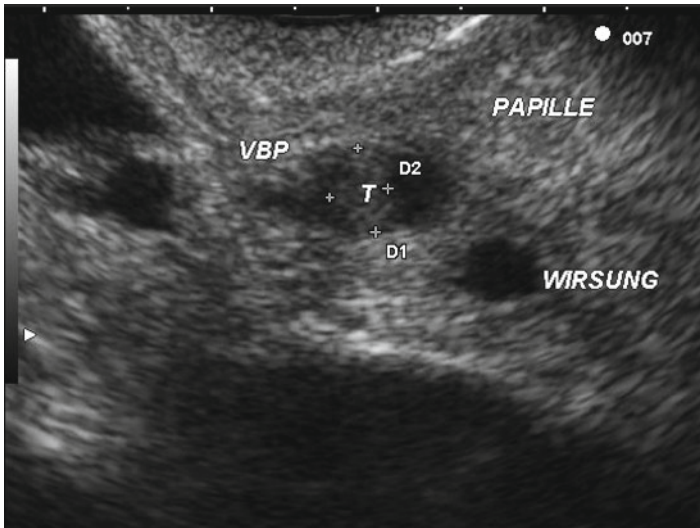


Fig. 12. Linear EUS image (7.5 MHz) showing a T1 cholangiocarcinoma as a hypoechoic mass (T) that measures 3.5 mm×5.1 mm in diameter and obstructs the common bile duct (VBP). Photograph courtesy from M. Giovannini.

found to have similar performances. Of note, the results of standard EUS (without FNA) were slightly inferior to those reported with magnetic resonance in another meta-analysis, with regard to both the detection of biliary obstruction (sensitivity, 97%; specificity, 98%) and the differentiation between benign and malignant biliary obstruction (sensitivity, 88%; specificity, 95%) (44).

Regarding lymph nodes, Faigel et al. have shown for pancreaticobiliary malignancies the size of lymph nodes was not associated with malignant involvement, while other commonly used parameters (i.e., a short distance between the tumor and the lymph node, a round shape and a hypoechoic, homogeneous, texture of the lymph node) were indicative of malignancy (45). For cholangiocarcinomas located at the hilum, Gleeson et al. have found that malignant and benign lymph nodes had a similar aspect, including size, roundness, echogenicity, and homogeneity (46). FNA is therefore necessary if the status of the visualized lymph nodes would alter clinical management.

SAMPLING

Table 3 summarizes the main results reported with EUS-FNA for suspected cholangiocarcinomas. Compared to pancreatic carcinomas,

Table 3
Results of EUS-FNA for suspected cholangiocarcinoma

<i>First author</i>	<i>Study design</i>	<i>N</i>	<i>On-site cytopathological examination</i>	<i>Proximal location^a</i>	<i>Mass at previous imaging</i>	<i>Sensitivity</i>
Fritscher-Ravens (43)	Prospective	44	NR	44 (hilum)	NR	0.89
Byrne (51)	Retrospective	35	Yes	3	NR	0.60
Eloubeidi (48)	Prospective	28	Yes	15	33%	0.86
DeWitt (47)	Retrospective	24	Yes	24	39%	0.77
Meara (49)	Prospective	44	Yes	NR	NR	0.87
Lee (42)	Prospective	40 ^b	Yes	1	0	0.47

NR not reported

^aLesions located at the hilum or common hepatic duct (those located in the common bile duct, distal to the cystic duct implantation, were defined as distal) (48)

^bA previously undiagnosed pancreatic head mass was evidenced at EUS in ten patients

cholangiocarcinomas may be more difficult to locate and to sample because they are usually smaller (mean size at the time of FNA, 19–24 mm) (42, 43, 47–49), and many of them are located in the proximal bile duct, including the hilum. Biliary stents may help to locate stricture-associated lesions, and usually pose no significant problem during FNA. Reported sensitivities for the detection of malignancy were $\geq 70\%$ in four out of six studies, and no sampling-related complications were reported in any of them. Factors that contributed to these results included the operators' expertise and the availability of an "on-site" cytopathologist. However, the interpretation of cytopathological reports and case selection were also likely important contributing factors. Generalizability of these results is uncertain because none of the studies listed in Table 3 reported the total number of patients who were eligible for inclusion during the investigation period, and these studies were performed in referral centers (a single operator performed all EUS-FNAs in at least one study) (48). Moreover, only three studies reported the number of failed attempts at FNA, a figure that is needed to calculate the sensitivity in an "intention to diagnose" analysis (89, 75, and 74% in these three studies) (43, 47, 48). These limitations are likely significant, as the single randomized study that has compared EUS-FNA vs. biliary brushing at ERCP for biliary strictures found that EUS-FNA had a relatively low sensitivity (43% vs. 46% for biliary brushing). However, if punctured lesions only were considered in that study ($n=28$), the sensitivity of EUS-FNA for cancer diagnosis was 75%, in line with other reports (50). Finally, in at least four of the studies listed in Table 3, specimens diagnosed as "suspicious for malignancy" were considered as equivalent to "malignant" to calculate the sensitivity for cancer diagnosis (43, 48, 49, 51). From a clinical point of view, this interpretation of cytopathological reports makes sense because no false-positive cases were reported (specificity, 100%). It seems, therefore, desirable that cytopathological reports of biliary FNA specimens include a "highly atypical suspicious for cancer" category, and to locally evaluate the clinical interpretation of this diagnosis (as is performed for biliary brushings in many centers) (52, 53). Finally, a serious drawback of EUS-FNA for cholangiocarcinoma is its low negative predictive value. This attained 70% in two studies only (49, 51), precluding reliable exclusion of malignancy following a negative FNA.

With regard to lymph nodes, these can also be sampled by EUS-FNA to better select patients for surgery (local lymph node metastasis is associated with shorter postresection survival) (54, 55). Gleeson et al. reported a retrospective series of 47 patients with unresectable hilar cholangiocarcinoma considered for liver transplantation who had lymph nodes detected at EUS (including 12 with previously undetec-

ted lymph nodes by CT and/or magnetic resonance) (46). FNA yielded malignant cells in 17% of cases.

LONGITUDINAL TUMOR EXTENT, TNM STAGE, AND RESECTABILITY

Longitudinal spreading is characteristic of cholangiocarcinomas, and tumor extension dictates the possibility (and extent) of surgical resection. Surgical management of cholangiocarcinomas is more problematic if liver hilum is involved compared to the pancreas. Criteria of nonresectability in the hilum classically include: bilateral tumor extension to secondary biliary radicals, encasement or occlusion of the main portal vein, lobar atrophy with contralateral portal vein involvement, advanced nodal disease or spread of tumor to adjacent organs (55, 56). If the tumor is thought to be resectable, negative resection margins should be achieved because this is an independent predictor of survival (54, 55). Depending on tumor extent and liver anatomy, achieving negative resection margins may require partial liver resection, possibly preceded by portal vein embolization to induce compensatory hypertrophy of the future remnant liver. Finally, some patients with an unresectable hilar cholangiocarcinoma <3 cm in diameter and no lymph-node metastases may be eligible for liver transplantation after neoadjuvant therapy, but this is proposed in a few high-volume transplant centers only (46). Accurate assessment of vascular invasion and tumor longitudinal spread is therefore necessary to select the best treatment strategy.

The new 2010 TNM classification of cholangiocarcinomas is different from the previous edition, in that extrahepatic bile duct cancer is now divided into two different staging systems: Perihilar bile ducts (Table 4a) and distal bile duct (Table 4b). This division is as a result of differences in anatomy of the bile duct and consideration of local factors that relate to resectability. Compared to the fifth edition of the TNM classification, the current seventh and previous sixth edition have introduced the T4 category, a modification that has improved the prediction of survival (57). However, several authors have reported that the distinction between the current T2 and T3 categories cannot reliably be performed, even by IDUS or histopathological examination (Fig. 13) (4).

In 1991, Tio et al. reported that the accuracy of EUS staging of carcinomas located in the extrahepatic bile ducts was excellent (84%) (Fig. 14) (58). However, these results were not confirmed and more recent studies have focused on IDUS, which is superior to EUS for T staging (correct T staging in a comparative study, 78% vs. 54%, IDUS vs. EUS, respectively; $P < 0.001$), and for the prediction of

Table 4
AJCC TNM classification of cholangiocarcinomas (a) perihilar bile ducts
and (b) distal bile duct

a. Perihilar bile ducts

T category

- Tis Carcinoma in situ
- T1 Tumor confined to the bile duct, with extension up to the muscle layer or fibrous tissue
- T2a Tumor invades beyond the wall of the bile duct to surrounding adipose tissue
- T2b Tumor invades adjacent hepatic parenchyma
- T3 Tumor invades unilateral branches of the portal vein or hepatic artery
- T4 Tumor invades main portal vein or its branches bilaterally; or the common hepatic artery; or the second-order biliary radicals bilaterally; or unilateral second-order biliary radicals with contralateral portal vein or hepatic artery involvement

N category

- N0 No regional lymph-node metastasis
- N1 Regional lymph-node metastasis (including nodes along the cystic duct, common bile duct, hepatic artery, and portal vein)
- N2 Metastasis to periaortic, pericaval, superior mesenteric artery, and/or celiac artery lymph nodes

b. Distal bile duct

T category

- Tis Carcinoma in situ
- T1 Tumor confined to the bile duct histologically
- T2 Tumor invades beyond the wall of the bile duct
- T3 Tumor invades the gallbladder, pancreas, duodenum, or other adjacent organs without involvement of the celiac axis, or the superior mesenteric artery
- T4 Tumor involves the celiac axis, or the superior mesenteric artery

N category

- N0 No regional lymph-node metastasis
- N1 Regional lymph-node metastasis
-

TNM Classification of Gastric Cancer. Used with the permission of the American Joint Committee on Cancer (AJCC), Chicago, Illinois. The original source for this material is the AJCC Cancer Staging Manual, Seventh Edition (2010) published by Springer Science and Business Media LLC

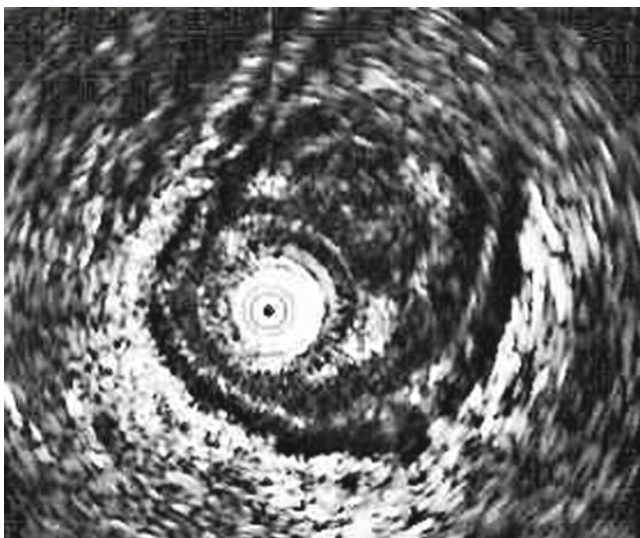


Fig. 13. Two-dimensional IDUS image (30 MHz) showing a T2 cholangiocarcinoma. The edge of the bile duct can often not be distinguished from the edge of the pancreatic parenchyma (2 o'clock position), making the distinction between T2 and T3 categories extremely difficult, even by histopathological means. Photograph courtesy from M. Giovannini.

resectability (59). EUS examination of tumors located at the hilum is limited by the long distance between the transducer and the proximal margin of the tumor. Conversely, its low penetration depth limits IDUS so that lymph nodes cannot be reliably assessed by this technique. Both techniques should therefore be combined in difficult cases.

IMPACT OF EUS-FNA ON PATIENT MANAGEMENT

Pathological diagnosis is required before embarking into neoadjuvant therapy of cholangiocarcinoma (e.g., portal vein embolization to induce compensatory hypertrophy of the future remnant liver), or in patients who are not eligible for surgery if aggressive treatments (e.g., photodynamic therapy) are considered (60, 61). This is critical because many patients who undergo resection for a suspected malignant biliary stricture have a final pathological diagnosis of benign disease (15% for hilar resections, 5–10% for pancreatic head resections) (62, 63). The proportion of inappropriate surgery is even >20% for hilar lesions, due

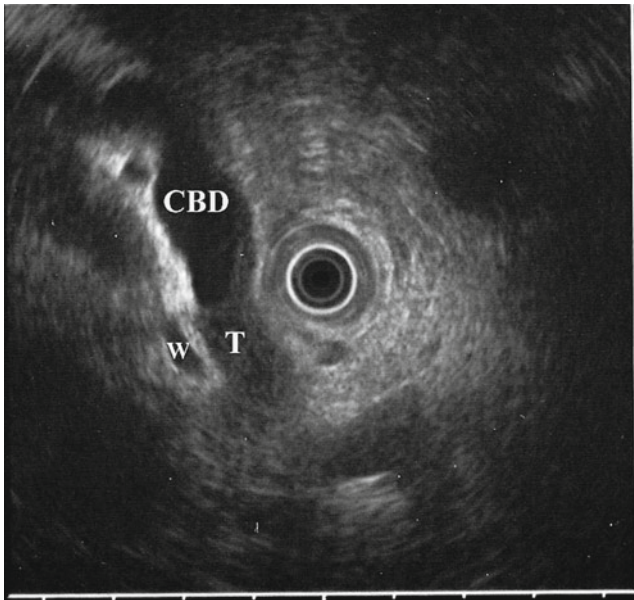


Fig. 14. Radial EUS image (7.5 MHz) showing a T3 cholangiocarcinoma (T) that invades the pancreas and causes upstream dilation of the common bile duct (CBD). The Wirsung's duct (W) is not dilated.

to erroneous preoperative diagnosis of metastases as primary hilar cholangiocarcinomas (64). As bile duct resection incurs 50% morbidity and a significant mortality (5–10% for hilar lesions, less for those treated by pancreaticoduodenectomy) (55), this possibility cannot be neglected.

The results of EUS-FNA have been reported to have a positive impact on patient management in 17–84% of patients in different series (43, 46, 48). Examples of management shift included avoidance of planned surgery in patients with previously undiagnosed Hodgkin's disease or hilar metastases (initially confounded as a primary tumor) or demonstration of malignant lymph node involvement. Conversely, the decision to embark on surgery is facilitated if the malignant etiology of a biliary stricture is demonstrated with FNA sampling. In this regard, the theoretical risk of peritoneal tumor seeding during EUS-FNA of hilar tumors (as has been reported after percutaneous transhepatic biliary drainage of cholangiocarcinomas) should be weighed against the potential benefit (65). Based on their personal experience, Gleeson et al. recommended not performing EUS-FNA in patients with a potentially resectable tumor (46).

Intraductal Ultrasonography

INTRODUCTION

Although IDUS does not provide a pathological diagnosis, it is more accurate than ERCP with transpapillary biopsies to distinguish between benign and malignant strictures (accuracy in a comparative study, 90% vs. 67%, respectively; $P < 0.02$) (66). In contrast with standard EUS, IDUS obtains high-resolution images of the bile duct stricture. For example, in a prospective comparative study of 56 patients, IDUS provided a diagnosis in 55/56 (98%) cases, as compared to only 45/56 (80%) cases for EUS ($P < 0.005$), due to the proximal location and/or to the small size of the tumors (59). This difference translated into a higher accuracy of IDUS for diagnosing biliary malignancy as compared with EUS (89% vs. 76%, $P < 0.002$).

DISTINCTION BETWEEN BENIGN AND MALIGNANT STRICTURES

Multiple echoendoscopic features have been proposed to discriminate benign from malignant biliary strictures (67), and this has often created some confusion. By using various combinations of these criteria, the few studies that have evaluated the performance of IDUS in the most relevant population (i.e., patients with a biliary stricture and no culprit mass identified at CT-Scan/magnetic resonance) have found sensitivities between 82 and 89%, and specificities between 64 and 85% (2, 68, 69). However, echoendoscopists were generally unblinded to both clinical data and ERCP findings, and neither the learning curve for biliary IDUS nor the interobserver agreement has been studied. To facilitate the interpretation of IDUS findings, Tamada et al. have identified three features that were independently associated with a malignant diagnosis in a prospective study that included 62 patients (Table 5) (70). If none of these three features were present, the negative predictive value of IDUS for malignancy was close to 90%. On the contrary, when IDUS showed two or three of these features, a final diagnosis of malignancy was made in 97% of cases. This

Table 5
IDUS features independently associated with malignancy
in biliary strictures

Presence of a sessile tumor (intraductal or outside of the bile duct)
Tumor size greater than 10.0 mm
Interrupted wall structure

indicates that patients with 2 IDUS features predictive of malignancy should be managed as having a malignancy even if preoperative pathological findings are benign.

Finally, as IDUS is limited by the lack of pathological diagnosis, some investigators have performed IDUS-directed biopsy sampling (with the IDUS probe and a biopsy forceps introduced together in the working channel of the duodenoscope). Using this approach in 21 patients, Moon et al. reported a higher sensitivity for cancer diagnosis with IDUS-guided in comparison with fluoroscopically-guided biopsy (83% vs. 56%, $P=0.14$) (71). New techniques are being developed to facilitate IDUS-guided bile duct biopsy.

STAGING OF CHOLANGIOMAS

Criteria used for staging purposes at IDUS in the largest series were as follows:

- Pancreas invasion was diagnosed if the hyperechoic layer between the bile duct and the pancreas was lost (72), or if the margin between the tumor and surrounding pancreatic tissue was not smooth (e.g., digitiform indentations) (73)
- Vessel invasion was diagnosed if the vessel-parenchymal sonographic interface was lost or if the tumor was detected within the vessel lumen (72, 73)
- Lymph nodes were considered as malignant if ≥ 2 of the following criteria were present: hypoechogenicity relative to periductal connective tissue, a round configuration, and conspicuous margins (see above comments about the validity of echoendoscopic criteria for assessment of lymph node metastasis) (2)
- Longitudinal tumor extent was assessed by defining tumor limits on the hepatic and duodenal sides as the disappearance of bile duct wall thickening; asymmetric wall thickening was considered a sign of tumor invasion (this should be assessed prior to biliary drainage to avoid stent-induced artifacts) (74).

For T staging, the accuracy of IDUS is superior to that of EUS, with the greatest difference noted for tumors located at the hilum (59). Tamada et al. also reported in pioneer studies, using various types of probes (7.5, 15, 20 and 30 MHz) a very high accuracy for T staging and for the diagnosis of vascular invasion (T staging, 82%; portal vein invasion, 100%; right hepatic artery invasion, 100%) (26, 27). These results were confirmed by other authors who reported accuracies close to 90% for the assessment of pancreas and portal vein invasion (the portal vein and the right hepatic artery are the most frequently invaded vessels, while the left and common hepatic arteries are less frequently invaded)

(72, 75–77). Compared to angiography, IDUS yielded slightly better results for the assessment of hepatic artery and portal vein invasion (nonsignificant differences) (75, 76). Resectability is better predicted by IDUS than by EUS (59).

For N staging, IDUS presents a lower accuracy than EUS, even without FNA (43% vs. 63%; $P < 0.05$). Due to the limited penetration depth (< 2 cm) of IDUS probes, this technique is currently considered as unreliable for complete lymph node assessment (59, 73). EUS coupled with FNA of lymph nodes is more useful for this purpose (46, 78).

The longitudinal extent of cholangiocarcinomas is a critical factor for the planning of surgical resection. IDUS coupled with biopsy sampling is likely the best technique currently available to assess this parameter. In a prospective study of 19 patients with a cholangiocarcinoma investigated by IDUS immediately after biliary cannulation, longitudinal spread was correctly assessed by IDUS in 84% of cases vs. 47% with ERC ($P < 0.05$) (74). Other studies have reported slightly less favorable results with IDUS, including 3D-IDUS (72). To overcome the shortcomings of IDUS, some authors have recently proposed to combine IDUS with transpapillary biopsy sampling: in a prospective study of 44 patients with a cholangiocarcinoma investigated preoperatively, the longitudinal tumor extent was correctly assessed on the hepatic and duodenal sides with IDUS in, respectively, 77 and 61% of cases. In the same patients, the corresponding figures with IDUS plus biopsy sampling were 93 and 82%, respectively (both P values < 0.05) (79).

Particular Case: Primary Sclerosing Cholangitis

The risk of developing a cholangiocarcinoma is markedly elevated in patients with PSC compared to the general population (prevalence, 5–36%, depending on the methods used for screening and follow-up duration) (80–82). As the development of a cholangiocarcinoma is not reliably heralded by symptomatic changes, surveillance strategies have been proposed for PSC patients. These include standard liver biochemistries every 3 months and dosage of serum tumor markers (CA 19-9 and CEA) plus magnetic resonance every 6 months. Worsening of liver biochemistries, elevation of the CA 19-9 above 200 IU/mL and/or CEA above 5 ng/mL, or the development of a new dominant stricture at magnetic resonance (i.e., a stricture < 1.5 mm on the CBD and/or < 1.0 mm on the common hepatic duct within 2 cm of the bifurcation) should prompt referral for ERCP and biliary sampling (56). IDUS may be performed at this time (no large series of PSC patients investigated with EUS has been reported to date).

The interpretation of 2 IDUS images in PSC patients may be difficult because the bile duct wall is thickened (at a mean of 2.5 mm vs. 0.6–0.8 mm in normal subjects) (7, 8), but this thickening is uniform along the extrahepatic bile ducts. In 34 PSC patients (41% of whom had a final diagnosis of malignancy), IDUS had a sensitivity and specificity for cancer detection of 77% and 55%, i.e. lower than those reported in 52 non-PSC patients in the same series (97% [P<0.05] and 74% [NS], respectively) (68). In that study, malignancy was diagnosed at IDUS if any one of the three following criteria was met: (1) hypoechoic stricture with irregular outer margin; (2) hypoechoic stricture with regular outer margin and one or both of the following: (a) abnormal stricture morphology (asymmetry, notching, or shelf-like), or (b) suspicious lymph nodes (hypoechoic, round, and smooth-border); or (3) stricture of intermediate echogenicity with irregular outer margin and one or both of following: (a) abnormal stricture morphology (asymmetry, notching, or shelf-like), or (b) suspicious lymph nodes (hypoechoic, round, and smooth border). The authors did not discuss why they chose criteria different from those listed in Table 5, but they explained that the comparison of strictures relative to one another allowed to make subjective diagnoses that were more accurate (sensitivity, 64%; specificity, 95%) than those strictly based on these three criteria.

Hyodo et al. have reported in a small case-series that the US contrast agents could help to differentiate PSC from cholangiocarcinoma (bile duct wall enhancement was observed 2 min after Levovist injection in sclerosing cholangitis but not in cholangiocarcinoma) (83). This approach merits further investigation with the US contrast agents of the current generation.

Therapeutic EUS for Biliary Strictures

PREAMBLE

Although EUS-guided biliary drainage seems promising, comparison with the current standard in case of ERCP failure, i.e., percutaneous drainage, has not yet been reported. Therefore, this technique should be reserved in patients in whom an endoscopist highly skilled at ERCP has failed to deeply cannulate the bile duct. An endoscopist skilled at both EUS and ERCP should perform EUS-guided biliary drainage, with interventional radiologists/biliary surgeons available in case of failure or complications. In hospitals where percutaneous biliary drainages are performed by radiologists, EUS-guided biliary drainage presents the advantage of requiring no coordination between interventional radiologists and endoscopists.

TECHNIQUE

See Chap. 16.

RESULTS

Eleven case series totaling 70 patients treated by EUS-guided biliary drainage have been published to date, with the largest experience reported by Kahaleh et al. (84–93). Overall, biliary drainage was successful in >90% of cases, with failures mostly related to difficulties in advancing the guidewire through the stricture. In one third of cases, a rendezvous procedure was performed and in two thirds of cases a stent was inserted into the bilioenteric access. Complications were reported in 11% of cases, and included cases of bile leak causing ascites and fever treated by paracentesis (extrahepatic approach), spontaneously resolving pneumoperitoneum, and cholangitis. Hemobilia was remarkably infrequent when the transhepatic route was used; this is likely related to the use of Doppler guidance to access the bile ducts.

GALLBLADDER

Normal Findings

Two or three layers are identified at EUS of the gallbladder wall. The inner hypoechoic layer corresponds to the mucosa, muscularis propria, and connective tissue of the subserosa (in some patients, little connective fibrous tissue is present and this layer mainly represents the muscularis propria); the outer hyperechoic layer represents the subserosal adipose tissue and serosa; if an additional (innermost) hyperechoic layer is visualized, it is associated with an echo interface or with the mucosa (94, 95). The thickness of the gallbladder wall is measured at a right angle to the transducer beam; it varies with its degree of distension but in a fasting patient the upper limit of normal is 3.5 mm (96).

Stones

EUS excels for the detection of gallbladder stones that are difficult to detect at percutaneous US due to their small size (<3 mm in diameter), location in the cystic duct, or because of the interposition of adipose tissue in obese patients. EUS is most beneficial in patients with “idiopathic” pancreatitis: in a study of 18 patients with negative findings at percutaneous US, 14 (78%) patients were found to have gallbladder

stones at EUS (36). In another study performed in patients with suspected gallbladder stones and ≥ 2 normal percutaneous US examinations, the sensitivity and specificity of EUS for the diagnosis of gallbladder stones were 96 and 86%, respectively (97).

Polypoid Lesions

DESCRIPTION

Gallbladder polypoid lesions (GBP), defined as lesions that protrude from the wall of the gallbladder into its lumen, are devoid from acoustic shadow and do not move with gravity or manipulation. Their presence should be confirmed by a second examination because GBP may be confused with a sludge ball or a blood clot (98, 99). According to two percutaneous US studies conducted in >6,000 subjects, the prevalence of GBP ranges between 4.5 and 6.9% of healthy subjects, with 85% of GBP being ≤ 5 mm in diameter (99, 100).

Lesions reported as GBP correspond to a spectrum of histopathological findings (Table 6):

- Cholesterol polyps account for the majority of GBP; they have no malignant potential and require no follow-up (101, 102). At pathological examination, they are often multiple and correspond to an accumulation of lipid-laden macrophages covered by a normal epithelium. At EUS, they are typically round or slightly lobulated, homogeneous, hyperechoic relative to liver parenchyma, and <10 mm in diameter.

Table 6
Principal histopathological findings associated with gallbladder polypoid lesions

Neoplastic
Malignant: adenocarcinoma, metastases
Benign: adenoma (rarely, leiomyoma, lipoma, hemangioma, hamartoma, neurofibroma, paragangliomas)
Non-neoplastic
Cholesterol polyp
Adenomyoma
Inflammatory polyp
Heterotopias (gastric, pancreatic)

Adapted from Albores-Saavedra et al. (135)

They may be difficult to distinguish from nonshadowing adherent stones. Large cholesterol polyps are typically pedunculated masses with a granular surface and contain hyperechoic spots corresponding to aggregates of foamy macrophages (103, 104).

- Adenomyomatous polyps, also called adenomyomas, are a variant of adenomyomatosis (an excessive proliferation of the biliary epithelium with invaginations into the thickened muscularis or beyond that may be diffuse, segmental, or focal, forming polyps). Gallbladder adenomyomatosis is common (2–33% of consecutive cholecystectomy specimens) and adenomyomas have been reported in up to 7% of unselected autopsies (105). At EUS, gallbladder adenomyomas appear as fundal masses that contain round anechoic or echogenic foci (corresponding to intramural diverticulae filled with bile or sludge, respectively), and may harbor a typical “comet tail” artifact originating from echogenic foci (106).
- Neoplasms account for up to 15% of all GBP (107). The distinction at EUS between the two most frequent forms, adenoma and adenocarcinoma, is not fundamental because adenomas may follow the adenoma-carcinoma sequence (108) and thus also need to be removed. At EUS, adenomas are typically smoothly marginated, intraluminal, sessile or pedunculated, polypoid masses. They are generally homogeneously hyperechoic (103), but larger polyps tend to be less echogenic and more heterogeneous (109). Adenocarcinomas are pedunculated or sessile, hypo- to isoechoic, homogeneous or heterogeneous masses (110, 111).

ROLE OF EUS IN THE MANAGEMENT OF GALLBLADDER POLYPOID LESIONS

Most authors have advocated cholecystectomy for GBP if these were (1) >10 mm in diameter, or (2) associated with gallstones or (3) found in patients >50 years (plus, more recently, in patients with PSC, although this is debated) (112, 113). Even though the morbidity of cholecystectomy is acceptable, findings at surgery argue in favor of a preoperative diagnosis more refined than simply assessing the GBP size and the presence or absence of gallbladder stones. This applies mainly for GBP in the 5–15 mm range because most GBPs <5 mm are non-neoplastic and most GBPs >15 mm are neoplastic (103, 111, 114, 115). In contrast, findings in the 5–15 mm range are mixed: adenomas and adenocarcinomas account for 8–29% of GBP measuring 5–10 mm, and non-neoplastic (mainly cholesterol) polyps account for 53–75% of GBP measuring 11–15 mm (104, 111, 114).

EUS is more effective than percutaneous US to image GBPs because it uses higher frequencies and, hence, has a higher resolution: Sugiyama

et al. have correctly diagnosed neoplastic vs. non-neoplastic GBPs in 97% vs. 71% of cases at EUS vs. percutaneous US, respectively ($P < 0.0001$), while using identical diagnostic criteria (115). Sadamoto et al. have identified in a retrospective EUS study three factors that were independently associated with a neoplastic (adenoma or adenocarcinoma) diagnosis in GBP < 20 mm in diameter, namely, the absence of internal hyperechoic spot, the presence of a heterogeneous echotexture and a greater maximum size (114). Based on these findings, scores were constructed to help differentiating neoplastic vs. non-neoplastic GBP (as was also done by Choi et al. (111)), but these scores are not very practical to use and have not been validated prospectively. (116) Therefore, it has been suggested that, in cases where GBPs appear different from either a cholesterol polyp (i.e., single tiny echogenic spot or containing at least a partial aggregation of echogenic spots) or an adenomyoma (i.e., containing multiple microcysts or with a comet tail artifact) at EUS, should be removed surgically. Other GBPs should be followed-up by percutaneous US every 6–12 months (104).

Finally, the ethnic origin of patients is likely an important factor that has been overlooked until recently. Gallbladder cancer is known to be more prevalent in Indians, American Indians, Japanese, and in some countries of Central and Eastern Europe (117). Based on a retrospective review of $> 70,000$ reports of percutaneous US, it has been calculated that, for similar gallbladder lesions, cholecystectomy would allow to detect an early cancer in 1/13 Indian patients vs. 1/670 Caucasian patients (117, 118).

Carcinoma

Gallbladder carcinoma (GBC) is the most common malignancy of the biliary tract. It may present as a GBP, a complex mass filling the gallbladder, or a wall thickening; this latter form represents 18% of GBC (119), and is difficult to differentiate from xanthogranulomatous cholecystitis and adenomyomatosis (120). GBC frequently invades the liver because of the continuity between the perimuscular connective tissue of the gallbladder and the interlobular connective tissue of the liver, and it disseminates to lymph nodes early in the course of the disease (even to nodes posterior to the portal vein or pancreatic head) (121, 122). Therefore, GBC is usually detected at an advanced stage and it has long had the reputation of having an extremely poor prognosis (except when it is discovered incidentally on a cholecystectomy specimen). Recently, progresses made in techniques of hepatic resection have allowed proposing a more aggressive surgical approach, and this has translated into

longer survivals. For T2 tumors, extended cholecystectomy (including resection of hepatic segments IV and V) plus extensive lymph node dissection are associated with 90–100% survivals at 3 years, as compared to 20–40% after a simple cholecystectomy. Importantly, simple cholecystectomy is sufficient for T1 tumors (at least T1a), and provides an almost 100% cure rate (123–125). It is thus of paramount importance to distinguish between T1 and T2 tumors preoperatively (i.e., cancer invasion limited to the muscle layer or to the perimuscular connective tissue).

The current, seventh edition of the TNM classification of GBC is shown in Table 7 (126). The main changes from the sixth edition is that the cystic duct is now included in the classification scheme, and the N classification now distinguishes hilar nodes (N1) from other regional nodes (N2). Although the majority of EUS studies have used the previous, fifth edition of the TNM classification, their results remain valid because the two categories that underwent modifications (T3 and T4) had been grouped in these EUS studies. Two retrospective studies have analyzed a total of 80 patients with GBC. Lesions were classified into four types, based on tumor characteristics (shape and surface) and

Table 7
2010 AJCC TNM classification of gallbladder carcinomas

T category	
Tis	Carcinoma in situ
T1a	Tumor invades lamina propria
T1b	Tumor invades muscle layer
T2	Tumor invades perimuscular connective tissue (no extension beyond serosa or into liver)
T3	Tumor perforates serosa and/or invades the liver and/or one other adjacent organ ^a
T4	Tumor invades main portal vein or hepatic artery or invades multiple extrahepatic organs or structures
N category	
N0	No regional lymph-node metastasis
N1	Metastases to nodes along the cystic duct, common bile duct, hepatic duct, hepatic artery, and/or portal vein
N2	Metastases to periaortic, pericaval, superior mesenteric artery, and/or celiac artery lymph nodes

^aFor example, stomach, duodenum, colon, pancreas, omentum, extrahepatic bile ducts

integrity of the outer hyperechoic layer of the gallbladder (127, 128). In the first study, the interobserver agreement was analyzed, and this was high (92%) (127). Correspondences between the four types of lesions described at EUS and T categories were proposed: type A (pedunculated mass with preserved adjacent wall structures) as pTis, type B (sessile and/or broad-based mass with a preserved outer hyperechoic layer of the gallbladder wall) as pT1, type C (sessile and/or broad-based mass with a narrowed outer hyperechoic layer) as pT2, and type D (sessile and/or broad-based mass with a disrupted outer hyperechoic layer) as pT3-4 (grouped). Using these correspondences, the accuracy of EUS was as follows: Tis, 100%; T1, 76%; T2, 85%; and T3-4, 93% (128). Distinction between T1 and T2 categories may be difficult because the difference between these two categories may be as slim as invasion up to the muscle layer or to the perimuscular connective tissue. As therapeutic planning between these two categories is markedly different, it is important to recognize a thinned outer hyperechoic layer as indicative of a T2 tumor. Fujimoto et al. have described in a case report another US feature that is suggestive of invasion into the subserosa (T2); this sign was confirmed by other authors to be valuable at EUS in patients with a GBC (it was identified in 11 of 13 patients with a type C lesion) (128).

During EUS, one should also look for previously undetected lymph nodes, liver metastases and carcinomatous ascites because up to 50% of the patients thought to have a resectable disease have metastasis at staging laparoscopy (129). Unfortunately, lymph nodes were not assessed in the two studies that have evaluated the accuracy of EUS staging (127, 128). Indeed, the value of EUS-FNA has not been thoroughly studied in patients with a GBC, likely because lesions located in the gallbladder can easily and safely be removed surgically, and it may not be justifiable to incur the risk of biliary peritonitis (a complication reported with both percutaneous and EUS-guided FNA of the gallbladder) or of a false-negative result (130). Two retrospective studies totaling 12 patients have reported the results of EUS-FNA for a suspected malignant gallbladder mass: no complication occurred, sensitivity for cancer detection was 90%, and lymph node involvement was demonstrated by FNA in three of ten malignant cases (131, 132). As always, FNA might be the most useful, when it demonstrates metastatic involvement of distant lymph nodes.

The role of EUS for staging GBC is challenged by recent advances in noninvasive imaging techniques. For example, 10 years ago, the sensitivity of CT-Scan to detect liver infiltration <2 cm in depth and lymph node metastases were 65 and <50%, respectively (133, 134). Recently, the improved spatial resolution of multidetector CT has

allowed to describe new CT criteria for T staging and to improve its overall accuracy (correct T staging, 84% in a recent retrospective study that included 118 patients) (135). In particular, the sensitivity and specificity for distinguishing T1 vs. \geq T2 lesions in that study were 79 and 99%, respectively (68 patients with pT1 or pT2 lesion were included).

In conclusion, EUS and IDUS are excellent imaging techniques to evaluate the biliary system. Because of its lower complication rate, it is preferred over ERCP for ruling out microlithiasis in somebody with low or intermediate clinical suspicion. EUS has become essential in clinical staging and managements of cholangiocarcinoma and gallbladder cancers.

REFERENCES

1. Technology Assessment Committee, Liu J, Carpenter S, Chuttani R, Croffie J, Disario J, et al. Endoscopic ultrasound probes. *Gastrointest Endosc.* 2006;63:751–4.
2. Stavropoulos S, Larghi A, Verna E, Battezzati P, Stevens P. Intraductal ultrasound for the evaluation of patients with biliary strictures and no abdominal mass on computed tomography. *Endoscopy.* 2005;37:715–21.
3. Sethi A, Chen KY, Austin GL, Brauer BC, Fukami N, Khan AH, et al. ERCP with cholangiopancreatography (CP) is associated with higher rates of endoscopic complications than ERCP alone. *Gastrointest Endosc.* 2008;67:AB102–3.
4. Domagk D, Diallo R, Menzel J, Schleicher C, Bankfalvi A, Gabbert HE, et al. Endosonographic and histopathological staging of extrahepatic bile duct cancer: time to leave the present TNM-classification? *Am J Gastroenterol.* 2005;100:594–600.
5. Noda Y, Fujita N, Kobayashi G, Kimura K, Yago A, Yuki T, et al. Comparison of echograms by a microscanner and histological findings of the common bile duct, in vitro study. *Jpn J Gastroenterol.* 1997;94:172–9.
6. Tamada K, Kanai N, Ueno N, Ichiyama M, Tomiyama T, Wada S, et al. Limitations of intraductal ultrasonography in differentiating between bile duct cancer in stage T1 and stage T2: in-vitro and in-vivo studies. *Endoscopy.* 1997;29:721–5.
7. Tamada K, Tomiyama T, Oohashi A, Aizawa T, Nishizono T, Wada S, et al. Bile duct wall thickness measured by intraductal US in patients who have not undergone previous biliary drainage. *Gastrointest Endosc.* 1999;49:199–203.
8. Mesenas S, Vu C, Doig L, Meenan J. Duodenal EUS to identify thickening of the extrahepatic biliary tree wall in primary sclerosing cholangitis. *Gastrointest Endosc.* 2006;63:403–8.
9. Tamada K, Tomiyama T, Ichiyama M, Oohashi A, Wada S, Nishizono T, et al. Influence of biliary drainage catheter on bile duct wall thickness as measured by intraductal ultrasonography. *Gastrointest Endosc.* 1998;47:28–32.
10. Levy MJ. The hunt for microlithiasis in idiopathic acute recurrent pancreatitis: should we abandon the search or intensify our efforts? *Gastrointest Endosc.* 2002;55:286–93.

11. Jünger C, Kullak-Ublick GA, Jünger D. Gallstone disease: microlithiasis and sludge. *Best Pract Res Clin Gastroenterol.* 2006;20:1053–62.
12. [No authors listed]. Gallstones and laparoscopic cholecystectomy. NIH Consensus Statement. 1992;10:1–28.
13. Everhart J. Digestive diseases in the United States: epidemiology and impact. Bethesda, MD: NIH, NIDDK; 1994. NIH publication no. 94-1447.
14. Soltan HM, Kow L, Toouli J. A simple scoring system for predicting bile duct stones in patients with cholelithiasis. *J Gastrointest Surg.* 2001;5:434–7.
15. Freeman ML, DiSario JA, Nelson DB, Fennerty MB, Lee JG, Bjorkman DJ, et al. Risk factors for post-ERCP pancreatitis: a prospective, multicenter study. *Gastrointest Endosc.* 2001;54:425–34.
16. Mazen Jamal M, Yoon EJ, Saadi A, Sy TY, Hashemzadeh M. Trends in the utilization of endoscopic retrograde cholangiopancreatography (ERCP) in the United States. *Am J Gastroenterol.* 2007;102:966–75.
17. Buscarini E, Tansini P, Vallisa D, Zambelli A, Buscarini L. EUS for suspected choledocholithiasis: do benefits outweigh costs? A prospective, controlled study. *Gastrointest Endosc.* 2003;57:510–8.
18. Solis-Caxaj CA. Treatment of Mirizzi syndrome. *J Am Coll Surg.* 2007;205:518–9.
19. Tse F, Liu L, Barkun A, Armstrong D, Moayyedi P. EUS: a meta-analysis of test performance in suspected choledocholithiasis. *Gastrointest Endosc.* 2008;67:235–44.
20. Garrow D, Miller S, Sinha D, Conway J, Hoffman BJ, Hawes RH, et al. Endoscopic ultrasound: a meta-analysis of test performance in suspected biliary obstruction. *Clin Gastroenterol Hepatol.* 2007;5:616–23.
21. Frossard JL, Hadengue A, Amouyal G, Choury A, Marty O, Giostra E, et al. Choledocholithiasis: a prospective study of spontaneous common bile duct stone migration. *Gastrointest Endosc.* 2000;51:175–9.
22. Ainsworth AP, Rafaelsen SR, Wamberg PA, Durup J, Pless TK, Mortensen MB. Is there a difference in diagnostic accuracy and clinical impact between endoscopic ultrasonography and magnetic resonance cholangiopancreatography? *Endoscopy.* 2003;35:1029–32.
23. Aubé C, Delorme B, Yzet T, Burtin P, Lebigot J, Pessaux P, et al. MR cholangiopancreatography versus endoscopic sonography in suspected common bile duct lithiasis: a prospective, comparative study. *AJR Am J Roentgenol.* 2005;184:55–62.
24. de Lédinghen V, Lecesne R, Raymond JM, Gense V, Amouretti M, Drouillard J, et al. Diagnosis of choledocholithiasis: EUS or magnetic resonance cholangiography? A prospective controlled study. *Gastrointest Endosc.* 1999;49:26–31.
25. Kondo S, Takada T, Miyazaki M, Miyakawa S, Tsukada K, Nagino M, et al. Guidelines for the management of biliary tract and ampullary carcinomas: surgical treatment. *J Hepatobiliary Pancreat Surg.* 2008;15:41–54.
26. Materne R, Van Beers BE, Gigot JF, Jamart J, Geubel A, Pringot J, et al. Extrahepatic biliary obstruction: magnetic resonance imaging compared with endoscopic ultrasonography. *Endoscopy.* 2000;32:3–9.
27. Scheiman JM, Carlos RC, Barnett JL, Elta GH, Nostrant TT, Chey WD, et al. Can endoscopic ultrasound or magnetic resonance cholangiopancreatography replace

- ERCP in patients with suspected biliary disease? A prospective trial and cost analysis. *Am J Gastroenterol.* 2001;96:2900–4.
28. Schmidt S, Chevallier P, Novellas S, Gelsi E, Vanbiervliet G, Tran A, et al. Choledocholithiasis: repetitive thick-slab single-shot projection magnetic resonance cholangiopancreatography versus endoscopic ultrasonography. *Eur Radiol.* 2007;17:241–50.
 29. Fernandez-Esparrach G, Gines A, Sanchez M, Pages M, Pellise M, Fernandez-Cruz L, et al. Comparison of endoscopic ultrasonography and magnetic resonance cholangiopancreatography in the diagnosis of pancreatobiliary diseases: a prospective study. *Am J Gastroenterol.* 2007;102:1632–9.
 30. Verma D, Kapadia A, Eisen GM, Adler DG. EUS vs MRCP for detection of choledocholithiasis. *Gastrointest Endosc.* 2006;64:248–54.
 31. Arguedas MR, Dupont AW, Wilcox CM. Where do ERCP, endoscopic ultrasound, magnetic resonance cholangiopancreatography, and intraoperative cholangiography fit in the management of acute biliary pancreatitis? A decision analysis model. *Am J Gastroenterol.* 2001;96:2892–9.
 32. McMahon CJ. The relative roles of magnetic resonance cholangiopancreatography (MRCP) and endoscopic ultrasound in diagnosis of common bile duct calculi: a critically appraised topic. *Abdom Imaging.* 2008;33:6–9.
 33. Wilcox CM, Varadarajulu S, Eloubeidi M. Role of endoscopic evaluation in idiopathic pancreatitis: a systematic review. *Gastrointest Endosc.* 2006;63:1037–45.
 34. Kohut M, Nowak A, Nowakowska-Duława E, Kaczor R, Marek T. The frequency of bile duct crystals in patients with presumed biliary pancreatitis. *Gastrointest Endosc.* 2001;54:37–41.
 35. Frossard JL, Sosa-Valencia L, Amouyal G, Marty O, Hadengue A, Amouyal P. Usefulness of endoscopic ultrasonography in patients with “idiopathic” acute pancreatitis. *Am J Med.* 2000;109:196–200.
 36. Liu CL, Lo CM, Chan JK, Poon RT, Fan ST. EUS for detection of occult cholelithiasis in patients with idiopathic pancreatitis. *Gastrointest Endosc.* 2000;51:28–32.
 37. Norton SA, Alderson D. Endoscopic ultrasonography in the evaluation of idiopathic acute pancreatitis. *Br J Surg.* 2000;87:1650–5.
 38. Tandon M, Topazian M. Endoscopic ultrasound in idiopathic acute pancreatitis. *Am J Gastroenterol.* 2001;96:705–9.
 39. Yusoff IF, Raymond G, Sahai AV. A prospective comparison of the yield of EUS in primary vs. recurrent idiopathic acute pancreatitis. *Gastrointest Endosc.* 2004;60:673–8.
 40. Frei GJ, Frei VT, Thirlby RC, McClelland RN. Biliary pancreatitis: clinical presentation and surgical management. *Am J Surg.* 1986;151:170–5.
 41. Goodman AJ, Neoptolemos JP, Carr-Locke DL, Finlay DB, Fossard DP. Detection of gall stones after acute pancreatitis. *Gut.* 1985;26:125–32.
 42. Lee JH, Salem R, Aslanian H, Chacho M, Topazian M. Endoscopic ultrasound and fine-needle aspiration of unexplained bile duct strictures. *Am J Gastroenterol.* 2004;99:1069–73.
 43. Fritscher-Ravens A, Broering DC, Knoefel WT, Rogiers X, Swain P, Thonke F, et al. EUS-guided fine-needle aspiration of suspected hilar cholangiocarcinoma in potentially operable patients with negative brush cytology. *Am J Gastroenterol.* 2004;99:45–51.

44. Romagnuolo J, Bardou M, Rahme E, Joseph L, Reinhold C, Barkun AN. Magnetic resonance cholangiopancreatography: a meta-analysis of test performance in suspected biliary disease. *Ann Intern Med.* 2003;139:547–57.
45. Faigel DO. EUS in patients with benign and malignant lymphadenopathy. *Gastrointest Endosc.* 2001;53:593–8.
46. Gleeson F, Rajan E, Levy M, Clain J, Topazian M, Harewood G, et al. EUS-guided FNA of regional lymph nodes in patients with unresectable hilar cholangiocarcinoma. *Gastrointest Endosc.* 2008;67:438–43.
47. DeWitt J, Misra VL, Leblanc JK, McHenry L, Sherman S. EUS-guided FNA of proximal biliary strictures after negative ERCP brush cytology results. *Gastrointest Endosc.* 2006;64:325–33.
48. Eloubeidi MA, Chen VK, Jhala NC, Eltoum IE, Jhala D, Chhieng DC, et al. Endoscopic ultrasound-guided fine needle aspiration biopsy of suspected cholangiocarcinoma. *Clin Gastroenterol Hepatol.* 2004;2:209–13.
49. Meara RS, Jhala D, Eloubeidi MA, Eltoum I, Chhieng DC, Crowe DR, et al. Endoscopic ultrasound-guided FNA biopsy of bile duct and gallbladder: analysis of 53 cases. *Cytopathology.* 2006;17:42–9.
50. Rösch T, Hofrichter K, Frimberger E, Meining A, Born P, Weigert N, et al. ERCP or EUS for tissue diagnosis of biliary strictures? A prospective comparative study. *Gastrointest Endosc.* 2004;60:390–6.
51. Byrne MF, Gerke H, Mitchell RM, Stiffler HL, McGrath K, Branch MS, et al. Yield of endoscopic ultrasound-guided fine-needle aspiration of bile duct lesions. *Endoscopy.* 2004;36:715–9.
52. Dumonceau JM. Biliary ERCP. *Endoscopy.* 2008;40:50–4.
53. Dumonceau JM, Macias Gomez C, Casco C, Genevay M, Marcolongo M, Bongiovanni M, et al. Grasp or brush for biliary sampling at endoscopic retrograde cholangiography? A blinded randomized controlled trial. *Am J Gastroenterol.* 2008;103:333–40.
54. DeOliveira ML, Cunningham SC, Cameron JL, Kamangar F, Winter JM, Lillemoen KD, et al. Cholangiocarcinoma: thirty-one-year experience with 564 patients at a single institution. *Ann Surg.* 2007;245:755–62.
55. Tsao JI, Nimura Y, Kamiya J, Hayakawa N, Kondo S, Nagino M, et al. Management of hilar cholangiocarcinoma: comparison of an American and a Japanese experience. *Ann Surg.* 2000;232:166–74.
56. Yachimski P, Pratt DS. Cholangiocarcinoma: natural history, treatment, and strategies for surveillance in high-risk patients. *J Clin Gastroenterol.* 2008;42:178–90.
57. Nishio H, Nagino M, Oda K, Ebata T, Arai T, Nimura Y. TNM classification for perihilar cholangiocarcinoma: comparison between 5th and 6th editions of the AJCC/UICC staging system. *Langenbecks Arch Surg.* 2005;390:319–27.
58. Tio TL, Cheng J, Wijers OB, Sars PR, Tytgat GN. Endosonographic TNM staging of extrahepatic bile duct cancer: comparison with pathological staging. *Gastroenterology.* 1991;100:1351–61.
59. Menzel J, Poremba C, Dietl KH, Domschke W. Preoperative diagnosis of bile duct strictures – comparison of intraductal ultrasonography with conventional endosonography. *Scand J Gastroenterol.* 2000;35:77–82.
60. Kahaleh M, Mishra R, Shami VM, Northup PG, Berg CL, Bashlor P, et al. Unresectable cholangiocarcinoma: comparison of survival in biliary stenting

- alone versus stenting with photodynamic therapy. *Clin Gastroenterol Hepatol.* 2008;6:290–7.
61. Ortner ME, Caca K, Berr F, Liebetruhl J, Mansmann U, Huster D, et al. Successful photodynamic therapy for nonresectable cholangiocarcinoma: a randomized prospective study. *Gastroenterology.* 2003;125:1355–63.
 62. Gerhards MF, Vos P, van Gulik TM, Rauws EA, Bosma A, Gouma DJ. Incidence of benign lesions in patients resected for suspicious hilar obstruction. *Br J Surg.* 2001;88:48–51.
 63. Wolfson D, Barkin JS, Chari ST, Clain JE, Bell RH, Alexakis N, et al. Management of pancreatic masses. *Pancreas.* 2005;31:203–17.
 64. Wetter LA, Ring EJ, Pellegrini CA, Way LW. Differential diagnosis of sclerosing cholangiocarcinomas of the common hepatic duct (Klatskin tumors). *Am J Surg.* 1991;161:57–63.
 65. Chapman WC, Sharp KW, Weaver F, Sawyers JL. Tumor seeding from percutaneous biliary catheters. *Ann Surg.* 1989;209:708–15.
 66. Vazquez-Sequeiros E, Baron TH, Clain JE, Gostout CJ, Norton ID, Petersen BT, et al. Evaluation of indeterminate bile duct strictures by intraductal US. *Gastrointest Endosc.* 2002;56:372–9.
 67. Tamada K, Ueno N, Tomiyama T, Oohashi A, Wada S, Nishizono T, et al. Characterization of biliary strictures using intraductal ultrasonography: comparison with percutaneous cholangioscopic biopsy. *Gastrointest Endosc.* 1998;47:341–9.
 68. Levy MJ, Baron TH, Clayton AC, Enders FB, Gostout CJ, Halling KC, et al. Prospective evaluation of advanced molecular markers and imaging techniques in patients with indeterminate bile duct strictures. *Am J Gastroenterol.* 2008;103:1263–73.
 69. Varadarajulu S, Eloubeidi MA, Wilcox CM. Prospective evaluation of indeterminate ERCP findings by intraductal ultrasound. *J Gastroenterol Hepatol.* 2007;22:2086–92.
 70. Tamada K, Tomiyama T, Wada S, Ohashi A, Satoh Y, Ido K, et al. Endoscopic transpapillary bile duct biopsy with the combination of intraductal ultrasonography in the diagnosis of biliary strictures. *Gut.* 2002;50:326–31.
 71. Moon JH, Choi HJ, Kim HK, Kwon KW, Cheon YK, Cho YD, et al. The usefulness of IDUS-guided transpapillary bile duct biopsy for the diagnosis of malignant biliary strictures. *Gastrointest Endosc.* 2008;67:AB208.
 72. Inui K, Yoshino J, Okushima K, Miyoshi H, Nakamura Y. Intraductal EUS. *Gastrointest Endosc.* 2002;56:S58–62.
 73. Tamada K, Ido K, Ueno N, Kimura K, Ichiyama M, Tomiyama T. Preoperative staging of extrahepatic bile duct cancer with intraductal ultrasonography. *Am J Gastroenterol.* 1995;90:239–46.
 74. Tamada K, Nagai H, Yasuda Y, Tomiyama T, Ohashi A, Wada S, et al. Transpapillary intraductal US prior to biliary drainage in the assessment of longitudinal spread of extrahepatic bile duct carcinoma. *Gastrointest Endosc.* 2001;53:300–7.
 75. Tamada K, Ido K, Ueno N, Ichiyama M, Tomiyama T, Nishizono T, et al. Assessment of hepatic artery invasion by bile duct cancer using intraductal ultrasonography. *Endoscopy.* 1995;27:579–83.

76. Tamada K, Ido K, Ueno N, Ichiyama M, Tomiyama T, Nishizono T, et al. Assessment of portal vein invasion by bile duct cancer using intraductal ultrasonography. *Endoscopy*. 1995;27:573–8.
77. Inui K, Miyoshi H, Yoshino J. Bile duct cancers: what can EUS offer? Intraductal us, 3d-IDUS? FNA – is it possible? *Endoscopy*. 2006;38:47–9.
78. Pollack MJ, Gholam PM, Chak A. EUS-FNA in unresectable cholangiocarcinoma: a novel indication. *Gastrointest Endosc*. 2008;67:444–5.
79. Noda Y, Fujita N, Kobayashi G, Ito K, Horaguchi J, Takasawa O, et al. Prospective study of intraductal ultrasonography before biliary drainage (IDUS-BD), transpapillary biopsy (TPB) and peroral cholangioscopy (POCS) in assessment of the longitudinal extent of bile duct cancer. *Gastrointest Endosc*. 2008;67:AB156–7.
80. Burak K, Angulo P, Pasha TM, Egan K, Petz J, Lindor KD. Incidence and risk factors for cholangiocarcinoma in primary sclerosing cholangitis. *Am J Gastroenterol*. 2004;99:523–6.
81. Farrant JM, Hayllar KM, Wilkinson ML, Karani J, Portmann BC, Westaby D, et al. Natural history and prognostic variables in primary sclerosing cholangitis. *Gastroenterology*. 1991;100:1710–7.
82. Rosen CB, Nagorney DM, Wiesner RH, Coffey RJ, LaRusso NF. Cholangiocarcinoma complicating primary sclerosing cholangitis. *Ann Surg*. 1991;213:21–5.
83. Hyodo T, Hyodo N, Yamanaka T, Imawari M. Contrast-enhanced intraductal ultrasonography for thickened bile duct wall. *J Gastroenterol*. 2001;36:557–9.
84. Ang TL, Teo EK, Fock KM. EUS-guided transduodenal biliary drainage in unresectable pancreatic cancer with obstructive jaundice. *JOP*. 2007;8:438–43.
85. Bories E, Pesenti C, Caillol F, Lopes C, Giovannini M. Transgastric endoscopic ultrasonography-guided biliary drainage: results of a pilot study. *Endoscopy*. 2007;39:287–91.
86. Burmester E, Niehaus J, Leineweber T, Huetteroth T. EUS-cholangio-drainage of the bile duct: report of 4 cases. *Gastrointest Endosc*. 2003;57:246–51.
87. Giovannini M, Moutardier V, Pesenti C, Bories E, Lelong B, Delperro JR. Endoscopic ultrasound-guided bilioduodenal anastomosis: a new technique for biliary drainage. *Endoscopy*. 2001;33:898–900.
88. Kahaleh M, Hernandez AJ, Tokar J, Adams RB, Shami VM, Yeaton P. Interventional EUS-guided cholangiography: evaluation of a technique in evolution. *Gastrointest Endosc*. 2006;64:52–9.
89. Mallery S, Matlock J, Freeman ML. EUS-guided rendezvous drainage of obstructed biliary and pancreatic ducts: report of 6 cases. *Gastrointest Endosc*. 2004;59:100–7.
90. Puspok A, Lomoschitz F, Dejaco C, Hejna M, Sautner T, Gangl A. Endoscopic ultrasound guided therapy of benign and malignant biliary obstruction: a case series. *Am J Gastroenterol*. 2005;100:1743–7.
91. Tarantino I, Barresi L, Repici A, Traina M. EUS-guided biliary drainage: a case series. *Endoscopy*. 2008;40:336–9.
92. Will U, Thieme A, Fueldner F, Gerlach R, Wanzar I, Meyer F. Treatment of biliary obstruction in selected patients by endoscopic ultrasonography (EUS)-guided transluminal biliary drainage. *Endoscopy*. 2007;39:292–5.

93. Yamao K, Bhatia V, Mizuno N, Sawaki A, Ishikawa H, Tajika M, et al. EUS-guided choledochoduodenostomy for palliative biliary drainage in patients with malignant biliary obstruction: results of long-term follow-up. *Endoscopy*. 2008;40:340–2.
94. Fujita NY. Analysis of the layer structure of the gallbladder wall delineated by endoscopic ultrasound using the pinning method. *Dig Endosc*. 1995;7:353–6.
95. Watanabe Y, Goto H, Naitoh Y, Hirooka Y, Itoh A, Taki T, et al. Usefulness of intra-ductal ultrasonography in gallbladder disease. *J Ultrasound Med*. 1998;17:33–9.
96. Engel JM, Deitch EA, Sikkema W. Gallbladder wall thickness: sonographic accuracy and relation to disease. *AJR Am J Roentgenol*. 1980;134:907–9.
97. Dahan P, Andant C, Lévy P, Amouyal P, Amouyal G, Dumont M, et al. Prospective evaluation of endoscopic ultrasonography and microscopic examination of duodenal bile in the diagnosis of cholecystolithiasis in 45 patients with normal conventional ultrasonography. *Gut*. 1996;38:277–81.
98. Cooperberg P, Golding RH. Advances in ultrasonography of the gallbladder and biliary tract. *Radiol Clin N Am*. 1982;20:611–33.
99. Jørgensen T, Jensen KH. Polyps in the gallbladder. A prevalence study. *Scand J Gastroenterol*. 1990;25:281–6.
100. Chen CY, Lu CL, Chang FY, Lee SD. Risk factors for gallbladder polyps in the Chinese population. *Am J Gastroenterol*. 1997;92:2066–8.
101. Kubota K, Bandai Y, Noie T, Ishizaki Y, Teruya M, Makuuchi M. How should polypoid lesions of the gallbladder be treated in the era of laparoscopic cholecystectomy? *Surgery*. 1995;117:481–7.
102. Owen CC, Bilhartz LE. Gallbladder polyps, cholesterosis, adenomyomatosis, and acute acalculous cholecystitis. *Semin Gastrointest Dis*. 2003;14:178–88.
103. Sugiyama M, Atomi Y, Kuroda A, Muto T, Wada N. Large cholesterol polyps of the gallbladder: diagnosis by means of US and endoscopic US. *Radiology*. 1995;196:493–7.
104. Sugiyama M, Atomi Y, Yamato T. Endoscopic ultrasonography for differential diagnosis of polypoid gall bladder lesions: analysis in surgical and follow up series. *Gut*. 2000;46:250–4.
105. Friess H, Holzinger F, Liao Q, Büchler MW. Surveillance of pre-malignant disease of the pancreatico-biliary system. *Best Pract Res Clin Gastroenterol*. 2001;15:285–300.
106. Raghavendra BN, Subramanyam BR, Balthazar EJ, Horii SC, Megibow AJ, Hilton S. Sonography of adenomyomatosis of the gallbladder: radiologic-pathologic correlation. *Radiology*. 1983;146:747–52.
107. Yang HL, Sun YG, Wang Z. Polypoid lesions of the gallbladder: diagnosis and indications for surgery. *Br J Surg*. 1992;79:227–9.
108. Kozuka S, Tsubone N, Yasui A, Hachisuka K. Relation of adenoma to carcinoma in the gallbladder. *Cancer*. 1982;50:2226–34.
109. Levy AD, Murakata LA, Abbott RM, Rohrmann CA. From the archives of the AFIP. Benign tumors and tumorlike lesions of the gallbladder and extrahepatic bile ducts: radiologic-pathologic correlation. *Armed Forces Institute of Pathology. Radiographics*. 2002;22:387–413.
110. Azuma T, Yoshikawa T, Araida T, Takasaki K. Differential diagnosis of polypoid lesions of the gallbladder by endoscopic ultrasonography. *Am J Surg*. 2001;181:65–70.

111. Choi WB, Lee SK, Kim MH, Seo DW, Kim HJ, Kim DI, et al. A new strategy to predict the neoplastic polyps of the gallbladder based on a scoring system using EUS. *Gastrointest Endosc.* 2000;52:372–9.
112. Boulton RA, Adams DH. Gallbladder polyps: when to wait and when to act. *Lancet.* 1997;349:817.
113. Karlsen TH, Schrupp E, Boberg KM. Gallbladder polyps in primary sclerosing cholangitis: not so benign. *Curr Opin Gastroenterol.* 2008;24:395–9.
114. Sadamoto Y, Oda S, Tanaka M, Harada N, Kubo H, Eguchi T, et al. A useful approach to the differential diagnosis of small polypoid lesions of the gallbladder, utilizing an endoscopic ultrasound scoring system. *Endoscopy.* 2002;34:959–65.
115. Sugiyama M, Xie XY, Atomi Y, Saito M. Differential diagnosis of small polypoid lesions of the gallbladder: the value of endoscopic ultrasonography. *Ann Surg.* 1999;229:498–504.
116. Chung JP, Lee SJ, Lee KS, Chung JB, Lee SI, Kang JK. EUS and the prediction of gallbladder neoplastic polyps: are polyps of 5 to 15 mm diameter really a homogenous group? *Gastrointest Endosc.* 2001;54:138–9.
117. Randi G, Franceschi S, La Vecchia C. Gallbladder cancer worldwide: geographical distribution and risk factors. *Int J Cancer.* 2006;118:1591–602.
118. Aldouri A, Malik H, Waytt J, Khan S, Ranganathan K, Kummaraganti S, et al. The risk of gallbladder cancer from polyps in a large multiethnic series. *Eur J Surg Oncol.* 2009;35:48–51. doi:10.1016/j.ejso.2008.01.036.
119. Chijiwa K, Sumiyoshi K, Nakayama F. Impact of recent advances in hepatobiliary imaging techniques on the preoperative diagnosis of carcinoma of the gallbladder. *World J Surg.* 1991;15:322–7.
120. Guermazi A. Are there other imaging features to differentiate xanthogranulomatous cholecystitis from gallbladder carcinoma? *Eur Radiol.* 2005;15:1271–2.
121. Levy AD, Murakata LA, Rohrmann CA. Gallbladder carcinoma: radiologic-pathologic correlation. *Radiographics.* 2001;21:295–314. questionnaire, 549–55.
122. Shirai Y, Yoshida K, Tsukada K, Ohtani T, Muto T. Identification of the regional lymphatic system of the gallbladder by vital staining. *Br J Surg.* 1992;79:659–62.
123. Bartlett DL. Gallbladder cancer. *Semin Surg Oncol.* 2000;19:145–55.
124. Bartlett DL, Fong Y, Fortner JG, Brennan MF, Blumgart LH. Long-term results after resection for gallbladder cancer. Implications for staging and management. *Ann Surg.* 1996;224:639–46.
125. Dixon E, Vollmer CM, Sahajpal A, Cattral M, Grant D, Doig C, et al. An aggressive surgical approach leads to improved survival in patients with gallbladder cancer: a 12-year study at a North American center. *Ann Surg.* 2005;241:385–94.
126. Edge SB, Byrd DR, Compton CC, et al. *AJCC Cancer Staging Manual.* 7th ed. New York: Springer; 2010.
127. Fujita N, Noda Y, Kobayashi G, Kimura K, Yago A. Diagnosis of the depth of invasion of gallbladder carcinoma by EUS. *Gastrointest Endosc.* 1999;50:659–63.
128. Sadamoto Y, Kubo H, Harada N, Tanaka M, Eguchi T, Nawata H. Preoperative diagnosis and staging of gallbladder carcinoma by EUS. *Gastrointest Endosc.* 2003;58:536–41.
129. Weber SM, DeMatteo RP, Fong Y, Blumgart LH, Jarnagin WR. Staging laparoscopy in patients with extrahepatic biliary carcinoma. Analysis of 100 patients. *Ann Surg.* 2002;235:392–9.

130. Jacobson BC, Waxman I, Parmar K, Kauffman JM, Clarke GA, Van Dam J. Endoscopic ultrasound-guided gallbladder bile aspiration in idiopathic pancreatitis carries a significant risk of bile peritonitis. *Pancreatology*. 2002;2:26–9.
131. Jacobson BC, Pitman MB, Brugge WR. EUS-guided FNA for the diagnosis of gallbladder masses. *Gastrointest Endosc*. 2003;57:251–4.
132. Varadarajulu S, Eloubeidi MA. Endoscopic ultrasound-guided fine-needle aspiration in the evaluation of gallbladder masses. *Endoscopy*. 2005;37:751–4.
133. Ootani T, Shirai Y, Tsukada K, Muto T. Relationship between gallbladder carcinoma and the segmental type of adenomyomatosis of the gallbladder. *Cancer*. 1992;69:2647–52.
134. Rodríguez-Fernández A, Gómez-Río M, Medina-Benítez A, Moral JV-D, Ramos-Font C, Ramia-Angel JM, et al. Application of modern imaging methods in diagnosis of gallbladder cancer. *J Surg Oncol*. 2006;93:650–64.
135. Kim SJ, Lee JM, Lee JY, Choi JY, Kim SH, Han JK, et al. Accuracy of preoperative T-staging of gallbladder carcinoma using MDCT. *AJR Am J Roentgenol*. 2008;190:74–80.

The Role of EUS in Rectal Cancer and Fecal Incontinence

*Uzma D. Siddiqui, MD
and Harry R. Aslanian, MD*

CONTENTS

EUS AND RECTAL CANCER

EUS AND FECAL INCONTINENCE

SUMMARY

Abstract

Endoscopic ultrasound (EUS) has emerged as an important imaging tool used in the locoregional staging of rectal cancer and assists in selecting patients with advanced disease that may benefit from neoadjuvant therapy. Studies have shown EUS to have a T staging accuracy of 80–95% and an N staging accuracy of 70–80%. EUS with fine needle aspiration (EUS-FNA) may improve accuracy in staging following surgery or neoadjuvant therapy by providing cytologic confirmation of malignancy. Future developments may include imaging with three-dimensional ultrasound and EUS-guided delivery of chemotherapeutic agents directly into tumors. In the evaluation of fecal incontinence, EUS provides information that is complementary to anorectal manometry and electromyography by providing direct views of the anal sphincter. EUS has been shown to be highly accurate (89–100%) in identifying internal or external anal sphincter defects. Furthermore, EUS has the potential to guide therapy with the delivery of injectable materials to fill sphincter defects.

Key Words: Rectal cancer, Fecal incontinence, Endoscopic ultrasound

From: *Clinical Gastroenterology: Endoscopic Ultrasound*,
Edited by: V. M. Shami and M. Kahaleh, DOI 10.1007/978-1-60327-480-7_15,
© Springer Science+Business Media, LLC 2010

EUS AND RECTAL CANCER

Background

The American Cancer Society predicts that there will be over 40,000 new cases of rectal cancer diagnosed in 2008 (1). The optimal management of rectal cancer is dependent upon accurate staging at the time of diagnosis. Patients with locally advanced disease may benefit from neoadjuvant chemoradiation to reduce tumor burden and perhaps allow for sphincter preserving surgeries. Better disease control has been seen in those patients with locally advanced disease (Tx with N1 or N2; T3 or T4 with N0) who undergo neoadjuvant chemoradiation followed by surgery (2). Furthermore, the Swedish Rectal Cancer Trials showed that preoperative radiotherapy decreased local recurrence rates and improved survival in this patient population (3).

EUS Technique

Rectal endoscopic ultrasound (EUS) has emerged as an important imaging tool in the pretreatment local staging of rectal cancer. Rectal EUS is most commonly performed with a flexible radial scanning echoendoscope, but rigid ultrasound probes can also be used. In our practice, we use a standard colonoscopy preparation and routinely utilize conscious sedation, although a sigmoidoscopy preparation without sedation is also acceptable. The patient is placed in the left lateral decubitus position for the procedure. An oblique viewing echoendoscope is passed up to 35 cm under endoscopic guidance to achieve sonographic visualization of the iliac vessels. We perform the initial imaging with radial echoendoscopes which provide a 360° view and generally utilize a linear echoendoscope when fine needle aspiration (FNA) is performed to sample lymph nodes. The scope is slowly withdrawn to assess for the presence of lymph nodes (N stage). The rectum can be filled with water to enhance acoustic coupling, and the patient may be rotated to completely submerge the rectal tumor. The depth of tumor penetration into the rectal wall is assessed with identification of the mucosa, submucosa, and muscularis propria to complete the T staging.

T Staging

EUS can provide detailed images of the various rectal wall layers and can accurately determine the depth of tumor invasion into the bowel wall to establish the T stage. The new 2010 American Joint Committee on Cancer (AJCC) TNM staging of colon and rectal cancers is shown in

Table 1
2010 American Joint Committee on Cancer (AJCC) TNM staging of colon and rectal cancers

T	Primary tumor
Tx	Primary tumor cannot be assessed
T0	No evidence of primary tumor
Tis	Carcinoma in situ: intraepithelial or invasion of lamina propria
T1	Tumor invades the submucosa
T2	Tumor invades the muscularis propria
T3	Tumor invades through the muscularis propria into perirectal tissues
T4a	Tumor penetrates to the surface of the visceral peritoneum
T4b	Tumor directly invades or is adherent to other organs or structures ^a
N	Regional lymph nodes
NX	Regional lymph nodes cannot be assessed
N0	No regional lymph node metastases
N1	Metastasis in 1–3 regional lymph nodes
N1a	Metastasis in one regional lymph node
N1b	Metastasis in 2–3 regional lymph nodes
N1c	Tumor deposit (s) in the perirectal tissues without regional nodal metastasis
N2	Metastasis in four or more regional lymph nodes
N2a	Metastasis in 4–6 regional lymph nodes
N2b	Metastasis in seven or more regional lymph nodes
M	Distant metastasis
M0	No distant metastasis
M1	Distant metastasis
M1a	Metastasis confined to one organ or site
M1b	Metastases in more than one organ/site or the peritoneum

^aInvasion of the prostate, seminal vesicles, cervix, or vagina
 TNM Classification of Rectal Cancer. Used with the permission of the American Joint Committee on Cancer (AJCC), Chicago, Illinois. The original source for this material is the AJCC Cancer Staging Manual, Seventh Edition (2010) published by Springer Science and Business Media LLC, <http://www.springerlink.com>

Table 1 (4). Figure 1 demonstrates the normal rectal wall layers by EUS. If a tumor involves the mucosal layers or the submucosa, this is a T1 lesion. T2 lesions extend beyond the submucosa and into (but not beyond) the muscularis propria. T3 tumors extend beyond the muscularis propria and into the perirectal tissues but not into adjacent organs (Fig. 2). T4 lesions penetrate beyond the perirectal tissues (Table 1). In males, the prostate and seminal vesicles can be well visualized and their

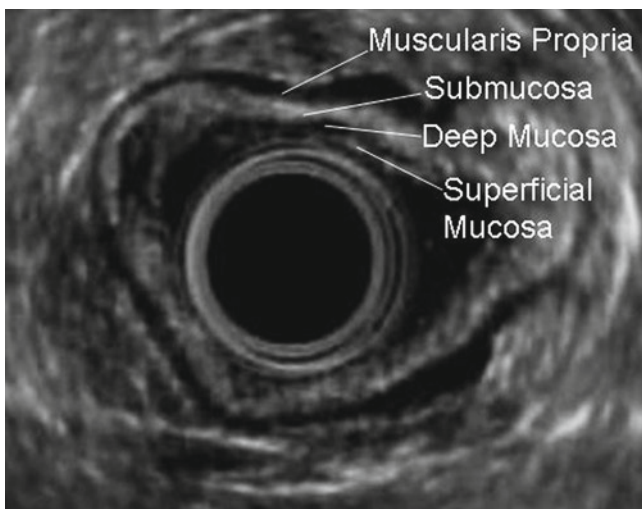


Fig. 1. Radial EUS images of the normal layers of the rectal wall.

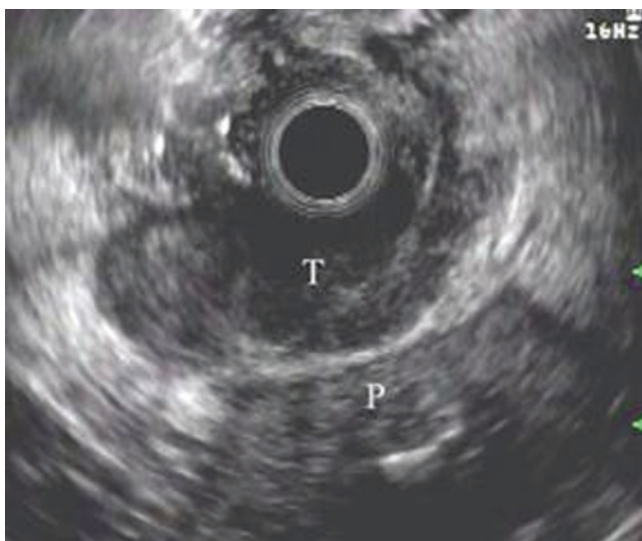


Fig. 2. Radial EUS image of a T3 rectal cancer with the hypoechoic tumor (T) extending beyond the rectal wall into surrounding fat and adjacent to, but separate from, the prostate (P).

relationship to the tumor is defined. Many studies have demonstrated the accuracy of EUS in T staging. Savides and Master examined results from 16 EUS studies (all included at least 70 patients) and calculated an overall EUS T staging accuracy of 83% (5). This review included earlier studies showing high EUS accuracies ranging between 76 and 90% and two more recent studies in 2002 that included over 900 patients and demonstrated lower accuracy rates of 63–69% (6, 7). Multiple comparison studies have shown that EUS has superior T staging accuracy (80–95%) when compared to CT (65–75%) (8–10). A trend toward greater accuracy versus MRI has been identified (MRI 75–85% vs. EUS 85–88%), but more studies are needed in comparison with the newer endorectal coil MRI (11–14). Differentiation between T2 and T3 tumors has presented the greatest challenge to accurate staging. Overstaging of T2 tumors has been occasionally recognized (15, 16). One study prospectively examined 80 patients with newly diagnosed rectal cancer and found that no patients were overstaged as T3 or T4, but 15% of those with T3 disease were actually understaged by EUS (17).

N Staging

Rectal EUS accuracy for regional nodal staging has been demonstrated to be between 70 and 80%, which is less accurate than EUS T staging and not significantly superior to the 65% reported accuracies of CT and MRI (9, 12, 13, 18). The presence of nodal spread is assessed in both the iliac and perirectal regions. The new 2010 AJCC staging system further delineates the N stage by the number of malignant nodes involved since this influences prognosis (Table 1) (4).

It has been previously suggested that simply visualizing lymph nodes in patients with rectal cancer indicated metastatic nodal spread and FNA was not warranted (19). We share this clinical viewpoint, and therefore do not routinely perform FNA of lymph nodes seen during rectal cancer EUS staging. However, the role of FNA in lymph node sampling remains controversial (this is discussed further in the FNA section below).

Fine Needle Aspiration

EUS-guided FNA (EUS-FNA) of visualized nodes performed via a linear echoendoscope may enhance rectal cancer staging accuracy (Figs. 3 and 4). While the addition of FNA has led to improved staging accuracy rates in tumors of the esophagus, pancreas, and lung

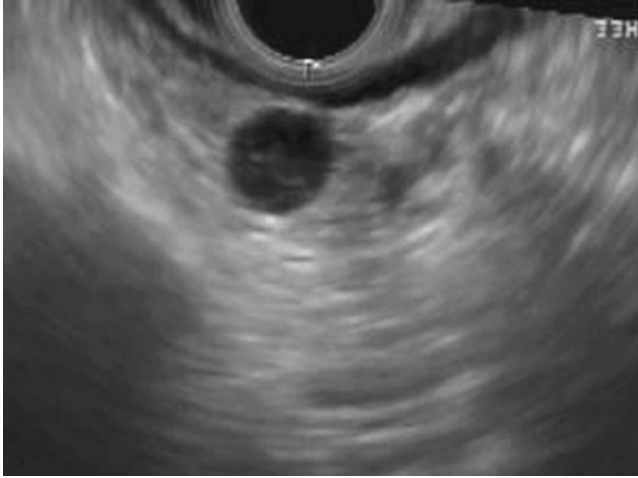


Fig. 3. Linear EUS view of a perirectal lymph node with worrisome features (hypoechoic and round with sharp borders).

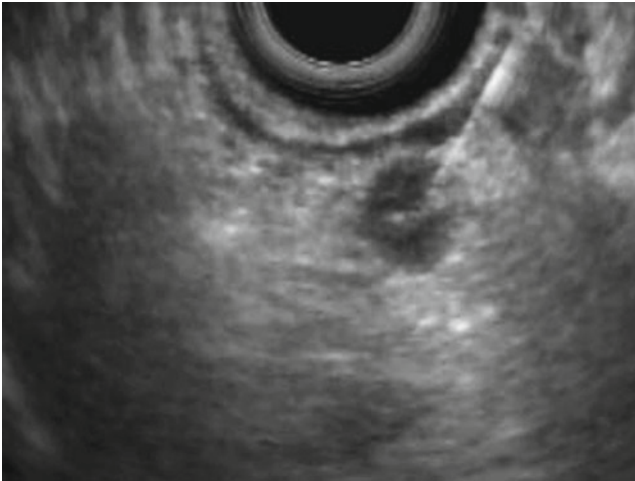


Fig. 4. Fine needle aspiration within the perirectal lymph node. Cytology confirmed the presence of malignancy.

(20–25), this has not been consistently shown with rectal cancer in the past (17, 26). A contributing factor may be that perirectal lymph nodes are usually too small to visualize and may only become significantly enlarged with the involvement of metastatic disease.

Harewood et al. demonstrated that visualization alone on EUS of enlarged perirectal nodes has a higher predictive value for metastases than for nodes elsewhere in the gastrointestinal tract. There were similarly high positive predictive values for both EUS (85%) and EUS-FNA (92%) (17). In esophageal cancer patients, there have been EUS nodal features identified that predict metastatic disease: hypoechoic echotexture, well-rounded shape, smooth/sharp border, and large size (typically >1 cm) (27). However, when these EUS nodal criteria were compared to FNA results in a recently published study by Gleeson et al., only 68% of malignant lymph nodes had ≥ 3 nodal features (28). The need for FNA of visualized lymph nodes will require further study.

EUS-FNA has been shown to be a feasible and safe technique for sampling both intramural and extraintestinal tumors, lymph nodes, and cystic lesions via the upper GI tract with a low risk of bacteremia, and does not routinely require administering prophylactic antibiotics (29–33). In contrast, the rectum is not a sterile field and prophylactic antibiotics are typically given with rectal EUS-FNA, despite the lack of data specifically supporting this practice. Levy et al. identified asymptomatic bacteremia in 2 of 100 patients undergoing EUS-FNA of the lower GI tract and concluded that the procedure should be considered low risk for infectious complications, and does not warrant prophylactic antibiotics for the prevention of bacterial endocarditis (33). Furthermore, if antibiotics are given, there is variation regarding the timing (before, during or after the procedure) and duration (one time dose or continue for 48–72 h following the procedure). Sasaki et al. showed that EUS-FNA of submucosal lesions and masses extrinsic to the rectum and colon could be safely performed without complications when a single dose of antibiotics was given following EUS-FNA (34). In contrast, a recent case report by Mezzi et al. described the formation of a pelvic abscess complicating EUS-FNA of a rectal lesion despite one dose of antibiotics being given during the procedure (35). The patient presented 5 days later complaining of rectal pain and fever, leading the authors to suggest continuing antibiotics for several days following the procedure. The most recent American Society of Gastrointestinal Endoscopy guideline regarding antibiotics prophylaxis for GI endoscopy states that there is “insufficient data to make firm recommendations” for antibiotic prophylaxis during EUS-FNA of solid lesions along the lower GI tract (36). Therefore, endoscopists should assess on a case by case basis. It is currently our practice to give a single dose of antibiotics prior to the performance of rectal EUS-FNA; however, more studies are needed to determine what role, if any, prophylactic antibiotics play in this setting.

Clinical Significance of EUS in Rectal Cancer Staging

Several studies have shown the clinical utility of EUS in the evaluation of rectal cancer. Harewood and Wiersema demonstrated that performing CT along with rectal EUS was the most cost-effective method for staging rectal cancer (37). Although this study showed EUS use to be associated with reduced tumor recurrence, there was no difference in mortality. Shami et al. evaluated 48 patients undergoing preoperative staging with CT and found that the addition of EUS changed management in 38% of the patients (38).

Factors Affecting EUS Accuracy

There are a number of factors that may influence rectal EUS staging accuracy. These include operator experience, stenotic tumors, and radiation therapy. Carmody and Otchy demonstrated a learning curve with rectal EUS, where accuracy rates improve with time (39). The accuracy of transrectal ultrasound staging improved from 58% during the first 12 studies to 87.5% in the remaining 24 exams. Stenotic tumors may prevent the echoendoscope from passing beyond the tumor, restricting the views obtained (40). EUS T staging accuracy has been shown to decrease following chemoradiation due to edema, necrosis, and fibrosis, which may distort the rectal wall architecture with changes that may be indistinguishable from malignancy (40, 41). It has been suggested that an influence of publication bias toward positive studies has led to the overestimation of EUS performance in rectal cancer staging (42); however, this has not been found to be a factor with EUS staging of upper gastrointestinal cancers (43).

Tumor Recurrence

Rectal cancer recurrence often develops outside the rectal wall, which makes early detection with standard endoscopy difficult. Two studies evaluated over 200 patients and showed that EUS is superior to CT in identifying local rectal cancer recurrence (100% detection rate vs. 82–85% detection rate) (44, 45). As previously noted, mucosal inflammation and fibrosis presenting after surgery or radiation therapy can obscure or mimic sonographic changes of tumor recurrence, limiting postradiation T and N staging of EUS. However, EUS-FNA provides cytologic confirmation that can improve accuracy (42). One study of 312 patients showed that accuracy rates for detecting tumor recurrence were higher for EUS-FNA versus EUS alone (92 vs. 75%) (46).

Future EUS Applications in Rectal Cancer

Advanced sonographic imaging has been reported using different forms of three dimensional (3D)-EUS. Some studies have used single rigid 3D-EUS probes, while others utilize standard equipment with 3D reconstruction software. However, the reported data is conflicting as to whether this technology significantly improves staging accuracy versus conventional rectal EUS (47–49). More studies are needed comparing 3D-EUS with standard EUS, CT, and MRI.

EUS may also play a therapeutic role in the future management of rectal cancer based on the studies of other malignancies. As has been shown in pancreatic and esophageal cancers, it is possible that biologic agents may be injected directly into rectal tumors to achieve local control (50). Further studies are needed to evaluate other possible applications of EUS guided therapeutics.

EUS AND FECAL INCONTINENCE

Background

Fecal incontinence is an emotionally devastating ailment where the inability to control bowel movements can cause embarrassment, significantly impact quality of life, and may lead to social isolation. Because of the social stigma attached to this condition, its prevalence is likely underestimated. Reported figures suggest that more than six million people and up to 2.2% of women in the United States are affected by fecal incontinence (51, 52). Although the etiology may be multifactorial, anal sphincter injury is a common cause (especially in women during childbirth) and if clearly identified, is amenable to medical and surgical therapies. In the past, the evaluation of fecal incontinence was based upon electromyography (EMG) and anal manometry. Anal EMG has fallen out of use because of poor patient tolerability due to the insertion of needles directly into the sphincter muscle. Anal manometry is commonly used to measure the sphincter's functional ability by placing a transducer across the anal canal into the rectum and having the patient voluntarily contract their anal sphincter. In patients with fecal incontinence, anal manometry has been shown to be 60% sensitive and 78% specific for detecting sphincter defects (53). The accuracy of these tests may be limited by their inability to directly view the anal sphincter. The addition of rectal EUS and MRI in the evaluation of fecal incontinence does provide detailed images of the anal sphincter.

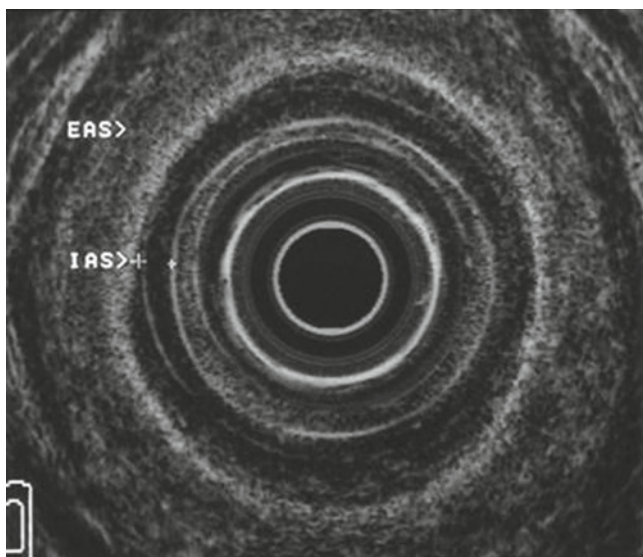


Fig. 5. Radial EUS view of normal external and internal anal sphincters (image provided by Dr. T. Savides).

Normal Anatomy of the Anal Sphincter

The anal sphincter consists of two distinct components, the internal and external sphincters (Fig. 5). The internal anal sphincter (IAS) consists of a 3–5 mm thick circular smooth muscle and the external anal sphincter (EAS) is a 6–10 mm thick ring of levator ani muscles (54). The IAS contributes 70–85% of the resting anal sphincter pressure and is mainly responsible for maintaining continence at rest. The IAS contributes 40% of the sphincter pressure generated after sudden distention of the rectum and the EAS reinforces anal tone during voluntary squeeze (55).

EUS Technique

With the patient in the left lateral decubitus position, the flexible radial echoendoscope (diameter of 12.7 mm) is passed into the rectum and then slowly pulled back through the anal canal with the balloon minimally inflated to minimize image distortion. As the scope is pulled out, the IAS is viewed first in the upper portion of the anal canal, and then the EAS is viewed in the lower portion. The IAS is an inner, hypoechoic ring of tissue that can become thicker and more hyperechoic with age

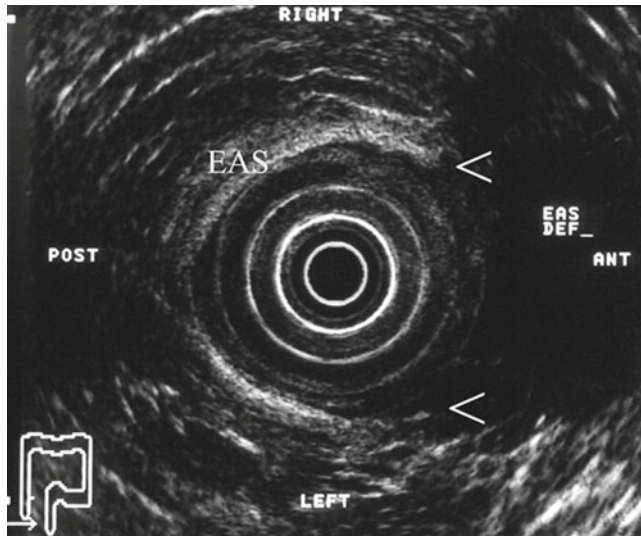


Fig. 6. Disruption of the hyperechoic external anal sphincter (EAS), with edge of tear marked with arrowheads (image provided by Dr. T. Savides).

due to collagen deposition (56–58). IAS tears appear as hyperechoic breaks in the ringed structure. The EAS is the outer, hyperechoic ring formed by the downward extension of the puborectalis muscle and tends to become thinner with age (59). Tears of the EAS appear as hypoechoic breaks (Fig. 6). A few differences between men and women should be considered when performing EUS. First, anal canal length varies from 25 mm for women to 33 mm for men (60). Second, the anterior part of the EAS is shorter, slopes more downward in women, and can make visualization of a complete ring in one plane difficult, which could lead to falsely identifying a sphincter defect (61).

EUS Accuracy in Identifying Sphincter Tears

Meyenberger et al. studied 28 patients with fecal incontinence that underwent rectal EUS prior to surgery (62). The etiology of incontinence was traumatic injury, about 50% were women, and some had both IAS and EAS defects. EUS correctly identified all 25 of IAS defects and all 10 EAS defects, but overall accuracy fell to 89% because an EAS defect was incorrectly diagnosed in three patients. Another study prospectively compared EUS to operative findings in 44 females undergoing

pelvic floor repair (63). All 23 EAS defects and 21 of 22 IAS defects identified on EUS were confirmed at surgery.

EUS Compared to Other Modalities

EUS has been compared to other diagnostic tools used in the evaluation of fecal incontinence. Initial studies of EUS compared to EMG demonstrated that it was much better tolerated by patients and could provide similarly accurate assessments of the anal sphincter (64–66). Another study compared EUS to anal manometry and EMG in 12 patients who underwent sphincter repair (67). EUS correctly identified all the sphincter injuries and had 100% accuracy versus 75% accuracies for EMG and manometry and 50% for clinical assessment. A few studies have compared rectal EUS with MRI in detecting sphincter injuries; however, the results have varied due to different patient populations, expertise at various institutions, and study design. One study by Malouf, using consensus opinion of the gastroenterologist and surgeon as a comparison, showed that MRI and EUS were concordant in 32 patients, EUS incorrect in 6 patients, and MRI incorrect in 15 patients (68). Another report of 22 women who underwent surgery for fecal incontinence showed that MRI had a better correlation with surgical findings than EUS (69). A more recent study of 19 women undergoing surgery for fecal incontinence showed that EUS and MRI were equivalent in diagnosing anal sphincter defects (70). More prospective studies will need to be done in a greater number of patients before definitive conclusions can be made regarding the accuracies of EUS and MRI in detecting sphincter injuries.

Clinical Impact of EUS on Fecal Incontinence

Multiple studies have examined the role of EUS in predicting the therapeutic response to sphincteroplasty. Three studies showed that 76% of patients with EUS detected anal sphincter defects had improvement in symptoms following surgery (62, 71, 72). Other studies demonstrated that performing EUS before and after sphincteroplasty to demonstrate the closure of sphincter defects correlated well with the improvement in symptoms of fecal incontinence (73, 74). One study examining 31 patients found that a persistent EAS defect seen on postoperative EUS predicted the failure of symptomatic improvement (75). Hill et al., however, showed that approximately 50% of patients had symptomatic improvement regardless of the results of EUS, anal manometry, or

whether surgery was performed (76). This study emphasized that while sphincter defects may have been correctly identified, conservative therapy may be effective in many cases. Additional studies are needed to determine the optimal management of patients with sphincter tears.

Future EUS Applications in Fecal Incontinence

The diagnostic accuracy in the identification of sphincter defects may potentially be improved with the application of 3D-EUS which can provide multiplanar imaging of the anal sphincter. To date, comparable results have been identified between 3D-EUS and MRI in detecting EAS defects (77). Tjandra et al. demonstrated a potential therapeutic use for EUS in fecal incontinence in a study evaluating different methods of treating patients with an injectable silicone biomaterial (PTP implants=Bioplastique™) (78). Injections into the intersphincteric space and IAS were performed and patients were randomized to delivery with EUS guidance (n=42) or simply by palpation (n=40). While both groups had significantly improved symptoms, this improvement was greater in the group with EUS-guided injections. Further studies are needed with long-term follow-up to see if EUS-guided therapies prove beneficial in fecal incontinence.

SUMMARY

Rectal EUS plays a significant role in the evaluation of malignant and benign diseases. EUS has emerged as an important tool used in the locoregional staging of rectal cancer and assists in selecting patients with advanced disease that may benefit from neoadjuvant therapy. Currently, EUS T staging has a high accuracy (80–95%) when performed prior to neoadjuvant therapy and in comparison to N staging (70–80%). EUS-FNA may improve accuracy but more studies are necessary to determine if this is significantly better than EUS alone. Future therapeutic roles may include EUS-guided delivery of chemotherapeutic agents directly into rectal tumors. In the evaluation of fecal incontinence, EUS provides the information that is complementary to anorectal manometry and electromyography by providing direct views of the anal sphincter. EUS has been shown to be highly accurate (89–100%) in identifying internal or EAS defects. Furthermore, EUS has the potential to guide therapy with the delivery of injectable materials to fill sphincter defects.

REFERENCES

1. American Cancer Society. What are the key statistics for colorectal cancer? <http://www.cancer.org> (2008). Accessed: March 9, 2010.
2. NIH consensus conference. Adjuvant therapy for patients with colon and rectal cancer. *JAMA*. 1990;264:1444–50.
3. Pahlman L, Glimelius B. Pre- or postoperative radiotherapy in rectal and rectosigmoid carcinoma. Report from a randomized multicenter trial. *Ann Surg*. 1990;211:187–95.
4. Edge SB, Byrd DR, Compton CC, Fritz AG, Greene FL, Trotti A. *AJCC Cancer Staging Manual*. 7th ed. New York: Springer; 2010.
5. Savides T, Master S. EUS in rectal cancer. *Gastrointest Endoscopy*. 2002;56(4):S12–17.
6. Garcia-Aguilar J, Pollack J, Lee SH, Hernandez de Anda E, Mellgren A, Wong WD, Finne CO, Rothenberger DA, Madoff RD. Accuracy of endorectal ultrasonography in preoperative staging of rectal tumors. *Dis Colon Rectum*. 2002;45:5–10.
7. Marusch F, Koch A, Schmidt U, Zippel R, Kuhn R, Wolff S, Pross M, Wierth A, Gastinger I, Lippert H. Routine use of transrectal ultrasound in rectal carcinoma: results of a prospective multicenter study. *Endoscopy*. 2002;34:385–90.
8. Herzog U, Von FM, Tondelli P, Schuppisser P. How accurate is endorectal ultrasound in the preoperative staging of rectal cancer? *Dis Colon Rectum*. 1993;36:127–34.
9. Tio TL, Coene PP, van Delden OM, Tytgat GN. Colorectal carcinoma: preoperative TNM classification with endosonography. *Radiology*. 1991;179:165–70.
10. Kwok H, Bisset IP, Hill GL. Preoperative staging of rectal cancer. *Int J Colorectal Dis*. 2000;15:9–20.
11. Waizer A, Powsner E, Russo I, Hadar S, Cytron S, Lombrozo R, et al. Prospective comparative study of magnetic resonance imaging versus transrectal ultrasound for preoperative staging and follow-up of rectal cancer. Preliminary Report. *Dis Colon Rectum*. 1991;34:1068–72.
12. Thaler W, Watzka S, Martin F, La GG, Psenner K, Bonatti G, et al. Preoperative staging of rectal cancer by endoluminal ultrasound vs. magnetic resonance imaging. Preliminary results of a prospective, comparative study. *Dis Colon Rectum*. 1994;37:1189–93.
13. Guinet C, Buy JN, Ghossain MA, Sezeur A, Mallet A, Bigot JM, et al. Comparison of magnetic resonance imaging and computed tomography in the preoperative staging of rectal cancer. *Arch Surg*. 1990;125:385–8.
14. Meyenberger C, Huch Boni RA, Bertschinger P, Zala GF, Klotz HP, Krestin GP. Endoscopic ultrasound and endorectal magnetic resonance imaging: a prospective comparative study for preoperative staging and follow-up of rectal cancer. *Endoscopy*. 1995;27:469–79.
15. Saitoh N, Okui K, Sarashina H, Suzuki M, Arai T, Nunomura M. Evaluation of echogenic diagnosis of rectal cancer using intrarectal ultrasonic examination. *Dis Colon Rectum*. 1986;29:234–42.
16. Dershaw DD, Enker WE, Cohen AM, Sigurdson ER. Transrectal ultrasonography of rectal carcinoma. *Cancer*. 1990;66:2336–40.

17. Harewood GC, Wiersema MJ, Nelson H, et al. A prospective blinded assessment of the impact of preoperative staging on the management of rectal cancer. *Gastroenterology*. 2002;123:24–32.
18. Rifkin MD, Ehrlich SM, Marks G. Staging of rectal carcinoma: prospective comparison of endorectal US and CT. *Radiology*. 1989;170:319–22.
19. Wiersema MJ, Harewood GC. Endoscopic ultrasound for rectal cancer. *Gastroenterol Clin North Am*. 2002;31:1093–105.
20. Giovannini M, Monges G, Seitz JF, Moutardier V, Bernardini D, Thomas P, Houvenaeghel G, Delpero JR, Giudicelli R, Fuentes P. Distant lymph node metastases in esophageal cancer: impact of endoscopic ultrasound-guided biopsy. *Endoscopy*. 1999;31(7):536–40.
21. Williams DB, Sahai AV, Aabakken L, Penman ID, van Velse A, Webb J, Wilson M, Hoffman BJ, Hawes RH. Endoscopic ultrasound guided fine needle aspiration biopsy: a large single centre experience. *Gut*. 1999;44:720–6.
22. Giovannini M, Seitz JF, Monges G, Perrier H, Rabbia I. Fine-needle aspiration cytology guided by endoscopic ultrasonography: results in 141 patients. *Endoscopy*. 1995;27(2):171–7.
23. Wiersema MJ, Vilmann P, Giovannini M, Chang KJ, Wiersema LM. Endosonography-guided fine-needle aspiration biopsy: diagnostic accuracy and complication assessment. *Gastroenterology*. 1997;112(4):1087–95.
24. Chang KJ, Nguyen P, Erickson RA, Durbin TE, Katz KD. The clinical utility of endoscopic ultrasound-guided fine-needle aspiration in the diagnosis and staging of pancreatic carcinoma. *Gastrointest Endosc*. 1997;45(5):387–93.
25. Gress FG, Savides TJ, Sandler A, Kesler K, Conces D, Cummings O, Mathur P, Ikenberry S, Bilderback S, Hawes R. Endoscopic ultrasonography, fine-needle aspiration biopsy guided by endoscopic ultrasonography, and computed tomography in the preoperative staging of non-small-cell lung cancer: a comparison study. *Ann Intern Med*. 1997;127(8):604–12.
26. Park HH, Nguyen PT, Tran Q, Chang KJ. Endoscopic ultrasound-guided fine needle aspiration in the staging of rectal cancer (abstract). *Gastrointest Endosc*. 2000;51:AB171.
27. Catalano MF, Sivak MV, Rice T, Gragg LA, Van Dam J. Endosonographic features predictive of lymph node metastasis. *Gastrointest Endosc*. 1994;40:442–6.
28. Gleeson FC, Clain JE, Papachristou GI, Rajan E, Topazian MD, Wang KK, Levy MJ. Prospective assessment of EUS criteria for lymphadenopathy associated with rectal cancer. *Gastrointest Endosc*. 2009;69(4):896–903.
29. Fusaroli P, Caletti G. Endoscopic ultrasonography: current clinical role. *Eur J Gastroenterol Hepatol*. 2005;17:293–301.
30. Chen VK, Eloubeidi MA. Endoscopic ultrasound-guided fine-needle aspiration of intramural and extrasintestinal mass lesions: diagnostic accuracy, complication assessment and impact on management. *Endoscopy*. 2005;37:984–9.
31. ASGE. ASGE Guideline: complications of EUS. *Gastrointest Endosc*. 2005;61:8–12.
32. Hirota WK, Petersen K, Baron TH, Goldstein JL, Jacobson BC, Leighton JA, Mallery JS, Waring JP, Fanelli RD, Wheeler-Harborough J, Faigel DO; Standards of Practice Committee of the American Society for Gastrointestinal Endoscopy. Guidelines for antibiotic prophylaxis for GI endoscopy. *Gastrointest Endosc*. 2003;58:475–82.

33. Levy MJ, Norton ID, Clain JE, Enders FB, Gleeson F, Limburg PJ, Nelson H, Rajan E, Topazian MD, Wang KK, Wiersema MJ, Wilson WR. Prospective study of bacteremia and complications with EUS FNA of rectal and perirectal lesions. *Clin Gastroenterol Hepatol*. 2007;5(6):684–9.
34. Sasaki Y, Niwa Y, Hirooka Y, Ohmiya N, Itoh A, Ando N, Miyahara R, Furuta S, Goto H. The use of endoscopic ultrasound-guided fine-needle aspiration for investigation of submucosal and extrinsic masses of the colon and rectum. *Endoscopy*. 2005;37(2):154–60.
35. Mezzi G, Arcidiacono PG, Carrara S, Freschi M, Boemo C, Testoni PA. Complication after endoscopic ultrasound-guided fine-needle aspiration (EUS-FNA) of rectal lesion. *Endoscopy*. 2007;39:E137.
36. ASGE. ASGE Guidelines: Antibiotic prophylaxis for GI endoscopy. *Gastrointest Endosc*. 2008;67(6):791–98.
37. Harewood GC, Wiersema MJ. Cost-effectiveness of endoscopic ultrasonography in the evaluation of proximal rectal cancer. *Am J Gastroenterol*. 2002;97:874–82.
38. Shami VM, Parmar KS, Waxman I. Clinical impact of endoscopic ultrasound and endoscopic ultrasound-guided fine needle aspiration in the management of rectal carcinoma. *Dis Colon Rectum*. 2004;47:59–69.
39. Carmody BJ, Otchy DP. Learning curve of transrectal ultrasound. *Dis Colon Rectum*. 2000;43:193–7.
40. Hunerbein M, Totkas S, Moesta KT, Ulmer C, Handke T, Schlag PM. The role of transrectal ultrasound-guided biopsy in the postoperative follow-up of patients with rectal cancer. *Surgery*. 2001;129(2):164–9.
41. Maor Y, Nadler M, Barshack I, Zmora O, Koller M, Kundel Y, Fidler H, Bar-Meir S, Avidan B. Endoscopic ultrasound staging of rectal cancer: diagnostic value before and following chemoradiation. *J Gastroenterol Hepatol*. 2006;21:454–8.
42. Harewood GC. Assessment of publication bias in the reporting of EUS performance in staging rectal cancer. *Am J Gastrol*. 2005;100:808–16.
43. van Vliet EPM, Eijkemans MJC, Kuipers EJ, Poley JW, Steyerberg EW, Siersema PD. Publication bias does not play a role in the reporting of endoscopic ultrasound staging of upper gastrointestinal cancers. *Endoscopy*. 2007;39:325–32.
44. Novell F, Pascual S, Viella P, Trias M. Endorectal ultrasonography in the follow-up of rectal cancer. Is it a better way to detect early local recurrence? *Int J Colorectal Dis*. 1997;12:78–81.
45. Rotondano G, Esposito P, Pellecchia L, Novi A, Romano G. Early detection of locally recurrent rectal cancer by endosonography. *Br J Radiol*. 1997;70:567–71.
46. Lohnert MS, Doniec JM, Henne-Bruns D. Effectiveness of endoluminal sonography in the identification of occult local rectal cancer recurrences. *Dis Colon Rectum*. 2000;43:483–91.
47. Vyslouzil K, Cwiertka K, Zboril P, Kucerova L, Starý L, Klementa I, Skalický P, Duda M. Endorectal sonography in rectal cancer staging and indication for local surgery. *Hepatogastroenterology*. 2007;54(76):1102–6.
48. Kim JC, Kim HC, Yu C, Han KR, Kim JR, Lee KH, Jang SJ, Lee SS, Ha HK. Efficacy of 3-dimensional endorectal ultrasonography compared with conventional ultrasonography and computed tomography in preoperative rectal cancer staging. *Am J Surg*. 2006;192:89–97.

49. Giovannini M, Bories E, Pesenti C, Moutardier V, Lelong B, Delpéro JR. Three-dimensional endorectal ultrasound using a new freehand software program: results in 35 patients with rectal cancer. *Endoscopy*. 2006;38(4):339–43.
50. Chang KJ. EUS guided fine needle injection (FNI) and anti-tumor therapy. *Endoscopy*. 2006;38(Suppl):S88–93.
51. Fecal incontinence: NIDDK (2008) <http://www.digestive.niddk.nih.gov/about/ddnews/win08/5.htm>. Accessed: March 9, 2010.
52. Nelson RL. Epidemiology of fecal incontinence. *Gastroenterology*. 2004;126 Suppl 1:S3–7.
53. Felt-Bersman RJ, Klinkenberg-Knoll EC, Meuwissen SGM. Anorectal function investigations in incontinent and continent patients. *Dis Colon Rectum*. 1990;33:479–86.
54. Rao S. Pathophysiology of adult fecal incontinence. *Gastroenterology*. 2004;126:S14–22.
55. Freckner B, Von Euler C. Influence of pudendal block on the function of the anal sphincter. *Gut*. 1975;16:482–9.
56. Gibbons CP, Bannister JJ, Trowbridge EA, Read NW. An analysis of anal sphincter pressure and anal compliance in normal subjects. *Int J Colorectal Dis*. 1986;1:231–7.
57. Nielson MB. Endosonography of the anal sphincter muscles in healthy volunteers and in patients with defecation disorders. *Acta Radiol Suppl*. 1998;416:1–21.
58. Papachrysostomou M, Pye SD, Wild SR, Smith AN. Anal endosonography in asymptomatic subjects. *Scand J Gastroenterol*. 1993;28:551–6.
59. Burnett SJ, Bartram CI. Endosonographic variations in the normal internal anal sphincter. *Int J Colorectal Dis*. 1991;6:2–4.
60. Gold DM, Bartram CI, Halligan S, Humphries KN. Three-dimensional endoanal sonography in assessing anal canal injury. *Br J Surg*. 1999;86:365.
61. Sultan AH, Kamm MA, Hudson CN, Nicholls JR, Bartram CI. Endosonography of the anal sphincters: normal anatomy and comparison with manometry. *Clin Radiol*. 1994;49:368.
62. Meyenberger C, Bertschinger P, Zala GF, Buchmann P. Anal sphincter defects in fecal incontinence: correlation between endosonography and surgery. *Endoscopy*. 1996;28:217–24.
63. Deen KI, Kumar D, Williams JG, Olliff J, Keighley MR. Anal sphincter defects. Correlation between endoanal ultrasound and surgery. *Ann Surg*. 1993;218:201–5.
64. Law PJ, Kamm MA, Bartram CI. A comparison between electromyography and anal endosonography in mapping external anal sphincter defects. *Dis Colon Rectum*. 1990;33:370.
65. Law PJ, Kamm MA, Bartram CI. Anal endosonography in the investigation of fecal incontinence. *Br J Surg*. 1991;78:312.
66. Burnett SJ, Speakman CT, Kamm MA, Bartram CI. Confirmation of endosonographic detection of external anal sphincter defects. *Br J Surg*. 1991;78:448.
67. Sultan AH, Kamm MA, Talbot IC, Nicholls RJ, Bartram CI. Anal endosonography for identifying external sphincter defects confirmed histologically. *Br J Surg*. 1994;81:463.
68. Malouf AJ, Williams AB, Halligan S, Bartram CI, Dhillon S, Kamm MA. Prospective assessment of accuracy of endoanal MR imaging and endosonography in patients with fecal incontinence. *AJR Am J Roentgenol*. 2000;175:741.

69. Rociu E, Stoker J, Eijkemans MJ, Schouten WR, Laméris JS. Fecal incontinence: endoanal US versus endoanal MR imaging. *Radiology*. 1999;212:453.
70. Pinta T, Kylanpää ML, Luukkonen P, Tapani E, Kivisaari A, Kivisaari L. Anal incontinence: diagnosis by endoanal US or endovaginal MRI. *Eur Radiol*. 2004;14(8):1472–7.
71. Jorge JMN, Wexner SD. Etiology and management fecal incontinence. *Dis Colon Rectum*. 1993;36:77–97.
72. Osterberg A, Graf W, Karlbom U, Pahlman L. Evaluation of a questionnaire in the assessment of patients with faecal incontinence and constipation. *Scand J Gastroenterol*. 1996;31:575–80.
73. Felt-Bersma RJ, Cuesta MA, Koorevaar M. Anal sphincter repair improves anorectal function and endosonographic image. A prospective clinical study. *Dis Colon Rectum*. 1996;39:878.
74. Ternent CA, Shashidharan M, Blatchford GJ, Christensen MA, Thorson AG, Sentovich SM. Transanal ultrasound and anorectal physiology findings affecting continence after sphincteroplasty. *Dis Colon Rectum*. 1997;40:462.
75. Savoye-Collet C, Savoye G, Koning E, Thoumas D, Michot F, Denis P, Benozio M. Anal endosonography after sphincter repair: specific patterns related to clinical outcome. *Abdom Imaging*. 1999;24:569.
76. Hill K, Fanning S, Fennerty MB, Faigal DO. Endoanal ultrasound compared to anorectal manometry for the evaluation of fecal incontinence: a study of the effect these tests have on clinical outcome. *Dig Dis Sci*. 2006;51(2):235–40.
77. West RL, Dwarkasing S, Briel JW, Hansen BE, Hussain SM, Schouten WR, Kuipers EJ. Can three-dimensional endoanal ultrasonography detect external anal sphincter atrophy? A comparison with endoanal magnetic resonance imaging. *Int J Colorectal Dis*. 2005;20:328–33.
78. Tjandra JJ, Lim JF, Hiscock R, Rajendra P. Injectable silicone biomaterial for fecal incontinence caused by internal anal sphincter dysfunction is effective. *Dis Colon Rectum*. 2004;47:2138–46.

Part III
Interventional EUS

Interventional Endoscopic Ultrasound-Guided Cholangiopancreatography

*Jennifer L. Maranki, MD,
Michel Kahaleh, MD, and
Vanessa M. Shami, MD*

CONTENTS

INTRODUCTION
LITERATURE REVIEW
SUMMARY

Abstract

Interventional endoscopic ultrasound-guided cholangiopancreatography (IEUCP) is an alternative to percutaneous drainage or surgery in patients with obstructive jaundice who have failed conventional ERCP. The techniques of biliary and pancreatic drainage are described. The literature regarding this novel technique including complications is reviewed. Due to the technical complexity associated with this procedure, it should be reserved for endoscopists with advanced training in EUS and ERCP at tertiary medical centers.

Key Words: Biliary obstruction, Pancreatic obstruction, Endoscopic ultrasound-guided cholangiopancreatography, Rendezvous, Endoscopic ultrasound, Biliary decompression, Pancreatogastric fistula, Hepaticogastrostomy, Choledochoduodenostomy

From: *Clinical Gastroenterology: Endoscopic Ultrasound*,
Edited by: V. M. Shami and M. Kahaleh, DOI 10.1007/978-1-60327-480-7_16,
© Springer Science+Business Media, LLC 2010

INTRODUCTION

Endoscopic retrograde cholangiopancreatography (ERCP) with stent placement is the procedure of choice for biliary decompression in patients with obstructive jaundice (1–3) and for strictures of the pancreas that are due to chronic pancreatitis (4–6) and other causes (7). Among experienced endoscopists, biliary and pancreatic duct decompression is successful in 90–95% of cases (8, 9). Failure to cannulate the bile duct may result from anatomic variation due to prior surgery, periampullary diverticula, tortuous ducts, impacted stones, or tumor infiltration (10–12). Pancreatic duct cannulation is typically successful in 90% of cases (9). Failures commonly result from pancreatic inflammation or surgically altered anatomy (12).

Following initial failed ERCP, the recommended next step is a reattempt by a more experienced endoscopist at a tertiary referral center (13, 14). Alternative means of achieving biliary decompression include percutaneous transhepatic drainage (PTC) (15–17), and surgical intervention (18). Both surgery and PTC followed by percutaneous or endoscopic drainage are associated with significant morbidity (19–21).

The evolution of the linear array echoendoscope as well as the ability to accurately guide a needle into the interventional field has greatly expanded the therapeutic potential of endoscopic ultrasound (EUS). EUS provides detailed imaging by approximating the frequency transducer to the area of interest. In the past decade, EUS has developed into a useful technique for fine needle aspiration (FNA) (22), pancreatic pseudocyst drainage (23–25), and celiac plexus block and neurolysis (26–32). Anatomically, the biliary tree and the pancreatic duct are in close proximity to the stomach and duodenum, thereby allowing visualization of the ducts from the EUS transducer. The natural progression was to extend the capabilities of EUS to the pancreaticobiliary system. The first cases describing Interventional EUS-guided cholangiopancreatography (IEUCP) were reported by Wiersema and colleagues in 1996 and involved 11 patients who had previously failed standard ERCP (33). More recently, IEUCP has been shown to be a feasible technique in achieving drainage of the respective system.

Patient Selection

Patients who present with biliary or pancreatic duct obstruction who have undergone and failed conventional ERCP at a tertiary care center by an experienced endoscopist are considered for candidacy for EUS-guided ERCP. Thorough imaging of the pancreaticobiliary tree, as well

as surrounding structures with CT or MRI is vital to identify the level of obstruction and outline the patient's anatomy. Since these procedures are typically longer in duration than standard ERCP, patients must undergo general anesthesia.

Endoscopist Selection

Since EUS-guided ERCP is a technically challenging procedure that bears a fair amount of risk when compared to conventional ERCP, ensuring adequate expertise in EUS and ERCP is mandatory. This goal can be accomplished either with a single operator who is highly skilled at both EUS and advanced endoscopy, or by two different endoscopists, one with experience in EUS, and the other in therapeutic ERCP. Furthermore, the procedure should be performed at a tertiary care center with experienced pancreatobiliary surgeons and interventional radiologists on hand in the event of a complication.

Patient Preparation

All patients should receive periprocedural antibiotics. Secondary to the longer duration and complexity of the procedure, patients should undergo general anesthesia for the procedure.

Techniques

Conventional ERCP should initially be reattempted on all patients. If it is unsuccessful again, then an EUS-guided technique should be considered. Patients should be consented specifically for the procedure.

A linear array echoendoscope with a working channel of at least 3 mm should be selected as this size accommodates stent placement when the procedure is performed in antegrade fashion. The Olympus GF-UCT 140 and the Pentax EG 38UT have working channels of 3.7 and 3.8 mm, respectively, and are ideal for the placement of a 10F stent, which is particularly useful when biliary drainage is attempted.

Puncture of the target duct is typically performed with either a 19- or 22-gauge needle (EUSN-19-T or EUS-1-CS; Cook Endoscopy). Despite being somewhat more difficult to use, the 19-gauge needle is preferred because it accommodates a 0.035-in. guidewire (Terumo; Microvasive), which provides more control than the 0.018-in. guidewire (Pathfinder; Microvasive Endoscopy, Boston Scientific Corp, Natick, MA).

Dilation of an enterocholedochal or pancreatic fistula can be accomplished with either a 4- or 6-mm wire-guided balloon catheter (MaxForce; Microvasive, Boston, MA) or a 6F or 7F bougie (SBDC-6 or -7; Wilson-Cook, Winston-Salem, NC).

EUS-GUIDED BILIARY DRAINAGE

EUS-guided biliary drainage is typically attempted with either a transgastric-transhepatic (intrahepatic) or transenteric-transcholedochal (extrahepatic) approach. If the intrahepatic ducts are significantly dilated, the intrahepatic approach is preferred as this technique can provide antegrade stent placement across the ampulla without the need for a rendezvous procedure. Once the echoendoscope is adequately positioned, color doppler should be used to identify regional vasculature.

Intrahepatic Approach

The intrahepatic approach is performed with the echoendoscope positioned in the cardia or along the lesser curvature of the stomach to allow visualization of the dilated left intrahepatic biliary system. Once color doppler has excluded overlying vasculature, the EUS needle is advanced into the intrahepatic duct, bile is aspirated, and a small amount of contrast is injected to opacify the biliary tree, confirming position inside the bile duct (Fig. 1). A guidewire is then advanced antegrade through the EUS needle and into the bile duct (Fig. 2). With fluoroscopic and EUS guidance, the guidewire is manipulated beyond the biliary obstruction and across the ampulla into the duodenum. Once the guidewire has traversed the ampulla, the procedure can be completed in either an antegrade fashion or with a rendezvous technique.

For completing the procedure in antegrade fashion, a 6 or 7F bougie is utilized to dilate the tract (Fig. 3), followed by antegrade stent deployment across the stricture (Fig. 4).

If the rendezvous technique is chosen, the echoendoscope must be carefully removed while leaving the guidewire in place. A duodenoscope is inserted and advanced to the duodenum, with visualization of the ampulla and the wire exiting the ampullary orifice (Fig. 5). The wire is grasped with a snare and withdrawn through the accessory channel. Since access to the common bile duct has been achieved, the procedure can be completed using standard ERC with stent placement.

If the guidewire cannot be advanced into the duodenum, a transenteric fistula can be created by dilating the tract with a 4–6 mm wire-guided balloon catheter or a 6–7F bougie, followed by stent placement.



Fig. 1. Injection of contrast through the endoscopic ultrasound needle, demonstrating successful opacification of the intrahepatic duct.

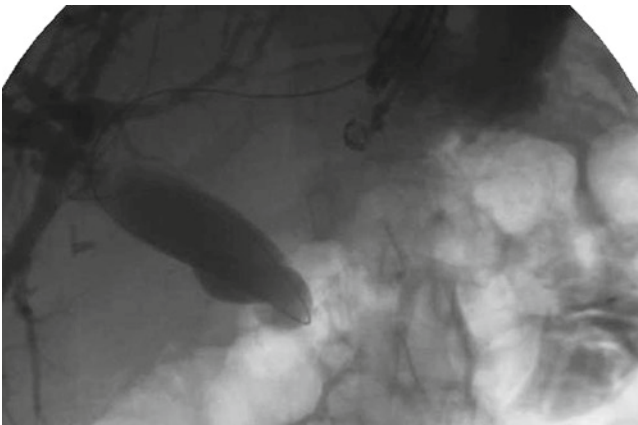


Fig. 2. A guidewire is advanced through the endoscopic ultrasound needle and into the biliary tree.

Extrahepatic Approach

To visualize the extrahepatic bile duct, the echoendoscope is typically positioned in the duodenum; it can also be positioned in the distal antrum, depending on the anatomy. After color doppler is used to identify adjacent vasculature, the EUS needle is then inserted into the bile

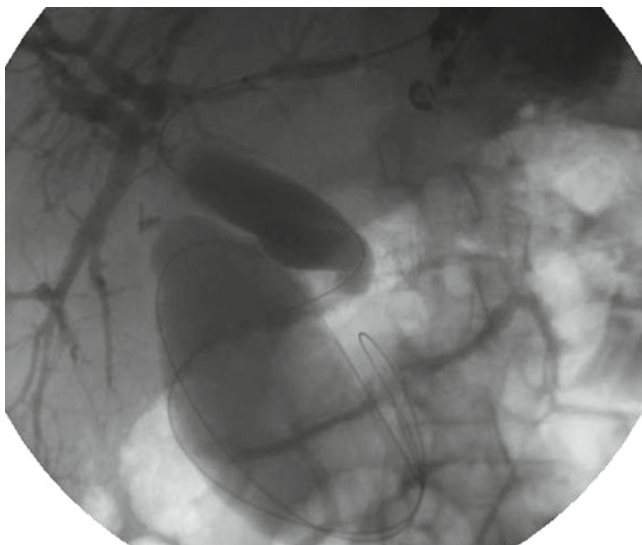


Fig. 3. Dilation of the tract between the stomach and the left intrahepatic duct in antegrade fashion.

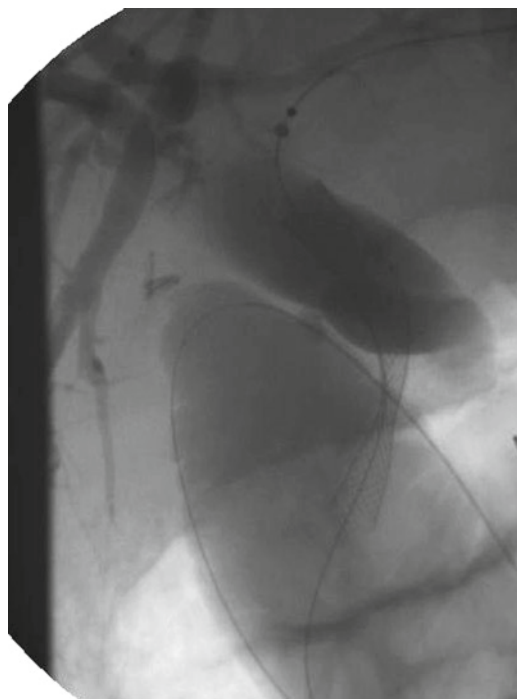


Fig. 4. Stent deployment into the left intrahepatic duct.

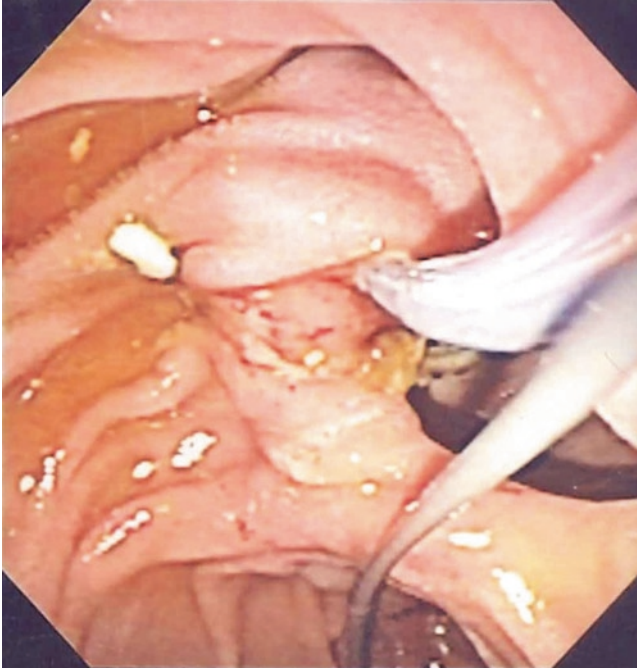


Fig. 5. Visualization of the wire exiting the ampullary orifice.

duct and the guidewire is advanced in an antegrade fashion across the ampulla and into the duodenum (Fig. 6). The remainder of the procedure is similar to that described above for the intrahepatic approach.

EUS-GUIDED PANCREATIC DRAINAGE

By positioning the echoendoscope in the stomach, the main pancreatic duct is identified with EUS guidance and punctured with the EUS needle. A small amount of contrast material is injected and a pancreatogram is performed to confirm successful access to the pancreatic duct (Fig. 7). A guidewire is advanced through the needle and into the pancreatic duct, with subsequent antegrade advancement of the wire into the duodenum, if possible. If the guidewire cannot be advanced in an antegrade fashion, it should be advanced retrograde into the pancreatic duct. After ductal access has been achieved, a pancreatogastric fistula is enlarged with a 6F or 7F bougie followed by balloon dilation with a 4- or 6-mm MaxForce dilator (Fig. 8). Intraductal strictures should be dilated with either the bougie or balloon catheter. A 7F stent is then placed through the pancreatogastric fistula (Fig. 9).



Fig. 6. Advancement of the guidewire into the extrahepatic bile duct, with advancement of the wire in an antegrade fashion.

LITERATURE REVIEW

EUS-Guided Biliary Drainage

Wiersema et al. described the use of EUS-guided cholangiography in ten patients in 1996 (24). In his series, biliary opacification guided repeat ERC with precut sphincterotomy in five of seven patients. In 2001, Giovannini et al. performed a choledochoduodenal fistula created under EUS guidance with a transbulbar stent placement (34). Two years later, Burmester et al. reported a series of four patients undergoing creation of an EUS enterobiliary fistula in three patients (35). EUS-guided drainage of obstructed biliary ducts via a rendezvous technique was performed in two patients by Mallery et al. (36). Kahaleh et al. reported a series of 23 patients undergoing EUS-guided ERC, with biliary decompression achieved in 21 patients (37). Most recently, our group has reported the largest study of EUS-guided ERC performed in 49 patients. The overall success rate was 84% (41/49), with an overall



Fig. 7. Pancreatogram demonstrating successful access into the pancreatic duct.

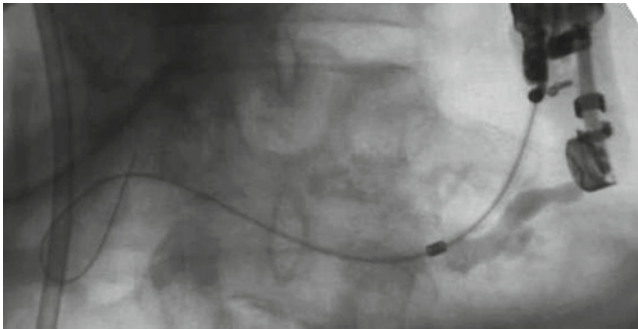


Fig. 8. Creation of pancreatogastric fistula followed by bougie dilation.

complication rate of 16%. Thirty-five patients underwent the intrahepatic approach, with a success rate of 83% (29/35). Fourteen patients underwent the extrahepatic approach (including 5 of whom had initially undergone the intrahepatic approach but were converted to the extrahepatic approach), with success in 12/14 patients, or 86% (38). Table 1 summarizes the published literature of EUS-guided biliary drainage to date.



Fig. 9. Placement of a 7F stent through the pancreaticogastrocystic fistula.

The main complications associated with EUS-guided biliary drainage include pneumoperitoneum, postprocedure pain, and bleeding, most of which tend to be managed conservatively or self-resolving. The risk of bile leak and perforation leading to biliary peritonitis was found to be fairly small based on the reported case series. Of the 93 cases reported, there were 5 cases of pneumoperitoneum, 1 biliary leak, 1 case of biliary peritonitis, 1 case where the wire was passed outside of the bile duct lumen (35, 36, 38, 39). There was also one ileus, two cases of stent shortening, one early blockage, one death from complications of cirrhosis, three episodes of pain, one case of cholangitis, one aspiration pneumonia, and one case of self-resolving bleeding (38, 40–43). The overall complication rate in these 93 cases was 20% (19/93).

EUS-Guided Pancreatic Drainage

In 1996, Wiersema (24) and Gress et al. (44) each reported one case of EUS-guided pancreatography. One approach to achieving pancreatic drainage involves the creation of a pancreaticoenteric fistula followed by rendezvous (36, 45, 46). Another technique requires the creation of a pancreaticogastrocystic fistula as the main method for duct drainage (47, 48). The rendezvous technique was described by Mallery and colleagues, in whose series successful drainage was reported in only 25% (1 of 4) of patients (36) (Table 1). In one case, the pancreatic duct could not be punctured, and in two of the cases, the wire could not be advanced

Table 1
Published series of IEUCP

<i>Author</i>	<i>Year</i>	<i>No. of patients</i>	<i>Technique</i>	<i>Complications</i>	<i>Rate of success^a</i>
Biliary drainage					
Burmester et al. (35)	2003	4	Intrahepatic (1), extrahepatic (2)	Bile leak (1)	75% (3 of 4)
Mallery et al. (36)	2004	2	Extrahepatic (2)	Wire passed out of biliary lumen (1)	100% (2 of 2)
Puspok et al. (40)	2005	6	Extrahepatic (6)	None	83% (5 of 6)
Bories et al. (41)	2007	11	Intrahepatic (11)	Ileus (1), stent shortening (2), early blockage (1)	91% (10 of 11)
Will et al. (42)	2007	8	Intrahepatic (7), extrahepatic (1)	Slight pain (2), cholangitis (1)	88% (7 of 8)
Tarantino et al. (43)	2008	8	Extrahepatic (8)	Death from cirrhosis (1)	100% (8 of 8)
Yamao et al. (39)	2008	5	Extrahepatic (5)	Pneumoperitoneum (1)	100% (5 of 5)
Maranki et al. (38)	2009	49	Intrahepatic (35), extrahepatic (14)	Biliary peritonitis (1), pain (1), pneumoperitoneum (4), aspiration pneumonia (1), self-resolving bleeding (1)	84% (41 of 49)

(continued)

Table 1
(continued)

<i>Author</i>	<i>Year</i>	<i>No. of patients</i>	<i>Technique</i>	<i>Complications</i>	<i>Rate of success^a</i>
Pancreatic drainage					
Francois et al. (47)	2002	4	Pancreaticogastrostomy (4)	Stent dislocation (1)	100% (4 of 4)
Kahaleh et al. (48)	2003	2	Pancreaticogastrostomy (2)	Hematemesis due to stent adjacent to vessel (1)	100% (2 of 2)
Mallery et al. (36)	2004	4	Rendezvous (4)	Transient fever (1)	25% (1 of 4)
Papachristou et al. (49)	2007	2	Rendezvous (2)	None	100% (2 of 2)
Kahaleh et al. (51)	2007	13	Pancreaticogastrostomy (10)	Bleeding (1), contained perforation (1)	77% (10 of 13)
Tessier et al. (52)	2007	36	Pancreaticogastrostomy (26), pancreaticobulbostomy (7)	Hematoma (1), pancreatitis (1)	92% (33 of 36)
Will et al. (53)	2007	12	Pancreaticogastrostomy (5), rendezvous (4)	Pain (4), bleeding (1), perforation (1), pseudocyst (1)	75% (9 of 12)

^aSuccess as defined by adequate drainage of the applicable duct

through the stricture. More recently, Papachristou et al. reported two cases of successful pancreatic drainage with the rendezvous technique in patients with nondilated pancreatic ducts (49). When the pancreatic duct cannot be decompressed from the second portion of the duodenum, creation of a pancreaticogastric fistula is the preferred method to achieve duct drainage (50). In a study at our institution, 13 patients with chronic pancreatitis and intractable pain were included; 7 of these patients had prior surgical diversions (51). Successful creation of a pancreaticogastric fistula was achieved in 10 (77%) patients, followed by stent placement. In two cases, the needle could not be oriented to allow the advancement of the guidewire for access, thus no endoprosthesis was placed. Complications of the procedures included one case of bleeding requiring hemoclip placement and one case of contained perforation that resolved spontaneously. Tessier and colleagues reported the largest retrospective series to date of 36 patients who underwent either pancreaticogastrostomy or pancreaticobulbostomy. Success was achieved in 92% of cases (33 of 36) and complications, including hematoma and severe pancreatitis, occurred in two patients (52). In 2007, Will and colleagues reported 12 patients through 14 interventions who underwent EUS-guided pancreatic duct drainage (53). Pancreatography was successful in all patients, and drainage of the pancreatic duct was achieved in nine patients. The transgastric approach, with creation of a pancreaticogastric fistula, was utilized in five patients, whereas four patients underwent the rendezvous technique with subsequent ERCP. The complication rate was 43%, with postprocedural pain occurring in four patients, bleeding in one patient, and perforation in one patient.

IEUCP has several advantages over percutaneous drainage, including the ability to visualize overlying vascular structures in real-time using color doppler while attempting needle puncture of the biliary or pancreatic ducts, potentially decreasing vascular injury. IEUCP provides the ability to achieve drainage without the need for an external drain, which can be a source of infection and discomfort. While the reported complication rate for EUS-guided pancreatic drainage is somewhat high, the complication rate for EUS-guided biliary drainage is more favorable, making it an attractive alternative to PTC.

SUMMARY

IEUCP should be considered as an alternative to PTC or surgery in patients with obstructive jaundice or pancreatic strictures who have failed conventional ERCP. Since the procedure is technically challenging, it should be performed by trained interventional endoscopists and at

a tertiary care center, with experienced pancreatobiliary surgeons and interventional radiologists available in the event of complications. In the presence of dilated intrahepatic ducts, the preferred method for biliary drainage is the intrahepatic approach with antegrade stent placement, avoiding the need for a rendezvous procedure. In the pancreatic duct, the antegrade approach is recommended for pancreatic drainage. IEUCP is a technique that is increasingly utilized in tertiary care centers and is evolving as a feasible alternative technique to PTC or surgery.

REFERENCES

1. Fogel EL, Sherman S, Devereaux BM, Lehman GA. Therapeutic biliary endoscopy. *Endoscopy*. 2001;33:31–8.
2. Schofl R. Diagnostic endoscopic retrograde cholangiopancreatography. *Endoscopy*. 2001;33:147–57.
3. Carr-Locke DL. Overview of the role of ERCP in the management of diseases of the biliary tract and the pancreas. *Gastrointest Endosc*. 2002;56:S157–60.
4. Dumonceau JM, Deviere J, Le Moine O, Delhaye M, Vandermeeren A, Baize M, et al. Endoscopic pancreatic drainage in chronic pancreatitis associated with ductal stones: long-term results. *Gastrointest Endosc*. 1996;43:547–55.
5. Ponchon T, Bory RM, Hedelius F, Roubein LD, Paliard P, Napoleon B, et al. Endoscopic stenting for pain relief in chronic pancreatitis: results of a standardized protocol. *Gastrointest Endosc*. 1995;42:452–6.
6. Cremer M, Deviere J, Delhaye M, Baize M, Vandermeeren A. Stenting in severe chronic pancreatitis: results of medium-term follow-up in seventy-six patients. *Endoscopy*. 1991;23:171–6.
7. Howard TJ, Moore SA, Saxena R, Matthews DE, Schmidt CM, Wiebke EA. Pancreatic duct strictures are a common cause of recurrent pancreatitis after successful management of pancreatic necrosis. *Surgery*. 2004;136:909–16.
8. Huibregtse K. Endoscopic retrograde cholangiopancreatography, endoscopic sphincterotomy and endoscopic biliary and pancreatic drainage. In: Yamada T, editor. *Textbook of gastroenterology*. Philadelphia: J.B. Lippincott, 1995. p. 2590–617.
9. Fink AS, Perez de Ayala V, Chapman M, Cotton PB. Radiologic pitfalls in endoscopic retrograde pancreatography. *Pancreas*. 1986;1:180–7.
10. Martin DF. Combined percutaneous and endoscopic procedures for bile duct obstruction. *Gut*. 1994;35:1011–2.
11. Lobo DN, Balfour TW, Iftikhar SY. Periampullary diverticula: consequences of failed ERCP. *Ann R Coll Surg Engl*. 1998;80:326–31.
12. Wright BE, Cass OW, Freeman ML. ERCP in patients with long-limb Roux-en-Y gastrojejunostomy and intact papilla. *Gastrointest Endosc*. 2002;56:225–32.
13. Kumar S, Sherman S, Hawes RH, Lehman GA. Success and yield of second attempt ERCP. *Gastrointest Endosc*. 1995;41:445–7.
14. Choudari CP, Sherman S, Fogel EL, Phillips S, Kochell A, Flueckiger J, et al. Success of ERCP at a referral center after a previously unsuccessful attempt. *Gastrointest Endosc*. 2000;52:478–83.

15. Ferrucci Jr JT, Mueller PR, Harbin WP. Percutaneous transhepatic biliary drainage: technique, results, and applications. *Radiology*. 1980;135:1–13.
16. Harbin WP, Mueller PR, Ferrucci Jr JT. Transhepatic cholangiography: complications and use patterns of the fine-needle technique: a multi-institutional survey. *Radiology*. 1980;135:15–22.
17. Calvo MM, Bujanda L, Heras I, Cabriada JL, Bernal A, Orive V, et al. The rendezvous technique for the treatment of choledocholithiasis. *Gastrointest Endosc*. 2001;54:511–3.
18. Smith AC, Dowsett JF, Russell RC, Hatfield AR, Cotton PB. Randomised trial of endoscopic stenting versus surgical bypass in malignant low bileduct obstruction. *Lancet*. 1994;344:1655–60.
19. Lameris JS, Stoker J, Nijs HG, Zonderland HM, Terpstra OT, van Blankenstein M, et al. Malignant biliary obstruction: percutaneous use of self-expandable stents. *Radiology*. 1991;179:703–7.
20. Beissert M, Wittenberg G, Sandstede J, Beer M, Tschammler A, Burghardt W, et al. Metallic stents and plastic endoprotheses in percutaneous treatment of biliary obstruction. *Z Gastroenterol*. 2002;40:503–10.
21. Kama NA, Coskun T, Yuksek YN, Yazgan A. Factors affecting post-operative mortality in malignant biliary tract obstruction. *Hepatogastroenterology*. 1999;46:103–7.
22. Wiersema MJ, Vilmann P, Giovannini M, Chang KJ, Wiersema LM. Endosonography-guided fine-needle aspiration biopsy: diagnostic accuracy and complication assessment. *Gastroenterology*. 1997;112:1087–95.
23. Grimm H, Binmoeller KF, Soehendra N. Endosonography-guided drainage of a pancreatic pseudocyst. *Gastrointest Endosc*. 1992;38:170–1.
24. Wiersema MJ. Endosonography-guided cystoduodenostomy with a therapeutic ultrasound endoscope. *Gastrointest Endosc*. 1996;44:614–7.
25. Kahaleh M, Shami VM, Conaway MR, Tokar J, Rockoff T, De La Rue SA, et al. Endoscopic ultrasound drainage of pancreatic pseudocyst: a prospective comparison with conventional endoscopic drainage. *Endoscopy*. 2006;38:355–9.
26. Wiersema MJ, Wiersema LM. Endosonography-guided celiac plexus neurolysis. *Gastrointest Endosc*. 1996;44:656–62.
27. Abedi M, Zfass AM. Endoscopic ultrasound-guided (neurolytic) celiac plexus block. *J Clin Gastroenterol*. 2001;32:390–3.
28. Gress F, Schmitt C, Sherman S, Ciaccia D, Ikenberry S, Lehman G. Endoscopic ultrasound-guided celiac plexus block for managing abdominal pain associated with chronic pancreatitis: a prospective single center experience. *Am J Gastroenterol*. 2001;96:409–16.
29. Collins D, Penman I, Mishra G, Draganov P. EUS-guided celiac block and neurolysis. *Endoscopy*. 2006;38:935–9.
30. Michaels AJ, Draganov PV. Endoscopic ultrasonography guided celiac plexus neurolysis and celiac plexus block in the management of pain due to pancreatic cancer and chronic pancreatitis. *World J Gastroenterol*. 2007;13:3575–80.
31. Schmulewitz N, Hawes R. EUS-guided celiac plexus neurolysis – technique and indication. *Endoscopy*. 2003;35:S49–53.
32. Levy MJ, Wiersema MJ. EUS-guided celiac plexus neurolysis and celiac plexus block. *Gastrointest Endosc*. 2003;57:923–30.

33. Wiersema MJ, Sandusky D, Carr R, Wiersema LM, Erdel WC, Frederick PK. Endosonography-guided cholangiopancreatography. *Gastrointest Endosc.* 1996;43:102–6.
34. Giovannini M, Moutardier V, Pesenti C, Bories E, Lelong B, Delpero JR. Endoscopic ultrasound-guided bilioduodenal anastomosis: a new technique for biliary drainage. *Endoscopy.* 2001;33:898–900.
35. Burmester E, Niehaus J, Leineweber T, Huetteroth T. EUS-cholangio-drainage of the bile duct: report of 4 cases. *Gastrointest Endosc.* 2003;57:246–51.
36. Mallery S, Matlock J, Freeman ML. EUS-guided rendezvous drainage of obstructed biliary and pancreatic ducts: report of 6 cases. *Gastrointest Endosc.* 2004;59:100–7.
37. Kahaleh M, Hernandez AJ, Tokar J, Adams RB, Shami VM, Yeaton P. Interventional EUS-guided cholangiography: evaluation of a technique in evolution. *Gastrointest Endosc.* 2006;64:52–9.
38. Maranki J, Hernandez A, Arlan B, Jaffan AA, Angle JF, Shami VM, et al. Interventional EUS-guided cholangiography (IEUC): long term experience of an emerging alternative to percutaneous transhepatic cholangiography (PTC) with video. *Endoscopy.* 2009;41:532–8.
39. Yamao K, Bhatia V, Mizuno N, Sawaki A, Ishikawa H, Tajika M, et al. EUS-guided choledochoduodenostomy for palliative biliary drainage in patients with malignant biliary obstruction: results of long-term follow-up. *Endoscopy.* 2008;40:340–2.
40. Puspok A, Lomoschitz F, Dejaco C, Hejna M, Sautner T, Gangl A. Endoscopic ultrasound guided therapy of benign and malignant biliary obstruction: a case series. *Am J Gastroenterol.* 2005;100:1743–7.
41. Bories E, Pesenti C, Caillol F, Lopes C, Giovannini M. Transgastric endoscopic ultrasonography-guided biliary drainage: results of a pilot study. *Endoscopy.* 2007;39:287–91.
42. Will U, Thieme A, Fueeldner F, Gerlach R, Wanzar I, Meyer F. Treatment of biliary obstruction in selected patients by endoscopic ultrasonography (EUS)-guided transluminal biliary drainage. *Endoscopy.* 2007;39:292–5.
43. Tarantino I, Barresi L, Repici A, Traina M. EUS-guided biliary drainage: a case series. *Endoscopy.* 2008;40:336–9.
44. Gress F, Ikenberry S, Sherman S, Lehman G. Endoscopic ultrasound-directed pancreatography. *Gastrointest Endosc.* 1996;44:736–9.
45. Will U, Meyer F, Manger T, Wanzar I. Endoscopic ultrasound-assisted rendezvous maneuver to achieve pancreatic duct drainage in obstructive chronic pancreatitis. *Endoscopy.* 2005;37:171–3.
46. Bataille L, Deprez P. A new application for therapeutic EUS: main pancreatic duct drainage with a “pancreatic rendezvous technique”. *Gastrointest Endosc.* 2002;55:740–3.
47. Francois E, Kahaleh M, Giovannini M, Matos C, Deviere J. EUS-guided pancreaticogastrostomy. *Gastrointest Endosc.* 2002;56:128–33.
48. Kahaleh M, Yoshida C, Yeaton P. EUS antegrade pancreatography with gastropancreatic duct stent placement: review of two cases. *Gastrointest Endosc.* 2003;58:919–23.

49. Papachristou GI, Gleeson FC, Petersen BT, Levy MJ. Pancreatic endoscopic ultrasound-assisted rendezvous procedure to facilitate drainage of nondilated pancreatic ducts. *Endoscopy*. 2007;39 Suppl 1:E324–5.
50. Shami VM, Kahaleh M. Endoscopic ultrasonography (EUS)-guided access and therapy of pancreatico-biliary disorders: EUS-guided cholangio and pancreatic drainage. *Gastrointest Endosc Clin N Am*. 2007;17:581–93.
51. Kahaleh M, Hernandez AJ, Tokar J, Adams RB, Shami VM, Yeaton P. EUS-guided pancreaticogastrostomy: analysis of its efficacy to drain inaccessible pancreatic ducts. *Gastrointest Endosc*. 2007;65:224–30.
52. Tessier G, Bories E, Arvanitakis M, Hittelet A, Pesenti C, Le Moine O, et al. EUS-guided pancreatogastrostomy and pancreatobulbostomy for the treatment of pain in patients with pancreatic ductal dilatation inaccessible for transpapillary endoscopic therapy. *Gastrointest Endosc*. 2007;65:233–41.
53. Will U, Fueeldner F, Thieme AK, Goldmann B, Gerlach R, Wanzar I, et al. Transgastric pancreatography and EUS-guided drainage of the pancreatic duct. *J Hepatobiliary Pancreat Surg*. 2007;14:377–82.

Endoscopic Ultrasound-Guided Drainage of Pancreatic Fluid Collections

*Jayant P. Talreja, MD
and Michel Kahaleh, MD*

CONTENTS

INTRODUCTION
MATERIALS AND METHODS
PROCEDURE DESCRIPTION
LITERATURE REVIEW
CONCLUSION

Abstract

Conventional transmural drainage of pancreatic fluid collections (PFCs) has been increasingly performed in tertiary care centers. The development of endoscopic ultrasonography (EUS) has expanded the safety and efficacy of endoscopic drainage of PFCs. The concept includes EUS-guided access into a PFC via creation of a transgastric or transduodenal fistula, followed by the deployment of a stent and/or placement of a nasocystic drain to decompress the fluid collection.

The current literature suggests that EUS-guidance should be recommended for draining PFCs in the following situations: unusual location of the collection, small window of entry, nonbulging collections, coagulopathy, intervening varices, or failed conventional

From: *Clinical Gastroenterology: Endoscopic Ultrasound*,
Edited by: V. M. Shami and M. Kahaleh, DOI 10.1007/978-1-60327-480-7_17,
© Springer Science+Business Media, LLC 2010

transmural drainage. The decision to use EUS-guidance should be based on local expertise and individual patient presentation. Here, the technique and review of current literature will be discussed.

Key Words: EUS, Pancreatic fluid collections, Pancreatic pseudocysts, Non-bulging pancreatic fluid collections

INTRODUCTION

Pancreatic fluid collections (PFCs) develop secondary to either fluid leakage or liquefaction of pancreatic necrosis (1) following acute pancreatitis, chronic pancreatitis, surgery, or abdominal trauma (2–5). The accepted nomenclature for classifying PFCs has been defined by the Atlanta classification (6, 7). The presence of underlying ductal damage, the severity of acute pancreatitis, and maturation of the collection in relation to the onset of acute pancreatitis are factors that influence formation and composition of the PFC (7–11). Indications for PFC drainage include infection, pain, gastric outlet or biliary obstruction, leakage, fistulization, and enlargement (7–11). Therapeutic options for PFCs include surgical, percutaneous, or endoscopic drainage. Morbidity rates of surgical drainage have ranged from 7% to 37% (7, 12–14). Percutaneous drainage under radiological guidance has been shown to be effective for all types of PFCs (15). The major disadvantages are the need for an indwelling catheter, which is a nidus for infection, and the significant rate of percutaneous fistula formation (16–18). Over the last decade, endoscopic drainage of PFCs has become the procedure of choice in many tertiary care institutions (7, 19, 20). Clinical success rates of 70–87% have been reported, with complication rates of 11–34% (20, 21). Drainage of PFCs, endoscopically, may be achieved by transmural or transpapillary placement of plastic endoprotheses (7, 22).

The limitation of endoscopic transmural drainage is its blind approach and the high risk of perforation when a visible bulge is absent (23). Complications may increase when the distance between the pseudocyst and the lumen exceeds 1 cm (24). The incidence of nonbulging fluid collections is approximately 42–48%; the management of these pancreatic fluid collections is particularly challenging using the conventional method of transmural drainage (25, 26). Under direct endosonographic control, puncture of cysts without bulging of the gastric or duodenal wall and also in patients with portal hypertension is safer (23). The evolution of endoscopic ultrasound (EUS) has extended the indications for transmural drainage to include pancreatic abscesses, organized liquefied necrosis, and nonbulging PFCs (1, 7, 27).

MATERIALS AND METHODS

Appropriate Candidates

Indications for drainage of pancreatic pseudocysts will differ depending on whether the cyst develops in the setting of acute or chronic pancreatitis (23). In acute pancreatitis, drainage is indicated when pancreatitis fails to resolve with conservative treatment. A general recommendation is to observe the pseudocyst for 6 weeks in case it spontaneously resolves. If there is not a well-known history of acute or chronic pancreatitis, suspicion should be high that the collection may be another entity such as a cystic neoplasm (28).

In chronic pancreatitis, drainage is symptom driven, and can manifest as abdominal pain, gastric outlet obstruction, or jaundice from biliary compression (23). There are currently no clear indications for PFC drainage exclusively based on size (29).

It is crucial to determine whether the fluid collection is primarily liquid or contains significant solid debris, therefore adequate cross-sectional imaging is required before the procedure. Most experts also recommend assessing the integrity of the main pancreatic duct with pancreatography when considering drainage (28). Most pancreatic ductal side branch leaks will resolve during transmural drainage; however, in patients with major main pancreatic ductal leaks, placement of pancreatic ductal stent may be necessary to restore ductal integrity.

The presence of nonbulging fluid collections, known portal hypertension/high pretest probability of bleeding, prior failed transmural entry using non-EUS-guided techniques, or the need to exclude cystic neoplasm are all reasons to consider EUS-guided drainage (29–32).

Cross-sectional imaging defining the patient's anatomy and "window of entry" (CT and/or MRI) prior to the procedure is highly recommended.

Appropriate Endoscopists

Only endoscopists skilled at both EUS and ERCP should perform this procedure. Additionally, it should be performed in a tertiary care center where pancreaticobiliary surgeons as well as interventional radiologists are available in the event of a complication.

Patient Preparation

EUS-guided drainage is a time-consuming and technically challenging procedure. Therefore, performance with the assistance of anesthesia is recommended. All patients should receive preprocedural antibiotics.

Instrumentation

Linear array echoendoscopes with a channel size of at least 3 mm should be used as this allows placement of larger ten French stents (23, 32). The GF-UCT140 (Olympus, Japan) has a working channel of 3.7 mm and the EG 38UT (Pentax, Japan) has a working channel of 3.8 mm. For pseudocyst puncture, it is preferable to use a 19-G FNA needle (Wilson-Cook, Winston-Salem, North Carolina), so a larger 0.035-in. guidewire can be inserted through the needle for pseudocyst drainage. Dilatation of the fistula created can be performed using a wire-guided balloon or cystenterostome (26).

The single step approach led to the development of instruments that consists of a 19-G stainless steel puncture needle (Grosse, Daldorf, Germany) loaded with a modified 7-Fr or 10-F stent and a Teflon pusher catheter (Wilson-Cook) (33, 34). A needle-wire device, introduced by Giovannini et al. (35) consists of a 0.035-in. needle wire suitable for cutting current, a 5.5-F dilator and an 8.5-F stent (length 6 cm) with a pusher preassembled on the same catheter (Giovannini Needle Wire Oasis, Cook Endoscopy, Winston-Salem, NC).

Predrainage Evaluation

Determining the presence of coagulopathy and thrombocytopenia should be done prior to considering transmural drainage. Contrast-enhanced abdominal CT or magnetic resonance imaging should be performed to ascertain whether the collection contains liquid or solid debris, to visualize the relationship of the collection to surrounding luminal and vascular structures, and to rule out underlying etiologies of true pancreatic pseudocyst, for which therapy may be different (23, 29). The combination of ultrasonographic features and analysis of cyst contents, allows one to confirm the diagnosis of a pseudocyst prior to performing drainage (36).

PROCEDURE DESCRIPTION

Initially, using EUS, the cyst is located (Fig. 1). Color Doppler ultrasound is then used to identify regional vasculature. A fistula between the pseudocyst and the stomach or duodenum is created by introducing a 19-G needle into the pseudocyst (Fig. 2). A sample of cyst contents is aspirated and submitted for biochemical analysis, and if infection is suspected, a sample should be sent for Gram stain and culture. Contrast filling of the pseudocyst can be carried out under fluoroscopy to document size, bound-

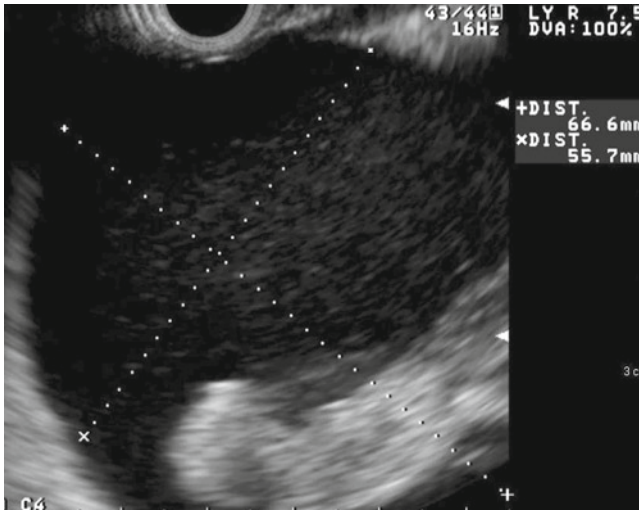


Fig. 1. EUS image and measurement of a large retrogastric pseudocyst.

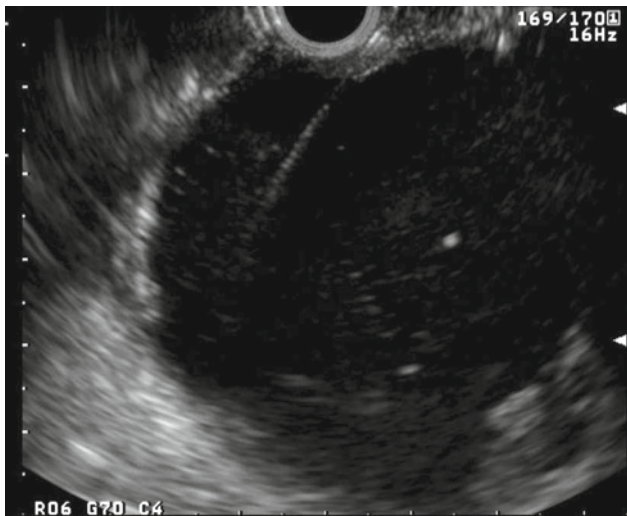


Fig. 2. EUS-guided puncture of the abscess, ultrasonographic view.

aries, and determine if communication with the pancreatic duct is seen. Drainage can be achieved by using either the needle-knife technique or the Seldinger technique. In the Seldinger technique, a 0.035-in guidewire is introduced through the needle and coiled within the pseudocyst (Fig. 3). Following this step, the fistula created is dilated with either a 6 mm or

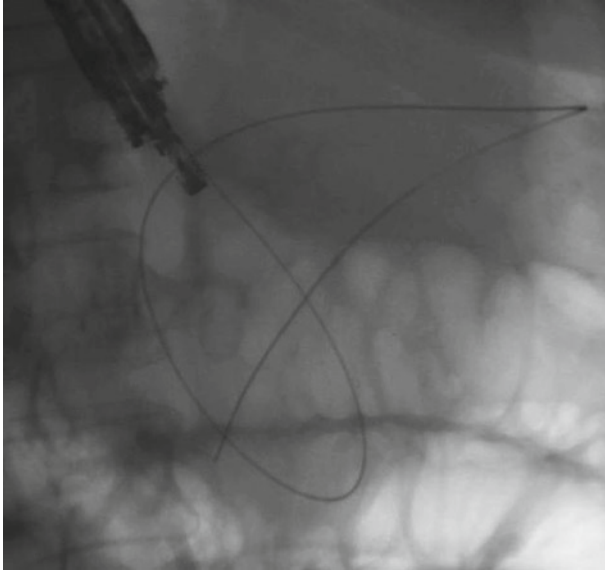


Fig. 3. Fluoroscopic image during placement of guidewire into the fluid collection.

8 mm balloon over the guidewire coiled into the pseudocyst (Fig. 4). The balloon is exchanged off the guidewire and one or two 10-Fr double-pigtail endoprotheses are placed (Figs. 5 and 6). At some institutions, a nasocystic drain may be placed to flush the fluid collection. An alternative to the balloon dilation technique is using a cystenterostome over the guidewire placed to enlarge the fistula using cautery (26). In cases where the pancreatic duct is disrupted or a dominant stricture is present, pancreatic duct stenting should be performed (27).

LITERATURE REVIEW

In 1992, Wiersema et al. reported the first EUS-guided drainage of a pancreatic pseudocyst using an interventional (i.e., large channel) EUS scope (37). Binmoeller et al. reported in 1995, an overall initial success rate of 78% (21/27 patients) after EUS-guided pseudocyst drainage (38). Giovannini et al. reported in 2001, a success rate of 88.5% in 35 patients who underwent EUS-guided drainage of a pancreatic pseudocyst or pancreatic abscess. In this study, four patients with pancreatic abscesses ultimately underwent surgery (39).

In 2006, Antillon et al. (25) reported that single-step EUS-guided transmural drainage, with large endoprotheses, is a safe and effective

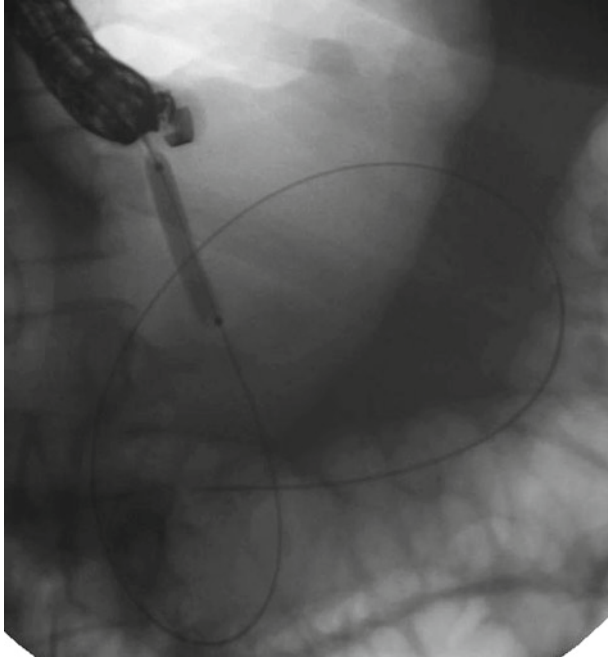


Fig. 4. Fluoroscopic image during dilation of the fistula created between the stomach and the abscess.

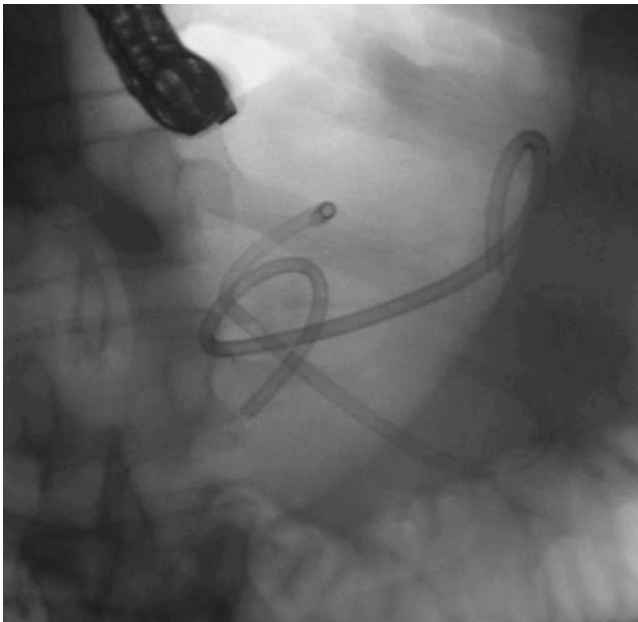


Fig. 5. Fluoroscopic images of deployment of a double pigtail 10 Fr stent across the fistula created.

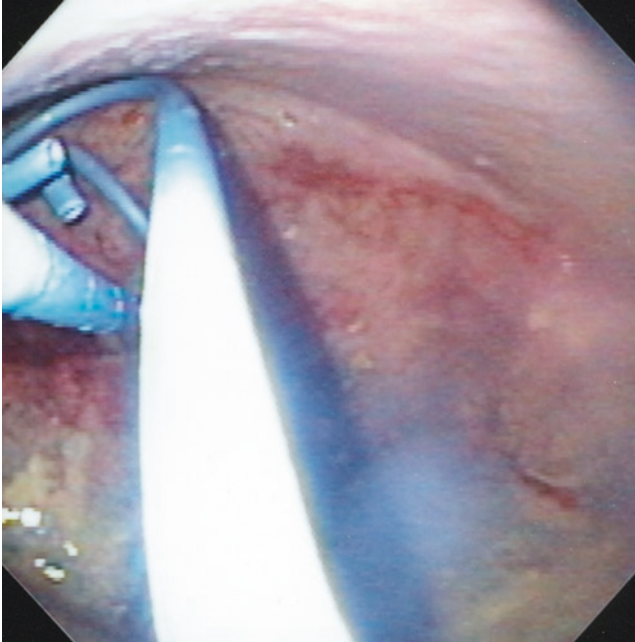


Fig. 6. Endoscopic view of a pseudocyst after decompression by two pigtailed.

therapy for patients with simple and complicated pancreatic pseudocysts. In this prospective cohort study, 82% (27/33) of patients had complete resolution of a pseudocyst, four had partial resolution with symptom relief, and there were only two major complications. Recurrence was observed in only one patient over 46 weeks of follow-up.

Kruger et al. (40) reported a prospective case series of 35 patients who underwent EUS-guided drainage with a single-step needle-wire device using 8.5 Fr stents. The overall resolution rate was 88% with a recurrence rate of 12% over 24 months. Fourteen patients (43%) had sustained clinical improvement and cyst resolution upon placement of the initial endoprosthesis. Cyst resolution was achieved by additional endoscopic cyst irrigation in ten patients (30%). This is probably related to the use of smaller diameter plastic stents.

In 2006, Hookey et al. (21) reported a total of 116 patients who presented with fluid collections varying from acute fluid collection, necrosis, acute pseudocyst, chronic pseudocyst, and pancreatic abscess. Of these patients, the drainage technique was transmural with EUS-guidance in 32 patients, and EUS-guidance was used in 19/41 patients who had a

combination of transpapillary and transmural drainage with EUS. EUS was used for a total of 44% (51/116) of the cases. The success rate for those who underwent EUS-guided transmural drainage was 90.6% (29/32). There was a recurrence rate of 12.5% (4/32) and three complications (9.4%). It is important to note that 12/32 (37.5%) patients in this subgroup had bulging fluid collections.

In 2007, Lopes et al. (41) published a retrospective review of 51 patients who underwent EUS-guided transmural drainage of pancreatic pseudocysts and abscesses; 94% (48/51) experienced successful drainage. The other three patients underwent surgery. Over 39 weeks of follow-up, recurrence was seen in 17.7% of patients, who then underwent subsequent endoscopic drainage. Interestingly, the placement of two stents decreased the complication rate for abscesses, while placement of a nasocystic drain did not.

Kahaleh et al. (32) reported a prospective study comparing 99 patients who underwent pseudocyst drainage using either conventional transmural drainage or EUS-guided drainage. Fifty-three patients who had a visible bulge and no obvious portal hypertension, underwent conventional drainage while the remaining 46 patients underwent EUS-guided drainage. A comparable number of patients in each group underwent transpapillary stent placement for pancreatic duct disruption or stricture. Both short-term success rates at one month (93% vs. 94%) and long-term success rates at 6 months (84% vs. 91%) were comparable. Complications occurred in 19% of EUS-guided drainage versus 18% of conventional transmural drainage, including bleeding(3), infection(8), stent migration(3), and pneumoperitoneum(5). No clear differences in efficacy or safety were observed between the two techniques. They concluded that the choice of technique is likely best predicted by individual patient presentation and local expertise, and recommended EUS for nonbulging collections and pseudocysts at risk for bleeding (i.e., intervening vessels or coagulopathy).

Barthet et al. (42) published a study assessing the clinical usefulness of a treatment algorithm for pancreatic pseudocysts. As per the algorithm, a CT scan should be performed first in patients with pancreatic pseudocyst-related symptoms to evaluate for the presence of portal hypertension. If there is no evidence of portal hypertension and there is clear bulging present, a conventional transmural drainage should be performed. If the pseudocyst is less than 5 cm without bulging and communication with the pancreatic duct, then transpapillary drainage should be performed. In patients who have portal hypertension with or without bulging, or in patients without bulging or ductal communication, EUS-guided drainage should be performed. Clinical success rates were achieved in 90% of the patients overall and EUS-guided

transmural drainage was performed on 28 patients (56%). Ninety percent of these patients achieved sustained response over a period of 12 months.

Varadarajulu et al. (31) published a prospective, nonrandomized study analyzing the characteristics that best predict the need for drainage of a pancreatic fluid collection by conventional transmural drainage versus EUS-guidance. In this study of 53 patients, conventional transmural drainage was technically successful in 30 patients (57%) and failed in 23 patients (43%). The causes of failed conventional drainage were the absence of luminal compression in 20, difficulty with scope positioning in two and bleeding with attempted drainage in one. All attempts at conventional drainage in the pancreatic tail were unsuccessful, but were successfully drained by EUS. When compared with conventional transmural drainage, EUS-guided drainage was longer in duration (40 min vs. 75 min), with similar rates of PFCs resolution. No complications were encountered in patients who underwent EUS-guided drainage, but bleeding occurred in one patient in the conventional transmural drainage group. The authors concluded that because a majority of pancreatic fluid collections can be drained by conventional transmural drainage in a shorter duration with comparable outcomes, EUS-guided drainage should be reserved mainly for collections located at the pancreatic tail.

In 2008, Varadarajulu et al. (43) published a prospective, randomized trial comparing, in 30 patients, the rate of technical success between EUS and EGD for transmural drainage of pancreatic pseudocysts. All patients randomized to EUS underwent successful drainage; however, only five of fifteen (33%) patients randomized to EGD had a technically successful procedure. All patients who failed drainage by EGD underwent successful drainage after crossover to EUS. After stenting, there was no significant difference in the rates of treatment success between EUS and EGD.

Two patients in whom drainage by EGD was attempted had major procedure-related bleeding, including one death. The authors concluded that when available, EUS should be considered as the first-line treatment modality for endoscopic drainage of pancreatic pseudocysts given its high technical success rate. It is important to note that a higher than average rate of failure in the conventional group was noted when compared to a previously published study (26). It is also important to note that the design of their study prevented EGD drainage without a stomach bulge. Consequently, their results, predictably, favor an EUS-guided approach. When attempted, 4/6 EGD-guided drainages were successful, compared to 23/24 EUS-guided drainages, which is not statistically significant. Although more complications were seen in the small number

Table 1
Outcomes in patients undergoing EUS-guided pancreatic fluid collection drainage

<i>EUS-guided drainage</i>	<i>Year</i>	<i>Number of patients</i>	<i>Procedure-related complications</i>	<i>Success rate</i>
Binmoeller (19)	1995	27	Bleeding (n=2)	21/27
Giovannini (39)	2001	35	Pneumoperitoneum (n=1)	31/35
Azar (46)	2006	23	Pneumoperitoneum (n=1)	21/23
Antillon (25)	2006	33	Bleeding (n=4), pneumoperitoneum (n=1)	31/33
Kruger (40)	2006	35	None	33/35
Kahaleh (32)	2006	46	Bleeding (n=2), stent migration (n=1), superinfection (n=4), pneumoperitoneum (n=2)	43/46
Barthet (42)	2008	28	Superinfection (n=5)	25/28
Hookey (21)	2006	32	Pneumoperitoneum (n=2), bleeding (n=1)	29/32
Lopes (41)	2007	51	Pneumoperitoneum (n=1), migration (n=1)	48/51
Varadarajulu (31)	2007	21	None	21/21
Varadarajulu (43)	2008	24	None	23/24
Total		368	Pneumoperitoneum (n=8), bleeding (n=9), superinfection (n=9), migration (n=2)	326/355 (91.8%)

of those undergoing EGD-guided drainage, the study was not powered to detect any difference in complications.

A summary of published data is presented in Table 1.

The absence of large randomized controlled trials comparing similar groups of patients undergoing conventional versus EUS-guided drainage

lead us to follow expert opinion when considering pseudocyst drainage. Other questions include the ideal number and size of stents that should be placed for adequate pancreatic drainage. Most authors recommend large plastic double pigtailed (20, 32). Talreja et al. (44) published a prospective case series in 18 patients who underwent drainage of pancreatic fluid collections by using covered self-expandable metallic stents (VIABIL; Conmed, Utica, NY). All but two of these patients underwent drainage with EUS-guidance. A total of 17 of 18 patients (95%) responded successfully, with 14 patients (78%) achieving complete resolution of their fluid collection. Another group has reported their experience on the use of metal stents for PFC drainage and facilitating necrosectomy, which is beyond the scope of this review (45). Further randomized studies need to be performed to confirm the safety and efficacy of these techniques.

CONCLUSION

The last decade has seen the rise of EUS-guidance in the drainage of PFCs. A variety of studies have been conducted and expert opinion has been reported to answer the question as to whether EUS-guidance is superior to conventional transmural drainage; however, a large prospective multicenter and randomized, controlled trial has not been reported that compares the two approaches. The advantages of using EUS-guided drainage include the ability to define the characteristics of the fluid collection, to rule out alternative diagnoses, and to assess for intervening vasculature. From a therapeutic stand point, one can access nonbulging collections, collections in challenging locations, or at high risk for complication (coagulopathy, intervening varices, or failed conventional transmural drainage). The disadvantages to this modality are that they are not readily available at all facilities and that procedure time is generally longer. Further progress in instrumentation is required to make this technique safer and more efficacious. In the meantime, EUS-guidance should be dictated by local expertise and the individual patient presentation.

REFERENCES

1. Baron TH, Thaggard WG, Morgan DE, Stanley RJ. Endoscopic therapy for organized pancreatic necrosis. *Gastroenterology*. 1996;111:755–64.
2. Baillie J. Pancreatic pseudocysts (part I). *Gastrointest Endosc*. 2004;59:873–9.
3. Yeo CL, Cameron JL, Sohn TA, Lillemoe KD, Pitt HA, Talamini MA, et al. Six hundred fifty consecutive pancreaticoduodenectomies in the 1990s: pathology, complications, and outcomes. *Ann Surg*. 1997;226:248–60.

4. Arvanitakis M, Delhaye M, Chamlou R, Matos C, Closset J, Medhi A, et al. Endoscopic therapy for main pancreatic duct rupture after silastic-ring vertical gastroplasty. *Gastrointest Endosc.* 2005;62:143–51.
5. Kloppel G. Pseudocysts and other non-neoplastic cysts of the pancreas. *Semin Diagn Pathol.* 2000;17:7–15.
6. Bradley III EL. A clinically based classification system for acute pancreatitis. Summary of the International Symposium on Acute Pancreatitis, Atlanta, GA, September 11 through 13, 1992. *Arch Surg.* 1993;128:586–90.
7. Baron TH, Harewood GC, Morgan DE, Yates MR. Outcome differences after endoscopic drainage of pancreatic necrosis, acute pancreatic pseudocysts, and chronic pancreatic pseudocysts. *Gastrointest Endosc.* 2002;56:7–17.
8. Baron TH, Morgan DE. The diagnosis and management of fluid collections associated with pancreatitis. *Am J Med.* 1997;102:555–63.
9. Yeo CJ, Bastidas JA, Lynch-Nyhan A, Fishman EK, Sinner MJ, Cameron JL. The natural history of pancreatic pseudocysts documented by computed tomography. *Surg Gyn Obstet.* 1990;170:411–7.
10. Bradley EL, Clements Jr JL, Gonzalez AC. The natural history of pancreatic pseudocysts: a unified concept of management. *Am J Surg.* 1979;137:135–41.
11. Gouyon B, Levy P, Ruzsniowski P, Zins M, Hammel P, Vilgrain V, et al. Predictive factors in the outcome of pseudocysts complicating alcoholic chronic pancreatitis. *Gut.* 1997;41:821–5.
12. Warsaw AL, Rattner DW. Timing of surgical drainage for pancreatic pseudocyst. Clinical and chemical criteria. *Ann Surg.* 1985;202:720–4.
13. Bradley III EL. A fifteen year experience with open drainage for infected pancreatic necrosis. *Surg Gyn Obstet.* 1993;177:215–22.
14. Boerma D, van Gulik TM, Obertop H, Gouma DJ. Internal drainage of infected pancreatic pseudocysts: safe or sorry? *Dig Surg.* 1999;16:501–6.
15. van Sonnenberg E, Wittich GR, Casola G, Brannigan TC, Karnel F, Stabile BE, et al. Percutaneous drainage of infected and noninfected pancreatic pseudocysts: experience in 101 cases. *Radiology.* 1989;170:757–61.
16. Ahearn PM, Baillie JM, Cotton PB, Baker ME, Meyers WC, Pappas TN. An endoscopic retrograde cholangiopancreatography (ERCP)-based algorithm for the management of pancreatic pseudocysts. *Am J Surg.* 1992;163:111–5.
17. Adams DB, Harvey TS, Anderson MC. Percutaneous catheter drainage of infected pancreatic and peripancreatic fluid collections. *Arch Surg.* 1990;125:1554–7.
18. Neff R. Pancreatic pseudocyst and fluid collections: percutaneous approaches. *Surg Clin North Am.* 2001;81:399–403.
19. Binmoeller KF, Seifart H, Walter A, Soehendra N. Transpapillary and transmural drainage of pancreatic pseudocysts. *Gastrointest Endosc.* 1995;42:219–24.
20. Cahen D, Rauws E, Fockens P, Weverling G, Huibregtse K, Bruno M. Endoscopic drainage of pancreatic pseudocysts; long-term outcome and procedural factors associated with safe and successful treatment. *Endoscopy.* 2005;37:977–83.
21. Hookey LC, Debroux S, Delhaye M, Arvanitakis M, Le Moine O, Deviere J. Endoscopic drainage of pancreatic fluid collections in 116 patients: a comparison of etiologies, drainage techniques, and outcomes. *Gastrointest Endosc.* 2006;63:635–43.
22. Delhaye M, Matos C, Deviere J. Endoscopic management of chronic pancreatitis. *Gastrointest Endosc Clin N Am.* 2003;13:717–42.

23. Giovannini M. EUS-guided pancreatic pseudocyst drainage. *Tech Gastrointest Endosc.* 2007;9(1):32–8.
24. Howell DA, Holbrook RF, Bosco JJ, Muggia RA, Biber BP. Endoscopic needle localization of pancreatic pseudocysts before transmural drainage. *Gastrointest Endosc.* 1993;39:693–8.
25. Antillon MR, Shah RJ, Stiegmann G, Chen YK. Single-step EUS-guided transmural drainage of simple and complicated pancreatic pseudocysts. *Gastrointest Endosc.* 2006;63(6):797–803.
26. Sanchez Cortes E, Maalak A, Le Moine O, Baize M, Delhaye M, Matos C, et al. Endoscopic cystenterostomy of nonbulging pancreatic fluid collections. *Gastrointest Endosc.* 2002;56:380–6.
27. Arvanitakis M, Delhaye M, Bali MA, Matos C, De Maertelaer V, Le Moine O, et al. Pancreatic fluid collections: a randomized controlled trial regarding stent removal after endoscopic transmural drainage. *Gastrointest Endosc.* 2007;65(4):609–19.
28. Baron TH. Endoscopic drainage of pancreatic pseudocysts. *J Gastrointest Surg.* 2008;12:369–72.
29. Andren-Sandberg A, Dervenis C. Pancreatic pseudocysts in the 21st century. Part II. Natural history. *JOP.* 2004;5:64–70.
30. Jacobson B, Baron T, Adler DG, Davila RE, Egan J, Hirota WK, et al. ASGE guideline: the role of endoscopy in the diagnosis and the management of cystic lesions and inflammatory fluid collections of the pancreas. *Gastrointest Endosc.* 2005;61:363–70.
31. Varadarajulu S, Wilcox CM, Tamhane A, Eloubeidi MA, Blakely J, Canon CL. Role of EUS in drainage of peripancreatic fluid collections not amenable for endoscopic transmural drainage. *Gastrointest Endosc.* 2007;66(6):1107–19.
32. Kahaleh M, Shami VM, Conway MR, Tokar J, Rockoff T, De La Rue SA, et al. Comparison of EUS and conventional endoscopic drainage of pancreatic pseudocyst. *Endoscopy.* 2006;38:355–9.
33. Seifert H, Dietrich C, Schmitt T, Caspary W, Wehrmann T. Endoscopic ultrasound-guided one-step transmural drainage of cystic abdominal lesions with a large-channel echoendoscope. *Endoscopy.* 2000;32:255–9.
34. Seifert H, Faust D, Schmitt T, Dietrich C, Caspary W, Wehrmann T. Transmural drainage of cystic peripancreatic lesions with a new large-channel echoendoscope. *Endoscopy.* 2001;33:1022–6.
35. Giovannini M, Bernardini D, Seitz JF. Cystogastrostomy entirely performed under endosonography guidance for pancreatic pseudocyst: results in six patients. *Gastrointest Endosc.* 1998;48:200–3.
36. Baron TH. Endoscopic drainage of pancreatic pseudocysts, abscesses and organized (walled-off) necrosis. In: ERCP Baron TH, Kozarek R, Carr-Locke DL, editors. Philadelphia: Saunders Elsevier; 2008, Chapter 45
37. Wiersema MJ. Endosonography-guided cystoduodenostomy with a therapeutic ultrasound endoscope. *Gastrointest Endosc.* 1996;44:614–7.
38. Binmoeller KF, Soehendra N. Endoscopic ultrasonography in the diagnosis and treatment of pancreatic pseudocysts. *Gastrointest Endosc Clin N Am.* 1995;5:805–16.
39. Giovannini M, Pesenti CH, Rolland AL, Moutardier V, Delpero JR. Endoscopic ultrasound guided drainage of pancreatic pseudocyst and pancreatic abscess using a therapeutic echoendoscope. *Endoscopy.* 2001;33:473–7.

40. Kruger M, Schneider AS, Manns MP, Meier PN. Endoscopic management of pancreatic pseudocysts or abscesses after an EUS-guided 1-step procedure for initial access. *Gastrointest Endosc.* 2006;63:409–16.
41. Lopes CV, Pesenti C, Bories E, Caillol F, Giovannini M. Endoscopic-ultrasound-guided endoscopic transmural drainage of pancreatic pseudocysts and abscesses. *Scan J Gastroenterol.* 2007;42:524–9.
42. Barthet M, Lamblin G, Gasmi M, Vitton V, Desjeux A, Grimaud JC. Clinical usefulness of a treatment algorithm for pancreatic pseudocysts. *Gastrointest Endosc.* 2008;67(2):245–52.
43. Varadarajulu S, Christein JD, Tamhane A, Drelichman ER, Wilcox CM. Prospective randomized trial comparing EUS and EGD for transmural drainage of pancreatic pseudocysts (with videos). *Gastrointest Endosc.* 2008;68(6):1102–11.
44. Talreja JP, Shami VM, Ku J, Morris TD, Ellen K, Kahaleh M. Transenteric drainage of pancreatic fluid collections with fully covered self-expanding metallic stents (with video). *Gastrointest Endosc.* 2008;68:1199–203.
45. Antillon MR, Bechtold ML, Bartalos CR, Marshall JB. Transgastric endoscopic necrosectomy with temporary metallic esophageal stent placement for the treatment of infected pancreatic necrosis. *Gastrointest Endosc.* 2009;69(1):178–80.
46. Azar RR, Oh YS, Janec EM, Early DS, Jonnalagadda SS, Edmundowicz SA. Wire-guided pancreatic pseudocyst drainage by using a modified needle knife and therapeutic echoendoscope. *Gastrointest Endosc.* 2006;63(4):688–92.

Endoscopic Ultrasound-Guided Celiac Plexus Block and Celiac Plexus Neurolysis

*Alejandra Castillo-Roth, MD
and Frank Gress, MD*

CONTENTS

INTRODUCTION
ANATOMICAL AND FUNCTIONAL
CONSIDERATIONS
CELIAC PLEXUS
TECHNIQUE
CPN
CELIAC PLEXUS BLOCK
PREPARATION PREPROCEDURE
POSTPROCEDURE MONITORING
SIDE EFFECTS AND COMPLICATIONS
OF THE PROCEDURE
PROCEDURE EFFICACY

Abstract

Celiac plexus neurolysis (CPN) and celiac plexus block (CPB) have been described as alternatives to increasing narcotic usage for patients with chronic abdominal pain due to pancreatic cancer and chronic pancreatitis. Endoscopic ultrasound (EUS) allows for direct and easy visualization of the celiac plexus region, and more recently, direct endosonographic views of the ganglia and interconnecting fibers have

From: *Clinical Gastroenterology: Endoscopic Ultrasound*,
Edited by: V. M. Shami and M. Kahaleh, DOI 10.1007/978-1-60327-480-7_18,
© Springer Science+Business Media, LLC 2010

been described. This technique provides a safer, more reliable and possibly cost-effective means of performing the procedure when compared with the percutaneous approach.

Although there are no strong randomized controlled trials or quality of life studies, there is some convincing evidence of the efficacy of EUS CPN and EUS CPB for the treatment of abdominal pain related to pancreatic cancer or chronic pancreatitis. Several small to medium-sized retrospective and prospective studies have reported significant data that supports the use of EUS-guided CPN and CPB procedures to provide safe delivery of pain relief.

Key Words: Pancreatic cancer, Pancreatitis, Celiac plexus, Celiac ganglia, Celiac plexus block, Celiac plexus neurolysis, Endoscopic ultrasound

INTRODUCTION

Chronic abdominal pain of pancreatic origin, from either malignancy or chronic pancreatitis, can be very incapacitating and associated with a significant decrease in the quality of life of these patients. There are many approaches used to treat these patients, including pancreatic enzymes, analgesics: escalating from acetaminophen and nonsteroidal anti-inflammatory drugs to increasingly potent narcotics, Celiac plexus block (CPB) or surgical ganglionectomy. Although administering analgesics in these patients is the main step in the management, their efficacy is limited and many concerns arise from their use. Particularly, with narcotics, side effects such as severe constipation, dependency, nausea, vomiting, lethargy, and delirium limits its use in patients with these conditions (1–5).

Since the visceral afferent neurons that transmit pain from the pancreas travel through the celiac plexus before synapsing in the spinal cord, blockage or destruction (neurolysis) of this pathway at the level of the celiac plexus has been attempted as a nonpharmacological method of mitigating pain related to chronic pancreatitis or pancreatic cancer, respectively.

The initial technique for performing celiac plexus neurolysis (CPN) was first described in 1914 by Kappis (6) who used a posterior transcutaneous approach, which was performed blindly (not guided by imaging modalities, since they were not available at that time).

As new imaging modalities developed, multiple methods for performing CPB or CPN have been described and are now being used. These include fluoroscopy, computed tomography and ultrasound guided techniques (7–17). More recently, with the development of endoscopic

ultrasound (EUS), EUS-guided injection of the celiac plexus was described. Initially, two studies were reported using this technique. Wiersema et al. first described EUS-guided CPN in patients with pancreatic cancer pain by injecting a local anesthetic (bupivacaine) and absolute alcohol at the level of the celiac plexus (18). Gress et al. first described EUS-guided CPB in patients with pain related to chronic pancreatitis by injecting a local anesthetic (bupivacaine) and a corticosteroid (triamcinolone) (19).

The EUS-guided approach, given anatomic considerations, offers the most direct nonsurgical approach to the celiac plexus. This chapter describes the techniques used for performing EUS-guided CPB and EUS-guided CPN, as well as reviews the current evidence in reference to its efficacy and safety.

ANATOMICAL AND FUNCTIONAL CONSIDERATIONS

Pancreas

The pancreas is a retroperitoneal endocrine, exocrine, and paracrine gland. It has an oblique orientation with the head of the gland at the level of the body of L2, and the tail of the gland located to the left at the level of the body of L1. Visceral pain from the pancreas is generally severe, located in the epigastrium and radiates to the back. The pathophysiology of pain in chronic pancreatitis and pancreatic cancer is complex and not well understood. Altered innervation with an increase in the number and diameter of nerve fibers (20) as well as destruction and invasion of intrapancreatic nerves by immune cells and malignant cells have been reported (21). Also brain-mediated mechanisms have been implicated (22).

CELIAC PLEXUS

The celiac plexus is a dense network of ganglia and interconnecting fibers that contain pre- and postganglionic sympathetic fibers, which connect within the celiac plexus. It also contains preganglionic parasympathetic fibers of the vagal trunk and afferent vagal fibers. Finally, nociceptive fibers that transmit pain travel through the celiac plexus as well. All these fibers innervate and transmit signals to and from the pancreas, hepatobiliary tree, spleen, mesentery, and large intestine up to the midtransverse colon.

The celiac plexus is located at the level of T12–L1, beneath the diaphragm, adjacent to the aorta, and surrounding the origin of the celiac

trunk. In general, the celiac plexus has two ganglia that lie on either side of the aorta in the above mentioned location although one to five ganglia distributed to the right and left of the celiac artery take-off have been described (23).

TECHNIQUE

The linear echoendoscope is used to perform the CPB and CPN. After oral intubation, the echoendoscope is slowly advanced down the esophagus into the esophagogastric junction and posterior lesser curve of the gastric fundus. At this level, longitudinal views of the aorta should be easily identified as a long anechoic tubular structure. Doppler can also be used to confirm this. The aorta is then traced down to the celiac artery take-off or celiac trunk, which is usually located between 40 and 50 cm from the incisors (see Figs. 1 and 2).

If the instrument is advanced slightly further caudally, the superior mesenteric artery take-off from the aorta can be seen. The exact location of the celiac plexus is controversial, however, it is believed to be located surrounding the celiac artery take-off or between the superior mesenteric artery and the celiac artery take-off.

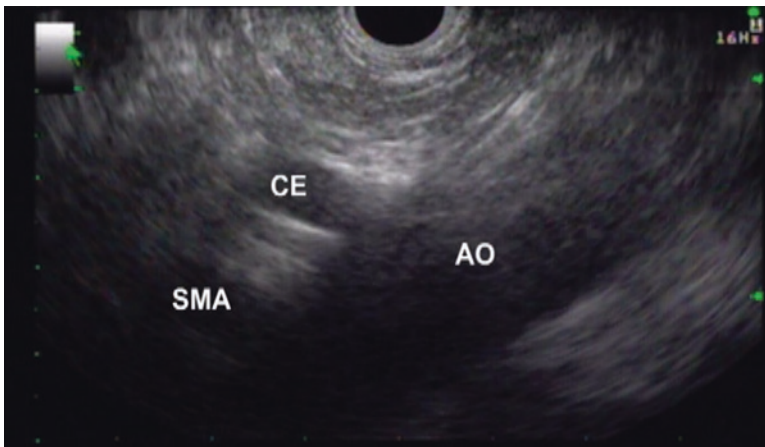


Fig. 1. Linear-array EUS imaging of aorta at the level of the celiac artery and superior mesenteric artery take-off. AO aorta, CE celiac trunk, SMA Superior mesenteric artery.

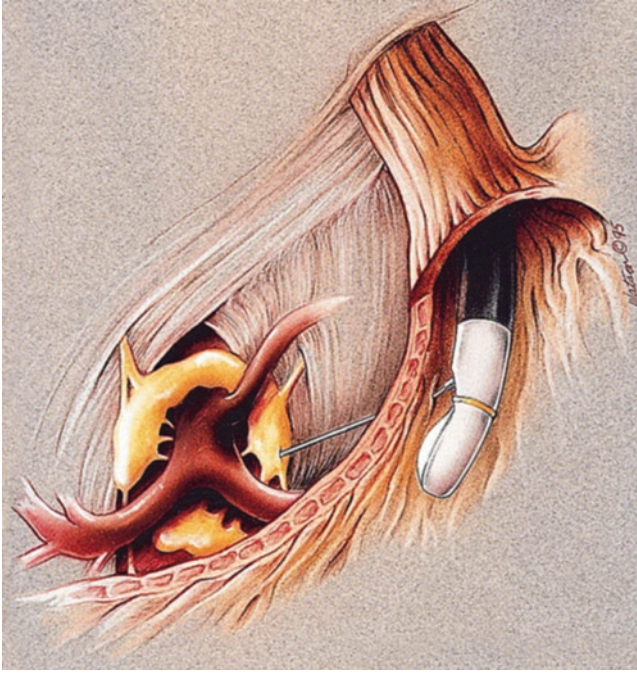


Fig. 2. Illustration of EUS-guided celiac plexus injection. The linear echoendoscope within the stomach and the needle is passing through the stomach wall into a celiac ganglion (Courtesy of Jane Watson, CMI. From ref (18). Copyright Elsevier (1996)).

Prior to performing the EUS CPB or neurolysis, it is advisable to visualize the remaining organs and structures in the area. Evaluation of the pancreas is particularly important to confirm the diagnosis of chronic pancreatitis or in the case of pancreatic cancer to determine the extent of disease.

After evaluation of the pancreas, the echoendoscope is slowly withdrawn to the level of the celiac artery take-off in order to perform the block or neurolysis. Doppler can be utilized during the block to better delineate the vessels and to ensure the absence of vessels in the path of the needle (see Fig. 3).

Two different injection techniques have been described. The initial bilateral injection technique, where each side – right anterolateral and left anterolateral – of the space immediately anterior to the aorta at the level of the celiac artery origin is injected (18, 19) and the one injection site technique, where the needle is placed just anterior to the take-off of

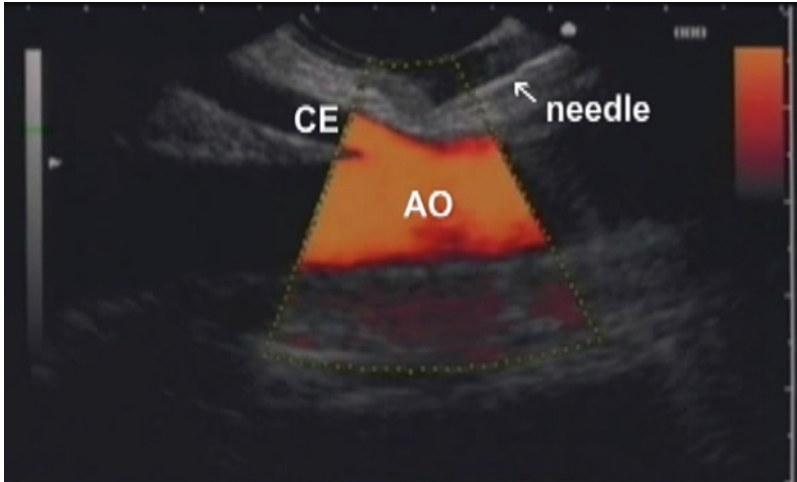


Fig. 3. Linear-array EUS imaging using doppler guidance for celiac plexus neurolysis in a patient with pancreatic cancer. AO aorta, CE celiac trunk.

the celiac artery and the entire solution is injected there with subsequent bilateral spread of solution (24, 25).

Recently, perhaps due to the advances in the quality of endosonographic imaging or increasing familiarity with the endosonographic anatomy of the celiac region, direct endosonographic visualization of the celiac ganglia has been described in 73–90% of a group of patients undergoing upper EUS for a variety of indications, including tumor staging, FNA of pancreatic lesions and the evaluation of subepithelial lesions (26–29). Histologic confirmation by FNA or Tru-cut needle biopsy with the intention of excluding malignant lymph nodes was performed in some of these cases (26–28).

Identification of celiac ganglia with EUS now allows direct injection into the ganglia rather than injection into the area of the celiac plexus, which in theory should enhance efficacy and safety. Endosonographic characteristics of ganglia have been consistently described as hypoechoic, oblong, comma-shaped or multilobulated structures with irregular margins that often contain hyperechoic focus or stranding. If more than one is present, they can be connected by thin hypoechoic threads, which likely represent nerve fibers (see Fig. 4). Its echogenicity is similar to the echogenicity of the adrenal gland. Color Doppler of the ganglia discloses little or no flow. Their size varied from 2 mm to 20 mm in depth by 7–20 mm in length (26–29).

Since the echoendoscope is located in the proximal stomach, which is situated to the left of the midline, most of the ganglia were seen

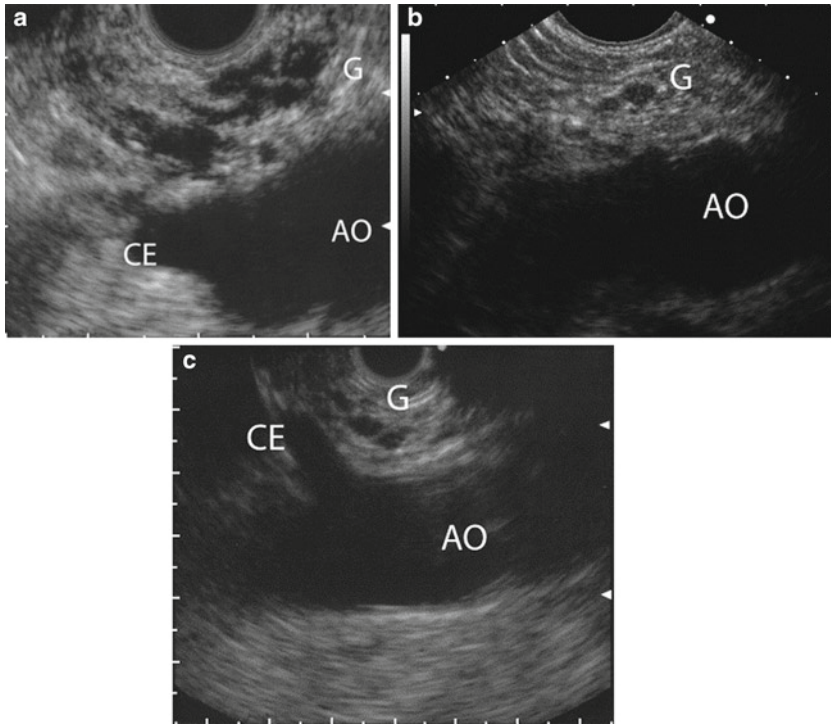


Fig. 4. (a–c) Linear-array EUS images of celiac ganglia (G) presenting as hypoechoic structures with lobulations, hyperechoic bands, or appearance of confluent spheres seen arising above the celiac artery (CE), anterior to the aorta (AO). From ref. (26) Copyright Elsevier (2006).

anterior to the aorta just above and to the left of the celiac artery take-off and medial to the left adrenal gland. Although on a few occasions ganglia were seen on the right side, visualizing these by EUS is more challenging. Celiac ganglia can be visualized with both the linear and radial echoendoscope (26–29).

Levy et al. (30) reported that direct ganglia injection was performed placing the needle tip in the center of ganglia that was smaller than 1.0 cm within the axis of the needle plane. While for ganglia > 1.0 cm or larger in the needle plane axis, the tip was advanced to the deepest point within the ganglia and slowly withdrawn as injection was given. The exact amount of injectate per ganglia was not specified, but as many ganglia as possible were injected in this study.

Regardless of the CPB technique used, once the echoendoscope is positioned to begin the procedure, a 22-gauge EUS fine needle

aspiration (FNA) needle is passed through the biopsy channel and attached to the echoendoscope. The needle is then advanced toward the celiac axis until the tip is inserted to the level of the celiac trunk (desired position). The stylet in the center of the needle is then withdrawn, taking care not to shift the position of the needle. This can be prevented by grasping the needle system's shaft tightly. Once the stylet is removed, a 10 cc syringe is attached to the top of the needle system and aspirated in order to confirm that the needle is not inside a blood vessel. Once this is confirmed, the agents (Bupivacaine and Triamcinolone for chronic pancreatitis or 98% Ethanol for pancreatic cancer) are individually injected in the celiac space. Each time a new syringe is exchanged, it should be aspirated prior to injection to confirm safe positioning. Inadvertent injection of these agents, especially Bupivacaine, into a blood vessel can be lethal.

CPN

The most common agent used for performing a CPN is dehydrated 98% absolute alcohol, although concentrations between 50% and 100% have been also described (31). Absolute alcohol is known to cause nerve damage by disruption of the cell membranes and precipitation of mucoprotein and lipoprotein. Given the potential for painful neuritis that can occur with alcohol injection a local anesthetic, 0.25% preservative-free bupivacaine, is also injected. Initial descriptions of this technique used separate injections, first 10 ml of bupivacaine followed by 10 ml of alcohol on each side if the Bilateral injection technique was performed (18); or 20 ml of bupivacaine, followed by 20 ml of alcohol if the single site injection was carried out (24, 25). However, mixing both agents prior to injections has also been used (30). It is important to flush with 3–5 cc of preservative-free saline after each injection. An echo dense cloud may also be seen in the area being injected with absolute alcohol. Alcohol blocks have typically been reserved for malignant pain as alcohol theoretically causes permanent fibrotic hyalinization and inflammatory damage of the celiac plexus area (32).

CELIAC PLEXUS BLOCK

The most common agents for performing a CPB are a combination of a local anesthetic, usually 0.25% preservative-free Bupivacaine; however, higher percentages have also been used; and a corticosteroid, either 80 mg of Triamcinolone or 80 mg of Solumedrol. The procedure is

performed using the same techniques described earlier. The rationale for using steroids instead of alcohol for the CPB in patients with chronic pancreatitis is based on the fact that this is a chronic rather than a terminal condition and absolute alcohol injection would in theory destroy the plexus causing permanent damage (32). In addition, in initial CPB studies using the percutaneous and surgical approaches, neurologic side effects such as paraplegia were noted likely due to the absolute alcohol spread over the spinal cord area (33–35). The risk of this happening has been reported to be much lower using an anterior approach, and theoretically even less under EUS guidance, therefore EUS-guided injection of alcohol in these patients has also been described (30). Finally, while some patients obtained relief, it was reported anecdotally that some of these patients later required surgical intervention for treating their chronic pancreatitis and were found to have extensive inflammatory response and scarring presumably due to the ethanol that made the surgical approach extremely difficult.

PREPARATION PREPROCEDURE

- The use of preprocedure laboratories has not been clearly defined, but initial papers recommended checking a blood count and coagulation profile prior to the procedure (18, 36).
- Patients should be well hydrated with intravenous normal saline between 500 ml and 1,000 ml prior to the procedure. Some endoscopists encourage patients to drink lots of fluids the day before the procedure to achieve the same effect.
- The patient is positioned in the left lateral decubitus, as is done with most upper endoscopic procedures.
- These patients need to be adequately sedated and their history of chronic narcotic use can make sedation a challenge. Consider the management of sedation by an anesthesiologist if necessary. Usually, monitored anesthesia care (MAC) can be successfully utilized; however, in some circumstances general anesthesia is required.
- Patients should have continuous monitoring of blood pressure and pulse oximetry throughout the procedure.
- The use of prophylactic antibiotics remains controversial, and its use is based on early reports of infection post EUS-guided CPB. In one such report, a patient with chronic pancreatitis on acid suppression therapy received bupivacaine and triamcinolone steroids using the bilateral injection technique and developed a pancreatic abscess after EUS CPB (37). The patient was treated with parenteral antibiotics and did well, being discharged in several days. Given the bactericidal properties of absolute

alcohol, the need for prophylactic antibiotics is probably not necessary for EUS CPN.

POSTPROCEDURE MONITORING

- Patients are usually monitored in recovery for 2 h after the procedure. Vital signs should be carefully monitored initially and then routinely once stable. Transient hypotension can occur and should be treated with bolus infusions of normal saline.
- Patients should be monitored for pain and symptoms suggestive of orthostatic hypotension.
- Patients are discharged when determined to be stable and able to leave for home.

SIDE EFFECTS AND COMPLICATIONS OF THE PROCEDURE

Most of the short-term side effect of EUS CPN and CPB are due to the sympathetic blockage, these include transient diarrhea which could last up to 2 weeks, described in 4–44% of the patients; and transient hypotension, seen in 20–40% of the patients. Hypotension in these patients generally responds rapidly to intravenous fluids (30, 35–39).

Transient pain increase can also occur. Initial studies reported about 9% of the patients experienced pain exacerbation immediately after the procedure, which generally starts while the patient is in the recovery room and could last up to 48 h and may require emergency visits and hospitalization in which a temporary increase of narcotics may be needed in some patients (30, 36–40).

More recently, with the description of EUS-directed injection into the celiac ganglion, pain or discomfort while the injectate is passing into the celiac ganglion has been described. This can manifest as an abrupt increase of patient movement, attempt to verbalize, and an increase in pulse and respiration even in patients undergoing deep sedation (30). This study also reported a higher rate of transient pain increase, which was seen in 36% of these patients.

Major complications are rare (less than 1% of patients) and have only been described using the percutaneous and surgical approaches (33–35), but they could potentially happen using EUS guidance as well and include lower extremity paresis and parathesia, pneumothorax, renal puncture, gastroparesis, and retroperitoneal bleeding.

Postprocedure infections are also uncommon. Development of peri-pancreatic abscess after EUS CPB as previously mentioned was described in a patient who was using a proton pump inhibitor; it resolved uneventfully with antibiotic therapy (37).

PROCEDURE EFFICACY

The evidence available for the efficacy of EUS CPN and CPB does not come from studies of superior quality and most of them have been for analgesia in patients with pancreatic cancer.

Eisenberg et al. (38) conducted a meta-analysis of percutaneous CPN for the treatment of cancer pain. Most of the patients had pancreatic cancer, but patients with pain related to other intraabdominal cancer were also included. Twenty-four studies were incorporated, only two were randomized controlled, one was prospective, and 21 were retrospective. The author concluded that although the evidence is not strong given the poor quality of most of the studies, his analysis suggests that regardless of the percutaneous technique used; CPB has long-lasting benefit for 70–90% of patients and a low rate of adverse effects from the procedure.

More recently, another meta-analysis (40) reported on five randomized controlled trials of CPN for pain control in unresectable pancreatic cancer. Four studies used the percutaneous approach under radiological guidance, and one study used an intraoperative approach. The conclusion was that CPN is associated with slightly improved pain control, reduced narcotic usage, and constipation as a side effect when compared with standard therapy using nonsteroidal anti-inflammatory drugs and/or narcotics. Three of these studies included a sham procedure in the control arm.

The initial study for EUS CPN for pain control in patients with pancreatic cancer included 30 patients, 25 patients with pancreatic cancer and five patients with metastatic intraabdominal cancer who underwent EUS CPN. No placebo control group was used in this study (18). Only 29 of these patients were followed for more than 2 weeks. The pain score measure by standardized visual analog scale (range: 0–10) improved from 6.6 ± 2.2 to 1.1 ± 1.5 at 2 weeks ($p=0.0002$), 1.5 ± 2.0 at 4 weeks ($p=0.0003$), 1.6 ± 2.8 at 8 weeks ($p=0.015$), and 1.2 ± 1.3 at 12 weeks ($p=0.004$). Almost 50% of the patients reported less narcotic use at week 12, while 42% reported the same narcotic usage (28).

A subsequent study from the same author (36) added 33 patients with pancreatic cancer to the initial series; statistical analysis revealed a significant decrease in the pain score, with 54% of the patients

experiencing a decline of greater than two points in their pain scores measured by standardized visual analog scale after having an EUS CPN. The greatest benefit was seen in those patients who received adjuvant therapy with chemotherapy alone or chemotherapy plus radiation. Reduction in the pain score from baseline was seen up until the end of the study at 24 weeks after CPN, at which point only data from 14 patients was available. Overall, narcotic usage did not differ over time during the study period.

The first study describing EUS CPB in patients with pain due to chronic pancreatitis was a prospective randomized comparison of EUS CPB and CT-guided CPB (19). Ten patients were randomized to the EUS technique, while eight patients had CT-guided CPB. The agents used and dosages for both techniques were identical. Fifty percent of the patients in EUS-guided CPB arm experienced decreased pain compared to 25% of the patients in the CT-guided CPB arm. The median pain score was measured using the visual analog scale (0 to 10) after EUS CPB and decreased from 8 to 1 at 4 weeks of follow-up versus a decrease of the median pain score from 10 to 9 at 4 weeks of follow-up after CT CPB. Also, significantly longer duration of effect was noted with EUS CPB, approximately 15 weeks when compared with approximately 4 weeks for CT CPB.

A cost analysis was also performed and concluded that cost per patient for pain control using CPB is lower with the EUS technique. A larger study by the same author (37) prospectively analyzed the results of EUS CPB in 90 patients with pain due to chronic pancreatitis. Overall, 55% of the patients reported a decrease of their pain after the block. The mean pain score after EUS CPB significantly decreased from 8 to 2 ($p < 0.005$) at both 4 and 8 weeks follow-up. Twenty-six percent of the subjects have persistent benefit at week 12 postprocedure and this decreased to 10% of the subjects at week 24. A subgroup analysis demonstrated that patients with prior pancreatic surgery due to chronic pancreatitis and patients less than 45 years of age were less likely to respond to the EUS CPB.

Two studies presented in abstract form have addressed the question of one site (just anterior to the celiac artery take-off) versus bilateral (each side of the celiac artery take-off) injection (24, 25). The initial report was a prospective study with 160 patients with pancreatic pain due to chronic pancreatitis or pancreatic cancer; 71 patients received injection in one site and 89 patients received bilateral injections; the percentage of pain reduction at seven days was significantly higher in the group with bilateral injections compared to the one site injection group, 70.4% versus 45.9%, but again follow-up was only 1 week. In general, the patients with pancreatic cancer pain responded better than

patients with chronic pancreatitis pain (24). The second study was a prospective randomized trial evaluating CPB for chronic pancreatitis pain. In this study, 23 patients received injection in one site and 28 patients received injection in two sites. Patients were followed until they no longer had pain relief (range 1–203 days). A total of 55% of the patients reported pain relief and no significant difference was seen in duration or onset of pain relief comparing one versus two injection sites (25).

All the above studies utilized the injection technique where the needle is placed in the area of the celiac plexus, either one site injection or bilateral injections, and not necessarily directly into the ganglia (see Technique section above). Levy et al. carried out the initial evaluation of efficacy and safety of EUS-guided direct ganglia neurolysis and block (30). This was a retrospective analysis in patients with pain related to chronic pancreatitis ($n=18$) or pancreatic cancer ($n=18$) that underwent direct EUS-guided ganglia injections. Sixteen out of seventeen of the cancer patients who received alcohol injection reported partial pain relief, while the only patient who received steroid injection in this group reported no response. Among the patients with chronic pancreatitis pain, 80% (4/5) of those who received alcohol injection reported either partial or complete resolution of pain versus 38% (5/13) of those who received steroid injection. Pain relief was more often noted in patients who developed transient pain after injection, a well-described side effect of this procedure (see Side Effect and Complications section). Interestingly, this initial transient pain increase was seen in 36% of the study's patients which is much higher than the 9% described by initial studies in which specific ganglia identification and injection was not performed. This is possibly related to a more accurate injection of the plexus.

A meta-analysis that reported on the effectiveness of the EUS-guided technique has been presented in abstract form (41). The study analyzed three studies of EUS CPN in patients with abdominal pain due to pancreatic cancer, two of which have been discussed above (30, 36). The three studies met strict criteria to be included in the meta-analysis and all had positive results. The authors concluded that EUS-guided CPN is effective in reducing abdominal pain due to pancreatic cancer in about 73% of patients without potentially life-threatening complications. However, narcotic usage did not change significantly after administering the EUS CPN.

In conclusion, EUS-guided CPB and CPN appear to be effective options for patients with intractable chronic abdominal pain due to pancreatic cancer or chronic pancreatitis that fails to respond to conservative treatment options. Particularly, it should be considered in those

with significant side effects from narcotic use or with pain unresponsive to medical management, including diet modification, pancreatic enzymes, and narcotics. The available evidence is more conclusive for patients with pain related to pancreatic cancer. That said, all existing studies have limitations and further research in this area is needed. The most conclusive evidence for EUS CPB and EUS CPN would derive from a randomized double-blinded placebo control study that not only takes into consideration the different techniques available (single or bilateral site injections versus direct injection into the ganglia) but also the medication injected: bupivacaine and alcohol versus bupivacaine and steroid. That study is yet to come.

REFERENCES

1. Lebovits AH, Lefkowitz M. Pain management of pancreatic carcinoma: a review. *Pain*. 1989;36:1–11.
2. Weissman DE, Haddox JD. Opioid pseudoaddiction – an iatrogenic syndrome. *Pain*. 1989;36:363–6.
3. Zenz M, Strumpf M, Tryba M. Long-term oral opioid therapy in patients with chronic nonmalignant pain. *J Pain Symptom Manage*. 1992;7:69–77.
4. Reidenberg MM, Portenoy RK. The need for an open mind about the treatment of chronic nonmalignant pain. *Clin Pharmacol Ther*. 1994;55:367–9.
5. Wehler M, Nichterlein R, Fischer B, Farnbacher M, Reulbach U, Hahn EG, et al. Factors associated with health-related quality of life in chronic pancreatitis. *Am J Gastroenterol*. 2004;99:138–46.
6. Kappis M. Sensibilitat und locale anasthesie im chirurgischen gebiet der bauchhohle mit besonderer berucksichtigung der splanchnicus-aasthesie. *Beitr Klin Chir*. 1919;115:161–75.
7. Hegedus V. Relief of pancreatic pain by radiography-guided block. *Am J Roentgenol*. 1979;133:1101–3.
8. Moore DC, Bush WH, Burnett LL. Celiac plexus block: a roentgenographic, anatomic study of technique and spread of solution in patients and corpses. *Anesth Analg*. 1981;60:369–79.
9. Ischia S, Luzzani A, Ischia A, Faggion S. A new approach to the neurolytic block of the coeliac plexus: the transaortic technique. *Pain*. 1983;16:333–41.
10. Herpels V, Kurdziel JC, Dondelinger RF. Percutaneous CT guided nerve block of the coeliac plexus and splanchnic nerves. *Ann Radiol*. 1988;31:291–6.
11. Derhy S, Couderc T, Begon C, Roche A. Celiac neurolysis. Anterior approach and x-ray computed tomographic guidance: a simple and logical technic. *Ann Radiol (Paris)*. 1989;32:230–3.
12. Mattia C, Laurenzi L, Caratozzolo M, Carassiti M, Scardella L, Pinto G. Echo-guided percutaneous celiac plexus block with alcohol with an anterior approach. *Minerva Anestesiol*. 1993;59:193–9.
13. Caratozzolo M, Lirici MM, Consalvo M, Marzano F, Fumarola E, Angelini L. Ultrasound-guided alcoholization of celiac plexus for pain control in oncology. *Surg Endosc*. 1997;11:239–44.

14. Polati E, Finco G, Gottin L, Bassi C, Pederzoli P, Ischia S. Prospective randomized double-blind trial of neurolytic coeliac plexus block in patients with pancreatic cancer. *Br J Surg*. 1998;85:199–201.
15. Marcy PY, Magne N, Descamps B. Coeliac plexus block: utility of the anterior approach and the real time colour ultrasound guidance in cancer patient. *Eur J Surg Oncol*. 2001;27:746–9.
16. Iki K, Fujita Y, Inada H, Satoh M, Tsunoda T. Celiac plexus block: evaluation of injectate spread by three-dimensional computed tomography. *Abdom Imaging*. 2003;28:571–3.
17. Wong GY, Schroeder DR, Carns PE, Wilson JL, Martin DP, Kinney MO, et al. Effect of neurolytic celiac plexus block on pain relief, quality of life, and survival in patients with unresectable pancreatic cancer: a randomized controlled trial. *JAMA*. 2004;291:1092–9.
18. Wiersema MJ, Wiersema LM. Endosonography-guided celiac plexus neurolysis. *Gastrointest Endosc*. 1996;44:656–62.
19. Gress F, Schmitt C, Sherman S, Ikenberry S, Lehman G. A prospective randomized ultrasound- and computed tomography-guided celiac plexus block for managing chronic pancreatitis pain. *Am J Gastroenterol*. 1999;94:900–5.
20. Yamada T, Alpers DH, Kaplowitz N, Lain L, Owyang C, Powel DW. Textbook of gastroenterology. 3th ed. Philadelphia: Lippincott Williams & Wilkins; 1999. Michale W. Mullholland and Diane M. Simone, Pancreas – anatomy and structural anomalies: 2107–2120.
21. Ceyhan GO, Michalski CW, Demir IE, Müller MW, Friess H. Pancreatic pain. *Best Pract Res Clin Gastroenterol*. 2008;22:31–44.
22. Fregni F, Pascual-Leone A, Freedman SD. Pain in chronic pancreatitis: a salutogenic mechanism or a maladaptive brain response? *Pancreatology*. 2007;7:411–22.
23. Ward EM, Rorie DK, Nauss LA, Bahn RC. The celiac ganglia in man: normal anatomic variations. *Anesth Analg*. 1979;58:461–5.
24. Lemelin V, Lam E, Sahai AA. Prospective trial of central versus bilateral celiac plexus block/neurolysis in 160 patients: bilateral injection is safe and is more effective. *Gastrointest Endosc*. 2005;61:AB77.
25. LeBlanc J, DeWitt J, Calley C, Symms M, McGreevy KA, McHenry L, et al. A prospective randomized trial of 1 versus 2 injections during a single EUS-guided celiac plexus block (CPB) procedure for chronic pancreatitis pain: final results. *Gastrointest Endosc*. 2008;67:AB224.
26. Gerke H, Silva Jr RG, Shamoun D, Johnson CJ, Jensen CS. EUS characteristics of celiac ganglia with cytologic and histologic confirmation. *Gastrointest Endosc*. 2006;64:35–9.
27. Levy MJ, Rajan E, Keeney G, Fletcher JC, Torpazian MD. Neural ganglia visualized by endoscopic ultrasound. *Am J Gastroenterol*. 2006;101:1787–91.
28. Gleeson FC, Levy MJ, Papachristou GI, Pelaez-Luna MC, Rajan E, Clain JE, et al. Frequency of visualization of presumed celiac ganglia by endoscopy ultrasound. *Endoscopy*. 2007;39:620–4.
29. HA TI, Kim GH, Song GA, Kim S, Lee JW. Detection of celiac ganglia with radial scanning endoscopic ultrasound. *Korean J Intern Med*. 2008;23:5–8.
30. Levy MJ, Topazian MD, Wiersema MJ, Clain JE, Rajan E, Wang KK, et al. Initial evaluation of the efficacy and safety of endoscopic ultrasound-guided direct ganglia neurolysis and block. *Am J Gastroenterol*. 2007;103:98–103.

31. Pusceddu C, Mameli S, Pili A, Podda G. Percutaneous neurolysis of the celiac plexus under CT guidance in the invasive treatment of visceral pain caused by cancer. *Tumori*. 2003;89:286–91.
32. Vranken JH, Zuurmond WW, Van Kemenade FJ, Dzoljic M. Neurohistopathologic findings after a neurolytic celiac plexus block with alcohol in patients with pancreatic cancer pain. *Acta Anaesthesiol Scand*. 2002;46:827–30.
33. Brown DL, Bulley CK, Quiel EL. Neurolytic celiac plexus block for pancreatic cancer pain. *Anesth Analg*. 1987;66:869–73.
34. Davies DD. Incidence of major complications of neurolytic coeliac plexus block. *J R Soc Med*. 1993;86:264–6.
35. Abdalla EK, Schell SR. Paraplegia following intraoperative celiac plexus injection. *J Gastrointest Surg*. 1999;3:668–71.
36. Gunaratham NT, Sarma AV, Norton ID, Wiersema MJ. A prospective study of EUS-guided celiac plexus neurolysis for pancreatic cancer. *Gastrointest Endosc*. 2001;54:316–24.
37. Gress F, Schmitt C, Sherman S, Ciaccia D, Ikenberry S, Lehman G. Endoscopic ultrasound-guided celiac plexus block for managing abdominal pain associated with chronic pancreatitis: a prospective singles center experience. *Am J Gastroenterol*. 2001;96:409–16.
38. Eisenberg E, Carr DB, Chalmers TC. Neurolytic celiac plexus block for treatment of cancer pain: a meta-analysis. *Anesth Analg*. 1995;80:290–5.
39. Noble M, Gress F. Techniques and results of neurolysis for chronic pancreatitis and pancreatic cancer. *Curr Gastroenterol Rep*. 2006;8:99–103.
40. Yan BM, Myers RP. Neurolytic celiac plexus block for pain control in unresectable pancreatic cancer. *Am J Gastroenterol*. 2007;102:430–8.
41. Singh G, Kaufman M, Das S, Micames C, Erber J, Cristescu B, et al. Efficacy of endoscopic ultrasound (EUS) guided celiac plexus neurolysis (CPN) for managing abdominal pain associated with pancreatic cancer: a systematic review and meta-analysis. *Gastrointest Endosc*. 2008;134:A45.

Part IV
Innovations in EUS

Fine Needle Injection Therapy

*Christopher J. DiMaio, MD
and William Brugge, MD*

CONTENTS

INTRODUCTION
TUMOR ABLATION
PRETREATMENT TUMOR IDENTIFICATION
PANCREATIC CYST ABLATION
SUMMARY

Abstract

Endoscopic ultrasound (EUS) has revolutionized many of the current diagnostic and treatment algorithms for patients with neoplastic lesions. The power of EUS is that it is a minimally invasive modality with the ability to provide real-time, high resolution imaging, in close proximity to organs, thus allowing for image-guided intervention. EUS allows us to utilize novel therapies by a minimally invasive approach to lesions that have traditionally required more invasive (i.e., surgical) or high risk (i.e., percutaneous) routes. This paper discusses the invaluable role of EUS-guided fine-needle injection (EUS-FNI) therapy.

Key Words: EUS-guided fine needle injection, Therapeutic EUS, EUS-guided pancreatic cyst ablation, EUS-guided fiducial placement

INTRODUCTION

Endoscopic ultrasound (EUS) has revolutionized many of the current diagnostic and treatment algorithms for patients with neoplastic pancreatic lesions. In its infancy, EUS was primarily a diagnostic modality,

From: *Clinical Gastroenterology: Endoscopic Ultrasound*,
Edited by: V. M. Shami and M. Kahaleh, DOI 10.1007/978-1-60327-480-7_19,
© Springer Science+Business Media, LLC 2010

allowing the endosonographer to identify and further characterize pancreatic lesions that were initially detected on cross-sectional imaging. With the development of linear array echoendoscopes and echoendoscope needles, the field quickly moved into one of tissue acquisitions by fine-needle aspiration (FNA) and now Tru-cut biopsies. The evolution of echoendoscopes and processors, as well as the growing expertise in endoscopic technique and image interpretation has led EUS to become a mainstay not only in the diagnosis of pancreatic neoplasms, but also in the staging of these lesions. Given our increasing comfort with and the demonstrated safety of inserting a needle into the pancreas, we have reached the final frontier of EUS-guided applications: therapy.

Pancreatic cancer is the fourth leading cause of cancer death (1). The mortality associated with this disease is dismal, with a 1-year survival rate of 24% and a 5-year survival of 5% for all stages (1). Disease is often advanced at the time of diagnosis, with only 7% of newly diagnosed cases being considered local, and therefore resectable (1). Furthermore, given the advanced age at which this cancer strikes, patients often have co-morbidities precluding surgical resection. Even for patients who undergo resection, the outlook is poor, as the recurrence rate is high and the 5-year survival rate in this group is only 20% (1).

Current therapies for pancreatic cancer, including chemotherapy, radiation, and combination therapy are largely ineffective. Management of these patients often turns toward palliation of biliary obstruction, duodenal obstruction, and pain. Clearly, new therapeutic options are needed.

The power of EUS is that it is a minimally invasive modality with the ability to provide real-time, high resolution imaging, in close proximity to the pancreas, thus allowing for image-guided intervention. There is a vast amount of literature reporting the feasibility and safety of EUS-guided needle insertion into the pancreas for tissue sampling. The natural evolution of this would be the use of these needles to guide local therapy to a target lesion. The following chapter focuses mainly on the role of EUS-guided fine-needle injection (EUS-FNI) therapy. Many of these novel approaches have been investigated and/or utilized in the management of neoplastic lesions in other organ systems. EUS allows us to utilize these novel therapies by a minimally invasive approach to lesions that have traditionally required more invasive (i.e., surgical) or high risk (i.e., percutaneous) routes.

TUMOR ABLATION

The ability of EUS to guide fine-needle injection in close proximity to the target lesion provides the foundation for therapeutic EUS. These therapies can be categorized as injectable, implantable, or energy-delivering.

Injection Therapy

BIOLOGICS

Biologic antitumor therapies are designed to change the biologic activity in the area of a tumor, ultimately leading to tumor cell destruction, and ideally tumor regression. These events may be mediated through numerous mechanisms, such as the host's own immune system, or the introduction of a genomic change to the cells in the diseased organ. One advantage to such an approach is a reduction in systemic exposure and toxicity experienced with traditional chemotherapeutic agents. A number of biologic therapies have been investigated as targeted tumor therapy for pancreatic malignancies.

One novel therapy makes use of the host's immune system to affect an antitumor response. The mixed lymphocyte reaction entails mixing allogeneic peripheral blood mononuclear cells with that of the host (i.e., patient). The ensuing release of cytokines results in the activation of the host's immune effector cells (2–6). If this cascade of events were to occur in a tumor, the destruction of tumor cells by the activated host immune effector cells might occur (7–9). The use of an allogeneic mixed lymphocyte culture, termed cytoimplant, delivered by EUS-FNI was investigated in eight patients with unresectable pancreatic adenocarcinoma (10). Patients received a single EUS-guided injection of no more than 10 ml of cytoimplant directly into the pancreatic tumor. There were two partial tumor responses and one minor tumor response, with an overall median survival of 13.2 months. There were no serious adverse events; however, 86% of subjects experienced fever lasting up to 4 weeks.

ONYX-015 (ONYX Pharmaceuticals, Richmond, CA) is a replication-selective adenovirus that preferentially replicates in and destroys tumor cells. These agents are able to spread throughout a tumor, and thus are an attractive weapon for the therapy of large solid tumors. Another advantage is their ability to spare normal peritumoral tissue, as has been demonstrated in Phase I and II clinical trials with patients with head and neck cancer (11, 12). The use of ONYX-015 has been investigated in patients with pancreatic adenocarcinoma. A Phase I trial involving the percutaneous CT-guided delivery of ONYX-015 in such patients demonstrated safety and tolerability, though with only minor objective tumor response (13). Improved efficacy may be dependent on the ability of the viral agent to spread diffusely throughout the tumor (14). Given that pancreatic adenocarcinomas frequently contain a significant amount of fibrosis, a single percutaneous intratumoral injection of an antitumor agent may be insufficient to allow for adequate distribution of the viral agent and thus ineffective tumor destruction. Multiple percutaneous injections would not be an ideal delivery modality for the patient.

On the other hand, EUS-guided injection would allow for a relatively easy approach for multiple targeted injections of this agent throughout a pancreatic tumor. Twenty-one patients with locally advanced, or metastatic, adenocarcinoma of the pancreas underwent eight EUS-guided injections of ONYX-015 over 8 weeks; the final four injections were given in combination with systemic gemcitabine. Two (10%) patients had a partial response and eight (38%) patients had stable disease, with an overall median survival of 7.5 months, and 67% demonstrating 6-month survival (15).

TNFERade (GenVec, Inc., Gaithersburg, MD) is another injectable antitumor agent that makes use of gene therapy. This replication-deficient adenoviral vector contains the human TNF-alpha gene, which is regulated by an upstream, radiation-inducible promoter region, early growth response 1 promoter (Egr-1). Previous trials in patients with various solid tumors, including those of the bile duct and colon, demonstrated that intratumoral injection of TNFERade with combined radiation therapy was well tolerated, without any dose-limiting toxicities encountered, and could result in complete pathologic response in a subset of patients (16, 17). Farrell et al. performed a phase II study evaluating the EUS-FNI or percutaneous delivery of TNFERade in combination with chemoradiation in patients with locally advanced pancreatic adenocarcinoma (18). Fifty patients received five weekly intra-tumoral injections of TNFERade, in addition to continuous infusion 5-Fu and external radiation therapy. The maximally tolerated dose of TNFERade was associated with significantly greater locoregional control of treated tumors, longer progression-free survival, and improved median survival compared to those patients who received a lower dose. Furthermore, there was no difference in disease control and survival in the EUS-FNI group when compared to the percutaneous delivery group. Similar experience of EUS-FNI delivery of TNFERade in patients with locally advanced esophageal cancer has also been reported (19).

The use of immature dendritic cells to directly activate cytotoxic antitumor T-cells has also been reported. The dendritic cells are harvested from the patient's own blood. Patients undergo leukapheresis in order to obtain a neutrophil-depleted fraction of peripheral mononuclear cells. This sample is further separated until a monocyte-rich fraction is obtained. This fraction is then stimulated using granulocyte-macrophage colony-stimulating factor and interleukin-4, resulting in the production of immature dendritic cells from the peripheral monocytes. These dendritic cells, when injected directly into tumor, can process tumor antigens and subsequently signal regional lymphoid tissue to initiate a specific T-cell mediated antitumor response (20–22). EUS-FNI delivery of this biologic agent into patients with unresectable pancreatic cancer

has not only been shown to be feasible, well tolerated, and safe, but can result in decreased levels of serum CA 19-9 and prolonged survival (23). Combination of chemotherapy with EUS-FNI immunotherapy with dendritic cells can also result in significant downstaging of tumor and thus allows for surgical resection (24).

Familiarity and comfort with these agents is growing. One group has reported their extensive experience in EUS-FNI of biologic antitumor agents. This includes the use of cytoimplant, TNFerade, and OncoVEX^{GM-CSF} (BioVex, Woburn, MA), a replication-selective oncolytic herpes simplex virus carrying the GM-CSF gene (25). Efficacy was not reported, though the safety and tolerability profile was described. Among the eight patients receiving cytoimplant, seven had low grade fever and three had Grade 3 GI toxicities. Of the 12 patients who received TNFerade, seven had GI toxicities (noted as either nausea or diarrhea), three developed a rash, and six had flu-like symptoms. A single vasovagal event and a single case of acute renal failure were observed. Among the four patients who received OncoVEX^{GM-CSF} group, three developed fever and all experienced myalgias. The authors reported no procedure-related complications or infections.

It should be noted that while the development of injectable biologic agents is exciting, most of the trials described in this section have been published only in abstract form, and all involve only a small number of patients. The approval and widespread use of these agents will be dependent on their validation in larger trials.

ETHANOL

Direct tumor destruction can be achieved by the injection of an ablative agent. The most commonly used ablative agent is 99% pure ethanol. Ethanol causes cell destruction by inducing cell membrane lysis and protein denaturation, and results in coagulative necrosis (26). There are numerous reports of its safety and efficacy in the ablation of solid or hyperplastic lesions in a variety of organs, including the thyroid, parathyroid, liver, kidney, and prostate (27–32).

Ethanol is commonly used for injection into the celiac ganglia for the palliation of pain as a result of pancreatic cancer or chronic pancreatitis (33). Although these injections are not designed to enter into the tissue of the pancreas, the site of injection is directly adjacent to the pancreas. Despite the injection of ethanol around the pancreatic gland, pancreatitis has not been reported after celiac neurolysis.

Currently, the use of ethanol ablation within the pancreas remains largely experimental. Initially, Aslanian et al. performed a pilot study to test the safety of this approach in the normal porcine pancreas (34).

Ethanol with a concentration of 50% (N=4) or 98% (N=4) was injected into the pancreas of eight pigs via EUS-FNI. The results of this study demonstrated that 0.5 ml of 50% ethanol caused localized changes in the porcine pancreas, with focal areas of inflammation, necrosis, and fibrosis measuring 2–6 mm in diameter. The injection of 0.5 ml of 98% ethanol resulted in larger areas (8–30 mm) of inflammation, necrosis, and fibrosis. All of the pigs tolerated the procedure well, without the evidence of distress or clinical pancreatitis. However, one pig, which received 1.0 ml of 98% ethanol, developed a fluid collection, while another pig in the 98% ethanol group developed an inflammatory colonic stricture. To further delineate the effects of an intrapancreatic ethanol injection, Matthes et al. performed EUS-FNI with increasing concentrations of ethanol in six live pigs (35). Injection of normal saline solution or 20% ethanol had little effect on the pancreatic tissue. The injection of 40–100% ethanol led to a visible necrotic area, which measured 20.8 ± 4.3 mm in diameter, and was readily visible on cross-sectional imaging as a low attenuation mass. Pathological analysis demonstrated fat necrosis, coagulation necrosis, granulation tissue with inflammatory cells, and foreign body giant cell reaction; there was no evidence of generalized pancreatitis in any of the histopathological specimens. Furthermore, all of the pigs tolerated the procedure without any clinical evidence of pancreatitis or elevations in serum amylase and lipase during the 7-day observation period. Experience with EUS-FNI of ethanol into mass lesions of the human pancreas has been limited. There are case reports of ethanol injection directly into the tumor mass arising from pancreatic cancers (36). Large volumes of ethanol are injected into the tumor mass with reported palliation from chronic pain arising from pancreatic cancer. At autopsy, areas of coagulation necrosis were found within the pancreatic tumor mass. There was no evidence of pancreatitis. A more recent report described the use of this modality as an alternative to surgery in a patient with an insulinoma (37). In one patient with a 13 mm insulinoma located in the pancreatic body, 8 ml of 95% ethanol was injected under EUS guidance. The patient experienced localized pain in the upper abdomen, with an associated mild increase of serum lipase, both of which resolved within 3 days. However, the patient did not experience any further episodes of hypoglycemia. Subsequent endosonographic imaging failed to demonstrate the insulinoma at its former position, and there was no evidence of tumor recurrence at 34 months of follow-up.

EUS-FNI of ethanol into a pancreatic tumor may provide a means for palliation of pain and/or tumor regression. Clearly, more phase I and II trials are needed to validate this therapy. One area where the use of ethanol holds promise has been in the treatment of pancreatic cystic neoplasms. This topic is covered in a later section.

Thermal/Energy Delivery

RADIOFREQUENCY ABLATION

Radiofrequency ablation (RFA) is an ablative therapy that makes use of thermal energy to induce localized cell death. A needle electrode with an uninsulated tip is inserted into the target lesion (Fig. 1). The electrode is then connected to an electrical generator, resulting in the emission of an RF current from the electrode tip. This current produces ion agitation in adjacent cells, which results in friction and heat generation, ultimately leading to coagulation necrosis and cell death. This modality is a mainstay in the management of both primary and metastatic hepatic tumors (38, 39). RFA is also employed in treating malignant lesions of the kidney, lung, brain, prostate, and breast (40–42).

The use of RFA in the pancreas has been previously established. However, its safety and utility are debated. Matsui et al. reported their experience of using RFA in 20 patients with unresectable pancreatic adenocarcinoma (43). Two patients (10%) died from critical complications, and there was no difference in average survival between the treated and control group. Elias et al. reported their experience in two patients with pancreatic tumors secondary to renal cancer, who both died secondary to severe necrotizing post-RFA pancreatitis (44). More promising reports describe the use of intraoperative RFA in patients with unresectable pancreatic cancer (45, 46). In a small pilot study, the treatment was well tolerated with no reported severe or clinically significant complications. A larger series demonstrated a significant survival benefit in patients with advanced pancreatic cancer undergoing combined palliative surgery and RFA vs. those having palliative surgery only (47).

EUS-guided RFA has been performed in a porcine model. Goldberg et al. investigated this technique in 13 swine using a specially designed

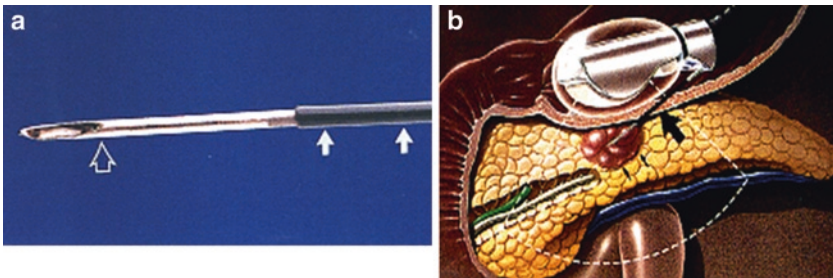


Fig. 1. Radiofrequency ablation in the pancreas. (a) Tip of the RF electrode needle. White arrows, insulated portion; open arrow, uninsulated tip. (b) RF electrode needle passing from within the instrument channel of an echoendoscope into the pancreas.

needle that was insulated for all but the distal 1.0–1.5 cm (48). Ablative sessions were performed in the thickest accessible portion of the pancreatic tail, with the intent to maintain needle tip temperature at $90 \pm 2^\circ\text{C}$. During an observation period of 9–14 days, none of the pigs experienced any signs of fever, distress, or agitation suggestive of pancreatitis. On necropsy, specimens demonstrated an area of necrosis 8–10 mm in diameter surrounding the site of needle insertion (Figs. 2 and 3). Furthermore, there was excellent correlation of these pathological findings to cross-sectional radiologic imaging (Fig. 4). In regards to safety, one pig developed a small peripancreatic fluid collection which proved to be a pseudocyst. Three transmural gastric burns were also found. These were determined to be a result of incomplete penetration of the gastric wall by the needle. Finally, one thermal injury was present on the small intestinal serosa of one pig.

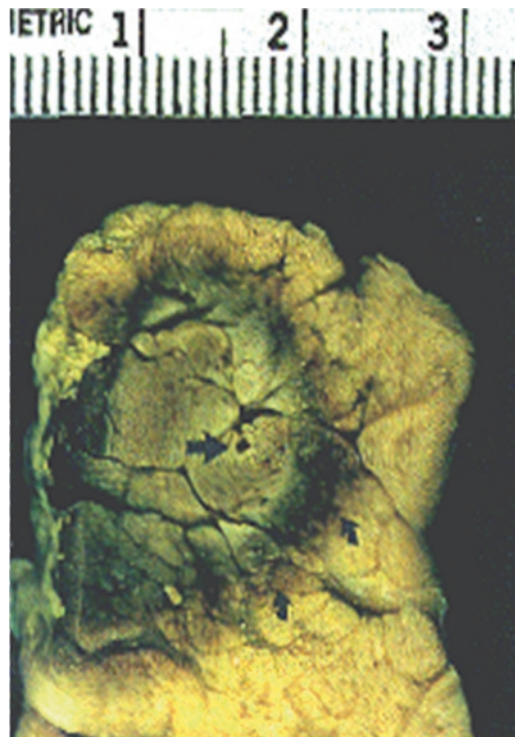


Fig. 2. Gross acute appearance of pancreatic tissue after RFA. The treatment site is a firm, beige area surrounded by reddish, brown rim (curved arrows). The electrode tract is visible within the treatment focus (straight arrow).

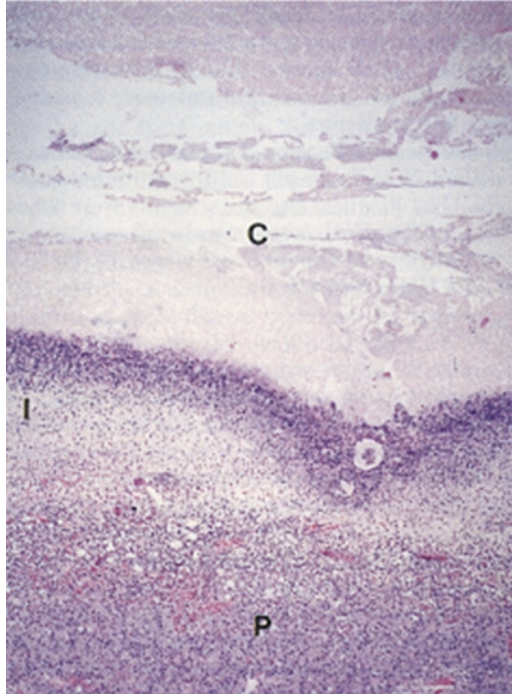


Fig. 3. Histology of pancreatic tissue 48 h after RFA (H&E, orig. mag. $\times 64$). There is a sharp demarcation between coagulated (C) and untreated pancreas (P) with a 1–2 mm watershed zone of an early inflammatory response (I) surrounding the coagulated tissue.

Unlike the liver or kidney, the pancreas has long been considered a “delicate” organ. The findings of peritarget burn injuries in an otherwise uncomplicated procedure, in addition to reports of severe complications and fatalities, signals that this modality may not be ready for widespread application in pancreatic tumors. Furthermore, such lesions offer unique considerations such as proximity to the intrapancreatic bile duct, involvement of adjacent vasculature structures, and retroperitoneal tumor extension. As such, the application of a local thermal ablative therapy may result in untoward consequences in regards to injury to these structures and/or an inability to directly ablate all tumor bulk (49). This has led some investigators to favor an intraoperative approach with prophylactic surgical biliary bypass to avoid this concern (50).

However, all hope should not be lost for EUS-guided RFA in the pancreas. The development of novel RFA needle electrodes and improvements in temperature control and monitoring should allow for continued

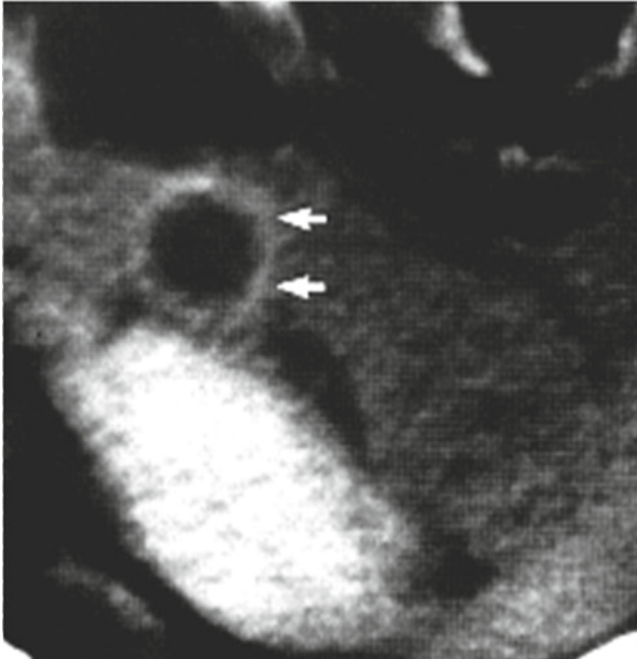


Fig. 4. CT appearance of pancreatic RFA. A well-defined, enhancing, 2–3 mm rim surrounds the treatment focus (14 days after treatment) (arrows).

investigation of this modality. Varadarajulu et al. reported their initial experience with an umbrella-shaped retractable needle electrode array (51). This device was connected to a generator that had an impedance-based feedback system designed to monitor the extent of tissue destruction and permit continued delivery of RF energy until complete ablation was achieved. Testing this device in the liver of two pigs, the authors produced a discrete spherical focus of coagulation necrosis, measuring 2.6 cm in diameter, without damage to adjacent structures. While these results are promising, clearly further animal studies evaluating its use in the pancreas must be performed prior to any human trials. Ultimately, given its ability to provide for focal ablation, EUS-guided RFA may prove to be a viable therapeutic option for small, discrete pancreatic lesions such as neuroendocrine tumors.

CRYOABLATION

Whereas RFA induces localized hyperthermia, cryotherapy induces cell death via localized hypothermia. Cryoablation has been used in the

management of both primary and metastatic liver tumors (52, 53). Given its similarities to RFA, a logical extension would be the development of EUS-guided cryoablation (Figs. 5 and 6). Recently, Carrara et al. evaluated this application in the pancreas of 14 swine using a new flexible bipolar ablation probe combining both RF and cryotechnology (54). A bipolar RF ablation system typically results in less effective ablation compared to a monopolar RF system (55, 56). However, by combining tissue cooling via cryotechnology, additional tissue devitalization is achieved (57). The overall result is effective tissue ablation, but with less power input (16 W for bipolar vs. 30–60 W for monopolar), and

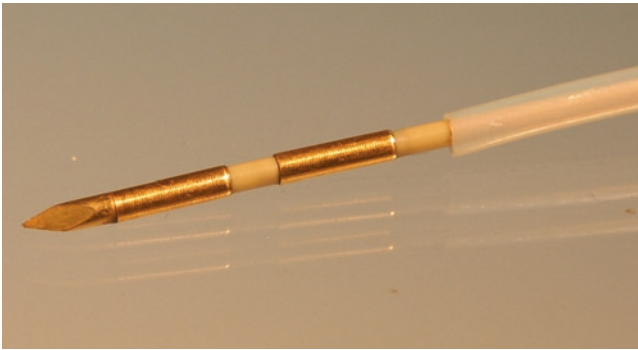


Fig. 5. Cryotherapy ablation probe.

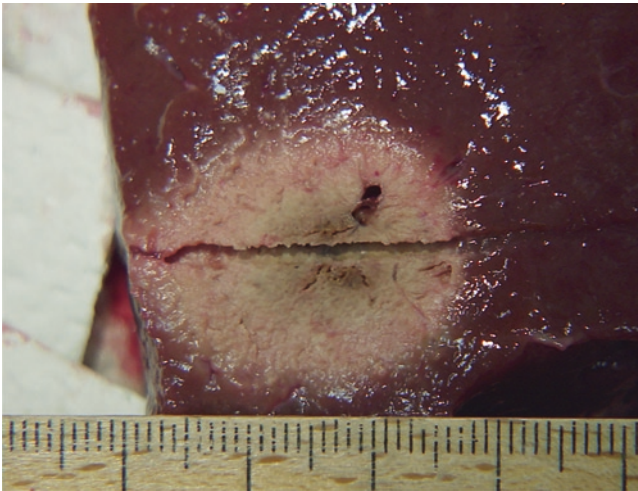


Fig. 6. Gross appearance of liver tissue after cryoablation.

ultimately less collateral damage (54). This technique was shown to be feasible. However, one pig developed clinically overt pancreatitis, and thermally induced adhesions to the stomach and gut were discovered at necropsy in four pigs. Mortality was negligible. The authors concluded that the risk of complications was associated with the duration of applied ablative energy. Furthermore, they proposed that the tissue response should be different and less pronounced in a tumor mass surrounded by a capsule of desmoplastic reaction, commonly seen in human pancreatic adenocarcinoma.

PHOTODYNAMIC THERAPY

Photodynamic therapy (PDT) involves the administration of a photosensitizing agent, followed by the exposure of the target tissue to an appropriate wavelength of light. The light activates the photosensitizing agent, which then reacts with oxygen to produce oxygen singlets. These oxygen singlets are highly destructive and result in localized tissue necrosis.

PDT has been used to treat Barrett's esophagus, as well as a variety of malignant lesions, including cancers of the esophagus and biliary tree (58, 59). The application of PDT in the pancreas has also been investigated. Studies have demonstrated that photosensitizers are not only taken up by the pancreas, but also that higher concentrations accumulate in malignant pancreatic tissue compared to normal tissue (60, 61). Successful PDT of pancreatic malignancies has been demonstrated in experimental animal models (62–64). Bown et al. performed PDT in 16 patients with locally advanced adenocarcinoma of the pancreatic head using percutaneous insertion of light fibers under CT-guidance (60). All patients demonstrated substantial tumor necrosis on subsequent imaging. Of note, two patients with tumor involving the gastroduodenal artery had significant bleeding, and three patients with suspected duodenal invasion developed duodenal obstruction. Despite these complications, the overall median survival time was 9.5 months.

EUS-guided PDT therapy may have a future role in the management of pancreatic neoplasms. Two studies led by one of the authors (WRB) have demonstrated the safety and feasibility of performing PDT by advancing a laser-light catheter through a 19-gauge echoendoscope needle into various organs, including the pancreas (65, 66) (Fig. 7). In the first study, three swine received an intravenous injection of the photosensitizing agent porfimer sodium. A small diameter quartz optical fiber with a 1 cm cylindrical light diffuser which emitted a 630-nm light was inserted via the EUS needle into liver, pancreas, spleen, and kidney. After 2 days of observation, there was no clinical evidence of peritoneal

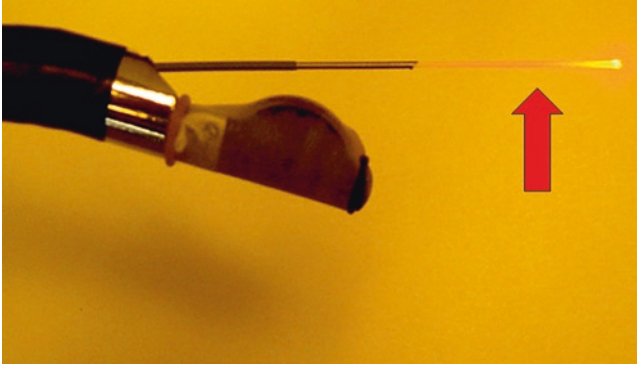


Fig. 7. Laser light fiber (arrow) passed through 19-gauge needle.

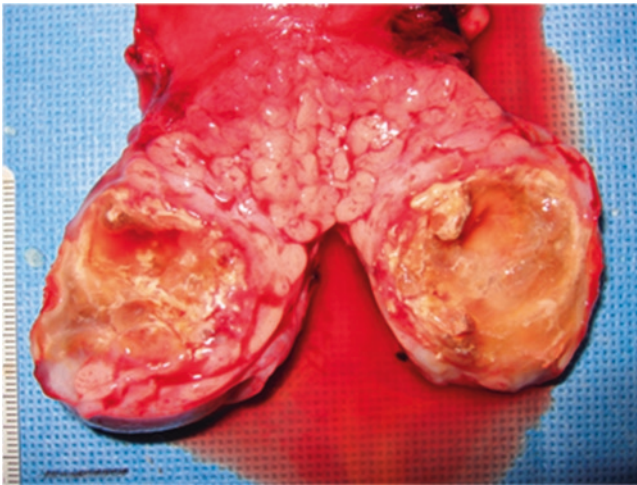


Fig. 8. Resected pancreas with focal necrotic area induced by PDT.

bleeding, infection, or pancreatitis. Furthermore, 100% tissue necrosis was demonstrated in all nine pancreas treatment locations (65) (Figs. 8 and 9). The second study examined the efficacy and safety of EUS-guided PDT of the porcine pancreas with a different photosensitizing agent, verteporfin. The investigators again demonstrated the safety of this modality, with none of the six swine experiencing clinical signs of pancreatitis, and none having objective evidence of infection, perforation, or bleeding. Local tissue necrosis was induced by PDT, and the size of the lesion corresponded with the length of exposure to laser light (66).

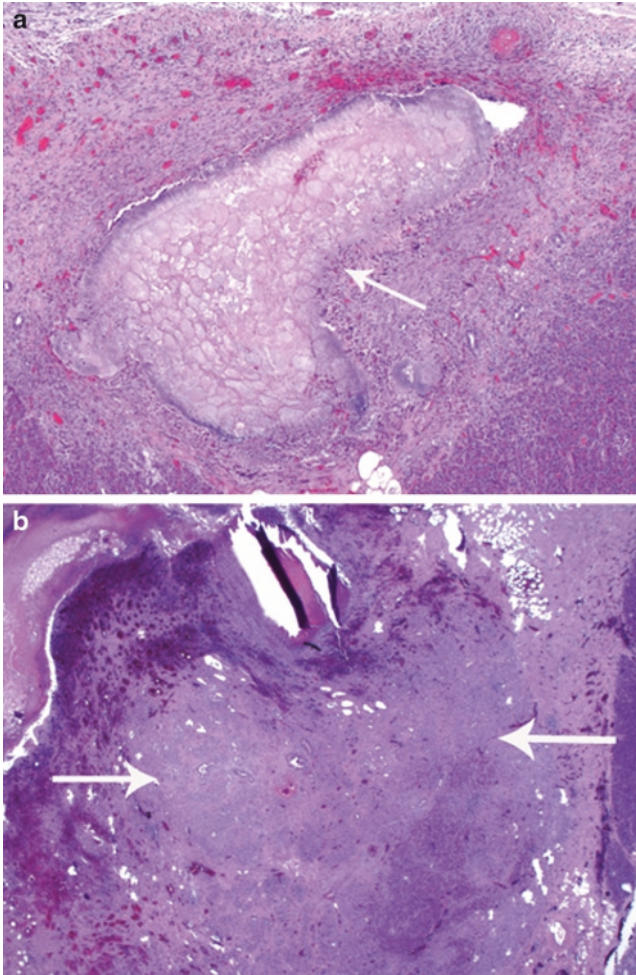


Fig. 9. (a) Histology of ablated pancreas, demonstrating focal fat necrosis (H&E, orig. mag. $\times 100$). (b) Histology of ablated pancreas, demonstrating granulation tissue (H&E, orig. mag. $\times 100$).

These few studies suggest that PDT may someday be part of the armamentarium of targeted therapy for pancreatic lesions. EUS may help identify ideal candidates for this therapy, as the human study described above suggests that those with invasion of the duodenum and/or gastroduodenal artery may be more prone to complications. Ultimately, EUS-guided PDT may prove to be a suitable definitive therapy for small, low grade malignancies, such as neuroendocrine

tumors. Further studies are needed to examine different photosensitizers, define the optimal dose of light therapy, and ultimately prove safety and feasibility in humans.

HIGH-INTENSITY FOCUSED ULTRASOUND

An emerging area of technology involves the use of therapeutic ultrasound. When applied to tissue, ultrasound can result in changes at the cellular level, including elevated temperature, cell membrane defects, and ultimately cell death (67, 68). In high-intensity focused ultrasound (HIFU), these energy waves are harnessed into a beam of high-intensity, and allow for the destruction a focal area of tissue or tumor. This modality has been employed in the management of solid malignancies involving the prostate, liver, breast, and kidneys (69–72). Histologic examination of such specimens demonstrates damage to the tumoral microvasculature as well coagulation necrosis of the malignant tissue (73). Because of the ability to control the depth and intensity of the ultrasound beam, HIFU has the advantage of limiting injury to normal surrounding tissue and structures (73).

The evaluation and use of HIFU thus far has largely been as a transcutaneous therapy. However, a transducer mounted onto an endoscope has been developed and has opened up the possibility of performing endoscopic HIFU (74). Prat et al. used a flexible catheter with an 8 by 2.8 mm ultrasound transducer containing a lumen that could be used to guide the placement of a catheter during ERCP (75). Ten patients with cholangiocarcinoma were treated with HIFU under fluoroscopic control. No adverse events occurred. Three patients had a complete tumor response while four patients had a partial response. Though this represents one early report, the results are clearly promising. The development of smaller probes that could be used in conjunction with EUS would herald an opportunity to expand the investigation and use of this therapeutic modality.

Implantable Therapy

CHEMOTHERAPY

Interstitial chemotherapy has been investigated and used for local control of tumors in the brain, breast, and prostate (76–79). By concentrating the chemotherapeutic agent within the tumor, this treatment has the potential advantage of eliminating systemic toxicity while simultaneously prolonging exposure of the lesion to the drug. Given the potential

for severe systemic toxicity with standard systemic chemotherapeutic agents used in the management of pancreatic carcinoma, EUS-guided delivery of a chemotherapeutic agent is an attractive alternative.

Investigation of this approach in animal models has been encouraging. A biodegradable polymer of sustained-release 5-fluorouracil was successfully implanted into the pancreas of six dogs (80). During a 14-day observation period, there were no signs of pancreatitis, infection, or peritoneal bleeding. Histopathological analysis at necropsy demonstrated an area of fibrous necrosis 5.2 mm in diameter surrounding the polymer implant, with mild inflammation surrounding this area. However, pancreatic tissue 20 mm from the focus, as well as tissue surrounding adjacent organs, was normal. Furthermore, a significant increase in the apoptotic index was demonstrated within 1 cm of the necrotic focus compared to an area 5 cm from the focus.

Oncogel is a new formulation of the drug paclitaxel. The drug is mixed with a thermosensitive, biodegradable polymer, which allows for slow, continuous release for up to 6 weeks (81, 82). The feasibility of EUS-guided delivery of Oncogel into a porcine pancreas model has been demonstrated (83) (Fig. 10). A recent study has demonstrated that this method can provide for high and sustained pancreatic tissue concentrations up to 14 days after injection (84). In pigs that received 3 or 4 ml injections of Oncogel (6 mg/ml), clinically significant tissue concentrations of drug were detected at distances of 30–50 mm from the initial depot (84).

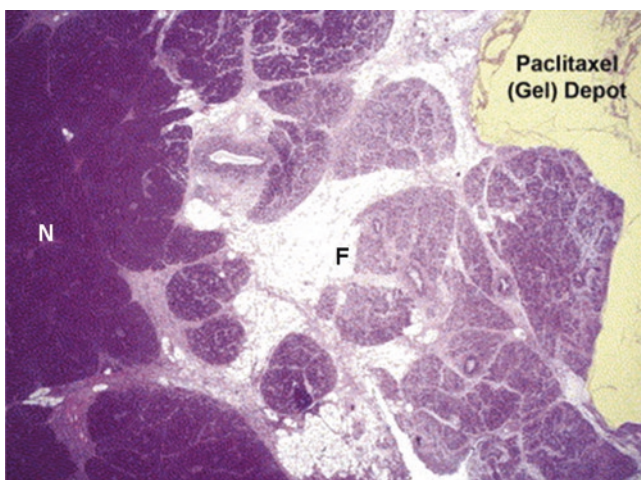


Fig. 10. Histology of pancreatic tissue 14-days after OncoGel depot implantation. Fibrotic tissue (F) surrounds the OncoGel depot (yellow area), while pancreatic tissue distant from the depot remains normal (N).

Furthermore, none of the pigs demonstrated any signs of systemic toxicity nor developed pancreatitis.

Clearly, further work is needed in this exciting area. In particular, improvements in the drug delivery technique and optimal drug volume and concentration need to be elucidated.

BRACHYTHERAPY

Interstitial brachytherapy involves the implantation of radioactive seeds directly into a tumor (Fig. 11). These seeds emit low-energy radiation within the tumor resulting in localized necrosis. This treatment limits the exposure of surrounding tissue and organs to the damaging radiation waves. Traditionally, seeds containing iodine-125 (I-125) or palladium-103 have been used owing to their low-energy emission and suitable half-lives (60 and 17 days, respectively). Brachytherapy has been used as either a single or combination therapy in cancers of the head, neck, breast, prostate, uterine cervix, and rectum (85–89). Brachytherapy has been used in the treatment and palliation of patients with pancreatic

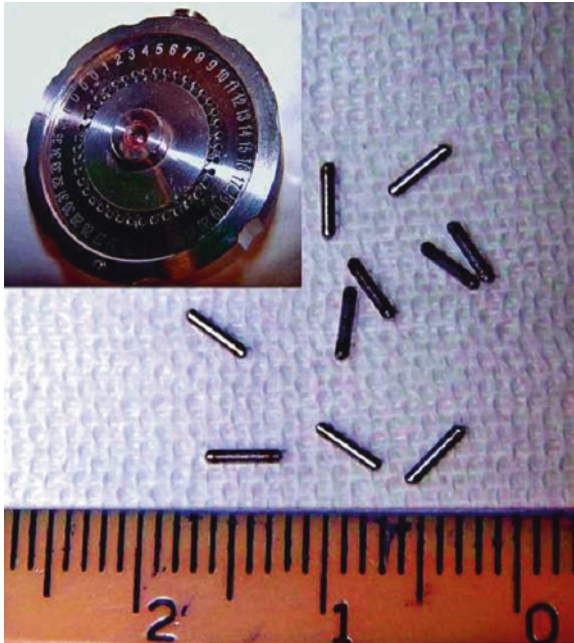


Fig. 11. Brachytherapy seeds.

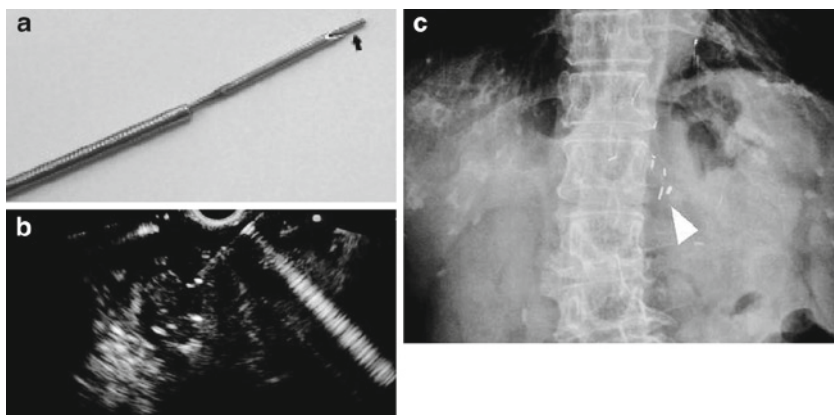


Fig. 12. (a) An iodine-125 radioactive seed (arrow) at the tip of an echoendoscope needle. (b) EUS-guided implantation of seeds in the pancreas. (c) Brachytherapy seeds visible on a radiograph (arrow head).

cancer for decades. Seeds are implanted either surgically or percutaneously and have been used in combination with either intraoperative radiation or external beam radiation. Numerous reports have demonstrated improvements in symptoms of pain, jaundice, and obstruction (90–93). However, survival benefit is modest at best.

EUS-guided implantation of radioactive seeds has been reported (Fig. 12). Sun et al. demonstrated the feasibility of this modality in a porcine model (94). Using a modified echoendoscope needle, an I-125 seed (4.5×0.84 mm) was loaded into the tip of an 18-gauge needle. Using a transgastric approach, the needle was inserted into normal pancreatic parenchyma under EUS-guidance. A stylet was used to deploy the seed out of the needle tip and into the desired location. The needle was then removed, reloaded, and EUS-guided implantation was repeated until a total of four seeds were placed. The authors reported technical success in all six swine. Over a 14-day observation period, there was no evidence of intraperitoneal bleeding, infection, or pancreatitis. At necropsy, a necrotic area measuring 3.5–4.5 cm in diameter was found surrounding the area of seed implantation. No seeds had migrated.

Investigation of EUS-guided brachytherapy in humans has been reported. Sun et al. implanted a mean number of 22 seeds into 15 patients with unresectable pancreatic cancer (95). Over a median follow-up time of 10.6 months, 27% of patients were noted to have a partial tumor response, while 33% patients were noted to have stable disease.

Clinical benefit in the form of pain control was demonstrated in 30% of patients. Local complications of pancreatitis and pseudocysts occurred in three patients. Jin et al. reported their experience in a larger series, which included 25 patients with unresectable pancreatic cancer (96). A median number of ten I-125 seeds were implanted in each patient. The authors demonstrated a significant improvement in pain scores without any serious complications.

One downside to performing this treatment is the potential need to insert a large number of seeds into a particular tumor. In the previously cited reports, up to a mean of 22 seeds were implanted within a particular tumor. Though it has not been demonstrated above, this would likely increase the procedure time, as well as raise the risk of complication, not to mention mechanical difficulties in assuring proper distribution and spatial orientation. Alternatively, the implantation or injection of a more fluid radioactive substance may circumvent this issue. ³²P BioSilicon is a radioactive-labeled 30 mm particle suspension. Initial studies have demonstrated the feasibility of EUS-guided brachytherapy with this substance in patients with advanced pancreatic adenocarcinoma (97). Furthermore, performance of this procedure with a single needle puncture and a median procedure duration time of 7 min was shown (97, 98).

Clearly, EUS-guided brachytherapy is a viable modality for both therapy and palliation in patients with advanced pancreatic malignancies. Its use can easily be expanded toward the management of other malignancies that are accessible by a transluminal GI approach. Lah et al. share their experience of implanting two I-125 seeds into malignant perigastric lymph nodes of a patient with recurrent esophageal cancer (99). As determined by imaging over an 8 month period, the lymph nodes were completely ablated.

PRETREATMENT TUMOR IDENTIFICATION

Fiducial Placement

The CyberKnife (Accuracy, Inc., Sunnyvale, CA, USA) frameless image-guided stereotactic radiosurgery system precisely delivers multiple small beams of high-dose radiation to a lesion. Compared to conventional external radiation therapy, the CyberKnife can limit the exposure and damage to the normal tissue and organs surrounding the target (100). In addition, when used with real-time respiratory tracking and compensatory Synchrony motion system, the CyberKnife can be applied to lesions that move during respiration.

CyberKnife is approved for the treatment of tumors anywhere in the body. For lesions in the central nervous system (CNS), bony landmarks are used as reference points to guide the beams. For non-CNS lesions, the system is dependent on the placement of a number of radiographic markers (fiducials) to guide the radiation beams in real-time. Fiducials are cylindrical gold seeds measuring 3–5 mm in length and 0.8–1.2 mm in diameter. Fiducials can be placed surgically or percutaneously, via ultrasound or CT guidance (101–105). EUS allows for close proximity to structures in the mediastinum and abdomen that are not readily accessible by percutaneous approaches and thus has the potential to provide for EUS-guided fiducial placement.

The feasibility and safety of EUS-guided fiducial placement has been reported. Pishvaian et al. report a series of 13 patients with various solid malignancies, including seven with pancreatic tumors (106). Optimal fiducial placement was defined by the placement of a minimum of three seeds in the area of the tumor or at the tumor edge, with a minimum angle of 15° between any two fiducials, and the minimum distance between any two fiducials being 2 cm. A standard 19-gauge echoendoscopy needle was used. After the needle tip was inserted into the target lesion, the stylet was removed and one fiducial was inserted into the needle channel. The stylet was then reinserted into the needle channel and used to push the fiducial out of the needle and into the lesion. The position of the fiducial was confirmed by both EUS and fluoroscopy. Technical success was reported in 11/13 (84.6%) cases. Three or four fiducials were able to be placed in each of nine patients, while five or six fiducials were placed in each of two patients. The investigators noted that placement of a 5-mm long fiducial was limited by bending of the scope tip. In such cases where the scope tip needed to be angulated to provide better approximation and optimal viewing of the lesion, a 3-mm long fiducial was able to be placed easily. There were no immediate complications noted, though one patient with a metastatic node in the porta hepatis developed cholangitis with pneumobilia 30 days postprocedure.

Subsequent studies examining a total of 77 patients have provided additional support to the feasibility and safety of this intervention (107–111). Two studies, with 16 and 23 subjects respectively, have demonstrated that virtually all patients will go on to have successful CyberKnife radiotherapy after fiducial placement (108, 109). Variations in technique include backloading the seed into a 19-gauge needle and holding it in place with sterile bone wax, or using a sterile water injection through the needle channel to deploy the seed (107–109, 111). Reported complications include one patient with mild acute pancreatitis and two patients with abdominal pain (111). One patient, at the time of

a treatment-planning CT scan was noted to have a seed that migrated along the SMA though this was clinically insignificant (107).

EUS-guided fiducial placement has also been successfully performed in patients with gastric cancer and cholangiocarcinoma, as well as patients with metastatic disease involving lymph nodes in the subcarinal, retrocrural, retrocardiac, porta hepatis, and para-spinal regions (106, 107). One group has even used this modality in the management of prostate cancer (110).

Tumor Marking

EUS-guided intervention for pretreatment tumor identification is not only limited to fiducial placement. EUS-guided injection of India ink into small pancreatic neuroendocrine tumors for tattooing can guide surgeons in locating the lesion and determining resection margins (112). Magno et al. demonstrated the safety and efficacy of implanting the radiopaque marker tantalum into mediastinal and celiac lymph nodes in a porcine model (113). The marked lesions were still visible 4 weeks postinjection. The authors propose that this technique would facilitate in the assurance of complete surgical resection of specimens, delineation of landmarks for radiation therapy, and surveillance for residual disease in irradiated fields that may not be optimal for EUS visualization. Finally, the development of new injectable contrast agents may allow for enhanced imaging of target organs and improved tumor detection. A new class of magnetic resonance (MR) contrast agents consisting of gadolinium encased inside ultra-short carbon nanotubes can result in a significantly stronger signal compared to conventional contrast agents. Vignesh et al. used EUS-FNI to inject the agent directly into the porcine pancreas, and established that this novel contrast agent resulted in a T1 MR signal that was 25-fold greater than that seen with standard gadolinium (114). The authors suggest that this agent may not only enhance pancreatic imaging, but may serve as a carrier for EUS-guided injectable therapy.

PANCREATIC CYST ABLATION

Pancreatic cystic lesions (PCL) represent an important opportunity to identify and treat an early form of pancreatic malignancy. Mucinous cystic lesions of the pancreas, which include intraductal papillary mucinous neoplasms and mucinous cystadenomas, contain an epithelial lining that produces the characteristic mucinous fluid. This epithelium can undergo dysplastic change, and result in histological findings

ranging from benign to borderline or malignant (115). The current standard of care is to resect all high-risk mucinous cystic lesions of the pancreas, as malignancy has been reported to be present in 17.5–60% of such lesions, and the long-term prognosis of these patients is better than patients with invasive carcinoma (116–118). However, the decision to perform surgery must be weighed against a number of patient factors as well as the known morbidity and mortality related to the surgery itself (119). Given that a large number of patients discovered to have such pancreatic lesions are not ideal surgical candidates, an alternative approach to managing such lesions is needed (120). The use of chemical injection for ablation of cystic lesions within different solid organs has been demonstrated to be both efficacious and safe. While various agents such as tetracycline and acetic acid have been used, the most commonly used agent is 99% ethanol. Renal cysts were one of the first lesions treated with percutaneous ethanol injection. Two injections into large, symptomatic renal cysts will result in successful ablation in all patients (121). Large volume hepatic cysts can be significantly reduced in volume after only one treatment with ethanol injection (122). The concentration of ethanol in the cyst cavity required for successful ablation appears to be approximately 40% (123). Ethanol (95%) injection into thyroid cysts results in shrinkage in a large percentage of cysts and successful ablation in 35% of patients (124). One report compared saline infusion to ethanol infusion and found that ethanol was more successful at cyst ablation (125). A long-term randomized trial demonstrated the effectiveness of ethanol injection and documented a low recurrence rate of benign thyroid cysts (126). Successful ablation with ethanol has also been reported in thyroglossal cysts, lymphoceles, pericardial cysts, and splenic cysts (127–129). Reported complications of ethanol cyst lavage include pain, abscess, hemorrhage into the cyst, transient hypotension during cyst injection, and ethanol intoxication (26).

EUS-guided ethanol lavage of PCL has been shown to be safe and efficacious. In a pilot study of 25 patients, varying concentrations of ethanol (5–80%) were used to ablate PCL (130). The cysts had a mean diameter of 19.4 mm and were located equally throughout the pancreas. A 22-gauge echoendoscope needle was used to puncture the cyst and evacuate the cyst of all fluid until collapse was achieved. With the cyst collapsed, ethanol was injected into the cyst, and the cyst was lavaged for 3–5 min, alternately filling and emptying the cavity. At the conclusion of the lavage, the cystic lesion was completely drained of all fluid. No short or long-term complications were reported. Of the 23/25 patients with complete follow-up, eight patients (35%) had complete resolution of their cystic lesion. Five patients underwent resection, and histologic evidence of epithelial ablation was seen. Based on the results

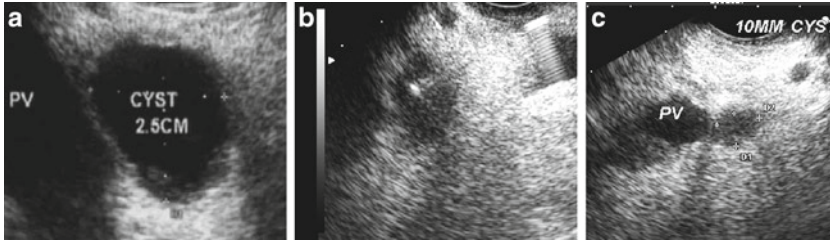


Fig. 13. Long-term follow-up of pancreatic cyst after ethanol ablation. The cyst decreases in size from 2.5 cm (a) to 1.9 cm (b) after one ethanol ablation session, and then to 1.0 cm (c) after a second ethanol ablation session.

of this pilot study, a multicenter, randomized, controlled, double-blind study was performed to evaluate the safety and efficacy of this technique (131). Subjects were randomized to receive the treatment with either EUS-guided ethanol lavage or EUS-guided saline lavage. Three months later, all subjects received an EUS-guided ethanol lavage (Fig. 13). Complete cyst resolution was seen in 10/18 (56%) of patients who received two sessions of ethanol lavage, compared to 3/12 (25%) ($p=0.14$) who received an initial saline lavage followed by ethanol lavage. Furthermore, in the small subset of patients who went on to have surgical resection between 50 and 100% of the cyst epithelium was shown to be ablated. The overall complication rate was low, as pancreatitis occurred in 3% of patients. Recently, the injection of paclitaxel (Taxol) into cystic lesions of the pancreas has been demonstrated to be a safe, feasible, and efficacious treatment modality (132). Paclitaxel is a chemotherapeutic agent utilized in the treatment of ovarian cancer, breast cancer, and nonsmall cell lung cancer. Its mechanism of action appears to involve the inhibition of the disassembly of microtubules during cell division and inducing apoptosis. The investigators demonstrated that a combination of ethanol and paclitaxel injected into a variety of pancreatic cystic lesions resulted in the complete resolution of cysts in 11 of 14 (79%) patients. One patient (7%) developed pancreatitis. In follow-up analysis, the authors concluded that complete resolution may be better achieved in smaller lesions (133).

SUMMARY

EUS-guided injection therapy represents the final step in transforming EUS into a truly interventional technique. Building upon the therapeutic principles developed by colleagues in oncology and radiation oncology,

and the technical fundamentals advanced by interventional radiologists, EUS-FNI is rapidly transforming the therapeutic and palliative options available to patients with pancreatic lesions. EUS-FNI provides a minimally invasive, real-time, image guided treatment alternative to a subset of patients who otherwise would have limited options available to them. Though it has yet to be shown, this technique will likely prove to be associated with a significantly lower morbidity compared to surgical interventions. The majority of these procedures will be able to be performed on an outpatient basis.

The clinical applications for EUS-FNI are plentiful. One likely role is as a neoadjuvant therapy for the downstaging of pancreatic tumors perhaps enabling surgical resection. For those patients who are not surgical candidates, EUS-FNI would be an attractive option to slow progression of primary or metastatic lesions, delay onset of intestinal or biliary obstruction, or to palliate pain. For those patients who may have already received chemotherapy and/or radiation therapy, EUS-FNI may provide a more tolerable approach for controlling their disease. One can envision the day when EUS-FNI will become part of the armamentarium of interventional endoscopic therapies, such as celiac plexus blockade, metal biliary stents, and enteral stents, which are presently in use to manage patients with pancreatic cancers.

However, a number of challenges remain before FNI therapy becomes a reality. Improvements in delivery systems and injection techniques are needed. Optimal duration, frequency, and dosing parameters need to be established. Furthermore, the treatment induced scarring and fibrosis may interfere with tumor surveillance by cross-sectional imaging or even repeat EUS. Clearly, further experimental animal studies and larger human trials will be needed to delineate these specifics. Ultimately, though the success of EUS-FNI is largely dependent on the collaboration of gastroenterologists and endoscopists with colleagues in oncology, surgery, and radiology in order to better understand how to develop and improve these techniques.

REFERENCES

1. American Cancer Society. Cancer facts and figures 2008. Atlanta: American Cancer Society; 2008.
2. Danzer SG, Kirchner H, Rink L. Cytokine interactions in human mixed lymphocyte culture. *Transplantation*. 1994;57:1638–42.
3. Ropke M, Ropke C, Claesson MH. T-cell activation. VI. Inhibitory and stimulatory effects of anti-major histocompatibility complex class I antibodies in allogeneic mixed lymphocyte culture. *Immunology*. 1993;79:263–9.
4. Leenaerts PL, Ceuppens JL, Van Damme J, et al. Evidence that stimulator cell-derived IL-6 and IL-1 are released in the mixed lymphocyte culture but are not requisite for responder T cell proliferation. *Transplantation*. 1992;54:1071–8.

5. Matthews SJ, Sullivan JS. A role for tumour necrosis factor-alpha in the human mixed lymphocyte culture reaction. *Immunol Cell Biol.* 1992;70:107–10.
6. Wang P, Vanky F, Klein E. MHC class I-restricted auto-tumor-specific CD4+CD8– T-cell clones established from autologous mixed lymphocyte-tumor cell culture (MLTC). *Int J Cancer.* 1992;51:962–7.
7. Golumbek PT, Lazenby AJ, Levitsky HI, et al. Treatment of established renal cancer by tumor cells engineered to secrete interleukin-4. *Science.* 1991; 254:713–6.
8. Jeffes III EW, Beamer YB, Jacques S, et al. Therapy of recurrent high-grade gliomas with surgery, autologous mitogen-activated IL-2-stimulated (MAK) killer lymphocytes, and rIL-2. Correlation of survival with MAK cell tumor necrosis factor production in vitro. *Lymphokine Cytokine Res.* 1991;10:89–94.
9. Lillehei KO, Mitchell DH, Johnson SD, et al. Long-term follow-up of patients with recurrent malignant gliomas treated with adjuvant adoptive immunotherapy. *Neurosurgery.* 1991;28:16–23.
10. Chang KJ, Nguyen PT, Thompson JA, et al. Phase I clinical trial of allogeneic mixed lymphocyte culture (Cytoimplant) delivered by endoscopic ultrasound-guided fine-needle injection in patients with advanced pancreatic carcinoma. *Cancer.* 2000;88:1325–35.
11. Nemunaitis J, Ganly I, Khuri F, et al. Selective replication and oncolysis in p53 mutant tumors with ONYX-015, an E1B-55kD gene-deleted adenovirus, in patients with advanced head and neck cancer: a Phase II trial. *Cancer Res.* 2000;60:6359–66.
12. Nemunaitis J, Khuri F, Ganly I, et al. Phase II trial of intratumoral administration of ONYX-015, a replication-selective adenovirus, in patient with refractory head and neck cancer. *J Clin Oncol.* 2001;19:289–98.
13. Mulvihill S, Warren R, Venook A, et al. Safety and feasibility of injection with an E1B-55 kDa gene-deleted, replication-selective adenovirus (ONYX-015) into primary carcinomas of the pancreas: a phase I trial. *Gene Ther.* 2001;8:308–15.
14. Heise CC, Williams A, Olesch J, Kirn DH. Efficacy of a replication-competent adenovirus (ONYX-015) following intratumoral injection: intratumoral spread and distribution effects. *Cancer Gene Ther.* 1999;6:499–504.
15. Hecht JR, Bedford R, Abbruzzese JL, et al. A phase I/II trial of intratumoral endoscopic ultrasound injection of ONYX-015 with intravenous gemcitabine in unresectable pancreatic carcinoma. *Clin Cancer Res.* 2003;9:555–61.
16. Mundt AJ, Vijayakumar S, Nemunaitis J, et al. A phase I trial of TNFerade biologic in patients with soft tissue sarcoma in the extremities. *Clin Cancer Res.* 2004;10:5747–53.
17. McLoughlin JM, McCarty TM, Cunningham C, et al. TNFerade, an adenovector carrying the transgene for human tumor necrosis factor alpha, for patients with advanced solid tumors: surgical experience and long-term follow-up. *Ann Surg Oncol.* 2005;12:825–30.
18. Farrell JJ, Senzer N, Hecht JR, et al. Long-term data for endoscopic ultrasound (EUS) and percutaneous (PTA) guided intratumoral TNFerade gene delivery combined with chemoradiation in the treatment of locally advanced pancreatic cancer (LAPC). *Gastrointest Endosc.* 2006;63:AB93.
19. Chang KJ, Senzer N, Swisher S, et al. Multi-center clinical trial using endoscopy (END) and endoscopic ultrasound (EUS) guided fine needle injection (FNI) of

- anti-tumor agent (TNFerade) in patients with locally advanced esophageal cancer. *Gastrointest Endosc.* 2006;63:AB84.
20. Banchereau J, Steinman RM. Dendritic cells and the control of immunity. *Nature.* 1998;392:245–52.
 21. Kugler A, Stuhler G, Walden P, et al. Regression of human metastatic renal cell carcinoma after vaccination with tumor cell-dendritic cell hybrids. *Nat Med.* 2000;6:332–6.
 22. Schnurr M, Galambos P, Scholz C, et al. Tumor cell lysate-pulsed human dendritic cells induce a T-cell response against pancreatic carcinoma cells: an in vitro model for the assessment of tumor vaccines. *Cancer Res.* 2001;61:6445–50.
 23. Irisawa A, Takagi T, Kanazawa M, et al. Endoscopic ultrasound-guided fine needle injection of immature dendritic cells into advanced pancreatic carcinoma refractory to gemcitabine: a pilot study. *Pancreas.* 2007;35:189–90.
 24. Nonogaki K, Hirooka Y, Itoh A, et al. Combined treatment with immunotherapy and chemotherapy using endoscopic ultrasonography: a phase I trial as first-line treatment in patients with locally advanced pancreatic carcinoma. *Gastrointest Endosc.* 2007;65:AB207.
 25. Muthusamy R, Ashida R, Lee JG, Chang K. The safety and feasibility of endoscopic ultrasound guided fine needle injection (EUS-FNI) of local biologic anti-tumor agents (BAA) in patients with advanced pancreatic carcinoma (APC). *Gastrointest Endosc.* 2008;67:AB109.
 26. Gelczer RK, Charboneau JW, Hussain S, et al. Complications of percutaneous ethanol ablation. *J Ultrasound Med.* 1998;17:531–3.
 27. Kim BM, Kim MJ, Kim EK, et al. Controlling recurrent papillary thyroid carcinoma in the neck by ultrasonographically-guided percutaneous ethanol injection. *Eur Radiol.* 2008;18:835–42.
 28. Lee SJ, Ahn IM. Effectiveness of percutaneous ethanol injection therapy in benign nodular and cystic thyroid diseases: long-term follow-up experience. *Endocr J.* 2005;52:455–62.
 29. Verges BL, Cercueil JP, Jacob D, et al. Results of ultrasonically guided percutaneous ethanol injection into parathyroid adenomas in primary hyperparathyroidism. *Acta Endocrinol (Copenh).* 1993;129:381–7.
 30. Lencioni R, Caramella D, Bartolozzi C, Mazzeo S, Di Coscio G. Percutaneous ethanol injection therapy of adenomatous hyperplastic nodules in cirrhotic liver disease. *Acta Radiol.* 1994;35(2):138–42.
 31. Fotiadis NI, Sabharwal T, Morales JP, et al. Combined percutaneous radiofrequency ablation and ethanol injection of renal tumours: midterm results. *Eur Urol.* 2007;52:777–84.
 32. Savoca G, De Stefani S, Gattuccio I, et al. Percutaneous ethanol injection of the prostate as minimally invasive treatment for benign prostatic hyperplasia: preliminary report. *Eur Urol.* 2001;40:504–8.
 33. Wiersema MJ, Wiersema LM. Endosonography-guided celiac plexus neurolysis. *Gastrointest Endosc.* 1996;44:656–62.
 34. Aslanian H, Salem R, Marginean C, et al. EUS-guided ethanol injection of normal porcine pancreas: a pilot study. *Gastrointest Endosc.* 2005;62:723–7.
 35. Matthes K, Mino-Kenudson M, Sahani DV, et al. Concentration-dependent ablation of pancreatic tissue by EUS-guided ethanol injection. *Gastrointest Endosc.* 2007;65:272–7.

36. Yamamoto S, Miyake I, Takatori K, Ohmoto K, Mitsui Y, Shimabara M. [Percutaneous ethanol injection for unresectable pancreatic cancer – report of two cases]. *Gan To Kagaku Ryoho*. 1998;25:1969–71.
37. Jurgensen C, Schuppan D, Nesper F, et al. EUS-guided alcohol ablation of an insulinoma. *Gastrointest Endosc*. 2006;63:1059–62.
38. Rossi S, Buscarini E, Garbagnati F, et al. Percutaneous treatment of small hepatic tumors by an expandable RF needle electrode. *AJR Am J Roentgenol*. 1998;170:1015–22.
39. Solbiati L, Goldberg SN, Ierace T, et al. Hepatic metastasis: percutaneous treatment of small hepatic tumors by an expandable RF needle electrode. *Radiology*. 1997;205:367–74.
40. Anzai Y, Lufkin R, DeSalles A, et al. Preliminary experience with MR-guided thermal ablation of brain tumors. *AJNR*. 1995;16:39–48.
41. Rosenthal DI, Springfield DS, Gebhart MC, et al. Osteoid osteoma: percutaneous radiofrequency ablation. *Radiology*. 1995;197:451–4.
42. Mirza AN, Fornage BD, Sneige N, et al. Radiofrequency ablation of solid tumors. *Cancer J*. 2001;7:95–102.
43. Matsui Y, Nakagawa A, Kamiyama Y, et al. Selective thermocoagulation of unresectable pancreatic cancer by using radiofrequency capacitive heating. *Pancreas*. 2000;20:14–20.
44. Elias D, Baton O, Sideris L, et al. Necrotizing pancreatitis after radiofrequency destruction of pancreatic tumours. *Eur J Surg Oncol*. 2004;30:85–7.
45. Hadjicostas P, Malakounides N, Varianos C, et al. Radiofrequency ablation in pancreatic cancer. *HPB*. 2006;8:61–4.
46. Varshney S, Sewkani A, Sharma S, et al. Radiofrequency ablation of unresectable pancreatic carcinoma: feasibility, efficacy, and safety. *JOP*. 2006;7(1 Suppl): 74–8.
47. Spiliotis JD, Datsis AC, Michalopoulos NV, et al. Radiofrequency ablation combined with palliative surgery may prolong survival of patients with advanced cancer of the pancreas. *Langenbecks Arch Surg*. 2007;392:55–60.
48. Goldberg SN, Mallery S, Gazelle GS, Brugge WR. EUS-guided radiofrequency ablation in the pancreas: results in a porcine model. *Gastrointest Endosc*. 1999; 50:392–401.
49. Siriwardena AK. Radiofrequency ablation for locally advanced cancer of the pancreas. *J Pancreas*. 2006;7:1–4.
50. Date RS, Siriwardena AK. Radiofrequency ablation of the pancreas II: intraoperative ablation of non-resectable pancreas cancer: a description of technique and initial outcome. *JOP*. 2005;6:588–92.
51. Varadarajulu S, Jhala N, Drelichman ER. Experimental study evaluating EUS-guided RFA using a prototype retractable needle electrode array. *Gastrointest Endosc*. 2008;67:AB110.
52. Tait IS, Yong SM, Cuschieri SA. Laparoscopic in situ ablation of liver cancer with cryotherapy and radiofrequency ablation. *Br J Surg*. 2002;89:1613–9.
53. Yan TD, Padang R, Morris DL. Longterm results and prognostic indicators after cryotherapy and hepatic arterial chemotherapy with or without resection for colorectal liver metastases in 224 patients: longterm survival can be achieved in patients with multiple bilateral liver metastases. *J Am Coll Surg*. 2006; 202:100–11.

54. Carrara S, Arcidiacono PG, Albarello L, et al. Endoscopic ultrasound-guided application of a new hybrid cryotherm probe in porcine pancreas: a preliminary study. *Endoscopy*. 2008;40:321–6.
55. Van Goethem BE, Rosenveldt KW, Kirpensteijn J. Monopolar versus bipolar electrocoagulation in canine laparoscopic ovariectomy: a non-randomized, prospective, clinical trial. *Vet Surg*. 2003;32:464–70.
56. Lee JM, Han JK, Choi SH, et al. Comparison of renal ablation with monopolar radiofrequency and hypertonic-saline-augmented bipolar radiofrequency: in vitro and in vivo experimental studies. *AJR Am J Roentgenol*. 2005;184:897–905.
57. Hines-Peralta A, Hollander CY, Solazzo S, et al. Hybrid radiofrequency and cryoablation device: preliminary results in an animal model. *J Vasc Interv Radiol*. 2004;15:1111–20.
58. Keeley SB, Pennathur A, Gooding W, et al. Photodynamic therapy with curative intent for Barrett's esophagus with high grade dysplasia and superficial esophageal cancer. *Ann Surg Oncol*. 2007;14:2406–10.
59. Ortner ME, Caca K, Berr F, et al. Successful photodynamic therapy for nonresectable cholangiocarcinoma: a randomized prospective study. *Gastroenterology*. 2003;125:1355–63.
60. Bown SG, Rogowska AZ, Whitelaw DE, et al. Photodynamic therapy for cancer of the pancreas. *Gut*. 2002;50:549–57.
61. Chatlani PT, Nuutinen PJ, Toda N, et al. Selective necrosis in hamster pancreatic tumours using photodynamic therapy with phthalocyanine photosensitization. *Br J Surg*. 1992;79:786–90.
62. Regula J, Ravi B, Bedwell J, et al. Photodynamic therapy using 5-aminolaevulinic acid for experimental pancreatic cancer: prolonged animal survival. *Br J Cancer*. 1994;70:248–54.
63. Mikvy P, Messman H, MacRobert AJ, et al. Photodynamic therapy of a transplanted pancreatic cancer model using meta-tetrahydroxyphenylchlorin (mTHRC). *Br J Cancer*. 1997;76:713–8.
64. Ayaru L, Wittmann J, MacRobert AJ, et al. Photodynamic therapy using verteporfin photosensitization in the pancreas and surrounding tissues in the Syrian golden hamster. *Pancreatol*. 2007;7:20–7.
65. Chan H-H, Nishioka NS, Mino M, et al. EUS-guided photodynamic therapy of the pancreas: a pilot study. *Gastrointest Endosc*. 2004;59:95–9.
66. Yusuf TE, Matthes K, Brugge WR. EUS-guided photodynamic therapy with verteporfin for ablation of normal pancreatic tissue: a pilot study in a porcine model (with video). *Gastrointest Endosc*. 2008;67:957–61.
67. Lubbe AS, Bergemann C. Ultrasound therapy for malignant tumors. A conceptual assessment. *J Clin Ultrasound*. 1994;22:113–7.
68. Wu F. Extracorporeal high intensity focused ultrasound in the treatment of patients with solid malignancy. *Minim Invasive Ther Allied Technol*. 2006;15:26–35.
69. Lee HM, Hong JH, Choi HY. High-intensity focused ultrasound therapy for clinically localized prostate cancer. *Prostate Cancer Prostatic Dis*. 2006;9:439–43.
70. Li YY, Sha WH, Zhou YJ, Nie YQ. Short and long term efficacy of high intensity focused ultrasound therapy for advanced hepatocellular carcinoma. *J Gastroenterol Hepatol*. 2007;22:2148–54.

71. Wu F, ter Haar G, Chen WR. High-intensity focused ultrasound ablation of breast cancer. *Expert Rev Anticancer Ther.* 2007;7:823–31.
72. Marberger M. Ablation of renal tumours with extracorporeal high-intensity focused ultrasound. *BJU Int.* 2007;99:1273–6.
73. Wu F, Chen WZ, Bai J, et al. Pathological changes in human malignant carcinoma treated with high-intensity focused ultrasound. *Ultrasound Med Biol.* 2001;27:1099–106.
74. Prat F, Chapelon J-Y, Arefiev A, et al. High-intensity focused ultrasound transducers suitable for endoscopy: feasibility study in rabbits. *Gastrointest Endosc.* 1997;46:348–51.
75. Prat F, Lafon C, DeLima DM, et al. Endoscopic treatment of cholangiocarcinoma and carcinoma of the duodenal papilla by intraductal high-intensity US: results of a pilot study. *Gastrointest Endosc.* 2002;56:909–15.
76. Yamanaka H, Imai K, Mashimo T, et al. Fundamental study on the implantable LH-RH agonist/polymer and its use in a randomized trial for prostate cancer. *Prog Clin Biol Res.* 1990;357:135–43.
77. Fournier C, Hecquet B, Bouffard P, et al. Experimental studies and preliminary clinical trials of vinorelbine-loaded polymeric bioresorbable implants for the local treatment of solid tumors. *Cancer Res.* 1991;51:5384–91.
78. Arica B, Calis S, Kas H, et al. 5-Fluorouracil encapsulated alginate beads for the treatment of breast cancer. *Int J Pharm.* 2002;242:267–9.
79. Brem H, Piantadosi S, Burger PC, et al. Placebo-controlled trial of safety and efficacy of intraoperative controlled delivery by biodegradable polymers of chemotherapy for recurrent gliomas. The polymer-brain tumor treatment group. *Lancet.* 1995;345:1008–12.
80. Sun S, Wang S, Ge N, et al. Endoscopic ultrasound-guided interstitial chemotherapy in the pancreas: results in a canine model. *Endoscopy.* 2007;39:530–4.
81. Zentner GM, Rathi R, Shih C, et al. Biodegradable block copolymers for delivery of proteins and water-insoluble drugs. *J Control Release.* 2001;72:203–15.
82. Jeong B, Bae YH, Lee DS, et al. Biodegradable block copolymers as injectable drug-delivery systems. *Nature.* 1997;388:860–2.
83. Linghu E, Matthes K, Mino-Kenudson M, et al. Feasibility of endoscopic ultrasound-guided Oncogel (ReGel/paclitaxel) injection into the pancreas in pigs. *Endoscopy.* 2005;37:1140–2.
84. Matthes K, Mino-Kenudson M, Sahani DV, et al. EUS-guided injection of paclitaxel (Oncogel) provides therapeutic drug concentrations in the porcine pancreas (with video). *Gastrointest Endosc.* 2007;65:448–53.
85. Schiefke F, Hildebrandt G, Pohlmann S, et al. Combination of surgical resection and HDR-brachytherapy in patients with recurrent or advanced head and neck carcinomas. *J Craniomaxillofac Surg.* 2008;36:285–92.
86. Benitez PR, Keisch ME, Vicini F, et al. Five year results: the initial clinical trial of MammoSite balloon brachytherapy for partial breast irradiation in early-stage breast cancer. *Am J Surg.* 2007;194:456–62.
87. Yoshioka Y, Konishi K, Oh RJ, et al. High-dose-rate brachytherapy without external beam irradiation for locally advanced prostate cancer. *Radiother Oncol.* 2006;80:62–8.

88. Patel FD, Rai B, Mallick I, Sharma SC. High-dose-rate brachytherapy in uterine cervical carcinoma. *Int J Radiat Oncol Biol Phys.* 2005;62:125–30.
89. Sakurai H, Mitsuhashi N, Harashima K, et al. CT-fluoroscopy guided interstitial brachytherapy with image-based treatment planning for unresectable locally recurrent rectal carcinoma. *Brachytherapy.* 2004;3:222–30.
90. Syed AM, Puthawala AA, Neblett DL. Interstitial iodine-125 implant in the management of unresectable pancreatic carcinoma. *Cancer.* 1983;52:808–13.
91. Shipley WU, Wood WC, Tepper JE, et al. Intraoperative electron beam irradiation for patients with unresectable pancreatic carcinoma. *Ann Surg.* 1984;200:289–96.
92. Peretz T, Nori D, Hilaris B, et al. Treatment of primary unresectable carcinoma of the pancreas with I-125 implantation. *Int J Radiat Oncol Biol Phys.* 1989;17:931–5.
93. Goertz SR, Ali MM, Parker GA. Local management of pancreatic carcinoma: iodine-125 implantation. *Clin Oncol (R Coll Radiol).* 1990;2:22–6.
94. Sun S, Qingjie L, Qiyong G, et al. EUS-guided interstitial brachytherapy of the pancreas: a feasibility study. *Gastrointest Endosc.* 2005;62:775–9.
95. Sun S, Xu H, Xin J, et al. Endoscopic ultrasound-guided interstitial brachytherapy of unresectable pancreatic cancer: results of a pilot trial. *Endoscopy.* 2006;38:399–403.
96. Jin Z, Du Y, Li Z, et al. Endoscopic ultrasonography-guided interstitial implantation of iodine 125-seeds combined with chemotherapy in the treatment of unresectable pancreatic carcinoma: a prospective pilot study. *Endoscopy.* 2008;40:314–20.
97. Meenan J, Mesenas S, Douglas N, et al. EUS-delivered therapy for pancreatic cancer: initial experience with targeted injection of 32P Biosilicon. *Gastrointest Endosc.* 2007;65:AB208.
98. Meenan J, Mesenas S, Mahon B, et al. Multi-center, feasibility study on the use of an EUS delivered P32-labeled liquid based brachytherapy implant in advanced pancreatic cancer. *Gastrointest Endosc.* 2008;67:AB109.
99. Lah JJ, Kuo JV, Chang KJ, Nguyen PT. EUS-guided brachytherapy. *Gastrointest Endosc.* 2005;62:805–8.
100. Hara W, Soltys SG, Gibbs IC. CyberKnife robotic radiosurgery system for tumor treatment. *Expert Rev Anticancer Ther.* 2007;7:1507–15.
101. Welsh JS, Berta C, Borzillary S, et al. Fiducial markers implanted during prostate brachytherapy for guiding conformal external beam radiation therapy. *Technol Cancer Res Treat.* 2004;3:359–64.
102. King CR, Lehmann J, Adler JR, et al. CyberKnife radiotherapy for localized prostate cancer: rationale and technical feasibility. *Technol Cancer Res Treat.* 2003;2:25–30.
103. Gerszten PC, Ozhasoglu C, Burton SA, et al. CyberKnife frameless single-fraction stereotactic radiosurgery for benign tumors of the spine. *Neurosurg Focus.* 2003;14:e16.
104. Whyte RI, Crownover R, Murphy MJ, et al. Stereotactic radiosurgery for lung tumors: preliminary report of a phase I trial. *Ann Thorac Surg.* 2003;75:1097–101.
105. Shirato H, Harada T, Harabayashi T, et al. Feasibility of insertion/implantation of 2.0-mm-diameter gold internal fiducial markers for precise setup and real-time tumor tracking in radiotherapy. *Int J Radiat Oncol Biol Phys.* 2003;56:240–7.

106. Pishvaian AC, Collins B, Gagnon G, et al. EUS-guided fiducial placement for CyberKnife radiotherapy of mediastinal and abdominal malignancies. *Gastrointest Endosc.* 2006;64:412–7.
107. Ellsmere JC, Mahadevan A, Kelleher T, et al. EUS-guided radiotherapy fiducials for upper gastrointestinal malignancies. *Gastrointest Endosc.* 2007;65:AB208.
108. Sanders MK, Khalid A, Fasanella KE, et al. EUS-guided fiducial placement for stereotactic radiosurgery in pancreatic cancer. *Gastrointest Endosc.* 2008;67:AB201.
109. Yan BM, Schellenberg D, Koong AC, Van Dam J. EUS guided gold fiducial insertion for image guided radiation therapy of pancreatic cancer. *Gastrointest Endosc.* 2008;67:AB225.
110. Yang J, Deshpande AR, Sussman DA, et al. EUS-guided fiducial placement (EUS FNF) prior to targeted radiation therapy in abdominal and pelvic tumors: a case series. *Gastrointest Endosc.* 2008;67:AB202.
111. Albashir S, Sawhney MS, Pleskow D, et al. EUS guided fiducial placement for CyberKnife treatment of pancreatic cancer. *Gastrointest Endosc.* 2008;67:AB223.
112. Gress FG, Barawi M, Kim D, Grendell JH. Preoperative localization of a neuroendocrine tumor of the pancreas with EUS-guided fine needle tattooing. *Gastrointest Endosc.* 2002;55:594–7.
113. Magno P, Giday SA, Gabrielson KL, et al. EUS-guided implantation of radiopaque marker into mediastinal and celiac lymph nodes is safe and effective. *Gastrointest Endosc.* 2007;66:387–92.
114. Vignesh S, Wilson L, Hartman K, et al. EUS FNI of gadolinium-loaded ultra-short carbon nanotubes (GDNT) into porcine pancreas boosts the MR T1 signal 25-fold. *Gastrointest Endosc.* 2007;65:AB195.
115. Moesinger RC, Talamini MA, Hruban RH, et al. Large cystic pancreatic neoplasms: pathology, resectability, and outcome. *Ann Surg Oncol.* 1999;6:682–90.
116. Salvia R, Fernandez-del Castillo C, Bassi C, et al. Main-duct intraductal papillary mucinous neoplasms of the pancreas: clinical predictors of malignancy and long-term survival following resection. *Ann Surg.* 2004;239:678–85.
117. Rodriguez JR, Salvia R, Crippa S, et al. Branch-duct intraductal papillary mucinous neoplasms: observations in 145 patients who underwent resection. *Gastroenterology.* 2007;133:72–9.
118. Crippa S, Salvia R, Warshaw AL, et al. Mucinous cystic neoplasm of the pancreas is not an aggressive entity: lessons from 163 resected patients. *Ann Surg.* 2008;247:571–9.
119. Porter GA, Pisters PW, Mansyur C, et al. Cost and utilization impact of a clinical pathway for patients undergoing pancreaticoduodenectomy. *Ann Surg Oncol.* 2000;7:484–9.
120. Lee CJ, Scheiman J, Anderson MA, et al. Risk of malignancy in resected cystic tumors of the pancreas < or =3 cm in size: is it safe to observe asymptomatic patients? A multi-institutional report. *J Gastrointest Surg.* 2008;12:234–42.
121. Hanna RM, Dahniya MH. Aspiration and sclerotherapy of symptomatic simple renal cysts: value of two injections of a sclerosing agent. *Am J Roentgenol.* 1996;167:781–3.
122. Larssen TB, Jensen DK, Viste A, Horn A. Single-session alcohol sclerotherapy in symptomatic benign hepatic cysts. Long term results. *Acta Radiol.* 1999;40:636–8.

123. Okano A, Hajiro K, Takakuwa H, Nishio A. Alcohol sclerotherapy of hepatic cysts: its effect in relation to ethanol concentration. *Hepatol Res.* 2000;17:179–84.
124. Monzani F, Lippi F, Goletti O, et al. Percutaneous aspiration and ethanol sclerotherapy for thyroid cysts. *J Clin Endocrinol Metab.* 1994;78:800–2.
125. Antonelli A, Campatelli A, Di Vito A, et al. Comparison between ethanol sclerotherapy and emptying with injection of saline in treatment of thyroid cysts. *Clin Investig.* 1994;72:971–4.
126. Verde G, Papini E, Pacella CM, et al. Ultrasound guided percutaneous ethanol injection in the treatment of cystic thyroid nodules. *Clin Endocrinol (Oxf).* 1994;41:719–24.
127. Fukumoto K, Kojima T, Tomonari H, et al. Ethanol injection sclerotherapy for Baker's cyst, thyroglossal duct cyst, and brachial cleft cyst. *Ann Plast Surg.* 1994;33:615–9.
128. Kinoshita Y, Shimada T, Murakami Y, et al. Ethanol sclerosis can be a safe and useful treatment for pericardial cyst. *Clin Cardiol.* 1996;19:833–5.
129. Akhan O, Baykan Z, Oguzkurt L, et al. Percutaneous treatment of a congenital splenic cyst with alcohol: a new therapeutic approach. *Eur Radiol.* 1997;7:1067–70.
130. Gan SI, Thompson CC, Lauwers GY, et al. Ethanol lavage of pancreatic cystic lesions: initial pilot study. *Gastrointest Endosc.* 2005;61:746–52.
131. Dewitt JM, McGreevy K, Schmidt CM, et al. Ethanol pancreatic injection of cysts (EPIC): preliminary results of a prospective multicenter, randomized, double blinded study. *Gastrointest Endosc.* 2007;65:AB106.
132. Oh H-C, Seo DW, Lee TY, et al. New treatment for cystic tumors of the pancreas: EUS-guided ethanol lavage with paclitaxel injection. *Gastrointest Endosc.* 2008;67:636–42.
133. Oh H-C, Seo DW, Lee SS, et al. EUS-guided ethanol lavage with paclitaxel injection (EUS-EP) for cystic tumors of the pancreas: follow-up study with analysis of response and its predictor. *Gastrointest Endosc.* 2008;67:AB222.

Contrast-Enhanced Endoscopic Ultrasound

Marc Giovannini, MD

CONTENTS

INTRODUCTION
GENERAL CONSIDERATIONS
COMMERCIALY AVAILABLE UCA IN EUROPE
PANCREATIC EUS AND US CONTRAST AGENTS
CONTRAST-ENHANCED EUS IN DISCRIMINATION
BETWEEN BENIGN AND MALIGNANT
MEDIASTINAL AND ABDOMINAL LYMPH NODES
CONCLUSION

Abstract

Endoscopic ultrasonography (EUS) has been widely used to assess tumors of the gastrointestinal tract as well as lymph nodes. However, EUS has its limitations in differentiating benign from malignant tumors. Microbubble imaging has allowed the observation of the vasculature of the abdominal organs on transabdominal US. Second-generation US contrast agents produce harmonic signals at lower acoustic powers that are suitable for EUS imaging and may help differentiate tumor types. This chapter reviews the current indications and limitations of this novel imaging and its potential future applications.

Key Words: Microbubbles, Enhancement of vascularization, Power-Doppler, Harmonic imaging, Pancreatic mass, Lymph nodes

From: *Clinical Gastroenterology: Endoscopic Ultrasound*,
Edited by: V. M. Shami and M. Kahaleh, DOI 10.1007/978-1-60327-480-7_20,
© Springer Science+Business Media, LLC 2010

INTRODUCTION

Among several technologies, endoscopic ultrasound (EUS) has been widely used to diagnose pancreatic lesions, lymph nodes, and GI tumors. EUS is superior to any other modality with respect to spatial resolution; however, EUS has limitations in evaluating vascularity by ultrasound (US) contrast when the color-Doppler or power-Doppler mode is used. Contrast-enhanced power-Doppler US is accompanied by artifacts (e.g., blooming) so that the width of a blood vessel visualized by the power-Doppler mode is magnified and wider than that visualized by fundamental B-mode imaging. Ten contrast harmonic imaging encompasses the intravenous (IV) infusion of Levovist (Schering AG, Berlin, Germany), an air-filled microbubble with an outer shell composed of 99.9% galactose and 0.1% palmitic acid. It allows the observation of the vasculature of the abdominal organs on transabdominal US. Contrast harmonic imaging detects signals from microbubbles and filters signals that originate from tissue by selectively detecting the harmonic components. This technology can detect signals from microbubbles in vessels with a very slow flow without Doppler-related artifacts and is used to characterize tumor vascularity in liver, pancreas, gallbladder, and the GI tract during transabdominal US. Until recently, there was no contrast harmonic imaging technique available for EUS examination because the transducer for current echoendoscopes with a limited frequency bandwidth and is too small to produce enough acoustic power for contrast harmonic imaging when using Levovist. Second-generation US contrast agents, e.g., SonoVue (Bracco Imaging, Milan, Italy), produce harmonic signals at lower acoustic powers and, therefore, are suitable for EUS imaging at low acoustic powers.

GENERAL CONSIDERATIONS

US contrast agents (UCAs), in conjunction with contrast specific imaging techniques, are increasingly accepted in clinical use for diagnostic imaging and workup in several organs. To those not familiar with the field, the rapid advances in technology and techniques can be difficult to follow. In March of 2003, at the EUROSON Congress in Copenhagen, it was agreed that it would be useful to produce a document providing a description of essential technical requirements, proposed investigator qualifications, suggested study procedures and steps, guidance on image interpretation, recommended and established clinical indications, and safety considerations (1).

The development of UCAs, which perform as blood pool tracers, have overcome the limitations of conventional B-Mode and color or

power-Doppler US and enable the display of parenchymal microvasculature (2). Dependent on the contrast agent and the US-mode, the dynamic lesion enhancement pattern is visualized during intermittent or continuous imaging. Enhancement patterns are described during subsequent vascular phases (e.g., arterial, portal venous, and late phase for liver lesions) similar to contrast-enhanced computer tomography (CECT) and/or contrast-enhanced magnetic resonance imaging (CEMRI). Contrast-enhanced ultrasound (CEUS) and CECT or CEMRI are not equivalent, as UCAs have different pharmacokinetics and are confined to the intravascular space. Whereas, the majority of currently approved contrast agents for CT and MRI are rapidly cleared from the blood pool into the extracellular space.

An inherent advantage of CEUS is the possibility to assess the contrast enhancement patterns in real time with a substantially higher temporal resolution than other imaging modalities, without the need to predefine scan time points or to perform bolus-tracking. Furthermore, administration can be repeated due to the excellent patient tolerance of UCAs.

In addition to IV use, UCAs intracavity applications such as intravesical administration can be performed.

UCA studies are subject to the same limitations as other types of US: as a general rule, if the baseline US is very suboptimal, CEUS may be disappointing.

COMMERCIALY AVAILABLE UCA IN EUROPE

Four transpulmonary UCA are currently approved and marketed within European countries:

1. Levovist® (air with a galactose and palmitic acid as a surfactant) (Schering, introduced in 1996). Main indications include heart, abdomen, vesico-ureteric reflux, and transcranial.
2. Optison® (octafluoropropane (perflutren) with an albumin shell) (GE Healthcare, introduced in 1998). Sole indication, to date, is cardiac.
3. SonoVue® (sulfur hexafluoride with a phospholipid shell) (Bracco, introduced in 2001). Approved indications are: cardiac-endocardial border delineation; macrovascular-cerebral and peripheral arteries, portal vein; and microvascular-characterization of focal lesions in liver, pancreas, and breast.
4. Luminity® (octafluoropropane perflutren with a lipid shell) (Bristol-Myers Squibb, introduced in 2006). Sole indication, to date, is cardiac.

There are other UCAs approved outside Europe or under investigation.

The UCAs which are currently used in diagnostic US are characterized by a microbubble structure consisting of gas bubbles stabilized

by a shell. UCAs act as blood pool agents. They strongly increase the US backscatter, and therefore are useful in the enhancement of echogenicity for the assessment of blood flow. While conventional US can detect high concentrations of microbubbles, in practice their assessment usually requires contrast specific imaging modes.

Contrast specific US modes are generally based on the cancelation and/or separation of linear US signals from tissue and utilization of the nonlinear response from microbubbles.

Nonlinear response from microbubbles is based on two different mechanisms:

1. Nonlinear response from microbubble oscillations at low acoustic pressure, chosen to minimize disruption of the microbubbles.
2. High-energy broadband nonlinear response arising from microbubble disruption. Nonlinear harmonic US signals may arise also in tissues themselves due to a distortion of the sound wave during its propagation through the tissue. The extent of this harmonic response from tissue at a given frequency increases with the acoustic pressure, which is proportional to the mechanical index (MI).

Low solubility gas UCAs (e.g., SonoVue®, Optison®, Luminity®) are characterized by the combination of improved stability with favorable resonance behavior at low acoustic pressure. This allows minimally disruptive contrast specific imaging at low MI and enables effective investigations over several minutes with the visualization of the dynamic enhancement pattern in real time. Low MI techniques, furthermore, lead to effective tissue signal suppression as the nonlinear response from the tissue is minimal when low acoustic pressures are used. US imaging with air-filled microbubbles (e.g., Levovist®) at high pressure is dependent on microbubble disruption which is a significant limitation for real-time imaging.

PANCREATIC EUS AND US CONTRAST AGENTS

Diagnosis between adenocarcinomas and nodular chronic pancreatitis can be problematic. All methods of diagnosis are limited. Histology remains the gold standard, but even biopsy can be difficult because cancers can produce a marked fibrotic reaction or necrosis and give false results. For endoscopic retrograde cholangiopancreatography (ERCP) with pancreatic duct brushing, sensitivity and specificity are, respectively, 85 and 66% when there is a stenosis of the main pancreatic duct (3).

MRCP gives a correct differentiation between malignant and benign lesions in 58% of cases (4, 5). MRCP remains an expensive procedure, is time consuming and is available only in a few centers.

There are few studies about contrast-enhanced EUS (CE-EUS). In one of the first studies, Bhutani et al. (6) evaluated the utility of SHU508 A (Levovist®) and concluded that it could potentially improve the accuracy of EUS in the diagnosis of malignant vascular invasion in the detection of occult pancreatic neoplasms and in the diagnosis of vascular thrombosis. Subsequently, Hirooka et al. (7) studied the presence or absence of enhancement of different lesions with Albutex® in 37 patients. An enhancement of the lesion was observed in 100% of the patients with islet cell tumors (Fig. 1), in 80% with intraductal papillary mucinous tumors (IPMT), in 75% with chronic pancreatitis, and no enhancement effect was observed in the patients with carcinoma (Fig. 2). All patients underwent angiography, and comparison between the images of CE-EUS and angiographic images showed similar results, except for three patients (two IPMT and one chronic pancreatitis) in whom angiograms were hypovascular, but enhancement effect was observed on EUS images. Finally, Becker et al. (8) showed their experience in 23 patients with another contrast agent (FS 069 Optison®) and evaluated CE-EUS as a method of differentiating inflammation and carcinoma based on perfusion characteristics. Markedly hyperperfused lesions were considered as inflammatory pseudotumors, whereas hypoperfused lesions compared to surrounding tissue were considered as carcinomas. Sensitivity for the differentiation of pancreatic carcinoma versus inflammatory changes was 94%, specificity 100%, positive predictive value (PPV) 100%, and negative predictive value (NPV) 88%. These results are very similar to our experience (9) (sensitivity 90.9%, specificity 88.8%, PPV 88.2%,

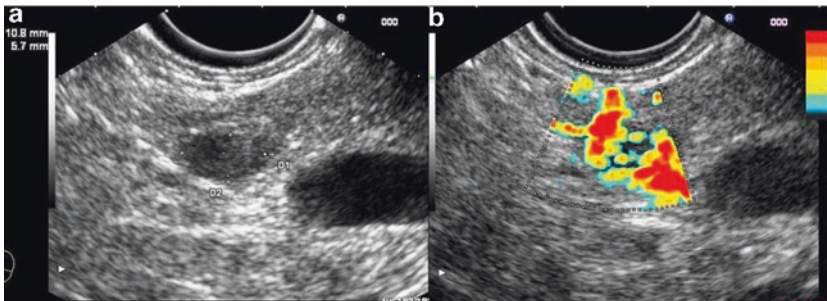


Fig. 1. (a) EUS image of an endocrine tumor of the pancreas. (b) Enhancement of the microvascularization occurs after Sonovue injection.

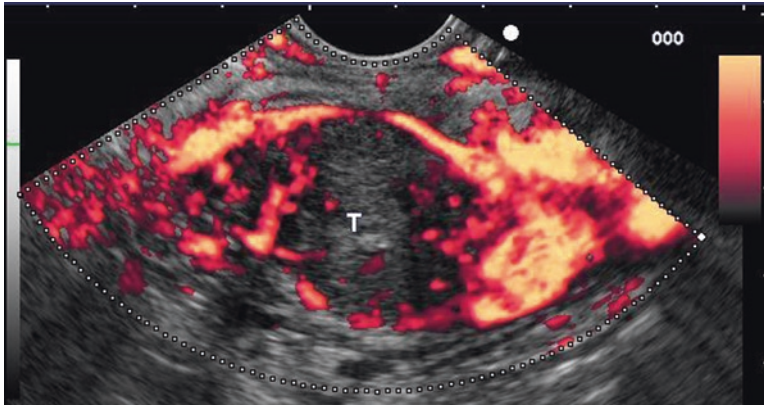


Fig. 2. EUS image of a pancreatic adenocarcinoma after Sonovue injection. Notice there is no enhancement of the tumor with peripheral hypervascularity.

and NPV 91.4%). In our study (9), we also studied hyperechoic lesions; sensitivity was 88.8%, specificity 90.9%, PPV 91.4%, and NPV 88.2%.

CE-EUS could be an interesting complement to EUS fine needle aspiration (FNA) by increasing diagnosis accuracy. EUS-FNA sensitivity and diagnosis accuracy are, respectively, 75–92% and 79–92% (8, 10–16). EUS-FNA is not reliable in 6–9% of cases due to vessel interpositions, duodenal stenosis, and tumoral hardness, particularly in chronic pancreatitis. Sensitivity of EUS-FNA can also be limited by uninterpretable material (bleeding or noncellular samples) ranging from 9 to 19%. Globally, the lack of sensitivity of EUS-FNA ranges from 8 to 25% of cases (8). In our work (3), sensitivity and diagnostic accuracy of this technique were comparable to cytopathology results guided by EUS (sensitivity 90.9%, specificity 88.8%, PPV 88.2%, and NPV 91.4%). In terms of final results, 97% of hypoechoic lesions were malignant tumors (30 adenocarcinoma, 1 endocrine tumor, 1 pancreatic lymphoma, and 1 pancreatic metastasis from colonic cancer). Therefore, CE-EUS may appear to be a reliable and complementary tool for EUS-FNA in the detection and classification of pancreatic lesions when EUS-FNA is challenging or biopsy uninterpretable. CE-EUS could improve accuracy and allow us to propose an appropriate treatment (surgery, follow-up, chemotherapy, etc.).

CE-EUS may allow us to differentiate malign tumor from pseudotumoral nodule. Chronic pancreatitis is also a limiting factor for the diagnosis of pancreatic masses. Several works have attempted to establish EUS imaging criteria, without tissue sampling, for the differentiation of benign inflammatory pseudotumors from cancerous tumors. Despite the

high resolution of EUS, it does not provide reliable differentiation of benign and malignant lesions of the pancreas (17). Fritscher-Ravens et al. (18) found that sensitivity of EUS-FNA in patients with a focal pancreatic lesion without chronic pancreatitis was 89%, while it was only 54% in patients with chronic pancreatitis. Nevertheless, the diagnosis of EUS-FNA influenced clinical management in nearly half of patients (19). CE-EUS could also play an important part in the case of lesions occurring within chronic pancreatitis. Indeed, in the study of Hocke et al. (3), adenocarcinoma developed in the setting of chronic pancreatitis was nonenhanced after contrast injection. Conversely, pseudotumoral nodule (benign masses) (91%) in chronic pancreatitis was hypervascularized after sonovue injection. For Takeda et al. (20), 100% pseudotumoral pancreatitis had an isoenhanced pattern, therefore, it was difficult to differentiate adenocarcinomas from inflammatory pancreatic masses (50% were not well classified).

CE-EUS could be useful in the case of negative results after EUS-FNA. In early studies, NPV of EUS-FNA was around 75% (13, 14), but most recent studies found NPV between 26 and 44% (8, 10–15). In the work by Oshikawa et al. (21), the rate of patients with negative results of the first biopsy, but with malignant tumor diagnosed a second time with a new puncture or with surgery, was 47%.

Globally, the NPV of pancreatic EUS-FNA is 30–33%. Theoretically, a new puncture is mandatory to confirm the absence of neoplasia. CE-EUS could possibly avoid this second procedure. With regard to false-negative results of Sonovue®, we found three adenocarcinomas that presented hyperechoic aspect (enhancement contrast pattern). Two were poorly differentiated adenocarcinoma and the third was associated with Intraductal papillary mucinous neoplasia (IPMN). This suggests that poorly differentiated adenocarcinoma could have different vascularity from well-differentiated adenocarcinoma. Concerning CE-EUS and endocrine tumors, there is only one case report using Levovist that seemed to be a useful diagnostic method for precise localization of small insulinoma (22). In our study (3), 87.5% (7/8) of endocrine tumors had a strong contrast enhancement pattern, indicating hypervascular lesions. These results were similar to CE-EUS (18, 23–25). These vascular images differed from those of almost all pancreatic ductal carcinomas. Thus, differentiation of enhancement pattern on CE-EUS between pancreatic adenocarcinomas and endocrine tumors is useful in the diagnosis of these lesions. In addition, “standard” EUS is already known to have a great value for localizing endocrine pancreatic tumors because of its excellent capacity to visualize small lesions and tumor vascularization at the same time (26, 27). Therefore, CE-EUS could increase sensitivity of diagnosis of pancreatic tumors.

Regarding IPMN, in our study (3), the only benign tumor was hyperechoic, whereas in malignant IPMN, one was hypoechoic and another was hyperechoic. In CE-EUS studies, malignancy could be associated with contrast enhancement. For Sofuni et al. (23), all four patients with IPMN showed hypervascularity of the nodules inside the tumors. For Nagase et al. (24), two of the five IPMN had solid components within the tumors and they were positive for enhancement effects. All five patients with IPMN underwent surgical resection and pathologic examination which revealed malignancy in the two lesions with solid components and positive enhancement. For Itoh et al. (28), when the patients with carcinoma were compared with those with adenoma, the postenhancement intensity was significantly higher in the carcinoma group. CE-EUS could be useful for the differential diagnosis of benign and malignant IPMN.

The small number of patients with IPMN in each study did not allow final conclusions.

Metastatic lesions of the pancreas are rare, between 5 and 10% (29), but an important cause of focal pancreatic lesions. There is only one description of one case of kidney metastasis analyzed in CE-EUS (30). Our work (9) is the first in the literature that describes the enhancement pattern of pancreatic metastasis in CE-EUS. All metastasis except one (4/5; 80%) showed an echo enhancement pattern, probably proving their hypervascularization. The only pancreatic metastasis nonenhanced was from colonic cancer. CE-EUS could provide a contribution to the differential diagnosis between a primary pancreatic carcinoma and a pancreatic metastasis, and therefore can have a decisive influence on the selection of appropriate therapeutic strategies such as chemotherapy versus surgery. In the future, CE-EUS could allow us to have a direct and reliable diagnosis without delay for histological findings. Perhaps it could also be time and cost-saving by limiting the use of expensive EUS needles.

CONTRAST-ENHANCED EUS IN DISCRIMINATION BETWEEN BENIGN AND MALIGNANT MEDIASTINAL AND ABDOMINAL LYMPH NODES

Enlarged mediastinal or abdominal lymph nodes, without symptomatic disease, has become a relevant clinical issue due to the rapid development of imaging techniques with an increasingly higher resolution of intrathoracic or intraabdominal structures. Current computed tomography scanners reliably recognize lymph nodes of 5–10 mm in size, but do not allow the ability to distinguish between malignant and benign lymph nodes in the majority of cases. EUS has an even higher local

resolution, but again, given a distinct visible lymph node, the investigator is frequently not able to assign this node to a malignancy whether or not a malignant tumor is already known. There are several US features such as size, round shape, hypoechoic appearance, missing “hilus sign”, and clear borders which cumulatively make a malignant lymph node most likely. The specificity for these signs is still below 90%, with the majority of malignant lymph nodes not exhibiting all these signs simultaneously. EUS-guided needle aspiration (FNA) represents the current “gold-standard” and has replaced more invasive procedures like mediastinoscopy at least for those groups of lymph nodes which are in reach of the EUS. In the hands of trained ultrasonographers, EUS-FNA reaches a sensitivity, specificity, and diagnostic accuracy of over 90%. Hocke et al. (31) had investigated a total of 122 patients with enlarged mediastinal and/or paraaortic lymph nodes diagnosed by CT scan which were included in the study. EUS-guided FNA was performed and cytologic specimens were diagnosed as representing a malignant or benign process in case of Papanicolaou IV and V, or Papanicolaou I and II, respectively. Based on cytology results, the investigated lymph nodes were classified as neoplastic (n=48) or nonneoplastic lymph nodes. Using the B-mode criteria, the preliminary diagnosis was confirmed in 64 out of 74 benign lymph nodes (specificity 86%). Regarding malignant lymph nodes, 33 of 48 were confirmed (sensitivity 68%). Using advanced contrast-enhanced EUS criteria, the diagnosis was confirmed in 68 of 74 benign lymph nodes (specificity 91%). However, in cases of malignant lymph nodes the number of correct diagnoses dropped to 29 of 48 (sensitivity 60%). The contrast-enhanced EUS criteria to identify benign lymph nodes and node enlargement in malignant lymphoma do not differ. If those ten patients with malignant lymphoma are excluded, the sensitivity of the contrast-enhanced EUS for malignant lymph nodes rises to 73%. Contrast-enhanced EUS improves the specificity in diagnosing benign lymph nodes as compared to B mode EUS. It does not improve the correct identification of malignant lymph nodes and cannot replace EUS-guided FNA (32).

CONCLUSION

CE-EUS could provide a contribution to the differential diagnosis between a primary pancreatic carcinoma, chronic pancreatitis, and a pancreatic metastasis, and therefore can have a decisive influence on the selection of appropriate therapeutic strategies. However, histology remains the standard in the differential diagnosis of pancreatic tumors. Regarding lymph nodes, CE-EUS cannot replace EUS-guided FNA.

REFERENCES

1. Claudon M, Cosgrove D, Albrecht T, Bolondi L, Bosio M, Calliada F, et al. Guidelines and good clinical practice recommendations for contrast enhanced ultrasound (CEUS) – update 2008. *Ultraschall Med.* 2008;29:28–44.
2. Masaki T, Ohkawa S, Amano A, Ueno M, Miyakawa K, Tarao K. Noninvasive assessment of tumor vascularity by contrast-enhanced ultrasonography and the prognosis of patients with nonresectable pancreatic carcinoma. *Cancer.* 2005;103:1026–35.
3. Hocke M, Schulze E, Gottschalk P, Topalidis T, Dietrich CF. Contrast-enhanced endoscopic ultrasound in discrimination between focal pancreatitis and pancreatic cancer. *World J Gastroenterol.* 2006;12:246–50.
4. Hintze RE, Adler A, Veltzke W, Abou-Rebyeh H, Hammerstingl R, Vogl T, et al. Clinical significance of magnetic resonance cholangiopancreatography (MRCP) compared to endoscopic retrograde cholangiopancreatography (ERCP). *Endoscopy.* 1997;29(3):182–7.
5. Domagk D, Wessling J, Reimer P, Hertel L, Poremba C, Senninger N, et al. Endoscopic retrograde cholangiopancreatography, intraductal ultrasonography, and magnetic resonance cholangiopancreatography in bile duct strictures: a prospective comparison of imaging diagnostics with histopathological correlation. *Am J Gastroenterol.* 2004;99(9):1684–9.
6. Bhutani MS, Hoffman BJ, van Velse A, Hawes RH. Contrast-enhanced endoscopic ultrasonography with galactose microparticles:SHU508 A (Levovist). *Endoscopy.* 1997;29(7):635–9.
7. Hirooka Y, Goto H, Ito A, Hayakawa S, Watanabe Y, Ishiguro Y, et al. Contrast-enhanced endoscopic ultrasonography in pancreatic diseases: a preliminary study. *Am J Gastroenterol.* 1998;93(4):632–5.
8. Becker D, Strobel D, Bernatik T, Hahn EG. Echo-enhanced color- and power-Doppler EUS for the discrimination between focal pancreatitis and pancreatic carcinoma. *Gastrointest Endosc.* 2001;53(7):784–9.
9. Giovannini M. Endosonography: new developments in 2006. *ScientificWorldJournal.* 2007;7:341–63. *362 Gastroenterol.* 2007;89(11):2038–41.
10. Voss M, Hammel P, Molas G, Palazzo L, Dancour A, O'Toole D, et al. Value of endoscopic ultrasound guided fine needle aspiration biopsy in the diagnosis of solid pancreatic masses. *Gut.* 2000;46(2):244–9.
11. Raut CP, Grau AM, Staerkel GA, Kaw M, Tamm EP, Wolff RA, et al. Diagnostic accuracy of endoscopic ultrasound-guided fine-needle aspiration in patients with presumed pancreatic cancer. *J Gastrointest Surg.* 2003;7(1):118–26. discussion 127–8.
12. Giovannini M, Seitz JF, Monges G, Perrier H, Rabbia I. Fine-needle aspiration cytology guided by endoscopic ultrasonography: results in 141 patients. *Endoscopy.* 1994;27(2):171–7.
13. Gress FG, Hawes RH, Savides TJ, Ikenberry SO, Lehman GA. Endoscopic ultrasound-guided fine-needle aspiration biopsy using linear array and radial scanning endosonography. *Gastrointest Endosc.* 1997;45(3):243–50.
14. Wiersema MJ, Vilmann P, Giovannini M, Chang KJ, Wiersema LM. Endosonography-guided fineneedle aspiration biopsy: diagnostic accuracy and complication assessment. *Gastroenterology.* 1997;112(4):1087–95.

15. Chang KJ, Nguyen P, Erickson RA, Durbin TE, Katz KD. The clinical utility of endoscopic ultrasound-guided fine-needle aspiration in the diagnosis and staging of pancreatic carcinoma. *Gastrointest Endosc.* 1997;45(5):387-93.
16. Williams DB, Sahai AV, Aabakken L, Penman ID, van Velse A, Webb J, et al. Endoscopic ultrasound guided fine needle aspiration biopsy: a large single centre experience. *Gut.* 1999;44(5):720-6.
17. Harewood GC, Wiersema MJ. Endosonography-guided fine needle aspiration biopsy in the evaluation of pancreatic masses. *Am J Gastroenterol.* 2000;97(6):1386-91.
18. Fritscher-Ravens A, Brand L, Knofel WT, Bobrowski C, Topalidis T, Thonke F, et al. Comparison of endoscopic ultrasound-guided fine needle aspiration for focal pancreatic lesions in patients with normal parenchyma and chronic pancreatitis. *Am J Gastroenterol.* 2002;97(11):2768-75.
19. Kaufman AR, Sivak Jr MV. Endoscopic ultrasonography in the differential diagnosis of pancreatic disease. *Gastrointest Endosc.* 1989;35(3):214-9.
20. Takeda K, Goto H, Hirooka Y, Itoh A, Hashimoto S, Niwa K, et al. Contrast-enhanced transabdominal ultrasonography in the diagnosis of pancreatic mass lesions. *Acta Radiol.* 2003;44(1):103-6.
21. Oshikawa O, Tanaka S, Ioka T, Nakaizumi A, Hamada Y, Mitani T. Dynamic sonography of pancreatic tumors: comparison with dynamic CT. *AJR Am J Roentgenol.* 2002;178(5):1133-7.
22. Kasono K, Hyodo T, Suminaga Y, Sugiura Y, Namai K, Ikoma A, et al. Contrast-enhanced endoscopic ultrasonography improves the preoperative localization of insulinomas. *Endocr J.* 2002;49(4):517-22.
23. Sofuni A, Iijima H, Moriyasu F, Nakayama D, Shimizu M, Nakamura K, et al. Differential diagnosis of pancreatic tumors using ultrasound contrast imaging. *J Gastroenterol.* 2005;40(5):518-25.
24. Nagase M, Furuse J, Ishii H, Yoshino M. Evaluation of contrast enhancement patterns in pancreatic tumors by coded harmonic sonographic imaging with a microbubble contrast agent. *J Ultrasound Med.* 2003;22(8):789-95.
25. Rickes S, Unkrodt K, Ocran K, Neye H, Wermke W. Differentiation of neuroendocrine tumors from other pancreatic lesions by echo-enhanced power Doppler sonography and somatostatin receptor scintigraphy. *Pancreas.* 2003;26(1):76-81.
26. Rosch T, Lightdale CJ, Botet JF, Boyce GA, Sivak Jr MV, Yasuda K, et al. Localization of pancreatic endocrine tumors by endoscopic ultrasonography. *N Engl J Med.* 1992;326(26):1721-6.
27. Ueno N, Tomiyama T, Tano S, Wada S, Aizawa T, Kimura K. Utility of endoscopic ultrasonography with color Doppler function for the diagnosis of islet cell tumor. *Am J Gastroenterol.* 1996;91(4):772-6.
28. Itoh T, Hirooka Y, Itoh A, Hashimoto S, Kawashima H, Hara K, et al. Usefulness of contrast-enhanced transabdominal ultrasonography in the diagnosis of intraductal papillary mucinous tumors of the pancreas. *Am J Gastroenterol.* 2005;100(1):144-52.
29. Fritscher-Ravens A, Sriram PV, Krause C, Atay Z, Jaeckle S, Thonke F, et al. Detection of pancreatic metastases by EUS-guided fine-needle aspiration. *Gastrointest Endosc.* 2001;53(1):65-70.

30. Flath B, Rickes S, Schweigert M, Lochs H, Possinger K, Wermke W. Differentiation of a pancreatic metastasis of a renal cell carcinoma from a primary pancreatic carcinoma by echo-enhanced power Doppler sonography. *Pancreatology*. 2003;3(4):349–51.
31. Hocke M, Menges M, Topalidis T, Dietrich CF, Stallmach A. Contrast-enhanced endoscopic ultrasound in discrimination between benign and malignant mediastinal and abdominal lymph nodes. *J Cancer Res Clin Oncol*. 2008;134:473–80.
32. Kanamori A, Hirooka Y, Itoh A, Hashimoto S, Kawashima H, Hara K, et al. Usefulness of contrast-enhanced endoscopic ultrasonography in the differentiation between malignant and benign lymphadenopathy. *Am J Gastroenterol*. 2006;101:45–51.

Endosurgical Applications of EUS

*Annette Fritscher-Ravens, MD
and Parupudi V.J. Sriram, MD*

CONTENTS

INTRODUCTION
ENDOLUMINAL ENDOSURGICAL METHODS
EXPERIMENTAL EUS-GUIDED ENDOSURGERY:
TOWARD NOTES
EUS-GUIDED ENDOSURGERY
CONCLUSION

Abstract

This article provides an overview of the currently practiced EUS-guided endoluminal surgical techniques, which are performed by a few centers throughout the world on a small number of patients. These include EUS-guided drainage of bile and pancreatic ducts, and necrosectomy. Some of the more experimental endosurgical techniques across the G-wall will be addressed, including those procedures that could potentially evolve into clinical routine such as EUS-guided vascular interventions as well as cardiac procedures. Currently, most of them are performed in the experimental animal and only a few in patients. NOTES procedures facilitated under EUS-guidance will be described and include those which can help to achieve safe transluminal access in difficult areas, target pathology with its unique ability to explore and examine the echomorphology of the organs prior to the intended intervention and detect the target within specific anatomy.

From: *Clinical Gastroenterology: Endoscopic Ultrasound*,
Edited by: V. M. Shami and M. Kahaleh, DOI 10.1007/978-1-60327-480-7_21,
© Springer Science+Business Media, LLC 2010

NOTES EUS-anastomosis, mediastinal procedures, and mediastinal and paragastric lymph-node inspection are some of the most sophisticated surgeries described.

Key Words: EUS, Endosurgery, NOTES, Intervention, EUS-drainage, Necrosectomy

INTRODUCTION

Advent of minimally invasive surgery has resulted in reduced scarring, shorter hospital stays, and a favorable cost-benefit ratio compared to conventional surgery. The recent trends to further minimize the surgical approach have led to natural orifice transluminal endoscopic surgery (NOTES) without any percutaneous access to the abdominal cavity (1–10). Two major limitations of such transluminal endoscopic interventions are (a) safe selection of a portal of entry into the body cavities avoiding vessels and (b) adequate closure of the transluminal access once the procedures are completed. Along with the evolution of interventional endoscopy, endoscopic ultrasound (EUS) remains a tool restricted to a minority of endoscopists due to lack of sufficient training facilities for EUS and inadequate reimbursement. For transluminal procedures like NOTES, EUS was initially thought to be a complicated procedure of limited value citing added cost and need for the exchange of endoscopes (11). But, in reality, EUS provides excellent transluminal imaging, allows interventions in the vicinity of vascular structures, facilitates precise targeting for injection of seeds for radiotherapy, and enables safe transmural interventions like aggressive endoscopic pancreatic necrosectomies (12–18). In the context of NOTES procedures, EUS could therefore serve as a guide for safe transluminal access, especially when access might be difficult (19). It may also have a place of its own by providing direct access to the peritoneal cavity and/or assist in performing endosurgical procedures from within the lumen (20–23). In addition, EUS can help target the pathology with its unique ability to explore and examine the echomorphology of the organs prior to the intended intervention (23). An EUS-based endoscopic suturing system laid the groundwork for the development of access closure methods in NOTES by offering the triangulation required during surgery (22–25). This article provides an overview on the currently practiced EUS-guided (EUS-g) endoluminal surgical techniques. Some of the more experimental EUS-g endosurgical techniques across the GI wall will also be addressed, including those with and without NOTES procedures that could potentially evolve into clinical routine practice.

ENDOLUMINAL ENDOSURGICAL METHODS

EUS-g fine needle aspiration (FNA) of periluminal structures through the GI tract has become routine. Endobronchial ultrasound-guided FNA has been recently introduced and is slowly gaining favor, mainly due to the limited availability of trained specialists. EUS-g celiac ganglion block/neurolysis have been performed for several years by endoscopists, although still underutilized. Operating in the vicinity of larger vessels may dissuade some endoscopists who do not perform high-risk interventions routinely, but as more therapeutic endoscopists adopt endosonography, these procedures are likely to become routine over time. For instance, EUS-g fluid collection drainage and cyst ablation have been considered some of the first major interventional therapies. Ethanol injection for cyst ablation has been performed by percutaneous ultrasonographers for many years. Although EUS-g cyst ablation has developed quite slowly, it has great potential to be adopted by more endosonographers in the future (26).

EUS-Guided Pancreatic Necrosectomy

Until recently, open pancreatic necrosectomy was the standard treatment for infected pancreatic necrosis, but is associated with significant morbidity, mortality, and prolonged hospitalization. Percutaneous or endoscopic necrosectomies are less invasive alternatives. EUS-guidance offers a definite advantage by imaging the necrosis, confirming adherence of the cavity to the gastric wall, and demonstrating the absence of intervening vessels in the lumen and pseudocyst walls prior to puncture. The typical approach involves EUS-g puncture, followed by balloon dilation of the cystoenterostomy and transmural drainage. Afterward, an endoscope is advanced through the gastric/duodenal wall into the necrotic cavity (Fig. 1). Repeated endoscopic necrosectomy and saline lavage are performed until the cavity appears clean (16, 17, 27). Possible coexisting pancreatic fistula can then be confirmed and sealed with N-butyl-2-cyanoacrylate (17). Some recent modifications include the use of a double percutaneous gastrostomy or temporary deployment of self-expanding metal stents to allow easier access and adequate drainage (28–30). However, published necrosectomy series were quite small until two recent abstracts describing 28 and 87 patients, respectively, with a success rate of up to 95% demonstrating the safety, efficacy, and minimally invasive nature of this procedure as an alternative to surgery (31, 32). One major limitation of EUS-g endoscopic necrosectomy is the lack of adequate tools for the removal of the necrotic material (Fig. 2).

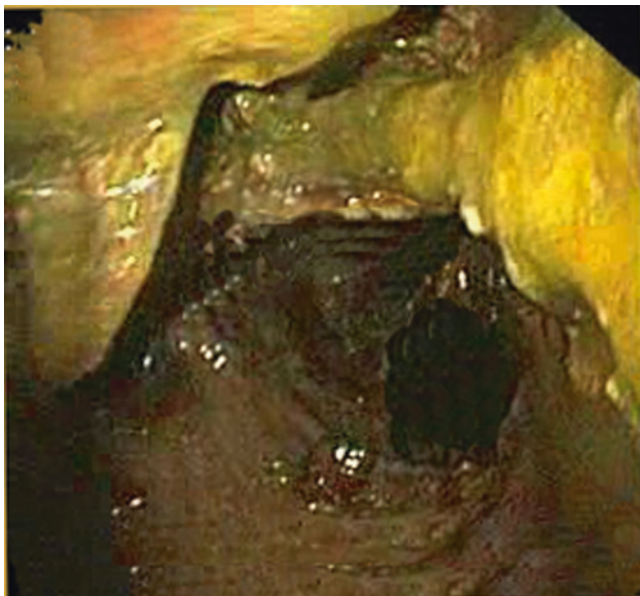


Fig. 1. An endoscope has been passed through an incision in the gastric wall into the necrotic cavity.

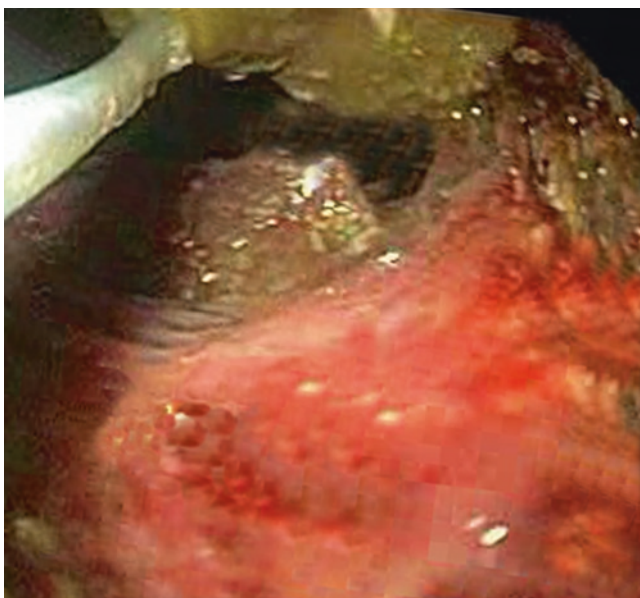


Fig. 2. After repeated necrosectomy, part of the cavity appears to be clean. An ERCP basket is used to remove remaining necrotic material (top).

In addition, the accessory channel and the angle of view are positioned obliquely to the shaft of the echoendoscope. This hinders adequate visualization and more importantly, results in a weakened transfer of pushing-force, difficult deployment of larger accessories, and occasional difficult passage of tools through the gastric wall. Therefore, exchange of the echoendoscope to a therapeutic endoscope is necessary to perform pseudocyst debridement, with potential loss of access. Recently, a new echoendoscope with straightforward view and accessory channel has been tested in six patients for cyst drainage. In four of these patients, the procedure could be performed without endoscope exchange (33).

EUS-Guided Drainage of the Biliary Tract

Due to the close proximity to the upper GI tract, the common bile duct (Fig. 3), the left intrahepatic ducts, and the main pancreatic duct are well visualized with EUS. Development of interventional EUS-g transgastric or duodenal cholangiography (IEUC), whenever ERCP fails seemed the next logical step toward EUS-g endosurgery (34–36) (Fig. 4a, b). Sahai et al. proved EUS-g hepaticogastrotomy feasible in animals (37). Subsequently, Giovannini et al. performed IEUC by widening the tract with biliary dilators to enable stent placement in a patient with biliary obstruction from pancreatic cancer (38). Burmester et al. modified this technique to a single step with the application of 8.5 F stents in three patients (39), before larger channel echoendoscopes were available (40).

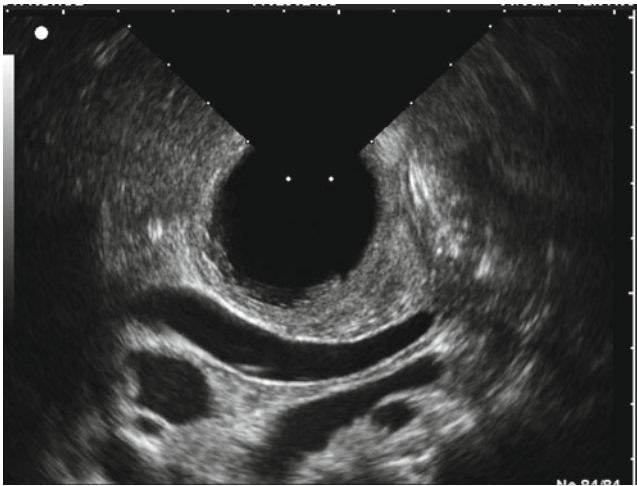


Fig. 3. The common bile duct is well visualized with EUS.

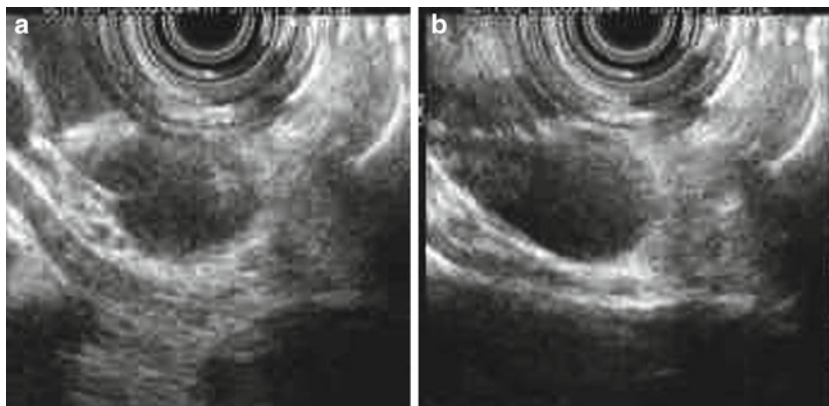


Fig. 4. (a) Early EUS image of an enlarged common bile duct with an EUS needle being advanced into it. (b): A guidewire has been pushed through the EUS needle into the enlarged common bile duct as a vehicle for stent advancement and eventual deployment.

Bile leakage into the peritoneal cavity is a risk with these procedures, and new stent designs may help to avoid this problem (41). Later, IEUC was successful in a larger series of 23 patients with transgastric ($n=13$) or transenteric approach ($n=10$), including stent deployment across the stricture in 18 cases (42, 43). Complications included one bile leak, two cases of self-limited pneumoperitoneum, and one with minor bleeding. The feasibility of this technique was recently confirmed in several case series in patients where ERCP had failed or was not an option (44–46). Although complications include postinterventional pain, cholangitis, stent occlusion, and migration, this method proved effective in the majority of cases and has the potential to serve as an alternative for failed or declined percutaneous transhepatic biliary drainage (PTD) (45, 46). An alternative to direct EUS-g transmural duct drainage is the EUS-g rendezvous technique (36). After EUS-g puncture of the bile duct, a guidewire is advanced through the needle, guided further distally and through the papilla under fluoroscopic control. The EUS scope is then exchanged for a duodenoscope, leaving the guidewire in place for ERCP and stent placement (Fig. 5a–c). Recently, 9-year and 5-year experiences have been reported in 12 and 47 patients, respectively (47, 48). The main advantage over PTD is the ability to complete therapy during the same procedure, under the same sedation. Recent developments have made it possible to perform the entire procedure, including dilatation and stent placement, solely with an echoendoscope (49). Finally, in a pilot study, the feasibility of a one-step technique of choledochoduodenostomy

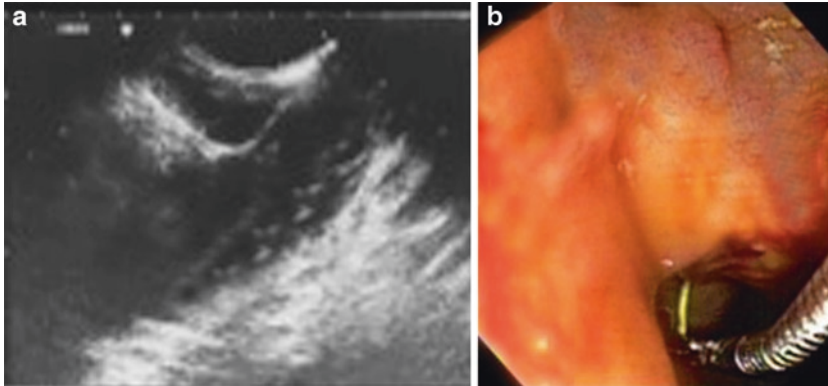


Fig. 5. (a) Similar to Fig. 4a, a guidewire has been passed through the EUS needle into the enlarged bile duct. (b) The wire has been passed through the papilla under fluoroscopy and is being captured with a forceps.

using a prototype-stretched coil delivery system was explored in an animal model (50).

EUS-Guided Bilioma Drainage

EUS-g interventions were further extended to drain bilomas. Kahaleh et al. described an innovative method of draining gallbladder fossa collections under EUS guidance in two patients (51). An EUS needle was inserted through the duodenal wall into the fluid collection, a guidewire coiled within, and an endoprosthesis placed, resulting in rapid symptomatic and radiographic improvement. EUS-g drainage offered a minimally invasive alternative to percutaneous treatment of persistent fluid collections following cholecystectomy. Long-term results are available in five symptomatic patients demonstrating EUS-g drainage to be an attractive alternative to percutaneous or surgical treatment (52).

EUS-Guided Pancreatic Duct Interventions

EUS-g pancreatography was first reported by Harada et al. in 1995 (34) and pancreatogastrostomy (EPG) in four patients by Francois et al. in 2002 (53). Five years later, the efficacy of EPG was shown in a case series of 13 patients with a significant decrease in pain score within a

mean follow-up of 14 months (54). EUS-g puncture and opacification of the pancreatic duct was performed transgastrically followed by guidewire and stent placement. Two complications included bleeding requiring hemoclips and perforation. The technique was also used in 12 cases of chronic pancreatitis with failed transpapillary approach (55). EPG was successful in all and drainage was achieved in 75% of patients, in four of whom a rendezvous was carried out. The overall complication rate was 42.9%, of which 28% were minor events such as pain. Bleeding and perforation were experienced in one case each. Mid-term outcome of EPG drainage in 36 patients with chronic pancreatitis showed a complete or "major" improvement in pain in 70% of patients (56). Two complications included acute pancreatitis with pseudocyst formation and a hematoma, both treated endoscopically. The approach of EUS-g biliary and pancreatic drainage provides an interesting treatment alternative when ERCP fails or is not an option. But the results also demonstrate the complexity of the procedures, requiring very experienced endoscopists and endosonographers in view of the fair success rate and high complication rate needing endoscopic management. Comparative, randomized studies are still missing.

EUS-Guided Vascular Interventions

Most major vessels can be visualized adequately, but are avoided in routine EUS as they present a threat for possible complication. However, the potential for performing vascular interventions is intriguing and has been pursued in several experimental studies. The extra hepatic portal vein (PV) is inaccessible to direct catheterization. EUS-g intervention has the potential to bridge this need in the future (57). Reports of EUS-g PV catheterization (Fig. 6) and pressure measurement in a portal hypertensive animal model are encouraging and show a close correlation between the mean PV pressures obtained by EUS and transhepatic catheterization (58). EUS-g intrahepatic PV puncture and pressure measurements also seem possible using a 5.5 F ERCP catheter over a wire into the PV (59). The feasibility and superiority of EUS-g PV angiography using carbon dioxide (CO₂) as a contrast agent was demonstrated in a porcine model and compared with iodinated contrast (60) (Figs. 7 and 8). An extension of this model to the thoracic and abdominal aorta, superior mesenteric and splenic artery, splenic, portal, and hepatic veins has been demonstrated under fluoroscopy (61). Possible future treatment options include EUS-g embolization of the PV using an ethylene-vinyl alcohol copolymer. Intact embolization was demonstrated in the main PV on CT scan and may have potential for minimally invasive, endoscopic preoperative treatment in patients

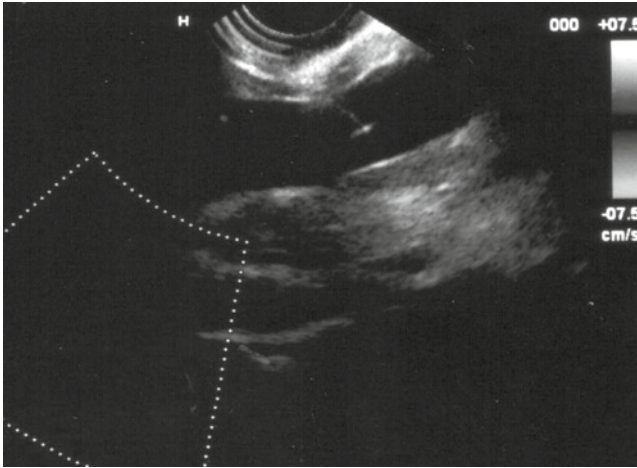


Fig. 6. In a porcine model, a needle can be seen within the portal vein.

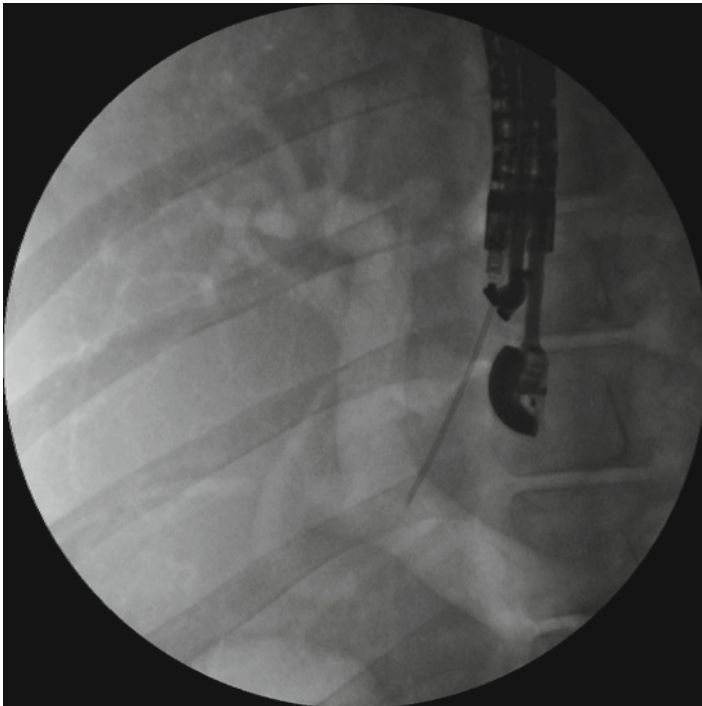


Fig. 7. EUS-g portal vein angiography using carbon dioxide (CO₂) as a contrast agent. Courtesy of Sergey Kantsevov, Department of Gastroenterology and Hepatology, Johns Hopkins University, Baltimore.

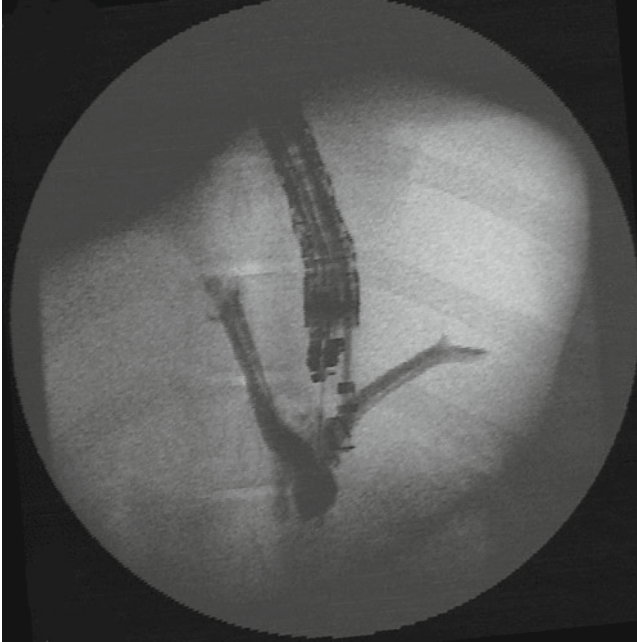


Fig. 8. Fundal Varices prior to therapy. Courtesy of Rafael Romero-Castro, Department of Gastroenterology, Virgen Macarena Hospital, Seville, Spain.

undergoing extensive hepatectomy (62). Most of the EUS-g interventions involving larger vessels have only been performed in animal studies. Romero-Castro et al., however, demonstrated a further treatment option, tested in five patients with recurrent bleeding from gastric varices. EUS-g injection of cyanoacrylate-lipiodol was performed to minimize the risk of rebleeding and was successful in all five patients, making this approach certainly worth further exploration (63) (Fig. 9a–d). A recent modification of the same group for this approach included the use of coil embolization instead of glue injection (Fig. 10).

EXPERIMENTAL EUS-GUIDED ENDOSURGERY: TOWARD NOTES

The major challenge to new techniques is developing complementary new tools and instrumentation. Such strides have made EUS-g techniques accessible to the peritoneal and mediastinal cavity. For example, in one study, lymph nodes were removed endoscopically using EUS for guidance (23) (Fig. 11a–c). After iatrogenic perforation of the gut wall, then followed by lymph node removal the created fistula is closed

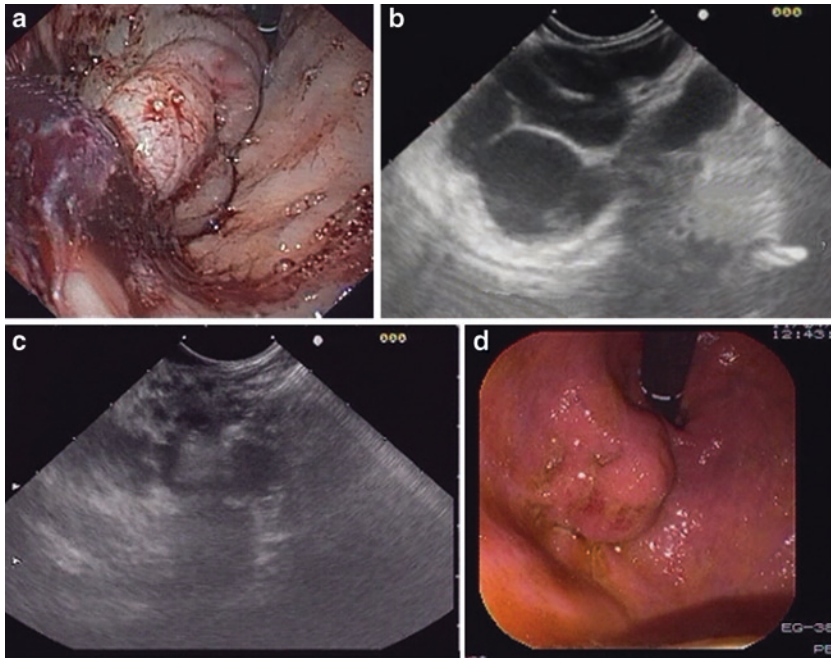


Fig. 9. (a) Endoscopic view of large gastric varices, which show signs of recent bleeding. (b) EUS view of the convolute of gastric varices. (c) EUS-g injection of cyanoacrylate-lipiodol into the feeding vessel. (d) Endoscopic view of the gastric varices after EUS-g injection of cyanoacrylate-lipiodol. Courtesy of Rafael Romero-Castro, Department of Gastroenterology, Virgen Macarena Hospital, Seville, Spain.

(Fig. 12a) this has been made possible thanks to the development of an endoscopic suturing device which was initially developed for EUS-g tissue apposition and has been used as a prototype for endoscopic closure of iatrogenic gut wall incisions. (TAS, Ethicon Endosurgery, Cincinnati, OH) (22, 64, 65) (Fig. 12b). Further advancement of invasive endoscopic endosurgery (IEE) is limited by the current single-channel instrument, lack of push force, and an accessory channel with a maximum diameter of 3.8 mm. For more sophisticated procedures, triangulation or a minimum of two channels are needed to perform complex techniques (Fig. 13). Structures could be held by instruments forwarded through one channel and IEE carried out through the second channel. The push force could be increased, and the spectrum and sophistication of IEE could be extended. A new double-channel linear array echoendoscope (Fig. 13) was tested and compared with the available single-channel scope in

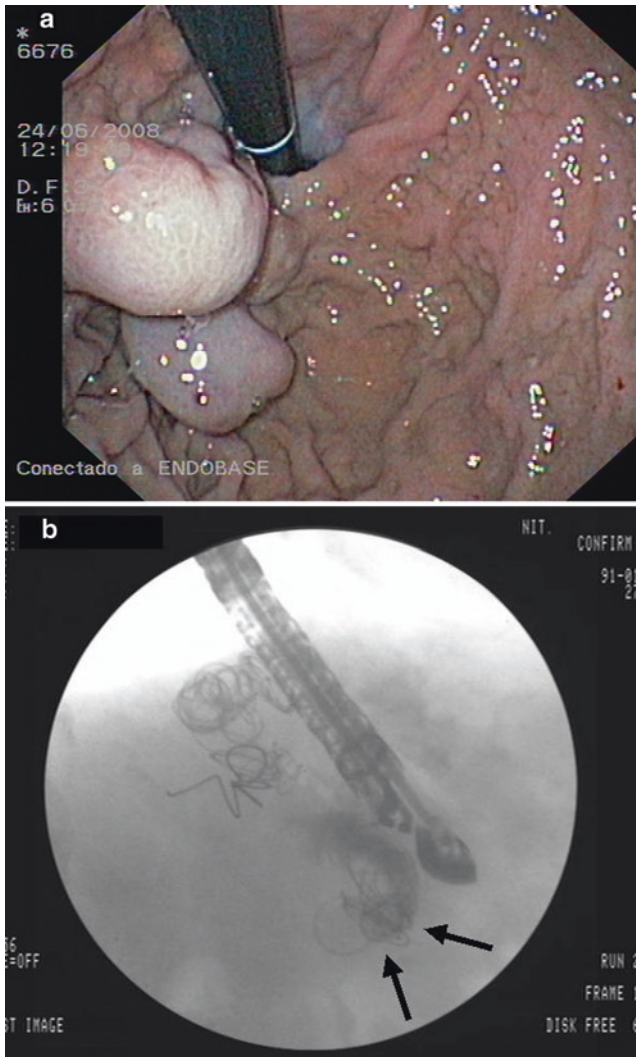


Fig. 10. (a) Filling of the venous system can be seen using CO₂ in a porcine model. (b) EUS-g coil embolization of gastric varices: radiographic view. Courtesy of Rafael Romero-Castro, Department of Gastroenterology, Virgen Macarena Hospital, Seville, Spain.

an animal survival study (66). EUS-g transesophageal biopsy and ablation of the aortic valve were performed. Procedure time, maneuverability, and ease of performance were better with the double-channel scope. Its limitations included lack of an elevator

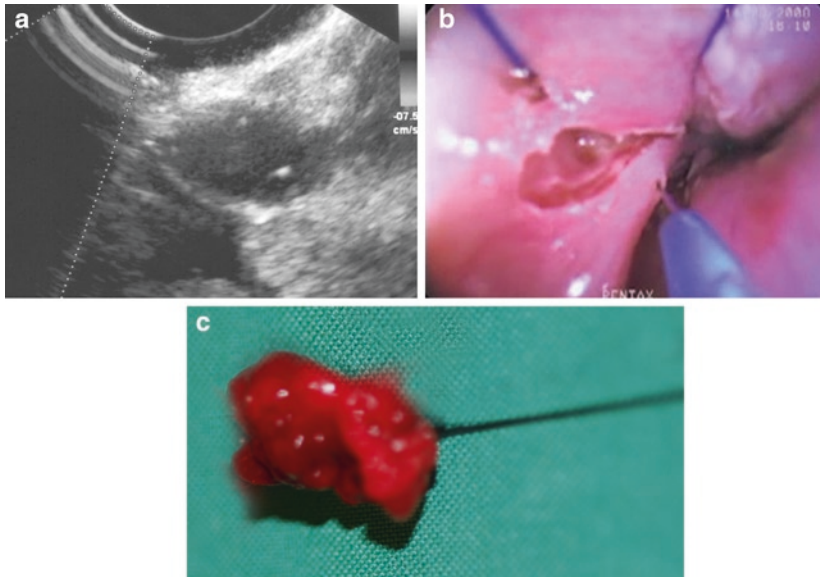


Fig. 11. (a) EUS-g placement of a metal anchor into a lymph node. (b) The thread with the anchor on its distal end can be seen in the endoscopic image appearing out of the GI wall. A needle knife has been used to cut the wall next to the threads open. (c) Photograph of an excised lymph node with the thread and anchor still in place.

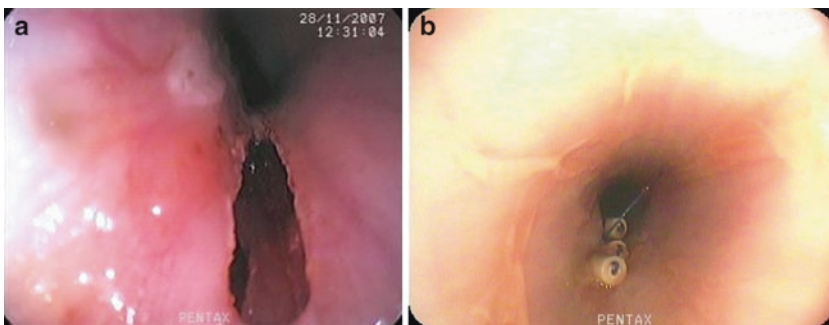


Fig. 12. (a) Large iatrogenic incision of the gut wall. (b) The iatrogenic incision has been closed with a prototype endoscopic suturing system (TAS, Ethicon Endosurgery, Cincinnati, OH).

preventing individual maneuverability of the needles and the difficulty to carry heavy instruments, especially when two needles were loaded. However, this new double lumen EUS scope has the potential to be of



Fig. 13. Prototype double channel echoendoscope with two EUS needles mounted onto both of the accessory channels.

great value in the future since the additional channel enables fixation of the target structure and allows planned complex interventions.

EUS-Guided Anastomosis

EUS-g creation of gastrojejunal anastomoses has been demonstrated to be feasible (24). The technique involves identification of an appropriate small bowel loop by transgastric EUS imaging and anchoring the targeted small bowel loop to the gastric wall by EUS-g deployment of a T-bar back loaded on a 19-gauge EUS needle. A guidewire is subsequently passed through the 19-gauge EUS needle, which served as a rail for deployment of devices (catheter, plate, balloon, etc.) into the small bowel. From the gastric side, a plate to spread the force, spring, and lock or a second balloon is pressed against the small bowel device, guided by the access catheter can serve as counter pressure. Creation of pressure greater than 200 mm Hg causes ischemic necrosis of the intervening tissue within a few days forming an anastomosis (Fig. 14), which can



Fig. 14. Autopsy of a pig showing patent gastrojejunal anastomosis.

subsequently be enlarged with a needle knife (67). Similar technique has been used to create cholecystogastrostomy for the removal of calculi (21). Several other clinical applications could be envisioned using these techniques, such as colo-colic anastomosis for inoperable obstructive colon cancer, bariatric surgery in morbidly obese individuals, and for the drainage of empyema of the gallbladder in inoperable patients.

One main drawback of this technique compared with a NOTES approach would be the invariable delay in the formation of the gastroenteric fistula.

EUS-Guided Cardiac Interventions

The proximity of the posterior mediastinum, left atrium, and the pulmonary trunk to the esophagus, and the extensive use of transesophageal echocardiography logically led to the exploration of EUS-g cardiac interventions (68). The primary concerns of cardiac interventions would be myocardial damage, bleeding, or arrhythmia. In acute experiments

(n=2) and survival experiments (n=6) on anesthetized pigs, a needle was introduced transesophageally through the posterior cardiac wall into the left atrium and beyond, as far as the aortic valve, under EUS-guidance. The smallest structure targeted was the coronary artery. Experimental procedures studied, included needle biopsy of the cardiac muscle; direct intracardiac recording of ECG; contrast injection into the left atrium, ventricle, and the coronary arteries. Cardiac conductive tissue ablation of the mitral valve and wire-guided radiofrequency interventions of the aortic and mitral valves were the most invasive procedures performed. The animals in the survival group were monitored clinically over a 2-week period and endoscopic and cardiac reevaluations were performed prior to autopsy. No visible damage was observed following acute experiments. One small hematoma was observed in one of the six surviving pigs. Reaching the aortic valve was more difficult because of the moving target, but ablation therapy was technically possible. The coronary artery was successfully punctured in three of the animals (weighing 40 kg or more); in smaller animals, the needle double-punctured these minute arteries. This technique was much easier, when a prototype double lumen echoendoscope was used, which enabled fixation of an arm of the valve with one instrument and ablation or puncture with the other. Furthermore in three patients, EUS-g access to the heart was used to obtain biopsies of left atrial mass or aspiration of pericardial fluid. The feasibility of EUS-g cardiac interventions was recently confirmed by Castro-Romero et al. who



Fig. 15. EUS-g/FNA of a pericardial tumor. Courtesy of Rafael Romero-Castro, Department of Gastroenterology, Virgen Macarena Hospital, Seville, Spain.

reported a case of EUS-g puncture of a pericardial mass lesion and was able to obtain a diagnosis (69) (Fig. 15).

EUS-GUIDED ENDOSURGERY

Recently, endoluminal interventions have expanded in the context of NOTES procedures. Although physicians performing NOTES have initially thought that EUS guidance might not be necessary, complications experienced have led to a reconsideration of this initial stance. At the recent third NOSCART meeting in San Francisco 2008, several presentations included reflections that EUS might play a role in the future. Although NOTES access is obtained without much complication when performed across the anterior wall of the stomach, this is not the case when another area is chosen for access into the peritoneal and/or thoracic cavity.

EUS-Guided Transluminal (NOTES) Access

Most NOTES procedures are being performed through the anterior gastric wall, based on the fact that larger vessels are not present in this area. The potential role of EUS-g vs. blind NOTES access was assessed in 32 procedures on 12 pigs in alternate areas, including the antrum, the posterior gastric wall, and the rectum. Blind NOTES access resulted in clinically relevant damage of organs and structures such as liver laceration, gallbladder puncture, and external iliac artery injury and thus was regarded as unsafe. Using EUS-g access no complications were experienced, when transgastric access was performed. But three complications occurred using the transrectal approach with superficial penetration into the lower abdominal wall muscle, puncture through the left mesosalpinx, and one small bowel perforation. The study demonstrated the superiority of EUS-g access vs. blind NOTES, which substantially reduced but not completely eliminated this risk (70). These findings were confirmed by another study, which used EUS-g access through the lesser curve and esophagus after major complications such as bleeding had occurred with blind NOTES access. Not only did EUS-guidance enable a safe access without bleeding, but it also enabled safe access to the adrenal gland, an organ which is difficult to be approached transgastrically. On the other hand, access through the anterior wall to perform gastrojejunal anastomosis was safe even without EUS-guidance (71). These initial pilot studies show that there may be a future role for EUS-guidance in NOTES procedures when access is attempted in areas other than the anterior gastric wall.

EUS-Guided Mediastinal Drainages and NOTES

The close proximity of major organs and blood vessels to the esophagus and potentially fatal mediastinal infections has precluded attempts at transesophageal procedures. However, with the advent of transesophageal EUS-FNA of lymph nodes, the mediastinum is no longer secluded from endoscopic interventions. The next step was EUS-FNA of mediastinal abscesses (72). This encompasses an iatrogenic full thickness incision into the esophageal wall and has been shown to be a feasible and a successful treatment option in select patients (73, 74). This represents a true endosurgical external EUS-g approach. Transesophageal iatrogenic perforation to access the mediastinum and thoracic cavity as described above is considered extremely invasive with potential for severe complications. Therefore, some groups created a submucosal tunnel after incision of the esophageal mucosa for access to the external space through the muscle layer at some distances distally from the mucosal incision (75, 76). However, if EUS-guidance was used, direct transmural incision of the esophageal wall seemed to provide a safe access to the mediastinum and thorax to perform interventions. In a 6 week survival study, our group performed transesophageal NOTES procedures in the mediastinum and thorax in a swine model (19). After an optimal incision site was chosen during EUS, a full-thickness esophageal incision of 2.5 cm diameter was performed endoscopically using a needle knife. Subsequently, an endoscope was passed through the access site into the mediastinum for minor procedures, including injection into the myocardium and pericardial fenestration. This was easier when the transesophageal access site was chosen near the heart by EUS. In six animals the pleura was incised for transesophageal thoracoscopy. The esophageal incision was closed using endoscopic suturing systems with anchor/locks, which provided excellent closure on histology, when compared with thoracoscopic sewing or clip closure (19, 77). However, when EUS was not used to guide through the esophageal wall, bleeding was experienced in 2/14 animals, loss of anatomical orientation in two, or inadvertent trauma to another organ in one (71, 77). Subsequent procedures were performed under EUS-guidance in nine consecutive animals successfully, avoiding injury to blood vessels or other organs in all cases. This leads one to think that direct transesophageal access without EUS-guidance would be unsafe. The risk of mediastinitis is present with these procedures, especially in the presence of reflux contamination from gastric residue into the mediastinum (78). The stomach should be completely empty for these procedures to avoid spillage into the mediastinum when the esophageal wall is open. The potential benefit of being able to incise the esophageal wall for further operative procedures has been shown in several

studies, and this approach might have some interesting future applications (71, 78–80). Even if NOTES is not intended, endoluminal full-thickness wall resection of the esophagus may make endoscopic removal of benign tumors entirely under EUS-guidance, possible. This would constitute a major benefit for patients in the future if the early animal experience could be translated into safe and efficacious procedures (79). Ryou et al. performed a systematic transesophageal exploration of the human mediastinum and thorax, and assessed the feasibility of advanced NOTES surgery in these compartments in two human cadavers (one male, one female) with video logs (81). A prototype double-channel endoscope (Olympus R-Scope) and the ERBE Hybrid knife were used to create a transesophageal access through a posterior submucosal flap, exploring the mediastinal, pleural, and pericardial compartments systematically. Lymph node sampling, pleural biopsy, vagotomy, thoracic duct ligation, pericardial window, and thymectomy could be successfully performed demonstrating that NOTES thoracic surgery via transesophageal access is technically feasible. However, for translation to patients, this approach would require a sterile conduit, novel tissue closure technique, EUS for anatomic mapping, and specialized ventilatory strategies.

Transluminal EUS

Preoperative detection of peritoneal and other small metastases can be difficult. Laparoscopy and laparoscopic ultrasonography (LUS) are frequently required to exclude metastases prior to resection. Voermans et al. assessed the feasibility of transluminal intraoperative EUS (iEUS) in an acute porcine model by the transgastric and transcolonic approach (82). Systematic peritoneoscopy with the evaluation of predetermined locations was compared with EUS-guided transluminal evaluation. Intraperitoneal EUS was found to be feasible during NOTES peritoneoscopy and resulted in an adequate US imaging of the liver with the transcolonic approach being superior to the transgastric approach.

CONCLUSION

Overall, endosurgical applications for EUS seem to have increased over the recent years. Although the endoluminal interventions performed are still limited in numbers, new generation endoscopists are more likely to adopt this technology and advance EUS-g interventions in future. The engagement of some in NOTES procedures has created further interest

to push the former boundaries of endoscopy. This will inevitably have an effect on the interventional potential of EUS. This will also further popularize interventional EUS when its potential for reducing the complications of NOTES, can be proven. However, the tools and instruments for more sophisticated interventions are missing and need to be developed. Lastly, reimbursement and training issues need to be addressed before endoscopists at large can learn, develop, and use EUS-g endosurgery.

Acknowledgments The authors wish to thank Rafael Romero-Castro, Department of Gastroenterology, Virgen Macarena Hospital, Seville, Spain and Sergey Kantsevov (The author initially held patents together with others for the TAS devices), Department of Gastroenterology and Hepatology, Johns Hopkins University, Baltimore for their kind supply with the images marked for publication in this article.

REFERENCES

1. Kalloo AN, Singh VK, Sanjay B, Jagannath SB, Niiyama H, Hill SL. Flexible transgastric peritoneoscopy: a novel approach to diagnosis and therapeutic intervention in the peritoneal cavity. *Gastrointest Endosc.* 2004;60:114–7.
2. Wagh MS, Thompson CC. Surgery Insight: natural orifice transluminal endoscopic surgery – an analysis of work to date. *Nat Clin Pract Gastroenterol Hepatol.* 2007;4:386–92.
3. Voermans RP, van Berge Henegouwen MI, Fockens P. Natural orifice transluminal endoscopic surgery (NOTES). *Endoscopy.* 2007;39:1013–7.
4. ASGE, SAGES. ASGE/SAGES Working Group on Natural Orifice Transluminal Endoscopic Surgery White Paper. *Gastrointest Endosc.* 2008;67:779–80.
5. Flora ED, Wilson TG, Martin IJ, O'Rourke NA, Maddern GJ. A review of natural orifice transluminal endoscopic surgery (NOTES) for intra-abdominal surgery experimental models, techniques, and applicability to the clinical setting. *Ann Surg.* 2008; 247:583–602.
6. Pearl JP, Ponsky JL. Natural orifice transluminal endoscopic surgery: a critical review. *J Gastrointest Surg.* 2008;12:1293–300.
7. Marescaux J, Dallemagne B, Perretta S, et al. Surgery without scars: report of transluminal cholecystectomy in a human being. *Arch Surg.* 2007;142:823–6.
8. Hazey JW, Narula VK, Renton DB, Reavis KM, Paul CM, Hinshaw KE, et al. Natural-orifice transgastric endoscopic peritoneoscopy in humans: initial clinical trial. *Surg Endosc.* 2008;22:16–20.
9. Zorron R, Maggioni LC, Pombo Loliveira AL, Carvalho GL, Filgueiras M. NOTES transvaginal cholecystectomy: preliminary clinical application. *Surg Endosc.* 2008;22:542–7.
10. Palanivelu C, Rajan PS, Rangarajan M, Parthasarathi R, Senthilnathan P, Prasad M. Transvaginal endoscopic appendectomy in humans: a unique approach to NOTES – world's first report. *Surg Endosc.* 2008;22:1343–7.
11. Access to the Peritoneal Cavity. Working Group Summary Presentations. International Conference on Natural Orifice Transluminal Endoscopic Surgery (NOTES)TM Scottsdale, Arizona. 9–11 Mar 2006.

12. Levy MJ, Topazian MD, Wiersema MJ, Clain JE, Rajan E, Wang KK, et al. Initial evaluation of the efficacy and safety of endoscopic ultrasound-guided direct ganglia neurolysis and block. *Am J Gastroenterol*. 2008;103:98–103.
13. Klapman JB, Chang KJ. Endoscopic ultrasound-guided fine-needle injection. *Gastrointest Endosc Clin N Am*. 2005;15:169–77.
14. Chang KJ, Lee JG, Holcombe RF, Kuo J, Muthusamy R, Wu ML. Endoscopic ultrasound delivery of an antitumor agent to treat a case of pancreatic cancer. *Nat Clin Pract Gastroenterol Hepatol*. 2008;5:107–11.
15. Magno P, Giday SA, Gabrielson KL, et al. EUS-guided implantation of radiopaque marker into mediastinal and celiac lymph nodes is safe and effective. *Gastrointest Endosc*. 2007;66:387–92.
16. Seifert H, Wehrmann T, Schmitt T, et al. Retroperitoneal endoscopic debridement for infected peripancreatic necrosis. *Lancet*. 2000;356(9230):653–5.
17. Seewald S, Groth S, Omar S, et al. Aggressive endoscopic therapy for pancreatic necrosis and pancreatic abscess: a new safe and effective treatment algorithm (with videos). *Gastrointest Endosc*. 2005;62:92–100.
18. Varadarajulu S, Mel Wilcox C, Tamhane A, Eloubeidi MA, Blakely J, Canon CL. Role of EUS in drainage of peripancreatic fluid collections not amenable for endoscopic transmural drainage. *Gastrointest Endosc*. 2007;66:1107–19.
19. Fritscher-Ravens A, Patel K, Ghanbari A, Kahle E, von Herbay A, Fritscher T, et al. Natural orifice transluminal endoscopic surgery (NOTES) in the mediastinum: long-term survival animal experiments in transesophageal access, including minor surgical procedures. *Endoscopy*. 2007;39:870–5.
20. Fritscher-Ravens A, Mosse CA, Mukherjee D, et al. Transgastric gastropexy and hiatus hernia repair for gastro-esophageal reflux disease under endoscopic ultrasound control: an experimental study in a porcine model. *Gastrointest Endosc*. 2004;59:89–95.
21. Fritscher-Ravens A, Mosse S, Mills T, Swain P. Endoscopic cholecystogastropexy, cholecystogastrotomy and gall stone removal under endoscopic ultrasound control. *Gut*. 2004;53(Suppl IV):A43.
22. Fritscher-Ravens A, Mosse CA, Mills TN, Mukherjee D, Park PO, Swain CP. A through-the-scope device for suturing and tissue approximation under EUS control. *Gastrointest Endosc*. 2002;56:737–42.
23. Fritscher-Ravens A, Mosse CA, Ikeda K, Swain P. Endoscopic transgastric lymphadenectomy by using EUS for selection and guidance. *Gastrointest Endosc*. 2006;63:302–6.
24. Fritscher-Ravens A, Mosse CA, Mukherjee D, et al. Transluminal endosurgery: single lumen access anastomotic device for flexible endoscopy. *Gastrointest Endosc*. 2003;58:585–91.
25. Ikeda K, Fritscher-Ravens A, Mosse CA, Mills T, Tajiri H, Swain CP. Endoscopic full-thickness resection with sutured closure in a porcine model. *Gastrointest Endosc*. 2005;62:122–9.
26. Gan SI, Thompson CC, Lauwers GY, Bounds BC, Brugge WR. Ethanol lavage of pancreatic cystic lesions: initial pilot study. *Gastrointest Endosc*. 2005;61:746–52.
27. Charnley RM, Lochan R, Gray H, O’Sullivan CB, Scott J, Oppong KE. Endoscopic necrosectomy as primary therapy in the management of infected pancreatic necrosis. *Endoscopy*. 2006;38:925–8.

28. Raczynski S, Teich N, Borte G, Wittenburg H, Mössner J, Caca K. Percutaneous transgastric irrigation drainage in combination with endoscopic necrosectomy in necrotizing pancreatitis. *Gastrointest Endosc.* 2006;64:420–4.
29. Antillon MR, Bechtold ML, Bartalos CR, Marshall JB. Transgastric endoscopic necrosectomy with temporary metallic esophageal stent placement for the treatment of infected pancreatic necrosis. *Gastrointest Endosc.* 2009;69(1):178–80.
30. Wang AY, Condrón SL, Gaylish R, Yeaton P. Fully-covered self-expandable metallic stents facilitate effective endoscopic pancreatic necrosectomy. *Gastrointest Endosc.* 2008;67:AB332.
31. Schmidt PN. Endoscopic ultrasound-guided transmural drainage and necrosectomy in complicated acute and chronic pancreatitis. *Gastrointest Endosc.* 2008;67:AB282.
32. Will U, Wanzar C, Gerlach R, Meyer F. Endoscopic interventions in pancreatic pseudocysts, abscesses and infected necroses – Experiences and treatment results of a large single centre case series (n=87). *Gastrointest Endosc.* 2008;67:AB285.
33. Kaltenbach TR, De Lusong MA, Soetikno RM, Shah JN, Binmoeller KF. Single-scope EUS guided cyst access, debridement and drainage using a novel therapeutic forward viewing echoendoscope. *Gastrointest Endosc.* 2008;67:AB202.
34. Harada N, Kouzu T, Arima M, et al. Endoscopic ultrasound guided pancreatography: a case report. *Endoscopy.* 1995;27:612–5.
35. Gress F, Ikenberry S, Sherman S, Lehman G. Endoscopic ultrasound directed pancreatography. *Gastrointest Endosc.* 1996;44:736–9.
36. Mallery S, Matlock J, Freeman ML. EUS-guided rendezvous drainage of obstructed biliary and pancreatic ducts: reports of 6 cases. *Gastrointest Endosc.* 2004;50:100–7.
37. Sahai AV, Hoffman BJ, Hawes RH. Endoscopic ultrasound guided hepatico-gastrostomy to palliate obstructive jaundice: preliminary results in pigs (abstract). *Gastrointest Endosc.* 1998;47:AB37.
38. Giovannini M, Moutardier B, Presenti C, Borries E, Lelong B, Delpero JR. Endoscopic ultrasound guided bilioduodenal anastomosis: a new technique for biliary drainage. *Endoscopy.* 2001;33:898–900.
39. Burmester E, Niehaus J, Leineweber T, Huetteroth T. EUS-cholangiodrainage of the bile duct: report of 4 cases. *Gastrointest Endosc.* 2003;57:246–50.
40. Seifert H, Faust D, Schmitt T, Dietrich C, Caspary W, Wehrmann T. Transmural drainage of cystic peripancreatic lesions with a new large-channel echo endoscope. *Endoscopy.* 2001;33:1022–6.
41. Fritscher-Ravens A, Mukherjee D, Mosse A, Swain PC. Push me pull you flexible plastic stents. *Gastrointest Endosc.* 2002;55:AB176.
42. Kahaleh M, Yoshida C, Kane L, Yeaton P. Interventional EUS cholangiography: a report of five cases. *Gastrointest Endosc.* 2004;60:138–42.
43. Kahaleh M, Hernandez AJ, Tokar J, Adams RB, Shami VM, Yeaton P. Interventional EUS-guided cholangiography: evaluation of a technique in evolution. *Gastrointest Endosc.* 2006;64:52–9.
44. Tarantino I, Barresi L, Repici A, Traina M. EUS-guided biliary drainage: a case series. *Endoscopy.* 2008;40:336–9.
45. Will U, Thieme A, Fueldner F, Gerlach R, Wanzar I, Meyer F. Treatment of biliary obstruction in selected patients by endoscopic ultrasonography (EUS)-guided trans-luminal biliary drainage. *Endoscopy.* 2007;39:292–5.

46. Bories E, Pesenti C, Caillol F, Lopes C, Giovannini M. Transgastric endoscopic ultrasonography-guided biliary drainage: results of a pilot study. *Endoscopy*. 2007;39:287–91.
47. Kim Y, Shawn Mallery J, Lai R, Kinney TP, Gupta K, Chau A, et al. EUS rendez-vous for transpapillary biliary access after unsuccessful ERCP – 9 years experience at a single center. *Gastrointest Endosc*. 2008;67:AB38.
48. Maranki JL, Shami VM, Hernandez AJ, Kahaleh M. Interventional EUS guided cholangiography (IEUS): Long term experience of an emerging alternative to percutaneous transhepatic cholangiography (PTC). *Gastrointest Endosc*. 2008;67:AB224.
49. Yamao K, Bhatia V, Mizuno N, Sawaki A, Ishikawa H, Tajika M, et al. EUS-guided choledochoduodenostomy for palliative biliary drainage in patients with malignant biliary obstruction: results of long-term follow-up. *Endoscopy*. 2008;40:340–2.
50. Chang K. Endoscopic choledochoduodenostomy (ECD) for the treatment of biliary obstruction using prototype compression coil and interventional endosonography (EUS): a “proof of principle” canine study. *Gastrointest Endosc*. 2008;67:AB109.
51. Kahaleh M, Wang P, Shami VM, Tokar J, Yeaton P. Drainage of gallbladder fossa fluid collections with endoprosthesis placement under endoscopic ultrasound guidance: a preliminary report of two cases. *Endoscopy*. 2005;37:393–6.
52. Shami VM, Talreja JP, Mahajan A, Phillips MS, Yeaton P, Kahaleh M. EUS-guided drainage of bilomas: a new alternative? *Gastrointest Endosc*. 2008;67:136–40.
53. François E, Kahaleh M, Giovannini M, Matos C, Devière J. EUS-guided pancreaticogastrostomy. *Gastrointest Endosc*. 2002;56:128–33.
54. Kahaleh M, Hernandez AJ, Tokar J, Adams RB, Shami VM, Yeaton P. EUS-guided pancreaticogastrostomy: analysis of its efficacy to drain inaccessible pancreatic ducts. *Gastrointest Endosc*. 2007;65:224–30.
55. Will U, Fuedner F, Thieme AK, Goldmann B, Gerlach R, Wanzar I, et al. Transgastric pancreatography and EUS-guided drainage of the pancreatic duct. *J Hepatobiliary Pancreat Surg*. 2007;14:377–82.
56. Tessier G, Bories E, Arvanitakis M, et al. EUS-guided pancreaticogastrostomy and pancreatobulbostomy for the treatment of pain in patients with pancreatic ductal dilatation inaccessible for transpapillary endoscopic therapy. *Gastrointest Endosc*. 2007;65:233–41.
57. Brugge WR. EUS is an important new tool for accessing the portal vein. *Gastrointest Endosc*. 2008;67:343–4.
58. Lai L, Poneris J, Santilli J, Brugge W. EUS-guided portal vein catheterization and pressure measurement in an animal model: a pilot study of feasibility. *Gastrointest Endosc*. 2004;59:280–3.
59. Giday SA, Clarke JO, Buscaglia JM, Shin EJ, Ko CW, Magno P, et al. EUS-guided portal vein catheterization: a promising novel approach for portal angiography and portal vein pressure measurements. *Gastrointest Endosc*. 2008;67:338–42.
60. Giday SA, Ko CW, Clarke JO, Shin EJ, Magno P, Jagannath SB, et al. EUS-guided portal vein carbon dioxide angiography: a pilot study in a porcine model. *Gastrointest Endosc*. 2007;66:814–9.
61. Magno P, Ko CW, Buscaglia JM, Giday SA, Jagannath SB, Clarke JO, et al. EUS-guided angiography: a novel approach to diagnostic and therapeutic interventions in the vascular system. *Gastrointest Endosc*. 2007;66:587–91.

62. Matthes K, Sahani D, Holalkere NS, Mino-Kenudson M, Brugge WR. Feasibility of endoscopic ultrasound-guided portal vein embolization with Enteryx. *Acta Gastroenterol Belg.* 2005;68:412–5.
63. Romero-Castro R, Pellicer-Bautista FJ, Jimenez-Saenz M, Marcos-Sanchez F, Caunedo-Alvarez A, Ortiz-Moyano C, et al. EUS-guided injection of cyanoacrylate in perforating feeding veins in gastric varices: results in 5 cases. *Gastrointest Endosc.* 2007;66:402–7.
64. Ikeda K, Mosse CA, Park PO, Fritscher-Ravens A, Bergström M, Mills T, et al. Endoscopic full-thickness resection (EFTR): circumferential cutting method. *Gastrointest Endosc.* 2006;64:82–9.
65. Raju GS, Fritscher-Ravens A, Rothstein R, Swain P, Gelrud A, Ahmed I, et al. Endoscopic closure of colon perforation compared to surgery in a porcine model: a randomized controlled trial. *Gastrointest Endosc.* 2008;68(2):324–32.
66. Fritscher-Ravens A, Ghanbari A, von Herbay A, Kahle E, Koehler P, Niemann H, et al. First experience with a new double channel linear array echoendoscope for advanced interventional EUS procedures compared to a single lumen instrument in a long-term animal survival study. *Gastrointest Endosc.* 2008;67(5):AB200.
67. Fritscher-Ravens A. EUS-guided drainage and anastomosis. In: Hawes RH, Fockens P, editors. *Endosonography*. Philadelphia: Saunders; 2006. p. 303–22.
68. Fritscher-Ravens A, Ganbari A, Mosse CA, et al. Transesophageal endoscopic ultrasound guided access to the heart. *Endoscopy.* 2007;39:385–9.
69. Romero-Castro R, Rios-Martin JJ, Gallego-Garcia de Vinuesa P, Castro-Fernandez AJ, Marques-Asin FJ, Pellicer-Bautista F, et al. Pericardial tumor diagnosed by EUS guided-FNA. *Gastrointest Endosc.* 2009;69(2):S255–6.
70. Elmunzer BJ, Schomisch SJ, Trunzo JA, Poulouse BK, Mcgee MF, Faulx AL, et al. Endoscopic ultrasound for localizing safe alternate access sites for NOTES: initial experience in a porcine model. *Gastrointest Endosc.* 2008;67(5):AB113.
71. Fritscher-Ravens A, Knoefel WT, Eisenberger CF, Schiffmann S, von Herbay A, Ghadimi MP, et al. Transesophageal access to the mediastinum: long term animal survival study using NOTES technique. *Gastrointest Endosc.* 2008;67(5):AB112.
72. Fritscher-Ravens A, Swain P, Schirrow L, et al. Urgent bedside endosonography and guided fine-needle aspiration for diagnosis and management of posterior mediastinitis. *Crit Care Med.* 2003;31:126–32.
73. Kahaleh M, Yoshida C, Kane L, Yeaton P. EUS drainage of a mediastinal abscess. *Gastrointest Endosc.* 2004;60(1):158–60.
74. Wehrmann T, Stergiou N, Vogel B, Riphaut A, Köckerling F, Frenz MB. Endoscopic debridement of paraesophageal, mediastinal abscesses: a prospective case series. *Gastrointest Endosc.* 2005;62(3):344–9.
75. Sumiyama K, Gostout CJ, Rajan E, et al. Transesophageal mediastinoscopy by submucosal endoscopy with mucosal flap safety valve technique. *Gastrointest Endosc.* 2007;65:679–83.
76. Willingham FF, Gee DW, Lauwers GY, Brugge WR, Rattner DW. Natural orifice transesophageal mediastinoscopy and thoracoscopy. *Surg Endosc.* 2008;22(4):1042–7.
77. Fritscher-Ravens A, Patel K, Kahle E, et al. Transesophageal access to and procedures within the mediastinum: a long-term animal survival study of NOTES procedures. *Endoscopy.* 2007;39:870–5.

78. Fritscher-Ravens A, Milla P, Schiffmann S, von Herbay A, Eisenberger CF, Ghanbari A, et al. Clip closure versus endoscopic suturing versus thoracoscopic repair of an esophageal perforation: randomized comparative long term survival study in a porcine model. *Gastrointest Endosc.* 2008;67(5):AB106.
79. Fritscher-Ravens A, Ghanbari A, Patel K, Koehler P, Kahle E, Niemann H, et al. Feasibility and safety of endoscopic full thickness esophageal wall resection and defect closure in a prospective long term survival animal study. *Gastrointest Endosc.* 2008;67(5):AB189.
80. Rothstein RI, Bergstrom M, Park PO, Mosse AC, Swain P. Mediastinoscopy and thoracoscopy: a next NOTES Frontier? *Gastrointest Endosc.* 2008;67(5):AB117.
81. Ryou M, Shaikh SN, Fernandez-Esparrach G, Ryan MB, Maurice D, Matthes EL, et al. NOTES thoracic surgery in a human cadaveric model: transesophageal exploration of the mediastinal, pericardial and pleural spaces followed by pleural biopsy, lymph node sampling, thoracic duct ligation, vagotomy, thymectomy and pericardial window. *Gastrointest Endosc.* 2008;67(5):AB111.
82. Voermans RP, van Berge Henegouwen MI, Bemelman WA, Fockens P. Feasibility of transgastric and transcolonic NOTES peritoneoscopy combined with intraperitoneal endoscopic ultrasonography. *Gastrointest Endosc.* 2008;67(5):AB114.

The Future of EUS

Thomas J. Savides, MD

CONTENTS

INTRODUCTION
FUTURE EUS EQUIPMENT
EUS INDICATIONS IN THE FUTURE
FUTURE TRAINING AND QUALITY ISSUES
CONCLUSIONS

Abstract

EUS has evolved from diagnostic imaging to tissue sampling, and most recently to therapy. This chapter provides thoughts about where the field of EUS may be headed over the next 5–10 years in terms of echoendoscope and accessory development, disease management, and training. The future of EUS is bright, and we should expect a number of creative new EUS therapies in the near future.

Key Words: Future of EUS, Therapeutic EUS, NOTES

INTRODUCTION

EUS has evolved over the past 20 years from a purely diagnostic imaging test, to having the ability to obtain tissue for diagnosis, and more recently to perform therapeutic interventions. During this period of time, we have constantly modified how we utilize EUS in response to changes in other technologies (endoscopic, radiographic, and surgical). The preceding chapters in the book provide discussion of the current state of the art of EUS, as well as cutting edge therapeutics. The purpose of this chapter is to provide an educated (and opinionated) guess

From: *Clinical Gastroenterology: Endoscopic Ultrasound*,
Edited by: V. M. Shami and M. Kahaleh, DOI 10.1007/978-1-60327-480-7_22,
© Springer Science+Business Media, LLC 2010

of the near future (5–10 years) based on our current technical needs, and how we may apply new tools to specific disease states and teach them to current and future endosonographers.

FUTURE EUS EQUIPMENT

EUS Scopes

The current “work horse” echoendoscopes in most units include both radial and linear scanning instruments. For diagnostic imaging purposes, one can argue the pros and cons of each. I personally see a role for both, as radial EUS gives excellent diagnostic information because of the 360° view. However, because linear scopes are needed to perform FNA, there will continue to be an increasing shift toward the use of linear echoendoscopes. Additionally, because more therapeutic EUS will be performed, there should be a significant increase in the use of large channel therapeutic linear echoendoscopes.

EUS scopes have evolved over the past 20 years. Mechanical sector scanning scopes have been replaced with electronic array scopes. Nonvision guided esophageal scopes have come and gone. Catheter probes were among the first devices we used, but have mostly been replaced now with dedicated scopes which provide a broader array of diagnostic and therapeutic capabilities. The most recent generation of scopes combine desirable features of standard videoendoscopes with EUS capability. Most notable is the use of forward viewing EUS scopes which combine a forward viewing EGD scope and EUS scope into one. These scopes allow more complete and efficient imaging, and may provide improved ability to perform some therapeutic procedures such as pseudocyst drainage.

Future scopes will hopefully continue combining scope functions with the ability to do EUS and ERCP in the same procedure. We frequently image a dilated bile duct first using EUS to determine if obstruction is due to a stone or mass, perform a EUS FNA if indicated, and then proceed to either ERCP with stone removal or stent placement in the same session. It would be desirable to have a scope system which combined EUS imaging, FNA, and ERCP features. This might take the form of a dedicated scope, or could involve a scope platform (similar to what is used in NOTES) through which we can place an EUS catheter probe and then switch out for ERCP accessories, and even possibly use cholangioscopy to complete the case without fluoroscopy.

As we do increasingly complex therapeutic interventions, we are more frequently using larger 3.8 mm diameter working channels to pass accessories. These therapeutic echoendoscopes are wider diameter and less flexible. It would be ideal to have larger working channels (even up

to 4.2 mm diameter) without the increased scope diameter size, with the ultimate goal of only large working channel scopes so that multiple types of linear echoendoscopes are not needed. Additionally, modifications to the scope tip and/or working channel diameter could improve the ease of needle passage, as discussed in the next section.

For those endosonographers who prefer the advantages of having both radial and linear array scopes, it would be nice to have a combined radial and linear scope, or possibly a multiplanar EUS scope in order to minimize the costs associated with having several different types of EUS scopes in a unit. This would also improve efficiency in terms of not switching from one scope to another. Again, it would be ideal if this could be done in either a forward viewing (EGD) or side viewing (ERCP) scope.

Endoscopic bronchoscopic ultrasound (EBUS) scopes are about a decade behind the state of the art GI EUS scopes, but we should see further advances in these scopes soon. These improvements will require better linear array scopes, and most importantly larger diameter working channels to allow increased use of therapeutic accessories. These scopes will also benefit gastroenterologists who can use them for stenotic esophageal tumors as well as patients who have a narrow cervical esophagus which occasionally prevents conventional echoendoscope passage.

Future EUS Ultrasound Processors

We currently have excellent quality EUS processors, which are often designed for high end transabdominal ultrasound imaging in radiology departments. These machines are quite large and take up significant floor space in our already cramped endoscopy units. Ideally, having smaller EUS processors which can fit onto the shelves of our standard endoscopy carts would be beneficial. This will save space in the unit as well as facilitate transportation of the equipment to the operating room and intensive care unit as needed.

Image quality should constantly improve, as has occurred over the past 20 years. We will likely see additional ways of visualizing lesions, as we have with Doppler and elastography. Additionally, contrast enhanced EUS will be further explored, although the widespread use may be limited because of the requirement for intravenous injection.

Future EUS Accessories

We have several FNA/FNI needles we use on a daily basis, consisting of 19, 22, and 25 gauge needles. In general, either the 22 or 25 gauge

needle is adequate to perform EUS FNA. The 19 gauge needle is useful for FNI and other therapeutic procedures. While improving EUS needle tip ultrasound visualization is always desirable; a trained endosonographer should be able to see all the current generation needles without difficulty.

A common problem for all needles is passage through an angulated or flexed distal part of the endoscope. It is unclear if this is a scope issue or a needle issue, but the reality is that commonly used needles will not pass through the distal end of the echoendoscope without pushing the up/down wheel forward (“looking down”) as far as possible to straighten the scope tip. When this is done, the target lesion is temporarily lost. With experience, one learns how to keep the scope very still during this maneuver such that when “looking up” again, the image comes back into view. However it would be advantageous to not have to perform endoscopic gymnastics by increasing the flexibility of both the needles and echoendoscope to facilitate needle passage.

Although EUS FNA is extremely good at obtaining tissue diagnosis, I suspect we will see increasing permutations to try to increase diagnostic yield. Perhaps some modification in needle design may result in more efficient diagnostic yield requiring just one to two passes rather than the three to five passes for diagnostic material. This would greatly help our efficiency and reduce cytopathology costs. We have seen attempts at different sized needles, different suction techniques, altered puncture forces, and brushes within needles to improve tissue diagnosis. None of these have made a dramatic impact in tissue diagnosis, and so we await further efforts.

The diagnostic accessory we need most is a device which can obtain large amounts of tissue for histopathologic, rather than cytopathologic, evaluation. This would assist in the diagnosis of certain challenging lesions such as autoimmune pancreatitis, lymphomas, and might also expand the utility of transgastric EUS into the realm of routine liver biopsies. We currently have a EUS-guided 19 gauge Tru-cut needle, but it is technically difficult to use (especially with the scope bent in the duodenum) and provides inconsistent amounts of tissue. However, if such a device were designed to work easily and reliably, this could significantly change what we do from obtaining cytology with several passes and using an in-room cytologist, to obtaining just one or two passes and sending them to Pathology for later analysis, as we do for mucosal or liver biopsies. This would be more time efficient and less expensive.

There is also a great need for industry to develop improved instruments for interventional EUS procedures. Perhaps most pressing is improved accessories for trans-intestinal drainage of fluid collections,

such as pseudocysts, obstructed bile ducts, bilomas, or perirectal abscesses. These would include items such as “one-step” drainage systems in which a single device could puncture through the intestinal tract into a fluid collection, followed by the advancement of a wire, dilating catheter, and stent assembly coaxially as a single device. Additionally, we could use either steerable catheters or steerable wires which would facilitate punctures into a dilated biliary system and manipulation of a wire through an obstructing mass for a rendezvous procedure.

Interventional procedures which involve injection of liquids, such as chemotherapy agents, might be improved by needles which can allow easier injection of viscous fluid. These needles might also have fenestrated tips which could allow the even distribution of fluid throughout a lesion. If cyst ablation were ever to become a proven management tool, one could also imagine double-channel catheters which allow simultaneous irrigation and aspiration.

EUS-guided metal fiducial placement for stereotactic radiosurgery is being increasingly performed into solid tumors (1, 2). The current limitation of this technique is that a 19 gauge needle is needed to accommodate the 0.8 mm diameter \times 3.0 mm long fiducials, which makes placement in the duodenum difficult. A 22 gauge needle with slightly thinner fiducials would be beneficial. Additionally, the ability to place multiple fiducials in a single puncture might be useful, perhaps with spacing material between the fiducials.

As an offshoot of NOTES procedures, it would be exciting to have a commercially available T-fastener device which we could use for tissue apposition. One could imagine a number of uses, such as endoscopic fundoplication, endoscopic gastric restriction for obesity, and anchoring of a pseudocyst, common bile duct, or gallbladder to adjacent intestinal wall to prevent leakage after drainage procedures.

EUS INDICATIONS IN THE FUTURE

Mediastinal EUS

Transesophageal EUS FNA for posterior mediastinal lesions should continue to be important, although probably less so with the more widespread use of PET scanning to assess mediastinal adenopathy for obvious malignancy and EBUS FNA by pulmonologists for tissue diagnosis. As more studies show the ease and effectiveness of EUS FNA for sampling mediastinal adenopathy, a combination of both EUS and EBUS FNA may eventually replace diagnostic surgical mediastinoscopy (3).

Luminal GI Tract Cancer

For the next few years, EUS will continue to have an important impact in local staging of esophageal and rectal tumors. It will help determine candidacy for endoscopic therapy as well as induction chemoradiation. However, as noninvasive imaging improves with CT and MRI for local staging, as well as PET for diagnosing metastatic disease, it is possible that EUS will be less utilized. Additionally, as we learn more about which patients benefit most from preoperative chemoradiation, we could see a trend to give nearly all patients with esophageal and rectal cancer preoperative chemoradiation regardless of stage, which would obviate the need for any local EUS staging. EUS for gastric and ampullary/duodenal cancer is mostly useful for identifying which tumors can undergo endoscopic management alone, and this will unlikely change. Endoscopic injection of chemotherapy agents may increase in the future, but it is uncertain if there will be an advantage to using EUS-guided FNA injection over injection using a sclerotherapy needle and a standard endoscope in luminal cancers (4).

Pancreatic Cancer

We are already seeing that improved noninvasive imaging studies such as multidetector CT and newer MRI scanners provide similar, but not perfect predictions of resectability of pancreatic cancer (5). In many expert centers, these less invasive studies are already the modality of choice for deciding surgical resectability of a lesion. However, EUS will continue to be needed to diagnose small lesions not visualized on CT or MRI, and most importantly to easily and safely obtain a tissue diagnosis. It is quite possible that future cancer therapies could be based on the analysis of tumor tissue for chemosensitivity testing, and this individualized therapy would increase demand for EUS FNA tissue acquisition, possibly before and during chemotherapy treatment (6).

We will see continued efforts toward injection of therapeutic agents into pancreatic cancers to try to impact tumor biology (7). These are still investigational, and hopefully one of the new agents such as modified viral vectors, radioactive material, or chemotherapy will prove to have a positive impact.

Pancreatic endocrine tumors are more frequently being diagnosed with routine use of CT scans. These tumors often have a much slower disease progression than adenocarcinoma, and might be amenable to EUS-guided ablation as described in the next section.

Pancreatic Cysts

Pancreatic cysts are perhaps the greatest challenge facing us over the next decade. The increasing use of highly sensitive CT and MRI scanners for a variety of abdominal conditions is leading to frequent detection of incidental and asymptomatic pancreatic cysts. The vast majority of these cysts will never result in pancreatic cancer death, but could result in large numbers of noninvasive tests as well as risky invasive testing and surgery.

A major problem we have is that we cannot predict the natural history of cysts. Most incidental cysts imaged with EUS, which are >2–3 cm and do not have an associated mass or dilated pancreatic duct, will not progress into cancer. Despite this, endosonographers frequently feel compelled to perform FNA aspiration of the cysts for amylase, lipase, CEA, and perhaps other biomarkers to try to stratify which patients are most likely to have mucinous lesions as a surrogate for developing cancer. However, at best, fluid analysis has an accuracy of 80% with a risk of approximately 1% of pancreatitis, bleeding, or infection secondary to the procedure (8, 9). We usually end up making a decision about cyst management based on factors other than cyst fluid analysis, such as patient age, symptoms, comorbidities, or family history. For these reasons, I rarely find it helpful to perform routine pancreatic cyst fluid analysis, and unless there is a dramatic breakthrough in either diagnostic markers or treatment, I suspect the rates of routine pancreatic cyst aspiration will decrease.

If the physician or patient is concerned about the risk of a pancreatic cyst developing into adenocarcinoma, the only way to reduce that risk is to have it surgically resected. Unfortunately, a partial pancreatectomy could have a higher mortality than the cyst posed. Where we are now with pancreatic cysts in many ways is analogous to where we were before endoscopic therapy existed for colon adenomas or Barrett's with high grade dysplasia. In the past, patients with colon polyps found on barium enema underwent surgical resection, but now they undergo less invasive colonoscopic polypectomy. In the past, all patients with Barrett's esophagus with high grade dysplasia or early carcinoma underwent esophagectomy, but now these patients are successfully undergoing endoscopic thermal ablation or mucosal resection. There is a need for a safe and effective endoscopic means to ablate high risk pancreatic cysts similar to what we have for colon adenomas and dysplastic Barrett's esophagus.

EUS-guided pancreatic cyst ablation could have great impact on endosonography in the future. There have been animal studies evaluating ablation of pancreatic parenchyma using radiofrequency ablation,

photodynamic therapy, and alcohol injection (10). Recent human studies described in a previous chapter have looked at absolute alcohol with or without paclitaxel and had promising results (11, 12). The main concern here is the risk of causing pancreatitis, or perhaps worse, causing permanent damage to the main pancreatic duct. This is an important and promising area of investigation, and hopefully we can learn from our interventional radiology and surgery colleagues who have used ablation modalities for a variety of solid and cystic lesions for years. It may be possible that in the future we use EUS to aspirate pancreatic cysts for biomarkers to determine which cysts are at highest risk for future malignancy and then use this information to decide which lesions will undergo EUS-guided cyst ablation.

EUS Pseudocyst Drainage

EUS has already become a standard part of many endoscopic pseudocyst drainage procedures. It allows cysts to be imaged that otherwise cannot be seen due to lack of mucosal bulging. Additionally, it can help diagnose potential malignant cysts and reduce bleeding risks by using ultrasound guidance of needle insertion. Hopefully, future scope and device development will allow easier one-step drainage of pseudocysts using either forward viewing linear scopes or possibly side viewing scopes with elevators. Additionally, one-step stent introducer kits would be an improvement, as discussed above.

One of the major problems with pseudocyst and pancreatic necrosis drainage is the relatively small (10mm) cystgastrostomy we create. I envision combined use of surgical and EUS techniques in the future, such as using EUS-guidance to enter a pseudocyst, then a flexible transoral (or laparoscopic transgastric) stapler to create a 40 mm cystgastrostomy. An endoscope or laparoscope could then enter the cyst for debridement (13).

EUS Celiac Plexus Neurolysis

Over the past decade pancreatic cancer pain management has significantly improved because of advances in medical oncology related to both pain management and newer chemotherapeutic agents. The need for celiac plexus neurolysis in most centers is decreasing. Additionally, celiac plexus blocks seem to have limited to no longterm efficacy for management of pain secondary to chronic pancreatitis.

CBD Stones

EUS should play an increasing role in the evaluation of patients with immediate probability for CBD stones. EUS can easily image the bile duct, and therefore potentially avoid exposure to the risks of diagnostic ERCP if no stones are present. The ability to use a single scope for both diagnostic (for detection of choledocholithiasis) as well as therapeutic (delivery of the stone) purposes would be ideal. It has been recently reported that small CBD stones can be removed by EUS-guidance alone, which would eliminate the use of fluoroscopy (14). The future could also include catheter ultrasound probes which can be passed down the ERCP scope working channel and be oriented to provide transduodenal imaging of the extrahepatic bile duct.

Biliary Drainage

As outlined in a previous chapter, EUS has tremendous potential to assist in biliary drainage. It is quite possible that with improved wires and catheters, we will have the ability to more easily do single session EUS-guided rendezvous procedures to place transpapillary biliary stents which will become more commonplace. Additionally, hepaticogastrostomies or choledochoduodenostomies will be increasingly performed (15, 16). While we are seeing these are technically feasible, we need to examine safety and efficacy outcomes. Important questions to ask are whether these biliary drainage procedures are best done using stents by creating permanent fistulas (i.e., via magnets). Alternatively, we may need to perform hepaticojejunostomies, to create the same longterm drainage as can be obtained surgically.

Hemostasis and Vascular EUS

There are two ways EUS can be used to assist in hemostasis. The least costly method would be to use a dedicated Doppler probe placed through the working channel of a therapeutic EGD scope. This probe can then be used to detect blood flow through an underlying vessel and direct standard hemostasis (thermal probes or clips) until no further signal is detected (17). However, given our current success at endoscopic hemostasis and the additional cost and time the use of doppler probes may add, it seems unlikely that they will ever gain widespread use.

The other means of EUS-guided hemostasis would be using linear echoendoscopes to find a bleeding site, such as varix, and then use EUS

FNI for embolization. This has been reported in a small number of cases with injection of alcohol, cyanoacrylate glue, and embolization coils (18). The concept of EUS-guided hemostasis may be useful in highly selected cases.

An intriguing use of EUS might be for the management of portal hypertension. Direct portal venous pressure measuring has been performed using direct EUS puncture in the portal vein in animal models (19). This has the potential in humans to provide direct portal pressure measurement, rather than the indirect measurement currently obtained via wedged hepatic vein pressures. Likewise, there is animal work suggesting that a EUS-guided procedure could be used to place a metal portocaval shunt (TIPS) via portal vein puncture (20). These are exciting areas of future investigation.

EUS and NOTES/Surgery

Therapeutic EUS FNA and Natural Orifice Transluminal Endoscopic Surgery (NOTES) are very similar. In both procedures, the outside of the luminal GI tract is accessed to obtain tissue or perform an intervention. NOTES clearly is more surgical, while therapeutic EUS FNA is more like interventional radiology being limited to needle-type devices. We might see a convergence of EUS and NOTES for access to the peritoneal cavity by using EUS to help find a safe place to enter.

The increasing prevalence of both GERD and obesity makes both of these diseases prime candidates for endoscopic therapies. As described in the previous chapter, it is quite possible that EUS-guided tissue apposition using T-fasteners could help create funduplications or assist with restrictive gastric procedures.

FUTURE TRAINING AND QUALITY ISSUES

Training in EUS will continue to be uniquely different from other endoscopic training in fellowship because it involves learning ultrasound imaging, detailed thoracic, abdominal and pelvic extraluminal anatomy, and GI and pulmonary oncology. Whether EUS, and for the matter ERCP, is learned during the standard 3-year fellowship or as part of a “4th-year” advanced endoscopy fellowship partially depends on the fellowship. Most GI fellows who want to become fully trained interventional endoscopists should do a 4th-year fellowship under the

mentorship of an experienced therapeutic endoscopist. Given that interventional endoscopy combines tools and techniques from a variety of endoscopist procedures, it is optimal to be trained in all aspects of therapeutic endoscopy, including EUS, ERCP, EMR, ablative techniques, deep enteroscopy, and complicated polypectomy. This cross-training is invaluable when using EUS to assist or perform therapeutic procedures. In addition to hands-on apprentice learning, trainees should also study anatomy atlases, EUS textbooks, educational videos, and attend regional/national courses.

In the future, there will be a need for practicing endosonographers who were previously trained in diagnostic EUS to learn the newer therapeutic maneuvers. These issues are now arising in terms of EUS-guided pseudocyst and fluid collection drainage, EUS-assisted biliary stent placement (rendezvous and transenteric stent placement), and EUS-guided Fine Needle Injection (FNI). Future training for these physicians will most likely involve training with inanimate models (pig stomachs, gelatin phantoms, etc.) or computer simulators during which the techniques can be learned in a safe and effective teaching environment.

We should consider training our pulmonary colleagues in transesophageal EUS FNA for access to mediastinal lymph nodes and central lung masses. Given that the pulmonary physicians have longterm management of these patients, it may be best for them to be adept at both EBUS and EUS, and have the back up of a gastroenterologist specially trained in transesophageal EUS.

As quality issues become increasingly important, so does the need for quality assessment. There have been initial attempts at monitoring appropriate indications and documentation. However, we may need to evaluate more objective outcomes, such as diagnostic rate of malignancy during EUS-guided FNA, or success rate for EUS-guided pseudocyst drainage (21).

CONCLUSIONS

The future of EUS is bright! There are exciting new echoendoscopes and accessories that will hopefully be available soon. These will lead to further innovations in therapeutic EUS procedures. New training methods will allow us to quickly learn these techniques in a safe and efficient manner. The creative interventional endoscopists who have embraced EUS will continue to push us into new frontiers.

REFERENCES

1. Pishvaian AC, Collins B, Gagnon G, Ahlawat S, Haddad NG. EUS-guided fiducial placement for CyberKnife radiotherapy of mediastinal and abdominal malignancies. *Gastrointest Endosc.* 2006;64(3):412–7.
2. Owens DJ, Savides TJ. EUS placement of metal fiducials by using a backloaded technique with bone wax seal. *Gastrointest Endosc.* 2009;69(4):972–3.
3. Wallace MB, Pascual JM, Raimondo M, et al. Minimally invasive endoscopic staging of suspected lung cancer. *JAMA.* 2008;299(5):540–6.
4. DuVall GA, Tarabar D, Seidel RH, Elstad NL, Fowers KD. Phase 2: a dose-escalation study of OncoGel (ReGel/paclitaxel), a controlled-release formulation of paclitaxel, as adjunctive local therapy to external-beam radiation in patients with inoperable esophageal cancer. *Anticancer Drugs.* 2009;20(2):89–95.
5. DeWitt J, Devereaux B, Chriswell M, et al. Comparison of endoscopic ultrasonography and multidetector computed tomography for detecting and staging pancreatic cancer. *Ann Intern Med.* 2004;141(10):753–63.
6. Michalski CW, Erkan M, Sauliunaite D, et al. Ex vivo chemosensitivity testing and gene expression profiling predict response towards adjuvant gemcitabine treatment in pancreatic cancer. *Br J Cancer.* 2008;99(5):760–7.
7. Chang KJ, Irisawa A. EUS 2008 Working Group document: evaluation of EUS-guided injection therapy for tumors. *Gastrointest Endosc.* 2009;69 Suppl 2:S54–8.
8. Brugge WR, Lewandrowski K, Lee-Lewandrowski E, et al. Diagnosis of pancreatic cystic neoplasms: a report of the cooperative pancreatic cyst study. *Gastroenterology.* 2004;126(5):1330–6.
9. Khalid A, Zahid M, Finkelstein SD, et al. Pancreatic cyst fluid DNA analysis in evaluating pancreatic cysts: a report of the PANDA study. *Gastrointest Endosc.* 2009;69(6):1095–102.
10. Brugge WR. EUS-guided tumor ablation with heat, cold, microwave, or radiofrequency: will there be a winner? *Gastrointest Endosc.* 2009;69 Suppl 2:S212–6.
11. Gan SI, Thompson CC, Lauwers GY, Bounds BC, Brugge WR. Ethanol lavage of pancreatic cystic lesions: initial pilot study. *Gastrointest Endosc.* 2005;61(6):746–52.
12. Oh HC, Seo DW, Lee TY, et al. New treatment for cystic tumors of the pancreas: EUS-guided ethanol lavage with paclitaxel injection. *Gastrointest Endosc.* 2008;67(4): 636–42.
13. Romanelli JR, Desilets DJ, Earle DB. Pancreatic pseudocystgastrostomy with a peroral, flexible stapler: human natural orifice transluminal endoscopic surgery anastomoses in 2 patients (with videos). *Gastrointest Endosc.* 2008;68(5):981–7.
14. Artifon EL, Kumar A, Eloubeidi MA, et al. Prospective randomized trial of EUS versus ERCP-guided common bile duct stone removal: an interim report (with video). *Gastrointest Endosc.* 2009;69(2):238–43.
15. Savides TJ, Varadarajulu S, Palazzo L. EUS 2008 Working Group document: evaluation of EUS-guided hepaticogastrostomy. *Gastrointest Endosc.* 2009;69 Suppl 2:S3–7.
16. Itoi T, Yamao K. EUS 2008 Working Group document: evaluation of EUS-guided choledochoduodenostomy (with video). *Gastrointest Endosc.* 2009;69 Suppl 2:S8–S12.

17. Wong RC. Endoscopic Doppler US probe for acute peptic ulcer hemorrhage. *Gastrointest Endosc.* 2004;60(5):804–12.
18. Levy MJ, Chak A. EUS 2008 Working Group document: evaluation of EUS-guided vascular therapy. *Gastrointest Endosc.* 2009;69 Suppl 2:S37–42.
19. Giday SA, Clarke JO, Buscaglia JM, et al. EUS-guided portal vein catheterization: a promising novel approach for portal angiography and portal vein pressure measurements. *Gastrointest Endosc.* 2008;67(2):338–42.
20. Buscaglia JM, Dray X, Shin EJ, et al. A new alternative for a transjugular intrahepatic portosystemic shunt: EUS-guided creation of an intrahepatic portosystemic shunt (with video). *Gastrointest Endosc.* 2009;69(4):941–7.
21. Savides TJ, Donohue M, Hunt G, et al. EUS-guided FNA diagnostic yield of malignancy in solid pancreatic masses: a benchmark for quality performance measurement. *Gastrointest Endosc.* 2007;66(2):277–82.

Index

A

Acinar cell carcinomas (ACCs), 141–142
American Cancer Society, 370
American Joint Committee
 on Cancer (AJCC), 184
American Society for Gastrointestinal
 Endoscopy (ASGE), 222, 375
Amine precursor uptake and decarboxylation
 (APUD), 282
Ampullary and duodenal lesions
 ampullary cancer
 diagnosis, 268
 TNM classification, 272, 274
 treatment, 275
 duodenal lesions
 benign lesions, 276
 Whipple's procedure, 276
 EUS examination technique
 EUS-guided FNA, 269
 intraductal ultrasound, 269–272
 radial echoendoscope, 268
 EUS staging accuracy, 272–274
 evaluation, 266
 TNM classification, 274
 treatment, 275
 vater
 benign lesions, 266–267
 malignant lesions, 267–268
 minor duodenal ampulla, 268
Aortopulmonary window (APW), 216

B

Balloon technique, 36
Barrett's esophagus, 198
B-cell lymphoma, 285
Benign lesions
 adenoma-carcinoma sequence, 266
 duodenal ampulla, 267
Biliary decompression

EUS-guided ERC, 396
percutaneous transhepatic drainage,
 390, 401
 surgical intervention, 390
Biliary imaging technique
 intraductal ultrasonography
 data acquisition, 332
 3D-IDUS probes, 331
 fluid irrigation, 332
 ultrasonic transducer, 331
 normal bile duct wall, 333–334
 standard endoscopic ultrasonography
 “*apical*” position, 329
 color Doppler examination, 331
 “*kissing the papilla*” position, 329
 liver hilum, 329, 331
 principal limitations, 331
 radial-and linear-scanning
 echoendoscope, 329
Biliary strictures
 standard endoscopic ultrasonography
 detection and characterization,
 342–343
 EUS-FNA impact, 348–349
 longitudinal tumor extent, TNM stage,
 and resectability, 346–348
 sampling, 343–346
 therapeutic EUS
 IDUS features, 350
 preamble, 353
 technique, 391–392
Biliary tract
 anatomy, 46–47
 bile duct strictures, 48
 cholangiocarcinoma, 48–49
 choledocholithiasis, 47–48
Biologic anti-tumor therapy
 dendritic cells, 444–445
 ONYX-015, 443–444
 TNFerade, 444

- Brachytherapy, 457–459
- Bronchogenic cysts, 207
- Bronchoscopy
vs. EUS, 216
TBNA, 216
- C
- Carcinoembryonic antigen (CEA), 304–305
- Carcinoid tumor, 257
- CBDS. *See* Common bile duct stones
- CEA. *See* Carcinoembryonic antigen
- Celiac plexus
block
chronic abdominal pain, 424
corticosteroid, 430
neurologic side effects, 431
preservative-free bupivacaine, 430
surgical intervention, 431
- neurolysis
absolute alcohol, 430
corticosteroid (triamcinolone), 425
local anesthetic (bupivacaine),
425, 430
posterior transcutaneous
approach, 424
preservative-free saline, 430
- Chemotherapy, 455–257
- Cholangiocarcinoma, 48–49
EUS-FNA results, 344
TNM classification, 346, 347
- Cholelithiasis, 47–48
- Colonoscopy, 21
- Common bile duct stones (CBDS), 79,
107–108, 269, 271. *See also*
Gallstone disease
EUS vs. magnetic resonance cholangio-
pancreatography, 339
risk factors, 334, 335
- Computed tomography (CT), 189, 211, 214,
231, 266
- Condom technique, 35–36
- Contrast-enhanced endoscopic ultrasound
benign and malignant mediastinal and
abdominal lymph nodes, 480–481
- CECT/CEMRI, 475
- contrast harmonic imaging, 474
- limitations, 474
- pancreatic cancer
angiographic images, 477–478
CE-EUS, 477–478
- endocrine tumors, 479
- EUS-FNA, 477–478
- fibrotic reaction, 476
- pancreatic tumors, 481
- spatial resolution, 474
- ultrasound contrast agents (UCAs)
advantage and limitations, 474–475
- IPMN, 479–480
- metastasis, 480
- microbubbles, 475–476
- transpulmonary UCA, 475
- Cryoablation, 450–452
- Curvilinear echoendoscope, 219
- Cyanoacrylate-lipiodol, 494, 495
- CyberKnife radiotherapy, 222, 459–460
- Cystic pancreatic lesions (CPLs)
characteristics, 299, 300
- cyst fluid evaluation
cytology, 303–304
genetic markers, 305–306
tumor markers, 304–305
- EUS guided fine needle aspiration
(EUS-FNA), 301–302
- EUS vs. imaging modalities, 299–301
- intraductal papillary mucinous
neoplasms (IPMN)
acute recurrent pancreatitis, 311–312
- ERCP appearance, 311, 313
- EUS sensitivity, 314
- fine needle aspiration cytology smear,
312, 314
- pancreas resection, 311, 313
- risk factors, 312, 314
- mucinous cystadenomas (MCN)
columnar epithelial cells, 309, 311
- morphology, 309
- peripheral calcifications, 309–310
- serous cystadenomas (SCA), 306–308
- solid pseudopapillary tumors (SPT),
315–317
- treatment
expectant management, 317
- non-operative therapies, 318–319
- surgical management, 318
- trucut biopsy (TCB), 302–303
- D
- Diagnostic ultrasonography, 4
- Duodenal lesions, 275–276
- Duplication cysts, 207

E

- EAS. *See* External anal sphincter
- Elastography, 22, 24, 25
- Electromyography (EMG), 377
- Electronic radial echoendoscopes, 66–67
- EMR. *See* Endoscopic mucosal resection
- Endobronchial ultrasound (EBUS), 15–17, 211, 216–217
- Endocrine tumor, 477
- Endoluminal endosurgical methods
 - biliary tract, 489–491
 - bilioma drainage, 491
 - pancreatic duct interventions, 491–492
 - pancreatic necrosectomy, 487–489
 - vascular interventions, 492–494
- Endoscopic bronchoscopic ultrasound (EBUS), 513
- Endoscopic mucosal resection (EMR), 191, 198
- Endoscopic retrograde
 - cholangiopancreatography (ERCP), 272, 329, 390, 476
- Endoscopic submucosal dissection (ESD), 241
- Endoscopic ultrasound-guided fine needle aspiration (EUS-FNA)
 - adrenal gland, 154–155
 - cytology principles, 112–114
 - extrahepatic biliary system and gallbladder, 152
 - liver biopsy, 152–154
 - luminal gut biopsy
 - adenocarcinomas, 115–117
 - carcinoid and neuroendocrine tumors, 119–121
 - duplication and bronchogenic cysts, 130
 - lymphomas, 125–128
 - melanomas, 128–130
 - mesenchymal neoplasms, 121–125
 - spindle cell carcinoma, 118–119
 - squamous cell carcinoma, 117–118
 - lung and mediastinum biopsy
 - large cell neuroendocrine carcinomas, 135–136
 - nonsmall cell carcinoma, 134
 - small cell neuroendocrine carcinoma, 136–137
 - well differentiated adenocarcinomas, 134–135
 - lymph nodes biopsy
 - adenopathy, 131–133
 - malignancy staging, 131
- pancreas biopsy
 - acinar cell carcinomas (ACCs), 142
 - cystic lesions, 147–152
 - lymphomas, 144
 - metastatic, 144–145
 - pancreatic ductal adenocarcinomas (PDAs), 139–141
 - pancreatic endocrine neoplasms (PENs), 142, 143
 - pancreatoblastomas, 143, 144
 - solid lesions, 145–146
 - solid pseudopapillary tumors (SPTs), 143, 144
- terminology, 114
- Endosonographers
 - accessories
 - EUS FNA, 515
 - EUS-guided metal fiducial placement, 515
 - gauge needles, 513–514
 - interventional procedures, 515
 - T-fastener device, 515
 - tissue diagnosis, 515
 - biliary drainage, 519
 - CBD stones, 519
 - celiac plexus neurolysis, 518
 - diagnostic imaging test, 507
 - hemostasis and vascular EUS, 519–520
 - luminal GI tract cancer, 516
 - mediastinal EUS, 515
 - pancreatic cancer, 516
 - pancreatic cysts
 - Barrett's esophagus, 517
 - endoscopic thermal ablation, 517
 - pseudocyst drainage, 518
 - scopes
 - linear echoendoscopes, 512, 513
 - pseudocyst drainage, 512
 - stenotic esophageal tumors, 513
 - therapeutic interventions, 511
 - training and quality issues, 520–521
 - ultrasound processors, 513
- Endosonographic instrumentation
 - echoendoscope design, 8–10
 - endobronchial ultrasound devices, 15–17
 - EUS colonoscope, 21
 - EUS needles
 - automated 22 gauge needle, 29, 30
 - disposable models, 26–28
 - 19 gauge core biopsy needle, 29

- Endosonographic instrumentation (*continued*)
- linear array echoendoscopes, 10–13
 - miniproboscopes, 21–23
 - Olympus MH 908 esophagoscope, 17, 19, 20
 - prototype end-viewing
 - echoendoscope, 20–21
 - radial echoendoscopes, 10, 14–15
 - radial vs. linear array, 5–8
 - ultrasound and rationale, 4–5
 - ultrasound console, 21–25
 - ultrasound transducer, 5
- Endosurgery
- endoluminal endosurgical methods
 - biliary tract, 489–491
 - bilioma drainage, 491
 - pancreatic duct interventions, 491–492
 - pancreatic necrosectomy, 487–489
 - vascular interventions, 492–494
 - EUS guided endosurgery
 - mediastinal drainages, 502–503
 - transluminal access, 501
 - transluminal EUS, 503
 - experimental EUS-guided endosurgery
 - cardiac interventions, 499–501
 - EUS-guided anastomosis, 498–499
 - instrument, 494–498
 - interventions, 503–504
- Enterochromaffin-like (ECL), 258
- ERCP. *See* Endoscopic retrograde cholangiopancreatography
- ESD. *See* Endoscopic submucosal dissection
- Esophageal cancer, 103–104
- Barrett's esophagus, 198
 - detecting tumor recurrence, 197
 - diagnosis, 184
- M staging, 195–196
- N staging
- accuracy, 192
 - elastography, 193
 - EUS-FNA, 193
 - FNA, 192–193
 - malignant strictures, 194–195
 - regional lymph nodes, 191–192
- quality indicators, 198
- restaging
- neoadjuvant chemoradiotherapy, 196
 - tumor, 197
- staging
- adenocarcinoma, 186
 - cell carcinoma, 185–186
 - TNM classifications, 184–185
- T staging
- celiac nodes, 189
 - classification, 190
 - hyperechoic layer, 187
 - mucosal and submucosal carcinoma, 191
 - regional staging, 187
 - transverse-or linear-array, 189
- Ethanol ablation, 445–446
- EUS-FNA. *See* Endoscopic ultrasound-guided fine needle aspiration
- EUS guided endosurgery
- mediastinal drainages, 502–503
 - transluminal access, 501
 - transluminal EUS, 503
- EUS-guided fiducial placement
- CyberKnife, 459–460
 - feasibility and safety, 460
- External anal sphincter (EAS), 85, 87
- F
- Familial adenomatous polyposis (FAP), 266
- FDG. *See* 18-Fluorodeoxyglucose
- Fecal incontinence
- anal sphincter, 378
 - clinical impact, 380–381
- EUS
- applications, 381
 - vs. diagnostic tools, 380
 - technique, 378–379
- Fiberoptic echoendoscopes, 65
- Fine needle aspiration, 184, 233, 478, 487.
- See also* Endoscopic ultrasound-guided fine needle aspiration (EUS-FNA)
- GI endoscopy, 375
- lymph nodes, 219
 - perirectal lymph node, 374
 - prophylactic antibiotics, 375
 - role, 208
- Fine needle injection therapy
- echoendoscopes, 442
 - pancreatic cystic lesions (PCL)
 - EUS-guided ethanol lavage, 462–463
 - mucinous cystic lesions, 461–462
 - paclitaxel, 463
 - pre-treatment tumor identification
 - fiducial placement, 459–461
 - tumor marking, 461
 - tumor ablation

- cryoablation, 450–452
 - high-intensity focused ultrasound (HIFU), 455
 - implantable therapy (*see* Implantable therapy)
 - injection therapy (*see* Injection therapy)
 - photodynamic therapy (PDT), 452–455
 - radiofrequency ablation (RFA), 447–450
- 18-Fluorodeoxyglucose (FDG), 238
- FNA. *See* Fine needle aspiration
- Follicular lymphoma, 127, 128
- Forward viewing endoscopy, 94

- G
- Gallbladder
 - carcinoma
 - cholecystectomy, 358
 - lymph nodes, 359
 - TNM classification, 358
 - polypoid lesions
 - adenomyomatous polyps, 356
 - cholesterol polyps, 355–356
 - EUS role, 356–357
 - histopathological findings, 355
 - neoplasms, 356
 - stones, 354–355
- Gallbladder polypoid lesions (GBP), 355
- Gallstone disease
 - CBD stones, 335
 - “idiopathic” acute pancreatitis, 340–342
 - non-invasive tests, 335
 - results
 - choledocholithiasis, 337
 - EUS vs. magnetic resonance cholangio-pancreatography, 339
 - gold-standard, 337
 - meta-analysis, 336
 - risk factors, 335
 - technique, 335–336
- Gastric cancer
 - adenocarcinoma, 228
 - diagnosis and staging, 231
 - EUS
 - comparison, 239
 - technical limitations, 238–239
 - technique, 231–233
 - evaluation
 - Borrmann classification, 241
 - ER techniques, 240
 - linitis plastica, 241–242
 - scirrhous, 241, 242
 - types, 241
 - M-staging, 238
 - N-staging
 - accuracy, 236
 - EUS vs. CT/MRI, 238
 - lymph nodes, 236–238
 - malignant vs. benign lymph nodes, 237
 - staging systems, 229–231
 - T-staging
 - accuracy, 233–234
 - endosonographers, 236
 - pooled sensitivities and specificities, 234
 - T1-T4 tumors, 233
- Gastric mucosa or submucosa, 239
- Gastric subepithelial mass, 250
- Gastric varices, 494, 496
- Gastric wall, 254. *See also* Pancreatic rest
- Gastrointestinal stromal tumor (GIST), 256
 - behavior, 122
 - epithelioid cells, 122
 - mutations, 123
 - spindle cells, 121
- GBP. *See* Gallbladder polypoid lesions
- GIST. *See* Gastrointestinal stromal tumor
- Glomus tumors, 259
- Granular cell tumors, 259

- H
- High frequency ultrasound sonography (HFUS). *See also* Intraductal ultrasonography (IDUS)
 - clinical indications
 - esophagus, 38
 - small bowel and colon, 42–45
 - stomach, 38–42
 - gastrointestinal wall anatomy, 36–37
 - instruments and examination techniques
 - balloon technique, 36
 - condom technique, 35–36
 - mechanical or electronic catheters, 35
- High-intensity focused ultrasound (HIFU), 455
- Hodgkin lymphomas, 132
- Hypoechoic pancreatic mass, 286, 290

I

- IAS. *See* Internal anal sphincter
- IEUCP. *See* Interventional endoscopic ultrasound-guided cholangiopancreatography
- Immunohistochemical (IHC), 261
- Implantable therapy
brachytherapy, 457–459
chemotherapy, 455–457
- Inflammatory fibroid polyp (IFP), 256
- Injection therapy. *See also* Fine needle injection therapy
biologics (*see* Biologic anti-tumor therapy)
ethanol ablation, 445
- Internal anal sphincter (IAS), 85, 87, 378
- Interventional endoscopic ultrasound-guided cholangiopancreatography
biliary decompression, 390
endoscopist selection, 391
enterocholedochal/pancreatic fistula, 392
- EUS-guided biliary drainage
biliary opacification, 396
biliary peritonitis, 398
choledochoduodenal fistula, 396
complications, 398
extrahepatic approach, 393–395
intrahepatic approach, 392–393
rendezvous procedure, 392
- EUS-guided pancreatic drainage
complication rate, 398
intraductal strictures, 395
pancreatic duct, 398
pancreatogastric fistula, 395, 398
pancreatogram, 395, 397
rendezvous technique, 401
- linear-array echoendoscope, 388, 389
pancreatic duct cannulation, 388
patient preparation, 389
patient selection, 388–389
stent placement, 390
target duct, 389
- Intraductal papillary mucinous neoplasms (IPMN)
acute recurrent pancreatitis, 312
ERCP appearance, 313
EUS sensitivity, 314
fine needle aspiration cytology smear, 314
pancreas resection, 313
risk factors, 312
- Intraductal papillary mucinous tumors (IPMT), 473

- Intraductal ultrasonography (IDUS), 269
benign and malignant strictures, 350
biliary tract anatomy, 44–45
cholangiocarcinomas staging, 351–352
clinical indications
bile duct strictures, 46
cholangiocarcinoma, 46–47
choledocholithiasis, 45–46
- pancreas
duct strictures and adenocarcinoma, 48
mucin-producing and Islet-cell tumors, 48–49
- papilla of Vater, 49
technical considerations, 44
- Intramural lesions
benign
duplication cyst, 256
inflammatory fibroid polyp, 256
leiomyoma, 253
lipoma, 252
pancreatic rest, 254–256
varices, 253–254
- malignant/premalignant
carcinoid tumor, 258
gastrointestinal stromal tumor, 256–258
glomus tumors, 258–259
granular cell tumors, 259
lymphoma, 258
metastasis, 259
- Intraoperative EUS (iEUS), 499
- Invasive endoscopic endosurgery (IEE), 492
- IPMN. *See* Intraductal papillary mucinous neoplasms
- Isoechoic lesion, 290

L

- Laparoscopic ultrasonography (LUS), 503
- Linear array echoendoscope
accessories
balloons, 99
buttons and caps, 99–100
chronic pancreatitis and pancreatic ductal anatomy, 104–105
common bile duct stones (CBDS), 105
esophageal cancer, 100–101
pancreatic cancer
evaluation, 103–104
primary staging, 102–103
vs. radial array, 3–6
rectal cancer, 105

- stomach cancer, 101–102
- techniques
 - ampulla, 98–99
 - celiac axis and adjacent structures, 94–95
 - forward viewing endoscopy, 92
 - liver and gallbladder, 96
 - maneuvering, 90–92
 - pancreas duct (PD), 97–98
 - posterior mediastinum, 92–94
 - rectum, 99
- Linitis plastica, 241
- Liver biopsy, 150–152
- Luminal gut biopsy
 - epithelial malignancy
 - adenocarcinomas, 113–115
 - carcinoid and neuroendocrine tumors, 117–119
 - duplication and bronchogenic cysts, 128
 - spindle cell carcinoma, 116–117
 - squamous cell carcinoma, 115–116
 - lymphomas, 125–128
 - melanomas, 128–130
 - mesenchymal neoplasms
 - gastrointestinal stromal tumors (GISTs), 121–123
 - immunohistochemistry, 124–126
 - leiomyomas, 123
 - leiomyosarcomas, 123, 124
 - peripheral nerve sheath and neural tumors, 124
 - schwannomas, 124, 125
- Lung
 - biopsy
 - large cell neuroendocrine carcinomas, 135–136
 - nonsmall cell carcinoma, 134
 - small cell neuroendocrine carcinoma, 136, 137
 - well differentiated adenocarcinomas, 134, 135
 - cancer
 - classification, 211, 212
 - cost effectiveness, 222
 - diagnosis, 223
 - EUS-FNA, 218
 - neo-adjuvant therapy, 208
 - non-small cell lung carcinoma (NSCLC), 210
 - staging, 211–213
- Lymph nodes biopsy
 - adenopathy
 - lymphoproliferative disease, 131
 - mycobacterial infection, 133
 - reactive/infectious causes, 132–133
 - sarcoidosis, 133
 - T-cell and Hodgkin lymphomas, 132
 - malignancy staging, 131
- Lymphoma, 257–259
- Lymphoproliferative disease, 131

- M
- MAC. *See* Monitored anesthesia care
- Magnetic resonance cholangio-pancreatography (MRCP), 328
- Magnetic resonance imaging (MRI), 238
- Malignant lesions, 267–268
- MALT. *See* Mucosa associated lymphoid tissue
- MCN. *See* Mucinous cystadenomas
- Mechanical radial echoendoscopes, 66
- Mediastinoscopy (MS), 216
- Mediastinum
 - biopsy
 - large cell neuroendocrine carcinomas, 135, 136
 - nonsmall cell carcinoma, 134
 - small cell neuroendocrine carcinoma, 136, 137
 - well differentiated adenocarcinomas, 135
 - cysts
 - bronchoscopy vs. EUS, 216
 - classification, 211
 - cost effectiveness, 222
 - cross sectional imaging, 214–215
 - endobronchial ultrasound, 216–217
 - EUS, 210–211
 - EUS and Mediastinoscopy, 216
 - EUS-FNA, role, 218
 - FNA, 208
 - FNA technique, 218–220
 - functional imaging, 215
 - induction therapy, 221–222
 - linear exam, 218
 - lung cancer, 210
 - lung mass, 208–210
 - medical mediastinoscopy, 216
 - new applications, 222
 - selective nodal targeting, 220–221
 - T4 disease, 221
 - Testing, 213–214
 - training, 222–223

- Meperidine, 166
- Mesenchymal neoplasms
 gastrointestinal stromal tumors (GISTs),
 121–123
 immunohistochemistry, 124–126
 leiomyomas, 123
 leiomyosarcomas, 123, 124
 peripheral nerve sheath
 and neural tumors, 124
 schwannomas, 124, 125
- Miniprobes, 21
- Mirizzi's syndrome, 336
- Monitored anesthesia care (MAC), 431
- MRCP. *See* Magnetic resonance
 cholangio-pancreatography
- MRI. *See* Magnetic resonance imaging
- M staging, 195–196, 238
- Mucinous cystadenomas (MCN)
 columnar epithelial cells, 309, 311
 morphology, 309
 peripheral calcifications, 309, 310
- Mucosa associated lymphoid tissue
 (MALT), 257
- N
- Natural orifice transluminal endoscopic
 surgery (NOTES), 520
- N-butyl-2-cyanoacrylate, 487
- Needles
 disposable models, 26–30
 19 gauge core biopsy needle, 29
 PowerShot, 29, 30
- Negative predictive value (NPV), 214
- Neoadjuvant chemotherapy, 210, 222
- Neoadjuvant therapy, 196
- Neuroendocrine tumor, 292
- Nonsmall cell lung carcinoma
 (NSCLC), 206
- N staging, cancer
 accuracy, 192, 236
 elastography, 193
 esophageal cancer, 191
 EUS-FNA, 193
 FNA, 192–193
 gastric cancer, 236
 lymph nodes, 236–237
 malignant strictures
 stricture dilation, 194
 TTS balloon, 194–195
 regional lymph nodes, 191–192
- O
- Olympus echoendoscope
 automated 22 gauge needle, 29, 30
 console, 22–24
 endobronchial ultrasound scope, 16
 linear array, 10, 13
 MH 908 esophagoprobe, 17, 19, 20
 prototype end-viewing echoendoscope,
 20–21
 radial array, 6, 8, 15
 therapeutic echoendoscopes, 13
 Olympus GF-UM160 model, 65, 66
- P
- Pancreas
 biopsy
 acinar cell carcinomas, 142
 cystic lesions, 147–152
 lymphomas, 144
 metastatic, 144–145
 pancreatic ductal adenocarcinomas,
 139–141
 pancreatic endocrine neoplasms,
 142, 143
 pancreatoblastomas, 143, 144
 solid lesions, 145–146
 solid pseudopapillary tumors (SPTs),
 143, 144
 duct strictures and adenocarcinoma, 50
 mucin-producing and islet-cell tumors,
 50–51
- Pancreatic cancer
 brain-mediated mechanisms, 425
 celiac plexus, 425–426
 clinical presentation and evaluation
 hormonally hyper-functioning and
 non-hyper functioning, 283
 hyperechoic mass, 283
 pancreatic lymphoma, 283
 symptoms, 282, 283
 endoscopic ultrasound (EUS)
 array system, 288
 vs CT, 291–292
 echoendoscope designs, 288
 EUS guided FNA, 292
 evaluation, 105–106
 post-procedure monitoring, 432
 pre-procedure preparation, 431–432
 primary staging, 105–106
 procedure efficacy

- CT-guided CPB, 434
- narcotic usage, 433
- one site vs. bilateral injection, 434
- pain control, EUS CPN for, 433, 435
- percutaneous CPN, 433
- subgroup analysis, 434
- radiographic imaging, 287
- side effects and complications, 432–433
- surgical resection, 282
- techniques
 - adrenal gland, echogenicity of, 428
 - bupivacaine, 430
 - celiac artery take-off, 426
 - celiac ganglia, 428, 429
 - CPB technique, 429
 - doppler guidance, 428
 - EUS-guided celiac
 - plexus injection, 427
 - linear echoendoscope, 426
 - Tru-cut needle biopsy, 428
- Pancreatic cystic lesion (PCL)
 - EUS-guided ethanol lavage, 462–463
 - mucinous cystic lesions, 461–462
 - paclitaxel, 463
- Pancreatic ductal adenocarcinoma (PDA), 139–141
- Pancreatic endocrine neoplasms (PENs), 142, 143
- Pancreatic fluid collections
 - Atlanta classification, 408
 - endoscopic drainage, 408
 - EUS-guided drainage
 - advantages, 418
 - clinical treatment, 415
 - conventional transmural drainage, 416
 - cyst resolution, 414
 - disadvantages, 418
 - first-line treatment modality, 416
 - outcomes, 417
 - pancreatic abscess, 412
 - plastic stents, 414
 - recurrence, 414, 415
 - transpapillary stent placement, 415
 - evolution of, 408
 - indications for, 408, 409
 - materials and methods
 - endoscopists, 409
 - instrumentation, 410
 - patient preparation, 409
 - pre-drainage evaluation, 410
 - procedure description, 410–412
 - transmural drainage, 409
 - therapeutic options for, 408
- Pancreatic rest
 - deep mucosa and submucosa, 254, 255
 - gastric antrum, 255
 - histologic diagnosis, 255
- Pancreatogastrostomy (EPG), 491
- Papilla of Vater IDUS, 51
- PCL. *See* Pancreatic cystic lesion
- PDA. *See* Pancreatic ductal adenocarcinoma
- PDT. *See* Photodynamic therapy
- PENs. *See* Pancreatic endocrine neoplasms
- Pentax echoendoscope
 - Hitachi console, 22, 24
 - linear array, 7, 10, 13
 - radial array, 10, 15, 16
- Peptic ulcer disease, 282
- Percutaneous transhepatic biliary drainage (PTD), 490
- Percutaneous transhepatic drainage (PTC), 390. *See also* Interventional endoscopic ultrasound-guided cholangiopancreatography
- Periapillary adenomas, 266
- Pericardial tumor, 500
- PFCs. *See* Pancreatic fluid collections
- Photodynamic therapy (PDT), 191, 198, 452–455
- Piezoelectric effect, 5
- Pitfalls
 - endoscope intubation and passage
 - EGD neck positioning maneuvers, 166
 - hydrostatic balloons, 167
 - equipment selection, 173–174
 - EUS indications
 - diagnostic limitations, 172
 - overstaging, 173
 - radiographic data, 172, 173
 - vascular involvement, 173
 - FNA considerations
 - anti-platelet agents, 174
 - EUS visualization, 175
 - FNA sheath, 175, 176
 - heparin and coumadin, 175
 - preparation and interpretation of specimens, 177
 - orientation
 - celiac axis, 171
 - duodenum, 167
 - extra-luminal structures, 167, 168
 - sedation, 166
 - technical issues
 - acoustic coupling, 171

- Pitfalls (*continued*)
 frequency settings, 172
 image quality, 171
 magnification, 172
 water instillation, 171
- Porcine model, 492
- Portal vein (PV), 492
- Positive predictive value (PPV), 215
- Positron emission tomography (PET), 173, 190, 211, 231, 238
- Primary sclerosing cholangitis (PSC), 352–353
- Probe ultrasonography
 HFUS (*see* High frequency ultrasound sonography (HFUS))
 IDUS (*see* Intraductal ultrasonography (IDUS))
 three-dimensional probes, 51–52
- Prototype end-viewing echoendoscope, 21–22
- R
- Radial endoscopic ultrasonography
 equipment
 fiberoptic echoendoscopes, 65
 mechanical and electronic, 66–67
 Olympus GF-UM160 model, 66
 technical specifications, 64, 66
 gastrointestinal tract wall, 69–70
 mediastinum and esophagus
 distal esophagus, 70–72
 mid-esophagus, 72–74
 proximal esophagus, 75
 pancreas and extrahepatic bile duct
 aorta, 79–82
 common bile duct (CBD), 81
 duodenal bulb, 80–82
 papilla, 80
 splenoportal confluence (SPC), 83
 ventral anlage, 80
 rectum
 fistulas and abscess, 85, 88
 iliac vessels, 85, 86
 internal and external sphincters, 85, 87
 prostate, 85, 86
 rigid probes, 84
 uterus, 85, 87
 stomach
 celiac trunk, 76, 78
 gallbladder, 73–75
 kidney, 75, 76
 left adrenal gland (LAD), 76, 79
 pancreatic body, 76, 78
 prepyloric antrum, 75, 76
- Radiofrequency ablation (RFA), 447
- Radiographic imaging, pancreatic cancer, 287
- RCC. *See* Renal cell carcinomas
- Rectal cancer
 chemotherapeutic agents, 381
 EUS
 accuracy, 376
 applications, 377
 FNA
 GI endoscopy, 375
 perirectal lymph node, 374
 prophylactic antibiotics, 375
 N staging, 373
 preoperative staging, CT, 376
 T staging, 370–373
- Rectal endosonography
 fistulas and abscess, 83, 85
 iliac vessels, 85, 86
 internal and external sphincters, 85, 87
 prostate, 85, 86
 rigid probes, 84
 uterus, 85, 87
- Renal cell carcinomas (RCC), 145
- Restaging
 neoadjuvant chemoradiotherapy, 196
 tumor, 197
- RFA. *See* Radiofrequency ablation
- S
- SCA. *See* Serous cystadenomas
- Serous cystadenomas (SCA), 306–308
- Signet ring carcinoma, 117
- α -Smooth muscle actin (SMA), 253
- Solid pseudopapillary tumors (SPT), 143, 147, 298–299
- SPC. *See* Splenoportal confluence
- Spindle cell carcinoma, 119–120
- Splenoportal confluence (SPC), 83
- SPT. *See* Solid pseudopapillary tumors
- Squamous cell carcinoma, 117–118
- Staging
 adenocarcinoma, 186
 cell carcinoma, 185
 esophageal cancer, 184
 TNM classifications, 185
- Stomach cancer, 104–105

- Subepithelial lesions
 - extramural lesions, 251
 - intramural lesions
 - benign, 252–256
 - malignant/premalignant, 256–259
- T
- TBC. *See* Trucut biopsy
- TBNA. *See* Trans-bronchial fine-needle aspiration
- T-cell lymphomas, 132
- T4 disease, 221
- Thickened gastric folds, 243
- TNM. *See* Tumor, node, and metastasis
- Trans-bronchial fine-needle aspiration (TBNA), 213
- Trans-esophageal endoscopic ultrasound, 206
- Trucut biopsy (TCB), 302–303
- T staging, cancer
 - accuracy, 233–234
 - celiac nodes, 189
 - classification, 190
 - endosonographers, 236
 - esophageal cancer, 189
 - gastric cancer, 231
 - hyperechoic layer, 187
 - mucosal and submucosal carcinoma, 191
 - pooled sensitivities and specificities, 234
 - regional staging, 187
 - transverse-or linear-array, 189
 - T1-T4 tumors, 233
- Tumor, node, and metastasis (TNM), 211, 229, 238–239
- U
- Ultrasonography (US), 266
- Ultrasound transducer, 4